WOMEN IN THORACIC ONCOLOGY: 2021

EDITED BY: Meng Xu Welliver and Ticiana A. Leal
PUBLISHED IN: Frontiers in Oncology

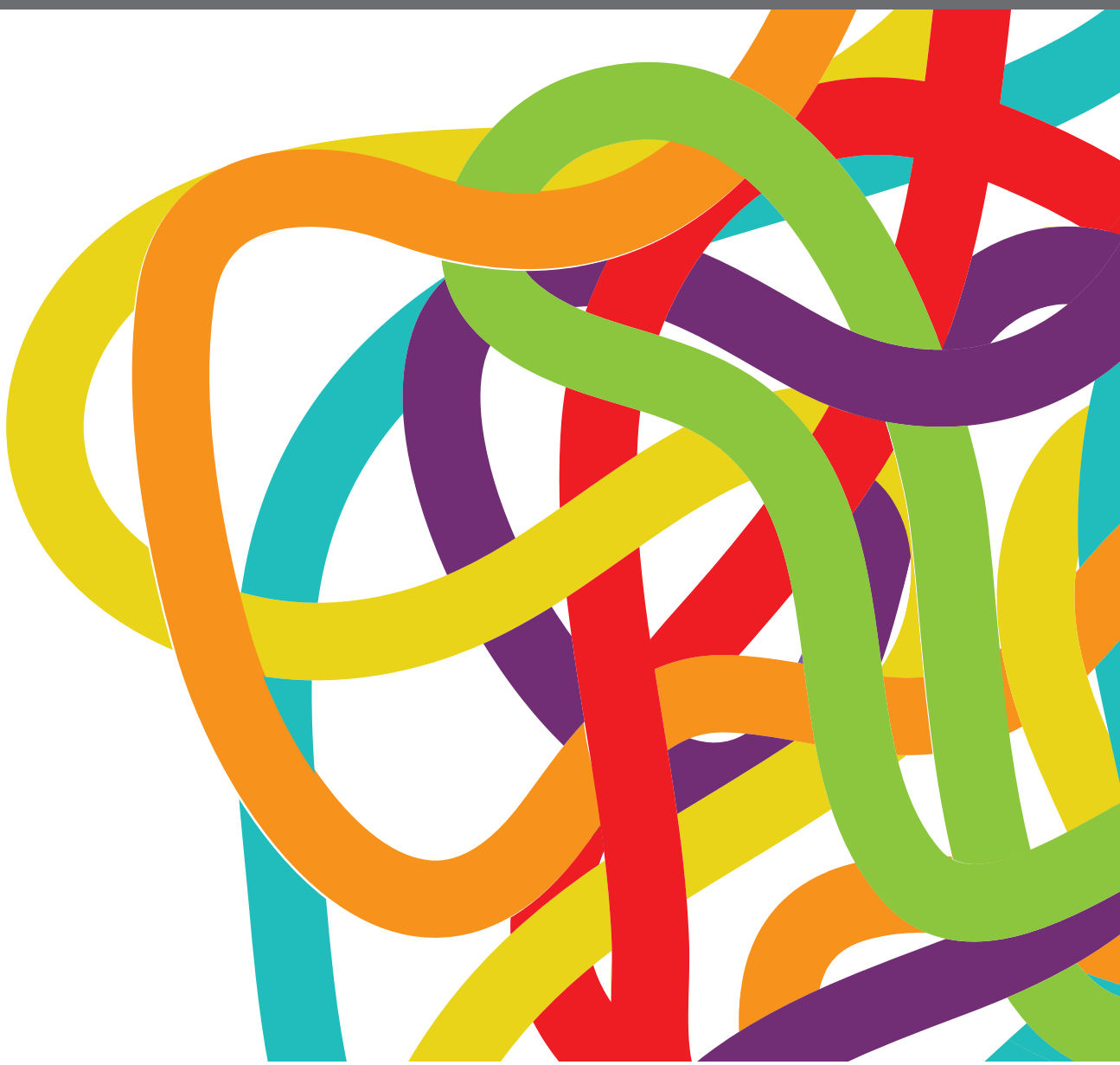

frontiers Research Topics

frontiers

ISSN 1664-8714
ISBN 978-2-83250-330-0
DOI 10.3389/978-2-83250-330-0

About Frontiers

Frontiers is more than just an open-access publisher of scholarly articles: it is a pioneering approach to the world of academia, radically improving the way scholarly research is managed. The grand vision of Frontiers is a world where all people have an equal opportunity to seek, share and generate knowledge. Frontiers provides immediate and permanent online open access to all its publications, but this alone is not enough to realize our grand goals.

Frontiers Journal Series

The Frontiers Journal Series is a multi-tier and interdisciplinary set of open-access, online journals, promising a paradigm shift from the current review, selection and dissemination processes in academic publishing. All Frontiers journals are driven by researchers for researchers; therefore, they constitute a service to the scholarly community. At the same time, the Frontiers Journal Series operates on a revolutionary invention, the tiered publishing system, initially addressing specific communities of scholars, and gradually climbing up to broader public understanding, thus serving the interests of the lay society, too.

Dedication to Quality

Each Frontiers article is a landmark of the highest quality, thanks to genuinely collaborative interactions between authors and review editors, who include some of the world's best academicians. Research must be certified by peers before entering a stream of knowledge that may eventually reach the public - and shape society; therefore, Frontiers only applies the most rigorous and unbiased reviews.
Frontiers revolutionizes research publishing by freely delivering the most outstanding research, evaluated with no bias from both the academic and social point of view. By applying the most advanced information technologies, Frontiers is catapulting scholarly publishing into a new generation.

What are Frontiers Research Topics?

Frontiers Research Topics are very popular trademarks of the Frontiers Journals Series: they are collections of at least ten articles, all centered on a particular subject. With their unique mix of varied contributions from Original Research to Review Articles, Frontiers Research Topics unify the most influential researchers, the latest key findings and historical advances in a hot research area! Find out more on how to host your own Frontiers Research Topic or contribute to one as an author by contacting the Frontiers Editorial Office: frontiersin.org/about/contact

WOMEN IN THORACIC ONCOLOGY: 2021

Topic Editors:
Meng Xu Welliver, The Ohio State University, United States
Ticiana A. Leal, University of Wisconsin-Madison, United States

Citation: Xu Welliver, M., Leal, T. A., eds. (2022). Women in Thoracic Oncology: 2021. Lausanne: Frontiers Media SA. doi: 10.3389/978-2-83250-330-0

Table of Contents

frontiers in Oncology

ORIGINAL RESEARCH
published: 15 April 2021
doi: 10.3389/fonc.2021.645352

Combination of Bempegaldesleukin and Anti-CTLA-4 Prevents Metastatic Dissemination After Primary Resection or Radiotherapy in a Preclinical Model of Non-Small Cell Lung Cancer

Amber M. Bates[1†], Ryan J. Brown[1†], Alexander A. Pieper[1], Luke M. Zangl[1], Ian Arthur[1], Peter M. Carlson[1], Trang Le[2], Gustavo A. Sosa[1], Paul A. Clark[1], Raghava N. Sriramaneni[1], KyungMann Kim[2], Ravi B. Patel[3‡] and Zachary S. Morris[1*‡]*

[1] Department of Human Oncology, University of Wisconsin School of Medicine and Public Health, University of Wisconsin-Madison, Madison, WI, United States, [2] Department of Biostatistics and Medical Informatics, University of Wisconsin School of Medicine and Public Health, University of Wisconsin-Madison, Madison, WI, United States, [3] Departments of Radiation Oncology and Bioengineering, University of Pittsburgh Hillman Cancer Center, Pittsburgh, PA, United States

Surgical resection or hypo-fractionated radiation therapy (RT) in early-stage non-small cell lung cancer (NSCLC) achieves local tumor control, but metastatic relapse remains a challenge. We hypothesized that immunotherapy with anti-CTLA-4 and bempegaldesleukin (BEMPEG; NKTR-214), a CD122-preferential IL2 pathway agonist, after primary tumor RT or resection would reduce metastases in a syngeneic murine NSCLC model. Mice bearing Lewis Lung Carcinoma (LLC) tumors were treated with combinations of BEMPEG, anti-CTLA-4, and primary tumor treatment (surgical resection or RT). Primary tumor size, mouse survival, and metastatic disease at the time of death were assessed. Flow cytometry, qRT-PCR, and cytokine analyses were performed on tumor specimens. All mice treated with RT or surgical resection of primary tumor alone succumbed to metastatic disease, and all mice treated with BEMPEG and/or anti-CTLA-4 succumbed to primary tumor local progression. The combination of primary tumor RT or resection and BEMPEG and anti-CTLA-4 reduced spontaneous metastasis and improved survival without any noted toxicity. Flow cytometric immunoprofiling of primary tumors revealed increased CD8 T and NK cells and decreased T-regulatory cells with the combination of BEMPEG, anti-CTLA-4, and RT compared to RT alone. Increased expression of genes associated with tumor cell immune susceptibility, immune cell recruitment, and cytotoxic T lymphocyte activation were observed in tumors of mice treated with BEMPEG, anti-CTLA-4, and RT. The combination of BEMPEG and anti-CTLA-4 with primary tumor RT or resection enabled effective control of local and metastatic disease in a preclinical murine NSCLC model. This therapeutic combination

OPEN ACCESS

Edited by:
Antonio Calles, Gregorio Marañón Hospital, Spain

Reviewed by:
Erik Wennerberg, Institute of Cancer Research (ICR), United Kingdom
Erik Henry Knelson, Dana–Farber Cancer Institute, United States

***Correspondence:**
Zachary S. Morris
zmorris@humonc.wisc.edu
Ravi B. Patel
patelr20@upmc.edu

[†]These authors have contributed equally to this work

[‡]These authors share senior authorship

Specialty section:
This article was submitted to Thoracic Oncology, a section of the journal Frontiers in Oncology

Received: *11 January 2021*
Accepted: *24 March 2021*
Published: *15 April 2021*

Citation:
Bates AM, Brown RJ, Pieper AA, Zangl LM, Arthur I, Carlson PM, Le T, Sosa GA, Clark PA, Sriramaneni RN, Kim K, Patel RB and Morris ZS (2021) Combination of Bempegaldesleukin and Anti-CTLA-4 Prevents Metastatic Dissemination After Primary Resection or Radiotherapy in a Preclinical Model of Non-Small Cell Lung Cancer. Front. Oncol. 11:645352. doi: 10.3389/fonc.2021.645352

has important translational potential for patients with early-stage NSCLC and other cancers.

Keywords: NSCLC, metastasis, radiation, bempegaldesleukin, immunotherapy, IL2

INTRODUCTION

Improvements in early detection (1–4) as well as advancements in surgery and radiation therapy (RT) have led to primary tumor control rates > 90% in early-stage non-small cell lung cancer (NSCLC) (5–10). Despite these improvements, the 5-year survival for patients with localized NSCLC remains below 60% (11) because many patients achieving primary tumor control nevertheless experience regional or metastatic recurrence of disease (12, 13). Treatment approaches that effectively control clinically occult metastatic disease are therefore needed in combination with primary tumor treatments for early-stage NSCLC.

Immunotherapies that activate a patient's own immune system to attack cancer cells have shown efficacy in the treatment of metastatic and regionally advanced NSCLC (14–18). Immune checkpoint inhibitors (ICI) are a class of monoclonal antibodies that modulate tumor tolerance among immune cells by blocking specific inhibitory receptor-ligand interactions to overcome immune exhaustion (e.g. anti-CTLA-4, anti-PD-1). In a clinical study combining hypofractionated palliative RT with ipilimumab (anti-CTLA-4) to treat patients with metastatic NSCLC, objective responses were observed in 18% of enrolled patients and 31% had disease control, but only 2 out of 39 patients had a complete response (19). Additional immunotherapy combinations that aid in preventing metastases should thus be further investigated. One promising immunotherapy is recombinant interleukin-2 (IL2) which expands antigen-specific CD8 T cell populations (20), and it has been shown to induce durable disease control in some patients with metastatic melanoma and renal cell carcinoma (21–23). However, clinical use of high-dose IL2 is limited due to its toxicity and short half-life (22, 24).

Bempegaldesleukin (BEMPEG; NKTR-214) is an investigational CD122-preferential IL2 pathway agonist that leverages the IL2 pathway to stimulate an antitumor immune response. BEMPEG, an IL2 protein with multiple releasable covalently attached polyethylene glycol (PEG) chains, is inactive upon administration, and overcomes the limitations of recombinant IL2 by providing active IL2 conjugate species *in vivo* as PEG chains are progressively released to achieve a sustained concentration of active drug and stable activity (24, 25). This drug delivery mechanism enables an improved safety profile, longer half-life, and outpatient dosing. IL2 stimulates proliferation of CD8 T cell and NK cells through the binding of the intermediate affinity IL2βγ receptor, but it also interacts with the high affinity trimeric IL2αβγ receptor leading to the expansion of regulatory T cells (Tregs), which can be immunosuppressive in the tumor microenvironment (TME) (20, 26). In patients with NSCLC, higher levels of Tregs in the TME are associated with a higher risk of recurrence (27, 28). Compared with native IL2, BEMPEG preferentially binds to the intermediate affinity IL2βγ receptor (CD122) and favors expansion for CD8 and NK cells without expansion of unwanted intratumoral Tregs (24, 29, 30).

In this preclinical study, we utilize a spontaneously metastasizing, immunologically "cold" Lewis lung carcinoma model (LLC) to test the capacity of anti-CTLA-4 and BEMPEG to prevent distant metastases after primary treatment with hypofractionated RT or surgical resection. We report a cooperative interaction between this combination of systemic immunotherapies and current standard local therapies employed against early-stage NSCLC and demonstrate the capacity of this combined treatment approach to elicit durable local and metastatic tumor control.

MATERIALS AND METHODS

Murine Tumor Models

Wild-type female C57BL/6 mice aged 6-8 weeks were obtained from Taconic Biosciences (Germantown, NY). Mice were housed and treated in accordance with the Guide for Care and Use of Laboratory Animals under a protocol approved by our Institutional Animal Care and Use Committee. All *in vivo* experiments were duplicated to demonstrate reproducible results.

Lewis Lung Carcinoma (LLC) cells were used in all experiments and were obtained from American Type Culture Collection (ATCC® CRL-1642). Cells were cultured in Dulbecco's Modified Eagle Medium with 100 U/mL penicillin-streptomycin and 10% fetal bovine serum (FBS, ThermoFisher). Cells were transferred to new flasks when they reached 80% confluency. Early passages after thaw (3-8) were used for all experiments. Before implantation, cells were washed and resuspended with PBS to remove all media, FBS, penicillin-streptomycin, and trypsin.

Tumors were generated from intradermal injections on the dorsal right flank of the mice with 1 x 10^6 LLC cells. Prior to each *in vivo* experiment, mice were randomized into their respective treatment. This was performed when the mean flank tumor size for the entire cohort reached ~80 mm^3. Tumor volume was approximated as ($width^2$ x length)/2 and measured biweekly using digital calipers. In the disseminated metastasis LLC model, lung metastasis was established by a tail veil injection of 2 x 10^5 LLC cells on day 10. Mice used for immunophenotyping experiments and lung metastasis quantification were euthanized at predetermined time points. For the survival experiments in **Figures 1** and **2**, cause of death graphs by day 60 are shown in **Figures 1** and **2** to depict how the mice in the survival experiments died, whether it was from metastatic disease

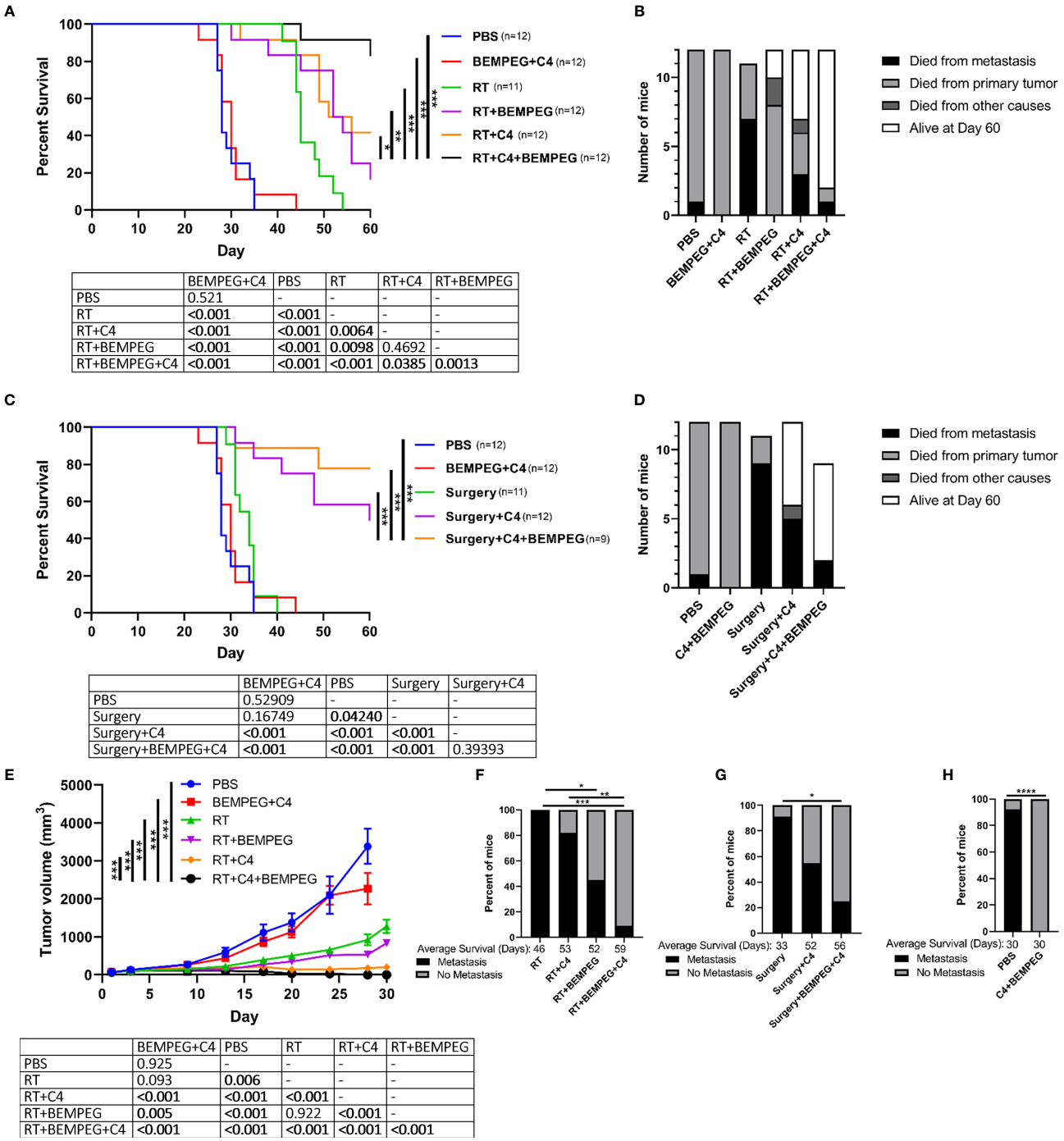

	BEMPEG+C4	PBS	RT	RT+C4	RT+BEMPEG
PBS	0.521	-	-	-	-
RT	<0.001	<0.001	-	-	-
RT+C4	<0.001	<0.001	0.0064	-	-
RT+BEMPEG	<0.001	<0.001	0.0098	0.4692	-
RT+BEMPEG+C4	<0.001	<0.001	<0.001	0.0385	0.0013

	BEMPEG+C4	PBS	Surgery	Surgery+C4
PBS	0.52909	-	-	-
Surgery	0.16749	0.04240	-	-
Surgery+C4	<0.001	<0.001	<0.001	-
Surgery+BEMPEG+C4	<0.001	<0.001	<0.001	0.39393

	BEMPEG+C4	PBS	RT	RT+C4	RT+BEMPEG
PBS	0.925	-	-	-	-
RT	0.093	0.006	-	-	-
RT+C4	<0.001	<0.001	<0.001	-	-
RT+BEMPEG	0.005	<0.001	0.922	<0.001	-
RT+BEMPEG+C4	<0.001	<0.001	<0.001	<0.001	<0.001

FIGURE 1 | BEMPEG and anti-CTLA-4 with local tumor treatment leads to tumor regression and increased survival in a single flank tumor model. In mice bearing a flank LLC tumor (~80 mm^3 on day 1), tumors were treated with 8 Gy x 3 daily fractions (days 1, 2, 3) or were surgically resected (day 16). Local treatment was combined with BEMPEG, anti-CTLA-4 (C4), or PBS control treatments. **(A, C)** Survival curves (Kaplan–Meier and Log-rank pairwise comparison with Benjamini-Hochberg adjustment for p-values, n≥10, 2 independent animal experiments) are shown comparing RT+C4+BEMPEG or surgery+BEMPEG+C4 to controls. **(B, D)** Cause of death is graphed for mice receiving the indicated treatments. **(E)** Tumor volume growth curves are shown comparing RT+C4+BEMPEG to controls (linear mixed effects model, mean ± SEM, n≥5, replicate experiment and individual mouse growth curves are shown in **Supplemental Figure 6**). **(F–H)** At the time of death, metastatic disease was determined *via* India ink staining of the lungs. Fisher's exact test and a post-hoc pairwise comparison with Benjamini-Hochberg adjustment for p-values were used for statistical analyses. **** = $P < 0.0001$; *** = $P < 0.001$; ** = $P < 0.01$; * = $P < 0.05$.

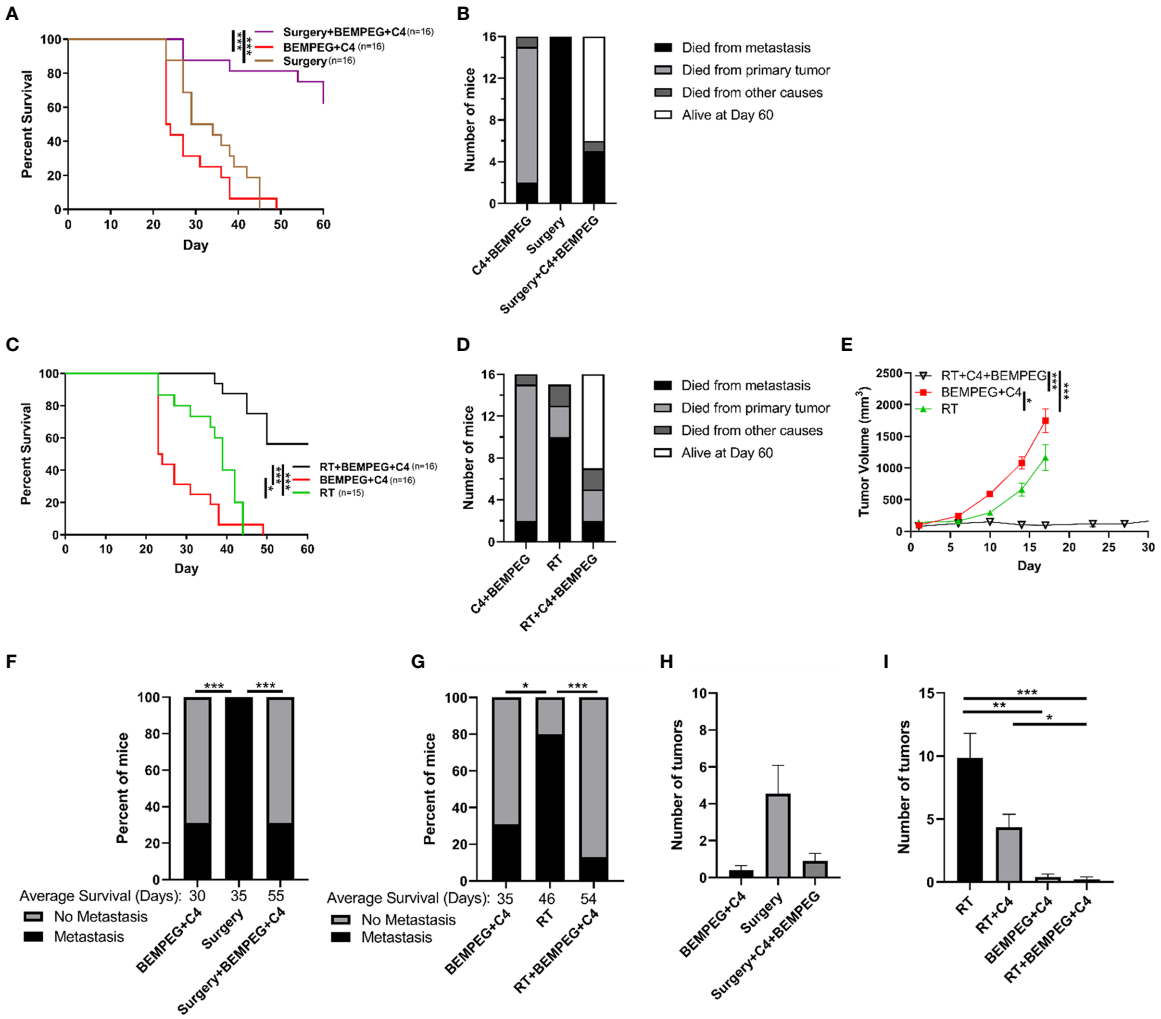

FIGURE 2 | BEMPEG and anti-CTLA-4 reduce metastatic spread in a disseminated LLC model. Mice bearing a LLC primary flank tumor (80 mm^3 on day 1) received an IV injection of $2x10^5$ LLC cells on day 10 after treatment initiation with 8 Gy x 3 daily fractions (days 1, 2, 3) or surgical resection (day 16). This local treatment was combined with BEMPEG and anti-CTLA-4 (C4) treatments. **(A, C)** Survival curves (Kaplan–Meier and Log-rank pairwise comparison with Benjamini-Hochberg adjustment for p-values, n≥9, 2 independent animal experiments) are shown. **(B, D)** Cause of death is graphed for mice receiving the indicated treatments. **(E)** Tumor volume growth curves are shown (linear mixed effects model, mean ± SEM, n=10, replicate experiment and individual mouse growth curves are shown in **Supplemental Figure 7**). **(F, G)** At the time of death, metastatic disease was determined *via* India ink staining of the lungs. Fisher's exact test and a post-hoc pairwise comparison with Benjamini-Hochberg adjustment for p-values were used for statistical analyses. At day 22 **(H)** and day 35 **(I)** mice were euthanized (replicate experiments in **Supplemental Figure 8**), lungs were harvested, and India ink stained as shown in **Supplemental Figure 1A**, and lung metastatic tumor burden was quantified. *** = P < 0.001; ** = P < 0.01; * = P < 0.05.

in which the mouse was euthanized or found dead with lung tumors (died from metastasis), euthanized due to the primary tumor size reaching 20 mm in any dimension (died from primary tumor), or if the mouse was euthanized by vet staff request due to moribund behavior or found dead with no lungs tumors (died from other causes).

After 90 days, mice from either model with a complete tumor response were rechallenged to evaluate for immune memory by an additional injection of 1 x 10^6 LLC cells intradermally in the opposite (left) flank. Age-matched naive mice were injected in the left flank with the same number of tumor cells.

Lung Staining

In order to visualize the lung metastasis, India ink staining was performed as previously described (31, 32). Blue India ink diluted 1:10 was injected intratracheally until the lungs were fully saturated with stain. Lungs were de-stained in Fekete's solution (580 mL 95% ethanol, 200 mL H_2O, 80 mL 37% formaldehyde, 40 mL glacial acidic acid) for 5 minutes after harvesting and then placed in 10% formalin to fix the tissue. After 48 hours, the stained lungs were transferred to 70% ethanol until quantification. Lung metastasis were determined by the absence of staining at tumor locations under a dissection

microscope. The entire surface of each lobe was examined thoroughly from multiple angles by two independent investigators who analyzed the lungs and were blinded to the treatment conditions. Lung metastases do not stain, while healthy lung tissue stains blue, allowing lung metastases to be grossly detectable and easily quantified (**Supplemental Figure 1A**). H&E-stained sections of these representative lungs revealed histological differences in the tissue indicative of tumor (**Supplemental Figure 1B**).

Treatments

Tumor targeted external beam RT was delivered using an XRad320 (PXi) irradiator (Precision X-Ray, Inc., North Branford, CT) in three daily fractions of 8 Gy on what was defined as treatment days 1, 2, and 3. Mice were immobilized and normal tissues outside of the right dorsal flank were shielded during RT using custom lead blocks. Surgical removal of tumors occurred on day 16. Mice were anesthetized *via* isoflurane and wounds were closed using staples. Anti-mouse-CTLA-4 mAb (IgG2c isotype of the 9D9 clone), provided by Bristol-Myers Squibb (Redwood City, CA), was administered *via* an intraperitoneal injection of 200 µg on treatment days 4, 7, and 10. Bempegaldesleukin (BEMPEG; NKTR-214), provided by Nektar Therapeutics (San Francisco, CA), was administered intravenously by a retro-orbital injection of 16 µg on treatment days 6, 15, and 24.

Gene Expression

Tumor samples harvested at day 20 were homogenized in trizol using a Bead Homogenizer (Bead Ruptor Elite, Omni International). RNA was extracted and isolated using RNeasy Mini Kit (Qiagen, Germany) according to the manufacturer's instructions and the concentrations were determined using a Nanodrop1000 Spectrophotometer (Thermo Scientific). cDNA was synthesized from total RNA using a QuantiTect Reverse Transcription Kit (Qiagen, Germany). Quantitative real-time polymerase chain reaction (qRT-PCR) was performed using PowerUp SYBR Green qPCR Master Mix (Life Technologies). The Labcyte Echo 550 and MANTIS liquid handling systems were used to load plates to reaction volume of 5 µL. Thermal cycling conditions were performed using the QuantStudio 6 Pro Real-Time PCR System (Applied Biosystems) which included a UDG activation stage at 50°C for 2 min, followed by a DNA polymerase activation stage at 95°C for 2 min followed by 40 cycles of each PCR step (denaturation), 95°C for 15s for annealing/extension and 60°C for 1 min. A melt curve analysis was done to ensure specificity of the corresponding qRT-PCR reactions. For data analysis, the Ct values were exported to an Excel file and fold change was calculated using the ΔΔCt method relative to the expression in the PBS controls (33). *Hprt*, *Pgk1*, and *Tbp* were used as endogenous controls. All reactions were performed in duplicate. Primer information can be found in **Supplemental Table 1**.

Tumor Cytokine Multiplex Immunoassay

At day 20, tumors were harvested and weighed. Tumor samples (5 µl/mg) were lysed in 20% Cell Lysis Buffer with PMSF (Cell Signaling Technology) and supplemented with Halt Protease and Phosphatase Inhibitor Cocktail (Thermo Scientific). Each tumor was homogenized in bead beater tubes, and the lysate was stored at -80°C. The concentration of 32 cytokines and chemokines in the tumor lysates (MILLIPLEX MAP Mouse Cytokine/Chemokine Magnetic Bead Panel, Millipore) were determined by a multiplex immunoassay following manufacturer's instructions. The MAGPIX System (Millipore) was used to read the multiplex plate. Concentrations were determined using a standard curve and their respective median fluorescence intensity (MFI) readings (Milliplex Analyst, Millipore). The data underwent log and Z-transformation followed by unbiased hierarchical clustering using Matlab R2019.

Flow Cytometry

Tumors harvested at day 20 after treatment initiation were processed for flow cytometric analysis as previously described (34). Briefly, tumors were enzymatically dissociated with DNAse and collagenase on a GentleMACS Octodissociator (Miltenyi Biotec) and then filtered through a 70 µm cell strainer. Single cell suspensions were stained with surface antibodies (**Supplemental Table 2**) and then fixed using the eBioscience Foxp3 fixation/permeabilization kit. UltraComp Beads eBeads (Invitrogen) were used for compensation. Flow cytometry was performed on an Attune (ThermoFisher), and compensation matrix and data was analyzed using FlowJo software following published flow cytometry guidelines (35).

Statistical Analysis

Tumor volume growth curves, displayed as means ± standard error of mean (SEM), were analyzed in a $\log_{10}$ transformation and compared between treatment groups using a linear mixed effects model. For survival analysis, Kaplan–Meier curves were generated, and a Log-rank pairwise comparison test with Benjamini-Hochberg (BH) adjustment for p-values was conducted to compare overall survival between treatment groups. To compare the presence of metastatic disease in the lungs at the time of death, Fisher's exact test followed by a post-hoc pairwise comparison with BH adjustment for p-values was used. A one-way ANOVA followed by a post-hoc multiple comparisons test with Tukey adjustment for p-values was used to determine the statistical significance among cell populations and in gene expression. All analyses were performed in GraphPad Prism or R (v.4.0.2). Adjusted p-values less than 0.05 were considered significant and are indicated in figures as **** = P <0.0001; *** = $P < 0.001$; ** = $P < 0.01$; * = $P < 0.05$.

RESULTS

BEMPEG and Anti-CTLA-4 With Local Tumor Treatment Leads to Tumor Regression and Increased Survival in a Single Flank Tumor Model

In mice bearing a flank LLC tumor (~80 mm^3 on day 1), we tested the efficacy of BEMPEG (16 µg, IV on days 6, 15, 24) and

anti-CTLA-4 treatments (200 μg, IP on days 4, 7, 10) combined with local treatment of the tumor through surgical resection (day 16) or delivering three fractions of 8 Gy RT (days 1, 2, 3). When local treatment was combined with BEMPEG and anti-CTLA-4, survival was significantly improved compared to RT or surgery alone (**Figures 1A–D**). BEMPEG and anti-CTLA-4 treatments without local treatment did not improve survival, and these mice died due to primary tumor burden (**Figure 1B**). Combining either BEMPEG or anti-CTLA-4 with RT slightly improved survival over RT alone ($p<0.01$), but the combination of BEMPEG, anti-CTLA-4, and RT significantly improved survival over either dual treatment ($p<0.001$, **Figure 1A**). Surgical resection alone only slightly ($p<0.05$) improved survival, but when combined with anti-CTLA-4 or BEMPEG and anti-CTLA-4, survival was significantly improved ($p<0.001$, **Figures 1C, D**). At day 90, 33% (4/12) of mice treated with BEMPEG, anti-CTLA-4, and RT were alive, while only 8% (1/12) of mice treated with RT and BEMPEG and 8% (1/12) of mice treated with RT and anti-CTLA-4 remained. An anti-tumor memory response was observed in 67% (2/3) of mice previously treated with BEMPEG, anti-CTLA-4, and RT – as determined by the rejection of re-engraftment with LLC (**Supplemental Figure 2**).

Tumor growth was significantly reduced in mice treated with RT, BEMPEG, and anti-CTLA-4 over dual therapy combinations or monotherapies ($p<0.001$, **Figure 1E**). At the time of death, lungs from these mice were India ink stained to evaluate metastatic disease. Most mice that received only local treatment to the primary tumor spontaneously developed lung metastases, but when combined with BEMPEG and anti-CTLA-4, this was significantly reduced ($p<0.05$, **Figures 1F, G**). Mice that received BEMPEG and anti-CTLA-4 treatments or PBS were euthanized at earlier time points due to primary tumor size (**Figure 1H**). Metastatic disease was not found in the lungs of these mice treated with BEMPEG and anti-CTLA-4, however a direct comparison with metastatic rates in the mice treated with RT, BEMPEG, and anti-CTLA-4 was not possible due to the longer time to death in the triple combination group. Note that anti-CTLA-4 and BEMPEG treatments were investigated separately and in combination in a preliminary experiment and did not appear to have a significant impact on tumor growth (**Supplemental Figure 3A**); however, the treatment combination of anti-CTLA-4 and BEMPEG did result in less metastatic disease (**Supplemental Figures 3B-C**).

BEMPEG and Anti-CTLA-4 Reduce Metastatic Spread in a Disseminated LLC Model

To test the prevention of metastatic disease in a more controlled manner, we tested the use of these combined local and immunotherapies in mice bearing an LLC primary flank tumor (80 mm^3 on day 1) and disseminated tumor cells administered by IV injection of $2x10^5$ LLC cells at day 10 after treatment initiation. The experiments in **Figure 1** demonstrate that the combination of local control with both anti-CTLA-4 and BEMPEG, and this combination was further investigated in **Figure 2** using a more focused approach. Local control of the primary tumor with three fractions of 8 Gy RT or surgical resection at day 16, when combined with BEMPEG and anti-CTLA-4 treatments, significantly improved survival as compared to local control alone or treatments of BEMPEG and anti-CTLA-4 without local control ($p<0.001$, **Figures 2A, C**). The mice treated with anti-CTLA-4 and BEMPEG were euthanized due to primary tumor burden, while most mice receiving only local treatment of the primary tumor with RT or surgery died from metastatic disease (**Figures 2B, D**). Again, the combination of BEMPEG and anti-CTLA-4 treatments with RT reduced tumor growth compared to BEMPEG and anti-CTLA-4 or RT alone ($p<0.001$, **Figure 2E**). At the time of death, in this disseminated metastasis model, significantly fewer mice developed lung tumors when treated with BEMPEG and anti-CTLA-4 than either local treatment alone ($p<0.05$, **Figures 2F, G**). The addition of BEMPEG and anti-CTLA-4 to local treatment prevented metastatic disease in the lungs as compared to local treatment alone ($p<0.001$). To further explore the prevention of lung metastases, mice that underwent either surgical resection of the primary tumor or received BEMPEG and anti-CTLA-4 treatments, or both, were euthanized at day 22 and lung metastases were quantified (**Figure 2H**). Mice that received RT, BEMPEG, and anti-CTLA-4 or a combination of these treatments were euthanized at day 35 and lung metastases were quantified (**Figure 2I**). On average, mice that received BEMPEG and anti-CTLA-4 treatments had fewer lung metastases, regardless of local treatment to the tumor (**Figures 2H, I**). Mice treated with RT, BEMPEG, and anti-CTLA-4 had significantly fewer lung metastases than those treated with RT alone or RT and anti-CTLA-4 ($p<0.05$, **Figure 2I**).

BEMPEG and Anti-CTLA-4 Combined With Local Radiation Creates a Favorable Adaptive Immune Microenvironment

The TME was assessed *via* flow cytometric and qRT-PCR to examine the anti-tumor immune response that we hypothesized to be responsible for the observed tumor regression, improved survival rates, and reduced metastases with these combinations of local therapy and BEMPEG plus anti-CTLA-4. LLC primary tumors were implanted on the right flank. Once average tumor size reached ~80 mm^3, mice were randomized and treated with combinations of three fractions of 8 Gy RT, BEMPEG, and/or anti-CTLA-4. At day 20 after initial treatment, tumors were dissected. Tumor infiltrating CD3 T cells, NK cells, CD8 T cells, CD4 T cells, and regulatory T cells (Tregs) were quantified using the gating strategy in **Supplemental Figure 4**, which shows a representative dot plot for each treatment group. A significant increase in CD3+ T cells, NK cells, CD8 T cells, and CD4 T cells was found in tumors of mice treated with RT, BEMPEG, and anti-CTLA-4 compared to those treated with RT alone ($p<0.01$, **Figures 3A, B**). These immunologically "cold" tumors have very low tumor infiltrating CD3 T cells, but CD3 T cells were significantly increased in tumors of mice treated with BEMPEG compared to PBS and RT (**Figure 3A**). The percentage of NK cells out of tumor infiltrating lymphocytes

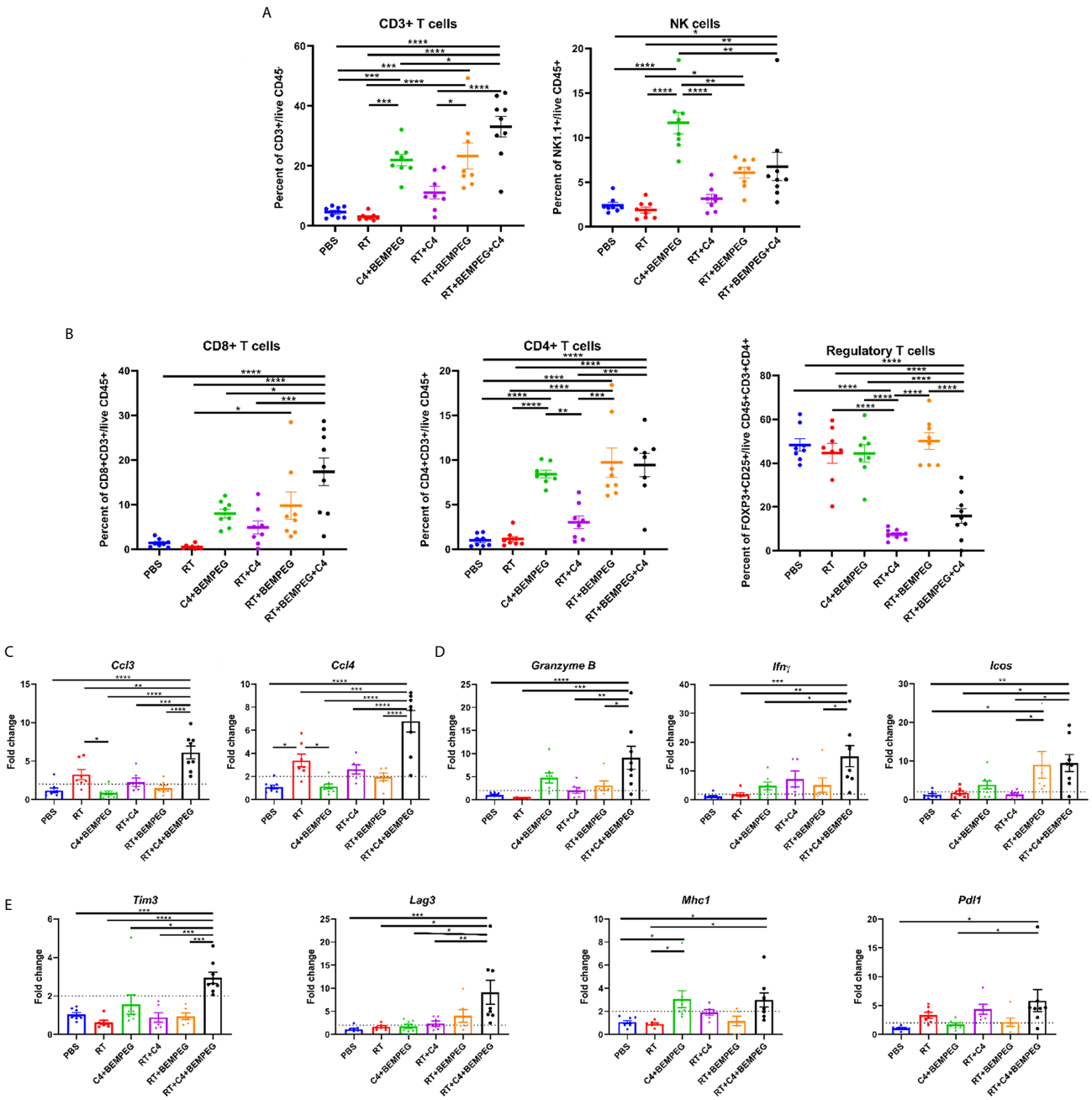

FIGURE 3 | BEMPEG and anti-CTLA-4 combined with local radiation creates a favorable adaptive immune microenvironment. Mice bearing a flank LLC tumor (~80 mm^3) were given 8 Gy x 3 locally combined with BEMPEG and anti-CTLA-4 (C4) treatments. At day 20 tumors were harvested and processed for qRT-PCR and flow cytometric analyses. **(A, B)** Flow cytometry tumor infiltrates are shown as a percent of parent or grandparent gate. **(C)** Expression of genes associated with immune cell recruitment, **(D)** cytotoxic T lymphocyte activation, and **(E)** immune susceptibility are displayed as fold change in expression relative to the PBS control (mean ± SEM, n≥8). A one-way ANOVA followed by a *post hoc* multiple comparisons test with Tukey adjustments for p-values was used to determine statistical differences among cell populations and gene expression (mean ± SEM, n≥8, **** = P <0.0001; *** = P < 0.001; ** = P < 0.01; * = P < 0.05).

(CD45+) was increased in tumors of mice treated with anti-CTLA-4 and BEMPEG as compared to all other groups ($p<0.01$, **Figure 3A**). IL2 expands NK cells (20), and NK cell infiltrate was highest in tumors of mice treated with BEMPEG. The percentage of CD8+ T cells out of overall immune cell infiltrate (CD45+) was also increased in tumors of mice treated with RT, BEMPEG, and anti-CTLA-4 over those treated with PBS, RT, anti-CLTA-4 and BEMPEG, or RT and anti-CTLA-4 ($p<0.05$, **Figure 3B**).

CD4+ T cells were increased in tumors from mice treated with BEMPEG compared to PBS, RT, or RT and anti-CTLA-4 (**Figure 3B**). The percentage of immunosuppressive Tregs (CD25+FOXP3+) out of CD4+ T cells was significantly decreased in tumors of mice treated with RT, BEMPEG, and anti-CTLA-4 or RT and anti-CTLA-4 compared to all other groups ($p<0.0001$, **Figure 3B**).

Using qRT-PCR, transcriptional differences in the bulk tumor mRNA were assessed. *Ccl3* (macrophage inflammatory protein-1α, MIP1α) and *Ccl4* (macrophage inflammatory protein-1β, MIP-1β), genes associated with recruitment and activation of immune cells, were significantly increased in the tumors of mice treated with RT, BEMPEG, and anti-CTLA-4 over all other groups ($p<0.01$, **Figure 3C**). *Ccl3* has been shown to recruit NK cells to the TME, and *Ccl4* can recruit dermal-resident CD103+ dendritic cells (DCs) (36). Expression of *Granzyme B, Ifnγ* (interferon gamma), and *Icos* (inducible co-stimulator), which are associated with activated cytotoxic T cells, was significantly increased in the tumors of mice treated with RT, BEMPEG, and anti-CTLA-4 over PBS and RT ($p<0.05$, **Figure 3D**). *Tim3* (T cell immunoglobulin and mucin domain-containing protein 3), *Lag3* (lymphocyte activation gene 3), *Pdl1* (programmed death ligand 1), and *Mhc1* (major histocompatibility complex-1), which are genes that regulate tumor cell immune susceptibility, were significantly increased in the tumors of mice treated with RT, BEMPEG, and anti-CTLA-4 (**Figure 3E**). *Pdl1* expression was significantly increased in the tumors of mice treated with RT, BEMPEG, and anti-CTLA-4 compared to mice treated with PBS or BEMPEG and anti-CTLA-4 ($p<0.05$). *Mhc1* expression was significantly increased in the tumors of mice treated with RT, BEMPEG, and anti-CTLA-4 or BEMPEG and anti-CTLA-4 compared to mice treated with PBS or RT ($p<0.05$).

Radiation, Anti-CTLA-4, and BEMPEG Combined Treatments Change the Cytokine Profiles of the TME

Further examination of the TME was performed using tumor fragments from these same mice as above by analyzing the concentrations of cytokines and chemokines in the TME. A multiplex cytokine assay was performed, and unsupervised hierarchal clustering was used to sort tumors based on detected levels of 25 cytokines and chemokines (**Figure 4A**, and **Supplemental Figure 5**). PBS samples had low levels of all markers and clustered together. Tumors from mice treated with BEMPEG in combination with RT, anti-CTLA-4, or both also clustered together. Significant differences were observed in several immune stimulating cytokines with the treatment of RT, anti-CTLA-4, and BEMPEG, including MIP1α, MIP1β, LIX, IL4, and IL5 ($p<0.05$, **Figure 4B**). IL-10 and IL-1α, cytokines associated with immunosuppressive or inhibitory functions, were significantly increased in tumors treated with RT alone compared to PBS ($p<0.05$), but not significantly increased in tumors from mice given the combination treatment of RT, anti-CTLA-4, and BEMPEG ($p>0.05$, **Figure 4C**).

DISCUSSION

In a spontaneously metastasizing immunologically "cold" model of early-stage NSCLC, we report that the combination of anti-CTLA-4 and BEMPEG inhibits the development of distant metastases and effectively eradicates IV injected tumor cells representing micro-metastatic disease. When combined with an effective local treatment (hypo-fractionated RT or surgery), this combination enables durable complete primary tumor response, long-term disease-free survival, and evidence of anti-tumor immune memory. While BEMPEG and anti-CTLA-4 alone do not control established primary tumors in this model, this combination of immunotherapy does augment local tumor control when combined with moderate dose hypo-fractionated RT or surgery. Similarly, with only primary tumor control, mice succumb to metastatic disease unless combined with BEMPEG and anti-CTLA-4. With recent studies showing safety for the combination of BEMPEG and anti-CTLA-4 or other ICIs in non-human primates (25) and humans with metastatic solid tumors (23), our findings highlight the exciting translational potential for testing the capacity of this treatment combination to improve the cure rates for patients receiving locally directed treatments for early-stage NSCLC and potentially other localized cancers with high-risk for occult metastatic disease.

Given the prominent role of Tregs in suppressing anti-tumor immunity in NSCLC and other tumor types (20, 26–28), we hypothesized that the efficacy of BEMPEG and anti-CTLA-4 in controlling micrometastatic NSCLC might result from overcoming Treg-mediated immune suppression with anti-CTLA-4 (37) and selectively stimulating clonal expansion of effector lymphocytes but not Tregs with BEMPEG (24). Our data from this immunologically "cold" LLC murine model of micrometastatic NSCLC supports these potential mechanisms. Immunologically "cold" tumors have few tumor infiltrating lymphocytes (TILs) as seen in the flow analysis of the CD3+ T cells in the PBS and RT alone controls (**Figure 3**). However, the composition of tumor infiltrating immune cells in these tumors was modified when BEMPEG or anti-CTLA-4 were added to local treatments. Specifically, we observed increased levels of CD8+ and CD4+ T cells as well as NK cells in tumor specimens following RT+BEMPEG, as compared to RT alone (**Figure 3**). We further confirmed a reduction of tumor infiltrating Tregs with the addition of anti-CTLA-4 to RT+BEMPEG, as compared to RT+BEMPEG alone (**Figure 3**).

Anti-CTLA4 has been shown to deplete Tregs *via* antibody-dependent cell-mediated cytotoxicity (ADCC) (37). Consistent with this, we observed that mice treated with RT and anti-CTLA4 with or without BEMPEG had significantly fewer Tregs in the TME than all other treatment groups, which suggests anti-CTLA-4 maintains a role in the depletion of Tregs in these combination treatment approaches (**Figure 3B**). Additionally, BEMPEG has been reported to selectively expand populations conventional effector T cells with relatively reduced effect on Tregs (29). Here, we also observe that mice treated with BEMPEG (anti-CTLA-4 +BEMPEG, RT+BEMPEG, and RT+anti-CTLA-4+BEMPEG) had tumors with significantly increased infiltration by CD4 but not Tregs (CD25+FOXP3+CD4+ T cells) (**Figure 3B**). Mice

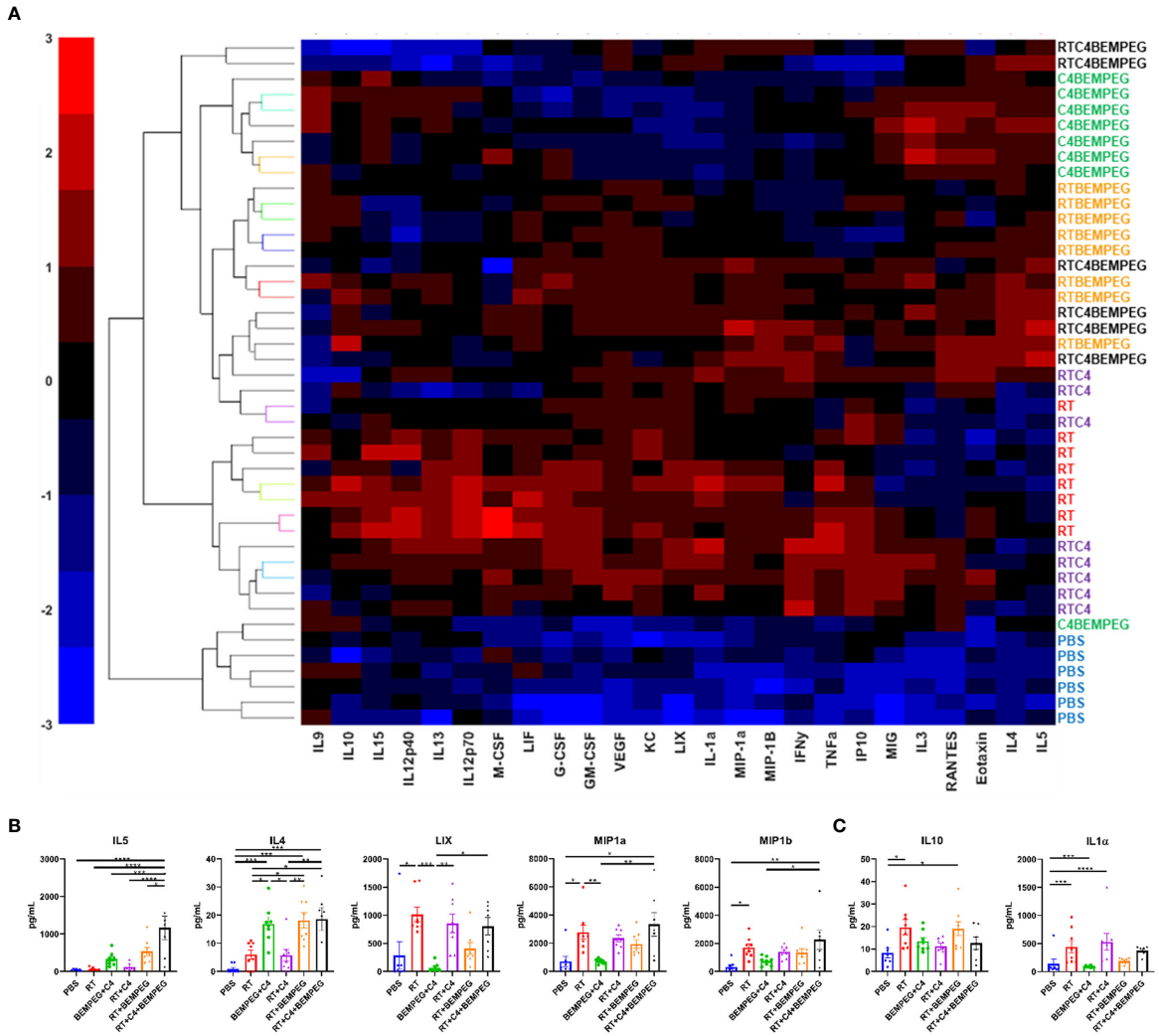

FIGURE 4 | Radiation, anti-CTLA-4, and BEMPEG combined treatments change the cytokine profiles of the TME. Mice bearing a flank LLC tumor (~80 mm^3) were given 8 Gy x 3 locally combined with BEMPEG and anti-CTLA-4 (C4) treatments. At day 20 tumors were collected and lysed. Multiplex immunoassay analysis was performed to determine concentrations of 25 cytokines and chemokines. **(A)** Unbiased hierarchal clustering was used to sort tumors based on detected levels of cytokines and chemokines. **(B, C)** A one-way ANOVA followed by a Tukey multiple comparisons test was used to determine statistical differences among cell populations, (mean ± SEM, n≥6, **** = P <0.0001; *** = P < 0.001; ** = P < 0.01; * = P < 0.05). **(B)** Concentrations of immune stimulating cytokines and **(C)** cytokines associated with immunosuppressive or inhibitory functions are shown.

treated with RT+BEMPEG or RT+BEMPEG+anti-CTLA-4 had significantly more CD8 T cells compared to the RT control. BEMPEG has been shown to increase CD8 T cells in the TME (29, 38). Together, this data suggests that the therapeutic mechanisms of anti-CTLA4 and BEMPEG are maintained and non-redundant when combined and delivered in conjunction with locally directed therapies like surgery or RT. This can provide a two-pronged approach to activating anti-tumor immunity against immunologically cold tumors by depleting immunosuppressive Tregs and driving increased infiltration by effector CD8 T cells in the TME. Our data also demonstrate that BEMPEG may increase NK cell recruitment to the TME, as all treatment groups with BEMPEG had increased NK cells compared to the RT and PBS controls (**Figure 3**). In other tumor models, studies have found that BEMPEG can increase NK cells in the peripheral blood (38) and in the tumor (25). However, *Ccl3* expression, which is associated with NK cell recruitment, did not follow this same trend. Future experiments should further investigate the mechanisms BEMPEG-induced recruitment of NK cells to the TME.

In addition to inducing an effector-dominated lymphocytic immune infiltrate in tumors, we observe that BEMPEG and anti-CTLA-4 increased the activation of tumor infiltrating immune cells, as measured by the increased expression of genes associated with cytotoxic T lymphocyte activation (*Icos*, *Granzyme B*, and *Ifnγ*) (**Figure 3**) and increased production of several immune stimulatory cytokines in the primary tumor microenvironment (**Figure 4**) following combined RT, BEMPEG, and anti-CTLA-4,

as compared to RT alone. Concurrent with these effects, we observed that combined BEMPEG and anti-CTLA-4 stimulated increased expression of *Mhc1* as well as upregulation of additional immune checkpoint ligands (*Pdl1*, *Tim3*, and *Lag3*). These expression changes may be secondary to the increased IFNγ production that we observed in the tumor microenvironment (39–41). In future studies it may be valuable to test this treatment approach in combination with inhibitors targeting these additional checkpoint ligands to further enhance the magnitude and/or duration of anti-tumor immunity stimulated by BEMPEG and anti-CTLA-4.

Our results support and expand upon several recently reported preclinical studies including one demonstrating that BEMPEG and ICIs synergize to augment T cell mediated anti-cancer immunity (29). A separate recent study suggested a cooperative therapeutic interaction between RT and BEMPEG in immunogenic tumor models, which sometimes exhibited strong response to BEMPEG alone (38). That study reported that combined RT and BEMPEG triggered an expanded CD8 T cell infiltrate. Here, we observe a similar effect and demonstrate that it may be further advanced by combination with anti-CTLA-4. Preclinical studies demonstrate that systemic effects of RT in priming a systemic anti-tumor T cell response are achieved more reliably when RT is combined with anti-CTLA-4 and/or anti-PD-1/PD-L1 checkpoint blockade (42, 43). A recent prospective single arm clinical study evaluating RT and anti-CTLA-4 in patients with NSCLC demonstrated safety and in favorably responding patients showed that RT-induced T cell recognition of tumor-specific neo-antigens (19).

Clinical studies are already underway integrating anti-PD1/PD-L1 into neo-adjuvant or adjuvant strategies for the treatment of early-stage NSCLC (e.g., NCT02504372, NCT02998528, NCT04025879, and NCT04214262). Given the response rates to anti-PD1/anti-PD-L1 therapies in other studies of patients with NSCLC, our expectation is that this approach will be effective in preventing metastatic progression for some, but not all early-stage NSCLC patients. As biomarkers emerge that can predict response to neo-adjuvant or adjuvant treatments with anti-PD1/PDL1, additional approaches will be needed for patients with tumors that are not responsive. The data we present here suggest that a combination of BEMPEG and anti-CTLA-4 with local control could be an effective alternative treatment option for patients with NSCLC that is not responsive to anti-PD1/PDL1 therapies, and clinical investigation is warranted to test this. LLC may be a good model for this type of disease, as it is immunologically "cold" and does not respond to anti-PDL1 (44).

While we investigated a model of early-stage localized cancer with occult micro-metastases, our findings may also have implications for advanced metastatic disease. We observe that combinations of anti-CTLA-4 and BEMPEG are powerful in eradicating micro-metastases but do not adequately control well-established macroscopic tumor sites. Rather, such tumors require locally directed therapies. Nearly all patients with metastatic NSCLC have more than one macroscopic tumor site. It is beyond the scope of the present study to evaluate whether targeting one tumor site with RT would prime effective anti-tumor immunity against other well-established macroscopic metastases or whether it would be beneficial to deliver local RT to all such tumor sites to achieve curative response when combined with anti-CTLA-4 and BEMPEG. Such approaches delivering RT to all tumor sites are increasingly practiced in patients with oligometastatic disease (45, 46). In settings of widespread metastatic disease this may be achieved using targeted radionuclide therapies (47, 48). In future studies, it will be interesting to test these approaches to combining radiation therapy with BEMPEG and ICIs in the treatment of macro-metastatic disease.

We acknowledge several weaknesses in this study including the exclusive use of heterotopic transplantable syngeneic murine models. Such models have clear value in translational immuno-oncology research because they enable *in vivo* hypothesis testing in settings of intact host immunity. However, it is understood that certain immune and radiobiological mechanisms in mice and heterotopic transplantable tumors may differ from those observed in human immune systems and tumors. Therefore, additional preclinical and clinical studies will be needed to establish the translational potential of the treatment approach developed here. In addition, the doses and conformality of RT delivered in this study do not directly replicate approaches used clinically for treatment of early-stage NSCLC. Specifically, we employ a hypofractionated dose of RT that has been reported to be optimal for activating a type I interferon response (49, 50). While similar, this regimen delivers a lower biologically equivalent dose than the stereotactic body RT (SBRT) regimens that are commonly employed clinically for treatment of early-stage NSCLC. Notably, for animal safety reasons we are not able to deliver the high dose SBRT clinical regimens to mice.

Despite such limitations, our results provide rationale for further preclinical and clinical testing of the combination of BEMPEG and anti-CTLA-4 together with local treatments like surgery or RT. Although testing of novel therapeutic combinations in cancer commonly begins in metastatic settings, our findings highlight an opportunity to potentially improve the treatment of high-risk early-stage cancers such as NSCLC. We advocate for increased testing of such novel treatments in these early stage patient populations with potentially curative cancers – a setting in which the impact of these therapeutic innovations may be greatest (51).

DATA AVAILABILITY STATEMENT

The original contributions presented in the study are included in the article/**Supplementary Material**, further inquiries can be directed to the corresponding authors.

ETHICS STATEMENT

The animal study was reviewed and approved by University of Wisconsin Institutional Animal Care and Use Committee.

AUTHOR CONTRIBUTIONS

RB, AB, and RP designed and performed experiments and analysed data. AP, LZ, IA, PMC, GS, PAC, and RS also performed experiments. ZM and RP contributed to experimental design and supervised the project. AB, TL, and KK analysed data. AB wrote the manuscript with input from all authors. All authors contributed to the article and approved the submitted version.

FUNDING

The authors' work is supported in part by grants from NIH P30 CA014520, NIH 1DP5OD024576, NIH U01CA233102, F30CA228315, Radiological Society of North America Research Fellow Grant RF1716, the Shaw Scientist Award, American Society of Clinical Oncology Hayden Family Foundation Young Investigator Award 12805, and K08CA241319. RP was supported in part by the Hillman Cancer Center Early Career Fellowship for Innovative Cancer Research and the Bentson Translational Research Fellowship.

ACKNOWLEDGMENTS

The authors thank Bristol Myers-Squibb and Nektar Therapeutics for the provision of anti-CTLA-4 and BEMPEG, respectively.

SUPPLEMENTARY MATERIAL

The Supplementary Material for this article can be found online at: https://www.frontiersin.org/articles/10.3389/fonc.2021.645352/full#supplementary-material

REFERENCES

1. Infante M, Cavuto S, Lutman FR, Passera E, Chiarenza M, Chiesa G, et al. Long-Term Follow-up Results of the DANTE Trial, a Randomized Study of Lung Cancer Screening with Spiral Computed Tomography. *Am J Respir Crit Care Med* (2015) 191(10):1166–75. doi: 10.1164/rccm.201408-1475OC
2. Pastorino U, Rossi M, Rosato V, Marchiano A, Sverzellati N, Morosi C, et al. Annual or biennial CT screening versus observation in heavy smokers: 5-year results of the MILD trial. *Eur J Cancer Prev* (2012) 21(3):308–15. doi: 10.1097/CEJ.0b013e328351e1b6
3. National Lung Screening Trial Research T, Aberle DR, Adams AM, Berg CD, Black WC, Clapp JD, et al. Reduced lung-cancer mortality with low-dose computed tomographic screening. *N Engl J Med* (2011) 365(5):395–409. doi: 10.1056/NEJMoa1102873
4. Saghir Z, Dirksen A, Ashraf H, Bach KS, Brodersen J, Clementsen PF, et al. CT screening for lung cancer brings forward early disease. The randomised Danish Lung Cancer Screening Trial: status after five annual screening rounds with low-dose CT. *Thorax* (2012) 67(4):296–301. doi: 10.1136/thoraxjnl-2011-200736
5. Higuchi M, Yaginuma H, Yonechi A, Kanno R, Ohishi A, Suzuki H, et al. Long-term outcomes after video-assisted thoracic surgery (VATS) lobectomy versus lobectomy via open thoracotomy for clinical stage IA non-small cell lung cancer. *J Cardiothorac Surg* (2014) 9:88. doi: 10.1186/1749-8090-9-88
6. Sakuraba M, Miyamoto H, Oh S, Shiomi K, Sonobe S, Takahashi N, et al. Video-assisted thoracoscopic lobectomy vs. conventional lobectomy via open thoracotomy in patients with clinical stage IA non-small cell lung carcinoma. *Interact Cardiovasc Thorac Surg* (2007) 6(5):614–7. doi: 10.1510/icvts.2007.157701
7. Shiraishi T, Shirakusa T, Hiratsuka M, Yamamoto S, Iwasaki A. Video-assisted thoracoscopic surgery lobectomy for c-T1N0M0 primary lung cancer: its impact on locoregional control. *Ann Thorac Surg* (2006) 82(3):1021–6. doi: 10.1016/j.athoracsur.2006.04.031
8. Fakiris AJ, McGarry RC, Yiannoutsos CT, Papiez L, Williams M, Henderson MA, et al. Stereotactic body radiation therapy for early-stage non-small-cell lung carcinoma: four-year results of a prospective phase II study. *Int J Radiat Oncol Biol Phys* (2009) 75(3):677–82. doi: 10.1016/j.ijrobp.2008.11.042
9. Timmerman R, Paulus R, Galvin J, Michalski J, Straube W, Bradley J, et al. Stereotactic body radiation therapy for inoperable early stage lung cancer. *JAMA* (2010) 303(11):1070–6. doi: 10.1001/jama.2010.261
10. Videtic GM, Hu C, Singh AK, Chang JY, Parker W, Olivier KR, et al. A Randomized Phase 2 Study Comparing 2 Stereotactic Body Radiation Therapy Schedules for Medically Inoperable Patients With Stage I Peripheral Non-Small Cell Lung Cancer: NRG Oncology RTOG 0915 (NCCTG N0927). *Int J Radiat Oncol Biol Phys* (2015) 93(4):757–64. doi: 10.1016/j.ijrobp.2015.07.2260
11. Siegel RL, Miller KD, Jemal A. Cancer statistics, 2019. *CA Cancer J Clin* (2019) 69(1):7–34. doi: 10.3322/caac.21551
12. Peterson J, Niles C, Patel A, Boujaoude Z, Abouzgheib W, Goldsmith B, et al. Stereotactic Body Radiotherapy for Large (> 5 cm) Non-Small-Cell Lung Cancer. *Clin Lung Cancer* (2017) 18(4):396–400. doi: 10.1016/j.cllc.2016.11.020
13. Verma V, Shostrom VK, Kumar SS, Zhen W, Hallemeier CL, Braunstein SE, et al. Multi-institutional experience of stereotactic body radiotherapy for large (>/=5 centimeters) non-small cell lung tumors. *Cancer* (2017) 123(4):688–96. doi: 10.1002/cncr.30375
14. Mok TSK, Wu YL, Kudaba I, Kowalski DM, Cho BC, Turna HZ, et al. Pembrolizumab versus chemotherapy for previously untreated, PD-L1-expressing, locally advanced or metastatic non-small-cell lung cancer (KEYNOTE-042): a randomised, open-label, controlled, phase 3 trial. *Lancet* (2019) 393(10183):1819–30. doi: 10.1016/S0140-6736(18)32409-7
15. Gandhi L, Rodriguez-Abreu D, Gadgeel S, Esteban E, Felip E, De Angelis F, et al. Pembrolizumab plus Chemotherapy in Metastatic Non-Small-Cell Lung Cancer. *N Engl J Med* (2018) 378(22):2078–92. doi: 10.1056/NEJMoa1801005
16. Garon EB, Rizvi NA, Hui R, Leighl N, Balmanoukian AS, Eder JP, et al. Pembrolizumab for the treatment of non-small-cell lung cancer. *N Engl J Med* (2015) 372(21):2018–28. doi: 10.1056/NEJMoa1501824
17. Paz-Ares L, Luft A, Vicente D, Tafreshi A, Gumus M, Mazieres J, et al. Pembrolizumab plus Chemotherapy for Squamous Non-Small-Cell Lung Cancer. *N Engl J Med* (2018) 379(21):2040–51. doi: 10.1056/NEJMoa1810865
18. Reck M, Rodriguez-Abreu D, Robinson AG, Hui R, Csoszi T, Fulop A, et al. Pembrolizumab versus Chemotherapy for PD-L1-Positive Non-Small-Cell Lung Cancer. *N Engl J Med* (2016) 375(19):1823–33. doi: 10.1056/NEJMoa1606774
19. Formenti SC, Rudqvist NP, Golden E, Cooper B, Wennerberg E, Lhuillier C, et al. Radiotherapy induces responses of lung cancer to CTLA-4 blockade. *Nat Med* (2018) 24(12):1845–51. doi: 10.1038/s41591-018-0232-2
20. Boyman O, Sprent J. The role of interleukin-2 during homeostasis and activation of the immune system. *Nat Rev Immunol* (2012) 12(3):180–90. doi: 10.1038/nri3156
21. Davar D, Ding F, Saul M, Sander C, Tarhini AA, Kirkwood JM, et al. High-dose interleukin-2 (HD IL-2) for advanced melanoma: a single center experience from the University of Pittsburgh Cancer Institute. *J Immunother Cancer* (2017) 5(1):74. doi: 10.1186/s40425-017-0279-5
22. Atkins MB, Lotze MT, Dutcher JP, Fisher RI, Weiss G, Margolin K, et al. High-dose recombinant interleukin 2 therapy for patients with metastatic

melanoma: analysis of 270 patients treated between 1985 and 1993. *J Clin Oncol* (1999) 17(7):2105–16. doi: 10.1200/JCO.1999.17.7.2105
23. Diab A, Tannir NM, Bentebibel SE, Hwu P, Papadimitrakopoulou V, Haymaker C, et al. Bempegaldesleukin (NKTR-214) plus Nivolumab in Patients with Advanced Solid Tumors: Phase I Dose-Escalation Study of Safety, Efficacy, and Immune Activation (PIVOT-02). *Cancer Discovery* (2020) 10:1158–73. doi: 10.1158/2159-8290.CD-19-1510
24. Charych D, Khalili S, Dixit V, Kirk P, Chang T, Langowski J, et al. Modeling the receptor pharmacology, pharmacokinetics, and pharmacodynamics of NKTR-214, a kinetically-controlled interleukin-2 (IL2) receptor agonist for cancer immunotherapy. *PloS One* (2017) 12(7):e0179431. doi: 10.1371/journal.pone.0179431
25. Charych DH, Hoch U, Langowski JL, Lee SR, Addepalli MK, Kirk PB, et al. NKTR-214, an Engineered Cytokine with Biased IL2 Receptor Binding, Increased Tumor Exposure, and Marked Efficacy in Mouse Tumor Models. *Clin Cancer Res an Off J Am Assoc Cancer Res* (2016) 22(3):680–90. doi: 10.1158/1078-0432.CCR-15-1631
26. Wang X, Rickert M, Garcia KC. Structure of the quaternary complex of interleukin-2 with its alpha, beta, and gammac receptors. *Science* (2005) 310 (5751):1159–63. doi: 10.1126/science.1117893
27. Petersen RP, Campa MJ, Sperlazza J, Conlon D, Joshi MB, Harpole DHJr., et al. Tumor infiltrating Foxp3+ regulatory T-cells are associated with recurrence in pathologic stage I NSCLC patients. *Cancer* (2006) 107 (12):2866–72. doi: 10.1002/cncr.22282
28. Shimizu K, Nakata M, Hirami Y, Yukawa T, Maeda A, Tanemoto K. Tumor-infiltrating Foxp3+ regulatory T cells are correlated with cyclooxygenase-2 expression and are associated with recurrence in resected non-small cell lung cancer. *J Thorac Oncol* (2010) 5(5):585–90. doi: 10.1097/JTO.0b013e3181d60fd7
29. Sharma M, Khong H, Fa'ak F, Bentebibel SE, Janssen LME, Chesson BC, et al. Bempegaldesleukin selectively depletes intratumoral Tregs and potentiates T cell-mediated cancer therapy. *Nat Commun* (2020) 11(1):661. doi: 10.1038/s41467-020-14471-1
30. Bentebibel SE, Hurwitz ME, Bernatchez C, Haymaker C, Hudgens CW, Kluger HM, et al. A First-in-Human Study and Biomarker Analysis of NKTR-214, a Novel IL2Rbetagamma-Biased Cytokine, in Patients with Advanced or Metastatic Solid Tumors. *Cancer Discovery* (2019) 9(6):711–21. doi: 10.1158/2159-8290.CD-18-1495
31. Wong RJ, Chan MK, Yu Z, Kim TH, Bhargava A, Stiles BM, et al. Effective intravenous therapy of murine pulmonary metastases with an oncolytic herpes virus expressing interleukin 12. *Clin Cancer Res an Off J Am Assoc Cancer Res* (2004) 10(1 Pt 1):251–9. doi: 10.1158/1078-0432.CCR-0197-3
32. Inoue M, Nakashima R, Enomoto M, Koike Y, Zhao X, Yip K, et al. Plasma redox imbalance caused by albumin oxidation promotes lung-predominant NETosis and pulmonary cancer metastasis. *Nat Commun* (2018) 9(1):5116. doi: 10.1038/s41467-018-07550-x
33. Livak KJ, Schmittgen TD. Analysis of relative gene expression data using real-time quantitative PCR and the 2(-Delta Delta C(T)) Method. *Methods* (2001) 25(4):402–8. doi: 10.1006/meth.2001.1262
34. Patel RB, Ye M, Carlson PM, Jaquish A, Zangl L, Ma B, et al. Development of an In Situ Cancer Vaccine via Combinational Radiation and Bacterial-Membrane-Coated Nanoparticles. *Adv Mater* (2019) 31(43):e1902626. doi: 10.1002/adma.201902626
35. Maecker HT, Trotter J. Flow cytometry controls, instrument setup, and the determination of positivity. *Cytometry A* (2006) 69(9):1037–42. doi: 10.1002/cyto.a.20333
36. Allen F, Bobanga ID, Rauhe P, Barkauskas D, Teich N, Tong C, et al. CCL3 augments tumor rejection and enhances CD8(+) T cell infiltration through NK and CD103(+) dendritic cell recruitment via IFNgamma. *Oncoimmunology* (2018) 7(3):e1393598. doi: 10.1080/2162402X.2017.1393598
37. Selby MJ, Engelhardt JJ, Quigley M, Henning KA, Chen T, Srinivasan M, et al. Anti-CTLA-4 antibodies of IgG2a isotype enhance antitumor activity through reduction of intratumoral regulatory T cells. *Cancer Immunol Res* (2013) 1 (1):32–42. doi: 10.1158/2326-6066.CIR-13-0013
38. Walker JM, Rolig AS, Charych DH, Hoch U, Kasiewicz MJ, Rose DC, et al. NKTR-214 immunotherapy synergizes with radiotherapy to stimulate systemic CD8(+) T cell responses capable of curing multi-focal cancer. *J Immunother Cancer* (2020) 8(1):e000464. doi: 10.1136/jitc-2019-000464
39. Philippou Y, Sjoberg HT, Murphy E, Alyacoubi S, Jones KI, Gordon-Weeks AN, et al. Impacts of combining anti-PD-L1 immunotherapy and radiotherapy on the tumour immune microenvironment in a murine prostate cancer model. *Br J Cancer* (2020) 123(7):1089–100. doi: 10.1038/s41416-020-0956-x
40. Lugade AA, Sorensen EW, Gerber SA, Moran JP, Frelinger JG, Lord EM. Radiation-induced IFN-gamma production within the tumor microenvironment influences antitumor immunity. *J Immunol* (2008) 180 (5):3132–9. doi: 10.4049/jimmunol.180.5.3132
41. Gerber SA, Sedlacek AL, Cron KR, Murphy SP, Frelinger JG, Lord EM. IFN-gamma mediates the antitumor effects of radiation therapy in a murine colon tumor. *Am J Pathol* (2013) 182(6):2345–54. doi: 10.1016/j.ajpath.2013.02.041
42. Pilones KA, Vanpouille-Box C, Demaria S. Combination of radiotherapy and immune checkpoint inhibitors. *Semin Radiat Oncol* (2015) 25(1):28–33. doi: 10.1016/j.semradonc.2014.07.004
43. Vanpouille-Box C, Pilones KA, Wennerberg E, Formenti SC, Demaria S. In situ vaccination by radiotherapy to improve responses to anti-CTLA-4 treatment. *Vaccine* (2015) 33(51):7415–22. doi: 10.1016/j.vaccine.2015.05.105
44. Chen JL, Pan CK, Huang YS, Tsai CY, Wang CW, Lin YL, et al. Evaluation of antitumor immunity by a combination treatment of high-dose irradiation, anti-PDL1, and anti-angiogenic therapy in murine lung tumors. *Cancer Immunol Immunother* (2021) 70(2):391–404. doi: 10.1007/s00262-020-02690-w
45. Tsao MN, Ven LI, Cheung P, Poon I, Ung Y, Louie AV. Stereotactic Body Radiation Therapy for Extracranial Oligometastatic Non-small-cell Lung Cancer: A Systematic Review. *Clin Lung Cancer* (2020) 21(2):95–105 e1. doi: 10.1016/j.cllc.2019.11.007
46. Palma DA, Olson R, Harrow S, Correa RJM, Schneiders F, Haasbeek CJA, et al. Stereotactic ablative radiotherapy for the comprehensive treatment of 4-10 oligometastatic tumors (SABR-COMET-10): study protocol for a randomized phase III trial. *BMC Cancer* (2019) 19(1):816. doi: 10.1186/s12885-019-5977-6
47. Jagodinsky JC, Morris ZS. Priming and Propagating Anti-tumor Immunity: Focal Hypofractionated Radiation for in Situ Vaccination and Systemic Targeted Radionuclide Theranostics for Immunomodulation of Tumor Microenvironments. *Semin Radiat Oncol* (2020) 30(2):181–6. doi: 10.1016/j.semradonc.2019.12.008
48. Sgouros G, Bodei L, McDevitt MR, Nedrow JR. Radiopharmaceutical therapy in cancer: clinical advances and challenges. *Nat Rev Drug Discovery* (2020) 19 (9):589–608. doi: 10.1038/s41573-020-0073-9
49. Dewan MZ, Galloway AE, Kawashima N, Dewyngaert JK, Babb JS, Formenti SC, et al. Fractionated but not single-dose radiotherapy induces an immune-mediated abscopal effect when combined with anti-CTLA-4 antibody. *Clin Cancer Res an Off J Am Assoc Cancer Res* (2009) 15(17):5379–88. doi: 10.1158/1078-0432.CCR-09-0265
50. Vanpouille-Box C, Alard A, Aryankalayil MJ, Sarfraz Y, Diamond JM, Schneider RJ, et al. DNA exonuclease Trex1 regulates radiotherapy-induced tumour immunogenicity. *Nat Commun* (2017) 8:15618. doi: 10.1038/ncomms15618
51. Morris ZS, Harari PM. Interaction of radiation therapy with molecular targeted agents. *J Clin Oncol* (2014) 32(26):2886–93. doi: 10.1200/JCO.2014.55.1366

Conflict of Interest: The authors declare that the research was conducted in the absence of any commercial or financial relationships that could be construed as a potential conflict of interest.

frontiers in Oncology

ORIGINAL RESEARCH
published: 28 April 2021
doi: 10.3389/fonc.2021.658395

Pleural Fluid Has Pro-Growth Biological Properties Which Enable Cancer Cell Proliferation

Rachelle Asciak[1,2,3†], Nikolaos I. Kanellakis[1,2,4,5*†], Xuan Yao[5,6], Megat Abd Hamid[5,6], Rachel M. Mercer[1], Maged Hassan[1], Eihab O. Bedawi[1], Melissa Dobson[7], Peter Fsadni[3], Stephen Montefort[3], Tao Dong[5,6], Najib M. Rahman[1,2,4,7‡] and Ioannis Psallidas[1,2,8‡]*

[1] Oxford Centre for Respiratory Medicine, Churchill Hospital, Oxford University Hospitals NHS Foundation Trust, Oxford, United Kingdom, [2] Laboratory of Pleural and Lung Cancer Translational Research, Nuffield Department of Medicine, University of Oxford, Oxford, United Kingdom, [3] Mater Dei Hospital, Msida, Malta, [4] National Institute for Health Research Oxford Biomedical Research Centre, University of Oxford, Oxford, United Kingdom, [5] Chinese Academy of Medical Sciences Oxford Institute, Nuffield Department of Medicine, University of Oxford, Oxford, United Kingdom, [6] MRC Human Immunology Unit, MRC Weatherall Institute of Molecular Medicine, University of Oxford, Oxford, United Kingdom, [7] Oxford Respiratory Trials Unit, Nuffield Department of Medicine, University of Oxford, Oxford, United Kingdom, [8] Research and Early Development, Respiratory & Immunology, AstraZeneca, Cambridge, United Kingdom

OPEN ACCESS

Edited by:
Lizza E. L. Hendriks, Maastricht University Medical Centre, Netherlands

Reviewed by:
Enrico Giarnieri, Sapienza University of Rome, Italy
Santiago Viteri, Instituto Oncológico Dr Rosell, Spain

***Correspondence:**
Rachelle Asciak
rachasciak@gmail.com
Nikolaos I. Kanellakis
nikolaos.kanellakis@ndm.ox.ac.uk

†These authors share first authorship

‡These authors share senior authorship

Specialty section:
This article was submitted to Thoracic Oncology, a section of the journal Frontiers in Oncology

Received: *25 January 2021*
Accepted: *15 March 2021*
Published: *28 April 2021*

Citation:
Asciak R, Kanellakis NI, Yao X, Abd Hamid M, Mercer RM, Hassan M, Bedawi EO, Dobson M, Fsadni P, Montefort S, Dong T, Rahman NM and Psallidas I (2021) Pleural Fluid Has Pro-Growth Biological Properties Which Enable Cancer Cell Proliferation. Front. Oncol. 11:658395. doi: 10.3389/fonc.2021.658395

Objectives: Patients with malignant pleural mesothelioma (MPM) or pleural metastases often present with malignant pleural effusion (MPE). This study aimed to analyze the effect of pleural fluid on cancer cells.

Materials and Methods: Established patient-derived cancer cell cultures derived from MPE (MPM, breast carcinoma, lung adenocarcinoma) were seeded in 100% pleural fluid (exudate MPM MPE, transudate MPE, non-MPE transudate fluid) and proliferation was monitored. In addition, the establishment of new MPM cell cultures, derived from MPE specimens, was attempted by seeding the cells in 100% MPE fluid.

Results: All established cancer cell cultures proliferated with similar growth rates in the different types of pleural fluid. Primary MPM cell culture success was similar with MPE fluid as with full culture medium.

Conclusions: Pleural fluid alone is adequate for cancer cell proliferation *in vitro*, regardless of the source of pleural fluid. These results support the hypothesis that pleural fluid has important pro-growth biological properties, but the mechanisms for this effect are unclear and likely not malignant effusion specific.

Keywords: pleural fluid, malignant pleural effusion (MPE), pleural metastases, malignant pleural mesothelioma, pleural cancer

INTRODUCTION

Malignant pleural effusion (MPE) is a common complication which affects patients with pleural metastases, or malignant pleural mesothelioma (MPM) (1, 2). The incidence of MPE is rising worldwide, driven by the increasing prevalence of cancer and advances in cancer management and treatment (3–5). The development of MPE has been linked with poor survival outcomes (5). MPE is an established prognostic factor for shorter life expectancy for patients with lung cancer (6).

Treatment options include observation, drainage and pleurodesis (5). Currently, treatment remains palliative and is mainly focused on symptom relief. Therefore, it is recommended to only drain symptomatic MPE (2, 5, 7), however, there is some early pre-clinical evidence that MPE may not simply be a bystander. It has been shown that MPE may have biological properties that contribute to MPM proliferation and promote resistance to chemotherapy (8, 9).

MPE is a protein-rich fluid including growth factors and cytokines, with pro-inflammatory, oncogenic and angiogenic properties such as vascular endothelial growth factor (VEGF) (10, 11), and immunosuppressive such as IL-10 (12). This suggests the hypothesis that MPE fluid provides a nutrient-rich microenvironment to support tumor growth, while suppressing anti-tumor immune activity.

Laboratory data support this view - Cheah et al. reported that MPM cells exposed to 30% MPM MPE fluid *in vitro* had increased cell viability compared to cells exposed to serum-free and serum-enriched medium. In addition, MPM cell death was significantly less likely after exposure to cisplatin/pemetrexed combination in the presence of 30% MPM MPE fluid, than cells that were only exposed to the chemotherapy (8). Although this data provides early evidence of the potential biological properties of pleural fluid the results have not been replicated and there were some experimental limitations (use of control and 30% MPE fluid does not necessarily reflect the *in vivo* pleural effusion environment).

Patient-derived cancer cell cultures are a faithful laboratory model with the potency to recapitulate the biology of the disease (13–15). Patient-derived MPM cancer cell cultures from MPE samples reflect tumor and patient heterogeneity and closely resemble native tumor specimens (16). There is a need to further understand the role of pleural fluid. Use of 100% pleural fluid in experimental models may bridge some of the gap between *in vitro* and *in vivo* settings, potentially providing a closer representative of cancer cells *in vivo* which are bathed in pleural fluid. This study aimed to analyze whether pleural fluid alone is adequate for cancer cell proliferation *in vitro*.

MATERIALS AND METHODS

Study Approval

Pleural fluid samples were collected from patients who gave consent for inclusion in the Oxford Radcliffe Pleural Biobank (Research ethics committee: South Central Oxford C 09/H0606/5 +5). This project was approved by the Oxford Radcliffe Biobank Central University Research Ethics Committee (CUREC) number: 19/A107. Pleural Biobank is a prospective collection of clinical specimens derived from patients presenting with pleural effusion of varied diagnoses.

Pleural Fluid Specimen Collection

Pleural fluid (50ml) was collected from patients with MPM who underwent pleural procedures as part of their standard medical care. The fluid was collected in sterile 50ml conical centrifuge tubes and processed for cell culture within 2-3 hours of sampling. The protocol used for cancer cell culture is described elsewhere (16). When pleural fluid was used as culture medium in the experiments, mostly fresh pleural fluid (kept in refrigerator at 3-4°C for up to 3 days) was used, but when this was not available, freshly-thawed-from-frozen unfiltered pleural fluid samples were used.

Seeding of Cells From Established Patient-Derived Cancer Cell Cultures in MPM Exudate MPE Fluid

1. The cells from established patient-derived MPM cell culture (MESO-163, epithelioid MPM) were seeded at 100,000 cells per well in a 6-well plate, in 2ml of MPM MPE pleural fluid.
2. The cells were incubated at 37°C and 5% CO_2.
3. Serial live images of the cells within the well were taken daily to monitor growth and proliferation.
4. The pleural fluid was refreshed every 48 hours.

Seeding of Cells From Established Patient-Derived Cancer Cell Cultures in Any Pleural Fluid

MPM cells from established patient-derived MPM cell cultures [MESO-163 (epithelioid MPM), MESO-024 (biphasic MPM), MESO-027 (epithelioid MPM), MESO-031 (epithelioid MPM) were seeded at 20,000 cells per well in a 96-well plate, in starvation medium (Dulbecco's modified eagle medium, Sigma-Aldrich®, D5671] for 12 hours before starvation medium was changed to 100µl of exudative MPM MPE fluid (biphasic MPM MPE fluid, with total fluid protein 39 g/l, glucose 2.3 mmol/l, LDH 679 IntUnit/l) or transudate MPE fluid (metastatic lung adenocarcinoma MPE (cytology positive for adenocarcinoma) with total fluid protein 8 g/l, glucose 5.7 mmol/l, LDH 190 IntUnit/l). There were at least 6 replicates for each cell culture at each time point. The pleural fluid was refreshed every 24 hours. Cell viability was assessed at 4, 8, 12, 24 and 48 hours using CellTiter-Glo®. A well-characterized, commercially available biphasic MPM cell line CRL-2081(MSTO-211H)™ (derived from human MPE fluid) was purchased from ATCC® and used as a control.

This experiment was then repeated, this time seeding cells directly in pleural fluid without using starvation medium, with patient-derived MPM [MESO-163 (epithelioid MPM), MESO-174 (biphasic MPM), MESO-024 (biphasic MPM), MESO-027 (epithelioid MPM)], breast cancer (BRST-156) and lung adenocarcinoma (LNG-183) cell cultures, and with exudate and transudate MPE fluid, as well as non-MPE pleural fluid from a patient with heart failure-related pleural effusion (total fluid protein 25 g/l, glucose 5.7 mmol/l, LDH 97 IntUnit/l) (minimum of 3 replicates per cell culture). Cells were incubated in an Incucyte® machine, and regular live images of the wells were obtained. For all experiments, cells were incubated at 37°C and 5% CO_2.

Calculation of Cell Size

Using Fiji (ImageJ) (17) version 2.0, the area of a sample of 3 cells from each image was calculated and a mean of the sizes obtained.

This enabled comparison of size of the cells seeded in different pleural fluid types.

Calculation of Cell Confluence

Pleural fluid was observed to have a tendency to adopt a gel-like texture *in vitro* (**Supplementary Figure 1**). Pleural fluid viscosity may lead to overestimation of the percentage confluence if this were to be calculated automatically, with viscous areas and fibrin strands being erroneously included as 'area covered by cells'. To avoid this, the percentage confluence was calculated by measuring the pixels in the area of the well covered by cells, and expressing it as a percentage of the pixels in the total area of the well in the image (18). This allowed manual setting of the threshold for each image, ensuring that only the area of the well covered by cells was included when calculating percentage confluence (**Supplementary Figure 2**).

Starting a New Cell Culture Without Using Culture Medium: Primary MPM Cell Culture in MPE Fluid, With Primary Culture in Full Culture Medium as a Control

Cells from MPM MPE fluid were seeded in full culture medium (Supplementary data) as per standard method used in our laboratory for primary cell culture, and in parallel, half the cells from the same MPE fluid sample were seeded in matched MPE fluid from the same patient instead of in full medium. The associated pleural fluid cytology result as reported by the clinical histopathologist as part of the patient's routine clinical care was collected from the medical records. The method used was as follows:

1. Pleural fluid samples from patients diagnosed with MPM were centrifuged at 800G for 10 minutes and the supernatant was aspirated and saved for later use.
2. The sedimented cells were resuspended in 3-5ml of red blood cell lysis solution (Qiagen®) and cells were kept at room temperature for 5 minutes.
3. The sample was then centrifuged again at 500G for 5 minutes. The supernatant was aspirated and discarded, and the pelleted cells washed with phosphate buffered saline (Sigma-Aldrich® MFCD00121855).
4. The sample was centrifuged one last time at 500G for 5 minutes. The pelleted cells were resuspended in 1ml of the MPE fluid saved from step 1 (or in 1ml full medium for the control), and then transferred to a cell culture treated plate with a further 9ml MPE fluid (or in 9ml full medium for the control) in it, and incubated at 37°C and 5% CO_2.
5. The MPE fluid (or full medium for the control) was refreshed every 48 hours, and the plates were monitored regularly under a light microscope.
6. The cells were allowed proliferate until >90% confluence. The cells were then split, and about 70% of the cells were transferred to a new culture dish this time in full medium.

Imaging

The serial live images of the cells within the wells were taken using ZEISS Axiocam 506 mono, to monitor growth and proliferation. The percentage confluence was calculated from the images using Fiji (ImageJ) (17) version 2.0.

Statistics

Kruskal-Wallis test was used to compare mean size of cells seeded in the different pleural fluid types. GraphPad PRISM version 8.3.0 (GraphPad Software, San Diego, California USA) was used for the growth curves and the statistics.

RESULTS

Cell Cultures Used in This Study

Table 1 shows the baseline demographics of the patients the cell cultures used in this study were derived from.

Cells From Established MPM Cell Cultures Proliferate in MPE Fluid Alone

The hypothesis that MPE fluid has biological properties was explored by first assessing whether cells from established MPM cell culture proliferate *in vitro*, obtaining nutrients solely from pleural fluid. Results revealed that the cells show increased levels of confluency with time (**Figure 1**).

Cells From Cancer Cell Cultures Proliferate *In Vitro* in Exudate and Transudate MPE Fluid, as Well as in Heart Failure Transudate Pleural Fluid

Subsequently, cells were seeded in pleural fluid in 96-well plates, and comparison of MPM cells' growth in exudative MPM MPE fluid and transudative MPE fluid showed similar growth rates (**Figure 2**).

Once it was clear that MPM cells were able to proliferate *in vitro* in 100% MPE fluid, the latter experiment was repeated with cells from four MPM cell cultures [MESO-163 (epithelioid), MESO-174 (biphasic), MESO-024 (biphasic), MESO-027 (epithelioid)] to compare exudate and transudate MPE fluid, and transudate non-MPE pleural fluid (**Figure 3**). Breast carcinoma and lung adenocarcinoma cells also proliferated *in vitro* in 100% pleural fluid alone (**Figure 4**). For cell cultures MESO-163 and MESO-027, there was decreased proliferation with transudate MPE and with non-MPE heart failure transudate

TABLE 1 | Shows the baselines demographics of the patients from whom the cell cultures used were derived from.

Cell culture	Patient age at fluid sampling	Patient gender	Histological diagnosis
MESO-163	63	F	Epithelioid MPM
MESO-174	69	M	Biphasic MPM
MESO-024	84	M	Biphasic MPM
MESO-027	56	M	Epithelioid MPM
MESO-031	78	M	Epithelioid MPM
BRST-156	NA	F	Breast carcinoma
LNG-183	NA	M	Lung adenocarcinoma

F, female; M, male; MPM, malignant pleural mesothelioma; NA, data not available.

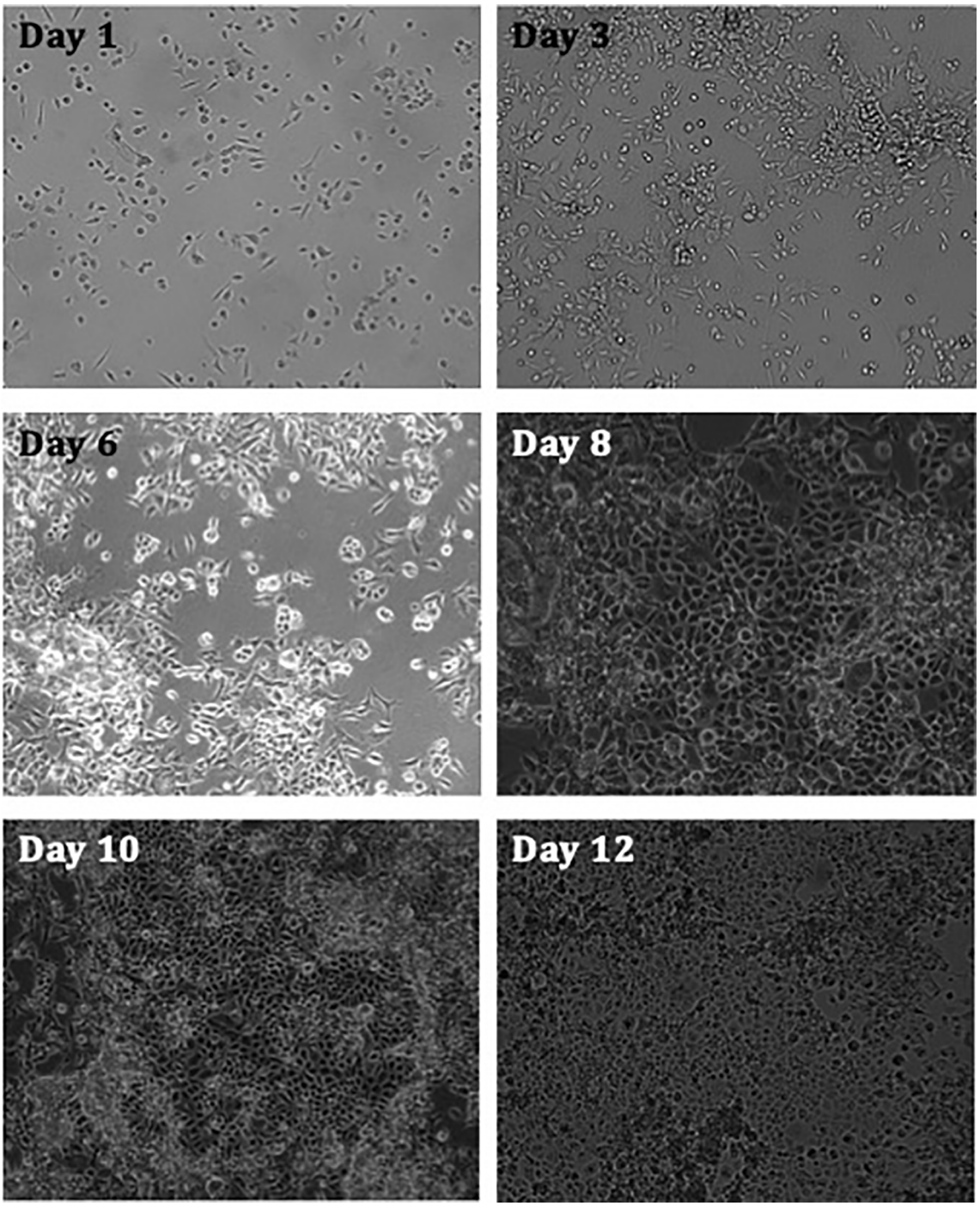

FIGURE 1 | Images taken of MPM cell culture MESO-163 (epithelioid MPM) seeded in 100% exudate MPM MPE fluid only, at 100,000 cells per well in a 6-well plate. The images were taken on days 1-12 after seeding, and were taken at 10x magnification [ZEISS Axiocam 506 mono]. The cells show increased levels of confluency with time. *MPE, malignant pleural effusion; MPM, malignant pleural mesothelioma.*

respectively, when compared to the proliferation with other types of pleural fluid tested. However, there was no clear decreased proliferation with any one pleural fluid type across all cell cultures tested.

There was no significant difference in cell morphology noted, and neither was there significant difference in size of cells seeded in the different types of pleural fluid (**Supplementary Figure 3**).

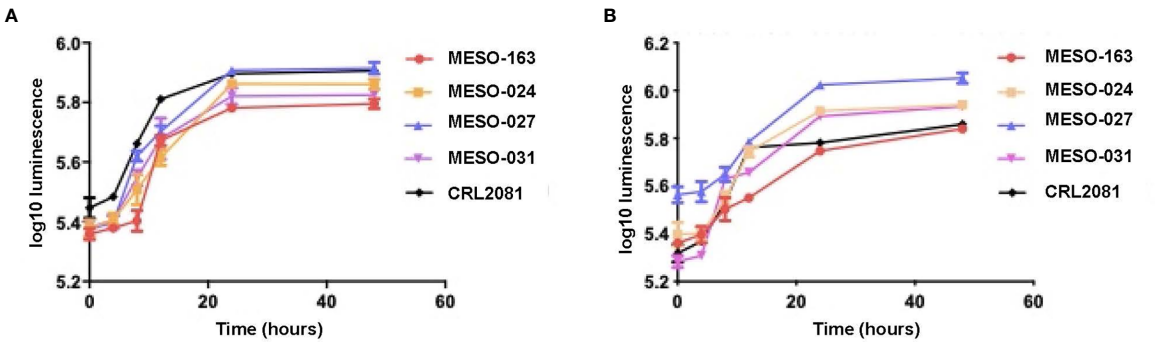

FIGURE 2 | The growth curves with mean and 95% confidence intervals for each time point, obtained after 20,000 MPM cells per well (96-well plate) were seeded in starvation medium for 12 hours, then starvation medium was replaced with **(A)** exudate MPM MPE fluid and **(B)** transudate MPE fluid from a patient with lung adenocarcinoma MPE (right sided graph). Cell viability was measured at 4, 8, 12, 24 and 48 hours using CellTiter-Glo®. *Cell cultures: MESO-163 (epithelioid MPM), MESO-024 (biphasic MPM), MESO-027 (epithelioid MPM), MESO-031 (epithelioid MPM); CRL2081(MSTO-211H)™ - a well-characterized, commercially available biphasic MPM cell line (derived from human MPE fluid) used as a control.*

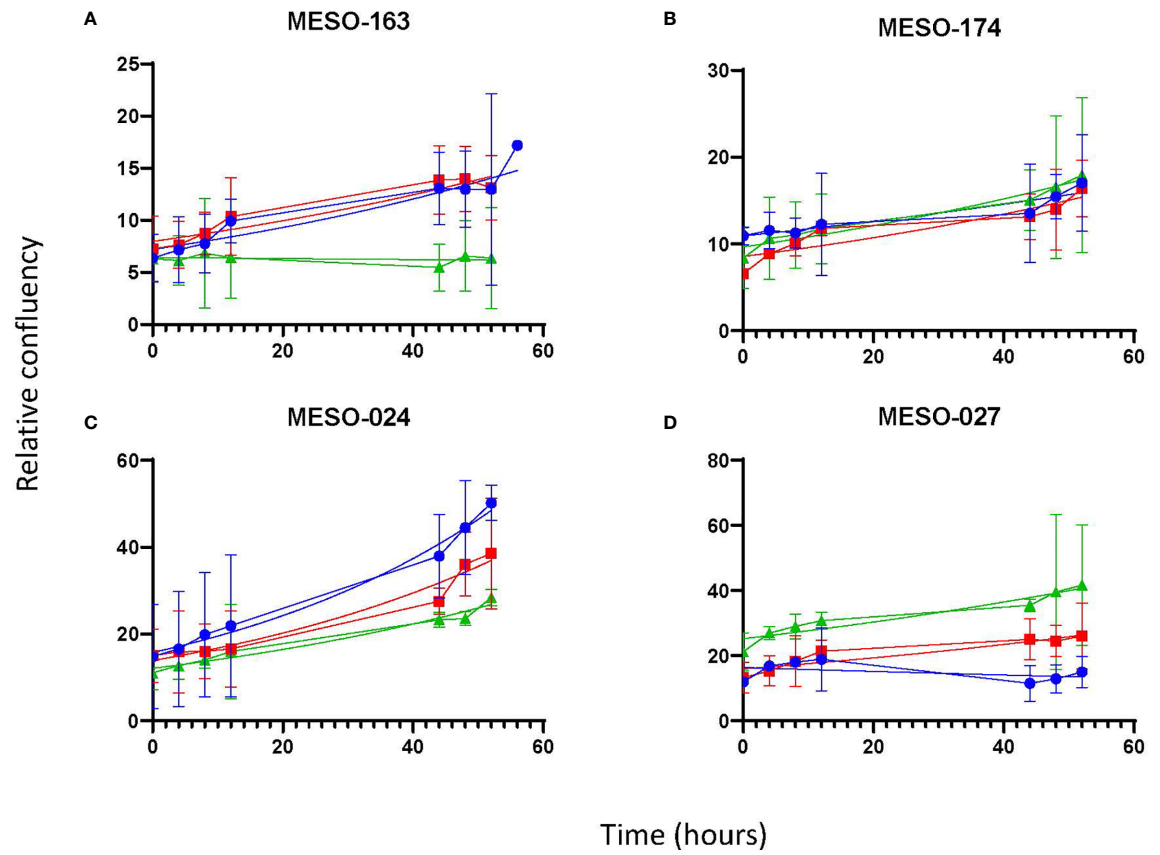

FIGURE 3 | The growth curves for cells from MPM cell cultures *in vitro*, seeded directly in pleural fluid. The curves show the mean and 95% confidence intervals, and a trendline for non-linear fit. *Cell cultures:* **(A)** *MESO-163 (epithelioid MPM)*, **(B)** *MESO-174 (biphasic MPM)*, **(C)** *MESO-024 (biphasic MPM)*, and **(D)** *MESO-027 (epithelioid MPM). HF, heart failure; MPE, malignant pleural effusion; MPM, malignant pleural mesothelioma.*

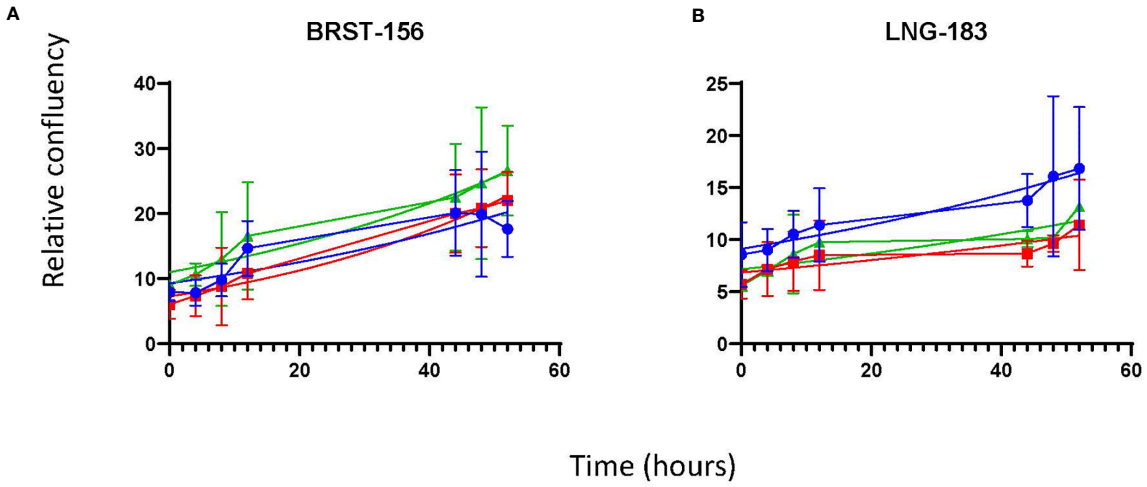

FIGURE 4 | The growth curves for non-MPM cell cultures *in vitro*, seeded directly in pleural fluid. The curves show the mean and 95% confidence intervals, and a trendline for non-linear fit. *Cells cultures:* **(A)** *BRST-156 (breast carcinoma)*, and **(B)** *LNG-183 (lung adenocarcinoma). HF, heart failure; MPE, malignant pleural effusion.*

Primary Culture of MPM Cells Can Be Achieved Using MPE Fluid Alone as Culture Medium

In order to further assess the biological properties of pleural fluid, primary MPM cell culture in MPE fluid was attempted in 6 MPM MPE fluid samples, with concurrent primary cell culture in the standard *in vitro* cell culture medium (DMEM enriched with 10%FBS) as a control. In 3 (3/6, 50%), cell culture was successful in both MPE fluid and cell culture medium, in 1/6 (16.7%) cell culture was unsuccessful from the start in cell culture medium and unsuccessful beyond passage 1 in pleural fluid, and 2 (2/6, 33.3%) attempts were unsuccessful in both MPE fluid and cell culture medium. These results and the associated pleural fluid cytology as reported by the clinical histopathologist as part of the patient's routine clinical care are shown in **Table 2**.

DISCUSSION

Cell culture is a time-consuming process, requiring several laboratory consumables, and an artificially produced cell culture medium containing a delicate balance of nutrients required for optimal *in vitro* cell growth. Despite this, MPM cells proliferated in 100% pleural fluid, to a similar degree in both exudative and transudative MPE fluid. This indicates that it is not simply the quantity of proteins within MPE fluid that gives the fluid the biological capabilities that support cancer cell proliferation *in vitro*. Furthermore, cancer cells proliferated in heart failure non-MPE transudative pleural fluid. It is possible that the heart failure transudate pleural fluid obtained the contains growth factors since it is a filtrate of blood *via* capillaries, and therefore is also able to support cancer cell proliferation *in vitro*. However, the cancer cells might have secreted the necessary growth factors.

TABLE 2 | Shows the outcomes of the MPM primary cell culture in MPE fluid and in full medium.

Cell cultures	MPM subtype	Pleural fluid cytology at time of MPE fluid sampling	Outcome of primary cell culture	
			Cells seeded in full medium	Cells seeded in MPE fluid
MESO-392	Biphasic	Negative	Grew well and frozen at P4 (after >2 months in culture)	Culture dish confluent, cells split and transferred to full medium on day 43. Went on to becoming an established cell culture beyond P5
MESO-051	Epithelioid	Not available	Cells discarded - no attached cells on day 3	Culture dish confluent, cells split and transferred to full medium on day 38. Cells stopped growing during P1 and were discarded.
MESO-397	Epithelioid	Positive	Cells discarded - no attached cells on day 3	Cells discarded - no attached cells on day 3
MESO-398	Biphasic	Negative	Cells discarded - no attached cells on day 3	Cells discarded - no attached cells on day 3
MESO-402	Epithelioid	Positive	Grew well and frozen at P2 (after >2 months in culture)	Culture dish confluent, cells split and transferred to full medium on day 39. Went on to becoming an established cell culture beyond P5
MESO-064	Epithelioid	Positive	Grew well and frozen at P2 (after >2 months in culture)	Culture dish confluent, cells split and transferred to full medium on day 40. Went on to becoming an established cell culture beyond P5

Cell culture success with MPE fluid was similar to that in full medium. MPE, malignant pleural effusion; MPM, malignant pleural mesothelioma; P, passage.

There have been no good quality studies assessing the components of transudates in this regard.

Cheah et al. reported that non-MPM MPE fluid and benign pleural effusion fluid were associated with increased MPM cell proliferation *in vitro*, by 1.4–2.8 fold and by 1.3–2.2 fold respectively, when compared to serum-free medium as a control (8). The difference in the present study is that cells were incubated with 100% pleural fluid as compared to 30% pleural fluid in culture medium, and therefore is more representative of the clinical scenario of pleural tumor cells bathed in 100% pleural fluid as would be found in the pleural space. Importantly, our findings indicate that the biological properties of pleural fluid are not seen solely in MPM cancer cells, but also in other non-MPM cancer cells including breast and lung carcinoma. Future studies further exploring this area should therefore also focus on other malignancies as well as MPM, and we postulate that there is a likely common pathway within the pleural environment to explain these findings.

Primary cell culture for cancer cells is traditionally performed using specifically manufactured artificial cell culture medium, containing all nutrients required to provide the optimal environment *in vitro* for cell proliferation. Despite this, the results show that 100% MPM MPE fluid has the ability to support the primary cell culture of MPM cells, extracted directly from pleural fluid, without addition of any other nutrients, at a similar rate to primary MPM cell culture in full culture medium.

Limitations

Pleural fluid viscosity limited the ability to demonstrate cell proliferation and cellular viability using the traditional ways applicable to cells cultured in clear full culture medium. To overcome this, a combination of methods were used to assess cellular proliferation, including live images, luminescence assay, and using bioinformatic algorithms to calculate relative confluence.

Cancer cells were able to survive and proliferate when seeded in 100% pleural fluid, and to our knowledge this is the first demonstration of this effect. Although the mechanism is unclear, any form of human pleural fluid (malignant, non-malignant, transudate, exudate) appears to have this effect, and this has potentially significant biological and clinical implications. If pleural fluid continuously bathing pleural cancer cells enables and sustains cell proliferation, the current management approach to MPE will need to be reconsidered. To this end, well-designed prospective clinical studies are now required to determine whether MPE fluid should be drained as early and completely as possible. Further translational studies are required to explore the biological mechanism of cancer cell proliferation when bathed in pleural fluid.

DATA AVAILABILITY STATEMENT

The original contributions presented in the study are included in the article/**Supplementary Material**. Further inquiries can be directed to the corresponding authors.

ETHICS STATEMENT

The studies involving human participants were reviewed and approved by Oxford Radcliffe Biobank Central University Research Ethics Committee (CUREC) number: 19/A107. The patients/participants provided their written informed consent to participate in this study.

AUTHOR CONTRIBUTIONS

RA, NK, NR and IP conceived and designed the study. RA and NK did laboratory assays and analyzed the data. XY, MH and TD provided resources and support for the laboratory assays. RA, NR, IP, EB, RM, and MH collected samples and clinical data. RA, NK and IP analyzed clinical data. RA, NK and MD provided resources and prepared the ethics protocols. NR and IP supervised the study. PF and SM supported and facilitating the conduction of the study. All authors contributed to the article and approved the submitted version.

FUNDING

This work was supported by an Oxfordshire Health Services Research Committee (OHSRC) Research Grant (ID 1247) and a Chinese Academy of Medical Sciences (CAMS) Innovation Fund for Medical Science (CIFMS, ID: 2018-I2M-2-002). NK and NR are supported by a National Institute for Health Research (NIHR) Oxford Biomedical Research Centre (BRC) grant. TD is supported by Medical Research Council, UK. XY and MH are supported by CAMS. The views expressed are those of the authors and not those of the NHS, or NIHR.

SUPPLEMENTARY MATERIAL

The Supplementary Material for this article can be found online at: https://www.frontiersin.org/articles/10.3389/fonc.2021.658395/full#supplementary-material

REFERENCES

1. Woolhouse I, Bishop L, Darlison L, De Fonseka D, Edey A, Edwards J, et al. British Thoracic Society Guideline for the investigation and management of malignant pleural mesothelioma. *Thorax* (2018) 73:i1–i30. doi: 10.1136/thoraxjnl-2017-211321
2. Bibby AC, Tsim S, Kanellakis N, Ball H, Talbot DC, Blyth KG, et al. Malignant pleural mesothelioma: an update on investigation, diagnosis and treatment. *Eur Respir Rev* (2016) 25:472–86. doi: 10.1183/16000617.0063-2016
3. Bibby AC, Dorn P, Psallidas I, Porcel JM, Janssen J, Froudarakis M, et al. ERS/EACTS statement on the management of malignant pleural effusions. *Eur J Cardiothorac Surg* (2019) 55:116–32. doi: 10.1093/ejcts/ezy258
4. Bibby AC, Dorn P, Psallidas I, Porcel JM, Janssen J, Froudarakis M, et al. ERS/EACTS statement on the management of malignant pleural effusions. *Eur Respir J* (2018) 52. doi: 10.1183/13993003.00349-2018

5. Roberts ME, Neville E, Berrisford RG, Antunes G, Ali NJ, and Group BTSPDG. Management of a malignant pleural effusion: British Thoracic Society Pleural Disease Guideline 2010. *Thorax* (2010) 65 Suppl 2:ii32–40. doi: 10.1136/thx.2010.136994
6. Porcel JM, Gasol A, Bielsa S, Civit C, Light RW, Salud A. Clinical features and survival of lung cancer patients with pleural effusions. *Respirology* (2015) 20:654–9. doi: 10.1111/resp.12496
7. Feller-Kopman DJ, Reddy CB, Decamp MM, Diekemper RL, Gould MK, Henry T, et al. Management of Malignant Pleural Effusions. An Official ATS/STS/STR Clinical Practice Guideline. *Am J Respir Crit Care Med* (2018) 198:839–49. doi: 10.1164/rccm.201807-1415ST
8. Cheah HM, Lansley SM, Varano Della Vergiliana JF, Tan AL, Thomas R, Leong SL, et al. Malignant pleural fluid from mesothelioma has potent biological activities. *Respirology* (2017) 22:192–9. doi: 10.1111/resp.12874
9. Hanahan D, Weinberg RA. Hallmarks of cancer: the next generation. *Cell* (2011) 144:646–74. doi: 10.1016/j.cell.2011.02.013
10. Stathopoulos GT, Kollintza A, Moschos C, Psallidas I, Sherrill TP, Pitsinos EN, et al. Tumor necrosis factor-alpha promotes malignant pleural effusion. *Cancer Res* (2007) 67:9825–34. doi: 10.1158/0008-5472.CAN-07-1064
11. Zebrowski BK, Yano S, Liu W, Shaheen RM, Hicklin DJ, Putnam JB Jr, et al. Vascular endothelial growth factor levels and induction of permeability in malignant pleural effusions. *Clin Cancer Res* (1999) 5:3364–8. doi: 10.1038/s41588-018-0209-6
12. Chen YM, Yang WK, Whang-Peng J, Kuo BI, Perng RP. Elevation of interleukin-10 levels in malignant pleural effusion. *Chest* (1996) 110:433–6. doi: 10.1378/chest.110.2.433
13. Lee JK, Liu Z, Sa JK, Shin S, Wang J, Bordyuh M, et al. Pharmacogenomic landscape of patient-derived tumor cells informs precision oncology therapy. *Nat Genet* (2018) 50:1399–411. doi: 10.1038/s41588-018-0209-6
14. McDermott U. Cancer cell lines as patient avatars for drug response prediction. *Nat Genet* (2018) 50:1350–1. doi: 10.1038/s41588-018-0245-2
15. Goodspeed A, Heiser LM, Gray JW, Costello JC. Tumor-Derived Cell Lines as Molecular Models of Cancer Pharmacogenomics. *Mol Cancer Res* (2016) 14:3–13. doi: 10.1158/1541-7786.MCR-15-0189
16. Kanellakis NI, Asciak R, Hamid MA, Yao X, Mccole M, Mcgowan S, et al. Patient-derived malignant pleural mesothelioma cell cultures: a tool to advance biomarker-driven treatments. *Thorax* (2020) 75:1004–8. doi: 10.1136/thoraxjnl-2020-215027
17. Schindelin J, Arganda-Carreras I, Frise E, Kaynig V, Longair M, Pietzsch T, et al. Fiji: an open-source platform for biological-image analysis. *Nat Methods* (2012) 9:676–82. doi: 10.1038/nmeth.2019
18. Busschots S, O'Toole S, O'Leary JJ, Stordal B. Non-invasive and non-destructive measurements of confluence in cultured adherent cell lines. *MethodsX* (2015) 2:8–13. doi: 10.1016/j.mex.2014.11.002

Conflict of Interest: IP was employed by AstraZeneca in a non-related field.

The remaining authors declare that the research was conducted in the absence of any commercial or financial relationships that could be construed as a potential conflict of interest.

frontiers in Oncology

ORIGINAL RESEARCH
published: 15 June 2021
doi: 10.3389/fonc.2021.643280

An EBC/Plasma miRNA Signature Discriminates Lung Adenocarcinomas From Pleural Mesothelioma and Healthy Controls

Alice Faversani[1†], Chiara Favero[2†], Laura Dioni[2], Angela Cecilia Pesatori[2,3], Valentina Bollati[2], Matteo Montoli[4], Valeria Musso[4], Andrea Terrasi[5], Nicola Fusco[1,6], Mario Nosotti[4,7], Valentina Vaira[1,7†] and Alessandro Palleschi[4,7*†]*

[1] Division of Pathology, Fondazione IRCCS Ca' Granda—Ospedale Maggiore Policlinico, Milan, Italy, [2] EPIGET Lab, Department of Clinical Sciences and Community Health, University of Milan, Milan, Italy, [3] Department of Preventive Medicine, Fondazione IRCCS Ca' Granda—Ospedale Maggiore Policlinico, Milan, Italy, [4] Division of Thoracic Surgery and Lung Transplantation, Fondazione IRCCS Ca' Granda Ospedale Maggiore Policlinico, Milan, Italy, [5] Division of Molecular Biology, Biomedical Center, Faculty of Medicine, LMU Munich, Martinsried, Germany, [6] Department of Biomedical, Surgical and Dental Sciences, University of Milan, Milan, Italy, [7] Department of Pathophysiology and Transplantation, University of Milan, Milan, Italy

Background: Despite significant improvement in screening programs for cancers of the respiratory district, especially in at-risk subjects, early disease detection is still a major issue. In this scenario, new molecular and non-invasive biomarkers are needed to improve early disease diagnosis.

Methods: We profiled the miRNome in exhaled breath condensate (EBC) and plasma samples from fourteen patients affected by lung AdCa, nine healthy subjects. miRNA signatures were then analyzed in another neoplasia of the respiratory district, i.e. pleural mesothelioma (n = 23) and subjects previously exposed to asbestos were used as controls for this cohort (n = 19). Selected miRNAs were analyzed in purified pulmonary neoplastic or normal epithelial and stromal cell subpopulation from AdCa patients. Finally, the plasmatic miRNA signature was analyzed in a publicly available cohort of NSCLC patients for data validation and *in silico* analysis was performed with predicted miRNA targets using the multiMiR tool and STRING database.

Results: miR-597-5p and miR-1260a are significantly over-expressed in EBC from lung AdCa and are associated with AdCa. Similarly, miR-1260a is also up-regulated in the plasma of AdCa patients together with miR-518f-3p and correlates with presence of lung cancer, whereas let-7f-5p is under-expressed. Analysis of these circulating miRNAs in pleural mesothelioma cases confirmed that up-regulation of miR-518f-3p, -597-5p and -1260a, is specific for lung AdCa. Lastly, quantification of the miRNAs in laser-assisted microdissected lung tissues revealed that miR-518f-3p, 597-5p and miR-1260a are predominantly expressed in tumor epithelial cells. Validation analysis confirmed miR-518f-3p as a possible circulating biomarker of NSCLC. *In silico* analysis of the potentially

OPEN ACCESS

Edited by:
Ferdinando Cerciello, Bern University Hospital, Switzerland

Reviewed by:
Ilaria Cavallari, Veneto Institute of Oncology (IRCCS), Italy
Jelena Kresoja-Rakic, University of Colorado Anschutz Medical Campus, United States

****Correspondence:***
Alessandro Palleschi
alessandro.palleschi@unimi.it
Valentina Vaira
valentina.vaira@unimi.it

[†]These authors have contributed equally to this work

Specialty section:
This article was submitted to Thoracic Oncology, a section of the journal Frontiers in Oncology

Received: *06 January 2021*
Accepted: *27 May 2021*
Published: *15 June 2021*

Citation:
Faversani A, Favero C, Dioni L, Pesatori AC, Bollati V, Montoli M, Musso V, Terrasi A, Fusco N, Nosotti M, Vaira V and Palleschi A (2021) An EBC/Plasma miRNA Signature Discriminates Lung Adenocarcinomas From Pleural Mesothelioma and Healthy Controls. Front. Oncol. 11:643280. doi: 10.3389/fonc.2021.643280

modulated biological processes by these three miRNAs, shows that tumor bioenergetics are the most affected pathways.

Conclusions: Overall, our data suggest a 3-miRNAs signature as a non-invasive and accurate biomarker of lung AdCa. This approach could supplement the current screening approaches for early lung cancer diagnosis.

Keywords: microRNA, lung cancer, malignant pleural mesothelioma, exhaled breath condensate, liquid biopsy, volatile biopsy

INTRODUCTION

Neoplasia of the respiratory district is among the leading cause of tumor related death worldwide. Among those are lung cancer and pleural mesothelioma, two diseases whose risk is further increased by environmental and occupational exposure to carcinogens, such as asbestos (1–3). Screening programs for such neoplasia are currently based on low-dose computed tomography (LDCT). The NELSON trial showed that the use of LDCT for lung cancer screening reduced lung cancer mortality of about 26% in men and 39–61% in women (4). Nevertheless, shared guidelines for nodules assessment and interpretation are still to be optimized to reduce the false-positive rate, limit the number of invasive procedures for benign disease and to avoid overtreatment of precancerous lesions (1, 3). Lastly, LDCT screening has important economical clues for National Health systems, and a selection of patients who might benefit more by LDCT is warranted (3).

Among lung cancers, the lung adenocarcinoma histotype represents the most frequent type of Non-Small Cell Lung Cancer (NSCLC) and it is characterized by a poor prognosis. In particular, patients affected by NSCLC have a 5-year predicted survival expectancy of 15.9% and a high recurrence rate (5). Despite advances in the field of tailored medical therapy in metastatic disease, an approach in the early stages is still the cornerstone of lung cancer treatment. Therefore, early diagnosis remains the most effective approach to detect the disease at an earlier, asymptomatic, and potentially curable stage. Similarly, although risk factors of MPM are well known, the current standard for MPM diagnosis relies on pleural biopsies.

In this scenario, the addition of non-invasive biomarkers to thoracic cancer screening protocols could reduce overtreatment rate and improve the eligibility selection for LDCT screening, overall reducing patients stress and sanitary costs. Further, biomarkers could support the clinical algorithm also in discriminating among different cancer types (3, 6). More efforts are needed to identify new molecular biomarkers to complement early NSCLC and MPM diagnosis by non-invasive techniques.

Abbreviations: A, alveoli; AdCa, Lung Adenocarcinonma; BMI, Body Mass Index; B, Bronchial epithelium; DECCS, Disposable Exhaled Condensate Collection System; EBC, Exhaled Breath Condensate; EV, Extracellular Vesicles; FC, Fold Change; FDR, False Discovery Rate; FFPE, Formalin-Fixed and Paraffin Embedded; miRNA, microRNA; NSCLC, Non-Small Cell Lung Cancer; RT, Reverse Transcription; TBC, Tubercolosis; T, Tumor Epithelium; Ts, Tumor Stroma.

microRNAs (miRNAs) are small non coding RNAs which regulate the translation of their targets mRNAs. miRNAs are involved in numerous physiological and pathological cellular processes (7); in particular, miRNAs participate in cancer progression with an oncogenic or tumor suppressor role (7). Further, miRNAs can be detected in normal and tumor tissues, but also in biological fluids such as serum and plasma (8), through their secretion *via* exosomes or as Ago2 protein complexes (9), where they can act as extracellular messengers. In this context, different studies showed the importance of miRNAs as circulating biomarkers in lung cancer and their use for liquid biopsy (10, 11).

Previously, we showed that two extracellular vesicles (EV)-associated plasmatic miRNAs distinguish patients with malignant pleural mesothelioma from cancer-free subjects previously exposed to asbestos (12) and that avatar mice of NSCLC retain tissue-specific and circulating miRNAs signatures of the primary tumor (13). Recently, it has been suggested that exhaled breath condensate (EBC)-miRNAs, the so-called volatile biopsy, could represent novel, non-invasive reliable biomarkers of respiratory diseases (14, 15), including lung cancer (16).

In this study, we aimed to identify miRNA signatures useful for lung cancer screening using minimally invasive procedures, such as EBC and plasma collection. To this end, we analyzed the EV-associated miRNome in EBC and plasma derived both from patients affected by NSCLC and healthy control subjects. Furthermore, we compared these signatures to the ones associated with malignant pleural mesothelioma to provide preliminary clues about the potential of circulating miRNA as a tool for diseases discrimination.

MATERIALS AND METHODS

Patients

From 2015 to 2016, we prospectively recruited a consecutive series of patients with early stage, i.e. stages I–II, AdCa and scheduled for pulmonary lobectomy at the Fondazione IRCCS Ca' Granda—Ospedale Maggiore Policlinico. Inclusion criteria were sex male, age ≥50 years, current or former smokers, ability to tolerate general anesthesia and cardiopulmonary reserve to tolerate a lobectomy. Exclusion criteria were previous thoracic surgery or previous personal history of any cancer. Fourteen patients were included in the study (**Figure 1**). After the usual clinical and disease-specific preoperative assessment, patients underwent pulmonary lobectomy and systematic lymphadenectomy. Preoperative clinical data and

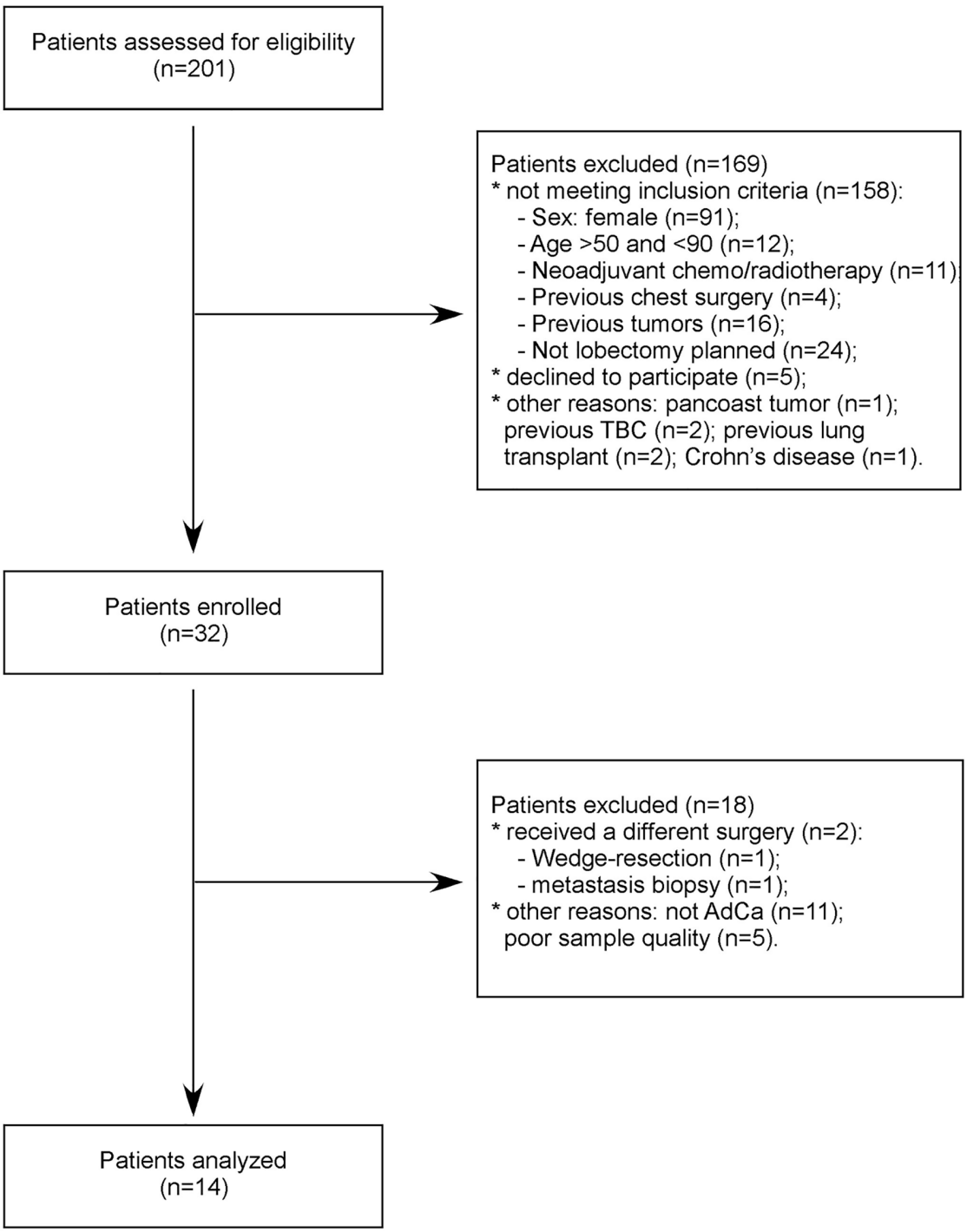

FIGURE 1 | Patients' selection flowchart.

postoperative histological report were recorded, anonymously, in a dedicated database (**Table 1**). One week before surgery, we collected EBC and plasma samples from all patients. As cancer-free controls, we collected EBC and plasma samples from nine age- and gender-matched voluntary subjects (**Supplementary Table 1**).

The protocol was approved by the Ethics local Committee of Fondazione IRCCS Ca' Granda-Ospedale Maggiore Policlinico, Milan, Italy (approval number: 879bis/11.12.2014) and was performed in agreement with the Helsinki Declaration. Informed consent was signed by each participant.

TABLE 1 | Clinicopathological features of the 14 patients affected by AdCa.

Sample	Sex	Age	Histotype	TNM[1]	Smoke[2]
AdCa1	M	77	Adenocarcinoma	T1bN0	Previous
AdCa2	M	63	Adenocarcinoma	T1aN2	Yes
AdCa4	M	79	Adenocarcinoma	T2aN2	Previous
AdCa6	M	59	Adenocarcinoma	T2aN1	Previous
AdCa7	M	79	Adenocarcinoma	T2aN1	Previous
AdCa8	M	66	Adenocarcinoma	T2aN2	Previous
AdCa9	M	67	Adenocarcinoma	T1bN0	Yes
AdCa11	M	68	Adenocarcinoma	T2aN0	Previous
AdCa12	M	73	Adenocarcinoma	T1bN2	Previous
AdCa14	M	57	Adenocarcinoma	T2bN0	Previous
AdCa15	M	71	Adenocarcinoma	T2N2	Previous
AdCa16	M	65	Adenocarcinoma	T1aN0	Yes
AdCa18	M	80	Adenocarcinoma	T1bN0	Previous
AdCa19	M	71	Adenocarcinoma	T1aN0	Previous

[1]*All patients were M0 at surgery (i.e. no distant metastasis were present at the diagnosis).*
[2]*The term previous, refers to at least 6 months before surgery.*

EBC- and plasmatic-miRNA profiles were also available for the previously described malignant pleural mesothelioma series (MPM; n = 23) and corresponding control subjects (asbestos-exposed, cancer-free individuals; n = 19) (12). For data validation we used a publicly available dataset of early stage NSCLCs and controls (GSE64591) annotated for gender, age and smoking habit (17). To remain strict to our study design, only males were included in the analysis. Accordingly, 86 NSCLCs and 71 controls were available.

EBC and Blood Collection

Samples from each study participant included: I) EBC, collected and processed according to American Thoracic Society/European Respiratory Society recommendations (18), using the DECCS (Disposable Exhaled Condensate Collection System) through a transportable unit for use in research (Medivac—Parma, Italy) as previously described (19, 20); II) About 7.5 ml blood sample, collected in EDTA Vacutainer tubes (Becton Dickinson, Franklin Lakes, NJ, USA) that was centrifuged within 3 h from collection at 1,200*g* for 15 min to separate the plasma fraction from the blood cells.

Tissue Microdissection and RNA Isolation

Tumor epithelium (TE), tumor-associated stroma (TS), non-neoplastic bronchial epithelium (BE) and alveolar parenchyma (A) were obtained by laser-assisted microdissection (Leica Microsystems, Milan, Italy) from formalin-fixed and paraffin embedded (FFPE) cancer and normal lung tissues of the enrolled patients (**Table 1**). Microdissection was performed as already described (21). Then, total RNA was isolated using the MasterPure RNA Purification Kit (Epicentre Biotechnologies, Madison, WI, USA) according to the supplier's protocol. To assess quality and quantity, all samples were analyzed by a 2100 Bioanalyzer (Agilent Technologies, Santa Clara, CA) using the Agilent RNA 6000 Pico Kit.

Extracellular Vesicles (EV) and miRNA Isolation

After collection, EBC and plasma samples were centrifuged three times at increasing speeds (1,000*g*, 2,000*g*, 3,000*g*) for 15 min at 4°C to remove cell debris and aggregates. Then, supernatants were ultracentrifuged using the BeckmanCoulter Optima-MAX-XP centrifuge (Beckman Coulter Life Sciences, Indianapolis, IN, USA) at 110,000×*g* for 75 min at 4°C and decanted. The EV pellet was kept at −80°C until use. miRNAs were isolated with the miRNeasy purification kit and the Rneasy MiniEluite spin column (all from Qiagen Hilden, Germany) to enrich for the miRNAs fraction, as suggested by the manufacturer. Finally, miRNAs were eluted in a final elution volume of 20 µl and stored at −80°C until processed for expression analysis.

EV-miRNAs Profiling

Reverse transcription (RT) was performed using Megaplex RT Primers, Pool A v2.1 and Pool B v3.0, with the TaqMan Micro RNA Reverse Transcriptase Kit (Thermo Fisher Scientific, Waltham, MA, USA) in a C1000 Thermal Cycler (Biorad, Hercules, CA, USA) as previously described (22). Then, converted miRNAs were pre-amplified before being analyzed using the TaqMan OpenArray Human miRNA Panel, with QuantStudio AccuFill System Robot and the QuantStudio 12K Flex Real-Time PCR System (Thermo Fisher Scientific). This platform contains 754 unique miRNAs and four internal controls (ath-miR159a, RNU48, RNU44 and U6). miRNAs with a threshold cycle (Ct) value >28, an AmpScore <1.24, or undetectable were considered not amplified and their Ct value was set to 29. Further, miRNAs that were not detected in all plasma or EBC samples (n = 438 and 590, respectively) were excluded from the analysis. Accordingly, 316 and 164 miRNAs were available for plasma or EBC study. The NormFinder (23) algorithm was applied to choose the best normalization strategy. The global mean, was selected as the best normalization method for data normalization and miRNA quantification in EBC and plasma samples and the miRNA expression was quantified using the relative quantification $2^{-\Delta\Delta Ct}$ formula (24).

Confirmation of miRNAs Expression by Individual qPCR

The top 11 miRNAs identified as associated with AdCa were validated in plasma and in tissue samples by qPCR performed in

triplicate using a custom primers pool. The U6 snRNA assay was added for data normalization. All reagents and instrument were from Thermo Fisher Scientifics. For this analysis, miRNAs with a Ct value >38, an AmpScore <1.1 were considered undetectable and their Ct value was set to 40. miRNA expression was quantified using the relative quantification $2^{-\Delta\Delta Ct}$ (24).

Statistical Analysis

Descriptive statistics were performed on all variables. Data are expressed as means ± SD or frequencies, as appropriate. To compare characteristics of the study patients by cases and controls we performed the chi-square test for categorical variables or the independent two-sample t-test for continuous variables. The mean value for each miRNA was calculated for AdCa and control groups and their ratio was used to obtain the Fold Change (FC). Then, miRNA expression values were log2 transformed to satisfy the linearity assumption. For each miRNA a logistic regression model adjusted for age, BMI (Body Mass Index) and smoking habits was run to assess miRNA discrimination between case and controls. The Odds Ratios (OR) were corrected for age, smoke and BMI and the standard error (SE) was computed as well. Due to the high number of comparisons, we applied a multiple comparison correction method based on the Benjamini–Hochberg False Discovery Rate (FDR) to calculate the FDR-adjusted p-value (p-FDR). In the screening analysis, a miRNA was considered to be differentially expressed if the p-value was <0.05, p-FDR was <0.25 and FC was <0.5 or >2. In the validation phase, miRNAs with raw p-value <0.05 were considered differentially expressed. To investigate the relationship between miRNA expression levels and type of tissues (A, BE, TE, TS) we performed linear mixed models for paired data. Analyses were performed using SAS 9.4 (SAS Institute, Cary, NC). To analyze EBC and plasma miRNAs levels in another type of cancer of the respiratory district, i.e. pleural mesothelioma, we used an already published dataset (12). Clustering analyses were performed either using the using the ComplexHeatmap package available within Bioconductor (https://bioconductor.org/packages/release/bioc/html/ComplexHeatmap.html) or the Heatmap tool available within GraphPad Prism software (Prism, La Jolla, CA, USA), as specified in each figure legend.

miRNA targets analysis was conducted using the multiMiR R package release 3.12 available within Bioconductor (http://multimir.ucdenver.edu), considering targets predicted by at least two algorithms. Then, predicted targets were imported in STRING and Gene Ontology analysis was performed to identify enriched Biological processes. The genome was used as background.

RESULTS

miRNAs Analysis in EBC and Plasma Samples Revealed a Distinctive miRNAs Expression Profile in AdCa Patients Compared to Healthy Subjects

We started the analyses profiling 754 miRNAs in the EBC derived from the lung cohort. To limit the biological variability of circulating miRNA signatures, lung cancer patients included in this study were selected following stringent criteria (**Figure 1**). Indeed patients had to be males, between the ages of 55 and 90, current or former smokers and affected by a non-metastatic lung adenocarcinoma. Following these criteria, we enrolled a homogeneous group of 14 AdCa patients. Similarly, control subjects (n = 9) were sex-, age- and habits-matched with cases. For two AdCa subjects, EBC-miRNAs could not be analyzed because of poor RNA quality.

One hundred and sixty-four (22%) miRNAs resulted expressed in at least one sample. When we performed an unsupervised hierarchical clustering, miRNAs expression levels showed a distinctive signature in patients compared to controls (**Supplementary Figure 1A**). In particular, miR-597-5p and miR-1260a were over-expressed in patients compared to healthy subjects (FC = 2.4 and 9.9, respectively; **Figure 2A**) and their levels were significantly associated with lung cancer (OR = 1.31, SE = 0.11, p = 0.019 and OR = 1.1, SE = 0.02, p = 0.031, for miR-597-5p and miR-1260a respectively; **Figure 2B**).

The same analysis was performed for the plasma samples. This time, 316 miRNAs (42%) were expressed in at least one sample (**Supplementary Figure 1B**), of which twelve miRNAs (miR-15a-5p, -34a-3p, -126-3p, -130b-3p, -135a-5p, -193b-3p, -195-5p, -342-3p, -345-5p, -362-5p, let-7e-5p and let-7f-5p) showed at least 2-fold down-regulation, whereas miR-302b-3p, -518f-3p and -1260a were at least 4-folds up-regulated in patients compared to healthy subjects (**Figure 2C**). Lastly, 23 plasma-miRNAs were significantly associated with lung cancer presence (**Figure 2D**).

At validation, we could confirm a significant deregulation of plasmatic miR-130b-3p, miR-302b-3p and miR-518f-3p in patients compared to controls (**Table 2**). A trend for let-7f-5p, miR-345-5p, and miR-362-5p under-expression in AdCa compared with controls could be detected along with up-regulation of miR-1260a (**Table 2**). No miRNAs was associated with patients' clinicopatological features, including tumor size or nodal metastasis.

Overall, from this miRNA screening we could detect that miR-1260a was significantly higher in patients compared with healthy controls both in EBC and plasma analyses, suggesting that it could be a circulating biomarker of lung AdCa.

miRNAs Analysis in Tumor and Normal Lung Tissues Components

In order to investigate the origin of the most relevant miRNAs deregulated in plasma and EBC of AdCa patients, we isolated by laser-microdissection different tumor cellular compartments, namely tumor epithelial cells (T) and tumor-associated stroma (Ts), as well as normal lung tissues, namely bronchial epithelium (B) and alveoli (A; **Supplementary Figure 2**) from archival blocks of our patients' series. Then, we analyzed the expression levels of the ten miRNAs (miR-130b-3p, -135a-5p, -302b-3p, -342-3p, -345-5p, -362-5p, -518f-3p, -597-5p, -1260a and let-7f-5p) in the microdissected tissues. This analysis highlighted distinctive miRNA profiles in the different tissues (**Figure 3A**). In line with the miRNA screening, the tumor suppressor miRNA

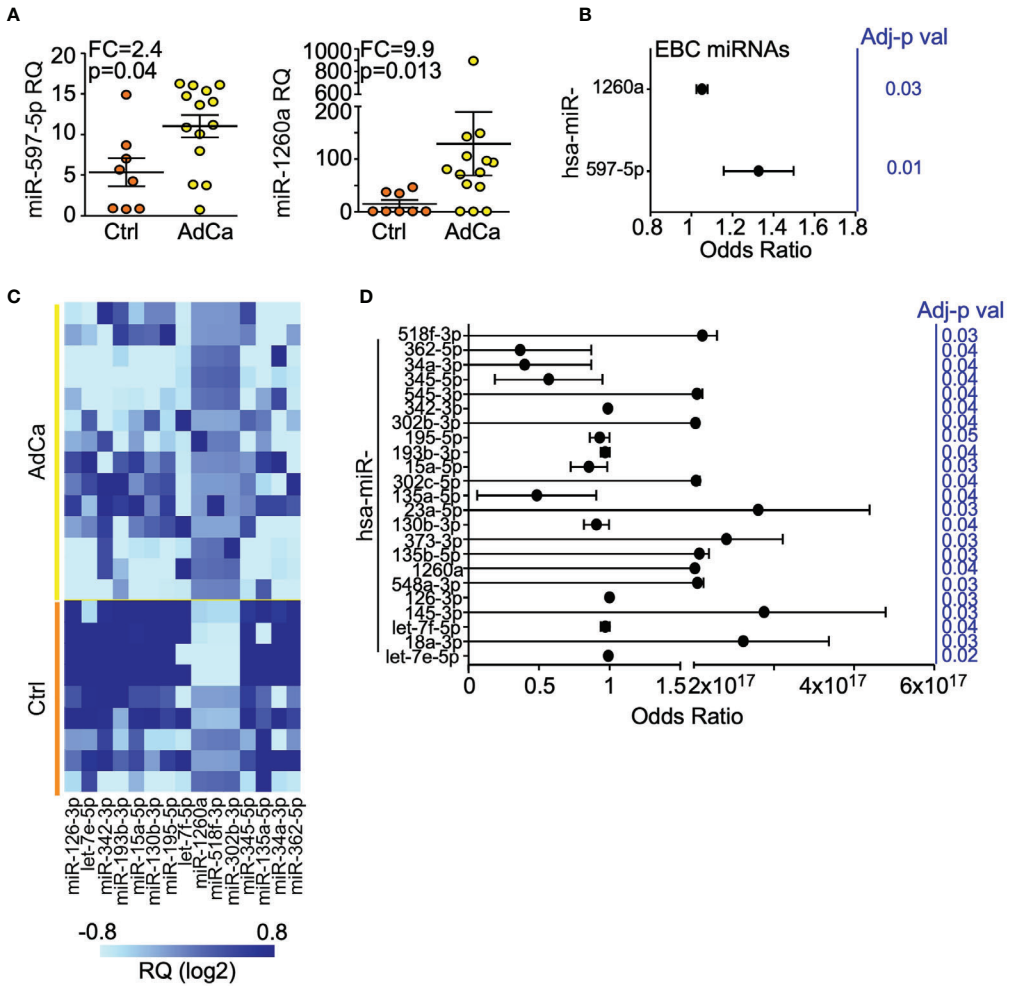

FIGURE 2 | miRNAs expression profile in EBC and plasma from AdCa patients and healthy controls. **(A)** miR-597-5p and miR-1260a expression levels in the EBC of patients with AdCa or healthy controls (Ctrl). Each dot is a case; lines, mean with interquartile range; FDR-adjusted *p* val <0.25; FC, fold-change; RQ, relative quantity. **(B)** Diagnostic value of EBC-miRNAs in identifying subjects with lung AdCa. Forest plot showing the odds ratio for the EBC miRNA miR-597-5p and miR-1260a. Bars, 95% confidence interval. Odds Ratio was adjusted for age, smoke and BMI; *p* values are from logistic regression analysis. **(C)** Heatmap of the plasma miRNAs differentially expressed (FC >2; FDR-adjusted p val <0.25) between AdCa patients and control (Ctrl) subjects. The heatmap was generated with GraphPad Prism software. **(D)** Diagnostic value of plasma-miRNAs in identifying subjects with lung AdCa. Forest plot showing the odds ratio for the indicated plasma miRNAs. Bars, 95% confidence interval. Odds Ratio was adjusted for age, smoke and BMI; *p* values are from logistic regression analysis; FC, fold change.

TABLE 2 | Validation analysis: the expression level and odds ratio (OR) of the plasmatic miRNAs is reported[3].

miRNA	CTRL (RQ mean)	AdCa (RQ mean)	OR	SE	P value
hsa-let-7f-5p	11.7	7.5	0.301	0.591	0.04
hsa-miR-130b-3p	6.7	2.3	0.410	0.430	0.03
hsa-miR-135a-5p	0.1	0.1	0.649	0.288	0.13
hsa-miR-302b-3p	1.07×10^{-5}	3.40×10^{-5}	2.849	0.595	0.08
hsa-miR-342-3p	292.2	359.7	0.561	0.519	0.26
hsa-miR-345-5p	4.4	3.0	0.406	0.488	0.06
hsa-miR-362-5p	0.5	0.3	0.390	0.487	0.05
hsa-miR-518f-3p	0.006	0.07	1.030	0.085	0.73
hsa-miR-597-5p	0.086	0.01	0.852	0.092	0.08
hsa-miR-1260a	8.2	13.8	1.615	0.644	0.46

[3]*OR was adjusted for age, smoking and body mass index (BMI). P values refer to the OR estimation using a linear regression model.*

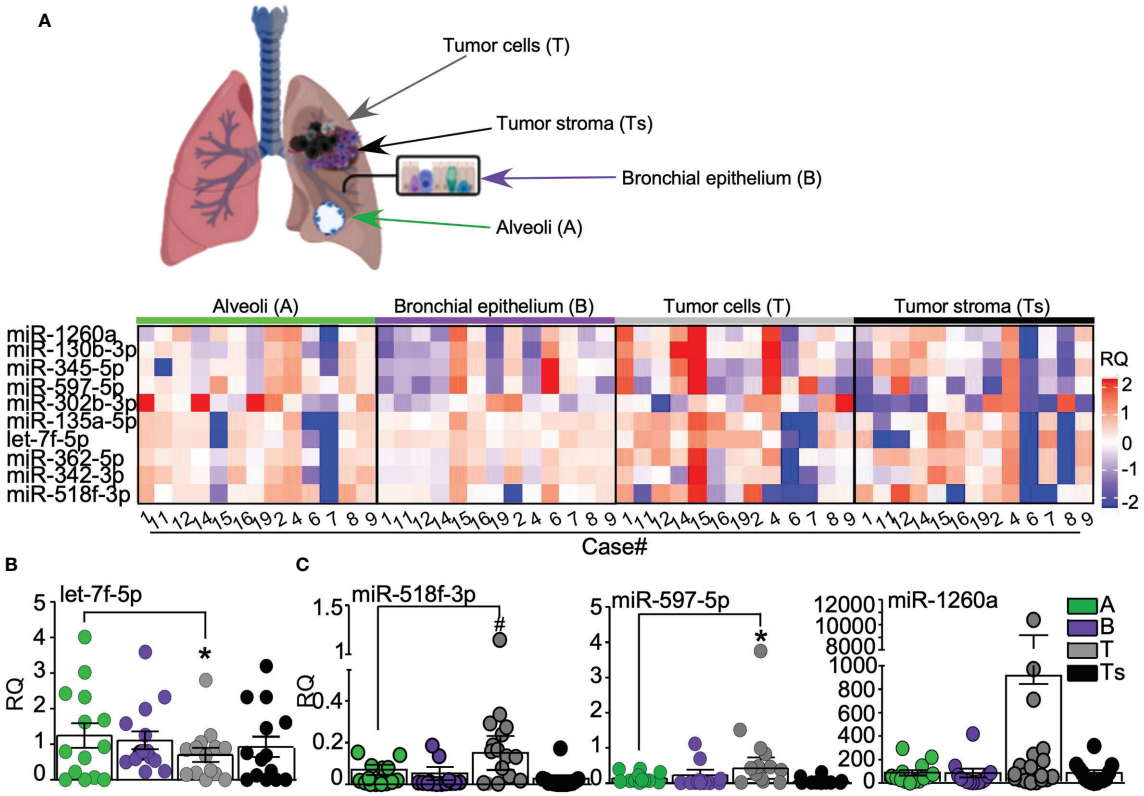

FIGURE 3 | miRNAs validation analysis. **(A)** Normal bronchial epithelium (B), alveoli (A) as well as lung tumor cells (T) and tumor-surrounding stroma (Ts) were laser-assisted microdissected from surgical specimens of 13 out of the 14 AdCa patients. Heatmap (generated with ComplexHeatmap package) shows the expression levels of the ten selected miRNAs in each case. *Upper panel*, representative images of the analyzed tissues. **(B, C)** The expression of the differentially regulated miRNAs in tumor cells is shown, with miRNA let-7f-5p being down regulated **(B)**, while miR-518f-3p, miR-597-5p, and miR-1260a **(C)** being up-regulated in lung tumor cells. Each dot is a sample; bars, mean ± SD. *p = 0.04, #p = 0.03 by Mann–Whitney U test.

let-7f-5p showed higher expression in normal tissues than in tumors (**Figure 3B**), whereas miR-518f-3p, miR-597-5p and -1260a, all up-regulated in plasma and EBC of AdCa, were more abundantly expressed in tumor cells than in the surrounding stroma or normal tissues (**Figure 3C**).

This experiment suggests the cell of origin of the differentially expressed miRNAs, and supports the concept that miR-1260a, miR-518f-3p and miR-597-5p could act as onco-miR in lung cancer environments.

Analysis of the Circulating miRNAs Signature in an Independent Series of Lung AdCa and in Patients Affected by Malignant Pleural Mesothelioma

To confirm if the identified plasmatic miRNA signature could be relevant and useful to identify male patients with lung adenocarcinoma, we used a publicly available dataset with annotated clinical information and miRNA profiles (17). From this analysis, we could identify that the plasmatic miRNAs, let-7f-5p and miR-518f-3p showed a trend in identifying patients with lung AdCa (**Supplementary Table 2**), as we found in the discovery phase.

To investigate whether our miRNA signature was specific for lung adenocarcinomas, we investigated the levels of the ten miRNAs in the EBC and plasma of the malignant pleural mesothelioma cohort (12). Neither miR-1260a, nor miR518f-3p or miR-597-5p was modulated in the EBC of the MPM patients with respect to control individuals (**Figure 4A** and **Supplementary Figure 3**). On the contrary, when we analyzed plasmatic miRNAs (**Figure 4B**), let-7f-5p levels were significantly down-regulated in the circulation of MPM patients compared to controls (**Figure 4C**), similarly to what observed for the lung AdCa cohort.

Therefore, we could conclude that the 3-miRNAs signature composed by miR-1260a, miR-597-5p and miR-518f-3p, could be specific for lung AdCa disease, whereas let-7f-5p decrease characterizes also other neoplasia of the respiratory district such as malignant pleural mesothelioma.

miRNAs Targets Analysis

In an attempt to preliminary speculate on potential signaling affected by the identified AdCa-upregulated miRNAs, namely miR-518f-3p, -597-5p, and miR-1260a, we performed an *in silico* analysis of predicted targets and potentially affected pathways. This

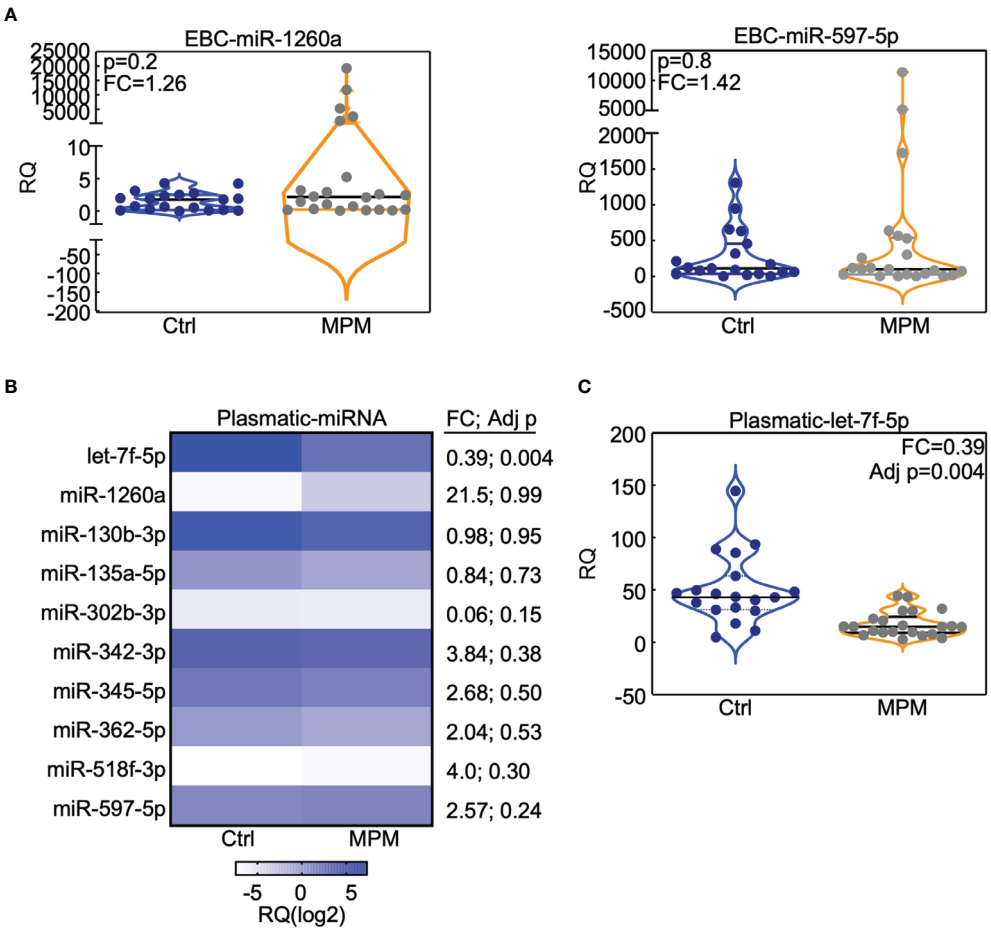

FIGURE 4 | miRNAs analysis in the MPM cohort. The indicated miRNAs were analyzed in the EBC **(A)** or in the plasma **(B, C)** obtained from 23 MPMs and 19 cancer-free subjects who were previously exposed to asbestos (Ctrl). **(B)** Heatmap (generated with GraphPad Prism software) indicates the expression level of the indicated plasmatic miRNA in MPM or control subjects. **(A, C)** Data are presented with violin plots where each case is a dot and lines indicate median with interquartile range. RQ, Relative quantity; FC, fold change; Adj p, FDR-adjusted p value.

analysis showed that tumor bioenergetics was the most affected signaling by the 3-miRNAs signature (**Supplementary Tables 3**, **4**). This analysis, although *in silico*, suggests that circulating onco-miRNAs might alter cell metabolism participating in promoting a pro-tumorigenic environment also in the lung.

DISCUSSION

Our study investigated the expression of 754 miRNAs in EBC and plasma samples of patients affected by AdCa and healthy control subjects. Both the EBC and plasma-miRNAs analyses highlighted a distinctive expression profile in patients compared to healthy subjects. In particular, miR-597-5p and -1260a were up-regulated in EBC of patients compared to controls and were associated with lung cancer presence. Interestingly, miR-1260a was upregulated also in the plasma of AdCa patients compared with controls.

The four miRNAs (let-7f-5p, miR-518f-3p, -597-5p and -1260a) signature resulted particularly interesting to discriminate patients affected by AdCa. Further, decreased le-7f-5p and increased miR-518f-3p levels were marginally associated to lung cancer in an independent series of male subjects (17). To test the specificity of this signature in identifying lung cancer patients, we analyzed circulating miRNAs in a second neoplasia of the respiratory district, namely the malignant pleural mesothelioma. This analysis showed that the onco-suppressor miRNA let-7f-5p was decreased also in the circulation of mesothelioma patients, highlighting the broad repression of this miRNA in different cancer settings. Indeed, members of the let-7 miRNAs family have been found down-regulated in different types of tumors targeting several oncogenes such as Ras, HMGA2 and cMyc (25).

On the other hand, miR-518f-3p, miR-597 and miR-1260 levels were unchanged in the plasma of mesothelioma patients compared with controls, and therefore, their up-regulation was specific for lung AdCa (**Figure 5**).

Further, we could document that these miRNAs are predominantly expressed by tumor epithelial cells and not by the stromal microenvironment. In line with its onco-suppressor role,

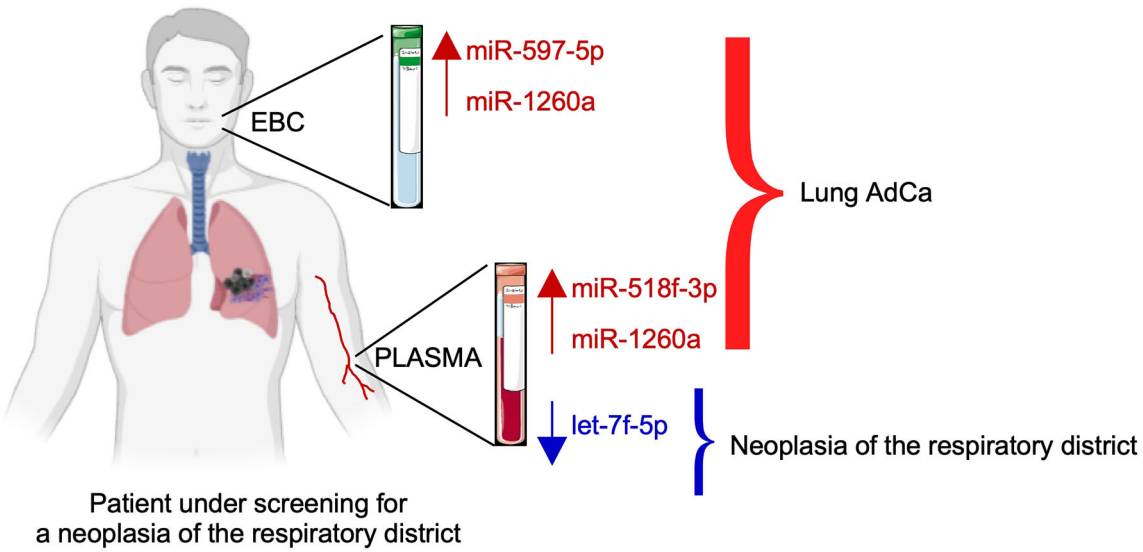

FIGURE 5 | Schematic of the proposed model of the three-miRNAs signature as an adjunct tool to screen subjects for lung cancer presence.

let-7f-5p was more expressed in normal alveolar cells than in the tumor compartments.

Finally, *in silico* analysis showed that these miRNAs target several transcripts involved in tumor bioenergetics. Data from literature, document that miR-1260 is correlated with poor prognosis in breast cancer (26) and in neuroblastoma (27), whereas miR-518f belongs to the oncogenic C19MC miRNA cluster (28).

A limitation of our study is the small number of patients enrolled. In order to reduce biological variability and to improve the results accuracy, we applied stringent criteria for patients' selection. On the other hand, we profiled two types of circulating miRNAs (EBC and plasma), and we verified the signatures in another cancer of the respiratory district, i.e. pleural mesothelioma to firstly provide a preliminary snapshot of non-invasive biomarkers of thoracic cancers that could implement differential diagnosis besides early detection.

The identification of biomarkers able to recognize the presence of lung cancer using non-invasive methods in addition to imaging analysis is one of the cancer research goals. Different studies have been focused on the detection of miRNAs in biological fluids, because the liquid biopsy is a valid, minimal-invasive method to explore pathological biomarkers (10, 11, 16, 29, 30). Several studies highlighted the potentiality of miRNAs detection in plasma, but few works investigated miRNAs in EBC (16, 30). EBC collection is a non-invasive and reproducible procedure which allows the analysis of molecules derived from lungs and lower respiratory tract (16, 30). Recently, a study reported that elevated miR-21 expression together with decreased miR-486 in EBC and plasma discriminates NSCLC patients from healthy subjects (16). This indicates that circulating miRNAs may have a diagnostic value and may serve as early non-invasive biomarkers in adjunct to the current screening methods. Nevertheless, to eventually confirm the use of miRNA as non-invasive biomarkers of lung AdCa or MPM in addition to LDCT in the clinical setting, larger cohort of patients are needed together with prospective studies on pre-diagnostic samples from longitudinally followed cohorts of at-risk subjects.

Altogether, our results and the recent literature support the use of the volatile biopsy as a reliable method to identify biomarkers useful in the clinical settings and propose a combined plasma/EBC 3-miRNAs signature to implement the screening protocols for cancers of the respiratory district.

DATA AVAILABILITY STATEMENT

The raw data supporting the conclusions of this article will be made available by the authors, without undue reservation.

ETHICS STATEMENT

The studies involving human participants were reviewed and approved by the Ethics Committee of Fondazione IRCCS Ca' Granda-Ospedale Maggiore Policlinico, Milan, Italy (approval number: 879bis/11.12.2014). The patients/participants provided their written informed consent to participate in this study.

AUTHOR CONTRIBUTIONS

MM, VM, MN, and ACP—patient selection. AF, CF, VB, VV, and AP—conceptualization and methodology. AF, CF, LD, AT, VM, NF, and MM—investigation. VM, MM, ACP, VB, and MN—data curation. AT, MM, ACP, CF, and NF—data analysis and interpretation. AF, NF, VV, and AP—manuscript drafting. VV and AP—manuscript finalization. All authors contributed to the article and approved the submitted version.

FUNDING

This work was supported by the Italian Minister of Health to VV (GR2011-02351626) and by Fondazione IRCCS Ca' Granda Project Competition program 2015/16 to AP.

SUPPLEMENTARY MATERIAL

The Supplementary Material for this article can be found online at: https://www.frontiersin.org/articles/10.3389/fonc.2021.643280/full#supplementary-material

REFERENCES

1. Tiitola M, Kivisaari L, Huuskonen MS, Mattson K, Koskinen H, Lehtola H, et al. Computed Tomography Screening for Lung Cancer in Asbestos-Exposed Workers. *Lung Cancer* (2002) 35(1):17–22. doi: 10.1016/s0169-5002(01)00294-x
2. Maisonneuve P, Rampinelli C, Bertolotti R, Misotti A, Lococo F, Casiraghi M, et al. Low-Dose Computed Tomography Screening for Lung Cancer in People With Workplace Exposure to Asbestos. *Lung Cancer* (2019) 131:23–30. doi: 10.1016/j.lungcan.2019.03.003
3. Veronesi G, Baldwin DR, Henschke CI, Ghislandi S, Iavicoli S, Oudkerk M, et al. Recommendations for Implementing Lung Cancer Screening With Low-Dose Computed Tomography in Europe. *Cancers (Basel)* (2020) 12(6):1672. doi: 10.3390/cancers12061672
4. de Koning HJ, van der Aalst CM, de Jong PA, Scholten ET, Nackaerts K, Heuvelmans MA, et al. Reduced Lung-Cancer Mortality With Volume CT Screening in a Randomized Trial. *N Engl J Med* (2020) 382(6):503–13. doi: 10.1056/NEJMoa1911793
5. Zappa C, Mousa SA. Non-Small Cell Lung Cancer: Current Treatment and Future Advances. *Transl Lung Cancer Res* (2016) 5(3):288–300. doi: 10.21037/tlcr.2016.06.07
6. Peled N, Hakim M, Bunn PAJr, Miller YE, Kennedy TC, Mattei J, et al. Non-Invasive Breath Analysis of Pulmonary Nodules. *J Thorac Oncol* (2012) 7 (10):1528–33. doi: 10.1097/JTO.0b013e3182637d5f
7. Peng Y, Croce CM. The Role of MicroRNAs in Human Cancer. *Signal Transduct Target Ther* (2016) 1:15004. doi: 10.1038/sigtrans.2015.4
8. Boeri M, Verri C, Conte D, Roz L, Modena P, Facchinetti F, et al. MicroRNA Signatures in Tissues and Plasma Predict Development and Prognosis of Computed Tomography Detected Lung Cancer. *Proc Natl Acad Sci USA* (2011) 108(9):3713–8. doi: 10.1073/pnas.1100048108
9. Arroyo JD, Chevillet JR, Kroh EM, Ruf IK, Pritchard CC, Gibson DF, et al. Argonaute2 Complexes Carry a Population of Circulating microRNAs Independent of Vesicles in Human Plasma. *Proc Natl Acad Sci USA* (2011) 108(12):5003–8. doi: 10.1073/pnas.1019055108
10. Sozzi G, Boeri M, Rossi M, Verri C, Suatoni P, Bravi F, et al. Clinical Utility of a Plasma-Based miRNA Signature Classifier Within Computed Tomography Lung Cancer Screening: A Correlative MILD Trial Study. *J Clin Oncol* (2014) 32(8):768–73. doi: 10.1200/JCO.2013.50.4357
11. Sestini S, Boeri M, Marchiano A, Pelosi G, Galeone C, Verri C, et al. Circulating microRNA Signature as Liquid-Biopsy to Monitor Lung Cancer in Low-Dose Computed Tomography Screening. *Oncotarget* (2015) 6 (32):32868–77. doi: 10.18632/oncotarget.5210
12. Cavalleri T, Angelici L, Favero C, Dioni L, Mensi C, Bareggi C, et al. Plasmatic Extracellular Vesicle microRNAs in Malignant Pleural Mesothelioma and Asbestos-Exposed Subjects Suggest a 2-miRNA Signature as Potential Biomarker of Disease. *PLoS One* (2017) 12(5):e0176680. doi: 10.1371/journal.pone.0176680
13. Russo MV, Faversani A, Gatti S, Ricca D, Del Gobbo A, Ferrero S, et al. A New Mouse Avatar Model of Non-Small Cell Lung Cancer. *Front Oncol* (2015) 5:52. doi: 10.3389/fonc.2015.00052
14. Maniscalco M, Fuschillo S, Paris D, Cutignano A, Sanduzzi A, Motta A, et al. Clinical Metabolomics of Exhaled Breath Condensate in Chronic Respiratory Diseases. *Adv Clin Chem* (2019) 88:121–49. doi: 10.1016/bs.acc.2018.10.002
15. Fesen K, Silveyra P, Fuentes N, Nicoleau M, Rivera L, Kitch D, et al. The Role of microRNAs in Chronic Pseudomonas Lung Infection in Cystic Fibrosis. *Respir Med* (2019) 151:133–8. doi: 10.1016/j.rmed.2019.04.012
16. Mozzoni P, Banda I, Goldoni M, Corradi M, Tiseo M, Acampa O, et al. Plasma and EBC microRNAs as Early Biomarkers of Non-Small-Cell Lung Cancer. *Biomarkers* (2013) 18(8):679–86. doi: 10.3109/1354750X.2013.845610
17. Wozniak MB, Scelo G, Muller DC, Mukeria A, Zaridze D, Brennan P, et al. Circulating MicroRNAs as Non-Invasive Biomarkers for Early Detection of Non-Small-Cell Lung Cancer. *PLoS One* (2015) 10(5):e0125026. doi: 10.1371/journal.pone.0125026
18. Horvath I, Hunt J, Barnes PJ, Alving K, Antczak A, Baraldi E, et al. Exhaled Breath Condensate: Methodological Recommendations and Unresolved Questions. *Eur Respir J* (2005) 26(3):523–48. doi: 10.1183/09031936.05.00029705
19. Carraro S, Giordano G, Piacentini G, Kantar A, Moser S, Cesca L, et al. Asymmetric Dimethylarginine in Exhaled Breath Condensate and Serum of Children With Asthma. *Chest* (2013) 144(2):405–10. doi: 10.1378/chest.12-2379
20. Carraro S, Andreola B, Alinovi R, Corradi M, Freo L, Da Dalt L, et al. Exhaled Leukotriene B4 in Children With Community Acquired Pneumonia. *Pediatr Pulmonol* (2008) 43(10):982–6. doi: 10.1002/ppul.20889
21. Faversani A, Amatori S, Augello C, Colombo F, Porretti L, Fanelli M, et al. miR-494-3p Is a Novel Tumor Driver of Lung Carcinogenesis. *Oncotarget* (2017) 8(5):7231–47. doi: 10.18632/oncotarget.13933
22. Pergoli L, Cantone L, Favero C, Angelici L, Iodice S, Pinatel E, et al. Extracellular Vesicle-Packaged miRNA Release After Short-Term Exposure to Particulate Matter Is Associated With Increased Coagulation. *Part Fibre Toxicol* (2017) 14(1):32. doi: 10.1186/s12989-017-0214-4
23. Andersen CL, Jensen JL, Orntoft TF. Normalization of Real-Time Quantitative Reverse Transcription-PCR Data: A Model-Based Variance Estimation Approach to Identify Genes Suited for Normalization, Applied to Bladder and Colon Cancer Data Sets. *Cancer Res* (2004) 64(15):5245–50. doi: 10.1158/0008-5472.CAN-04-0496
24. Livak KJ, Schmittgen TD. Analysis of Relative Gene Expression Data Using Real-Time Quantitative PCR and the 2(-Delta Delta C(T)) Method. *Methods* (2001) 25(4):402–8. doi: 10.1006/meth.2001.1262
25. Kumar MS, Erkeland SJ, Pester RE, Chen CY, Ebert MS, Sharp PA, et al. Suppression of Non-Small Cell Lung Tumor Development by the Let-7 microRNA Family. *Proc Natl Acad Sci USA* (2008) 105(10):3903–8. doi: 10.1073/pnas.0712321105
26. Madhavan D, Peng C, Wallwiener M, Zucknick M, Nees J, Schott S, et al. Circulating miRNAs With Prognostic Value in Metastatic Breast Cancer and for Early Detection of Metastasis. *Carcinogenesis* (2016) 37(5):461–70. doi: 10.1093/carcin/bgw008
27. Khan FH, Pandian V, Ramraj S, Aravindan S, Herman TS, Aravindan N. Reorganization of MetastamiRs in the Evolution of Metastatic Aggressive Neuroblastoma Cells. *BMC Genomics* (2015) 16(1):501. doi: 10.1186/s12864-015-1642-x
28. Augello C, Colombo F, Terrasi A, Trombetta E, Maggioni M, Porretti L, et al. Expression of C19MC miRNAs in HCC Associates With Stem-Cell Features and the Cancer-Testis Genes Signature. *Dig Liver Dis* (2018) 50(6):583–93. doi: 10.1016/j.dld.2018.03.026
29. Zhu H, Fan GC. Extracellular/Circulating microRNAs and Their Potential Role in Cardiovascular Disease. *Am J Cardiovasc Dis* (2011) 1(2):138–49.
30. Kostikas K, Koutsokera A, Papiris S, Gourgoulianis KI, Loukides S. Exhaled Breath Condensate in Patients With Asthma: Implications for Application in Clinical Practice. *Clin Exp Allergy* (2008) 38(4):557–65. doi: 10.1111/j.1365-2222.2008.02940.x

Conflict of Interest: The authors declare that the research was conducted in the absence of any commercial or financial relationships that could be construed as a potential conflict of interest.

frontiers in Oncology

ORIGINAL RESEARCH
published: 28 June 2021
doi: 10.3389/fonc.2021.669786

How the COVID-19 Pandemic Impacted on Integrated Care Pathways for Lung Cancer: The Parallel Experience of a COVID-Spared and a COVID-Dedicated Center

Giulia Pasello[1,2†], Jessica Menis[1,2†], Sara Pilotto[3], Stefano Frega[1], Lorenzo Belluomini[3], Federica Pezzuto[4], Anna Caliò[5], Matteo Sepulcri[6], Nunzia Luna Valentina Cernusco[7], Marco Schiavon[4], Maurizio Valentino Infante[8], Marco Damin[4], Claudio Micheletto[8], Paola Del Bianco[1], Riccardo Giovannetti[8], Laura Bonanno[1], Umberto Fantoni[4], Valentina Guarneri[1,2], Fiorella Calabrese[4], Federico Rea[4], Michele Milella[3‡] and PierFranco Conte[1,2‡]*

[1] Medical Oncology Department, Istituto Oncologico Veneto IRCCS, Padova, Italy, [2] Department of Surgery, Oncology and Gastroenterology, University of Padova, Padova, Italy, [3] Section of Oncology, Department of Medicine, University of Verona School of Medicine and Verona University Hospital Trust, Verona, Italy, [4] University of Padova, Medical School, Department of Cardiac, Thoracic, Vascular Sciences and Public Health, Padova, Italy, [5] Department of Diagnostics and Public Health, University of Verona School of Medicine and Verona University Hospital Trust, Verona, Italy, [6] Radiation Oncology Department, Istituto Oncologico Veneto IRCCS, Padova, Italy, [7] Radiation Oncology Department, University of Verona School of Medicine and Verona University Hospital Trust, Verona, Italy, [8] Cardiovascular and Thoracic Department, University of Verona School of Medicine and Verona University Hospital Trust, Verona, Italy

Introduction: The COVID-19 pandemic has proved to be a historic challenge for healthcare systems, particularly with regard to cancer patients. So far, very limited data have been presented on the impact on integrated care pathways (ICPs).

Methods: We reviewed the ICPs of lung cancer patients who accessed the Veneto Institute of Oncology (IOV)/University Hospital of Padua (Center 1) and the University Hospital of Verona (Center 2) before and after the COVID-19 pandemic, through sixteen indicators chosen by the members of a multidisciplinary team (MDT).

Results: Two window periods (March and April 2019 and 2020) were chosen for comparison. Endoscopic diagnostic procedures and major resections for early stage NSCLC patients increased at Center 1, where a priority pathway with dedicated personnel was established for cancer patients. A slight decrease was observed at Center 2 which became part of the COVID unit. Personnel shortage and different processing methods of tumor samples determined a slightly longer time for diagnostic pathway completion at both Centers. Personnel protection strategies led to a MDT reshape on a web basis and to a significant selection of cases to be discussed in both Centers. The optimization of patient access to healthcare units reduced first outpatient oncological visits, patient enrollment in clinical trials, and end-of-life cancer systemic treatments; finally, a higher

OPEN ACCESS

Edited by:
Marco Lucchi,
University of Pisa, Italy

Reviewed by:
Farzad Taghizadeh-Hesary,
Shahid Beheshti University of Medical Sciences, Iran
Jeffrey Tuan,
National Cancer Centre Singapore, Singapore

***Correspondence:**
Giulia Pasello
giulia.pasello@iov.veneto.it

[†]These authors have contributed equally to this work

[‡]These authors share last authorship

Specialty section:
This article was submitted to Thoracic Oncology, a section of the journal Frontiers in Oncology

Received: 19 February 2021
Accepted: 07 June 2021
Published: 28 June 2021

Citation:
Pasello G, Menis J, Pilotto S, Frega S, Belluomini L, Pezzuto F, Caliò A, Sepulcri M, Cernusco NLV, Schiavon M, Infante MV, Damin M, Micheletto C, Del Bianco P, Giovannetti R, Bonanno L, Fantoni U, Guarneri V, Calabrese F, Rea F, Milella M and Conte P (2021) How the COVID-19 Pandemic Impacted on Integrated Care Pathways for Lung Cancer: The Parallel Experience of a COVID-Spared and a COVID-Dedicated Center. Front. Oncol. 11:669786. doi: 10.3389/fonc.2021.669786

proportion of hypofractionation was delivered as a radiotherapy approach for early stage and locally advanced NSCLC.

Conclusions: Based on the experience of the two Centers, we identified the key steps in ICP that were impacted by the COVID-19 pandemic so as to proactively put in place a robust service provision of thoracic oncology.

Keywords: lung cancer, COVID-19, multidisciplinary team discussion, integrated care pathway, pandemic

INTRODUCTION

A novel disease caused by the coronavirus, COVID-19, causing severe acute respiratory syndrome (SARS), named SARS-CoV-2, was classified as a pandemic by the World Health Organization (WHO) on 12 March 2020 (1). COVID-19 has proved to be a historic challenge for healthcare systems around the world (2, 3).

In particular, the management of cancer care soon became a crucial issue to which national and international oncology organizations replied with recommendations concerning patients receiving anticancer treatments. Recommendations included delaying active treatment administration based on a case-by-case risk/benefit evaluation, planning remote follow-up assessments, and limiting caregiver access to hospitals (4, 5).

Lung cancer is still the leading cause of cancer death worldwide, and it has been associated with a high risk of pulmonary complications and mortality linked to SARS-CoV2 infection (6).

Lung cancer patient care involves several health professionals and different units joined together in multidisciplinary teams. Integrated Care Pathways (ICPs) have been identified as an adequate tool for improving the management of lung cancer patient care (7–9). ICPs are currently widely used in hospitals for a structured and detailed planning of care, since they facilitate a systematic and continuous audit of clinical practices through quality indicators that investigate the three dimensions of quality: professional, organizational, and patient-oriented care (7–10).

Raising evidence on lung cancer care was published during the COVID-19 pandemic, but, to the best of our knowledge, very limited data were presented on the impact on ICP. The ICP for lung cancer has been active in the Veneto region since 2017 and measures these patients' quality of care (11).

We joined the experience of two Centers in the Veneto region, one of the regions in Italy that was most hit by the COVID-19 pandemic, with the primary aim of investigating the impact of COVID-19 on the regional ICP for lung cancer patients.

MATERIALS AND METHODS

The study was designed on 30 April 2020 with the primary aim of investigating the difference in terms of diagnostic and therapeutic procedure volumes and timings in a two-month observation period: 1 March–30 April 2019, and 1 March–30 April 2020.

This time frame has been selected in order to catch the different impact of the pandemic on two different centers, at the beginning of the infection curve rise in Italy; indeed, the pandemic curve reached a peak between March and April 2020, while a significant decrease was observed at the beginning of May.

The working group comprised all the physicians and healthcare researchers involved in the management of lung cancer patients in the two Veneto Region Centers: medical oncologists, pulmonologists, thoracic surgeons, pathologists, and radiation oncologists from the Veneto Institute of Oncology (IOV) and the University Hospital of Padua (named Center 1) and the University Hospital of Verona (named Center 2). While Center 1 one was only partially dedicated to COVID-19 patient care, Center 2 became a COVID-dedicated hospital on 13 March 2020 (12).

Indicators were identified by using group facilitation techniques designed to explore the level of consensus among a group of experts and to aggregate judgments into refined agreed opinions. Facilitation includes a set of functions or activities carried out before, during, and after a meeting to help the group achieve its own outcomes. Facilitative functions may be accomplished by group members or leaders or by an external facilitation specialist. This method is usually used during the meetings by the ICP working groups in order to assess among all specialists which indicators are best suitable for different purposes.

A total of sixteen indicators (**Supplementary Table 1**) were selected taking into account their availability, reproducibility, significance, and measurability. These indicators were agreed upon and also chosen based on the Veneto ICP (11), literature evidence (7–10), international guidelines (13–15), and the expert opinion of the hospital's multidisciplinary lung cancer team. The deadline for data collection was set for 22 May 2020.

We retrospectively reviewed the ICPs of consecutive lung cancer patients who were referred to the two Centers during the two-month observation period. The last follow-up was 30 April 2020.

The clinical features of referred patients were not this study's primary interest. Therefore, all data were collected in an anonymous form.

Data on activity volumes from oncology, pulmonology, radiation therapy, and thoracic surgery were derived from electronic medical records, institutional electronic tracking systems usually employed for administrative purposes, and multidisciplinary team registries. Data on patients' enrollment

in clinical trials were gathered through our electronic database by data managers fully dedicated to lung cancer clinical trials. Data of activity volumes of the Center 1 pathology unit were extracted through Armonia Software (Dedalus Healthcare Systems Group) version 15.0.7.1, while those of the Center 2 pathology unit were gathered through Pathos Software. All data were further confirmed by manually examining daily activity lists.

Indicators to assess each Center's activity volumes were reported as total numbers, percentages, or ratios; indicators to assess different performance times were calculated as median and mean with working day ranges. The total number of patients evaluated for each indicator (*i.e.* the denominator) varied depending on the indicator's content.

A web meeting for data sharing and discussion took place on 29 May 2020 before manuscript writing and submission. The study design and timeline are summarized in **Figure 1**.

The performance time in 2019 and 2020 was calculated through median values and compared by means of the Mann–Whitney Rank Sum Test. Activity volumes were compared through a two-tailed binomial test used to determine whether the probability of each indicator is equal to 1/2 in the two periods and a Pearson's Chi-squared test with simulated p-value to compare two observed proportions. Specifically, when comparing the 2019 and 2020 activity volumes we supposed that, of the total number of procedures (y1 + y2), a portion y1 was performed in the first year and a portion y2 in the second year.

RESULTS

The Veneto Institute of Oncology, which includes medical and radiation oncology, was not defined as a COVID-19 hospital during the entire pandemic; the thoracic surgery, pneumology, and pathology units of the University Hospital of Padua were partially involved in the diagnosis and care of COVID-19 patients, even though some personnel were specifically dedicated to endoscopic diagnostic procedures for cancer patients.

On the other hand, the Verona University Hospital Trust was converted into a COVID hospital during the pandemic's peak. The thoracic surgery, pneumology, and oncology units were heavily involved in COVID-19 patient care.

Activity Volumes of Pneumology Units and Timing for NSCLC Patients

The absolute number of diagnostic bronchoscopies performed at the Center 1 pneumology unit was 29 in 2019, increasing to 43 in 2020 (p value = 0.1249), while those performed at Center 2 decreased from 16 in 2019 to 8 in 2020 (p value = 0.1516).

The second indicator was differentiated between the two Centers in order to have a reliable assessment of the activities in the two time periods. The absolute number of thoracoscopies showed a slight non-significant decrease in Center 1, with 18 procedures in 2019 and 13 in 2020 (p value = 0.4731). Similarly, pre-surgical spirometries in Center 2 numbered 24 in 2019, decreasing to 16 in 2020 (p = 0.2682) (**Figure 2A**).

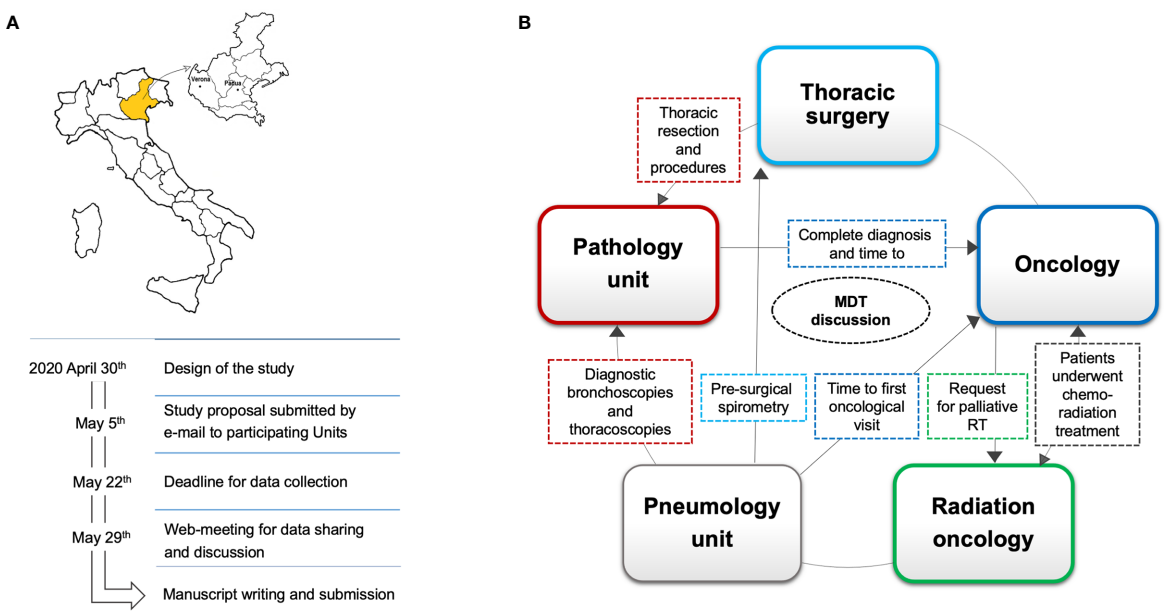

FIGURE 1 | Study design and data collection involving two Centers (Center 1 in Padua; Center 2 in Verona) in the Veneto region, marked here in yellow. The study's main steps were pursued *via* telematics, from the study design to data collection and sharing results, in compliance with pandemic containment measures **(A)**. The impact of COVID-19 on lung cancer patient care was assessed through indicators (dashed lines), identified and selected from regional Integrated Care Pathways (ICPs) and from an expert panel on the basis of relevance to healthcare providers' workloads. The direction of the arrows depicts how these cancer specialists interact with each other in the context of ICPs, while the color of the indicator is the same as that of the healthcare provider whose activity is influenced by **(B)**. MDT, multidisciplinary team.

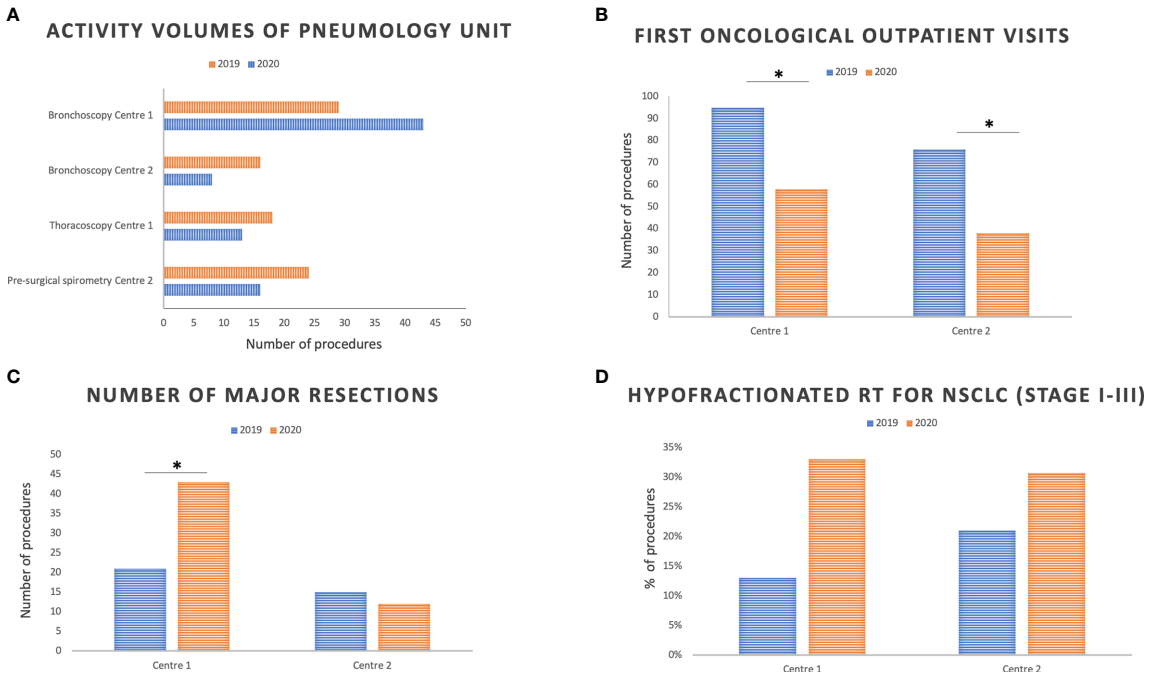

FIGURE 2 | Pneumology **(A)**, medical oncology **(B)**, thoracic surgery **(C)**, and radiation oncology **(D)** activity volumes at the two Centers in March and April 2019 compared with March and April 2020. RT, radiotherapy. *Indicates statistically significant differences between 2019 and 2020; *p* significance level: 0.05.

Finally, the median time between the first visit to the pneumologist and the first oncological visit in Center 1 was 20.5 days in 2019 and 27 in 2020 (p value = 0.160), while this was 30 days in 2019 and 45 days in 2020 in Center 2 (p value < 0.0001) (**Figure 3A**). The benchmark established by the Regional ICP for this indicator is 28 working days.

Histological Diagnosis and Molecular Characterization Timing

The Center 1 pathology unit observed a median time from biopsy procedure to histological diagnosis of 5 working days (wd) in 2019 and 6 wd in 2020 (p value < 0.001); in Center 2, the median time from biopsy to histological diagnosis was 6 days in 2019 and 5 days in 2020 (p value = 0.014). In both sites, a significant reduction in diagnoses from biopsy samples was observed. Indeed, in Center 1, histological samples from tumor biopsies totalled 215 in 2019 and 171 in 2020 (p value = 0.0285), with an overall 20% reduction; in Center 2, biopsy samples decreased from 79 in 2019 to 37 in 2020 (p value = 0.0001), with an overall 53% reduction.

Conversely, the diagnostic process from surgical specimens did not change significantly in the two Centers in 2020 compared to 2019, both in terms of the number of surgical specimens analyzed and in terms of the median time from surgical procedure to histological diagnosis. In both Centers, the median time for a histological report was within the 20 days set as a benchmark by the Regional ICP: 6 wd in 2019 and 7 wd in 2020 at Center 1 (p = 0.058), 12 wd in both periods at Center 2 (p value = 0.94).

In the same way, molecular analyses (ROS1, ALK, and PD-L1 immunohistochemistry; ALK and ROS1 FISH, EGFR mutational analysis through real-time PCR) overlapped numerically in 2019 and 2020 in both Centers; the median time between histological diagnosis and molecular characterization results was only slightly longer in Center 2 (from 8 to 9 days, p value = 0.02) while in Center 1, this was 7 days in both periods (p value = 0.440) (Regional ICP benchmark: 10 wd) (**Figure 3B**).

Oncological Activity Volumes and the Therapeutic Pathway of NSCLC Cancer Patients

We analyzed the absolute number of first oncological outpatient visits at the two Centers, and we observed a significant reduction in 2020 compared to 2019. Indeed, first visits in Center 1 amounted to 95 in 2019 and 58 in 2020 (p value = 0.0035), a 39% reduction; in Center 2, 76 first visits were held in 2019 and 38 in 2020, with a 50% reduction (p value = 0.0005) (**Figure 2B**).

In the same way, the number of patients enrolled in clinical trials, calculated as the ratio between the number of patients enrolled in clinical trials and the number of active clinical trials, decreased in 2020. Forty-nine patients were enrolled in 13 active trials at Center 1 in 2019 (ratio 3.8), while 34 patients were enrolled in 14 active clinical trials in 2020 (ratio 2.4). Center 2 enrolled 10 patients in 10 clinical studies in 2019 (ratio 1), and eight patients in 10 clinical trials in 2020 (ratio 0.8).

Access prioritization, soon established for both Centers, led to a reduction in the proportion of patients who received systemic anticancer treatment 30 days before death, calculated as the ratio

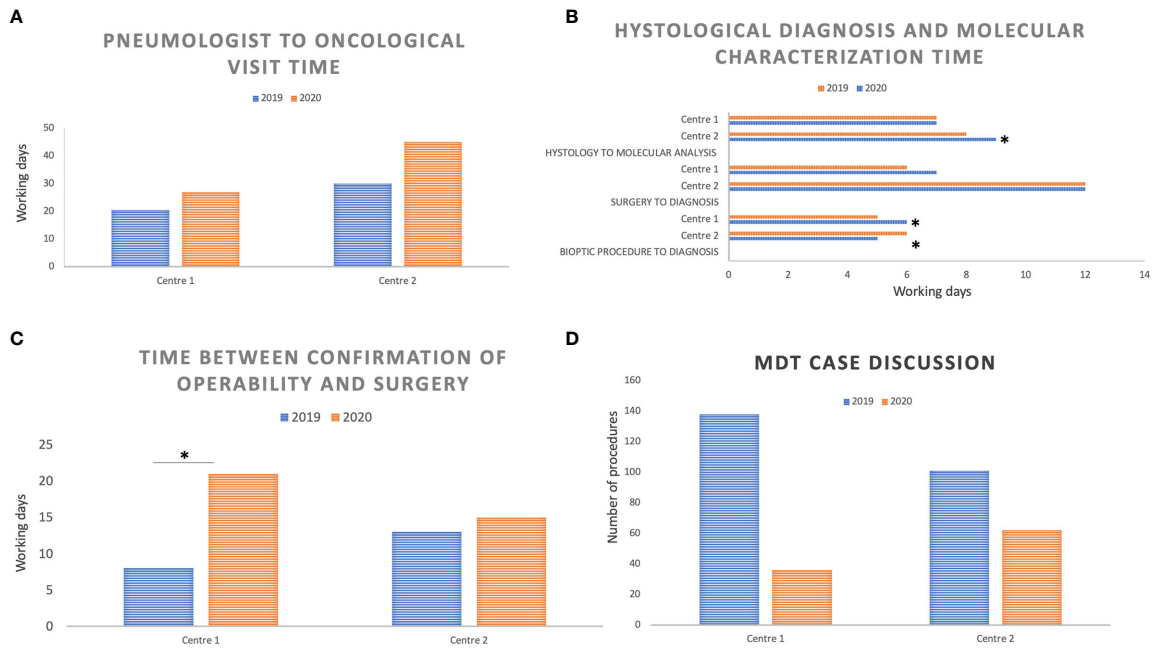

FIGURE 3 | Median performance time reported in working days and compared between March and April 2019 *versus* March and April 2020 at the two Centers: **(A)** Time interval between the pneumology assessment and the first oncological visit; **(B)** Time interval between the biopsy or surgical procedure and the histological diagnosis, and between the histological diagnosis and molecular results; **(C)** Time interval between the confirmation of operability based on functional assessment and surgery (lobectomy or pneumonectomy); **(D)** Number of cases discussed by the multidisciplinary team (MDT) at the two Centers in March and April 2019 compared with March and April 2020. *Indicates statistically significant differences between 2019 and 2020; *p* significance level: 0.05.

between the number of patients who died within 30 days from the last systemic treatment administration and the number of patients undergoing active systemic treatment. From among 296 active treatments ongoing at Center 1 in 2019 and 335 in 2020, 12 patients (4%) died within 30 days from the last treatment administration in 2019 and eight (2%) in 2020 (p value = 0.2684). In Center 2, seven patients (3%) out of 222 in 2019 and four (2%) out of 213 in 2020 died within 30 days from the last treatment administration (p value = 0.5517) (Regional ICP benchmark: lower than 10%).

Activity Volumes, Timings and Mortality Rates From Thoracic Surgical Procedures

As far as timing and activity volumes of thoracic surgery units are concerned, we first assessed an indicator from the ICPs of the Veneto region, namely the median time between the confirmation of operability based on functional assessment and surgery (lobectomy or pneumonectomy).

While the median time in Center 1 was prolonged from 8 working days in 2019 to 21 working days in 2020 (p value = 0.009), times overlapped in Center 2 (13 working days in 2019, range 2–35; 15 working days in 2020, range 4–43; p value = 0.557) (**Figure 3C**).

Moreover, thoracic surgery in Center 1 saw an increase in the percentage of major resections, calculated as the number of NSCLC major resections out the total number of procedures: from 21 in 2019 to 43 in 2020 (p value = 0.0081). Conversely, a 20% reduction in major resections was observed in Center 2: from 15 in 2019 to 12 in 2020 (p value = 0.7011) (**Figure 2C**). No difference in mortality rates, calculated within 30 days from major anatomical resection, was observed in the two Centers between 2019 and 2020 (0%) (Regional ICP benchmark: lower than 10%).

Radiation Therapy in Locally Advanced and Palliative Locoregional Treatments in Metastatic NSCLC

Radiation oncologists carefully assessed three performance indicators which were potentially impacted by the COVID-19 pandemic. No significant difference in terms of percentage of concomitant chemo-radiotherapy (cCTRT) in stage III NSCLC patients was observed. This was calculated as the ratio between the concomitant chemo-radiotherapy treatments and the overall chemo-radiotherapy treatments (concomitant *plus* sequential: cCTRT). Center 1 observed seven cCTRT (78%) out of nine cCTRT in 2019, and six (86%) out of seven in 2020 (p value = 1), while Center 2 experienced four (50%) out of eight cCTRT in 2019 and three (60%) out of five in 2020 (p value = 1). Both Centers increased the percentage of hypofractionated regimens on overall treatment plans: from 13 (3/23) to 33% (8/24) in Center 1 between 2019 and 2020 (p value = 0.1684), and from 21 (10/48) to 31% (10/32) in Center 2 (p value = 0.4233) in the same time periods (**Figure 2D**).

Finally, a reduction in palliative treatments (namely, disease relief symptoms on the brain, bone, and chest) was observed in

both Centers during the COVID peak period. While palliative treatments in 2019 totalled 54 in Center 1 and 21 in Center 2, these dropped to 44 (p value = 0.3634) and 17 (p value = 0.6271) in 2020, respectively, in the two Centers.

Multidisciplinary Team Discussion

Across March and April 2019, eight MDT meetings took place in Center 1 (in an 8 week period) wherein 138 patients were discussed. In March–April 2020, four meetings took place (one physical and three web-based) in a 9 week period, during which 36 patients were discussed ($p < 0.0001$). The COVID-19 pandemic determined a 74% reduction in the number of patients discussed. Similarly, in Center 2, eight MDT meetings took place in 2019 (in an 8 week period) wherein 101 patients were discussed, while seven MDT meetings took place in 2020, during which 62 patients were discussed ($p = 0.0028$), with a final 39% reduction in the number of patients discussed (**Figure 3D**).

DISCUSSION

By the end of April 2020, Italy had already been badly hit by COVID-19, with 201,505 overall confirmed cases and 27,359 deaths since the beginning of this pandemic (source: National Health System data) (15). Cancer patients are more susceptible to this infection compared to healthy people and non-cancer patients due to the systemic malignancy-related immunosuppressive state and to active disease-oriented treatments, such as chemotherapy or immunotherapy, radiotherapy and surgery (16–20). Therefore, cancer care professionals were called upon to cautiously manage this emergency in the everyday balance between risks and benefits in treatment planning (21, 22). Nevertheless, such uncertainty caused patients to feel abandoned, worsened disease-related distress, and led to patients leaving life-saving treatments, as recently reported in 15–20% of cases (23).

To build and share knowledge, several real-world data was collected with the aim of counting the number of infected patients, hospital and Intensive Care Unit admissions, and to measure the mortality and acquirement of immunity (24, 25).

However, to the best of our knowledge, no focused effort has been made to date to retrospectively measure the impact on local cancer management and to assess possible shortages of non-COVID-19-related healthcare provisions (26). Moreover, the majority of reports focused on single-center experiences (27, 28).

The present work focuses on the integrated care pathways of NSCLC management. The aim is to report data on multidisciplinary performance volumes and timing of NSCLC patients referred to two Italian Centers, one COVID-spared and one COVID-dedicated, in March and April 2020 and to compare the data with the same 2019 period.

Even though both pneumology units had to reorganize their activities to cope with the management of COVID-19 patients, a different impact of the pandemic on performance volumes and timings was observed between the two Centers. The Center 1 pneumology unit had a slight decrease in the number of thoracoscopy procedures requiring an operating theater. However, since a priority pathway for cancer patients with dedicated specialized personnel for endoscopic diagnostic procedures was established, the pure number of procedures actually increased in 2020 compared to 2019. On the other hand, the Center 2 unit was entirely involved in COVID-positive patient diagnoses and care and, subsequently, had a higher volume of bronchoscopy and spirometry procedures.

For both Centers, the time between the first pulmonologist and the first oncological visits was slightly prolonged due to the longer time needed for staging and diagnostic pathway completion. Similar to the experience of pathological departments in other Italian Centres (29), the activities of both pathology departments were affected since technical and administrative personnel were reduced on-site and moved to smart working, thus limiting the workforce available for sample processing. Pathologists and technicians were also involved in the *post-mortem* examination of suspected or certain COVID-19-positive patients, which was time-consuming and personnel-intensive. Moreover, cytological samples from bronchoalveolar lavage (BAL) were first processed through alcohol and formalin treatment and only analyzed later in order to avoid potential exposure to the virus (30–32).

A significant reduction in first oncological evaluations was observed at both Centers, and this was mostly due to a decrease in visits from outside the region and the optimization of patient access to the oncological unit, which led medical oncologists to postpone clinical evaluation when all diagnostics and staging was complete. In accordance with the recommendations of the main national and European guidelines (4, 5), a careful evaluation of treatment administration was performed for frail patients on the basis of age and comorbidities, and also for further lines of treatment, with particular reference to those regimens lacking strong evidence of survival benefits. As a consequence, we observed a reduction in patient deaths within 30 days from the last anticancer treatment administration, which was established as a relevant indicator by Regional ICPs.

Once again, the different trend in major resection numbers between the two Centers was a consequence of the two units' different levels of involvement in COVID-19-positive patient care. Indeed, while the availability of operating rooms increased in Center 1, where priority was given to cancer patients suitable for major interventions, operating rooms were temporarily closed to cancer patients and subsequently opened with a limited flow in Center 2. The longer time observed in Center 1 between the operability indication and surgical resection was mainly due to the minimization of patient access to preoperative tests and anesthesiological assessment.

Departmental reorganization and limiting patient access to the hospital also involved the radiation therapy unit, leading to an increase in hypofractionated regimens (33). This was in line with the Italian experience recently reported by the Italian Association of Radiotherapy and Clinical Oncology (AIRO), where hypofractionation was considered as one of the basic strategies to efficiently cope with the disruption caused by the pandemic (34).

Additionally, some patients showed reduced compliance to repeated access to hospital for locoregional treatments with palliative intent, thus leading to the optimization of best supportive care at home.

Overall, the indicators established by the Regional ICP and selected for the purpose of this study confirmed an adequate management and diagnostic–therapeutic pathway for cancer patients; indeed, from the six of them, only one indicator exceeded the recommended benchmark, and this involved the Center 2 pneumology unit which was converted into a COVID-dedicated unit.

MDT meetings at Center 1 were more impacted than Center 2, even because the earlier spread of COVID-19 was focused in Padua; moreover, in Center 2, MDT was promptly switched to the web-based format thus allowing a higher number of web meetings to take place. The decrease observed in the number of discussion cases was overall in line with the reduction in oncological visits and diagnostic procedures during the pandemic's peak and to a better selection of cases to be discussed where more than two specialists were needed.

In order to reduce patient access to healthcare units and to select patients for locoregional and systemic treatments, multidisciplinary team discussion should be maintained as a basic requirement for good clinical practice in lung cancer patient management, potentially impacting patients' survival (35, 36).

The optimization of telemedicine and resource allocation for easy-to-use software would allow patients' clinical documents and iconography to be transferred between physicians and between physicians and patients. These are starting points for innovative healthcare practice and would also help to reassure patients on the presence and reliability of oncologists.

Worldwide teamwork in the sharing of clinical and autoptic data on lung cancer patients affected by COVID-19 and a longer follow-up of such patients may help clinicians to efficiently shape their practice for continuous care in oncology and the protection of frail subpopulations (26).

Based on the experience of the two Centers, we identified the key determinants for a robust provision of thoracic procedures: pre-defined plans for epidemic response; aggressive early action to "flatten the curve"; the ability to separate resources between the management of COVID-19 (or any epidemic) and routine clinical services; prioritization of thoracic surgery; and, the volume of COVID-19 cases in that region.

Although the impact of health reorganization measures on patients' survival is not the aim of the present study, this issue is currently under investigation at national level where lung cancer patients' outcome has been investigated with longer follow-up.

The limitations of this analysis are certainly related to the study's retrospective nature and the limited number of Centers involved; nevertheless, in our opinion, this analysis presents a good picture of the experience acquired by the two Centers in one of the Italian regions worst-hit by the COVID-19 pandemic.

Some approaches for facing the impact of pandemic on health system, which were improved only in subsequent months of 2020 and finally became routine strategies during the second peak of 2021, include a prompt plan for protection and monitoring of personnel, who should also be divided into different paths according to access to COVID or no-COVID departments; production of time and personnel-sparing procedures for patients' sample management, which take under consideration the central role of the pathologist and pulmonologist both in COVID infection and cancer diagnostic process; dynamic update of guidelines on systemic and locoregional treatment of lung cancer patients in order to warrant early start of the diagnostic–therapeutic pathway and to avoid hospital access not finalized to survival improvement; finally, patients' empowerment to early cancer symptoms and signs referral and diagnostic and staging procedure compliance in order to limit advanced stages at the clinical presentation.

To conclude, the lessons learned will improve the ICP through more flexibility and awareness of pivotal points and will go a long way to ensure continuity of care by caregivers to cancer patients.

DATA AVAILABILITY STATEMENT

The raw data supporting the conclusions of this article will be made available by the authors without undue reservation.

ETHICS STATEMENT

Ethical review and approval was not required for the study on human participants in accordance with the local legislation and institutional requirements. Written informed consent for participation was not required for this study in accordance with the national legislation and the institutional requirements.

AUTHOR CONTRIBUTIONS

All authors listed have made a substantial, direct, and intellectual contribution to the work and approved it for publication.

SUPPLEMENTARY MATERIAL

The Supplementary Material for this article can be found online at: https://www.frontiersin.org/articles/10.3389/fonc.2021.669786/full#supplementary-material

REFERENCES

1. Available at: http://www.euro.who.int/en/health-topics/health-emergencies/coronavirus-covid-19/news/news/2020/3/who-announces-covid-19-outbreak-a-pandemic.
2. Rosenbaum L. The Untold Toll - The Pandemic's Effects on Patients Without Covid-19. *N Eng J Med* (2020) 382(24):2368–71. doi: 10.1056/NEJMms2009984
3. Rosenbaum L. Facing Covid-19 in Italy: Ethics, Logistics, and Therapeutics on the Epidemic's Front Line. *N Engl J Med* (2020) 382:1873–5. doi: 10.1056/NEJMp2005492
4. Associazione Italiana di Oncologia Medica (AIOM). *Coronavirus Covid19 Infectious Risk: Indications for Oncology* (2020). Available at: https://www.aiom.it/wp-content/uploads/2020/03/20200313_COVID- 19_indicazioni_AIOM-CIPOMO-COMU.pdf.

5. Available at: https://www.esmo.org/guidelines/cvancer-patient-management-during-the-covid-19-pandemic.
6. Garassino MC, Whisenant JG, Huang LC, Trama A, Torri V, Agustoni F, et al. Covid-19 in Patients With Thoracic Malignancies (TERAVOLT): First Results of an International, Registry-Based, Cohort Study. *Lancet Oncol* (2020). doi: 10.1016/S1470-2045(20)30314-4
7. Fasola G, Rizzato S, Merlo V, Aita M, Ceschia T, Giacomuzzi F, et al. Adopting Integrated Care Pathways in Non Small Cell Lung Cancer From Theory to Practice. *J Thorac Oncol* (2012) 7(8):1283–90. doi: 10.1097/JTO.0b013e318257fbfe
8. Ouwens MM, Hermens RR, Termeer RA, Vonk-Okhuijsen SY, Tjan-Heijnen VC, Verhagen AF, et al. Quality of Integrated Care for Patients With Nonsmall Cell Lung Cancer: Variations and Determinants of Care. *Cancer* (2007) 110:1782–90. doi: 10.1002/cncr.22986
9. Tanvetyanon T. Quality of Care Indicators for Non Small Cell Lung Cancer. *Cancer Control* (2009) 16:335–41. doi: 10.1177/107327480901600408
10. Fasola G, Menis J, Follador A, De Carlo E, Valent F, Aresu G, et al. Integrated Care Pathways in Lung Cancer: A Quality Improvement Project. *Int J Technol Assess Health Care* (2018) 34(1):3–9. doi: 10.1017/S026646231700441X
11. Available at: https://salute.regione.veneto.it/web/rov/polmone.
12. Zuliani S, Zampiva I, Tregnano D, Casali M, Cavaliere A, Fumagalli A, et al. Organizational Challenges, Volumes of Oncological Activity, and Patients' Perception During the SARS-Cov-2 Epidemic. *Eur J Cancer* (2020). doi: 10.1016/j.ejca.2020.05.029
13. Available at: https://www.nccn.org/professionals/physician_gls/default.aspx.
14. Available at: https://www.esmo.org/guidelines/lung-and-chest-tumours.
15. Available at: https://www.aiom.it/linee-guida-aiom-neoplasie-del-polmone-2019/.
16. Kamboj M, Sepkowitz KA. Nosocomial Infections in Patients With Cancer. *Lancet Oncol* (2009) 10:589–97. doi: 10.1016/S1470-2045(09)70069-5
17. Li J-Y, Duan X-F, Wang L-P, Xu Y-J, Huang L, Zhang TF, et al. Selective Depletion of Regulatory T Cell Subsets by Docetaxel Treatment in Patients With Nonsmall Cell Lung Cancer. *J Immunol Res* (2014) 2014:286170. doi: 10.1155/2014/286170
18. Longbottom ER, Torrance HDT, Owen HC, Fragkou PC, Hinds CJ, Pearse RM, et al. Features of Postoperative Immune Suppression Are Reversible With Interferon Gamma and Independent of Interleukin-6 Pathways. *Ann Surg* (2016) 264:370–77. doi: 10.1097/SLA.0000000000001484
19. Sica A, Massarotti M. Myeloid Suppressor Cells in Cancer and Autoimmunity. *J Autoimmun* (2017) 85:117–25. doi: 10.1016/j.jaut.2017.07.010
20. Davis AP, Boyer M, Lee JH, Kao SC. Covid-19: The Use of Immunotherapy in Metastatic Lung Cancer. *Immunotherapy* (2020) 12(8):545–8. doi: 10.2217/imt-2020-0096
21. Lewis MA. Between Scylla and Charybdis — Oncologic Decision Making in the Time of Covid-19. *NEJM* (2020) 382:2285–7. doi: 10.1056/NEJMp2006588
22. Banna G, Curioni-Fontecedro A, Friedlandlaender A, Addeo A. How We Treat Patients With Lung Cancer During the SARS-CoV-2 Pandemic: Primum non Nocere. *ESMO Open* (2020) 4:e000765. doi: 10.1136/esmoopen-2020-000765
23. Available at: https://www.repubblica.it/oncologia/qualita-di-vita/2020/04/22/news/coronavirus_la_solitudine_dei_malati_di_cancro_a_chi_rivolgersi_per_un_aiuto_psicologico-254686860/.
24. Lee LYW, Cazier JB, Angelis V, Arnold R, Bisht V, Campton NA, et al. Covid-19 Mortality in Patients With Cancer on Chemotherapy or Other Anticancer Treatments: A Prospective Cohort Study. *Lancet* (2020) 395(10241):1919–26. doi: 10.1016/S0140-6736(20)31173-9
25. Luo J, Rizvi H, Egger JV, Preeshagul IR, Wolchok JD, Hellmann MD. Impact of PD-L1 Blockade on Severity of COVID-19 in Patients With Lung Cancer. *Cancer Discov* (2020) 10(8):1121–8. doi: 10.1158/2159-8290.CD-20-0596
26. Portmans P, Guarneri V, Cardoso M. Cancer and COVID-19: What do We Really Know? *Lancet* (2020) 395(10241):1884–5. doi: 10.1016/S0140-6736(20)31240-X
27. Zuliani S, Zampiva I, Tregnago D, Miriam Casali M, Cavaliere A, Fumagalli A, et al. Organisational Challenges, Volumes of Oncological Activity and Patients' Perception During the Severe Acute Respiratory Syndrome Coronavirus 2 Epidemic. *Eur J Cancer* (2020) 135:159–69. doi: 10.1016/j.ejca.2020.05.029
28. De Marinis F, Attili I, Morganti S, Stati V, Spitaleri G, Gianoncelli L, et al. Results of Multilevel Containment Measures to Better Protect Lung Cancer Patients From COVID-19: The IEO Model. *Front Oncol* (2020) 10(665):1–8. doi: 10.3389/fonc.2020.00665
29. Vigliar E, Iaccarino A, Bruzzese D, Malapelle U, Bellevicine C, Troncone G. Cytology in the Time of Coronavirus Disease (COVID-19): An Italian Perspective. *J Clin Pathol* (2020) 0:1–3. doi: 10.1136/jclinpath-2020-206614
30. Centers for Disease Control and Prevention (CDC). *Interim Laboratory Biosafety Guidelines for Handling and Processing Specimens Associated With Coronavirus Disease 2019 (COVID-19)*. (2020).
31. World Health Organization. *Laboratory Biosafety Guidance Related to the Novel Coronavirus (2019-nCoV): Interim Guidance*. (2020).
32. Iwen PC, Stiles KL, Pentella MA. Safety Considerations in the Laboratory Testing of Specimens Suspected or Known to Contain the Severe Acute Respiratory Syndrome Coronavirus 2 (SARS-Cov-2). *Am J Clin Pathol* (2020) 51(3):239–42. doi: 10.1093/ajcp/aqaa047.
33. Faivre-Finn C, Fenwick JD, Francks KN, Harrow S, Hatton MQF, Hiley C. Reduced Fractionation in Lung Cancer Patients Treated With Curative-Intent Radiotherapy During the COVID-19 Pandemic. *Clin Oncol* (2020) 32(8):481–9. doi: 10.1016/j.clon.2020.05.001
34. Jerekzeck-Fossa BA, Pepa M, Marvaso G, Bruni A, Buglione di Monale E Bastia M, Catalano G, et al. Covid-19 Outbreak and Cancer Radiotherapy Disruption in Italy: Survey Endorsed by the Italian Association of Radiotherapy and Clinical Oncology (Airo). *Radiother Oncol* (2020) 149:89–93. doi: 10.1016/j.radonc.2020.04.061
35. Kumar S, Chmura S, Robinson C, Lin SH, Gadgeel SM, Donington J, et al. Alternative Multidisciplinary Management Options for Locally Advanced NSCLC During the Coronavirus Disease 2019 Global Pandemic. *J Thoracic Oncol* (2020) 15(7):1137–46. doi: 10.1016/j.jtho.2020.04.016
36. Stone E, Rankin N, Kerr S, Fong K, Currow DC, Phillips J, et al. Does Presentation at Multidisciplinary Team Meetings Improve Lung Cancer Survival? Findings From a Consecutive Cohort Study. *Lung Cancer* (2018) 124:199–204. doi: 10.1016/j.lungcan.2018.07.032

Conflict of Interest: The authors declare that the research was conducted in the absence of any commercial or financial relationships that could be construed as a potential conflict of interest.

frontiers in Oncology

ORIGINAL RESEARCH
published: 30 August 2021
doi: 10.3389/fonc.2021.645623

Pulmonary Neuroendocrine Neoplasms Overexpressing Epithelial-Mesenchymal Transition Mechanical Barriers Genes Lack Immune-Suppressive Response and Present an Increased Risk of Metastasis

Tabatha Gutierrez Prieto[1], Camila Machado Baldavira[1], Juliana Machado-Rugolo[1,2], Cecília Farhat[1], Eloisa Helena Ribeiro Olivieri[3], Vanessa Karen de Sá[3], Eduardo Caetano Abilio da Silva[4], Marcelo Luiz Balancin[1], Alexandre Muxfeldt Ab´Saber[1], Teresa Yae Takagaki[5], Vladmir Cláudio Cordeiro de Lima[6,7] and Vera Luiza Capelozzi[1]**

[1] Department of Pathology, University of São Paulo Medical School (USP), São Paulo, Brazil, [2] Health Technology Assessment Center (NATS), Clinical Hospital (HCFMB), Medical School of São Paulo State University (UNESP), Botucatu, Brazil, [3] International Center of Research/CIPE, AC Camargo Cancer Center, São Paulo, Brazil, [4] Molecular Oncology Research Center, Barretos Cancer Hospital, Barretos, São Paulo, Brazil, [5] Division of Pneumology, Instituto do Coração (Incor), Medical School of University of São Paulo, São Paulo, Brazil, [6] Oncology, Rede D'Or São Paulo, São Paulo, Brazil, [7] Department of Clinical Oncology, Instituto do Câncer do Estado de São Paulo (ICESP), São Paulo, Brazil

Typical carcinoids (TC), atypical carcinoids (AC), large cell neuroendocrine carcinomas (LCNEC), and small cell lung carcinomas (SCLC) encompass a bimodal spectrum of metastatic tumors with morphological, histological and histogenesis differences, The hierarchical structure reveals high cohesiveness between neoplastic cells by mechanical desmosomes barrier assembly in carcinoid tumors and LCNEC, while SCLC does not present an organoid arrangement in morphology, the neoplastic cells are less cohesive. However, the molecular mechanisms that lead to PNENs metastasis remain largely unknown and require further study. In this work, epithelial to mesenchymal transition (EMT) transcription factors were evaluated using a set of twenty-four patients with surgically resected PNENs, including carcinomas. Twelve EMT transcription factors (*BMP1*, *BMP7*, *CALD1*, *CDH1*, *COL3A1*, *COL5A2*, *EGFR*, *ERBB3*, *PLEK2*, *SNAI2*, *STEAP1*, and *TCF4*) proved to be highly expressed among carcinomas and downregulated in carcinoid tumors, whereas upregulation of *BMP1*, *CDH2*, *KRT14* and downregulation of *CAV2*, *DSC2*, *IL1RN* occurred in both histological subtypes. These EMT transcription factors identified were involved in proliferative signals, epithelium desmosomes assembly, and cell motility sequential steps that support PNENs invasion and metastasis in localized surgically resected primary tumor. We used a two-stage design where we first examined the candidate EMT transcription factors using a whole-genome screen, and subsequently, confirmed EMT-like changes by transmission electron

OPEN ACCESS

Edited by:
Paul Takam Kamga,
Université de Versailles Saint-Quentin-en-Yvelines, France

Reviewed by:
Tamás Zombori,
University of Szeged, Hungary
Ryota Kurimoto,
Tokyo Medical and Dental University, Japan
Helmut H. Popper,
Medical University of Graz, Austria

***Correspondence:**
Tabatha Gutierrez Prieto
tabathaprieto@yahoo.com.br
Vera Luiza Capelozzi
vera.capelozzi@fm.usp.br

Specialty section:
This article was submitted to Thoracic Oncology, a section of the journal Frontiers in Oncology

Received: *06 January 2021*
Accepted: *10 August 2021*
Published: *30 August 2021*

Citation:
Prieto TG, Baldavira CM, Machado-Rugolo J, Farhat C, Olivieri EHR, de Sá VK, da Silva ECA, Balancin ML, Ab´Saber AM, Takagaki TY, Cordeiro de Lima VC and Capelozzi VL (2021) Pulmonary Neuroendocrine Neoplasms Overexpressing Epithelial-Mesenchymal Transition Mechanical Barriers Genes Lack Immune-Suppressive Response and Present an Increased Risk of Metastasis. Front. Oncol. 11:645623. doi: 10.3389/fonc.2021.645623

microscopy and then, the EMT-related genes that were differentially expressed among PNENs subtypes were predicted through a Metascape analysis by in silico approach. A high expression of these EMT transcription factors was significantly associated with lymph node and distant metastasis. The sequential steps for invasion and metastasis were completed by an inverse association between functional barrier created by PD-L1 immunosuppressive molecule and EMT transcriptional factors. Our study implicates upregulation of EMT transcription factors to high proliferation rates, mechanical molecular barriers disassembly and increased cancer cell motility, as a critical molecular event leading to metastasis risk in PNENs thus emerging as a promising tool to select and customize therapy.

Keywords: pulmonary neuroendocrine neoplasms, epithelial to mesenchymal transition transcriptional factors, desmosomes, desmocollin, collagen, metastasis

INTRODUCTION

Currently, neuroendocrine neoplasms (NENs) are categorized into differentiated neuroendocrine tumors (NETs), also named as carcinoid tumors (TC, typical carcinoid and AC, atypical carcinoid), and poorly differentiated neuroendocrine carcinomas (NECs), including large cell neuroendocrine carcinoma (LCNEC) and small cell lung carcinoma (SCLC) (1). Patients with PNENs have tumors sufficiently localized to be considered treatable by surgical resection, and among those whose tumors are successfully resected, approximately 90-98% of patients with typical carcinoid, and 50-60% of atypical carcinoid, survive 5 years (2, 3) even developing local invasiveness, dissemination to regional lymph nodes, and distant metastasis (4, 5) which occur in 3% of typical carcinoids and 21% for atypical carcinoids (6–8). In contrast, only 20-30% of the patients with large cell neuroendocrine carcinoma survive 5 years after surgical resection and adjuvant chemotherapy (9), and only 10% of the patients with small cell lung carcinoma survive 5 years after Cisplatin + Carboplatin + Etoposide (10).

In addition to morphological and histological differences, PNENs encompass a bimodal spectrum of metastatic tumors with differences in histogenesis. For instance, normal lung contains a population of neuroendocrine cells (NE), referred as Kulchitsky cell, within the bronchial tree and neuroendocrine bodies in the periphery, which also might give rise to carcinoids, a specific group of tumors based on their secretory products, distinct staining characteristics, and ability to uptake and decarboxylate amine precursors (11). In contrast, SCLC do not arise from Kulchitzky cells, but from multipotent or undifferentiated neuroendocrine NE cells in the central bronchial tree (12–14) as previously demonstrated in experimental models genetically modified (15). Given these unusual characteristics of PNENs, not only is it still often difficult to oncologist predicts which tumors will invade, metastasize, and abbreviate the patient's life, nevertheless, effective adjuvant treatments still depend on identifying these tumors shortly after biopsy or surgery as well.

The tissue availability for genome investigation, looking for biomarkers that signal the risk of metastasis and cancer specific death, has primarily focused on tumor epithelial compartment (16–18) and not on their effects on molecular events for invasion more lethal, and more therapeutically relevant for metastatic lesion. Furthermore, genome-based studies that have preliminarily explored in metastatic tumors were done using small sample biopsies (19–23). Thus, the molecular mechanisms that lead to PNENs metastasis remain largely unknown and require further study. The identification of EMT-related genes in tumor epithelial compartment and their effects on metastasis steps as new biomarkers and therapeutic targets for PNENs is promising.

In order to address these gaps in the literature, we evaluated epithelial to mesenchymal transition (EMT) transcription factors, most of them involved in cancer cell proliferation signals, mechanical molecular barriers, and cell block motility that support PNENs invasion and metastasis in localized surgically resected primary tumor. Overall, we performed an analysis of EMT transcription factors expression data generated using mRNA in two approaches, where we first utilized gene expression microarray technology to identify candidate genes that are associated with PNENs metastasis, confirmed EMT-like changes by transmission electron microscopy and validation in a similar independent cohort using in silico analysis. To complete the sequential steps for invasion and metastasis by PNENs, we evaluated the functional barrier created by the PD-L1 immunosuppressive molecule.

MATERIALS AND METHODS

Patients and Samples

Discovery Cohort

We analyzed tumor samples collected from 65 patients diagnosed with either a carcinoid tumor or LCNEC confirmed by surgical resection, or with SCLC confirmed by surgical resection or a biopsy, between 2007 and 2016. 24 fresh frozen tumor-normal pairs (10 SCLC, 4 LCNEC, 5 AC, and 5 TC) from A. C. Camargo Cancer Center, in São Paulo, Brazil, and Hospital do Amor, in Barretos, Brazil, and 41 archival formalin-fixed

paraffin-embedded histological sections samples (13 SCLC, 9 LCNEC, 5 AC, and 14 TC) from the Hospital das Clínicas and from the Heart Institute of the University of São Paulo (USP). The neoplastic area was delimited during the frozen section procedure to ensure the exclusion of non-neoplastic tissue. At the time of resection, random samples of tumor were diced, fixed in 2.5% buffered glutaraldehyde, embedded in Araldite, and cut into thin sections that were then stained with uranyl acetate and lead citrate and examined by transmission electron microscopy (TEM) to confirm EMT-like changes. The histologic diagnosis and immunohistochemistry results were then reviewed and confirmed by two experienced lung pathologists in accordance with the WHO 2015 classification (24). The main histologic criteria for tumor re-classification were the mitotic count and the presence of an organoid pattern (rosettes, pseudo rosettes, palisading, spindle cells) or necrosis. The cohort included 29 carcinoid tumors (19 TC and 10 AC), 13 LCNEC, and 23 SCLC. Patient's demographics and clinicopathological characteristics were obtained from medical records and included age, sex, smoking history, tumor size, tumor stage (according to the International Association for the Study of Lung Cancer classification system, 8th edition), and follow-up information (24). The internal ethics committees of all the participating institutions approved this study's protocol (process number 1.077.100) with a waiver for informed consent by their review boards.

Evaluation of Biological Function of EMT-Related Gene Expressions

To validate our data and to investigate which EMT biological process were involved, we conducted an interactive analysis on the Metascape[1], a tool for gene annotation and gene list enrichment analysis, to analyze the genes whose expression differed among PNEN subtypes (25). For the gene list used, we carried out a pathway and process enrichment analysis using the following ontology sources: KEGG Pathway, GO Biological Processes, Reactome Gene Sets, Canonical Pathways, CORUM, DisGeNET. With the purpose of identifying EMT-related protein interactions, we used the Search Tool for the Retrieval of Interacting Genes/Proteins (STRING) database (26) to explore the protein-protein interaction (PPI) of the EMT-related genes that were investigated in our study. A heatmap was created to verify the association between the relative expression of the EMT transcription factors and histological subtypes using the Heatmapper platform[2]. Then, we used the average distance and the Euclidean distance between elements to perform an unsupervised hierarchical grouping.

Epithelial-Mesenchymal Transition (EMT) Transcription Factors Identification

Total RNA was extracted from fresh-frozen tumor and normal tissues using the QIAsymphony miRNA CT 400 kit (Qiagen, CA, USA) according to the manufacturer's instructions. RNA integrity and quality were determined using the Bioanalyzer 2100 (Agilent Technologies). Complementary DNA was synthesized using the c-DNA – RT² First Strand Kit (Qiagen Sample & Assay Technologies) according to the manufacturer's protocol. The difference of expression in EMT genes was evaluated by the real-time PCR method. Quantitative reverse transcription-polymerase chain reaction (qRT-PCR) was performed using the RT² Profiler PCR Array System (PAHS-090Z; Qiagen, Dusseldorf, Germany) kit for the human EMT pathway with 84 target genes. The array includes a total of 84 EMT genes, 5 housekeeping genes (*ACTB*, *B2M*, *GAPDH*, *HPRT1*, *RPLP0*), 1 genomic DNA control (GDC) to assess contamination, 3 reverse transcriptase controls (RTC) that certify the efficiency of the reverse transcription step, and 3 positive PCR controls (PPC) consisting of an artificial DNA sequence certifying the test accuracy (see **Supplementary Table S1**). Each 96-well plate includes SYBR® Green-optimized primer assays for a thoroughly researched panel of 84 EMT genes, that also are included the collagen and integrin genes. Furthermore, the high-quality primer design and RT² SYBR® Green qPCR Mastermix formulation enable the PCR array to amplify 96 gene-specific products simultaneously under uniform cycling conditions. The samples were amplified using Applied Biosystems Step One Plus (Applied Biosystems, California, USA). The cycling conditions were as follows: 95°C for 10 minutes, 40 cycles at 95°C for 15 seconds, 60°C for 1 minute, followed by the dissociation period. The data were then analyzed in the StepOne software (v. 2.0, Applied Biosystems) using the Δ threshold cycle (Ct) method ($2^{-\Delta\Delta Ct}$) (27). All data were normalized by the housekeeping genes, and normal lung tissue specimens were used as case control. The Ct cutoff was set to 35, and Fold-Change (FC) cutoff was set to ≥2.0.

Programmed Cell Death Ligand 1 (PD-L1) Detection

PD-L1 expression was automatically detected using the Ventana Benchmark Ultra Platform (Roche, Ventana Medical Systems Inc., Tucson, USA) with an OptiView DAB IHD Detection Kit and OptiView Amplification Kit according to proprietary protocols and using the primary anti-PD-L1 antibody SP263 (prediluted; Roche). Samples were considered positive to antigen expression at the presence of a fully membranous brownish staining.

PD-L1 Tumor Proportion Score (TPS) Determination

The TMP of membranous PD-L1 expression in cancer cells was determined by digital image analysis. The images were captured using a Nikon camera attached to a Nikon microscope and sent to an LG monitor by means of a computer-controlled (Pentium 1330 MHz) digitalizing system (Oculus TCX, Coreco Inc., St. Laurent, Quebec, Canada). All slides were fully analyzed at a magnification of ×400 and submitted to an automatic staining vector analysis, followed by total tissue area detection, separation of tumor from non-tumor areas in each slide, and finally, automatic cellular detection. We then used a membrane algorithm to obtain the H-score of the PD-L1 membranous staining. This algorithm consisted of multiplying each staining membrane score, i.e., 0 (no staining), 1+ (weak staining), 2+ (moderate staining), or 3+ (strong staining), by the percentage of

[1] https://metascape.org/
[2] http://www.Heatmapper.ca/expression/

positive cell (0-100%) at that intensity to reach a final H-score ranging between 0-300 (**Figure 5**). If the H-score was equal to or higher than the mean value of all samples, PD-L1 protein expression was classified as positive, whereas an H-score lower than the mean value was classified as negative PD-L1 protein expression (28, 29).

Data Management and Statistical Analysis

Data were collected and managed using REDCap electronic data capture tools hosted at A. C. Camargo Cancer Center, in São Paulo, Brazil, Hospital do Amor, in Barretos, Brazil, and Hospital das Clínicas and from the Heart Institute of the University of São Paulo (USP). Considering the non-normal distribution of our data, all statistical tests used in this study to examine the difference between categories and groups were non-parametric tests as follows: the chi-square test or Fisher's exact test was used to examine differences in categorical variables, whereas either the Kruskal-Wallis test or the Mann–Whitney U test was used to detect differences in continuous variables between groups of patients. Qualitative data were described using relative frequencies. Overall survival (OS) was defined as the interval from the date of biopsy or surgical resection to death and OS curves were estimated using the Kaplan–Meier method. The Cox proportional hazards model was then used to analyze the association between OS rate and other covariances, and only parameters that presented $P \leq 0.2$ in a univariate analysis were considered for multivariate analysis. We used the Statistical Package of Social Science (SPSS) version 18 for all statistical analysis. All tests with $P<0.05$ were deemed statistically significant and a Bonferroni correction was used when necessary.

RESULTS

Functional Enrichment Analysis of EMT-Related Genes in PNENs

As shown in **Figure 1**, we first created a heatmap distribution of the 17 EMT transcription factors studied in our cohort among PNENs histological types, which showed different levels of expression (FC≥ 2.0). We observed that *BMP1*, *CDH2*, and *KRT14* were upregulated, whereas *CAV2*, *DSC2*, and *IL1RN* were downregulated in all histological subtypes. Furthermore, 12 genes (*BMP1*, *BMP7*, *CALD1*, *CDH1*, *COL3A1*, *COL5A2*, *EGFR*, *ERBB3*, *PLEK2*, *SNAI2*, *STEAP1*, and *TCF4*) were differentially expressed among histological subtypes and were all overexpressed in SCLC and LCNEC when compared to TC and AC.

To assess the function and the biological process that EMT-related genes presented in our cohort, the Metascape analysis were performed. The heatmap of enriched terms across input gene lists included: "extracellular structure organization", "salivary gland morphogenesis", "PID A6B1 A6B4 Integrin Pathway", "endocardial cushion development", "PID AJDISS 2Pathway", "skin development", "heterotypic cell-cell adhesion", "PID Beta Catenin NUC Pathway", "muscle tissue development", and "regulation of neuron differentiation" (**Figure 2A**).

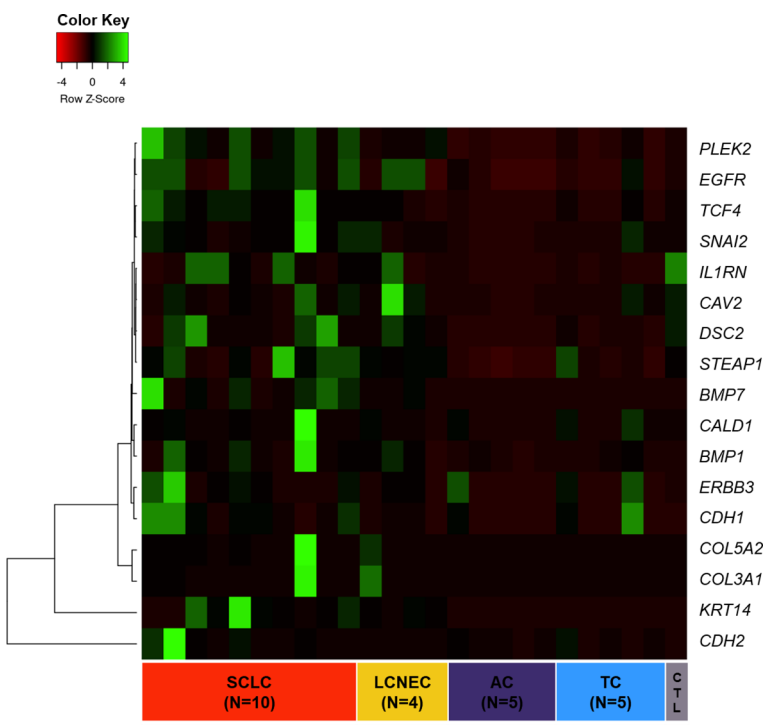

FIGURE 1 | Heatmap of 17 EMT-related genes differentially expressed across PNET histological subtypes.

Figure 2B shows the network formed by these enriched terms. We then consulted the enrichment analysis in DisGeNET and observed that these 17 EMT-related genes are involved in many types of cancers, as shown in **Figure 2C**. Furthermore, we analyzed our gene list using PPI enrichment analyses carried out in the following databases: BioGrid6, InWeb_IM7, and OmniPath. In the resultant network, the three best-scoring terms by p-value were "degradation of the extracellular matrix", "extracellular matrix organization", and "extracellular structure organization". In a second analysis, we investigated the PPI network of these EMT-related genes using the STRING database. Its molecular organization can be visualized as a network of differentially connected nodes shown in **Figure 3**. Each node stands for a protein and the edges represent dynamic interactions.

Association Between EMT Gene Expression and Histological Subtypes

The next step was to explore the association between EMT genes and histotypes as can be appreciated in **Table 1**. We found a significant association between all histological subtypes and 11 differentially expressed EMT transcription factors, including *BMP7*, *COL3A1*, *COL5A2*, *DSC2*, *EGFR*, *IL1RN*, *KRT14*, *PLEK2*, *SNAI2*, *STEAP1*, and *TCF4* (P<0.05). It is worth noting that less differentiated tumors overexpressed of EMT genes, as is the case of SCLC when compared to TC, AC, and LCNEC, except for *DSC2* and *IL1RN* that were underexpressed in PNENs. LCNEC showed intermediate EMT gene expression, with average gene expression levels falling between that of SCLC and carcinoid tumors. TC and AC presented low expression of all the 11 EMT genes when compared to LCNEC and SCLC.

EMT-Like Changes by Transmission Electron Microscopy (TEM)

Subsequently, we examined the PNENs cancer cells by transmission electron microscopy and optical microscopy to find morphologic evidence to correlate with the molecular changes, as shown in **Figure 4**. In TC and AC (**Figures 4A, C**, respectively) the cancer cells were intimately associated with each other through desmosomes located in the lateral membrane although they showed a tenuous disassembly. In contrast, SCLC and LCNEC (**Figures 4B, D**, respectively) showed an intense loss of desmosome morphology and disassembly of cell-cell contacts. The ultrastructure changes revealing mechanical barriers disassembly coincided with loss of cohesiveness between cancer cells visualized at hematoxylin-eosin in PNENs (**Figures 5A–D**).

Association Between PD-L1 Signal and Clinicopathological Features

The next step was to investigate whether PD-L1 functional immune suppressive barrier was also compromised in these tumors (**Figure 5**). In fact, the observation of a negative signal intensity of PD-L1 was associated with high malignant potential tumors, such as SCLC (**Figure 5H**). Furthermore, membranous signal intensity of PD-L1 increased progressively as tumor malignancy, being higher in LCNEC, lower in AC, and lowest in TC (**Figures 5E–G**, respectively). These findings coincided with a significant difference in PD-L1 H-score signal intensity in PNEN tumor cells (P<0.01). A PD-L1 H-score < 1.021 was detected in 13 TC (68.4%), 4 AC (44.4%) and 4 LCNEC (33.3%), whereas a PD-L1 H-score > 1.021 was found in 6 TC (31.6%), 5 AC (55.6%), and 8 LCNEC (66.7%). Moreover, when

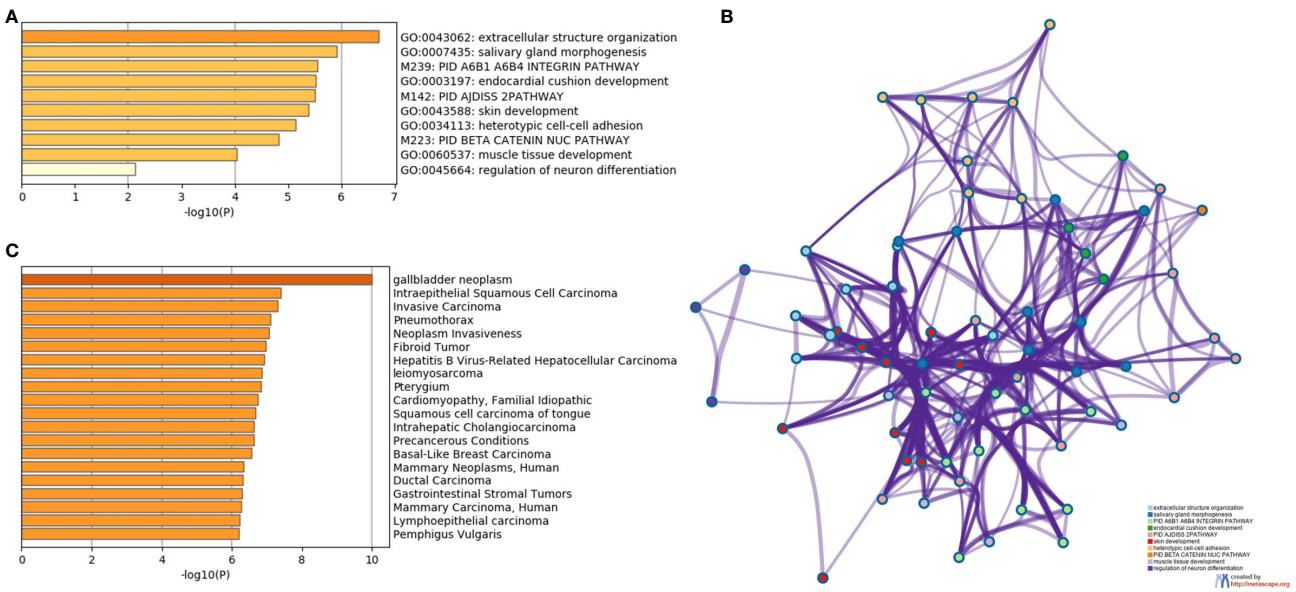

FIGURE 2 | The enrichment analysis of 17 EMT-related genes using Metascape. **(A)** Heatmap of enriched terms colored by P-values. **(B)** Protein-protein interaction network. **(C)** Summary of enrichment analysis in DisGeNET colored by P-values.

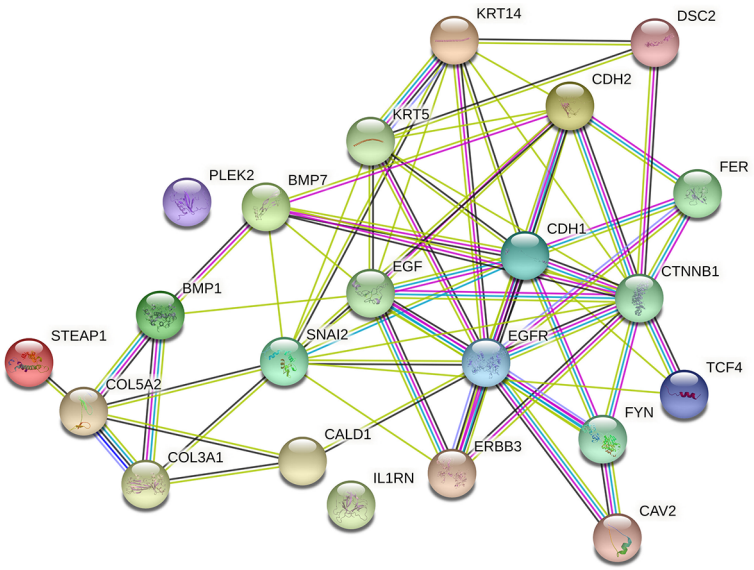

FIGURE 3 | Cluster analysis of the PPI network using STRING database for EMT proteins interactions. The network included the 22 functional partners with the highest interaction confidence score, namely, STEAP1, COL5A2, COL3A1, BMP1, CALD1, IL1RN, ERBB3, SNAI2, BMP7, PLEK2, CAV2, FYN, EGFR, EGF, KRT5, KRT14, CDH1, CTNBB1, TCF4, FER, CDH2, DSC2, (score ≥ 0.9).

the Kruskal-Wallis test was performed, a significant correlation emerged between PD-L1 expression and histological types (P=0.0001). In addition, PD-L1 H-score > 1.021 was significantly associated with advantageous clinicopathologic parameters, such as early stage (I and II) (P=0.03) and N0 status (P=0.02) (**Table 2**).

Of note, we observed a significant inverse association between PD-L1 H-score and the expression of *COL5A2* (R= -0.45; P=0.03), *DSC2* (R= -0.51; P=0.01), *KRT14* (R= -0.46; P=0.02), *IL1RN* (R= -0.53, P=0.01), and *STEAP1* (R= -0.45; P=0.03) by a nonparametric Spearman's rank correlation coefficient. These associations confer an opposite effect between EMT and PD-L1 and might influence the neoplastic cells to control invasion and tumor metastasis.

Association Between EMT Gene Expression and Clinical Characteristics of PNENs Patients

Last but not least, the functional and mechanical molecular barriers players intensifies the clinical scenario of the theatrical course of PNENs. The clinical characteristics of the patients enrolled in our study are summarized in **Table 3**. Patients had a median age at diagnosis of 58 years and were evenly distributed between genders, 34 female and 30 males. Most of the patients were diagnosed at the early stage of disease (32/29) and were smokers (38), mainly in SCLC (21). However, in our cohort, of the 19 TC patients, 9 were smokers, contradicting the fact that in majority of the cases, these patients are never-smokers. Since smoking history was obtained from the patients' electronic

TABLE 1 | Association between median EMT gene expression and histological subtypes of PNENs patients by non-parametric Kruskal-Wallis test, (P<0.05).

EMT mRNA expression	High-grade neuroendocrine tumors		Carcinoid tumors		Control	*P-value*
	SCLC	LCNEC	AC	TC	Lung normal tissue	
BMP7	13.39	4.23	0.41	0.78	2.14	0.003
COL3A1	9.46	5.05	0.59	1.18	2.97	0.006
COL5A2	15.54	3.24	0.64	0.65	2.58	0.005
DSC2	1.10	1.63	0.10	0.54	2.18	0.005
EGFR	9.26	6.90	0.10	0.78	3.09	0.036
IL1RN	0.49	0.49	0.07	0.04	2.57	0.009
KRT14	112.77	76.11	10.55	2.32	2.00	0.010
PLEK2	11.87	3.97	0.25	1.13	2.02	0.002
SNAI2	4.35	2.17	0.38	1.09	2.18	0.005
STEAP1	2.72	2.67	0.67	1.34	2.40	0.010
TCF4	7.74	3.86	0.33	0.65	2.58	0.004

PNENs, pulmonary neuroendocrine neoplasms; TC, typical carcinoid; AC, atypical carcinoid; LCNEC, large cell neuroendocrine carcinoma; SCLC, small cell lung carcinoma.

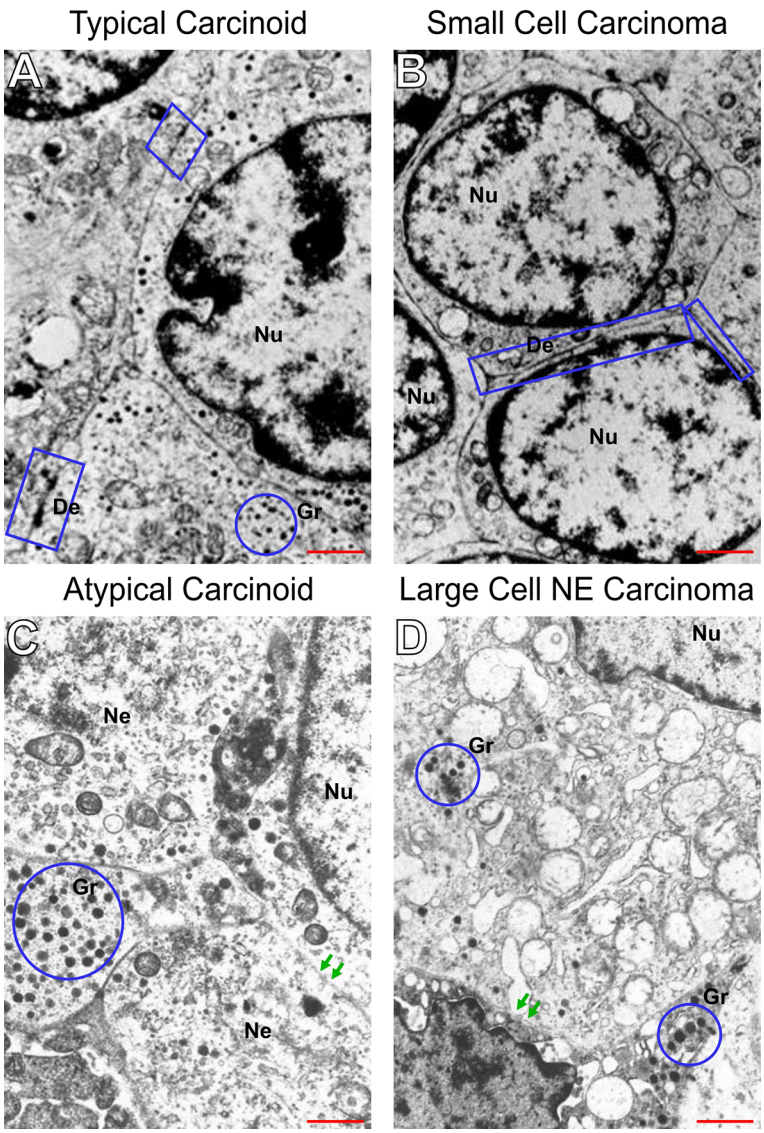

FIGURE 4 | Disruption of intercellular junctional complexes of PNENs cells and enhanced breakdown of the basement membrane. Transmission electron micrographs of PNENs cells in typical carcinoid **(A)**, small cell lung carcinoma **(B)**, atypical carcinoid **(C)**, and large cell neuroendocrine carcinoma **(D)**. Ultrastructural, the TC and SCLC present nucleus with condensed chromatin on the periphery, whereas in AC and LCNEC the nucleus are more vesiculous with sparse distribution of chromatin. The neuroendocrine origin of the four subgroups is evident by different amounts of the NE granules (blue circles) inside of cytoplasmic processes or dispersed in the cytoplasm. In SCLC, the tumor cells were loosely dissociated with each other through tenues desmosomes compared to TC (the electron-dense materials at the lateral side, blue circle). Note that the intercellular junctional complex are not prominent in SCLC compared to TC, suggesting abnormal levels of desmocolin. In contrast, diminishing of electron-dense materials, indicating disruptions of intercellular junctional complexes, and enhanced breakdown of the basement membrane indicating the opening of cell-cell contacts in AC and LCNEC (red arrows). The micrographs are representative PNENs sections from 24 patients. Scale bars: 1 mm. De, desmosomes; Nu, nucleus; Gr, granules; Ne, neuroendocrine.

medical records, this discrepancy was observed and that somehow needs to be proven in the current studies that we are conducting. Fourteen patients of our cohort developed distant metastasis. The median follow-up of the patients was 36 (0–100) months.

We observed statistical differences between the expression of some EMT genes (*BMP1*, *BMP7*, *COL3A1*, *CDH1*, *EGFR*, *EBB3*, *PLEK2*, and *TCF4*) and the clinical stage of patients, especially at the presence of overexpression of these genes. Patients with advanced stage (III/IV) at diagnosis presented tumors that significant overexpressed *BMP1* (61.9%, P=0.042), *BMP7* (47.6%, P=0.008), *CDH1* (57.1%, P=0.002), *COL3A1* (52.4%, P=0.002), *EGFR* (47.6%, P=0.008), *ERBB3* (61.9%, P=0.001), *PLEK2* (57.1%, P=0.003), and *TCF4* (57.1%, P=0.003) (see **Supplementary Figure S1**). Patients with a smoking history also presented a significant difference in gene expression. Their tumors overexpressed *BMP7* (43.5%, P=0.027), *COL3A1* (47.8%, P=0.009), *EGFR* (43.5%, P=0.027), *PLEK2* (56.5%, P=0.001), and

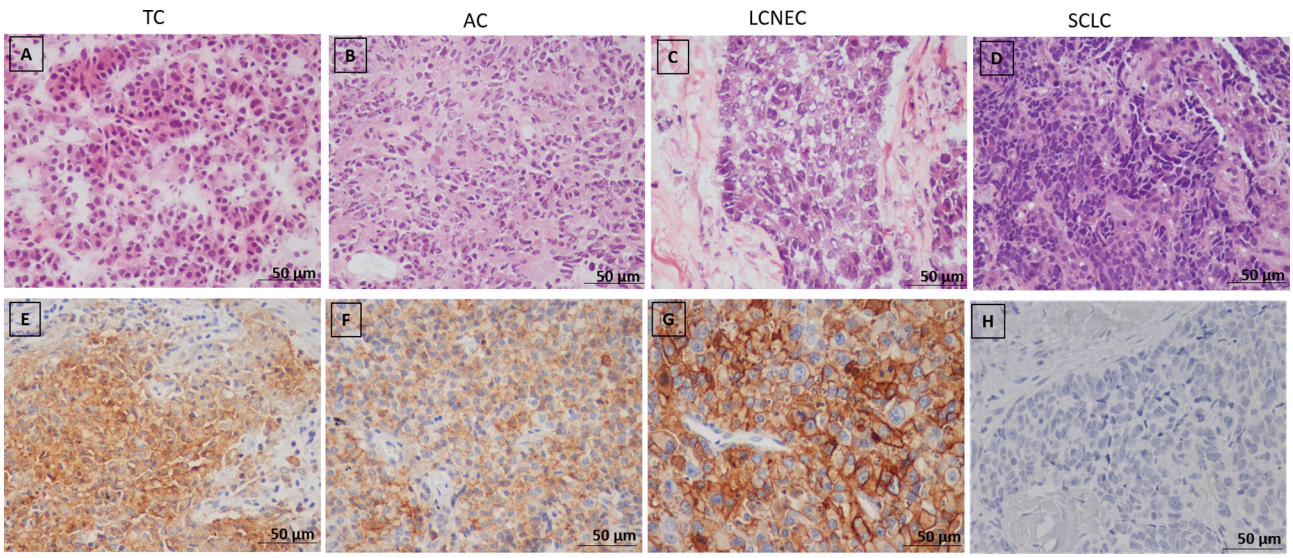

FIGURE 5 | **(A–D)** Representative microphotographs of pulmonary neuroendocrine neoplasms subtypes (H&E), **(A)** Typical carcinoid (TC), **(B)** Atypical carcinoid, **(C)** Large cell neuroendocrine carcinoma (LCNEC), **(D)** Small cell lung carcinoma (SCLC); **(E–H)** Immunohistochemical staining of PD-L1 in PNENs, **(E, F)** Moderate PD-L1 immunostaining in typical (TC) and atypical carcinoid (AC), respectively; **(G)** Strong PD-L1 immunostaining in large cell neuroendocrine carcinoma (LCNEC), **(H)** Negative PD-L1 immunostaining in small cell lung carcinoma (SCLC).

SNAI2 (47.8%, P=0.039) (see **Supplementary Figure S2**). We also found a significant association between patients with lymph node metastasis and overexpression of *BMP7* (47.4%, P=0.005), *CALD1* (42.1%, P=0.020), *CDH1* (52.6%, P=0.001), *COL3A1* (42.1%, P=0.020), *EGFR* (47.4%, P=0.005), *ERBB3* (57.9%, P=0.000), *PLEK2* (47.4%, P=0.024), and *TCF4* (52.6%, P=0.001) (see **Supplementary Figure S3**). Finally, patients with distant metastasis had tumors that overexpressed *COL3A1* (38.9%, P=0.013), and *COL5A2* (38.9%, P=0.038)

TABLE 2 | Correlation between PD-L1 expression in neuroendocrine tumor cells and clinicopathological characteristics of PNENs patients, by Mann-Whitney test, (P<0.05).

Variables	Neuroendocrine tumor cells PD-L1 Expression (mean)	*P*-value*
Gender		
Male	0.71	0.30
Female	1.33	
Age, median (years)		
< 58	0.34	**0.01**
≥ 58	1.80	
Smoking Status		
Yes	0.55	0.80
No	0.77	
Histological subtypes		
CT	1.02	0.05
LCNEC	2.83	
Clinical Stage†		
I-II	0.80	**0.03**
III-IV	0.001	
Lymph node Metastasis		
Yes	0.5	**0.02**
No	1.97	

CT, carcinoid tumors; LCNEC, large cell neuroendocrine carcinoma; PD-L1, programmed death-ligand 1.
†8th Edition International Association for the Study of Lung Cancer (24).
**Bolded values refers to a statistical significance of p-value (P<0.05).*

TABLE 3 | Frequency of demographic and clinical characteristics of PNENs patients.

Characteristics	Number of Patients (N=65)
[a]**Age, years**	
Median (range)	58 (19-80)
<58	34 (52.3%)
≥58	30 (46.2%)
Sex	
[a]*Male*	30 (46.2%)
Female	34 (52.3%)
[a]**Smoking status**	
Yes	38 (58.5%)
No	20 (30.8%)
Histological subtype	
SCLC	23 (35.4%)
LCNEC	13 (20.0%)
AC	10 (15.4%)
TC	19 (29.2%)
[a]**TNM stage**†	
I/II	32 (49.2%)
III/IV	29 (44.6%)
[a]**Distant metastasis**	
M0	32 (49.2%)
M1	14 (21.5%)
Follow-up (months)	36 (0-100)

PNENs, pulmonary neuroendocrine neoplasms; TC, typical carcinoid; AC, atypical carcinoid; LCNEC, large cell neuroendocrine carcinoma; SCLC, small cell lung carcinoma.
[a]Some cases lacked follow-up information: gender (1); age (1); smoking status (7); TNM stage (4); Distant metastasis (19).

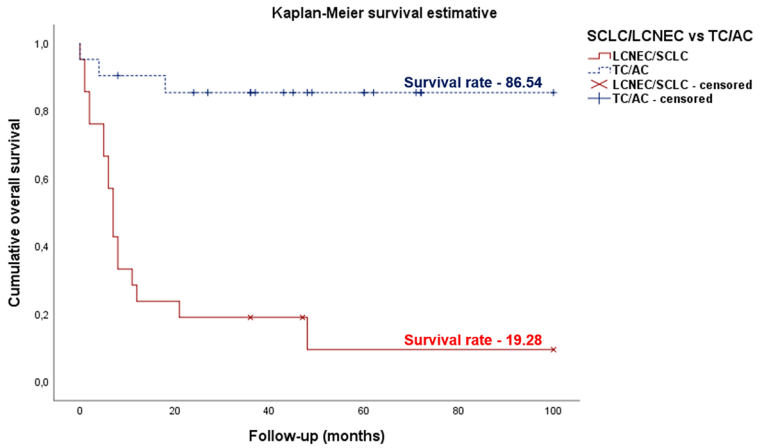

PNET Subtypes	HR (95% CI)	*P*
SCLC	1.62 (0.63-4.12)	0.31
Carcinoid tumors (AC/TC)	0.11 (0.03-0.45)	0.00
LCNEC (reference)	-	0.00

SCLC/LCNEC vs TC/AC	Overall Survival (months)		95% CI	Chi-Square (Log Rank)	*P*
	Mean	Standard Error			
SCLC/LCNEC	19.28	6.83	5.88-32.68	21.21	0.00
TC/AT	86.54	7.02	72.42-100.66		

FIGURE 6 | Kaplan-Meier curve according to the PNENs histological subtypes. Patients diagnosed with carcinoid tumors (TC/AC) appears as top curve (median survival 86.54 months), while those who were diagnosed with high-grade neuroendocrine tumors (SCLC and LCNEC) (bottom curve) had median survival time of 19.28 months (P<0.01 by log-rank test).

(see **Supplementary Figure S4**). We found no statistical differences between these genes and adjuvant treatment, age, or gender in our cohort.

Survival Analysis

As expected, the cumulative survival rate of patients stratified by PNEN morphologic types was significantly higher in carcinoid tumors (86.54 months) than in the LCNEC and SCLC (19.28 months) (log-rank = 21.21, P<0.01) (**Figure 6**). In the Cox univariate analysis, the following variables were significantly associated with low risk of death: tumor T1 stage, N0 stage, M0 stage, and early clinical stage. The down-expression of *CDH1*, *COL3A1*, *DSC2*, *EGFR*, *PLEK2*, and *TCF4* was also associated with a low risk of death (**Table 4**, P<0.01).

EMT gene expression was different between patients of different PNEN variants, who showed distinctly different average survival times in our Kaplan-Meier curve. The group with lower expression of *CDH1*, *COL3A1*, *DSC2*, *EGFR*, *PLEK2*, and *TCF4* (top curve) had a median survival time between 40-63 months. By contrast, those with higher expression of these genes (bottom curve) had a median survival time between just 4-15 months (P ≤ 0.01), as determined by log-rank test (**Figure 7**). Once these variables were accounted for in a multivariate analysis, where the mathematical model was controlled by histology, we found that patients who presented low expression of *COL3A1*, *DSC2*, *EGFR* and *TCF4* as co-dependent variables, as well as low expression of *PLEK2* as an independent variable, were at low risk of death. The chi-square including the covariates was 24.16, (P<0.01).

DISCUSSION

We evaluated EMT-related genes, using a set of twenty-four patients with surgically resected PNENs, including SCLC. These EMT transcription factors were involved in proliferative signals, epithelium desmosomes assembly, and cell motility that support PNENs sequential steps for invasion and metastasis in localized surgically resected primary tumor. We used a two-stage design where we first examined the candidate EMT genes using a whole-genome screen, and subsequently, we analyze the upregulation of these genes through Metascape analysis *in silico* approach. Additionally, high expression of EMT genes involved in cellular proliferation, epithelium desmosomes barrier, and cell motility were significantly associated with lymph node metastasis, and distant metastasis. To complete the sequential steps for invasion and metastasis by PNENs, we evaluated the PD-L1 immune checkpoint status and found an inverse association between EMT genes and PD-L1 expression. Our findings suggest that

TABLE 4 | Variables associated with overall survival (OS) in PNENs patients.

	Univariate Analysis			Multivariate Analysis	
	HR (95% CI)	**HR**	***P*-value**	**HR (95% CI)**	***P*-value***
Clinicopathological Characteristics					
Age, median (yrs): <58 *vs* ≥58	0.60 (0.25-1.41)	0.52	0.24		
Gender					
Male	1.69 (0.71-4.00)	0.52	0.23		
Smoking status					
Yes	4.78 (1.38-16.50)	1.56	**0.01**		
T Stage (Tumor invasion)†					
T1	0.16 (0.04-0.66)	-1.77	**0.01**		
T2	0.51 (0.16-1.63)	0.65	0.26		
T3	0.46 (0.05-3.80)	0.76	0.47		
T4 (reference)			0.08		
Lymph Node Status (N)†					
N_0	0.12 (0.03-0.47)	-2.10	**0.00**		
N_1	0.43 (0.10-1.83)	0.83	0.25		
N2	0.99 (0.26-3.78)	0.00	0.99		
N3 (reference)			**0.00**		
M stage (Distant Metastasis)†					
Absence	0.32 (0.12-0.84)	-1.12	**0.02**		
Clinical stage					
Early (I/II)					
Advanced (III/IV) (reference)	0.16 (0.06-0.43)	-1.81	**0.00**		
Histological subtypes					
SCLC	1.62 (0.63-4.12)	0.48	0.31	3.75 (0.54-25.91)	0.17
	0.11 (0.03-0.45)	-2.12	**0.00**	0.03 (0.001-0.91)	**0.04**
Carcinoid tumors (AC/TC)					
LCNEC (reference)			**0.00**		**0.01**
PD-L1 protein expression (mean)					
< 1.021	1.35 (0.31-5.84)	0.30	0.68		
≥ 1.021 *(reference)*					
EMT gene expression (median)					
***CDH1* mRNA**					
< 2.82 (N=8)	0.06 (0.008-0.53)	-2.71	**0.01**		
≥ 2.82 (N=15) *(reference)*					
***COL3A1* mRNA**					
< 2.97 (N=11)	0.17 (0.04-0.65)	-1.72	**0.00**	0.99 (0.97-1.02)	0.81
≥ 2.97 (N=13) *(reference)*					
***DSC2* mRNA**					
< 2.18 (N=18)	0.16 (0.04-0.59)	-1.79	**0.00**	1.05 (0.82-1.34)	0.66
≥ 2.18 (N=3) *(reference)*					
***EGFR* mRNA**					
< 3.09 (N=12)	0.25 (0.07-0.83)	-1.36	**0.02**	1.07 (0.88-1.31)	0.46
≥ 3.09 (N=11) *(reference)*					
***PLEK2* mRNA**				0.82 (0.69-0.98)	**0.02**
< 2.02 (N=9)	0.14 (0.03-0.68)	-1.92	**0.01**		
≥ 2.02 (N=14) *(reference)*					
***TCF4* mRNA**				1.09 (0.86-1.38)	0.44
< 2.58 (N=9)	0.13 (0.03-0.65)	-1.97	**0.01**		
≥ 2.58 (N=14) *(reference)*					

Univariate and multivariate analysis employed a Cox proportional hazards model. Chi-square 24.16, P=0.001.

HR, hazard ratio (β coefficient); CI, confidence interval; PD-L1, Programmed death-ligand; EMT, epithelial-to-mesenchymal transition.

†8th Edition International Association for the Study of Lung Cancer (24).

**Bolded values refers to a statistical significance of p-value (P<0.05).*

One case lacked follow-up information about survival.

incorporation of EMT-related gene expression profile to routine genome-wide examination of biomarkers helps to predict metastasis in PNENs and may be a promising tool to select and customize therapy.

Over the past decade, treatment options for metastatic PNENs have increased, although mortality and 5-year survival remain little altered for PNETs (30) and PNECs (31, 32). Molecular studies identified somatic mutations, somatic copy numbers, and pathway alterations in primary PNENs tumors (16–18); however, less is known regarding the steps of the molecular events for invasion and metastasis by PNENs, more lethal and therapeutically relevant. It is worth emphasizing that PNENs, unlike other lung tumors, are solid tumors basically composed of highly cohesive epithelial cells intermingled by thin

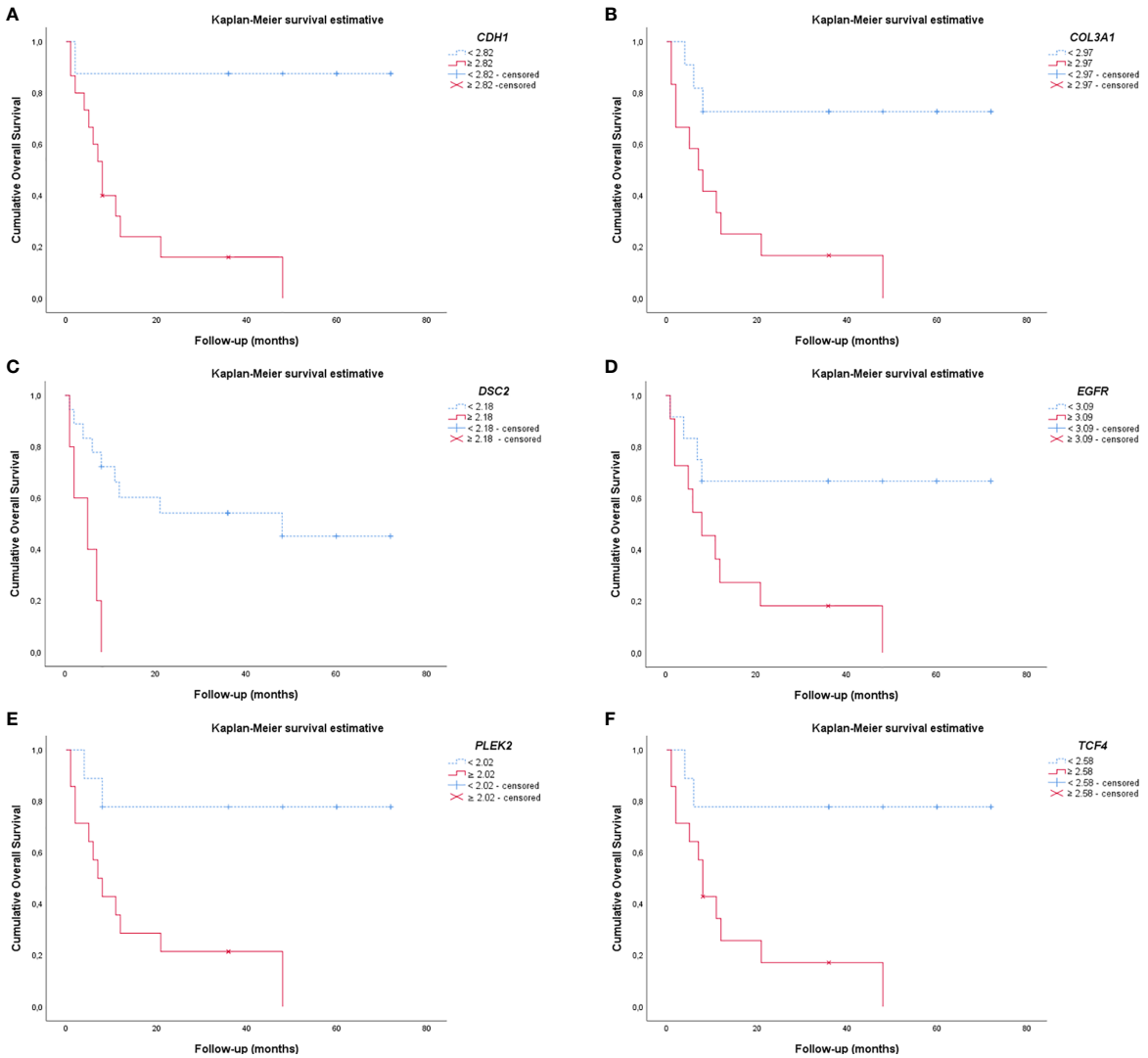

FIGURE 7 | Kaplan-Meier curves show the difference in EMT gene expression between patients regarding the PNENs variants and the risk of death. **(A)** *CDH1*; **(B)** *COL3A1*; **(C)** *DSC2*; **(D)** *EGFR*; **(E)** *PLEK2* and **(F)** *TCF4*. For all these EMT genes, patients that had lower expression appeared as the top curve, and their median survival time ranged between 40-63 months. In contrast, patients with higher expression of these genes (bottom curve) had a median survival time range of 4-15 months ($P \leq 0.01$ by log-rank test).

connective tissue septa and thin-walled vessels with a limited number of immune cells. In this context, the matricellular and vascular structure of the adjacent lung parenchyma represents the scenario for invasion. Therefore, studies that interrogate genes in tumors associated with cohesiveness of neoplastic cells, and their motility, are critical to understanding the biology of invasion and metastasis in these tumors, the major cause of patient mortality.

The process of cancer cell invasion and metastasis undoubtedly comprises a series of complex multistep process in which phenotype differences are mediated by a network of transcription factors. Among these, the EMT process signalized by tumor cells is thought to be important because facilitates cancer cell detachment, motility and penetration into blood and lymphatic vessels. Thus, a clear knowledge of EMT underlying molecular mechanism is crucial for effective targeted therapies. Despite extensive efforts, the regulatory mechanism of EMT in most cell/tissue types is not fully resolved as in case of the complex PNENs (33, 34). In order to understand the roles of EMT transcription factors in metastatic process, we explored the mRNA level in PNENs. Overall, we observed that the EMT-related genes were upregulated in SCLC, downregulated in carcinoid tumors, and presented an intermediate level of expression in LCNEC. In fact, the expression of EMT genes was much lower in carcinoid tumors when compared to SCLC and LCNEC, offering a plausible explanation for their progressive changes in phenotype and clinical spectrum, discussed below.

We found that EMT-related genes including cadherin, desmocollin, collagen, and tyrosine kinase receptors were overexpressed in PNENs. Actually, Gene Ontology and functional enrichment analysis confirmed that these highly enriched and overrepresented genes are implicated in cellular and extracellular barriers to mediate motility, invasion, and metastasis. In agreement with other studies, our results support the notion that the synergistic action of these EMT master transcription factors, functioning as invasion oncogenes in PNENs (35–37).

Notably, by transmission electron microscopy we showed that desmosomes disassembly barrier intensity was the expression phenotype factor that coincided with the levels of EMT genes encoding six barrier molecules, including *BMP1*, *BMP7*, *CALD1*, *KRT14*, *CAV2*, *IL1RN*, and three adherent junctions proteins (CDH1, CDH2, DSC2), associated to risk of lymph node and distant metastasis in PNENs. Accordingly, we have found that PNETs and PNECs expressed high levels of *BMP1*, *CDH2*, and low levels of *CAV2*, *DSC2*, *IL1RN*, whereas *BMP7*, *CALD1*, and *CDH1*, were overexpressed by PNECs and low expressed by PNETs, suggesting a positive autogenous transcriptional regulation involving activation of the EMT-related genes by phosphorylation (38) to maintain the mechanical barriers between neoplastic cells. Actually, barriers can be mediated through both tight junctions and desmosomal adhesion. Desmosomes, or macula adherens, are intermediate filament-based cell–cell adhesions using desmosomal cadherins anchored to intermediate filaments *via* desmoplakins. Expression of desmosomal barrier molecules has been observed in several solid tumors, with mixed prognostic associations. In melanoma, elevated levels of the cadherin desmocollin 3 (DSC3) has been associated with increased metastatic risk, but in colon and lung cancer, it has been associated with a better prognosis (39–41).

Remarkably, we have also found that the expression of PD-L1, which has an immunosupressive function in the anti-tumor immune reaction, correlated inversely with EMT transcription factors related to barriers (*CDH2*, *CAV2*, *DSC2*, and *IL1RN*). This inverse relationship was previously demonstrated in melanoma and ovary cancer in a well-designed study done by Salerno and colleagues (42). According to those authors, physical or mechanical barriers created by endothelial or epithelial cells with tight junctions, or functional barriers created by immunosuppressive molecules including PD-L1 (43) can also limit the immune cell infiltration valued as immune escape by tumors which can otherwise be targeted effectively with immunotherapy (44). Here, we provide two important evidence. First, carcinoids and large cell neuroendocrine carcinomas can express functional barriers created by immunosuppressive PD-L1 thus limiting the immune cell infiltration to reward the low expression of the desmosomes disassembly barrier, justifying the longer survival of the patients even with metastasis. Second, small cell lung carcinomas are associated with the lack of PD-L1 immunosuppressive barrier allowing the immune cell infiltration, but with high expression of desmosomes disassembly barrier, both facilitators of distant metastasis and shorter overall patient survival, otherwise be targeted effectively with immunotherapy PD-L1 expression. Third, the high levels of EMT transcriptions factors expressed by SCLC cells can confer mesenchymal properties, on the one hand justifying its histologic fusiform pattern, and on the other hand the acquisition of immune regulatory capacities for checkpoint blockade immunotherapy, as recently demonstrated in an elegant work made by Kursunel and colleagues (14).

Our current understanding of EMT may also be associated to the established transcriptional regulators that are classically studied separately. Therefore, the synergistic action among cooperative transcriptional factors, which has emerged as a general characteristic of enhancers (45), has not been included in the transcriptional programs of EMT. In sharp divergence to the established EMT model, in which a single transcriptions factor such as *SNAI2* controls the EMT program, we identified other master transcriptional factors suggesting a synergistical control of the EMT transcriptional program in metastatic behavior of PNENs, reinforcing the idea that EMT is a phenomenon highly dependent on the PNENs cellular machinery in which it occurs.

String database analysis confirmed the PPI network of these EMT-related genes, its molecular organization as a network of differentially connected nodes, and dynamic synergism. We found that *EGFR* and *ERBB3* were also upregulated in PNECs and downregulated in PNETs and may synergistically determine a positive feedback with desmosomes disassembly barrier. This finding gains strength in the literature by demonstrating that inhibition of *EGFR* promotes desmosome assembly by upregulation of desmosomal proteins such as desmoglein 2 and desmocollin 2 in squamous cell carcinoma of head and neck (46). In another study, activation of *EGFR* led to decreased protein levels of *DSC3*, whereas *EGFR* inhibition resulted in enhanced expression of *DSC3*, indicating an *EGFR*-dependent regulation of *DSC3* in lung cancer. Interestingly, these authors also found the inhibition of *EGFR* by gefitinib increased the expression of *DSC3* (39).

Importantly, EMT genes are involved in crucial processes, such as cellular development and differentiation, cellular growth and proliferation, cell migration and motility, and extracellular matrix invasion and cellular adhesion. Regarding *TCF4* transcription factor, it has been reported that it plays a key role in the initiation of colorectal cancer progression through the upregulation of β-catenin/*TCF4* target genes, such as c-*MYC*, *AXIN2*, and *LGR5*, regulating cell proliferation and stemness in epithelial stem and progenitor cells (47). In lung adenocarcinoma, *STEAP1* is reported to be involved in processes closely associated with cancer cell proliferation, such as cell division, cytokine production, cytokine signaling, and DNA replication (48). In addition, *PLEK2* interacts with the actin cytoskeleton to induce cell spreading, whereas *IL1RN* modulates immune and inflammatory responses, and *SNAI2* facilitate microenvironment invasion and dissemination (49, 50). However, there is limited knowledge of the role of these EMT-related genes in neuroendocrine tumors.

In our cohort, EMT genes as *COL3A1*, *COL5A2*, *PLEK2*, and *SNAI2* presented high expression in PNECs and low expression

in PNETs. As PNENs are tumors with a limited stroma, the question is how the tumor cells migrate to gain access into vessels? Recently, mechanical properties of tissue have growing sympathy for tissue stiffness, defined as the resistance to deformation in response to applied force, in a multitude of biological processes (51). Gene expression is controlled by spatial and temporal variability of tissue stiffness and, ultimately, determine the differentiation lineages of stem cells (52). Not least important, different gradients in tissue stiffness works as powerful signal to guide migrating cells during cancer dissemination (53, 54).

Therefore, we speculate that neuroendocrine cancer cells transformed by EMT process acquire stem-like and mesenchymal properties to upregulate tissue stiffness by increasing ECM deposition facilitating motility and permeation in vessels. This powerful feedforward loop raises numerous possibilities for drug development and warrants further investigation into the mechanisms specific to different PNENs.

Taken together, the molecular and ultrastructural events described here may justify the progressive changes in phenotype and clinical spectra of PNENs. The dysregulated expression of *BMP1*, *BMP7*, *CALD1*, *KRT14*, *CAV2*, *IL1RN*, and adherent junctions proteins (CDH1, CDH2, DSC2), promotes the primordial detachment between the distal cancer cells, depriving the central cancer cells of the blood supply leading to comedonecrosis in AC and LCNEC and "geographic" in SCLC. *EGFR* and *ERBB3* were also upregulated in PNECs and downregulated in PNETs promoting the cancer cell proliferation, justifying the progressive increase of Ki67 antigen detected within the nucleus during interphase, and increased mitosis index after the protein relocation to the surface of the chromosomes. In this context, the Ki-67 protein increases during all active phases of the cell cycle (G1, S, G2, and mitosis) from TC to SCLC.

Evidently, these molecular biomarkers may justify the differences between the clinicopathologic features and survival analysis of SCLC/LCNEC and carcinoid tumors. In fact, a Cox multivariate analysis showed that when the mathematical model was controlled by histology, patients that presented low expression of *COL3A1*, *DSC2*, *EGFR*, and *TCF4*, as co-dependent factors, and low expression of *PLEK2*, as an independent factor, lead to a significantly low risk of death and better survival in PNENs patients.

In summary, the results presented herein provide important molecular evidence that EMT-related genes are involved in cancer cell proliferative signals, desmosomes disassembly, and cell motility that support PNENs sequential steps for invasion and metastasis in localized surgically resected primary tumor. Specifically, our study indicates that PNENs overexpressing EMT-mechanical molecular barriers, genes lack functional immune suppressive barrier and present increased patient mortality risk due to metastasis and thus potentially offer insight into novel therapeutic targets. Overall, these EMT genes may represent partially an EMT 'remodeling' program to drive metastatic establishment.

DATA AVAILABILITY STATEMENT

The original contributions presented in the study are publicly available. This data can be found here: https://www.ncbi.nlm.nih.gov/geo/query/acc.cgi?acc=GSE181381.

ETHICS STATEMENT

The study was approved in accordance with the ethical standards of the responsible committee on human experimentation local (Research Ethics Committee of University of São Paulo Medical School - CAAE:17436113.9.0000.0068; opinion number: 1.0077.100) and with the 1964 Helsinki declaration. A waiver of the requirement for informed consent was obtained from committee, and to identity of the subjects under this retrospective analysis was omitted and anonymized. Written informed consent for participation was not required for this study in accordance with the national legislation and the institutional requirements.

AUTHOR CONTRIBUTIONS

Conception and design: VLC and TP. Writing, review, and editing: VLC, TP, CB, and JM-R. Data analysis and interpretation: VLC, TP, and CB. Statistical analysis: CF, VLC, and TP. Provision of study materials or patients: MB, AA, ES, EO, VS, and TT. Administrative support: VLC. All authors contributed to the article and approved the submitted version.

FUNDING

This work was supported by Sao Paulo Research Foundation (FAPESP; 2018/20403-6, 2019/12151-0) and the National Council for Scientific and Technological Development (CNPq; 483005/2012-6). The SP263 antibody was granted as courtesy by Roche Diagnostics (Roche-Ventana, Tucson, USA).

ACKNOWLEDGMENTS

We are grateful to Ms. Esmeralda Miristeni Eher and Ms. Sandra de Morais Fernezlian for their expertise on immunohistochemical protocols. Funding/Support: This work was supported by Sao Paulo Research Foundation (FAPESP; 2018/20403-6, 2019/12151-0) and the National Council for Scientific and Technological Development (CNPq; 483005/2012-6). The SP263 antibody was granted as courtesy by Roche Diagnostics (Roche-Ventana, Tucson, USA).

SUPPLEMENTARY MATERIAL

The Supplementary Material for this article can be found online at: https://www.frontiersin.org/articles/10.3389/fonc.2021.645623/full#supplementary-material

Supplementary Figure 1 | Box plot of the associations between EMT gene expression and Clinical stage – Early (I/II) *vs* Advanced (III/IV) in a log scale. The top and bottom of the box plot represents the 25th and 75th percentile range. The line across the box shows the median of gene expression and the top and bottom bars show the maximum and minimum values, outliers were showed. The association between EMT gene expression and Clinical stage was calculated by Fisher's exact test. **(A)** *BMP1*mRNA (P=0.042); **(B)** *BMP7*mRNA (P=0.008); **(C)** *CDH1*mRNA (P=0.002); **(D)** *COL3A1*mRNA (P=0.002); **(E)** *EGFR* mRNA (P=0.008); **(F)** *ERBB3*mRNA (P=0.001); **(G)** *PLEK2*mRNA (P=0.003) and **(H)** *TCF4*mRNA (P=0.003).

Supplementary Figure 2 | Box plot of the associations between EMT gene expression and smoking status (smoker *vs* non-smoker) in a log scale. The top and bottom of the box plot represents the 25th and 75th percentile range. The line across the box shows the median of gene expression and the top and bottom bars show the maximum and minimum values, outliers were showed. The association between EMT gene expression and smoking status was calculated by Fisher's exact test. **(A)** *BMP7*mRNA (P=0.027); **(B)** *COL3A1*mRNA (P=0.009); **(C)** *EGFR*mRNA (P=0.027); **(D)** *PLEK2*mRNA (P=0.001) and **(E)** *SNAI2*mRNA (P=0.039).

Supplementary Figure 3 | Box plot of the associations between EMT gene expression and lymph node metastasis (absence *vs* presence) in a log scale. The top and bottom of the box plot represents the 25th and 75th percentile range. The line across the box shows the median of gene expression and the top and bottom bars show the maximum and minimum values, outliers were showed. The association between EMT gene expression and lymph node metastasis was calculated by Fisher's exact test. **(A)** *BMP7* mRNA (P=0.005); **(B)** *CALD1*mRNA (P=0.020); **(C)** *CDH1*mRNA (P=0.001); **(D)** *COL3A1*mRNA (P=0.020); **(E)** *EGFR*mRNA (P=0.005); **(F)** *ERBB3*mRNA (P=0.000); **(G)** *PLEK2*mRNA (P=0.024) and **(H)** *TCF4*mRNA (P=0.001).

Supplementary Figure 4 | Box plot of the associations between EMT gene expression and distant metastasis (absence *vs* presence) in a log scale. The top and bottom of the box plot represents the 25th and 75th percentile range. The line across the box shows the median of gene expression and the top and bottom bars show the maximum and minimum values, outliers were showed. The association between EMT gene expression and distant metastasis was calculated by Fisher's exact test. **(A)** *COL3A1*mRNA (P=0.013) and **(B)** *COL5A2*mRNA (P=0.038).

REFERENCES

1. Rindi G, Klimstra DS, Abedi-Ardekani B, Asa SL, Bosman FT, Brambilla E, et al. A Common Classification Framework for Neuroendocrine Neoplasms: An International Agency for Research on Cancer (IARC) and World Health Organization (WHO) Expert Consensus Proposal. *Mod Pathol* (2018) 31:1770–86. doi: 10.1038/s41379-018-0110-y
2. Derks JL, Leblay N, Thunnissen E, van Suylen RJ, den Bakker M, Groen HJM, et al. Molecular Subtypes of Pulmonary Large-Cell Neuroendocrine Carcinoma Predict Chemotherapy Treatment Outcome. *Clin Cancer Res* (2018) 24:33–42. doi: 10.1158/1078-0432.CCR-17-1921
3. Derks JL, van Suylen RJ, Thunnissen E, den Bakker MA, Groen HJ, Smit EF, et al. Chemotherapy for Pulmonary Large Cell Neuroendocrine Carcinomas: Does the Regimen Matter? *Eur Respir J* (2017) 49:1601838. doi: 10.1183/13993003.01838-2016
4. Dasari A, Mehta K, Byers LA, Sorbye H, Yao JC. Comparative Study of Lung and Extrapulmonary Poorly Differentiated Neuroendocrine Carcinomas: A SEER Database Analysis of 162,983 Cases. *Cancer* (2018) 124:807–15. doi: 10.1002/cncr.31124
5. Wang J, Ye L, Cai H, Jin M. Comparative Study of Large Cell Neuroendocrine Carcinoma and Small Cell Lung Carcinoma in High-Grade Neuroendocrine Tumors of the Lung: A Large Population-Based Study. *J Cancer* (2019) 10:4226–36. doi: 10.7150/jca.33367
6. Cives M, Rizzo F, Simone V, Bisceglia F, Stucci S, Seeber A, et al. Reviewing the Osteotropism in Neuroendocrine Tumors: The Role of Epithelial-Mesenchymal Transition. *Neuroendocrinology* (2015) 103:321–34. doi: 10.1159/000438902
7. Van Loon K, Zhang L, Keiser J, Carrasco C, Glass K, Ramirez MT, et al. Bone Metastases and Skeletal-Related Events From Neuroendocrine Tumors. *Endocr Connect* (2015) 4:9–17. doi: 10.1530/EC-14-0119
8. Cives M, Quaresmini D, Rizzo FM, Felici C, D'Oronzo S, Simone V, et al. Osteotropism of Neuroendocrine Tumors: Role of the CXCL12/CXCR4 Pathway in Promoting EMT *In Vitro*. *Oncotarget* (2017) 8:22534–49. doi: 10.18632/oncotarget.15122
9. May MS, Kinslow CJ, Adams C, Saqi A, Shu CA, Chaudhary KR, et al. Outcomes for Localized Treatment of Large Cell Neuroendocrine Carcinoma of the Lung in the United States. *Transl Lung Cancer Res* (2021) 10:71–9. doi: 10.21037/tlcr-20-374
10. Yao Y, Zhou Y, Yang Z, Huang H, Shen H. Adjuvant Chemotherapy Following Surgical Resection Improves Survival in Patients With Early Stage Small Cell Lung Cancer. *Oncol Res* (2019) 27:203–10. doi: 10.3727/096504018X15202953107093
11. Pearse AG. The Cytochemistry and Ultrastructure of Polypeptide Hormone-Producing Cells of the APUD Series and the Embryologic, Physiologic and Pathologic Implications of the Concept. *J Histochem Cytochem* (1969) 17:303–13. doi: 10.1177/17.5.303
12. Gould VE, Memoli VA, Dardi LE. Multidirectional Differentiation in Human Epithelial Cancers. *J Submicrscopic Cytol* (1981) 13:97–115.
13. Lloyd RV. Overview of Neuroendocrine Cells and Tumors. *Endocr Pathol* (1996) 7:323–8. doi: 10.1007/BF02739840
14. Kursunel MA, Taskiran EZ, Tavukcuoglu E, Yanik H, Demirag F, Karaosmanoglu B, et al. Small Cell Lung Cancer Stem Cells Display Mesenchymal Properties and Exploit Immune Checkpoint Pathways in Activated Cytotoxic T Lymphocytes. *Cancer Immunol Immunother* (2021). doi: 10.1007/s00262-021-02998-1
15. George J, Lim JS, Jang SJ, Cun Y, Ozretić L, Kong G, et al. Comprehensive Genomic Profiles of Small Cell Lung Cancer. *Nature* (2015) 524:47–53. doi: 10.1038/nature14664
16. Lee JK, Lee J, Kim S, Kim S, Youk J, Park S, et al. Clonal History and Genetic Predictors of Transformation Into Small-Cell Carcinomas From Lung Adenocarcinomas. *J Clin Oncol* (2017) 35:3065–74. doi: 10.1200/JCO.2016.71.9096
17. Rekhtman N, Pietanza MC, Hellmann MD, Naidoo J, Arora A, Won H, et al. Next-Generation Sequencing of Pulmonary Large Cell Neuroendocrine Carcinoma Reveals Small Cell Carcinoma-Like and Non-Small Cell Carcinoma-Like Subsets. *Clin Cancer Res* (2016) 22:3618–29. doi: 10.1158/1078-0432.CCR-15-2946
18. Peifer M, Fernández-Cuesta L, Sos ML, George J, Seidel D, Kasper LH, et al. Integrative Genome Analyses Identify Key Somatic Driver Mutations of Small-Cell Lung Cancer. *Nat Genet* (2012) 44:1104–10. doi: 10.1038/ng.2396
19. Baine MK, Rekhtman N. Multiple Faces of Pulmonary Large Cell Neuroendocrine Carcinoma: Update With a Focus on Practical Approach to Diagnosis. *Transl Lung Cancer Res* (2020) 9:860–78. doi: 10.21037/tlcr.2020.02.13
20. Le Loarer F, Watson S, Pierron G, de Montpreville VT, Ballet S, Firmin N, et al. SMARCA4 Inactivation Defines a Group of Undifferentiated Thoracic Malignancies Transcriptionally Related to BAF-Deficient Sarcomas. *Nat Genet* (2015) 47:1200–5. doi: 10.1038/ng.3399
21. Makise N, Yoshida A, Komiyama M, Nakatani F, Yonemori K, Kawai A, et al. Dedifferentiated Liposarcoma With Epithelioid/Epithelial Features. *Am J Surg Pathol* (2017) 41:1523–31. doi: 10.1097/PAS.0000000000000910
22. Sauter JL, Graham RP, Larsen BT, Jenkins SM, Roden AC, Boland JM. SMARCA4-Deficient Thoracic Sarcoma: A Distinctive Clinicopathological Entity With Undifferentiated Rhabdoid Morphology and Aggressive Behavior. *Mod Pathol* (2017) 30:1422–32. doi: 10.1038/modpathol.2017.61

23. Rekhtman N, Montecalvo J, Chang JC, Alex D, Ptashkin RN, Ai N, et al. Smarca4-Deficient Thoracic Sarcomatoid Tumors Represent Primarily Smoking-Related Undifferentiated Carcinomas Rather Than Primary Thoracic Sarcomas. *J Thorac Oncol* (2020) 15:231–47. doi: 10.1016/j.jtho.2019.10.023
24. Goldstraw P, Chansky K, Crowley J, Rami-Porta R, Asamura H, Eberhardt WE, et al. The IASLC Lung Cancer Staging Project: Proposals for Revision of the TNM Stage Groupings in the Forthcoming (Eighth) Edition of the TNM Classification for Lung Cancer. *J Thorac Oncol* (2016) 11:39–51. doi: 10.1016/j.jtho.2015.09.009
25. Zhou Y, Zhou B, Pache L, Chang M, Khodabakhshi AH, Tanaseichuk O, et al. Metascape Provides a Biologist-Oriented Resource for the Analysis of Systems-Level Datasets. *Nat Commun* (2019) 10:1523. doi: 10.1038/s41467-019-09234-6
26. Szklarczyk D, Gable AL, Lyon D, Junge A, Wyder S, Huerta-Cepas J, et al. STRING V11: Protein-Protein Association Networks With Increased Coverage, Supporting Functional Discovery in Genome-Wide Experimental Datasets. *Nucleic Acids Res* (2019) 47:D607–D13. doi: 10.1093/nar/gky1131
27. Livak KJ, Schmittgen TD. Analysis of Relative Gene Expression Data Using Real-Time Quantitative PCR and the 2(-Delta Delta C(T)) Method. *Methods* (2001) 25:402–8. doi: 10.1006/meth.2001.1262
28. Balancin ML, Teodoro WR, Baldavira CM, Prieto TG, Farhat C, Velosa AP, et al. Different Histological Patterns of Type-V Collagen Levels Confer a Matrices-Privileged Tissue Microenvironment for Invasion in Malignant Tumors With Prognostic Value. *Pathol Res Pract* (2020) 216:153277. doi: 10.1016/j.prp.2020.153277
29. Balancin ML, Teodoro WR, Farhat C, de Miranda TJ, Assato AK, de Souza, et al. An Integrative Histopathologic Clustering Model Based on Immuno-Matrix Elements to Predict the Risk of Death in Malignant Mesothelioma. *Cancer Med* (2020b) 9:4836–49. doi: 10.1002/cam4.3111
30. Lenotti E, Alberti A, Spada F, Amoroso V, Maisonneuve P, Grisanti S, et al. Outcome of Patients With Metastatic Lung Neuroendocrine Tumors Submitted to First Line Monotherapy With Somatostatin Analogs. *Front Endocrinol (Lausanne)* (2021) 12:669484. doi: 10.3389/fendo.2021.669484
31. Ferrara MG, Stefani A, Simbolo M, Pilotto S, Martini M, Lococo F, et al. Large Cell Neuro-Endocrine Carcinoma of the Lung: Current Treatment Options and Potential Future Opportunities. *Front Oncol* (2021) 11:650293. doi: 10.3389/fonc.2021.650293
32. Riess JW, Jahchan NS, Das M, Zach Koontz M, Kunz PL, Wakelee HA, et al. A Phase Iia Study Repositioning Desipramine in Small Cell Lung Cancer and Other High-Grade Neuroendocrine Tumors. *Cancer Treat Res Commun* (2020) 23:100174. doi: 10.1016/j.ctarc.2020.100174
33. Hanahan D, Weinberg RA. Hallmarks of Cancer: The Next Generation. *Cell* (2011) 144:646–74. doi: 10.1016/j.cell.2011.02.013
34. Thiery JP, Sleeman ,JP. Complex Networks Orchestrate Epithelial-Mesenchymal Transitions. *Nat Rev Mol Cell Biol* (2006) 7:131–42. doi: 10.1038/nrm1835
35. Chang H, Liu Y, Xue M, Liu H, Du S, Zhang L, et al. Synergistic Action of Master Transcription Factors Controls Epithelial-to-Mesenchymal Transition. *Nucleic Acids Res* (2016) 44:2514–27. doi: 10.1093/nar/gkw126
36. Salon C, Moro D, Lantuejoul S, Brichon PY, Drabkin H, Brambilla C, et al. E-Cadherin-Beta-Catenin Adhesion Complex in Neuroendocrine Tumors of the Lung: A Suggested Role Upon Local Invasion and Metastasis. *Hum Pathol* (2004) 35:1148–55. doi: 10.1016/j.humpath.2004.04.015
37. Pelosi G, Scarpa A, Puppa G, Veronesi G, Spaggiari L, Pasini F, et al. Alteration of the E-Cadherin/Beta-Catenin Cell Adhesion System is Common in Pulmonary Neuroendocrine Tumors and is an Independent Predictor of Lymph Node Metastasis in Atypical Carcinoids. *Cancer* (2005) 103:1154–64. doi: 10.1002/cncr.20901
38. Mitrophanov AY, Groisman EA. Positive Feedback in Cellular Control Systems. *Bioessays* (2008) 30:542–55. doi: 10.1002/bies.20769
39. Cui T, Chen Y, Yang L, Knosel T, Huber O, Pacyna-Gengelbach M, et al. The P53 Target Gene Desmocollin 3 Acts as a Novel Tumor Suppressor Through Inhibiting EGFR/ERK Pathway in Human Lung Cancer. *Carcinogenesis* (2012) 33:2326–33. doi: 10.1093/carcin/bgs273
40. Cui T, Chen Y, Yang L, Knosel T, Zoller K, Huber O, et al. DSC3 Expression is Regulated by P53, and Methylation of DSC3 DNA is a Prognostic Marker in Human Colorectal Cancer. *Br J Cancer* (2011) 104:1013–9. doi: 10.1038/bjc.2011.28
41. Rezze GG, Fregnani JH, Duprat J, Landman G. Cell Adhesion and Communication Proteins are Differentially Expressed in Melanoma Progression Model. *Hum Pathol* (2011) 42:409–18. doi: 10.1016/j.humpath.2010.09.004
42. Salerno EP, Bedognetti D, Mauldin IS, Deacon DH, Shea SM, Pinczewski J, et al. Human Melanomas and Ovarian Cancers Overexpressing Mechanical Barrier Molecule Genes Lack Immune Signatures and Have Increased Patient Mortality Risk. *Oncoimmunology* (2016) 5:e1240857. doi: 10.1080/2162402X.2016.1240857
43. Shechter R, London A, Schwartz M. Orchestrated Leukocyte Recruitment to Immune-Privileged Sites: Absolute Barriers *Versus* Educational Gates. *Nat Rev Immunol* (2013) 13:206–18. doi: 10.1038/nri3391
44. Topalian SL, Hodi FS, Brahmer JR, Gettinger SN, Smith DC, McDermott DF, et al. Safety, Activity, and Immune Correlates of Anti-PD-1 Antibody in Cancer. *N Eng J Med* (2012) 366:2443–54. doi: 10.1056/NEJMoa1200690
45. Spitz F, Furlong EE. Transcription Factors: From Enhancer Binding to Developmental Control. *Nat Rev Genet* (2012) 13:613–26. doi: 10.1038/nrg3207
46. Lorch JH, Klessner J, Park JK, Getsios S, Wu YL, Stack MS, et al. Epidermal Growth Factor Receptor Inhibition Promotes Desmosome Assembly and Strengthens Intercellular Adhesion in Squamous Cell Carcinoma Cells. *J Biol Chem* (2004) 279:37191–200. doi: 10.1074/jbc.M405123200
47. Satoh K, Yachida S, Sugimoto M, Oshima M, Nakagawa T, Akamoto S, et al. Global Metabolic Reprogramming of Colorectal Cancer Occurs at Adenoma Stage and is Induced by MYC. *Proc Natl Acad Sci USA* (2017) 114:E7697–706. doi: 10.1073/pnas.1710366114
48. Guo Q, Ke X, Liu Z, Gao W-L, Fang S-X, Chen C, et al. Evaluation of the Prognostic Value of STEAP1 in Lung Adenocarcinoma and Insights Into its Potential Molecular Pathways *via* Bioinformatic Analysis. *Front Genet* (2020) 11:242. doi: 10.3389/fgene.2020.00242
49. Otsuki Y, Saya H, Arima Y. Prospects for New Lung Cancer Treatments That Target EMT Signaling. *Dev Dynam* (2018) 247:462–72. doi: 10.1002/dvdy.24596
50. Movva S, Wen W, Chen W, Millis SZ, Gatalica Z, Reddy S, et al. Multi-Platform Profiling of Over 2000 Sarcomas: Identification of Biomarkers and Novel Therapeutic Targets. *Oncotarget* (2015) 6:12234–47. doi: 10.18632/oncotarget.3498
51. Yang S, Plotnikov SV. Mechanosensitive Regulation of Fibrosis. *Cells* (2021) 10:994. doi: 10.3390/cells10050994
52. Engler AJ, Sen S, Sweeney HL, Discher DE. Matrix Elasticity Directs Stem Cell Lineage Specification. *Cell* (2006) 126:677–89. doi: 10.1016/j.cell.2006.06.044
53. Kai F, Drain AP, Weaver VM. The Extracellular Matrix Modulates the Metastatic Journey. *Dev Cell* (2019) 49:332–46. doi: 10.1016/j.devcel.2019.03.026
54. Oudin MJ, Weaver VM. Physical and Chemical Gradients in the Tumor Microenvironment Regulate Tumor Cell Invasion, Migration, and Metastasis. *Cold Spring Harb Symp Quant Biol* (2016) 81:189–205. doi: 10.1101/sqb.2016.81.030817

Conflict of Interest: The author VCL was employed by the company Rede D'Or São Luiz S.A.

The remaining authors declare that the research was conducted in the absence of any commercial or financial relationships that could be construed as a potential conflict of interest.

Publisher's Note: All claims expressed in this article are solely those of the authors and do not necessarily represent those of their affiliated organizations, or those of the publisher, the editors and the reviewers. Any product that may be evaluated in this article, or claim that may be made by its manufacturer, is not guaranteed or endorsed by the publisher.

frontiers in Oncology

ORIGINAL RESEARCH
published: 09 September 2021
doi: 10.3389/fonc.2021.729765

Prevalence of Delta-Like Protein 3 in a Consecutive Series of Surgically Resected Lung Neuroendocrine Neoplasms

Greta Alì[1†], Iosè Di Stefano[2†], Anello Marcello Poma[2], Stefano Ricci[3], Agnese Proietti[1], Federico Davini[4], Marco Lucchi[5], Franca Melfi[4] and Gabriella Fontanini[2]*

[1] Unit of Pathological Anatomy, University Hospital of Pisa, Pisa, Italy, [2] Department of Surgical, Medical, Molecular Pathology and Critical Area, University of Pisa, Pisa, Italy, [3] Pathology Unit, Azienda Unità Sanitaria Locale-IRCCS di Reggio Emilia, Reggio Emilia, Italy, [4] Multispecialty Centre for Surgery, Minimally Invasive and Robotic Thoracic Surgery, University Hospital of Pisa, Pisa, Italy, [5] Unit of Thoracic Surgery, University Hospital of Pisa, Pisa, Italy

OPEN ACCESS

Edited by:
Elena Levantini,
Beth Israel Deaconess Medical Center and Harvard Medical School, United States

Reviewed by:
Vincenzo L'Imperio,
University of Milano-Bicocca, Italy
Shigeki Umemura,
National Cancer Center Hospital East, Japan

***Correspondence:**
Gabriella Fontanini
gabriella.fontanini@med.unipi.it

[†]These authors have contributed equally to this work and share first authorship

Specialty section:
This article was submitted to Thoracic Oncology, a section of the journal Frontiers in Oncology

Received: 23 June 2021
Accepted: 13 August 2021
Published: 09 September 2021

Citation:
Ali G, Di Stefano I, Poma AM, Ricci S, Proietti A, Davini F, Lucchi M, Melfi F and Fontanini G (2021) Prevalence of Delta-Like Protein 3 in a Consecutive Series of Surgically Resected Lung Neuroendocrine Neoplasms. Front. Oncol. 11:729765. doi: 10.3389/fonc.2021.729765

Delta-like protein 3 (DLL3) is a protein of the Notch pathway, and it is a potential therapeutic target for high-grade lung neuroendocrine tumors (NETs), i.e., small cell lung carcinoma (SCLC) and large cell neuroendocrine carcinoma (LCNEC). However, DLL3 prevalence in lung NETs and its association with clinicopathological characteristics and prognosis remained unclear. We analyzed the immunohistochemical expression of DLL3 and its prognostic role in a consecutive series of 155 surgically resected lung NETs, including typical carcinoid (TC), atypical carcinoid (AC), LCNEC, and SCLC patients. The DLL3 expression was categorized as high (>50% positive tumor cells) or low (<50%). In addition, tumors were categorized by H-score (i.e., percentage of positive cells by staining intensity, ≥150 *vs.* <150). DLL3 staining was positive in 99/155 (64%) samples, and high DLL3 expression was frequently observed in high-grade tumors. In detail, 46.9% and 75% of SCLC and 48.8% and 53.7% of LCNEC specimens showed a high DLL3 expression by using H-score and percentage of positive tumor cells, respectively. Regarding low-grade NETs, only 4.9% and 12.2% TCs and 19.5% and 24.4% ACs had high DLL3 expression considering H-score and percentage of positive tumor cells, respectively. High DLL3 expression was associated with advanced American Joint Committee on Cancer (AJCC) stage, peripheral location, and chromogranin A expression in high-grade tumors ($p < 0.05$). In low-grade NETs, high DLL3 expression was associated with female sex, peripheral location, a higher number of mitoses, higher Ki-67 index, presence of necrosis, and pleural infiltration ($p < 0.05$). No association was observed between high DLL3 expression and overall survival (OS) and disease-free survival (DFS) in high-grade NETs, whereas high DLL3 expression was associated with lower DFS in ACs ($p = 0.01$). In conclusion, our study demonstrated a high prevalence of DLL3 expression in high-grade lung NET patients and its association with aggressive clinicopathological features. These findings confirm that DLL3 could represent a useful biomarker for target therapy in high-grade tumors. Our results also suggest that the DLL3 expression could identify a subset of

AC tumors with more aggressive behavior, thus providing the basis for new therapeutic options in this group of patients.

Keywords: lung neuroendocrine tumors, delta-like protein 3, immunohistochemistry, prognosis, biomarker

INTRODUCTION

Neuroendocrine (NE) tumors (NETs) are a heterogeneous group of neoplasms found most commonly in the lung and in the gastrointestinal tract (1, 2). The 2021 WHO classification of lung tumors identifies four distinct histological variants of lung NETs by using diagnostic criteria similar to those used since the 1999 WHO classification. These lung NETs have been categorized as typical carcinoid (TC), atypical carcinoid (AC), large cell NE carcinoma (LCNEC), and small cell lung carcinoma (SCLC); and they are differentiated on the basis of mitotic rate, presence of necrosis, and cytomorphological details, which allow to distinguish between low-grade (TC and AC) and high-grade (LCNEC and SCLC) tumors (3–5).

Low-grade NETs of the lung have a favorable prognosis compared with the more common high-grade NETs, i.e., LCNECs and SCLCs (6, 7).

The correct classification of lung NETs allows to select the most effective treatment regimen; surgery is often curative for both TC and AC, and for LCNECs. On the contrary, surgery is rarely used for SCLC patients, who are generally treated with chemotherapy. However, the rapid acquisition of chemoresistance in these patients and the substantial lack of alternative treatment options contribute to clinical failures (8–10). In carcinoid patients with metastatic disease, adjuvant therapy should be considered only in selected cases, since no studies have convincingly proved a benefit in terms of risk of local or distant recurrence (11–13). Therefore, more effective therapies and predictive biomarkers are needed both in carcinoid tumor patients who are not curable with surgery alone and in high-grade pulmonary NE carcinoma patients.

Delta-like protein 3 (DLL3), a member of the Notch family, has been identified as an inhibitory ligand of the Notch signalling pathway. DLL3 might function as an oncogenic driver in high-grade NETs, not only in the lung (14) but also in the gastrointestinal area (15), where DLL3 appears to be a downstream transcriptional target of the Achaete-scute homolog 1 (ASCL1) transcription factor (16–20). In particular, DLL3 is frequently expressed in the cell membrane of high-grade NETs, and it has low to no expression in most normal tissue (21); therefore, DLL3 could represent a potential therapeutic target in these tumors. Recently, some preclinical and clinical studies have used rovalpituzumab tesirine (Rova-T), a humanized monoclonal antibody against DLL3 in SCLCs (22–24). In these studies, the DLL3 expression seemed to identify patients who are more likely to achieve a response and a better long-term benefit after treatment with Rova-T (23, 24). Other DLL3-targeting agents, such as T cell-redirecting therapies and immuno-oncology therapies (AMG 757 and AMG 119), may have a high effect and specificity for DLL3-positive SCLC tumor cells (25–27).

For these reasons, recent studies have focused on the immunohistochemical DLL3 expression in lung NETs. However, most of them concern high-grade neoplasms, whereas few data are available for carcinoid tumors (23, 24, 28–32). In this study, we analyzed the immunohistochemical expression of DLL3 in a cohort of 155 patients with lung NETs including TCs, ACs, SCLCs, and LCNECs. This cohort included only limited-stage lung NETs treated with surgery; and for all cases, clinicopathological characteristics and prognostic factors were retrospectively reviewed. The aim of this paper was to investigate clinical features that might be associated with the DLL3 expression and to explore the prognostic role of this marker in pulmonary NETs.

MATERIALS AND METHODS

Patient Selection

This study was approved by the Ethics Committee "Comitato Etico di Area Vasta Nord Ovest" (CEAVNO) for Clinical Experimentation. A total of 155 lung NET specimens were retrospectively collected from the archives of the Operative Unit of Pathological Anatomy III of the University Hospital of Pisa. In detail, we collected 41 TC, 41 AC, 41 LCNEC, and 32 SCLC samples obtained from patients who had been submitted to surgical resection at the Unit of Thoracic Surgery of the University Hospital of Pisa from December 2007 to December 2019. Participation in this study required informed consent. Patients did not receive neoadjuvant chemotherapy nor radiation therapy. Clinical information, including sex, age, smoking status, disease-free survival (DFS), and overall survival (OS) were reviewed for each patient.

Lung Tissue Specimens

All tumor samples were formalin-fixed and paraffin-embedded (FFPE). The most representative paraffin block of tumor was selected for immunohistochemical analysis for each case. Histological diagnoses and pathological features were obtained by two pathologists (GA and ID), according to the WHO 2015 histological and immunohistochemical criteria (4).

In detail, the NET specimens were evaluated for growth patterns (organoid, trabecular, follicular, palisading, rosette, spindle-cell, and diffuse lymphoma-like), mitosis number per 2 mm^2, presence of necrosis and its pattern (absent, punctate, extensive, and geographic), vascular invasion (none, present focal, present extended), and tumor-infiltrating lymphocytes (TILs), both intra-tumoral and stromal lymphocytes (none <1%, focal <10%, moderate <50%, and diffused ≥50%). In detail, the presence of necrosis was determined by semiquantitative analysis evaluating necrosis percentage in the tumor area. We also evaluated the immunohistochemical expression of the NE markers (chromogranin A, synaptophysin, and CD56). At least

one positive NE marker was required for diagnosis. Furthermore, the immunohistochemical results for thyroid transcription factor 1 (TTF1) and Ki-67 proliferative index were available for all samples. The NE markers, Ki-67, and TTF1 were scored as negative or positive (negative, weakly 1+, moderately 2+, or strongly 3+), as described before (33). Ki-67 was evaluated as the percentage of positively stained tumor cell-nuclei.

For each tumor sample, data concerning site, size, lymph node (LN) status, pleural involvement, and stage were also collected. For all lung NETs, the eighth edition of the TNM classification was applied for pathological staging (34).

DFS was calculated from the date of tumor resection and diagnosis to the date of either disease recurrence including local recurrence or metastasis; otherwise, data were censored at the time of last follow-up or death. OS was calculated from the date of tumor resection to the date of death, or data were censored at the last follow-up.

Immunohistochemistry

DLL3 immunohistochemical analysis was performed on 4-µm-thick tissue sections that were deparaffinized in xylene and rehydrated using a graded series of ethanol solutions. The sections were then subjected to immunohistochemical staining with anti-DLL3 antibody, Rabbit Monoclonal Primary Antibody (clone SP347) (Ventana Medical Systems, Inc. Tucson, AZ, USA) by incubating the sections at 36°C for 32 min. Analysis was conducted with the BenchMark ULTRA semiautomated staining instrument (Ventana Medical Systems) using the OptiView DAB IHC Detection Kit (Ventana Medical Systems). Following a series of washes, the sections were counterstained with Hematoxylin II for 4 min and with Bluing Reagent (Ventana Medical Systems) for 4 min, dehydrated by passages in ethanol with increasing concentration from 70% to 100%, and then mounted.

In all cases, immunohistochemical evaluation was performed independently by two pathologists (GA and ID) who were blinded to all the clinical and pathological data. Selected cases were discussed with a third pathologist (GF) for confirmation. In our study, DLL3 expression was scored for any cytoplasmic and/or membranous staining at any intensity in total tumor cells. In literature, the evaluation of DLL3 immunohistochemical expression has widely varied by using different scores and thresholds for defining positivity (21–23, 28–30, 32, 35). Therefore, in our study, DLL3 positivity was determined based on the proportion of cells expressing DLL3 out of the total number of cells defining the level of expression of DLL3. Subsequently, we categorized DLL3 staining by using the following threshold for DLL3 scoring, which is used in the first clinical trial (23): high expression (>50% positive tumor cells) or low expression (<50%). We also determined the staining intensity as weak (1), intermediate (2), and strong (3) for each sample (**Figure 1**). Therefore, in order to determine the best evaluation system for DLL3 expression and to take in account the different intensities of the staining we observed in our samples, we further evaluated the DLL3 immunohistochemical results by a semiquantitative approach used to assign an H-score to tumor samples. H-score was calculated by multiplying the percentage of positive cells by the predominant staining intensity, with 300 possible values (0–300), as previously described (22, 29). As well as for the score based on the proportion of DLL3 positive cells, the tumors were ranked according to the median theoretical value as high DLL3 expressors (H-score ≥150) and low DLL3 expressors (H-score <150) by using H-score.

Statistical Analysis

Pearson's chi-squared test or Fisher's exact test was used for categorical variables. Continuous variables were analyzed by the Mann–Whitney or the Kruskal–Wallis tests, and by the Dunn test for multiple comparisons with the Benjamini–Hochberg correction. Survival curves were computed by the Kaplan–Meier method. Cox's proportional hazard model was used for both univariate and multivariate analyses. All analyses were performed in R environment (version 4.0.2, https://www.r-project.org/, last accessed in January 2021).

A p-value below 0.05 was considered significant.

RESULTS

Clinicopathological Characteristics of Patients

The present study included 155 patients with lung NETs, 41 (26.5%) TCs, 41 (26.5%) ACs, 41 (26.5%) LCNECs, and 32 (20.5%) SCLCs. Clinicopathological characteristics of patients and morphological findings are summarized in **Table 1**.

Patients with high-grade LCNEC and SCLC tumors were more frequently males and smokers. High-grade NETs were more often peripheral. SCLCs, LCNECs, and ACs were larger than TC tumors.

Patients with TC were more often pT1 without regional LN involvement.

Therefore, TC tumors were more commonly resected at stage I (N = 38; 92.7%) in contrast to other histotypes. As regards pleural involvement, high-grade NETs often presented invasion of the pleura, and SCLC showed more frequent vascular invasion than all the other NETs.

Necrosis presence and mitosis number were used as criteria to differentiate the different lung NETs (4). No TC tumors had necrosis, while some AC tumors had punctate necrosis (N = 17; 41.5%), and almost all high-grade NETs showed extensive or geographic necrosis. As expected, the Ki-67 index value was significantly higher in LCNECs and SCLCs compared with low-grade NETs.

With regard to architectural patterns, organoid was the most frequent pattern in low-grade NETs (TCs and ACs) and in LCNECs. The peripheral palisading pattern was observed only in LCNECs; similarly, the diffused lymphoma-like pattern was observed only in SCLCs. High-grade NETs presented significantly more TILs than low-grade tumors.

DLL3 Immunohistochemistry in Lung NETs

DLL3 staining was positive in 99/155 (64%) samples, and high DLL3 expression was frequently observed in high-grade tumors.

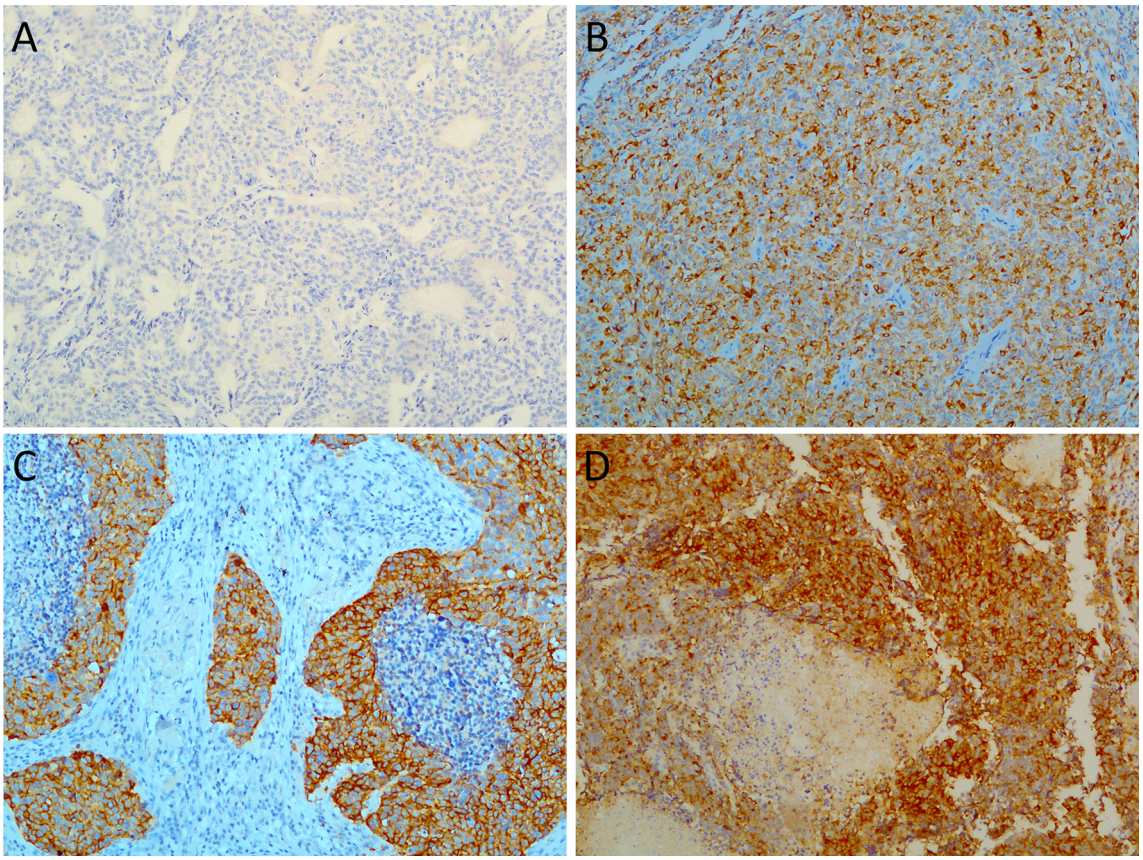

FIGURE 1 | Representative images showing variable percentages of delta-like protein 3 (DLL3) immunohistochemical staining in lung neuroendocrine tumors: **(A)** typical carcinoid DLL3 negative; **(B)** a case of atypical carcinoid showing combined cytoplasmic and membranous staining with moderate intensity; **(C)** large cell neuroendocrine carcinoma with strong and diffuse DLL3 staining; **(D)** high immunohistochemical expression level of DLL3 in a small cell lung carcinoma specimen. Magnification, ×20.

In particular, 20/41 (48.8%) LCNECs and 15/32 (46.9%) SCLCs showed a DLL3 H-score ≥150, whereas only 2/41 (4.9%) TCs and 8/41 (19.5%) ACs had an H-score as high as 150. Considering the percentage of tumor cells, 22/41 (53.7%) LCNECs, 24/32 (75%) SCLCs, 5/41 (12.2%) TCs, and 10/41 (24.4%) ACs showed more than 50% of stained tumor cells (**Figures 2A, B**). There were no significant differences in DLL3 expression within low-grade and high-grade tumors. Detailed DLL3 immunohistochemistry (IHC) results are shown in **Table 2**.

DLL3 Immunohistochemistry and Clinicopathological Data

The association between DLL3 expression and clinicopathological patient characteristics and morphological findings is summarized in **Table 2**.

Overall, patients with high DLL3 expression were more frequently smokers, both current and former; high DLL3 expression was also associated with peripheral tumors.

Considering high- and low-grade tumors as separate groups (**Tables 3** and **4**), the high DLL3 expression was again associated with the peripheral site of the neoplasm ($p = 0.01$ for high-grade and $p < 0.001$ for low-grade tumors). In the high-grade neoplasm group, high DLL3 H-score was associated with advanced pathological American Joint Committee on Cancer (AJCC) stage and younger age.

In the low-grade neoplasm group, the DLL3 expression was higher in females ($p < 0.001$). The high DLL3 expression correlated with histological parameters typically associated with high-grade NETs such as high mitosis number ($p < 0.001$), Ki-67 index ($p < 0.0001$), and presence of necrosis ($p < 0.001$). These correlations hold true for the low-grade tumor group, while no significant associations were observed between the DLL3 expression and these variables in the high-grade group.

A greater DLL3 expression was also observed in tumors with visceral pleura infiltration, where 23/35 (65.7%) had ≥50% positive tumor cells and 18/35 (51.4%) had H-score ≥150. On the other hand, considering cases with no pleural involvement, 82/120 (68.3%) had <50% positive tumor cells and 93/120 (77.5%) had H-score <150. These findings were confirmed in the low-grade group of tumors.

The high DLL3 expression in all samples correlates with the presence of moderate or diffuse TIL infiltration ($p < 0.001$),

TABLE 1 | Clinicopathological characteristics of patients with lung neuroendocrine tumors.

Features	All patients (N = 155)	Typical carcinoid (N = 41)	Atypical carcinoid (N = 41)	Large cell neuroendocrine carcinoma (N = 41)	Small cell carcinoma (N = 32)	p-Value
Age, median (range)	67 (16–84)	67 (16–82)	64 (20–81)	69 (48–84)	70 (57–82)	0.05
Sex, N (%)						<0.001
Male	92 (59.4)	10 (24.4)	22 (53.7)	35 (85.4)	25 (78.1)	
Female	63 (40.6)	31 (75.6)	19 (46.3)	6 (14.6)	7 (21.9)	
Smoking status, N (%)						<0.001
Never	45 (29.0)	22 (53.7)	20 (48.8)	3 (7.3)	0 (0)	
Current	41 (26.5)	5 (12.2)	9 (22.0)	18 (43.9)	9 (28.1)	
Former	69 (44.5)	14 (34.1)	12 (29.2)	20 (48.8)	23 (71.9)	
Site of tumor, N (%)						<0.001
Peripheral	89 (57.4)	20 (48.8)	17 (41.5)	34 (82.9)	18 (56.3)	
Central	64 (41.3)	21 (51.2)	24 (58.5)	7 (17.1)	12 (37.5)	
Peripheral + central*	2 (0.7)	0 (0)	0 (0)	0 (0)	2 (6.2)	
Size of tumor (cm), median (range)	2.7 (0.5–15)	2.2 (0.7–8)	3 (0.8–8.5)	2.8 (0.5–15)	2.9 (1–9.5)	0.01
pT, N (%)						<0.001
T1	85 (54.8)	35 (85.3)	20 (48.8)	19 (46.3)	11 (34.4)	
T2	36 (23.2)	4 (9.8)	14 (34.1)	8 (19.6)	10 (31.2)	
T3–T4	34 (22.0)	2 (4.9)	7 (17.1)	14 (34.1)	11 (34.4)	
pN, N (%)						<0.001
N0	113 (72.9)	40 (97.6)	28 (68.3)	27 (65.8)	18 (56.3)	
N1	22 (14.2)	1 (2.4)	10 (24.4)	5 (12.2)	6 (18.7)	
N2	20 (12.9)	0 (0)	3 (7.3)	9 (22.0)	8 (25.0)	
pM, N (%)						0.21
M0	150 (96.8)	41 (100)	38 (92.7)	39 (95.1)	32 (100)	
M1	5 (3.2)	0 (0)	3 (7.3)	2 (4.9)	0 (0)	
Pleural involvement, N (%)						<0.001
Absent	120(77.4)	41 (100)	36 (87.8)	24 (58.5)	19 (59.4)	
Present	35 (22.6)	0 (0)	5 (12.2)	17 (41.5)	13 (40.6)	
Vascular invasion, N (%)						<0.001
Absent	126(81.3)	39 (95.1)	35 (85.4)	36 (87.8)	16 (50.0)	
Present	29 (18.7)	2 (4.9)	6 (14.6)	5 (12.2)	16 (50.0)	
Pathological AJCC stage, N (%)						<0.001
I	87 (56.1)	38 (92.7)	20 (48.8)	19 (46.3)	10 (31.2)	
II	35 (22.6)	2 (4.9)	14 (34.1)	8 (19.6)	11 (34.4)	
III	28 (18.1)	1 (2.4)	4 (9.8)	12 (29.2)	11 (34.4)	
IV	5 (3.2)	0 (0)	3 (7.3)	2 (4.9)	0 (0)	
Pattern of necrosis, N (%)						<0.001
Absent	66 (42.6)	41 (100)	24 (58.5)	0 (0)	1 (3.1)	
Punctate	31 (20.0)	0 (0)	17 (41.5)	5 (12.2)	9 (28.1)	
Extensive	39 (25.2)	0 (0)	0 (0)	24 (58.6)	15 (46.9)	
Geographic	19 (12.2)	0 (0)	0 (0)	12 (29.2)	7 (21.9)	
Growth patterns, N (%)						<0.001
Organoid	92 (59.4)	26 (63.4)	26 (63.4)	25 (61.0)	15 (46.9)	
Rosettes	11 (7.1)	3 (7.3)	7 (17.1)	1 (2.4)	0 (0)	
Spindle	16 (10.3)	2 (4.9)	3 (7.3)	0 (0)	11 (34.4)	
Trabecular	9 (5.8)	6 (14.6)	1 (2.4)	2 (4.9)	0 (0)	
Follicular	11 (7.1)	4 (9.8)	4 (9.8)	3 (7.3)	0 (0)	
Palisading	10 (6.5)	0 (0)	0 (0)	10 (24.4)	0 (0)	
Diffuse-lymphoma like	6 (3.8)	0 (0)	0 (0)	0 (0)	6 (18.7)	
TILs, N (%)						<0.001
None	44 (28.4)	24 (58.5)	19 (46.3)	1 (2.4)	0 (0)	
Focal	45 (29.0)	15 (36.6)	16 (39.1)	9 (22.0)	5 (15.6)	
Moderate	63 (40.6)	2 (4.9)	6 (14.6)	29 (70.7)	26 (81.3)	
Diffuse	3 (2.09	0 (0)	0 (0)	2 (4.9)	1 (3.1)	
Number of mitosis, median (range)	6 (0–90)	1 (0–1)	3 (2–9)	35 (17–90)	44 (25–78)	<0.001
Immunohistochemistry						
% Ki-67 median, (range)**	33 (1–95)	5 (1–15)	15 (5–45)	70 (40–90)	90 (50–95)	<0.001
Chromogranin A pos, N (%)**	146 (94.2)	41 (100)	41 (100)	36 (87.8)	28 (87.5)	<0.001
Synaptophysin pos, N (%)**	141 (91.0)	40 (97.6)	41 (100)	34 (82.9)	26 (81.3)	<0.001
CD56 pos, N (%)**	155 (100)	41 (100)	41 (100)	41 (100)	32 (100)	0.01
TTF-1 pos, N (%)**	71 (45.8)	0 (0)	2 (4.9)	38 (92.7)	31 (96.9)	<0.001

The table shows only the number of positive samples (intensity > 0).

TILs, tumor-infiltrating lymphocytes; pos, positive; AJCC, American Joint Committee on Cancer.

**Not considered for statistics.*

***For the statistical studies, all immunohistochemical variables were considered as linear.*

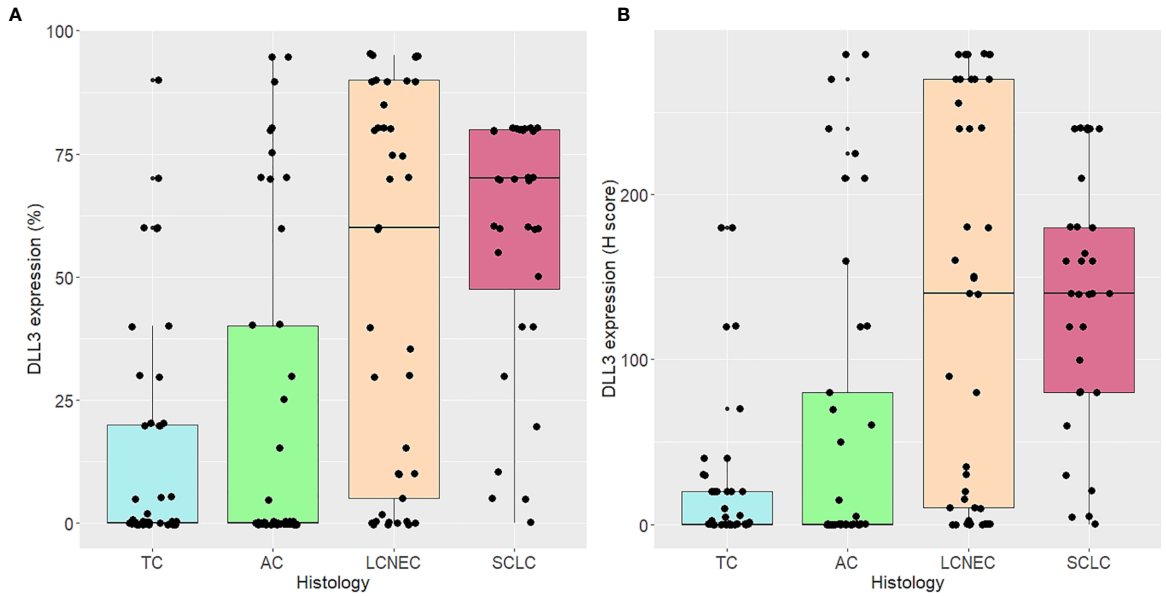

FIGURE 2 | Delta-like protein 3 (DLL3) expression according to histological types. DLL3 expression is indicated as percentage of tumor cells **(A)** and H-score **(B)**.

palisading growth pattern ($p = 0.01$), and positive TTF-1 immunohistochemical staining ($p < 0.001$).

Among the neoplasms with high DLL3 expression, 40/61 (65.6% using percentage value) and 31/45 (68.9% using H-score) presented a moderate-to-severe inflammatory infiltrate.

In the high-grade neoplasm group (total = 73), DLL3 H-score positively correlated with chromogranin A expression ($p = 0.04$).

DLL3 H-Score and Survival Data

The prognostic value of DLL3 was tested using an H-score cutoff of 150. Overall, the high DLL3 expression is associated with lower OS ($p = 0.001$) and DFS ($p < 0.001$) (**Figure 3**). Similarly, in low-grade tumors, the high DLL3 expression correlates with poorer DFS ($p < 0.01$) (**Figure 4**). As expected, the majority of adverse events in low-grade tumors occurred in AC patients. We tested the prognostic impact of DLL3 in this histological category, and again, the high DLL3 expression predicted a worse DFS ($p = 0.01$). To better understand the prognostic impact of DLL3, we tested it in multivariate settings, including histology and AJCC stage. DLL3 H-score (cutoff 150) showed a suggestive trend for poor DFS ($p = 0.06$, hazard ratio (HR) = 1.90, 95% CI 0.98–3.70), independently of the other parameters.

DISCUSSION

In the last few years, DLL3 has been identified as a novel therapeutic target gene mostly in SCLCs, but also in LCNECs (23, 36). Moreover, the literature data have demonstrated a relationship between DLL3 expression and sensitivity of platinum-based adjuvant chemotherapy, suggesting a predictive role of the DLL3 expression (37).

To the best of our knowledge, this is the first article investigating the DLL3 immunohistochemical expression and its prognostic role in a consecutive series of limited-stage lung NETs treated with surgery and including all four histological types (TCs, ACs, LCNECs, and SCLCs).

Higher DLL3 expression was more frequent in high-grade neoplasms. In detail, 46.9% and 75% of SCLC specimens showed a high DLL3 expression by using H-score and percentage of positive tumor cells, respectively. Our DLL3 prevalence data are consistent with those in the literature, showing that the DLL3 protein is highly expressed in SCLCs (21–23, 30, 35, 38, 39).

However, two studies reported a high DLL3 expression in only 32% of SCLCs (28). These discrepancies could depend on technical differences, on DLL3 score computation, and on the analysis of bioptic specimens.

We also demonstrated a high DLL3 expression in 48.8% of LCNECs by using H-score and 53.7% of LCNECs by using percentages of positive tumor cells, comparable with previous studies in LCNECs (29, 35). Only Ogawa and colleagues found lower rates of DLL3 expression (37.1% of LCNECs) by immunohistochemistry, but the results of their data could be due to the non-homogeneous study cohort, which included pure and combined LCNECs as well as different antibody clones (37).

The DLL3 expression has not been fully elucidated in lung carcinoid tumors. In our study, among the low-grade NETs, 20%–25% of ACs and 5%–12% of TCs—assessed by H-score and percentage of positive tumor cells, respectively—have high DLL3 expression. Only two other studies explored the DLL3 immunohistochemical expression in low-grade NETs. Alcala et al. reported a high expression in 40% of carcinoid samples (31); however, the authors included 20 low-grade NE neoplasms without specifying the TC and AC proportion, nor the DLL3

TABLE 2 | Demographics and clinical and pathological features of all neuroendocrine tumors based on high DLL3 expression.

	DLL3 score %			DLL3 H-score		
	Low (<50%) 94/155	**High (≥50%) 61/155**	**p-Value**	**Low (<150) 110/155**	**High (≥150) 45/155**	**p-Value**
Histological diagnosis			<0.001			<0.001
TC, N (%)	36 (38.3)	5 (8.2)		39 (35.5)	2 (4.4)	
AC, N (%)	31 (33)	10 (16.4)		33 (29.9)	8 (17.8)	
LCNEC, N (%)	19 (20.2)	22 (36.1)		21 (19.1)	20 (44.5)	
SCLC, N (%)	8 (8.5)	24 (39.3)		17 (15.5)	15 (33.3)	
Age, median (range)	68 (16–84)	67 (40–79)	0.24	66 (16–84)	70 (40–79)	0.26
Male sex, N (%)	54 (57.4)	38 (62.3)	0.79	60 (54.6)	32 (71.1)	0.48
Smoking status, N (%)			<0.001			<0.001
Never	37 (39.4)	8 (13.1)		42 (38.1)	3 (6.7)	
Current	16 (17)	25 (41)		17 (15.5)	24 (53.3)	
Former	41 (43.6)	28 (45.9)		51 (46.4)	18 (40)	
Peripheral site of tumor, N (%)	41 (43.6)	48 (78.7)	<0.001	52 (47.3)	37 (82.2)	<0.001
Size of tumor (cm), median (range)	2.8 (0.7–9.5)	2.5 (0.5–15)	0.83	2.8 (0.7–9.5)	2.5 (0.5–15)	0.67
pT, N (%)			0.66			0.51
T1	55 (58.5)	30 (49.2)		61 (55.5)	24 (53.3)	
T2	21 (22.3)	15 (24.6)		27 (24.5)	9 (20)	
T3–T4	18 (19.2)	16 (26.2)		22 (20)	12 (26.7)	
pN, N (%)			0.20			0.27
N0	71 (75.5)	42 (68.9)		83 (75.5)	30 (66.7)	
N1	12 (12.8)	10 (16.4)		13 (11.8)	9 (20)	
N2	11 (11.7)	9 (14.7)		14 (12.7)	6 (13.3)	
pM1, N (%)	2 (2.1)	3 (4.9)	0.10	2 (1.8)	3 (6.7)	0.07
Pleural involvement, N (%)			<0.001			<0.001
Presence	12 (12.8)	23 (37.7)		17 (15.5)	18 (40)	
Absence	82 (87.2)	38 (62.3)		93 (84.5)	27 (60)	
Vascular invasion, N (%)	13 (13.8)	16 (26.2)	0.22	20 (18.2)	9 (20)	0.09
Pathological AJCC stage, N (%)			0.39			0.35
I	57 (60.6)	30 (49.2)		65 (59.1)	22 (48.9)	
II	19 (20.3)	16 (26.2)		23 (20.9)	12 (26.7)	
III	16 (17)	12 (19.7)		20 (18.2)	8 (17.8)	
IV	2 (2.1)	3 (4.9)		2 (1.8)	3 (6.6)	
Necrosis, median (range)	0 (0–60)	20 (0–60)	<0.001	0 (0–60)	20 (0–60)	<0.001
Pattern of necrosis, N (%)			<0.001			<0.001
Absent	56 (59.6)	10 (16.4)		62 (56.4)	4 (8.9)	
Punctate	13 (13.8)	18 (29.5)		18 (16.3)	13 (28.9)	
Extensive	17 (18.1)	22 (36.1)		20 (18.2)	19 (42.2)	
Geographic	8 (8.5)	11 (18)		10 (9.1)	9 (20)	
Growth patterns, N (%)			0.01			0.01
Organoid	57 (60.6)	35 (57.4)		66 (60)	26 (57.8)	
Rosettes	9 (9.6)	2 (3.3)		9 (8.2)	2 (4.4)	
Spindle	7 (7.4)	9 (14.8)		10 (9.1)	6 (13.3)	
Trabecular	8 (8.5)	1 (1.6)		9 (8.2)	0 (0)	
Follicular	9 (9.6)	2 (3.3)		10 (9.1)	1 (2.2)	
Palisading	3 (3.2)	7 (11.5)		3 (2.7)	7 (15.6)	
Diffuse-lymphoma like	1 (1.1)	5 (8.2)		3 (2.7)	3 (6.6)	
TILs, N (%)			<0.001			<0.001
Diffuse	0 (0)	3 (4.9)		1 (0.9)	2 (4.4)	
Moderate	26 (27.7)	37 (60.7)		34 (30.9)	29 (64.4)	
Focal	32 (34)	13 (21.3)		36 (32.7)	9 (20)	
None	36 (38.3)	8 (13.1)		39 (35.5)	5 (12.1)	
Number of mitosis, median (range)	3 (0–90)	35 (1–78)	<0.001	3 (0–90)	33 (1–78)	<0.001
Immunohistochemistry						
% Ki-67 median (range)*	10 (1–95)	80 (2–95)	<0.001	15 (1–95)	75 (2–95)	<0.001
Chromogranin A pos, N (%)*	85 (90.4)	51 (83.6)	0.27	97 (88.2)	39 (86.7)	0.40
Synaptophysin pos, N (%)*	87 (92.6)	54 (88.5)	0.24	101 (91.8)	40 (88.9)	0.20
CD56 pos, N (%)*	94 (100)	61 (100)	0.16	110 (100)	45 (100)	0.06
TTF-1 pos, N (%)*	28 (29.8)	43 (70.5)	<0.001	39 (35.5)	32 (71.1)	<0.001

The table shows only the number of positive samples (intensity > 0).

TILs, tumor-infiltrating lymphocytes; pos, positive; DLL3, delta-like protein 3.

TC, typical carcinoid; AC, atypical carcinoid; LCNEC, large cell neuroendocrine carcinoma; SCLC, small cell lung carcinoma; AJCC, American Joint Committee on Cancer.

**For the statistical studies, all immunohistochemical variables were considered as linear.*

TABLE 3 | Demographics and clinical and pathological features of high-grade neuroendocrine tumors (73/155) based on high DLL3 expression.

	DLL3 score %			DLL3 H-score		
	Low (<50%) 27/73	High (≥50%) 46/73	p-Value	Low (<150) 38/73	High (≥150) 35/73	p-Value
Age, median (range)	73 (58–84)	67 (48–79)	<0.01	72 (58–84)	69 (48–79)	0.01
Male sex, N (%)	24 (88.9)	36 (78.3)	0.25	30 (78.9)	30 (85.7)	0.76
Smoking status, N (%)			0.12			0.06
Never	1 (3.7)	2 (4.3)		2 (5.3)	1 (2.8)	
Current	8 (29.6)	19 (41.3)		8 (21.1)	19 (54.3)	
Former	18 (66.7)	25 (54.3)		28 (73.7)	15 (42.9)	
Peripheral site of tumor, N (%)	16 (59.3)	36 (78.3)	0.05	23 (60.5)	29 (82.9)	0.01
Size of tumor (cm), median (range)	3.5 (1–9.5)	2.6 (0.5–15)	0.60	3.4 (1–9.5)	2.5 (0.5–15)	0.34
pT, N (%)			0.27			0.10
T1	10 (37.0)	20 (43.5)		13 (34.2)	17 (48.6)	
T2	8 (29.6)	10 (21.7)		12 (31.6)	6 (17.1)	
T3–T4	9 (33.4)	16 (34.8)		13 (34.2)	12 (34.3)	
pN, N (%)			0.61			0.23
N0	13 (48.1)	32 (69.6)		20 (52.6)	25 (71.4)	
N1	5 (18.5)	6 (13.0)		6 (15.8)	5 (14.3)	
N2	9 (33.4)	8 (17.4)		12 (31.6)	5 (14.3)	
pM1, N (%)	0 (0)	2 (4.3)	0.07	0 (0)	2 (5.7)	0.10
Pleural involvement, N (%)			0.93			0.60
Presence	10 (37.0)	20 (43.5)		15 (39.5)	15 (42.9)	
Absence	17 (63.0)	26 (56.5)		23 (60.5)	20 (57.1)	
Vascular invasion, N (%)	6 (22.2)	15 (32.6)	0.29	13 (34.2)	8 (22.9)	0.70
Pathological AJCC stage, N (%)			0.06			0.04
I	9 (33.3)	20 (43.5)		12 (31.6)	17 (48.6)	
II	7 (25.9)	12 (26.1)		11 (28.9)	8 (22.9)	
III	11 (40.7)	12 (26.1)		15 (39.5)	8 (22.9)	
IV	0 (0)	2 (4.3)		0 (0)	2 (5.7)	
Necrosis, median (range)	30 (5–60)	20 (0–60)	0.52	30 (0–60)	20 (10–60)	0.76
Pattern of necrosis, N (%)			0.74			1
Absent	0 (0)	1 (2.2)		1 (2.7)	0 (0)	
Punctate	2 (7.4)	12 (26.1)		7 (18.4)	7 (20.0)	
Extensive	17 (63.0)	22 (47.8)		20 (52.6)	19 (54.3)	
Geographic	8 (29.6)	11 (23.9)		10 (26.3)	9 (25.7)	
Growth patterns, N (%)			0.24			0.30
Organoid	17 (63.0)	23 (50.0)		22 (57.9)	18 (51.4)	
Rosettes	0 (0)	1 (2.2)		0 (0)	1 (2.8)	
Spindle	2 (7.4)	9 (19.6)		5 (13.1)	6 (17.1)	
Trabecular	1 (3.7)	1 (2.2)		2 (5.3)	0 (0)	
Follicular	3 (11.1)	0 (0)		3 (7.9)	0 (0)	
Palisading	3 (11.1)	7 (15.2)		3 (7.9)	7 (20.0)	
Diffuse-lymphoma like	1 (3.7)	5 (10.8)		3 (7.9)	3 (8.7)	
TILs, N (%)			0.12			0.28
Diffuse	0 (0)	3 (6.5)		1 (2.7)	2 (5.7)	
Moderate	19 (70.4)	36 (78.3)		27 (71.1)	28 (80.0)	
Focal	7 (25.9)	7 (15.2)		9 (23.5)	5 (14.3)	
None	1 (3.7)	0 (0)		1 (2.7)	0 (0)	
Number of mitosis, median (range)	35 (17–90)	40 (20–78)	0.60	38 (17–90)	39 (20–78)	0.67
Immunohistochemistry						
% Ki-67 median (range)*	80 (40–95)	80 (40–95)	0.30	80 (40–95)	80 (40–95)	0.28
Chromogranin A pos, N (%)*	18 (66.7)	36 (78.3)	0.07	25 (65.8)	29 (82.9)	0.04
Synaptophysin pos, N (%)*	21 (77.8)	39 (84.8)	0.44	30 (78.9)	30 (85.7)	0.53
CD56 pos, N (%)*	27 (100.0)	46 (100.0)	0.91	38 (100.0)	35 (100.0)	0.66
TTF-1 pos, N (%)*	26 (96.3)	43 (93.5)	0.17	37 (97.3)	32 (91.4)	0.08

The table shows only the number of positive samples (intensity > 0).

TILs, tumor-infiltrating lymphocytes; pos, positive; DLL3, delta-like protein 3; AJCC, American Joint Committee on Cancer.

**For the statistical studies, all immunohistochemical variables were considered as linear.*

immunohistochemical expression cutoff used. The other study by Xie et al. showed higher DLL3 immunoreactivity in 37% of AC and 32.8% of TC samples by using the cutoff of >50% positive tumor cells to define the high DLL3 expression (30). However, we do not have a straightforward explanation for the DLL3 prevalence discrepancies observed in carcinoid cohorts. For this reason, the DLL3 expression in low-grade NETs needs to be evaluated in larger cohorts in order to define the possible prognostic-therapeutic role in this category of tumors.

The association between DLL3 expression and clinicopathological characteristics has not been thoroughly explored, and it is still largely uncertain. In our study, in the entire cohort, NE neoplasms with high

TABLE 4 | Demographics and clinical and pathological features of low-grade neuroendocrine tumors (82/155) based on high DLL3 expression.

	DLL3 score %			DLL3 H-score		
	Low (<50%)67/82	**High (≥50%) 15/82**	**p-Value**	**Low (<150)72/82**	**High (≥150) 10/82**	**p-Value**
Age, median (range)	65 (16–82)	66 (40–79)	0.54	65 (16–82)	71 (40–79)	0.54
Female sex, N (%)	37 (55.2)	13 (86.7)	<0.001	42 (58.3)	8 (80)	<0.001
Smoking status, N (%)			0.06			0.07
Never	36 (53.7)	6 (40)		40 (55.6)	2 (20)	
Current	8 (11.9)	6 (40)		9 (12.5)	5 (50)	
Former	23 (34.3)	3 (20)		23 (31.9)	3 (30)	
Peripheral site of tumor, N (%)	25 (37.3)	12 (80)	<0.001	29 (40.3)	8 (80)	<0.001
Size of tumor (cm), median (range)	2.5 (0.7–8.5)	2.3 (0.9–4.4)	0.09	2.5 (0.7–8.8)	1.9 (0.9–4.4)	0.16
pT, N (%)			0.15			0.16
T1	45 (67.2)	10 (66.7)		48 (66.7)	7 (70)	
T2	13 (19.4)	5 (33.3)		15 (20.8)	3 (30)	
T3–T4	9 (13.4)	0 (0)		9 (12.5)	0 (0)	
pN, N (%)			0.89			0.89
N0	58 (86.6)	10 (66.7)		63 (87.5)	5 (50)	
N1	7 (10.4)	4 (26.7)		7 (9.7)	1 (10)	
N2	2 (3)	1 (6.7)		2 (2.8)	4 (40)	
pM1, N (%)	0 (0)	2 (13.3)	0.30	0 (0)	2 (20)	0.21
Pleural involvement, N (%)			0.01			<0.01
Presence	2 (3)	3 (20)		2 (2.8)	3 (30)	
Absence	65 (97)	12 (80)		70 (97.2)	7 (70)	
Vascular invasion, N (%)	7 (10.4)	1 (6.7)	0.82	7 (9.7)	1 (10)	0.88
Pathological AJCC stage, N (%)			0.38			0.32
I	48 (71.6)	10 (66.7)		53 (73.6)	5 (50)	
II	12 (17.9)	4 (26.7)		12 (16.7)	4 (40)	
III	5 (7.5)	0 (0)		5 (6.9)	0 (0)	
IV	2 (3)	1 (6.7)		2 (2.8)	1 (10)	
Necrosis %, median (range)	0 (0–30)	0 (0–5)	0.66	0 (0–30)	5 (0–5)	0.25
Pattern of necrosis, N (%)			0.01			<0.001
Absent	56 (83.6)	9 (60)		61 (84.7)	4 (40)	
Punctate	11 (16.4)	6 (40)		11 (15.3)	6 (60)	
Extensive	0 (0)	0 (0)		0 (0)	0 (0)	
Geographic	0 (0)	0 (0)		0 (0)	0 (0)	
Growth patterns, N (%)			0.64			0.63
Organoid	40 (59.7)	12 (80)		44 (61.1)	8 (80)	
Rosettes	9 (13.4)	1 (6.7)		9 (12.5)	1 (10)	
Spindle	5 (7.5)	0 (0)		5 (6.9)	0 (0)	
Trabecular	7 (10.4)	0 (0)		7 (9.7)	0 (0)	
Follicular	6 (9)	2 (13.3)		7 (9.7)	1 (10)	
Palisading	0 (0)	0 (0)		0 (0)	0 (0)	
Diffuse-lymphoma like	0 (0)	0 (0)		0 (0)	0 (0)	
TILs, N (%)			0.34			0.34
Diffuse	0 (0)	0 (0)		0 (0)	0 (0)	
Moderate	7 (10.4)	1 (6.7)		7 (9.7)	1 (10)	
Focal	25 (37.3)	6 (40)		27 (37.5)	4 (40)	
None	35 (52.2)	8 (53.3)		38 (90.5)	5 (50)	
Number of mitosis, median (range)	1 (0–9)	3 (1–8)	0.11	1 (0–9)	3 (1–8)	0.04
Immunohistochemistry						
% Ki-67 median (range)*	7 (1–45)	15 (2–80)	0.11	8 (1–45)	20 (2–75)	0.02
Chromogranin A pos, N (%)*	67 (100)	15 (100)	0.66	72 (100)	10 (100)	0.72
Synaptophysin pos, N (%)*	66 (98.5)	15 (100)	0.43	71 (98.6)	10 (100)	0.35
CD56 pos, N (%)*	67 (100)	15 (100)	0.16	72 (100)	10 (100)	0.10
TTF-1 pos, N (%)*	2 (3)	0 (0)	0.85	2 (2.8)	0 (0)	0.84

The table shows only the number of positive samples (intensity > 0).

TILs, tumor-infiltrating lymphocytes; pos, positive; DLL3, delta-like protein 3; AJCC, American Joint Committee on Cancer.

**For the statistical studies, all immunohistochemical variables were considered as linear.*

DLL3 expression more often belonged to smoking patients. The neoplasms were mainly peripheral, and more than half of the high DLL3 expression neoplasms had pleural infiltration at microscopic evaluation. Samples with high immunoreactivity had higher numbers of mitosis, higher Ki-67 index, and greater necrosis; moreover, they generally presented palisade growth pattern and moderate-to-severe TILs and expressed TTF-1.

As regards high-grade NETs, those with high DLL3 expression tended to have advanced AJCC stage, peripheral location, and chromogranin A expression. The association of

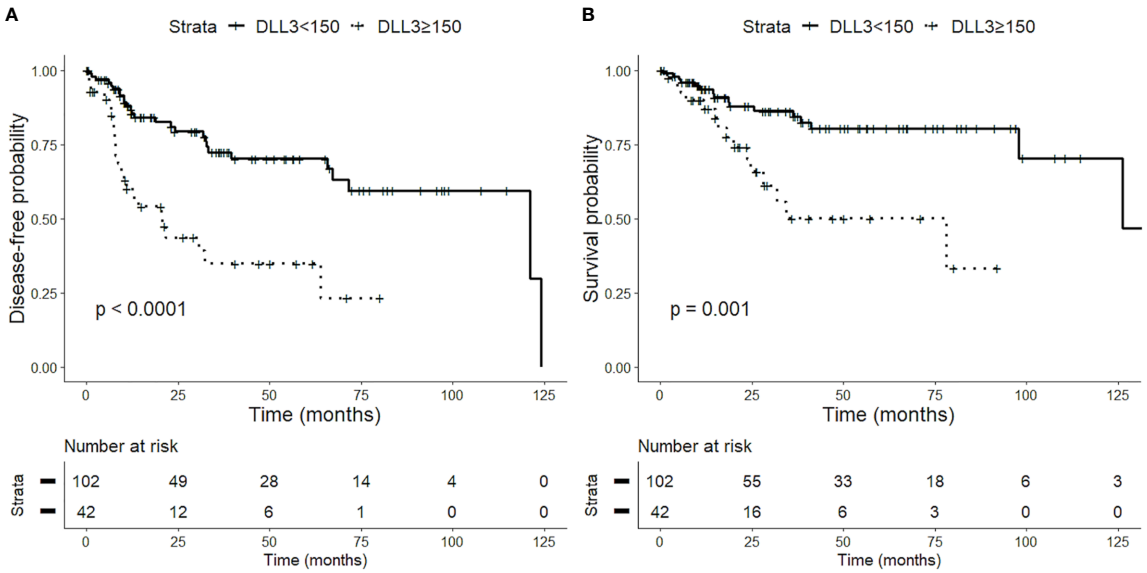

FIGURE 3 | Impact of delta-like protein 3 (DLL3) expression on prognosis of patients with lung neuroendocrine tumors. High levels of DLL3 expression (H-score > 150) are associated with a worse disease-free survival (DFS) **(A)** and overall survival (OS) **(B)**.

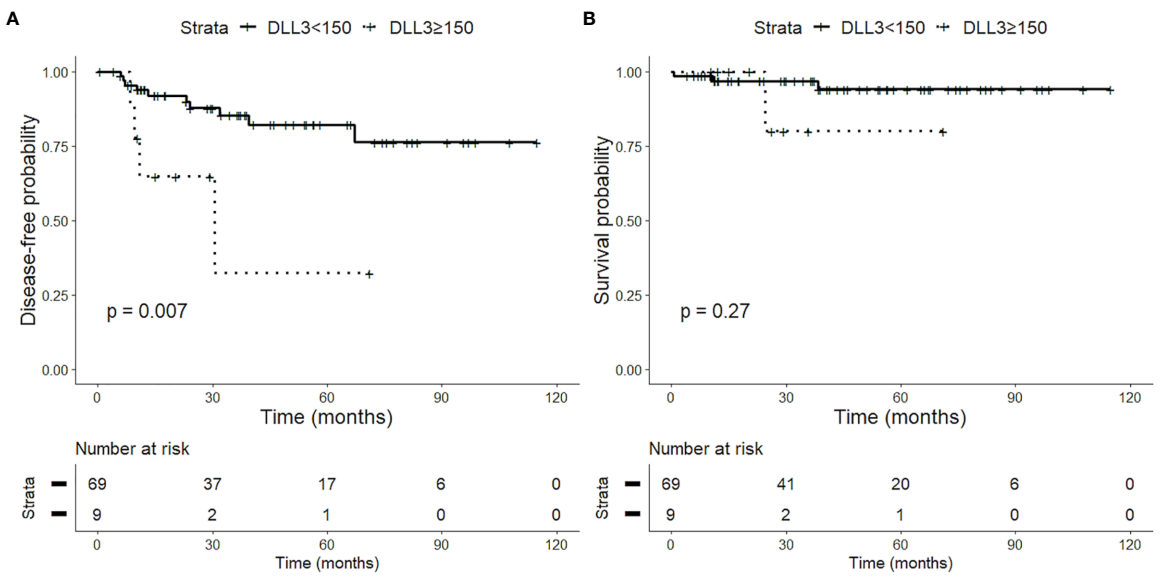

FIGURE 4 | Impact of delta-like protein 3 (DLL3) staining on prognosis of patients with low-grade lung neuroendocrine tumors. High DLL3 expression (H-score > 150) is associated with a reduced disease-free survival (DFS) **(A)** but not with overall survival (OS) **(B)**, probably due to the low number of events.

DLL3 expression with more aggressive tumor behavior was also found in patients with other high-grade tumor types, such as endometrial carcinoma, lung adenocarcinoma, and small cell bladder cancer (40–42), as well as in SCLC patients (39). However, other studies did not find any association between DLL3 expression and clinicopathological characteristics in high-grade NE lung tumors (28, 37, 38).

As regards low-grade NETs, neoplasms with high DLL3 expression frequently belonged to female patients, as previously described (30), and generally presented with a peripheral location. Interestingly, high DLL3 expression was also associated with aggressive histological characteristics, such as a higher number of mitoses, higher Ki-67 index, presence of punctate necrosis, and greater predisposition to pleural infiltration.

As regards survival data, high DLL3 expression was associated with lower OS and DFS in the entire cohort. The significant association with lower DFS was confirmed also independently of the histology and AJCC stage, which are the most useful prognostic indices. The association between high DLL3 expression and lower OS and DFS suggests that this marker might be associated with more aggressive tumors, even if this association has not been confirmed for high-grade tumors. The high proportion of patients with positive DLL3 tumor expression, despite the absence of prognostic implications, confirms previous results in SCLC and LCNEC patients (28, 37–39). A study by Huang et al. (43) found an association between high level of the DLL3 expression and low progression-free survival (PFS) and OS rates in biopsy from primary tumors and metastatic LNs in advanced SCLC patients. However, a larger multicenter study, evaluating DLL3 expression in biopsy samples collected from 1,073 SCLC patients with limited and extensive stage disease, did not find any association between DLL3 expression and survival data (32). Therefore, the DLL3 prognostic role needs to be further investigated in biopsy from SCLC patients, which represent the most frequent type of specimen in these patients. Only Xie and collaborators observed a significant association between high DLL3 expression and better OS and small size of tumors in both SCLC and AC patients, suggesting that the DLL3 expression might represent a favorable prognostic factor in lung NETs. However, in their study, only a relatively small percentage of lung NETs had low expression of DLL3. Therefore, prognostic data need to be interpreted with caution (30).

The DLL3 expression has not yet been associated with OS in low-grade NETs. We observed a significant association between high DLL3 expression and lower DFS in ACs. This finding as well as the association between DLL3 expression and aggressive histological characteristics suggests that DLL3 expression could identify a subgroup of ACs with worse prognosis and more clinically aggressive behavior.

Several recent studies suggest the existence of low-grade lung NETs with proliferative capacities higher than those currently accepted for TC and AC (5, 44, 45). These cases could be the lung equivalent of gastro-entero-pancreatic (GEP) NET G3. This new category has a prognostic and therapeutic significance: G3 NETs show a more aggressive behavior than G1–G2 NETs and a lower response rate to platinum-based chemotherapy, which remains a therapeutic signature of NE carcinomas (46). However, actually, this entity is not included in lung NET classification since only a limited number of cases have been reported so far, with different terminologies, different inclusion criteria, and few therapeutic information; and more data about these cases are needed. In this context, DLL3 expression could add useful prognostic information to histological subtyping in low-grade lung NETs.

Cardnell and collaborators found a correlation between TTF1 and DLL3 expression in SCLCs, suggesting that TTF1 could be used as a surrogate marker for DLL3 (47). However, we did not observe this association in high-grade tumors, which confirms previous results from the literature (29). In accordance with previous reports (29, 37), we observed a significant correlation between higher DLL3 expression and increased staining intensity of chromogranin A in high-grade tumors, which supported the hypothesis that the DLL3 expression is related to NE differentiation and could promote NE tumorigenesis in high-grade lung NETs.

Several limitations associated with the present study should be mentioned. Firstly, this was a retrospective, non-randomized single-center study that concerned only resected specimens. However, in clinical practice, the vast majority of SCLCs are diagnosed by biopsy procedure without any need for subsequent surgery resection. Nevertheless, we evaluated DLL3 expression by using a homogeneous cohort composed of only surgically resected pulmonary NETs. Our results thus need to be confirmed in a prospective cohort, by evaluating the DLL3 expression in biopsies from SCLC patients. Our cohort selection may also have led to a bias to evaluate the association between DLL3 expression and prognosis (OS and DFS) in SCLC patients, since the better outcome of the early-stage SCLC patients in our study. However, our results are similar to those of other studies that used biopsies of SCLC to assess for DLL3 expression (23, 32). Secondly, although our report is referred to a large series in terms of surgically resected SCLCs, the overall number of TCs, ACs, and LCNECs is relatively small; and further validation studies should be warranted.

However, despite these limitations, our study demonstrated a high prevalence of DLL3 expression in high-grade lung NET patients and its association with aggressive clinicopathological features. These findings confirm that DLL3 could represent a useful biomarker for target therapy in high-grade tumors. Our results also suggest that the DLL3 expression could identify a subset of ACs tumors with more aggressive behavior, thus providing the basis for new therapeutic options in this group of patients.

DATA AVAILABILITY STATEMENT

The original contributions presented in the study are included in the article/supplementary files. Further inquiries can be directed to the corresponding author.

ETHICS STATEMENT

The study was approved by the Ethics Committee "Comitato Etico di Area Vasta Nord Ovest" (CEAVNO) for Clinical experimentation. Informed written consent for publication was not asked, since no data that can potentially and clearly identify patients were used and reported in the manuscript.

AUTHOR CONTRIBUTIONS

Conception of the work and result interpretation: GA, IDS, and GF. Immunohistochemistry and data analysis: AMP, SR, and AP. Sample collections and result interpretation: FD, ML, and FM. Pathological diagnosis: GA, IDS, and GF. All authors contributed to the article and approved the submitted version.

REFERENCES

1. Yao JC, Hassan M, Phan A, Dagohoy C, Leary C, Mares JE, et al. One Hundred Years After "Carcinoid": Epidemiology of and Prognostic Factors for Neuroendocrine Tumors in 35,825 Cases in the United States. *J Clin Oncol* (2008) 26(18):3063–72. doi: 10.1200/JCO.2007.15.4377
2. Dasari A, Shen C, Halperin D, Zhao B, Zhou S, Xu Y, et al. Trends in the Incidence, Prevalence, and Survival Outcomes in Patients With Neuroendocrine Tumors in the United States. *JAMA Oncol* (2017) 3 (10):1335–42. doi: 10.1001/jamaoncol.2017.0589
3. Travis W, Colby T, Corrin B, Shimosato Y, Brambilla E. In collaboration with Sobin LH and Pathologists From 14 Countries. WHO International Histological Classification of Tumours. In: *Histological Typing of Lung and Pleural Tumours*. New York: Springer-Verlag (1999).
4. Travis WD BE, Burke AP, Marx A, Nicholson AG. *WHO Classification of Tumours of the Lung, Pleura, Thymus and Heart. 4th ed*. Lyon, France: International Agency for Research on Cancer (2015).
5. Board WCoTE. *Thoracic Tumours*. Lyon (France): International Agency for Research on Cancer (2021).
6. Filosso PL, Falcoz PE, Solidoro P, Pellicano D, Passani S, Guerrera F, et al. The European Society of Thoracic Surgeons (ESTS) Lung Neuroendocrine Tumors (NETs) Database. *J Thorac Dis* (2018) 10(Suppl 29):S3528–S32. doi: 10.21037/jtd.2018.04.104
7. Rekhtman N. Neuroendocrine Tumors of the Lung: An Update. *Arch Pathol Lab Med* (2010) 134(11):1628–38. doi: 10.1043/2009-0583-RAR.1
8. Ramirez RA, Chauhan A, Gimenez J, Thomas KEH, Kokodis I, Voros BA. Management of Pulmonary Neuroendocrine Tumors. *Rev Endocr Metab Disord* (2017) 18(4):433–42. doi: 10.1007/s11154-017-9429-9
9. Fasano M, Della Corte CM, Papaccio F, Ciardiello F, Morgillo F. Pulmonary Large-Cell Neuroendocrine Carcinoma: From Epidemiology to Therapy. *J Thorac Oncol* (2015) 10(8):1133–41. doi: 10.1097/JTO.0000000000000589
10. Wang S, Zimmermann S, Parikh K, Mansfield AS, Adjei AA. Current Diagnosis and Management of Small-Cell Lung Cancer. *Mayo Clin Proc* (2019) 94(8):1599–622. doi: 10.1016/j.mayocp.2019.01.034
11. Hung YP. Neuroendocrine Tumors of the Lung: Updates and Diagnostic Pitfalls. *Surg Pathol Clin* (2019) 12(4):1055–71. doi: 10.1016/j.path.2019.08.012
12. Caplin ME, Baudin E, Ferolla P, Filosso P, Garcia-Yuste M, Lim E, et al. Pulmonary Neuroendocrine (Carcinoid) Tumors: European Neuroendocrine Tumor Society Expert Consensus and Recommendations for Best Practice for Typical and Atypical Pulmonary Carcinoids. *Ann Oncol* (2015) 26(8):1604–20. doi: 10.1093/annonc/mdv041
13. Uprety D, Halfdanarson TR, Molina JR, Leventakos K. Pulmonary Neuroendocrine Tumors: Adjuvant and Systemic Treatments. *Curr Treat Options Oncol* (2020) 21(11):86. doi: 10.1007/s11864-020-00786-0
14. Furuta M, Kikuchi H, Shoji T, Takashima Y, Kikuchi E, Kikuchi J, et al. DLL3 Regulates the Migration and Invasion of Small Cell Lung Cancer by Modulating Snail. *Cancer Sci* (2019) 110(5):1599–608. doi: 10.1111/cas.13997
15. Matsuo K, Taniguchi K, Hamamoto H, Ito Y, Futaki S, Inomata Y, et al. Delta-Like 3 Localizes to Neuroendocrine Cells and Plays a Pivotal Role in Gastrointestinal Neuroendocrine Malignancy. *Cancer Sci* (2019) 110 (10):3122–31. doi: 10.1111/cas.14157
16. Chapman G, Sparrow DB, Kremmer E, Dunwoodie SL. Notch Inhibition by the Ligand DELTA-LIKE 3 Defines the Mechanism of Abnormal Vertebral Segmentation in Spondylocostal Dysostosis. *Hum Mol Genet* (2011) 20 (5):905–16. doi: 10.1093/hmg/ddq529
17. Bray SJ. Notch Signalling in Context. *Nat Rev Mol Cell Biol* (2016) 17(11):722–35. doi: 10.1038/nrm.2016.94
18. George J, Lim JS, Jang SJ, Cun Y, Ozretic L, Kong G, et al. Comprehensive Genomic Profiles of Small Cell Lung Cancer. *Nature* (2015) 524(7563):47–53. doi: 10.1038/nature14664
19. Crabtree JS, Singleton CS, Miele L. Notch Signaling in Neuroendocrine Tumors. *Front Oncol* (2016) 6:94. doi: 10.3389/fonc.2016.00094
20. George J, Walter V, Peifer M, Alexandrov LB, Seidel D, Leenders F, et al. Integrative Genomic Profiling of Large-Cell Neuroendocrine Carcinomas Reveals Distinct Subtypes of High-Grade Neuroendocrine Lung Tumors. *Nat Commun* (2018) 9(1):1048. doi: 10.1038/s41467-018-03099-x
21. Huang RSP, Holmes BF, Powell C, Marati RV, Tyree D, Admire B, et al. Delta-Like Protein 3 Prevalence in Small Cell Lung Cancer and DLL3 (SP347) Assay Characteristics. *Arch Pathol Lab Med* (2019) 143(11):1373–7. doi: 10.5858/arpa.2018-0497-OA
22. Saunders LR, Bankovich AJ, Anderson WC, Aujay MA, Bheddah S, Black K, et al. A DLL3-Targeted Antibody-Drug Conjugate Eradicates High-Grade Pulmonary Neuroendocrine Tumor-Initiating Cells *In Vivo*. *Sci Transl Med* (2015) 7(302):302ra136. doi: 10.1126/scitranslmed.aac9459
23. Rudin CM, Pietanza MC, Bauer TM, Ready N, Morgensztern D, Glisson BS, et al. Rovalpituzumab Tesirine, a DLL3-Targeted Antibody-Drug Conjugate, in Recurrent Small-Cell Lung Cancer: A First-in-Human, First-in-Class, Open-Label, Phase 1 Study. *Lancet Oncol* (2017) 18(1):42–51. doi: 10.1016/S1470-2045(16)30565-4
24. Morgensztern D, Besse B, Greillier L, Santana-Davila R, Ready N, Hann CL, et al. Efficacy and Safety of Rovalpituzumab Tesirine in Third-Line and Beyond Patients With DLL3-Expressing, Relapsed/Refractory Small-Cell Lung Cancer: Results From the Phase II TRINITY Study. *Clin Cancer Res* (2019) 25(23):6958–66. doi: 10.1158/1078-0432.CCR-19-1133
25. Owen DH, Giffin MJ, Bailis JM, Smit MD, Carbone DP, He K. DLL3: An Emerging Target in Small Cell Lung Cancer. *J Hematol Oncol* (2019) 12(1):61. doi: 10.1186/s13045-019-0745-2
26. Giffin MJ, Cooke K, Lobenhofer EK, Estrada J, Zhan J, Deegen P, et al. AMG 757, A Half-Life Extended, DLL3-Targeted Bispecific T-Cell Engager, Shows High Potency and Sensitivity in Preclinical Models of Small-Cell Lung Cancer. *Clin Cancer Res* (2021) 27(5):1526–37. doi: 10.1158/1078-0432.CCR-20-2845
27. Owonikoko TK, Borghaei H. Immunotherapy of Lung Cancer. *J Thorac Dis* (2018) 10(Suppl 3):S395–S6. doi: 10.21037/jtd.2018.01.142
28. Tanaka K, Isse K, Fujihira T, Takenoyama M, Saunders L, Bheddah S, et al. Prevalence of Delta-Like Protein 3 Expression in Patients With Small Cell Lung Cancer. *Lung Cancer* (2018) 115:116–20. doi: 10.1016/j.lungcan.2017.11.018
29. Hermans BCM, Derks JL, Thunnissen E, van Suylen RJ, den Bakker MA, Groen HJM, et al. DLL3 Expression in Large Cell Neuroendocrine Carcinoma (LCNEC) and Association With Molecular Subtypes and Neuroendocrine Profile. *Lung Cancer* (2019) 138:102–8. doi: 10.1016/j.lungcan.2019.10.010
30. Xie H, Boland JM, Maleszewski JJ, Aubry MC, Yi ES, Jenkins SM, et al. Expression of Delta-Like Protein 3 is Reproducibly Present in a Subset of Small Cell Lung Carcinomas and Pulmonary Carcinoid Tumors. *Lung Cancer* (2019) 135:73–9. doi: 10.1016/j.lungcan.2019.07.016
31. Alcala N, Leblay N, Gabriel AAG, Mangiante L, Hervas D, Giffon T, et al. Integrative and Comparative Genomic Analyses Identify Clinically Relevant Pulmonary Carcinoid Groups and Unveil the Supra-Carcinoids. *Nat Commun* (2019) 10(1):3407. doi: 10.1038/s41467-019-11276-9
32. Rojo F, Corassa M, Mavroudis D, Aysim Büge Öz, Biesma B, Brcic L, et al. International Real-World Study of DLL3 Expression in Patients With Small Cell Lung Cancer. *Lung Cancer* (2020) 147:237–43. doi: 10.1016/j.lungcan.2020.07.026
33. Liu L, Wei J, Teng F, Zhu Y, Xing P, Zhang J, et al. Clinicopathological Features and Prognostic Analysis of 247 Small Cell Lung Cancer With Limited-Stage After Surgery. *Hum Pathol* (2021) 108:84–92. doi: 10.1016/j.humpath.2020.11.007
34. Brierley JD, Wittekind C, Gospodarowicz MK. *TNM Classification of Malignant Tumours*. Oxford, UK: Wiley Blackwell (2017).
35. Brcic L, Kuchler C, Eidenhammer S, Pabst D, Quehenberger F, Gazdar AF, et al. Comparison of Four DLL3 Antibodies Performance in High Grade Neuroendocrine Lung Tumor Samples and Cell Cultures. *Diagn Pathol* (2019) 14(1):47. doi: 10.1186/s13000-019-0827-z
36. Lashari BH, Vallatharasu Y, Kolandra L, Hamid M, Uprety D. Rovalpituzumab Tesirine: A Novel DLL3-Targeting Antibody-Drug Conjugate. *Drugs R D* (2018) 18(4):255–8. doi: 10.1007/s40268-018-0247-7
37. Ogawa H, Sakai Y, Nishio W, Fujibayashi Y, Nishikubo M, Nishioka Y, et al. DLL3 Expression is a Predictive Marker of Sensitivity to Adjuvant Chemotherapy for Pulmonary LCNEC. *Thorac Cancer* (2020) 11(9):2561–9. doi: 10.1111/1759-7714.13574
38. Tendler S, Kanter L, Lewensohn R, Ortiz-Villalon C, Viktorsson K, De Petris L. The Prognostic Implications of Notch1, Hes1, Ascl1, and DLL3 Protein Expression in SCLC Patients Receiving Platinum-Based Chemotherapy. *PloS One* (2020) 15(10):e0240973. doi: 10.1371/journal.pone.0240973
39. Furuta M, Sakakibara-Konishi J, Kikuchi H, Yokouchi H, Nishihara H, Minemura H, et al. Analysis of DLL3 and ASCL1 in Surgically Resected Small Cell Lung Cancer (Hot1702). *Oncologist* (2019) 24(11):e1172–e9. doi: 10.1634/theoncologist.2018-0676

40. Wang J, Zhang K, Liu Z, Wang T, Shi F, Zhang Y, et al. Upregulated Delta-Like Protein 3 Expression Is a Diagnostic and Prognostic Marker in Endometrial Cancer: A Retrospective Study. *Med (Baltimore)* (2018) 97(51): e13442. doi: 10.1097/MD.0000000000013442
41. Liu ZY, Wu T, Li Q, Wang MC, Jing L, Ruan ZP, et al. Notch Signaling Components: Diverging Prognostic Indicators in Lung Adenocarcinoma. *Med (Baltimore)* (2016) 95(20):e3715. doi: 10.1097/MD.0000000000003715
42. Koshkin VS, Garcia JA, Reynolds J, Elson P, Magi-Galluzzi C, McKenney JK, et al. Transcriptomic and Protein Analysis of Small-Cell Bladder Cancer (SCBC) Identifies Prognostic Biomarkers and DLL3 as a Relevant Therapeutic Target. *Clin Cancer Res* (2019) 25(1):210–21. doi: 10.1158/1078-0432.CCR-18-1278
43. Huang J, Cao D, Sha J, Zhu X, Han S. DLL3 is Regulated by LIN28B and miR-518d-5p and Regulates Cell Proliferation, Migration and Chemotherapy Response in Advanced Small Cell Lung Cancer. *Biochem Biophys Res Commun* (2019) 514(3):853–60. doi: 10.1016/j.bbrc.2019.04.130
44. Volante M, Mete O, Pelosi G, Roden AC, Speel AJM, Uccella S. Molecular Pathology of Well-Differentiated Pulmonary and Thymic Neuroendocrine Tumors: What Do Pathologists Need to Know? *Endocr Pathol* (2021) 32 (1):154–68. doi: 10.1007/s12022-021-09668-z
45. Marchiò C, Gatti G, Massa F, Bertero L, Filosso P, Pelosi G, et al. Distinctive Pathological and Clinical Features of Lung Carcinoids With High Proliferation Index. *Virchows Arch* (2017) 471(6):713–20. doi: 10.1007/s00428-017-2177-0
46. Klimstra D, Kloppel G, La Rosa Salas B. The WHO Classification of Tumours Editorial (Ed.), Classification of Neuroendocrine Neoplasms of the Digestive System. In: *WHO Classification of Digestive System Tumours, 5th ed*. Lyon: IARC Press (2019). p. 16–21.
47. Cardnell RJ, Li L, Sen T, Bara R, Tong P, Fujimoto J, et al. Protein Expression of TTF1 and cMYC Define Distinct Molecular Subgroups of Small Cell Lung Cancer With Unique Vulnerabilities to Aurora Kinase Inhibition, DLL3 Targeting, and Other Targeted Therapies. *Oncotarget* (2017) 8(43):73419–32. doi: 10.18632/oncotarget.20621

Conflict of Interest: The authors declare that the research was conducted in the absence of any commercial or financial relationships that could be construed as a potential conflict of interest.

Publisher's Note: All claims expressed in this article are solely those of the authors and do not necessarily represent those of their affiliated organizations, or those of the publisher, the editors and the reviewers. Any product that may be evaluated in this article, or claim that may be made by its manufacturer, is not guaranteed or endorsed by the publisher.

frontiers in Oncology

REVIEW
published: 21 October 2021
doi: 10.3389/fonc.2021.757323

Alternative Energy: Breaking Down the Diverse Metabolic Features of Lung Cancers

Kasey R. Cargill, William L. Hasken, Carl M. Gay and Lauren A. Byers *

Department of Thoracic/Head and Neck Medical Oncology, University of Texas MD Anderson Cancer Center, Houston, TX, United States

Metabolic reprogramming is a hallmark of cancer initiation, progression, and relapse. From the initial observation that cancer cells preferentially ferment glucose to lactate, termed the Warburg effect, to emerging evidence indicating that metabolic heterogeneity and mitochondrial metabolism are also important for tumor growth, the complex mechanisms driving cancer metabolism remain vastly unknown. These unique shifts in metabolism must be further investigated in order to identify unique therapeutic targets for individuals afflicted by this aggressive disease. Although novel therapies have been developed to target metabolic vulnerabilities in a variety of cancer models, only limited efficacy has been achieved. In particular, lung cancer metabolism has remained relatively understudied and underutilized for the advancement of therapeutic strategies, however recent evidence suggests that lung cancers have unique metabolic preferences of their own. This review aims to provide an overview of essential metabolic mechanisms and potential therapeutic agents in order to increase evidence of targeted metabolic inhibition for the treatment of lung cancer, where novel therapeutics are desperately needed.

Keywords: lung cancer, metabolism, metabolic inhibitors, glycolysis (Warburg effect), oxidative phosphorylation

OPEN ACCESS

Edited by:
Meng Xu Welliver, The Ohio State University, United States

Reviewed by:
Loredana Urso, University of Padua, Italy
Natasha A. Jain, Deaconess Henderson Clinic, United States

***Correspondence:**
Lauren A. Byers
lbyers@mdanderson.org

Specialty section:
This article was submitted to Thoracic Oncology, a section of the journal Frontiers in Oncology

Received: *12 August 2021*
Accepted: *29 September 2021*
Published: *21 October 2021*

Citation:
Cargill KR, Hasken WL, Gay CM and Byers LA (2021) Alternative Energy: Breaking Down the Diverse Metabolic Features of Lung Cancers. Front. Oncol. 11:757323. doi: 10.3389/fonc.2021.757323

INTRODUCTION

Lung cancer continues to be recognized as the leading cause of cancer-related deaths in the United States (1). Non-small cell lung cancer (NSCLC) accounts for around 85% of all lung cancers and includes adenocarcinoma (40-50%), squamous cell carcinoma (SCC; 25-30%), and large cell carcinoma (3-10%) (2, 3). Approximately 25% of these tumors are diagnosed early in disease progression when surgical resection is the primary treatment leaving them with a 60% five year survival rate (2, 4). Unfortunately the remaining diagnoses are ineligible for surgery due to advanced disease and receive frontline chemotherapy or radiation and have a five year survival rate of 23% (2). In comparison, SCLC accounts for 15% of all lung tumors, but has a substantially lower five year survival rate of only 7% (1). SCLC is not routinely resected due to frequently advanced staging at the time of diagnosis, therefore despite recent advances in chemo- and immunotherapies, prognosis remains poor. The dismal survival rates and rapid relapse among all types of lung cancer, highlights the importance of research into personalized therapeutic strategies.

Many cancer investigations have underscored the significance of altered metabolic phenotypes in both the tumor and tumor microenvironment (TME), however few studies in lung cancer (both NSCLC and SCLC) have been aimed at understanding the contribution of metabolic dysregulation

to disease progression and therapy response. This review aims to provide an overview of essential metabolic mechanisms and potential therapeutic agents in order to increase evidence of targeted metabolic inhibition for the treatment of lung cancer.

LUNG CANCER AS A METABOLIC DISEASE

Cancer metabolism has been a prominent avenue of investigation since the 1920s when Dr. Otto Warburg classified what is now known as the Warburg effect (5, 6). This observation that cancer cells exhibit enhanced glucose metabolism over the more efficient oxidative metabolism became a hallmark of the disease and is still a widely accepted and investigated phenomenon. The Warburg effect is comprised of three main aspects: 1) enhanced glucose uptake 2) increased lactate secretion and 3) decreased oxidative metabolism (**Figure 1**) (7–9). Dr. Warburg originally attributed the decrease in oxidative metabolism to mitochondrial dysfunction; however this hypothesis has since been disputed. While some tumors do exhibit loss of mitochondrial density or altered dynamics rendering the organelle non-functional, other types retain their oxidative metabolic capacity entirely and may even up-regulate oxidative mechanisms of nutrient production, particularly in chemoresistant tumors (8, 10). This suggests that cancer cells are adaptive in terms of the metabolic pathways needed for tumorigenesis and cancer persistence. Therefore, today it is realized that each cancer needs to be independently evaluated for metabolic pathway utilization. These crucial differences in the metabolic preference of cancer are at the forefront of investigation and may hold the key to identifying novel molecules for therapeutic targeting with broad application to the personalization of cancer medicine.

Metabolic Pathways Contributing to Cancer

Increased aerobic glycolysis characterized by uptake of glucose and lactate secretion is the most notable effect described by Warburg (7, 8, 11). This phenomenon is observed in many cancers, however the mechanisms driving this phenotype are significantly more complex. For example, several oncogenic pathways have been implicated in the up-regulation of glycolysis, including MYC, PI3K-Akt-mTOR, and stabilized HIF-1/2α to name a few (**Table 1**) (8, 29–31). Collectively, these pathways are involved in increased expression of almost every enzyme in the glycolysis pathway. More recently, mechanisms such as HIF stabilization have been shown to concurrently down regulate mitochondrial pyruvate oxidation (32, 33). Other such mechanisms also exist including regulation through reactive oxygen species (ROS) (34). Apart from suppression of mitochondrial respiration, several reports have revealed that mitochondria may also be crucial for energy and biosynthetic precursor generation as well (35–37), but this has been less readily interrogated. Because of the complexity and differences of metabolic regulation in cancer cells, an emerging

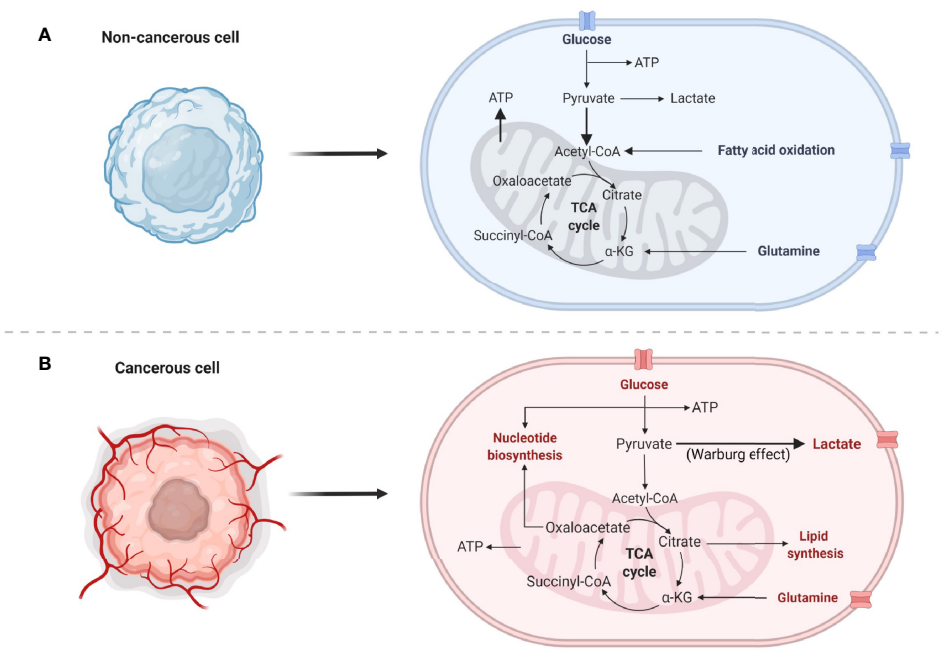

FIGURE 1 | Normal and cancer cell metabolisms. **(A)** Common normal, non-cancerous metabolic pathways predominantly utilized by the cells. Bold arrows indicate increased flux of pyruvate into the mitochondria for the generation of ATP. **(B)** Highly proliferative cancer cell metabolism utilizes numerous pathways to generate energy, nucleotides, lipids, and amino acids. Bold arrow indicates preferential conversion of pyruvate to lactate, known as the Warburg effect.

TABLE 1 | The effect of genetic mutation on metabolism.

Gene Mutation	Expression Change	Altered Pathway	References
EGFR	↑	Glycolysis Nucleotide metabolism	Jin et al. (12); Bethune et al. (13)
KEAP1	↓	Glutaminolysis	Romero et al. (14)
KRAS	↑	Fatty acid metabolism GlycolysisPPP	Jin et al. (12); Pupo et al. (15); Jančík et al. (16); Padanad, et al. (17)
LKB1	↓	Glutaminolysis	Galan-Cobo et al. (18)
MYC	↑	Fatty acid metabolism Glutaminolysis Glycolysis	Chalishazar et al. (19); Rapp et al. (20); Marengo et al. (21)
NOTCH1	↑	Glutaminolysis GlycolysisOxidative phosphorylation	Sellers et al. (22); Zou et al. (23)
NTRK1	↑	Glutaminolysis GlycolysisOxidative phosphorylation	Vaishnavi et al. (24); Yang et al. (25)
P53	↓	Glycolysis	Jin et al. (12)
PTEN	↓	Glycolysis	Jin et al. (12); Georgescu (26)
RB1	↓	Amino acid metabolism GlycolysisNucleotide metabolism	Bhateja et al. (27); Mandigo et al. (28)

Lung cancers typically acquire specific genetic mutations leading to tumor formation and progression. Several commonly mutated genes lead to metabolic changes that result in therapy resistance. ↑ indicates increased expression; ↓ indicates decreased expression.

hypothesis is that the metabolic profiles of individual cancer cells may be as heterogeneous as the tumor itself.

Metabolic reprogramming is just one hallmark of cancer that serves to facilitate rapid cellular proliferation, avoidance of cell death, and mitigation of stress responses. Although non-cancerous, terminally differentiated cells rely on oxidative phosphorylation (OXPHOS) to meet energy demands, cancer cells require nucleotides [generated by the pentose phosphate pathway (PPP)], reducing equivalents [generated by glycolysis, the PPP, and the tricarboxylic acid cycle (TCA)], and amino acids (taken in from the TME or generated predominantly from the PPP or TCA) in addition to energy produced from glycolysis and OXPHOS to adapt to constant changes in their environment (**Figure 1**). See the following review for an in-depth overview of the aforementioned metabolic pathways in lung cancer (38). In addition to these biomolecules supporting tumor growth, many metabolites also play a role in anti-apoptotic signaling and interaction with the TME (39, 40). The current literature depicting the metabolic processes provides insight into why lung cancers exhibit aggressive tumor growth, making it the number one cause of cancer-related deaths (1, 41).

Non-Small Cell Lung Cancer

Although the morphological and genetic components leading to NSCLC are largely known, long-term survival of disease remains inadequate despite recent advances in personalized treatment and immunotherapies (42, 43). Thus, recent studies have been aimed at elucidating the metabolic properties and vulnerabilities driving NSCLC (44). Unlike some cancers that exhibit clear-cut dependence on a particular metabolic pathway, NSCLC utilizes multiple pathways to drive proliferation (44)—however it is unclear whether these pathways operate simultaneously or arise due to the heterogeneous cell population found in the diverse tumor environment. Studies investigating the mechanisms that dictate tumor growth have shed light on the importance of cellular metabolism in driving disease and have become the focus of several therapeutic opportunities (17, 18). While these reports show metabolic reprogramming is a contributor to cancer, few treatment options have progressed through early stage clinical trials despite promising pre-clinical results. In NSCLC specifically, recurrently mutated oncogenes and tumor suppressors (*TP53*, *EGFR*, *KEAP1*, and others) have been implicated as regulators of metabolism and major drivers of metabolic reprogramming (**Table 1**) (44).

To determine whether metabolic heterogeneity is related to increases in both glycolysis and TCA cycle intermediates, one study profiling 80 NSCLC human cell lines found that the ratio of glucose utilization and lactate secretion varied greatly between samples indicating that the Warburg effect is not a universal characteristic of NSCLC (44). In fact, NSCLC can be divided into at least glycolysis-dependent and OXPHOS-dependent subtypes (45). NSCLC cell lines subjected to Seahorse extracellular flux analysis treated with either metformin (OXPHOS inhibitor) or a MCT4 (lactate) inhibitor found that OXPHOS-dependent cells were sensitive to metformin, whereas cellular proliferation was attenuated by MCT4 inhibition specifically in the glycolysis-dependent cells (45). Other investigations have shown that NSCLC cells also take in lactate through MCT1 lactate transporters to utilize as a carbon source in the TCA cycle and lipid biosynthesis (36, 38, 46). This suggests that an increased flux through glycolysis may directly supply lactate for paracrine reuptake to meet both aerobic and anaerobic cellular demands. Although cell lines are a valuable tool for investigating the complexities of metabolism, the differences between immortalized cell lines and primary resected tumors adds difficulty to teasing apart metabolic discrepancies between studies.

Several studies have interrogated the cellular and genetic discrepancies among the most common subsets of NSCLC—adenocarcinoma and squamous cell carcinoma (SCC) (2), therefore is likely that there are metabolic differences as well. Resected human adenocarcinoma and SCC tumors subjected to stable isotope tracing indicated that squamous cell carcinoma relies on NOTCH1-driven glucose and glutamine catabolism to a greater extent than adenocarcinoma, suggesting enhanced glycolysis is a crucial driver for the quick progression of SCC (22, 47). A 24-gene signature comprised of glycolysis (ALDOC, GAPDH, PGAM, and TPI), PPP (G6PDH and TALDO1), nucleotide synthesis (CTPS1, GMPS, PAICS, and UMPS), amino acid biosynthesis (AHCY, ASNS, BDH1, CKMT1, GCLM, GGH, GSS, MTHFD2, PSAT1, and SHMT2), and TCA cycle (GOT2, IDH2, MDH2, and ME1) genes was elucidated between SCC and adenocarcinoma and conferred a worse outcome in SCC patients (22). In addition to gene expression,

enzymatic activity was enhanced across 10 glycolytic enzymes in SCC compared to adenocarcinoma, which correlated to the NOTCH pathway (including MYC expression) (22). Interestingly, in addition to glycolysis, TCA cycle intermediates, fatty acid synthesis biomolecules, and reducing equivalents were all increased in SCC, however it is hypothesized that this is to regenerate NAD+ for glycolysis (22). Another explanation is that NSCLC has uniformly enhanced bioenergetics or more likely, it is comprised of glycolytic and oxidative regions that are challenging to delineate and will require more sophisticated single cell analysis.

Other recent clinical work performed ^{13}C-glucose diffusion in nine NSCLC patients and found an increase in glucose and TCA-derived metabolites (i.e. lactate, citrate, glutamate, and malate) (48). Of these patients, four had EGFR mutations, two harbored KRAS mutations, and the remaining three did not have either mutation (48). The group further showed that neither mutation status conferred unique metabolic alternations (48). Although mutational status was not predictive of the exact metabolic changes that would be induced in a patient, which may in part be due to the small sample size, these mutations are quite common among NSCLC. In fact, lung adenocarcinoma can be classified by genetic mutations in *TP53* (46%), *KRAS* (32%), *EGFR* (27%), and *KEAP1* (23%), among others (14, 49, 50) and SCC may have mutations in *TP53* (90%), *KEAP1* (31%), and *PTEN* (15%) and others (**Table 1**) (50–52). Further, these mutations may provide insight into the metabolic state of each cancer type.

TP53 mutations, implicated in both adenocarcinoma and SCC, have profound significance in altering metabolism. Wild type p53 plays a role in maintaining OXPHOS by assembling complexes of the electron transport chain while simultaneously inhibiting glycolytic enzyme transcription and the oxidative branch of the PPP (38). In line with these observations, p53 expression has been identified as a biomarker of resistance to the glycolysis inhibitor 2-deoxy-D-glucose (2DG) such that p53-deficient NSCLC cells (H358) exhibit significantly reduced ATP levels accompanied by profound oxidative stress when treated with 2DG (53) suggesting that glycolysis inhibition would be preferentially beneficial in tumors lacking p53.

EGFR mutations occur most often in lung adenocarcinomas and play an important part in mediating global metabolic reprogramming. Alterations in *EGFR* commonly result in the Warburg effect through stabilization of glucose transporters. Further, signaling through the PI3K/AKT/mTOR pathway promotes glycolysis by regulating the localization of glucose transporter GLUT1 to the plasma membrane in *EGFR*-mutated NSCLC (54). Moreover, glutaminolysis is increased and inhibition with erlotinib in combination with CB-839 (glutaminase inhibitor) in *EGFR*-mutated tumors resulted in tumor regression (55). This sets precedence for combinatorial approaches targeted at altered metabolism and genetic mutations in lung cancer.

KRAS activating mutations are common and mutually exclusive to *EGFR* mutations. *In vivo* lung tumors with depleted KRAS exhibit reduced glycolysis and lipid gene expression leading to reduced uptake of these associated metabolites, consistent with reports that show KRAS overexpression up-regulates these pathways (17, 56). Further, inhibition of the glycolysis pathway with 2DG in KRAS mutant NSCLC models significantly attenuated cell line and tumor growth (57). Because the mutant form of KRAS has thus far been untargetable by conventional chemotherapeutic agents, it is advantageous to identify targets enhanced by this *KRAS* mutation (51). To this affect, studies have been aimed at investigating targetable mechanisms downstream of the mutation, including the consequential metabolic reprogramming that occurs. This serves as yet another example of how targeting major metabolic pathways may lead to treatment options capable of reducing tumor growth regardless of mutation status.

KEAP1 mutations often occur concurrently with *KRAS* mutations in adenocarcinomas, however can occur independent of *KRAS* particularly in SCC (14, 58). Although *KRAS* mutant tumors are largely characterized by glucose and lipid metabolizing pathways, *KEAP1* mutations are also highly dependent on glutamine (14). This glutamine dependence has been therapeutically targeted with CB-839 in lung adenocarcinoma xenografts which revealed decreased tumor growth rates (14). Interestingly, *KEAP1* loss also decreases the production of ROS and enhances resistant to oxidative stress (58). This is through the regulation of NRF2 protein stability, a mediator of pathways including cellular stress, autophagy, proliferation, and metabolism. Together, KEAP1/NRF2 coordinate to reprogram cancer cells towards pathways that support glycolysis, mitochondrial respiration, and amino acid biosynthesis (14, 59).

Lastly, *LKB1* inactivation or mutation occurs in nearly 20% of NSCLC cases, and, similarly to KEAP1 mutations, occur concurrently with KRAS mutations in 7-10% of NSCLCs (60). LKB1 canonically phosphorylates the family of AMP-related kinases, which are major sensors of cellular energy that target mitochondria and fatty acid metabolism pathways. Due to this, LKB1-deficient lung cancer cells were preferentially susceptible to the mitochondrial electron transport chain complex I inhibitor phenformin (60). This effect was not seen with the similar agent metformin nor the glycolysis inhibitor 2DG, due to an induction of ROS leading to increased mitophagy (60). In addition to LKB1 and KRAS concurrent mutations, KEAP1 inactivating mutations are also often enriched for simultaneous KEAP1 mutations. Collectively, these three mutations cooperatively drive dependence on glutamine and thus, are sensitive to CB-839 *in vitro* and *in vivo* (18). These data indicate that LKB1 mutations do not reprogram towards glycolysis and instead are reliant on OXPHOS to drive tumor progression.

Studies such as these, that elucidate the contribution of mutational status to metabolic rewiring, lay the foundation for use of metabolic modulators in NSCLC. Although, it is clear that additional phenotyping across cell lines and primary tumors is required to identify biomarker predictors of metabolic pathway utilization. In addition to this, it is likely that metabolic signatures of tumors may be regulated by addition mechanisms including DNA methylation (44). It is evident that there are numerous contributors to cellular metabolism. Much like the

genetic heterogeneity seen in solid tumors, there is growing evidence that NSCLCs exhibit localized regions in the tumors that may have different nutrient requirements, which may be dependent on various factors including nutrient availability, oxygenation, and immune infiltration (48).

Small Cell Lung Cancer

Unlike NSCLC, SCLC is characterized by universal loss of *RB1* and *TP53* and traditionally diagnosed, classified, and treated as a single disease (**Table 1**) (51, 61–64). The evolution of SCLC subtyping has occurred over the past 30 years starting with the observation that SCLC cell lines had two prominent biochemical signatures, which resulted in classification of *classical* and *variant* subtypes (65). Moreover, the variant subtype was further divided into categories dependent on unique biochemical, morphological, and growth properties (66). Once this initial characterization was established, several studies began looking at the unique molecular signatures (67, 68), which included the identification of the neuroendocrine transcription factor subtypes ASCL1 (67, 69, 70) and NEUROD1 (67, 79), the non-neuroendocrine, tuft-cell variant classified by POU2F3 (67, 71), *MYC*-driven populations (19, 68), and *YAP/TAZ* variant phenotype (67, 72). Although much effort has been directed towards finding an appropriate characterization system, less is known about the metabolic preferences and pathway utilization, which may further delineate SCLC.

SCLC is most notably characterized by loss of *RB1* and *P53*, both of which regulate various metabolic pathways (**Table 1**) (28, 73–75), therefore the observation of metabolic differences based on these alone would not provide unique and targetable pathways. Metabolically, the most well studied subcategories of SCLC are driven by ASCL1 and MYC expression. ASCL1 is a transcription factor dictating neuroendocrine lineage that can be stratified into $ASCL1^{high}$ and $ASCL1^{low}$ populations (76). Interestingly, $ASCL1^{low}$ cell lines and tumors often highly express the transcription factor MYC, which is implicated in approximately 20% of SCLC (68, 73, 76). The $ASCL1^{Low}/MYC^{High}$ phenotype also typically has high NEUROD1 [in cell lines and genetically engineered mouse models (GEMMs)] or POU2F3 (in patient tumors) expression, however this discrepancy between cell lines, mouse models, and patient tumors is not well understood (73, 74, 77, 78).

Combined metabolic and transcriptional profiling of a panel of 29 SCLC cell lines and 47 primary SCLC tumors revealed that *ASCL1* was the top differential gene delineating two major metabolomics profiles (76, 79). The identified metabolites were linked to nucleotide biosynthesis, amino acid metabolism, and the TCA (76). Interestingly, several purine, but not pyrimidine, nucleotides were significantly elevated only in the $ASCL1^{Low}$ cell lines (76). Similarly, transcriptional data from 81 patient tumors (74) revealed that genes linked to purine synthesis (*IMPDH1* and *IMPDH2*) were also enriched in approximately 20% of the tumors that also had low *ASCL1* expression (76). Moreover, *MYC* expression strongly correlated with *IMPDH1* and *IMPDH2* and ChIP-seq experiments confirmed direct MYC binding to the promoter region of these genes (76). This led to a hypothesis that IMPDH may be a targetable biomolecule and CRISPR/Cas9 *IMPDH1* knockdown and treatment with the IMPDH inhibitor mycophenolic acid (MPA) both lead to significant decreases in cellular viability in treatment-naïve and chemoresistant SCLC (76, 79). Clinically, this provides a basis for investigation into the use of IMPDH inhibitors such as MPA and mizoribine, but also may in part explain why anti-folates and nucleoside analogues are moderately successful in NEUROD1 and POU2F3-expressing SCLC, which commonly exhibit MYC overexpression (78, 80).

In addition to nucleotide synthesis, the $ASCL1^{Low}MYC^{High}$ phenotype has also been implicated in alterations in amino acid and polyamine synthesis in SCLC (19, 76). Tumors from ASCL1-driven $Rb1^{fl/fl};p53^{fl/fl};Pten^{fl/fl}$ (RPP) mice and MYC-driven (NEUROD1 phenotype) $Rb1^{fl/fl};p53^{fl/fl};MycT58A^{LSL/LSL}$ mice exhibit metabolically distinct patterns with particular enrichment in the arginine and proline biosynthesis pathways (19). In line with this, inhibition of polyamine biosynthesis with NOS, ODC1, or mTOR inhibitors and siRNAs against *ODC1* reduced cellular proliferation and viability in MYC-driven SCLC cell lines (19). Moreover, metabolic distinctions between treatment-naïve and chemo-resistance revealed that chemo-resistant cell lines exhibited a dependence on arginine and polyamine biosynthetic pathways as well as the mTOR pathway that was directly modulated by MYC expression (19). Not only does MYC play a key role in the metabolic phenotype of SCLC, but also in the evolution of the molecular subtype profile (19). MYC has been shown to regulate the dedifferentiation of ASCL1+ neuroendocrine cells through promotion of Notch signaling to support the evolution of NEUROD1+ and YAP1+ cells (19). While MYC has not been directly implicated in the emergence of chemo-resistance, MYC-driven fluctuations in Notch signaling activation and metabolic alterations may contribute to the plasticity of SCLC subtypes and appearance of subtype evolution or tumor heterogeneity (19, 78, 81, 82)

Nucleotides and amino acids are essential for the rapid proliferation that characterizes cancer; however, the specific pathways that generate these biomolecules are relatively understudied in SCLC. With the recent introduction of molecular subtyping and the initiative to discover subtype-specific therapies, metabolic profiling may offer valuable insight into new therapeutic targets. Although, current pathway analysis is limited, Morita et al. performed an investigation into the role of the glycolysis enzymes PKM1 and PKM2 in neuroendocrine SCLC (80). PKM1 is often expressed in terminally differentiated cells, while PKM2 is more commonly expressed by proliferating cells and cancer regulated by MYC (83). PKM2 is therefore likely favored by cells exhibiting the Warburg effect, whereas PKM1 is preferred by more oxidative tumors in most cases (84, 85). In a pan-cancer analysis, the PKM1/PKM2 ratio was higher in SCLC compared to several other types of cancer, however it is important to note that PKM1 was still not the major PK isoform expressed (only 16-38%) (80). PKM1 was also found to be required for PKM2 activation leading to cellular proliferation and exclusive expression of PKM1 facilitated active flux of glucose-derived carbons into the TCA with reduced lactate production (80). With the regulation of both glucose catabolism and OXPHOS by PK isozymes, inhibitors of these crucial pathways may prove effective. Unfortunately, there are no

current investigations into the use of glycolysis inhibitors, however a Phase II clinical trial with CP-613 has been conducted in a small cohort of 12 patients with relapsed SCLC (86). CP-613 is a lipoate analogue that targets pyruvate dehydrogenase (PDH) and alpha-ketoglutarate dehydrogenase (KGDH), two key mitochondrial enzymes. Although efficacy was poor with no partial or complete responses, all 3 patients who subsequently were treated with topotecan exhibited robust response (86). Moreover, *in vitro* combination of CP-613 with topotecan was synergistic and offers evidence for a combinatorial approach of metabolic inhibitors and chemotherapy in future investigations (86).

Large cell neuroendocrine carcinoma (LCNEC) is a rare form of lung cancer (approximately 3%) associated with *TP53* (86%) and/or *RB1* (36%) gene alterations (**Table 1**) (3, 87). While LCNEC is classified as a variant of NSCLC, the transcriptional properties and clinical treatment regimen is quite similar to SCLC (3, 88). An integrative genomic and transcriptomic profiling of LCNEC revealed two subclasses: Type I ($ASCL1^{High}/DLL3^{High}/Notch^{Low}$) and Type II ($ASCL1^{Low}/DLL3^{Low}/Notch^{High}$). Type I LCNEC shared closest similarities with classic ASCL1-driven SCLC and exhibited increased expression of genes involved in energy generation, OXPHOS, ETC/ATP synthase pathways (88). This suggests that ASCL1-driven SCLC and Type I LCNEC are more reliant on mitochondrial respiration rather than the Warburg effect (88). While we can extrapolate that Type II LCNEC is more similar to variant NEUROD1- or MYC-driven SCLC, further metabolomic profiling is required.

NUTRIENT COMPETITION AND THE TUMOR MICROENVIRONMENT

With the recent emergence of immunotherapies (specifically, immune checkpoint blockade; ICB) and their usage in both NSCLC and SCLC, it is crucial to understand the role of metabolism in the regulation of an immune response in cancer. As previously demonstrated in this review, therapeutics for cancer have the ability to alter cellular metabolic programs used by cancer cells. Understanding the metabolic changes that occur as a result of therapy may shed light on new opportunities for combinatorial treatments that are more beneficial than front line therapies. Importantly, immune cell activation, expansion, and function require the same nutrients and metabolic pathways as cancer cells, with a specific dependence on glycolysis (40). Since tumor cells are often highly glycolytic, they outcompete immune cells for glucose, amino acids, and fatty acids leading to immune dysfunction and an inability to clear tumor antigens (**Figure 2**). This nutrient competition has also been implicated in driving tumor progression (40, 89). In addition to hoarding glucose, cancer cells have the unique ability to evade the immune system *via* metabolite secretion (lactate) and expression of immune checkpoint molecules (PD-L1), both of which decrease immune cell cytokine production (IFN-γ), glycolysis, and immune cell expansion (**Figure 2**) (90). This environment favors cancer persistence and leads to decreased immune cell function while promoting an anti-inflammatory environment that confers tolerance to the growing tumor.

The major product of the Warburg effect, lactate, is secreted into the tumor microenvironment (TME) by rapidly proliferating tumors (3, 36, 46, 91). This serves to acidify the TME region, which 1) fuels mitochondria 2) suppresses the immune system and 3) promotes metastasis through therapy resistance (**Figure 2**) (91). The metabolic heterogeneity of tumors allows for glycolytic and oxidative cells to work symbiotically through a bidirectional pyruvate to lactate conversion (91). As previously discussed in NSCLC, glycolytic cells secrete lactate through MCT4 while oxidative cells uptake lactate through MCT1 (46, 91), which maintains an acidic TME while providing fuel for *de novo* amino acid, nucleotide, and fatty acid synthesis. Moreover, a result of oxidative metabolism is ROS, which act as signaling molecules to suppress immune function (92, 93). More directly however, a decreased pH, due to lactate secretion, augments signaling pathways of immune cells, rendering them incapable of efficient activation through the down regulation of glycolysis-promoting mechanisms, leading to T cell exhaustion, apoptosis, and a pro-tumoral M2 macrophage phenotype (**Figure 2**) (91).

Current investigations have examined the efficacy of ICB as a single agent and in combination with chemotherapy and glycolysis inhibitors and found that glycolysis inhibition does not negatively affect immune function, since these drugs are taken in most rapidly by glucose-addicted cancer cells (94). Together, metabolism and nutrient availability are important factors that dictate the microenvironment's ability to promote immune evasion and tumor progression. In addition to altering the metabolic reprogramming required for proper immune cell activation, many tumors, including NSCLC and SCLC, express immune checkpoint molecules, such as PD-L1 (89). PD-L1-expressing tumor cells engage with PD-1 on lymphocytes to actively suppress immune cell expansion and effector function (**Figure 2**) (89). Apart from this, PD-L1 and glycolysis have been shown to be positively correlated, although it is currently unclear whether PD-L1 expression enhances glycolysis or vice versa. One study has shown that glucose deprivation lead to an up-regulation of PD-L1, while siRNA knockdown of PD-L1 likewise decreased expression of glycolysis enzymes (specifically PFKFB3) in NSCLC cell lines (95). Further, another investigation found that PD-L1 increased expression of the glycolysis enzyme HK2 in SCC NSCLC (96). These studies suggest that PD-L1 may be directly involved in the up-regulation of glycolysis and elude to potential signaling mechanisms such as PI1K/AKT/mTOR, EGFR, and HIF-1α (95–98). Interestingly, other investigations have concluded that the metabolic switch towards glycolysis is essential for PD-L1 overexpression (99, 100). Regardless of the mechanisms leading to synergy between glycolysis and PD-L1, it is clear that their up-regulation facilitates immune dysfunction and is associated with poorer survival (99, 101). Due to this, it would be interesting to investigate the ability of PD-L1 to be a potential biomarker of highly glycolytic tumors, which would allow for metabolic intervention with inhibitors of the glycolysis pathway. While

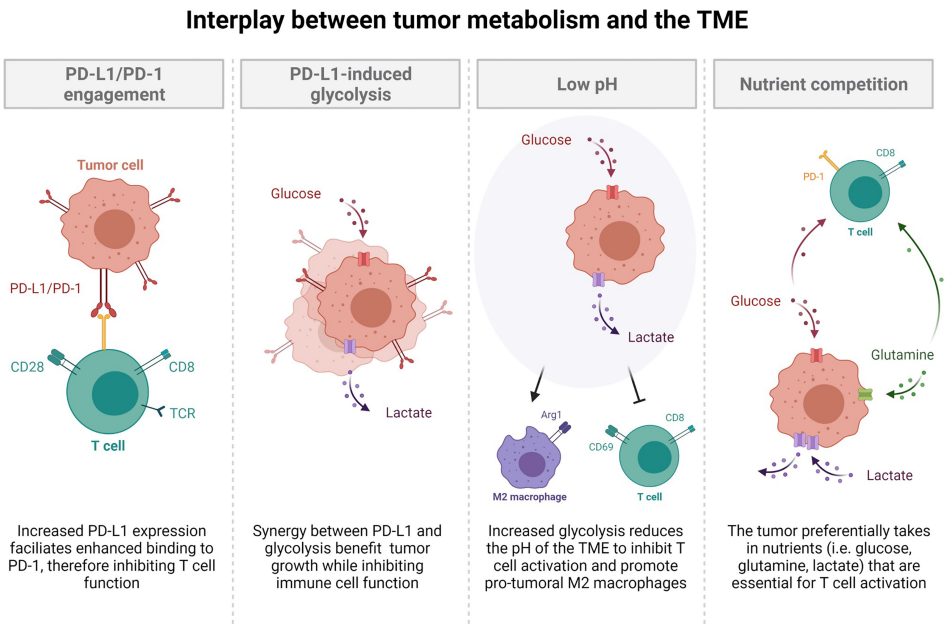

FIGURE 2 | The interplay between tumor metabolism and the tumor microenvironment. Increased PD-L1 expression facilitates enhanced binding to PD-1, thereby inhibiting T cell function. Synergy between PD-L1 and glycolysis benefit tumor growth while inhibiting immune cell function. Increased glycolysis reduces the pH of the tumor microenvironment to inhibit T cell activation and promotion of pro-tumoral M2 macrophages. The tumor preferentially takes in nutrients such as glucose, glutamine, and lactate, which are all essential for T cell activation. This nutrient competition leaves resources scarce for optimal T cell activation.

use of ICBs have variable success in the clinic, combinatorial therapies utilizing frontline chemotherapy and ICB plus glycolysis inhibitors may be more effective to restore the nutrient balance in the TME and promote reinvigoration of the immune system to promote tumor clearance.

METABOLIC IMPLICATIONS OF THERAPY IN LUNG CANCER

Fueling Resistance: Metabolic Alterations and Standard of Care

Current frontline efforts aimed at mitigating lung cancer is highly dependent on the subtype of disease and stage of progression at the time of diagnosis. Regardless of the treatment regimen, the baseline metabolic profile of the tumor plays a role in therapy sensitivity and rate of relapse. Cisplatin (a common platinum-based chemotherapy) resistance in particular is thought to be a result of lung cancer with a more oxidative phenotype, characterized by increased mitochondrial density, ROS, and dependence on glutamine and fatty acid oxidation mechanisms (102–105). Carboplatin (another platinum-based chemotherapy) resistance, however is associated with a greater dependence on glycolysis, possibly mediated by MYC expression (102, 106, 107). It is unclear whether these profound differences in resistance mechanisms are due to metabolic reprogramming events triggered by the treatment or whether the treatment selectively targets cells utilizing specific pathways from a metabolically heterogeneous population.

The recent approval of immunotherapies to be used as a standard of care has offered benefit to only subsets of patients (108). Understanding the role of immunotherapy in altering both tumor and immune metabolisms could provide key insights into why the rates of relapse for NSCLC and SCLC have not dramatically changed since this advancement. As previously discussed, the tumor and the immune system are in constant competition for access to the essential nutrients required for expansion of both cell populations. Therefore, optimal inhibition would block nutrient flux into the tumor leaving the essential molecules in the TME for immune activation. The addition of immunotherapy enhances mitochondrial activity and ROS production in tumor cells, which serves to divert glucose to the immune cells, and thus promoting activation unless terminal exhaustion has been attained (40, 109). ROS, however, can act as a double- edged sword for the immune system. While the canonical role is often associated with cytotoxic capabilities and promotion of DNA damage, another emerging role for ROS is as critical secondary messengers important for T cell differentiation and function (110). Metabolically, low to moderate levels of ROS are required for T cell metabolic reprogramming towards aerobic glycolysis upon T cell activation, and use of a manganese metalloporphyrin (ROS scavenger) significantly reduced function and engagement in the glycolysis pathway (111). In the TME, similar studies suggest that ROS levels exceed an advantageous amount, therefore a strict balance is required for

inducing T cell activation without causing functional inhibition (110). Although ICB attempts to facilitate immune activation, infiltration into large tumor masses often remains futile due to high ROS levels, lack of proper nutrients, and an acidic environment. This necessitates additional management of tumor growth and metabolic inhibitors would be a prime course of action. In fact, ongoing studies have seen improvement in ICB intervention with the addition of glycolysis, metabolite, and OXPHOS inhibitors in pre-clinical investigations (109, 112, 113).

Antimetabolites as Anticancer Drugs

While a portion of lung cancers have been meticulously characterized by alterations in gene expression and oncogene/tumor suppressor mutations, there has been little progress in developing therapies that target these mutations and effectively achieve adequate therapeutic outcomes in all patients. Because of this, it may be beneficial to explore treatment options that target the accelerated DNA replication that occurs in lung cancer cells. First employed clinically in the 1940's by Dr. Sidney Farber, antimetabolites work by mimicking substrates to irreversibly inhibit enzymes needed for DNA replication (114, 115). The effects of antimetabolites are generally cytotoxic, conferring the most pronounced effects on cells that are most metabolically active (116). While this class of drugs was originally used to treat lymphoblastic leukemia in children nearly a century ago, the use of antimetabolites as broad anti-cancer drugs did not achieve substantial popularity until much more recently (114, 115). What started as a single class of synthetic folate analogues has since expanded to a much broader collection of drugs targeting a larger array of enzymes essential to cellular metabolism. Two agents – gemcitabine and pemetrexed – are examples of antimetabolites used clinically today that may give way to new, more efficacious therapies in lung cancer. These antimetabolites, if any, may bear more exploration.

The nucleoside analogue gemcitabine is a potent pyrimidine antimetabolite that has historically been used as a first-line therapy for pancreatic adenocarcinoma, but has also been used to treat solid tumors in patients with breast, ovarian, and lung cancers (117). In its active form, gemcitabine interferes with cellular metabolism by acting as a nucleoside analogue to inhibit DNA synthesis (117). Gemcitabine has been particularly useful as an anti-cancer therapy because of additional effects that preferentially stimulate apoptotic signaling pathways in malignant cells through caspase activation. While this treatment offers a seemingly reliable way to target distinctly metabolically active cancer cells through restriction in DNA synthesis, literature shows chemoresistance develops quickly in a large subset of patients (117, 118). Although resistance often occurs within just weeks of initial treatment response, the mechanisms contributing to resistance are multifactorial stemming from genetic expression of the tumor and the immune cell profile. Interestingly however, a study evaluating chemoresistant SCLC patient's response to gemcitabine exhibited an overall response rate of 13% (119). Furthermore, clinical trials in NSCLC comparing gemcitabine alone and in combination with other classic therapies have shown little difference in treatment groups (120). Together, these studies suggest that metabolic intervention to delay nucleoside biosynthesis may be most effective as a late-stage treatment for patients that have acquired resistance to front-line therapies.

Another antimetabolite that has been in use clinically over the past two decades is pemetrexed. A synthetic folate analogue akin to the drugs Farber originally employed to treat lymphoblastic leukemia, pemetrexed acts in at least three mechanisms to disrupt production of both purines and pyrimidines, thus reducing cellular proliferation. Specifically, inhibiting thymidylate synthase, dihydrofolate reductase, and GAR formyl-transferase broadly depletes folate conferring anti-tumor effects against an assortment of cancers (121). Several clinical trials have sought to discern if pemetrexed is suitable for use as a single agent or combinatorial therapy for those with NSCLC. In clinical trial, pemetrexed exhibited a significantly increased progression free survival rate compared to placebo and was relatively well tolerated by patients (122). Similarly, Karayama et al. treated chemo-naïve non-squamous NSCLC patients with either pemetrexed or docetaxel and found a significantly increased period of toxicity free survival in pemetrexed-treated patients (123). Other studies have evaluated pemetrexed in combination with platinum-based chemotherapy as front-line treatment, with no discernable added efficacy to traditional chemotherapy (124). Although pemetrexed is a common front-line therapy for lung adenocarcinoma NSCLC, resistance is common (125).

Gemcitabine and pemetrexed are just two examples of the many chemotherapeutic agents under the broad category of antimetabolites. As single agents, antimetabolites have not proven incredibly successful for the treatment of lung cancer (126), however in combination with other chemotherapy agents there is least modest improvement of efficacy *in vitro* and *in vivo* (118, 126–128). Antimetabolites that interfere with cellular metabolism by inhibiting the synthesis of the building blocks of nucleotides appears as an ideal method of slowing tumor growth. In clinical practice, however, antimetabolites require high therapeutic dosages leading to toxic side effects in some NSCLC and SCLC patients (126, 127, 129), although toxicity has been partially mitigated through the addition of chemotherapy protective drugs (129). The progress seen in clinical trials, as well as experiments with adjuvant agents that increase efficacy, offer promise for the use of antimetabolites, however further research into patient stratification and biomarkers of efficacy should be considered.

Are Metabolic Inhibitors Effective in Lung Cancer Treatment?

Cellular metabolism consists of intricate pathways with the regulating molecules often rendered dysfunctional in tumors. Although signaling cascade pathways are potential therapeutic targets, toxicity in non-cancerous cells is often detrimental. To overcome this, directly modulating the metabolic pathways may prove advantageous, as the most metabolically active cells tend to be targeted by their increased uptake of nutrients—known as cellular selectivity based on demand (130). This provides several avenues for intervention by 1) stopping glucose/glutamine/lactate transport into the cell or 2) inhibiting enzymatic conversions in glycolysis and OXPHOS pathways (**Figure 3**).

Several studies have been aimed at blocking the major energy-producing carbon sources (glucose, glutamine, and lactate) from initial transport into a cancer cell (**Table 2**). Based on the predominant physiological need for glucose to support cancer cell proliferation, glucose transport inhibitors may be useful in limiting the amount of glucose taken in by the tumor. In human-derived NSCLC A549 cells, siRNA against GLUT1 inhibited colony formation, reduced proliferation, and increased apoptosis (131). When compared to non-tumorigenic lung (NL20) cells, A549 cells treated with the GLUT1 inhibitor WZB117 exhibited far less proliferation, indicating that A549 cells are inherently more glucose-dependent (**Table 2** and **Figure 3**) (132). Moreover, xenografts with A549-derived tumors that were treated with WZB117 had a 70% reduction in tumor growth compared to vehicle controls (132).

Another molecule relied on by cancer is glutamine, which is transported into the cell through amino acid transporters including SLC1A5 (133). SLC1A5 is highly expressed in NSCLC cell lines and human tumor samples (133). Studies in NSCLC using the glutamine analogue L-γ-Glutamyl-p-nitroanilide (GPNA) revealed that glutamine is transported through SLC1A5 and that this transporter is required for proliferation in glutamine-dependent cell lines (A549, HCC15, and H520), which was confirmed using siRNA against SLC1A5 (**Table 2** and **Figure 3**) (133). Inhibition of SLC1A5 using GPNA also showed a marked increase in ROS generation due to a blockade of the glutamine to glutathione (ROS scavenger) conversion (133).

The last carbon source discussed is lactate, which is transported by MCT1/MCT4. Treatment with the MCT1 inhibitor SR13800 decreased lactate transport and enhanced OXPHOS in SCLC cell lines (**Table 2** and **Figure 3**) (134). Another small molecule inhibitor of MCT1, AZD3965, has been tested in SCLC cell lines and human-derived H526 xenograft models, which both exhibited a notable delay in cell proliferation and tumor growth, respectively (**Table 2** and **Figure 3**) (135, 136). Similarly, metabolites analyzed from *in vitro* experimentation with AZD3965 had alterations in amino acid and nucleotide biosynthesis and increased ROS generation (135), contributing to reduction in proliferation. Although a number of pathways are used by cancer cells, blocking the initial transport of carbon-source molecules have shown promise and deserve further attention of research in the treatment of lung cancer, where new treatment options are desperately needed to improve patient outcome and survival.

In addition to blockade of nutrient transport, inhibitors have been produced to target many enzymes in the glycolysis pathway, have high potential for efficacy, but have not been introduced into clinical practice as lung cancer therapies. When targeting the glycolysis pathway, the most well characterized inhibitor is 2DG (**Table 2** and **Figure 3**). In H23 human-derived NSCLC cells, treatment with 2DG inhibited cell growth and induced cell cycle arrest (57). Another study using human-derived H460 NSCLC cells found treatment with 2DG also activated PI3K/AKT signaling and phosphorylated Raf/MEK/ERK kinases, cell cycle and DNA damage molecules, and JAK/STAT proteins suggesting that the off target effects are far reaching and affect multiple pathways (137). Therefore, while promising, exploration into other enzymatic glycolysis inhibitors with fewer off targets would be more optimal. For that reason, inhibitors of PFKFB3 (rate-limiting enzyme of glycolysis) and LDHA (pyruvate to lactate converter) have been developed. Among the PFKFB3 inhibitors PFK-15 and the more potent PFK-158 have been the most encouraging and progressed into preclinical and clinical trials

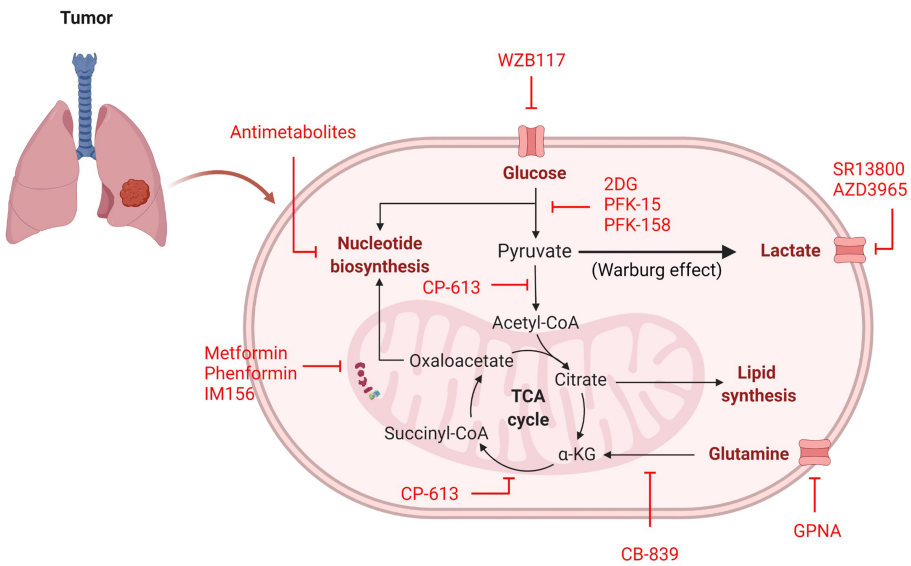

FIGURE 3 | Inhibitors of cancer cell metabolism. Inhibitors (red) can target many metabolic pathways in an attempt to stop or delay energy and nutrient generation necessary for cellular proliferation.

TABLE 2 | Inhibitors of cancer cell metabolism.

Name of Drug	Target Pathway	Lung Cancer Clinical Trail (Clinicaltrials.gov)
AZD3965	MCT1 (Lactate transport)	NCT01791595
CB-839 (Telaglenastat)	GLS (Glutaminolysis)	NCT02771626
CD-613 (Devimistat)	Mitochondrial PDH/KGDH	N/A
IM156	Mitochondrial ETC Complex 1	NCT03272256
L-γ-Glutamyl-p-nitroanilide (GPNA)	Glutamine transport	N/A
Metformin	Mitochondrial ETC Complex 1	NCT02285855 NCT01997775
PFK-15	PFKFB3 (Glycolysis)	N/A
PFK-158	PFKFB3 (Glycolysis)	NCT02044861
Phenformin	Mitochondrial ETC Complex 1	NCT03026517
SR13800	MCT1 (Lactate transport)	N/A
WZB 117	GLUT1 (Glycolysis)	N/A
2– Deoxy-d-Glucose (2DG)	HK2 (Glycolysis)	NCT00096707 NCT00633087

Many metabolic inhibitors have been utilized in clinical trials, however few have led to FDA approval. This table provides a list of the inhibitors described in ***Figure 3*** *and any associated clinical trials that have accepted lung cancer patients.*
N/A, not applicable.

(**Table 2** and **Figure 3**) (38, 138). Unfortunately, these studies have not been conducted in NSCLC or SCLC models, however lung metastasis was reduced in head and neck squamous cell carcinoma (HNSCC) Cal27 xenografts treated with PFK-15 (139). Moreover, mesothelioma (a cancer that affects the pleural lining of the lungs and is linked to asbestos exposure) cells treated with PFK-158 exhibited reduced glycolysis and cell proliferation and this treatment alone was sufficient in reducing tumor growth without associated toxicities in xenograft mice (140). PFK-158 is currently undergoing clinical trial (NCT02044861) (141). Similarly to PFKFB3 inhibitors, several LDHA inhibitors have be produced, yet none of been extensively evaluated in preclinical or clinical trials. Although LDHA inhibition has not been previously examined, LDHA knockout NSCLC models have decreased tumor formation and even show regression of stablished tumors (142), providing evidence that LDHA may be a future viable target for lung cancer therapies.

Lastly, several reports on lung cancer metabolism suggest these tumors, particularly NSCLC, may be more oxidative, which provides an opportunity for metabolic intervention of mitochondrial respiration. Surprisingly, one of the most studied OXPHOS inhibitors in lung cancer is metformin, a common diabetes mellitus medication that blocks complex I of the ETC (**Table 2** and **Figure 3**) (42, 143). The anti-cancer activity of metformin has been documented in numerous cancer studies (143) and studies have found that diabetic patients with NSCLC on metformin even experience prolonged survival (144–146). While data investigating the therapeutic benefit of metformin in cancer may be encouraging, some evidence suggests that metformin use increases adaptive glycolysis activity (147), which would be counterproductive in metabolically-heterogeneous tumors and could increase therapy resistance. Additionally, it requires high dosing to achieve therapeutic advantage. Similar ETC complex I have been developed to overcome these drawbacks. phenformin, a structurally-similar anti-diabetic drug, was developed in an attempt to increase potency, however a therapeutic dose could not be achieved due to toxicity (**Table 2** and **Figure 3**) (42). Currently, a third ETC complex I inhibitor, IM156, with heightened potency and attainable therapeutic dosing is in Phase I clinical trial (**Table 2** and **Figure 3**) (148).

With the inherent metabolic nature of cancer, metabolism inhibitors are an underutilized category of therapy and should be considered as effective anti-cancer agents. Most metabolism-altering agents have displayed strong efficacy in cell lines and mouse models and those that have progressed into clinical trial, have been well tolerated. Further, metabolic inhibitors are actively taken in by the most metabolically active cells (i.e. the tumor) and therefore do not negatively affect cellular processes in non-malignant cells. With this knowledge future investigations of metabolic inhibition alone and in combination with the standard-of-care is essential for driving personalized lung cancer treatment options for all patients.

DISCUSSION

Cancer is an inherently metabolic disease, however cell origin, mutation status, oxygenation, and nutrient availability all contribute to the utilization of a particular metabolic program. To date, few metabolic inhibitors have progressed to clinical trial and those that have been clinically evaluated show moderate efficacy at best. Unfortunately, there has only been limited effort to metabolically characterize patient lung tumors or identify patients most likely to benefit. This is, in part, due to the difficulty of obtaining clinical samples since many lung cancers are not routinely surgically resected. Further difficulties may stem from the transient nature of metabolic pathway preference and differences between *in vitro* and *in vivo* cancer cells. These pitfalls highlight the urgency to identify viable biomarkers corresponding to the tumor metabolic profile.

We and others have previously shown that tumor heterogeneity exists in both NSCLC and SCLC and the administration of frontline treatment further exacerbates this phenotype (82, 149–151). It can be hypothesized that tumoral metabolism is also heterogenic, which would likewise enable clusters of glycolytic and oxidative cells that would become more profound after chemotherapy (**Figure 4**). For this reason, methods for patient metabolic phenotyping should be developed to assist with selecting the optimal combination of metabolic inhibitor in addition to frontline chemotherapy and ICB to delay tumor growth.

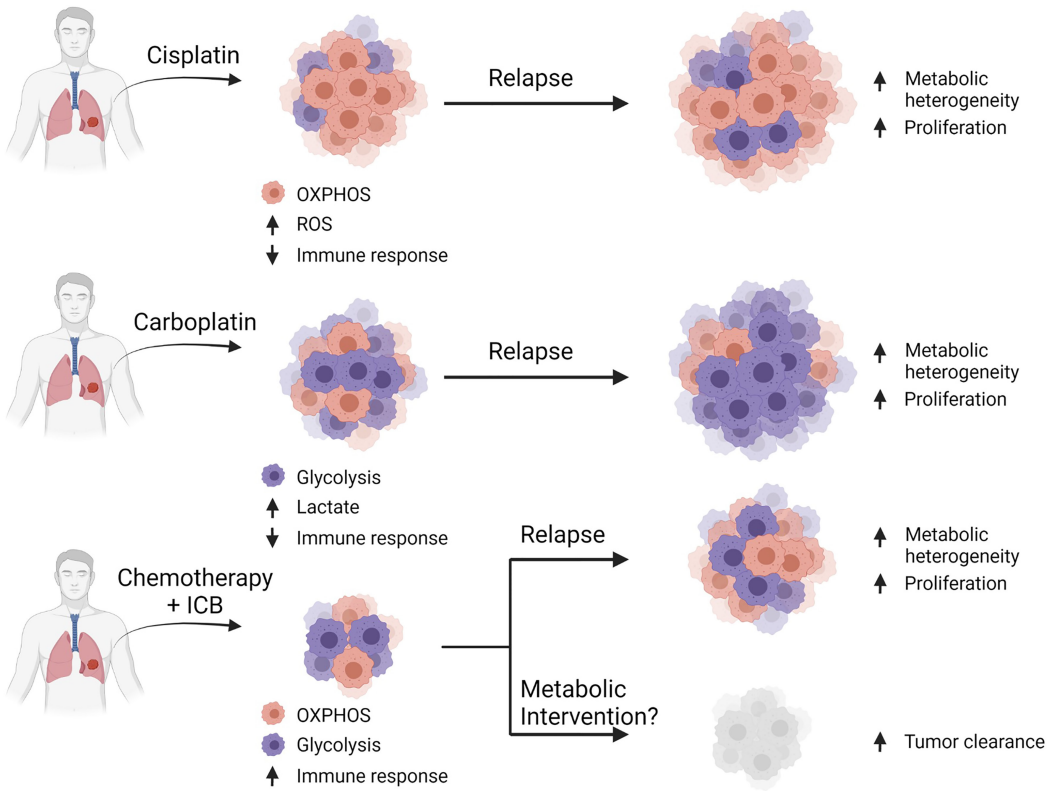

FIGURE 4 | Combinatorial approaches for standard-of-care with metabolic inhibition. Hypothesis that common platinum-based chemotherapies select for cells dependent on their particular metabolic profiles. Cisplatin-based therapy selects for cells that are mostly oxidative, which leads to enhanced ROS production and reduced immune function leading to relapse. Carboplatin-based therapy selects for glycolytic cells leading to enhanced lactates production and reduced immune function resulting in relapse. A general chemotherapy plus immune checkpoint blockade provides some benefit in a few patients, but often ultimately leads to relapse, however metabolic intervention may provide additional efficacy by targeting pathways required for cellular proliferation.

In conclusion, the effort to characterize lung cancer metabolism is at the forefront of investigation. There is ample evidence in support for targeting metabolic pathways to delay tumor growth as second-line single agents or in combination with frontline chemotherapy plus ICB. It is of utmost importance, however, to identify specific patient populations that would respond to such treatment efforts through biomarker analysis of cell surface or secreted molecules. Since cellular metabolism is a transient phenomenon, time course monitoring of identified biomarkers would be critical. If this can be achieved, the road will be paved for personalized therapies for targeted inhibition of metabolic pathways in lung cancer.

AUTHOR CONTRIBUTIONS

KC conceived and wrote the manuscript. WH wrote and edited the manuscript. KC and WH generated the figures and tables. LB and CG acquired funding and oversaw the writing and editing of the manuscript. All authors contributed to the article and approved the submitted version.

FUNDING

The authors of this work are supported by the following funding agencies and fellowships: University of Texas SPORE in Lung Cancer P5-CA070907 (KC, CG, LB); NIH/NCI R01-CA207295 (LB); NIH/NCI U01-CA213273 (LB); NIH/NCI T32 CA009666 (CG); IALSC ILCF Fellowship (KC); ASCO Young Investigator Award (CG); The Khalifa Bin Zayed Al Nahyan Foundation (CG); through generous philanthropic contributions to The University of Texas MD Anderson Lung Cancer Moon Shot Program (LB); The Andrew Sabin Family Fellowship (LB); CG and LB were supported by the Abell Hangar Foundation, the LUNGevity Foundation Career Development Award (CG), and the Rexanna Foundation for Fighting Lung Cancer (CG, LB).

ACKNOWLEDGMENTS

Figures were generated through licensing with BioRender.

REFERENCES

1. Howlader N, Noone AM, Krapcho M, Miller D, Brest A, Yu M, et al. *SEER Cancer Statistics Review (CSR) 1975-2016*. Bethesda, MD: National Cancer Institute (2019). Available at: https://seer.cancer.gov/csr/1975_2016/.
2. Zappa C, Mousa SA. Non-Small Cell Lung Cancer: Current Treatment and Future Advances. *Transl Lung Cancer Res* (2016) 5(3):288–300. doi: 10.21037/tlcr.2016.06.07
3. Fasano M, Della Corte CM, Papaccio F, Ciardiello F, Morgillo F. Pulmonary Large-Cell Neuroendocrine Carcinoma: From Epidemiology to Therapy. *J Thorac Oncol* (2015) 10(8):1133–41. doi: 10.1097/JTO.0000000000000589
4. Dransfield MT, Lock BJ, Garver RIJr. Improving the Lung Cancer Resection Rate in the US Department of Veterans Affairs Health System. *Clin Lung Cancer* (2006) 7(4):268–72. doi: 10.3816/CLC.2006.n.005
5. Warburg OH. The Classic: The Chemical Constitution of Respiration Ferment. *Clin Orthop. Relat Res* (2010) 468(11):2833–9. doi: 10.1007/s11999-010-1534-y
6. Warburg OH. The Metabolism of Carcinoma Cells. *Cancer Res* (1925) 9 (1):148–63. doi: 10.1158/jcr.1925.148
7. Liberti MV, Locasale JW. The Warburg Effect: How Does it Benefit Cancer Cells? *Trends Biochem Sci* (2016) 41(3):211–8. doi: 10.1016/j.tibs.2015.12.001
8. Zheng J. Energy Metabolism of Cancer: Glycolysis *Versus* Oxidative Phosphorylation (Review). *Oncol Lett* (2012) 4(6):1151–7. doi: 10.3892/ol.2012.928
9. Feron O. Pyruvate Into Lactate and Back: From the Warburg Effect to Symbiotic Energy Fuel Exchange in Cancer Cells. *Radiother. Oncol* (2009) 92(3):329–33. doi: 10.1016/j.radonc.2009.06.025
10. Emmings E, Mullany S, Chang Z, Landen CN, Linder S, Bazzaro M. Targeting Mitochondria for Treatment of Chemoresistant Ovarian Cancer. *Int J Mol Sci* (2019) 20(229):229. doi: 10.3390/ijms20010229
11. Seyfried TN, Shelton LM. Cancer as a Metabolic Disease. *Nutr Metab (Lond)* (2010) 7:7. doi: 10.1186/1743-7075-7-7
12. Jin G, Kim MJ, Jeon HS, Choi JE, Kim DS, Lee EB, et al. PTEN Mutations and Relationship to EGFR, ERBB2, KRAS, and TP53 Mutations in Non-Small Cell Lung Cancers. *Lung Cancer* (2010) 69(3):279–83. doi: 10.1038/s43018-020-0046-2
13. Bethune G, Bethune D, Ridgway N, Xu Z. Epidermal Growth Factor Receptor (EGFR) in Lung Cancer: An Overview and Update. *J Thorac Dis* (2010) 2(1):48–51.
14. Romero R, Sayin VI, Davidson SM, Bauer MR, Singh SX, LeBoeuf SE, et al. Keap1 Loss Promotes Kras-Driven Lung Cancer and Results in Dependence on Glutaminolysis. *Nat Med* (2017) 23(11):1362–8. doi: 10.1038/nm.4407
15. Pupo E, Avanzato D, Middonti E, Bussolino F, Lanzetti L. KRAS-Driven Metabolic Rewiring Reveals Novel Actionable Targets in Cancer. *Front Oncol* (2019) 9:848. doi: 10.3389/fonc.2019.00848
16. Jin S, Drábek J, Radzioch D, Hajdúch M. Clinical Relevance of KRAS in Human Cancers. *J Biomed Biotechnol* (2010) 2010(3):1–13. doi: 10.1155/2010/150960
17. Padanad MS, Konstantinidou G, Venkateswaran N, Melegari M, Rindhe S, Mitsche M, et al. Fatty Acid Oxidation Mediated by Acyl-CoA Synthetase Long Chain 3 Is Required for Mutant KRAS Lung Tumorigenesis. *Cell Rep* (2016) 16(6):1614–28. doi: 10.1016/j.celrep.2016.07.009
18. Galan-Cobo A, Sitthideatphaiboon P, Qu X, Poteete A, Pisegna MA, Tong P, et al. LKB1 and KEAP1/NRF2 Pathways Cooperatively Promote Metabolic Reprogramming With Enhanced Glutamine Dependence in KRAS-Mutant Lung Adenocarcinoma. *Cancer Res* (2019) 79(13):3251–67. doi: 10.1158/0008-5472.CAN-18-3527
19. Chalishazar MD, Wait SJ, Huang F, Ireland AS, Mukhopadhyay A, Lee Y, et al. MYC-Driven Small-Cell Lung Cancer Is Metabolically Distinct and Vulnerable to Arginine Depletion. *Clin Cancer Res* (2019) 25(16):5107–21. doi: 10.1158/1078-0432.CCR-18-4140
20. Rapp UR, Korn C, Ceteci F, Karreman C, Luetkenhaus K, Serafin V, et al. Myc Is a Metastasis Gene for Non-Small-Cell Lung Cancer. *PLoS One* (2009) 4(6):e6029. doi: 10.1371/journal.pone.0006029
21. Marengo B, Garbarino O, Speciale A, Monteleone L, Traverso N, Domenicotti C. MYC Expression and Metabolic Redox Changes in Cancer Cells: A Synergy Able to Induce Chemoresistance. *Oxida Med Cell Longev* (2019) 2019:1–9. doi: 10.1155/2019/7346492
22. Sellers K, Allen TD, Bousamra M 2nd, Tan J, Mendez-Lucas A, Lin W, et al. Metabolic Reprogramming and Notch Activity Distinguish Between Non-Small Cell Lung Cancer Subtypes. *Br J Cancer* (2019) 121(1):51–64. doi: 10.1038/s41416-019-0464-z
23. Zou B, Zhou XL, Lai SQ, Liu JC. Notch Signaling and Non-Small Cell Lung Cancer. *Oncol Lett* (2018) 15(3):3415–21. doi: 10.3892/ol.2018.7738
24. Zou A, Zhou M, Lai AT, Liu S, Liu M, Liu D, et al. Oncogenic and Drug-Sensitive NTRK1 Rearrangements in Lung Cancer. *Nat Med* (2013) 19(11):1469–72.
25. Yang X, Shen H, Buckley B, Chen Y, Yang N, Mussell AL, et al. NTRK1 Is a Positive Regulator of YAP Oncogenic Function. *Oncogene* (2019) 38 (15):2778–87.
26. Georgescu MM. PTEN Tumor Suppressor Network in PI3K-Akt Pathway Control. *Genes Cancer* (2010) 1(12):1170–7. doi: 10.1177/1947601911407325
27. Bhateja P, Chiu M, Wildey G, Lipka MB, Fu P, Yanf MCL, et al. Retinoblastoma Mutation Predicts Poor Outcomes in Advanced Non Small Cell Lung Cancer. *Cancer Med* (2019) 8(4):1459–66. doi: 10.1002/cam4.2023
28. Mandigo AC, Yuan W, Xu K, Gallagher P, Pang A, Guan YF, et al. RB/E2F1 as a Master Regulator of Cancer Cell Metabolism in Advanced Disease. *Cancer Discov* (2021) 11(9). doi: 10.1158/2159-8290.CD-20-1114
29. Al Tameemi W, Dale TP, Al-Jumaily RMK, Forsyth NR. Hypoxia-Modified Cancer Cell Metabolism. *Front Cell Dev Biol* (2019) 7:4. doi: 10.3389/fcell.2019.00004
30. Camarda R, Williams J, Goga A. *In Vivo* Reprogramming of Cancer Metabolism by MYC. *Front Cell Dev Biol* (2017) 5:35. doi: 10.3389/fcell.2017.00035
31. Stine ZE, Walton ZE, Altman BJ, Hsieh AL, Dang CV. MYC, Metabolism, and Cancer. *Cancer Discov* (2015) 5(10):1024–39. doi: 10.1158/2159-8290.CD-15-0507
32. Nagao A, Kobayashi M, Koyasu S, Chow CCT, Harada H. HIF-1-Dependent Reprogramming of Glucose Metabolic Pathway of Cancer Cells and Its Therapeutic Significance. *Int J Mol Sci* (2019) 20(2):238. doi: 10.3390/ijms20020238
33. McFate T, Mohyeldin A, Lu H, Thakar J, Henriques J, Halim ND, et al. Pyruvate Dehydrogenase Complex Activity Controls Metabolic and Malignant Phenotype in Cancer Cells. *J Biol Chem* (2008) 283(33):22700–8. doi: 10.1074/jbc.M801765200
34. Kumari S, Badana AK, Murali MG, Shailender G, Malla R. Reactive Oxygen Species: A Key Constituent in Cancer Survival. *Biomark Insights* (2018) 13:1177271918755391. doi: 10.1177/1177271918755391
35. Scalise M, Pochini L, Galluccio M, Console L, Indiveri C. Glutamine Transport and Mitochondrial Metabolism in Cancer Cell Growth. *Front Oncol* (2017) 7:306. doi: 10.3389/fonc.2017.00306
36. Chen YJ, Mahieu NG, Huang X, Singh M, Crawford PA, Johnson SL, et al. Lactate Metabolism is Associated With Mammalian Mitochondria. *Nat Chem Biol* (2016) 12(11):937–43. doi: 10.1038/nchembio.2172
37. Scatena R. Mitochondria and Cancer: A Growing Role in Apoptosis, Cancer Cell Metabolism, and Dedifferentiation. In: R S., P B., B G., editors. *Advances in Mitochondrial Medicine. Advances in Experimental Medicine and Biology*. Dordrecht: Springer (2012). p. 287–308.
38. Vanhove K, Graulus GJ, Mesotten L, Thomeer M, Derveaux E, Noben JP, et al. The Metabolic Landscape of Lung Cancer: New Insights in a Disturbed Glucose Metabolism. *Front Oncol* (2019) 9:1215. doi: 10.3389/fonc.2019.01215
39. Sharma A, Boise LH, Shanmugam M. Cancer Metabolism and the Evasion of Apoptotic Cell Death. *Cancers (Basel)* (2019) 11(8):1–20. doi: 10.3390/cancers11081144
40. Chang CH, Qiu J, O'Sullivan D, Buck MD, Noguchi T, Curtis JD, et al. Metabolic Competition in the Tumor Microenvironment Is a Driver of Cancer Progression. *Cell* (2015) 162(6):1229–41. doi: 10.1016/j.cell.2015.08.016
41. Organization, W.H. *Cancer* (2020). Available at: https://www.who.int/news-room/fact-sheets/detail/cancer (Accessed 20 May 2020).
42. Majem B, Nadal E, Munoz-Pinedo C. Exploiting Metabolic Vulnerabilities of Non Small Cell Lung Carcinoma. *Semin Cell Dev Biol* (2019) 2020:54–62. doi: 10.1016/j.semcdb.2019.06.004
43. Nadal E, Massuti B, Domine M, Garcia-Campelo R, Cobo M, Felip E. Immunotherapy With Checkpoint Inhibitors in Non-Small Cell Lung

Cancer: Insights From Long-Term Survivors. *Cancer Immunol Immunother* (2019) 68(3):341–52. doi: 10.1007/s00262-019-02310-2
44. Chen PH, Cai L, Huffman K, Yang C, Kim J, Faubert B, et al. Metabolic Diversity in Human Non-Small Cell Lung Cancer Cells. *Mol Cell* (2019) 76 (5):838–51.E5. doi: 10.1016/j.molcel.2019.08.028
45. Lindsay CR, Blackhall FH, Carmel A, Gazzaniga P, Groen HJM, Krebs MG, et al. The Metabolic Phenotypes of Non-Small Cell Lung Cancer Cells in Association With Clinical Treatment Strategies. *Ann Oncol* (2019) 30 (Supplement_2). doi: 10.1093/annonc/mdz073.019
46. Faubert B, Li KY, Cai L, Hensley CT, Kim J, Zacharias LG, et al. Lactate Metabolism in Human Lung Tumors. *Cell* (2017) 171(2):358–371 e9. doi: 10.1016/j.cell.2017.09.019
47. Chen M, Liu X, Du J, Wang XJ, Xia L. Differentiated Regulation of Immune-Response Related Genes Between LUAD and LUSC Subtypes of Lung Cancers. *Oncotarget* (2017) 8(1):133–44. doi: 10.18632/oncotarget.13346
48. Hensley CT, Faubert B, Yuan Q, Lev-Cohain N, Jin E, Kim J, et al. Metabolic Heterogeneity in Human Lung Tumors. *Cell* (2016) 164(4):681–94. doi: 10.1016/j.cell.2015.12.034
49. Chen Z, Fillmore CM, Hammerman PS, Kim CF, Wong KK. Non-Small-Cell Lung Cancers: A Heterogeneous Set of Diseases. *Nat Rev Cancer* (2014) 14 (8):535–46. doi: 10.1038/nrc3775
50. Herbst RS, Morgensztern D, Boshoff C. The Biology and Management of Non-Small Cell Lung Cancer. *Nature* (2018) 553(7689):446–54. doi: 10.1038/nature25183
51. Inamura K. Lung Cancer: Understanding Its Molecular Pathology and the 2015 WHO Classification. *Front Oncol* (2017) 7:193. doi: 10.3389/fonc.2017.00193
52. Cancer Genome Atlas Research, N. Comprehensive Genomic Characterization of Squamous Cell Lung Cancers. *Nature* (2012) 489 (7417):519–25. doi: 10.1038/nature11404
53. Sinthupibulyakit C, Ittarat W, St. Clair WH, St. Clair DK. P53 Protects Lung Cancer Cells Against Metabolic Stress. *Int J Oncol* (2010) 37(6):1575–81. doi: 10.3892/ijo_00000811
54. Makinoshima H, Takita M, Saruwatari K, Umemura S, Obata Y, Ishii G, et al. Signaling Through the Phosphatidylinositol 3-Kinase (PI3K)/Mammalian Target of Rapamycin (mTOR) Axis Is Responsible for Aerobic Glycolysis Mediated by Glucose Transporter in Epidermal Growth Factor Receptor (EGFR)-Mutated Lung Adenocarcinoma. *J Biol Chem* (2015) 290(28):17495–504. doi: 10.1074/jbc.M115.660498
55. Momcilovic M, Bailey ST, Lee JT, Fishbein MC, Magyar C, Braas D, et al. Targeted Inhibition of EGFR and Glutaminase Induces Metabolic Crisis in EGFR Mutant Lung Cancer. *Cell Rep* (2017) 18(3):601–10. doi: 10.1016/j.celrep.2016.12.061
56. Maschek G, Savaraj N, Priebe W, Braunschweiger P, Hamilton K, Tidmarsh GF, et al. 2-Deoxy-D-Glucose Increases the Efficacy of Adriamycin and Paclitaxel in Human Osteosarcoma and Non-Small Cell Lung Cancers *in Vivo*. *Cancer Res* (2004) 64(1):31–4. doi: 10.1158/0008-5472.CAN-03-3294
57. Wang H, Wang L, Zhang Y, Wang J, Deng Y, Lin D. Inhibition of Glycolytic Enzyme Hexokinase II (HK2) Suppresses Lung Tumor Growth. *Cancer Cell Int* (2016) 16:9. doi: 10.1186/s12935-016-0280-y
58. Gong M, Li Y, Ye X, Zhang L, Wang Z, Xu X, et al. Loss-Of-Function Mutations in KEAP1 Drive Lung Cancer Progression *via* KEAP1/NRF2 Pathway Activation. *Cell Commun Signal* (2020) 18(1):98. doi: 10.1186/s12964-020-00568-z
59. Panieri E, Telkoparan-Akillilar P, Suzen S, Saso L. The NRF2/KEAP1 Axis in the Regulation of Tumor Metabolism: Mechanisms and Therapeutic Perspectives. *Biomolecules* (2020) 10(5):791. doi: 10.3390/biom10050791
60. Shackelford DB, Abt E, Gerken L, Vasquez DS, Seki A, Leblanc M, et al. LKB1 Inactivation Dictates Therapeutic Response of Non-Small Cell Lung Cancer to the Metabolism Drug Phenformin. *Cancer Cell* (2013) 23(2):143–58. doi: 10.1016/j.ccr.2012.12.008
61. Park KS, Liang MC, Raiser DM, Zamponi R, Roach RR, Curtis SJ, et al. Characterization of the Cell of Origin for Small Cell Lung Cancer. *Cell Cycle* (2011) 10(16):2806–15. doi: 10.4161/cc.10.16.17012
62. Wildey G, Dowlati A. Genomic Alterations in Small Cell Lung Cancer and Their Clinical Relevance. *Transl Lung Cancer Res* (2016) 5(4):450–1. doi: 10.21037/tlcr.2016.07.05
63. Sameshima Y, Matsuno Y, Hirohashi S, Shimosato Y, Mizoguchi H, Sugimura T, et al. Alterations of the P53 Gene Are Common and Critical Events for the Maintenance of Malignant Phenotypes in Small-Cell Lung Carcinoma. *Oncogene* (1992) 7(3):451–7.
64. Takahashi T, Takahashi T, Suzuki HI, Hida T, Sekido Y, Ariyoshi Y, et al. The P53 Gene Is Very Frequently Mutated in Small-Cell Lung Cancer With a Distinct Nucleotide Substitution Pattern. *Oncogene* (1991) 6(10):1775–8.
65. Carney D, Gazdar A, Guccion J, Marangos P, Moody T, Zweig M, et al. Establishment and Identification of Small Cell Lung Cancer Cell Lines Having Classic and Variant Features. *Cancer Res* (1985) 45:2913–23.
66. Gazdar A, Carney D, Nau M, Minna J. Characterization of Variant Subclasses of Cell Lines Derived From Small Cell Lung Cancer Having Distinctive Biochemical, Morphological, and Growth Properties. *Cancer Res* (1985) 45:2924–30.
67. Rudin CM, Poirier JT, Byers LA, Dive C, Dowlati A, George J, et al. Molecular Subtypes of Small Cell Lung Cancer: A Synthesis of Human and Mouse Model Data. *Nat Rev Cancer* (2019) 19(5):289–97. doi: 10.1038/s41568-019-0133-9
68. Cardnell RJ, li L, Sen T, Bara R, Tong P, Fujimoto J, et al. Protein Expression of TTF1 and cMYC Define Distinct Molecular Subgroups of Small Cell Lung Cancer With Unique Vulnerabilities to Aurora Kinase Inhibition, DLL3 Targeting, and Other Targeted Therapies. *Oncotarget* (2017) 8(43):73419–32. doi: 10.18632/oncotarget.20621
69. Borromeo MD, Savage TK, Kollipara RK, He M, Augustyn A, Osborne JK, et al. ASCL1 and NEUROD1 Reveal Heterogeneity in Pulmonary Neuroendocrine Tumors and Regulate Distinct Genetic Programs. *Cell Rep* (2016) 16(5):1259–72. doi: 10.1016/j.celrep.2016.06.081
70. Augustyn A, Borromeo M, Wang T, Fujimoto J, Shao C, Dospoy PD, et al. ASCL1 Is a Lineage Oncogene Providing Therapeutic Targets for High-Grade Neuroendocrine Lung Cancers. *Proc Natl Acad Sci USA* (2014) 111 (41):14788–93. doi: 10.1073/pnas.1410419111
71. Huang YH, Klingbeil O, He XY, Wu XS, Arun G, Lu B, et al. POU2F3 Is a Master Regulator of a Tuft Cell-Like Variant of Small Cell Lung Cancer. *Genes Dev* (2018) 32(13-14):915–28. doi: 10.1101/gad.314815.118
72. Horie M, Saito A, Ohshima M, Suzuki HI, Nagase T. YAP and TAZ Modulate Cell Phenotype in a Subset of Small Cell Lung Cancer. *Cancer Sci* (2016) 107 (12):1755–66. doi: 10.1111/cas.13078
73. Mollaoglu G, Guthrie MR, Bohm S, Bragelmann J, Can I, Ballieu PM, et al. MYC Drives Progression of Small Cell Lung Cancer to a Variant Neuroendocrine Subtype With Vulnerability to Aurora Kinase Inhibition. *Cancer Cell* (2017) 31(2):270–85. doi: 10.1016/j.ccell.2016.12.005
74. George J, Lim JS, Jang SJ, Cun Y, Ozretic L, Kong G, et al. Comprehensive Genomic Profiles of Small Cell Lung Cancer. *Nature* (2015) 524(7563):47–53. doi: 10.1038/nature14664
75. Peifer M, Fernandez-Cuesta L, Sos ML, George J, Seidel D, Kasper LH, et al. Integrative Genome Analyses Identify Key Somatic Driver Mutations of Small-Cell Lung Cancer. *Nat Genet* (2012) 44(10):1104–10. doi: 10.1038/ng.2396
76. Huang F, Ni M, Chalishazar MD, Huffman KE, Kim J, Cai L, et al. Inosine Monophosphate Dehydrogenase Dependence in a Subset of Small Cell Lung Cancers. *Cell Metab* (2018) 28(3):369–82.e5. doi: 10.1016/j.cmet.2018.06.005
77. Ghandi M, Huang FW, Jane-Valbuena J, Kryukov GV, Lo CC, McDonald ER 3rd, et al. Next-Generation Characterization of the Cancer Cell Line Encyclopedia. *Nature* (2019) 569(7757):503–8. doi: 10.1038/s41586-019-1186-3
78. Gay CM, Stewart CA, Park EM, Diao L, Groves SM, Heeke S, et al. Patterns of Transcription Factor Programs and Immune Pathway Activation Define Four Major Subtypes of SCLC With Distinct Therapeutic Vulnerabilities. *Cancer Cell* (2021) 39(3):346–60.E7. doi: 10.1016/j.ccell.2020.12.014
79. Huang F, Huffman KE, Wang Z, Wang X, Li K, Cai F, et al. Guanosine Triphosphate Links MYC-Dependent Metabolic and Ribosome Programs in Small-Cell Lung Cancer. *J Clin Invest* (2021) 131(1). doi: 10.1172/JCI139929
80. Morita M, Sato T, Nomura M, Sakamoto Y, Inoue Y, Tanaka R, et al. PKM1 Confers Metabolic Advantages and Promotes Cell-Autonomous Tumor Cell Growth. *Cancer Cell* (2018) 33(3):355–367 e7. doi: 10.1016/j.ccell.2018.02.004
81. Lim JS, Ibaseta A, Fischer MM, Cancilla B, O'Young G, Cristea S, et al. Intratumoural Heterogeneity Generated by Notch Signalling Promotes

Small-Cell Lung Cancer. *Nature* (2017) 545(7654):360–4. doi: 10.1038/nature22323
82. Stewart CA, Gay CM, Xi Y, Sivajothi S, Sivakamasundari V, Fujimoto J, et al. Single-Cell Analyses Reveal Increased Intratumoral Heterogeneity After the Onset of Therapy Resistance in Small-Cell Lung Cancer. *Nat Cancer* (2020) 1:423–36. doi: 10.1038/s43018-019-0020-z
83. David CJ, Chen M, Assanah M, Canoll P, Manley JL. HnRNP Proteins Controlled by C-Myc Deregulate Pyruvate Kinase mRNA Splicing in Cancer. *Nature* (2010) 463(7279):364–8. doi: 10.1038/nature08697
84. Zhang Z, Deng X, Liu Y, Liu Y, Sun L, Chen F. PKM2, Function and Expression and Regulation. *Cell Biosci* (2019) 9:52. doi: 10.1186/s13578-019-0317-8
85. Zheng X, Boyer L, Jin M, Mertens J, Kim Y, Ma L, et al. Metabolic Reprogramming During Neuronal Differentiation From Aerobic Glycolysis to Neuronal Oxidative Phosphorylation. *Elife* (2016) 5:e13374. doi: 10.7554/eLife.13374
86. Lycan TW, Pardee TS, Petty WJ, Bonomi M, Alistar A, Lamar ZS, et al. A Phase II Clinical Trial of CPI-613 in Patients With Relapsed or Refractory Small Cell Lung Carcinoma. *PloS One* (2016) 11(10):e0164244. doi: 10.1371/journal.pone.0164244
87. Zhou Z, Zhu L, Niu X, Shen S, Zhao Y, Zhang J, et al. Comparison of Genomic Landscapes of Large Cell Neuroendocrine Carcinoma, Small Cell Lung Carcinoma, and Large Cell Carcinoma. *Thorac Cancer* (2019) 10(4):839–47. doi: 10.1111/1759-7714.13011
88. George J, Walter V, Peifer M, Alexandrov LB, Seidel D, Leenders F, et al. Integrative Genomic Profiling of Large-Cell Neuroendocrine Carcinomas Reveals Distinct Subtypes of High-Grade Neuroendocrine Lung Tumors. *Nat Commun* (2018) 9(1):1048. doi: 10.1038/s41467-018-03099-x
89. Kishton RJ, Sukumar M, Restifo NP. Metabolic Regulation of T Cell Longevity and Function in Tumor Immunotherapy. *Cell Metab* (2017) 26(1):94–109. doi: 10.1016/j.cmet.2017.06.016
90. Lim S, Phillips JB, Madeira da Silva L, Zhou M, Fodstad O, Owen LB, et al. Interplay Between Immune Checkpoint Proteins and Cellular Metabolism. *Cancer Res* (2017) 77(6):1245–9. doi: 10.1158/0008-5472.CAN-16-1647
91. de la Cruz-Lopez KG, Castro-Munoz LJ, Reyes-Hernandez DO, Garcia-Carranca A, Manzo-Merino J. Lactate in the Regulation of Tumor Microenvironment and Therapeutic Approaches. *Front Oncol* (2019) 9:1143. doi: 10.3389/fonc.2019.01143
92. Chen X, Song M, Zhang B, Zhang Y. Reactive Oxygen Species Regulate T Cell Immune Response in the Tumor Microenvironment. *Oxid Med Cell Longev 2016* (2016) p:1580967. doi: 10.1155/2016/1580967
93. Weinberg F, Ramnath N, Nagrath D. Reactive Oxygen Species in the Tumor Microenvironment: An Overview. *Cancers (Basel)* (2019) 11(8):1–20. doi: 10.3390/cancers11081191
94. Renner K, Bruss C, Schnell A, Koehl G, Becker HM, Fante M, et al. Restricting Glycolysis Preserves T Cell Effector Functions and Augments Checkpoint Therapy. *Cell Rep* (2019) 29(1):135–50.e9. doi: 10.1016/j.celrep.2019.08.068
95. Yu Y, Liang Y, Li D, Wang L, Liang Z, Chen Y, et al. Glucose Metabolism Involved in PD-L1-Mediated Immune Escape in the Malignant Kidney Tumour Microenvironment. *Cell Death Discov* (2021) 7(1):15. doi: 10.1038/s41420-021-00401-7
96. Kim S, Jang JY, Koh J, Kwon D, Kim YA, Paeng JC, et al. Programmed Cell Death Ligand-1-Mediated Enhancement of Hexokinase 2 Expression Is Inversely Related to T-Cell Effector Gene Expression in Non-Small-Cell Lung Cancer. *J Exp Clin Cancer Res* (2019) 38(1):462. doi: 10.1186/s13046-019-1050-1
97. Noman MZ, Desantis G, Janji B, Hasmim M, Karray S, Dessen P, et al. PD-L1 is a Novel Direct Target of HIF-1alpha, and its Blockade Under Hypoxia Enhanced MDSC-Mediated T Cell Activation. *J Exp Med* (2014) 211(5):781–90. doi: 10.1084/jem.20131916
98. Cui Y, Li Y, Li X. The Impact of PD-L1 on Glucose Metabolism of Lung Adenocarcinoma Cells. *J Nucl Med* (2018) 59(Supplement 1):1252.
99. Long L, Chen M, Yuan Y, Ming AL, Guo W, Wu K, et al. High Expression of PKM2 Synergizes With PD-L1 in Tumor Cells and Immune Cells to Predict Worse Survival in Human Lung Adenocarcinoma. *J Cancer* (2020) 11(15):4442–52. doi: 10.7150/jca.42610
100. Jiang Z, Liu Z, Li M, Chen C, Wang X. Increased Glycolysis Correlates With Elevated Immune Activity in Tumor Immune Microenvironment. *EBioMedicine* (2019) 42:431–42. doi: 10.1016/j.ebiom.2019.03.068
101. El-Guindy DM, Helal DS, Sabry NM, Abo El-Nasr M. Programmed Cell Death Ligand-1 (PD-L1) Expression Combined With CD8 Tumor Infiltrating Lymphocytes Density in Non-Small Cell Lung Cancer Patients. *J Egypt. Natl Canc. Inst.* (2018) 30(4):125–31. doi: 10.1016/j.jnci.2018.08.003
102. Zaal EA, Berkers CR. The Influence of Metabolism on Drug Response in Cancer. *Front Oncol* (2018) 8:500. doi: 10.3389/fonc.2018.00500
103. Wangpaichitr M, Wu C, Li YY, Nguyen DJM, Kandemir H, Shah S, et al. Exploiting ROS and Metabolic Differences to Kill Cisplatin Resistant Lung Cancer. *Oncotarget* (2017) 8(30):49275–92. doi: 10.18632/oncotarget.17568
104. Sullivan EJ, Kurtoglu M, Brenneman R, Liu H, Lampidis TJ. Targeting Cisplatin-Resistant Human Tumor Cells With Metabolic Inhibitors. *Cancer Chemother Pharmacol* (2014) 73(2):417–27. doi: 10.1007/s00280-013-2366-8
105. Jeon JH, Kim DK, Shin Y, Kim HY, Song B, Lee EY, et al. Migration and Invasion of Drug-Resistant Lung Adenocarcinoma Cells Are Dependent on Mitochondrial Activity. *Exp Mol Med* (2016) 48(12):e277. doi: 10.1038/emm.2016.129
106. Liu Y, He C, Huang X. Metformin Partially Reverses the Carboplatin-Resistance in NSCLC by Inhibiting Glucose Metabolism. *Oncotarget* (2017) 8(43):75206–16. doi: 10.18632/oncotarget.20663
107. Ireland AS, Micinski AM, Kastner DW, Guo B, Wait SJ, Spainhower KB, et al. MYC Drives Temporal Evolution of Small Cell Lung Cancer Subtypes by Reprogramming Neuroendocrine Fate. *Cancer Cell* (2020) 80(21). doi: 10.1158/1538-7445.TUMHET2020-PO-120
108. Massarelli E, Papadimitrakopoulou V, Welsh J, Tang C, Tsao AS. Immunotherapy in Lung Cancer. *Transl Lung Cancer Res* (2014) 3(1):53–63. doi: 10.3978/j.issn.2218-6751.2014.01.01
109. Daneshmandi S, Wegiel B, Seth P. Blockade of Lactate Dehydrogenase-A (LDH-A) Improves Efficacy of Anti-Programmed Cell Death-1 (PD-1) Therapy in Melanoma. *Cancers (Basel)* (2019) 11(4):1–11. doi: 10.3390/cancers11040450
110. Yarosz EL, Chang CH. The Role of Reactive Oxygen Species in Regulating T Cell-Mediated Immunity and Disease. *Immune Netw* (2018) 18(1):e14. doi: 10.4110/in.2018.18.e14
111. Previte DM, O'Connor EC, Novak EA, Martins CP, Mollen KP, Piganelli JD. Reactive Oxygen Species are Required for Driving Efficient and Sustained Aerobic Glycolysis During CD4+ T Cell Activation. *PloS One* (2017) 12(4):e0175549. doi: 10.1371/journal.pone.0175549
112. Kouidhi S, Ben Ayed F, Benammar Elgaaied A. Targeting Tumor Metabolism: A New Challenge to Improve Immunotherapy. *Front Immunol* (2018) 9:353. doi: 10.3389/fimmu.2018.00353
113. Joshi S, Durden DL. Combinatorial Approach to Improve Cancer Immunotherapy: Rational Drug Design Strategy to Simultaneously Hit Multiple Targets to Kill Tumor Cells and to Activate the Immune System. *J Oncol* (2019) p:5245034. doi: 10.1155/2019/5245034
114. Farber S, Diamond LK, Mercer RD, Sylvester RF, Wolff JA. Temporary Remissions in Acute Leukemia in Children Produced by Folic Acid Antagonist, 4-Aminopteroyl-Glutamic Acid (Aminopterin). *N Engl J Med* (1948) 238:787–93. doi: 10.1056/NEJM194806032382301
115. Kaye SB. New Antimetabolites in Cancer Chemotherapy and Their Clinical Impact. *Br J Cancer* (1998) 78(3):1–7. doi: 10.1038/bjc.1998.747
116. Mehrmohamadi M, Jeong SH, Locasale JW. Molecular Features That Predict the Response to Antimetabolite Chemotherapies. *Cancer Metab* (2017) 5:8. doi: 10.1186/s40170-017-0170-3
117. de Sousa Cavalcante L, Monteiro G. Gemcitabine: Metabolism and Molecular Mechanisms of Action, Sensitivity and Chemoresistance in Pancreatic Cancer. *Eur J Pharmacol* (2014) 741:8–16. doi: 10.1016/j.ejphar.2014.07.041
118. Hatami E, Nagesh PKB, Jaggi M, Chauhan SC, Yallapu MM. Gambogic Acid Potentiates Gemcitabine Induced Anticancer Activity in Non-Small Cell Lung Cancer. *Eur J Pharmacol* (2020) 888:173486. doi: 10.1016/j.ejphar.2020.173486
119. van der Lee I, Smit EF, van Putten JW, Groen HJ, Schlosser NJ, Postmus PE, et al. Single-Agent Gemcitabine in Patients With Resistant Small-Cell Lung Cancer. *Ann Oncol* (2001) 12(4):557–61. doi: 10.1023/A:1011104509759

120. Karampeazis A, Vamvakas L, Kotsakis A, Christphyllakis C, Kentepozidis N, Chandrinos V, et al. Docetaxel Plus Gemcitabine *Versus* Gemcitabine in Elderly Patients With Advanced Non-Small Cell Lung Cancer and Use of a Geriatric Assessment: Lessons From a Prematurely Closed Hellenic Oncology Research Group Randomized Phase III Study. *J Geriatr Oncol* (2016) 8(1):23–30. doi: 10.1016/j.jgo.2016.05.002
121. Adjei AA. Pemetrexed: A Multitargeted Antifolate Agent With Promising Activity in Solid Tumors. *Ann Oncol* (2000) 11(10):1335–41. doi: 10.1023/A:1008379101017
122. Belani CP, Wu YL, Chen YM, Kim JH, Yang SH, Zhang L, et al. Efficacy and Safety of Pemetrexed Maintenance Therapy *Versus* Best Supportive Care in Patients From East Asia With Advanced, Nonsquamous Non-Small Cell Lung Cancer: An Exploratory Subgroup Analysis of a Global, Randomized, Phase 3 Clinical Trial. *J Thorac Oncol* (2012) 7(3):567–73. doi: 10.1097/JTO.0b013e31823d4f9d
123. Karayama M, Inui N, Kuroishi S, Yokomura K, Toyoshima M, Shirai T, et al. Maintenance Therapy With Pemetrexed *Versus* Docetaxel After Induction Therapy With Carboplatin and Pemetrexed in Chemotherapy-Naive Patients With Advanced Non-Squamous Non-Small-Cell Lung Cancer: A Randomized, Phase II Study. *Cancer Chemother Pharmacol* (2013) 72(2):445–52. doi: 10.1007/s00280-013-2218-6
124. Niho S, Yoshida T, Akimoto T, Sakamaki K, Ono A, Seto T, et al. Randomized Phase II Study of Chemoradiotherapy With Cisplatin + S-1 *Versus* Cisplatin + Pemetrexed for Locally Advanced Non-Squamous Non-Small Cell Lung Cancer: SPECTRA Study. *Lung Cancer* (2020) 141:64–71. doi: 10.1016/j.lungcan.2020.01.008
125. Tanino R, Tsubata Y, Harashima N, Harada M, Isobe T. Novel Drug-Resistance Mechanisms of Pemetrexed-Treated Non-Small Cell Lung Cancer. *Oncotarget* (2018) 9(24):16807–21. doi: 10.18632/oncotarget.24704
126. Morere JF, Duran A, Tcherakian F, Boaziz C, Valeyre D, Battesti JP, et al. Cisplatin-5-Fluorouracil in Small Cell Lung Cancer. A Phase II Study in 109 Patients. *Lung Cancer* (1994) 11(3-4):275–81. doi: 10.1016/0169-5002(94)90547-9
127. Dazzi C, Cariello A, Casanova C, Verlicchi A, Montanari M, Papiani G, et al. Gemcitabine and Paclitaxel Combination as Second-Line Chemotherapy in Patients With Small-Cell Lung Cancer: A Phase II Study. *Clin Lung Cancer* (2013) 14(1):28–33. doi: 10.1016/j.cllc.2012.03.003
128. Stewart DJ, Tomiak EM, Goss G, Gertler SZ, Logan D, Huan S, et al. Paclitaxel Plus Hydroxyurea as Second Line Therapy for Non-Small Cell Lung Cancer. *Lung Cancer* (1996) 15(1):115–23. doi: 10.1016/0169-5002(96)00576-4
129. Neijstrom ES, Capizzi RL, Rudnick SA, Kirsch M, Delaney D, Kahn L, et al. High-Dose Methotrexate in Small Cell Lung Cancer. Lack of Efficacy in Preventing CNS Relapse. *Cancer* (1983) 51(6):1056–61. doi: 10.1002/1097-0142(19830315)51:6<1056::AID-CNCR2820510614>3.0.CO;2-V
130. Patel CH, Leone RD, Horton MR, Powell JD. Targeting Metabolism to Regulate Immune Responses in Autoimmunity and Cancer. *Nat Rev Drug Discov* (2019) 18(9):669–88. doi: 10.1038/s41573-019-0032-5
131. Zhao H, Sun J, Shao J, Zou Z, Qiu X, Wang E, et al. Glucose Transporter 1 Promotes the Malignant Phenotype of Non-Small Cell Lung Cancer Through Integrin Beta1/Src/FAK Signaling. *J Cancer* (2019) 10(20):4989–97. doi: 10.7150/jca.30772
132. Liu Y, Cao Y, Zhang W, Bergmeier S, Qian Y, Akbar H, et al. A Small-Molecule Inhibitor of Glucose Transporter 1 Downregulates Glycolysis, Induces Cell-Cycle Arrest, and Inhibits Cancer Cell Growth *In Vitro* and *In Vivo*. *Mol Cancer Ther* (2012) 11(8):1672–82. doi: 10.1158/1535-7163.MCT-12-0131
133. Hassanein M, Hoeksema MD, Shiota M, Qian J, Harris BK, Chen H, et al. SLC1A5 Mediates Glutamine Transport Required for Lung Cancer Cell Growth and Survival. *Clin Cancer Res* (2013) 19(3):560–70. doi: 10.1158/1078-0432.CCR-12-2334
134. Grass GD, Scott KEN, Fernandez MR, Stewart PA, Kang YP, Yang C, et al. Targeting Lactate Transport in Small-Cell Lung Cancer. *Int J Radiat Oncol* (2018) 102(3):e182. doi: 10.1016/j.ijrobp.2018.07.670
135. Bola BM, Chadwick AL, Michopoulos F, Blount KG, Telfer BA, Williams KJ, et al. Inhibition of Monocarboxylate Transporter-1 (MCT1) by AZD3965 Enhances Radiosensitivity by Reducing Lactate Transport. *Mol Cancer Ther* (2014) 13(12):2805–16. doi: 10.1158/1535-7163.MCT-13-1091
136. Polanski R, Hodgkinson CL, Fusi A, Nonaka D, Priest L, Kelly P, et al. Activity of the Monocarboxylate Transporter 1 Inhibitor AZD3965 in Small Cell Lung Cancer. *Clin Cancer Res* (2014) 20(4):926–37. doi: 10.1158/1078-0432.CCR-13-2270
137. Zhong D, Xiong L, Liu T, Liu X, Liu X, Chen J, et al. The Glycolytic Inhibitor 2-Deoxyglucose Activates Multiple Prosurvival Pathways Through IGF1R. *J Biol Chem* (2009) 284(35):23225–33. doi: 10.1074/jbc.M109.005280
138. Yi M, Ban Y, Tan Y, Xiong W, Li G, Xiang B. 6-Phosphofructo-2-Kinase/Fructose-2,6-Biphosphatase 3 and 4: A Pair of Valves for Fine-Tuning of Glucose Metabolism in Human Cancer. *Mol Metab* (2019) 20:1–13. doi: 10.1016/j.molmet.2018.11.013
139. Li HM, Yang JG, Liu ZJ, Wang WM, Yu ZL, Ren JG, et al. Blockage of Glycolysis by Targeting PFKFB3 Suppresses Tumor Growth and Metastasis in Head and Neck Squamous Cell Carcinoma. *J Exp Clin Cancer Res* (2017) 36(1):7. doi: 10.1186/s13046-016-0481-1
140. Sarkar Bhattacharya S, Thirusangu P, Jin L, Roy D, Jung D, Xiao Y, et al. PFKFB3 Inhibition Reprograms Malignant Pleural Mesothelioma to Nutrient Stress-Induced Macropinocytosis and ER Stress as Independent Binary Adaptive Responses. *Cell Death Dis* (2019) 10(10):725. doi: 10.1038/s41419-019-1916-3
141. Redman RA, Pohlmann PR, Kurman MR, Tapolsky G, Chesney JA. A Phase I, Dose-Escalation, Multi-Center Study of PFK-158 in Patients With Advanced Solid Malignancies Explores a First-in-Man Inhbibitor of Glycolysis. *J Clin Oncol* (2015) 33(15_suppl):TPS2606–TPS2606. doi: 10.1200/jco.2015.33.15_suppl.tps2606
142. Xie H, Hanai J, Ren JG, Kats L, Burgess K, Bhargava P, et al. Targeting Lactate Dehydrogenase–a Inhibits Tumorigenesis and Tumor Progression in Mouse Models of Lung Cancer and Impacts Tumor-Initiating Cells. *Cell Metab* (2014) 19(5):795–809. doi: 10.1016/j.cmet.2014.03.003
143. Saraei P, Asadi I, Kakar MA, Moradi-Kor N. The Beneficial Effects of Metformin on Cancer Prevention and Therapy: A Comprehensive Review of Recent Advances. *Cancer Manag Res* (2019) 11:3295–313. doi: 10.2147/cmar.s200059
144. Lin JJ, Gallagher EJ, Sigel K, Mhango G, Galsky MD, Smith CB, et al. Survival of Patients With Stage IV Lung Cancer With Diabetes Treated With Metformin. *Am J Respir Crit Care Med* (2015) 191(4):448–54. doi: 10.1164/rccm.201407-1395OC
145. Xu T, Li D, He Y, Zhang F, Qiao M, Chen Y. Prognostic Value of Metformin for Non-Small Cell Lung Cancer Patients With Diabetes. *World J Surg Oncol* (2018) 16(1):60. doi: 10.1186/s12957-018-1362-1
146. Medairos RA, Clark J, Holoubek S, Kubasiak JC, Pithadia R, Hamid F, et al. Metformin Exposure Is Associated With Improved Progression-Free Survival in Diabetic Patients After Resection for Early-Stage Non-Small Cell Lung Cancer. *J Thorac Cardiovasc Surg* (2016) 152(1):55–61.e1. doi: 10.1016/j.jtcvs.2016.03.094
147. Andrzejewski S, Siegel PM, St-Pierre J. Metabolic Profiles Associated With Metformin Efficacy in Cancer. *Front Endocrinol (Lausanne)* (2018) 9:372. doi: 10.3389/fendo.2018.00372
148. Rha SY, Boem SH, Kim GM, Shin YG, Yim DS, Kim HS, et al. Phase I Study of an Oxidative Phosphorylation Inhibitor IM156 in Patients With Advanced Solid Tumors. In: *AACR*. Atlanta, GA (2019).
149. Wu F, Fan J, He Y, Xiong A, Yu J, Li Y, et al. Single-Cell Profiling of Tumor Heterogeneity and the Microenvironment in Advanced Non-Small Cell Lung Cancer. *Nat Commun* (2021) 12(1):2540. doi: 10.1038/s41467-021-22801-0
150. Zhang Y, Chang L, Yang Y, Fang W, Guan Y, Wu A, et al. Intratumor Heterogeneity Comparison Among Different Subtypes of Non-Small-Cell Lung Cancer Through Multi-Region Tissue and Matched ctDNA Sequencing. *Mol Cancer* (2019) 18(1):7. doi: 10.1186/s12943-019-0939-9
151. Simpson KL, Frese KK, Simms N, Rowe W, Pearce SP, Humphrey S, et al. A Biobank of Small Cell Lung Cancer CDX Models Elucidates Inter- and Intratumoral Phenotypic Heterogeneity. *Nat Cancer* (2020) 1:437–51. doi: 10.1038/s43018-020-0046-2

Conflict of Interest: CG serves in a consulting and advisory capacity for AstraZeneca, Kisoji Biotechnology, and Bristol Myers Squibb. CG is also a part of Speaker's Bureau for AstraZeneca and Beigene. LB serves on advisory committees for AstraZeneca, AbbVie, GenMab, BergenBio, Pharma Mar SA, Sierra Oncology, Merck, Bristol Myers Squibb, Genentech, and Pfizer. LB also

receives research support from AbbVie, AstraZeneca, GenMab, Sierra Oncology, Tolero Pharmaceuticals.

The remaining authors declare that the research was conducted in the absence of any commercial or financial relationships that could be construed as a potential conflict of interest.

Publisher's Note: All claims expressed in this article are solely those of the authors and do not necessarily represent those of their affiliated organizations, or those of the publisher, the editors and the reviewers. Any product that may be evaluated in this article, or claim that may be made by its manufacturer, is not guaranteed or endorsed by the publisher.

frontiers in Oncology

SYSTEMATIC REVIEW
published: 22 November 2021
doi: 10.3389/fonc.2021.774081

Managing Severe Dysgeusia and Dysosmia in Lung Cancer Patients: A Systematic Scoping Review

Ana Sofia Spencer[1], David da Silva Dias[2,3,4], Manuel Luís Capelas[3,5], Francisco Pimentel[6], Teresa Santos[3,4,7,8], Pedro Miguel Neves[3,4], Antti Mäkitie[9,10,11] and Paula Ravasco[3,4,11,12]*

[1] Department of Medical Oncology, Centro Hospitalar Universitário de Lisboa Central, Hospital de Santo António dos Capuchos, Lisbon, Portugal, [2] Department of Medical Oncology, Centro Hospitalar Universitário do Algarve, Hospital de Faro, Faro, Portugal, [3] Centre for Interdisciplinary Research in Health of Universidade Católica Portuguesa (UCP), Lisbon, Portugal, [4] CatolicaMed Platform of of Universidade Católica Portuguesa (UCP), Lisbon, Portugal, [5] Universidade Católica Portuguesa (UCP), Institute of Health Sciences, Centre for Interdisciplinary Research in Health (CIIS), Lisbon, Portugal, [6] BlueClinical, Matosinhos, Portugal, [7] European University, Lisbon, Portugal, [8] Católica Medical School, Universidade Católica Portuguesa (UCP), Lisbon, Portugal, [9] Department of Otorhinolaryngology-Head and Neck Surgery, Helsinki University Hospital and University of Helsinki, Helsinki, Finland, [10] Research Program in Systems Oncology, Faculty of Medicine, University of Helsinki, Helsinki, Finland, [11] Division of Ear, Nose and Throat Diseases, Department of Clinical Sciences, Intervention and Technology, Karolinska Institute and Karolinska University Hospital, Stockholm, Sweden, [12] Centro de Investigação Interdisciplinar Egas Moniz (CiiEM), Instituto Universitário Egas Moniz (IUEM), Quinta da Granja, Monte de Caparica, Caparica, Portugal

OPEN ACCESS

Edited by:
Jeroen Hiltermann, University Medical Center Groningen, Netherlands

Reviewed by:
Xu Tian, University of Rovira i Virgili, Spain
Natasha A. Jain, Deaconess Henderson Clinic, United States

***Correspondence:**
Ana Sofia Spencer
ana.spencer@campus.ul.pt

Specialty section:
This article was submitted to Thoracic Oncology, a section of the journal Frontiers in Oncology

Received: *10 September 2021*
Accepted: *04 November 2021*
Published: *22 November 2021*

Citation:
Spencer AS, da Silva Dias D, Capelas ML, Pimentel F, Santos T, Neves PM, Mäkitie A and Ravasco P (2021) Managing Severe Dysgeusia and Dysosmia in Lung Cancer Patients: A Systematic Scoping Review. Front. Oncol. 11:774081. doi: 10.3389/fonc.2021.774081

Introduction: Lung cancer (LC) is highly prevalent worldwide, with elevated mortality. In this population, taste and smell alterations (TSAs) are frequent but overlooked symptoms. The absence of effective therapeutic strategies and evidence-based guidelines constrain TSAs' early recognition, prevention and treatment (Tx), promoting cancer-related malnutrition and jeopardizing survival outcomes and quality of life.

Objectives: To systematically review the literature on TSAs in LC patients, understand the physiopathology, identify potential preventive and Tx strategies and to further encourage research in this area.

Methods: Literature search on English language articles indexed to PubMed, CINALH, SCOPUS and Web of Science using MeSH terms "Lung neoplasms","Dysgeusia", "Olfaction Disorders", "Carcinoma, Small Cell","Carcinoma, Non- Small-Cell Lung "Adenocarcinoma of Lung","Carcinoma, Large Cell", and non-MeSH terms "Parageusia", "Altered Taste", "Smell Disorder", "Paraosmia", "Dysosmia","Lung Cancer" and "Oat Cell Carcinoma".

Results: Thirty-four articles were reviewed. TSAs may follow the diagnosis of LC or develop during cancer Tx. The estimated prevalence of self-reported dysgeusia is 35-38% in treatment-naïve LC patients, and 35-69% in those undergoing Tx, based on studies involving LC patients only. One prospective pilot trial and 1 RCT demonstrated a clinically significant benefit in combining flavor enhancement, smell and taste training and

individualized nutritional counselling; a systematic review, 1 RCT and 1 retrospective study favored using intravenous or oral zinc-based solutions (150mg 2-3 times a day) for the prevention and Tx of chemotherapy (CT) and radiotherapy (RT) -induced mucositis and subsequent dysgeusia.

Conclusions: This is the first review on dysgeusia and dysosmia in LC patients to our knowledge. We propose combining taste and smell training, personalized dietary counselling and flavor enhancement with oral zinc-based solutions (150mg, 2-3 times a day) during CT and/or RT in this population, in order to prevent and help ameliorate Tx-induced dysgeusia and mucositis. However due to study heterogeneity, the results should be interpreted with caution. Developing standardized TSA measurement tools and performing prospective randomized controlled trials to evaluate their effect are warranted.

Keywords: dysgeusia, dysosmia, taste and smell alterations (TSAs), lung cancer, dietary counselling, zinc, weight loss

INTRODUCTION

The second most frequently occurring cancer globally is lung cancer, with an incidence of 2,206.77 (excluding non-melanoma skin cancers), only surpassed by breast cancer. Also, it has the highest mortality of any cancer, accounting for 1,796,144 deaths in 2020 (1).

Whilst many symptoms are associated with lung cancer, clinicians frequently observe taste and smell alterations (TSAs). TSAs can be present upon initial diagnosis or develop during the course of cancer treatment, and can lead to a change in food preferences, resulting in reduced nutrient intake, a higher probability of weight loss and impact on patient's health-related quality of life (HRQoL) through a decrease in the pleasure of eating (2).

Although taste and smell belong to anatomically distinct systems, they are intimately connected in the sensory perception of food (3).

The chemical interplay between taste and smell senses is critical in helping humans gather information about themselves and their surrounding environment, from aiding social interaction, detecting potential dangers and the enjoyment of food consumption (4).

When consuming food or drinks, saliva helps dissolve tastant molecules facilitating their interaction with taste receptors in the mouth, leading to the activation of subsequent cascades that send signals to the brain through specialized nerve cells. The signals generated by the five basic tastes – bitter, salty, sour, sweet and umami - interact with other signals triggered by eating and drinking, such as smell and the trigeminal sensations of irritancy, temperature and texture. Together, these combine to create the sensations associated with flavor. Upon stimulation, taste bud cells trigger the activation of proximal gustatory afferent fibers that convey signals, *via* the facial (VII), glossopharyngeal (IX) and vagal (X) nerves, to the rostral division of the solitary tract nucleus in the brain stem. Additional taste neurons of a higher-order project these signals to the thalamus and subsequently to the gustatory cortex. The taste signals are then projected to a variety of brain structures *via* neurons in the gustatory cortex, including the mid-brain dopaminergic regions, amygdala, and orbitofrontal cortex. The orbitofrontal cortex is also targeted by neurons involved in olfaction and oral mouth-feel which is thought to be central in perceiving flavour (5).

The axons of olfactory sensory neurons project signals to the olfactory bulb. The piriform cortex is the main recipient of afferents from the olfactory bulb. The axons of neurons projected from the olfactory bulb are broadly dispersed across the surface of the piriform cortex, and individual piriform cortex neurons respond to numerous, chemically distinct odorants, clustering odor representations and enabling them to preferentially signify odor relationships (6).

The olfactory and taste systems can be damaged in multiple ways that reduce their function, including age, bacterial and viral illnesses, trauma, surgical damage, severe allergies, chronic rhinosinusitis, inborn genetic disorders, neurological diseases, some medications and cancer treatments (4).

Both quantitative and qualitative changes can occur as a result of taste disorders. Quantitative changes include ageusia (total taste loss), hypogeusia (partial taste loss) and hypergeusia (increased taste responsiveness). Qualitative changes include phantogeusia (the sensation of taste with stimuli absent, also known as "oral phantoms") and dysgeusia (the persistence in the mouth of slaty, bitter, rancid or metallic taste sensations after finishing a meal (3, 5).

Typically, smell disorders are divided into four categories, depending on their odor perception impact. Firstly, the absence of smell perception, or Anosmia. Secondly, a quantitatively reduced ability to perceive smells, or Hyposmia. Thirdly, a qualitative distortion of the normally perceived smell, or Parosmia. And finally, the perception of smells in the absence of an odor, or Phantosmia (4).

TSAs can be evaluated through quantitative analysis, chemical stimuli or surveys (6). As described above, the nature of the chemical senses is incredibly complex and interconnected,

therefore being important to assess smell and taste together (7).

However, a limiting factor to the evaluation of TSAs arises from the heterogeneity of the systems used to measure them and the fact that these symptoms are often underestimated and overlooked, probably due to their non-life-threatening nature (8).

Dysgeusia affects 46-77% of patients with cancer, from roughly 53% of patients receiving treatment with chemotherapeutic drugs, to 66% of those receiving radiotherapy (RT) and 76% of those patients prescribed both treatments (2, 8–11).

One review reported a prevalence of 12-84% of self-reported taste problems among cancer patients (12).

Another review of patients receiving chemotherapy (CT) reported a prevalence of alterations to taste of 45-84% and of alterations to smell of 5-60%. It also found that in patients with advanced cancer, almost 80% reported TSAs (13).

One unicentric study involving 239 patients with different cancer types undergoing cancer treatment (including nine patients with lung cancer) reported a 54% rate of dysphagia, 62% rate of taste changes and 35% rate of smell changes (14).

These wide ranges relate to study heterogeneity and the absence of standardized questionnaires and methodologies for patients to self-report the presence of chemosensory alterations (3, 12).

Malnutrition is a common finding in cancer patients, with an incidence varying between 31–87%. Undernutrition and weight loss may result from reduced energy intake, increased energy requirements, impaired nutrient absorption, tumor-related catabolism and inflammation leading to muscle wasting, anticancer treatment side effects and patient's poor psychological state (15).

A study by Joseph P.V. et al. performed with 1,329 cancer patients of various types undergoing CT, concluded that patients reporting treatment-related taste alterations suffered significantly from neuropsychological symptoms. These included higher levels of depression, anxiety, sleep disturbance and fatigue when compared to patients with no change in taste (16).

In line with the psychosocial impact of CT, Sasaki et al. evaluated the perception of symptoms through a 94-item questionnaire in 49 patients receiving chemotherapy in a hospital in Japan. It was concluded that the most frequent and troublesome non-physical concern of patients was the fact that "it affected their families or partner" (17).

Multiple studies have highlighted that poor prognosis and quality of life (QoL) in cancer patients is intimately associated with weight loss, which in turn raises the probability of adverse side-effects from treatment and impairing the response of a tumor to therapy (15).

This is reflected by the fact that malnutrition, and not malignancy, is responsible for 20% of cancer patients deaths, meaning it is essential for patients to maintain an appropriate dietary intake throughout their cancer treatment (18).

This scoping review aims to comprehensively understand the pathophysiology, impact, prevention, and treatment of TSAs in lung cancer patients, and to identify gaps in our current scientific knowledge so as to encourage further research in those areas. A preliminary search on Pubmed and the Cochrane Database of Systematic Reviews was conducted and no existing or in progress systematic reviews on this topic were identified.

METHODS

Inclusion Criteria

This scoping review was built on the basis of "The Joanna Briggs Institute" methodology. The inclusion criteria for this review were based upon the PCC elements (Population, Concept and Context). This review examined all studies and reports focusing on TSAs occurring in adult lung cancer patients, either being treatment-naïve or submitted to cancer treatment, even if the studies were not limited to this specific cancer type. Studies focusing on the pathophysiology, management and treatment approaches of TSAs were also considered.

Types of Sources

This scoping review considered experimental and quasi-experimental study designs, including randomized controlled trials, non-randomized controlled trials, before and after studies and interrupted time-series studies. Analytical observational studies, including prospective and retrospective cohort studies and analytical cross-sectional studies; and descriptive observational study designs including case series, individual case reports and descriptive cross-sectional studies, were considered for inclusion. Text and opinion papers that met the inclusion criteria were also considered.

Search Strategy

A literature search was performed in July 2021 including English language papers indexed to Pubmed, CINALH, SCOPUS and Web of Science, using the MeSH terms "Dysgeusia", "Olfaction Disorders", "Lung neoplasms", "Carcinoma, Non-Small-Cell Lung", "Carcinoma, Small Cell", "Adenocarcinoma of Lung", "Carcinoma, Large Cell", and the additional search terms "Altered Taste"; "Parageusia", "Smell Disorder", "Dysosmia", "Paraosmia", "Lung Cancer" and "Oat Cell Carcinoma", with no date range filter (**Table 1**). Articles from other sources were also searched to complement the review. Additionally, bibliography lists of all retrieved articles were searched for relevant studies.

Data Extraction and Presentation

Data were extracted from papers by two authors independently, using the Rayyan data extraction tool. The data extracted included specific details about TSAs in cancer patients in general and in lung cancer patients, as well as key relevant information to the review questions. Where there was disagreement between authors, the issues were discussed to reach a consensus. Following extraction, all full texts were subsequently independently screened by the reviewers. The extracted data are presented in tabular form, to align with the

TABLE 1 | Summary of the search strategy.

Search Strategy	
Pubmed	[((((((((((Taste Disorders[MeSH Terms)] OR Taste Disorders[Title/Abstract]) OR Dysgeusia[MeSH Terms]) OR Dysgeusia[Title/Abstract]) OR Olfaction Disorders [MeSH Terms]) OR Olfaction Disorders[Title/Abstract]) OR Altered Taste[Title/Abstract]) OR Parageusia[Title/Abstract]) OR Smell Disorder[Title/Abstract]) OR Dysosmia[Title/Abstract]) OR Paraosmia[Title/Abstract])) AND ((((((((((Carcinoma, Large Cell[MeSH Terms]) OR Carcinoma, Large Cell[Title/Abstract]) OR Adenocarcinoma of Lung[MeSH Terms]) OR Adenocarcinoma of Lung[Title/Abstract]) OR Carcinoma, Small Cell[MeSH Terms]) OR Carcinoma, Small Cell [Title/Abstract]) OR Carcinoma, Non-Small-Cell Lung[MeSH Terms]) OR Carcinoma, Non-Small-Cell Lung[Title/Abstract]) OR Lung neoplasms[MeSH Terms]) OR Lung neoplasms[Title/Abstract]) OR Lung Cancer[Title/Abstract]) OR Oat Cell Carcinoma[Title/Abstract])
CINAHL	(MM Lung neoplasms OR TI Lung neoplasms OR AB Lung neoplasms OR MM Carcinoma, non-small cell lung OR TI Carcinoma, non-small cell lung OR AB Carcinoma, non-small cell lung OR MM Carcinoma, Small Cell OR TI Carcinoma, Small Cell OR AB Carcinoma, Small Cell OR MM Adenocarcinoma of Lung OR TI Adenocarcinoma of Lung OR AB Adenocarcinoma of Lung OR TI Carcinoma, Large Cell OR AB Carcinoma, Large Cell OR TI Lung Cancer OR AB Lung Cancer OR TI Oat Cell Carcinoma OR AB Oat Cell Carcinoma) AND (MM Dysgeusia OR TI Dysgeusia OR AB Dysgeusia OR MM Olfaction disorders OR TI Olfaction disorders OR AB Olfaction disorders OR MM Taste Disorders OR TI Taste Disorders OR AB Taste Disorders OR TI Altered Taste OR AB altered states of consciousness OR TI Parageusia OR AB Parageusia OR TI Smell Disorder OR AB Smell Disorder OR TI Dysosmia OR AB Dysosmia OR TI Paraosmia OR AB Paraosmia)
Web Of Science	Search similar to the two search engines above
SCOPUS	Search similar to the two search engines above

objectives of this scoping review. We attached a narrative summary to accompany the tabulated results to describe the relationship between the results and the review's objective and questions.

RESULTS

Study Inclusion

A total of 1,960 citations were identified. After duplicate removal (n=159), 1,802 titles and abstracts meeting the inclusion criteria remained for analysis. 1,752 references were then excluded, with 50 full texts retrieved for analysis. Sixteen studies were excluded, leaving 34 articles to be included in this review. The PRISMA flowchart (**Figure 1**) describes the flow of decisions of this process. **Table 5** records studies ineligible following the full text review.

Review findings

Factors Influencing TSAs

The exact underlying mechanisms behind chemosensory alterations in cancer patients is not fully known, due to odor and taste abnormalities having a multifactorial etiology, heterogeneous cancer population studies, variability of the definition of "taste" and on the endpoints used in the studies, as well as the lack of standardized measurement tools to evaluate TSAs (3, 12).

A study by Belqaid et al. demonstrated that the intensity of TSAs tends to change over time within the course of lung cancer treatment. Additionally, TSAs are influenced by the presence of additional symptoms, side-effects of treatment and other individual and contextual factors (19).

Additional factors can also contribute to reduced smell and taste perception, including, poor oral hygiene, lack of saliva and alcohol or nicotine abuse (20).

Eating-related symptoms such as nausea, dry mouth, premature satiety, appetite loss and fatigue also interrelate with TSAs (21).

Xerostomia is highly related to taste alteration, as food particles stimulate taste bud taste receptor cells within the lingual papillae, when in solution. Therefore, reduced secretion and increased saliva viscosity may interfere with flavor molecules being transported to taste and olfactory receptors (3).

In addition, changes in cell volume or osmolar content of any of the central nervous system neurons implicated in the sense of taste are influenced by extracellular hypo-osmolality and may potentially inhibit the sense of taste (22).

In a systematic review by Nolden et al., the majority of the reviewed articles identified no significant relationship between measures of smell or taste and intake of food and enjoyment. However, it was suggested that where lower taste sensitivity is experienced by patients (higher detection thresholds), incidences of food avoidance also increase. The most common taste alterations were observed for sweet and, to some extent, bitter perception, whereas alterations in cancer patients to salt and sour perception where less frequent. The alterations were associated with lower consumption, appetite, and patients avoiding certain foods (12).

Williams and Cohen compared the taste threshold levels of 30 male lung cancer subjects before the start of RT or CT with a healthy control group, demonstrating a significant reduction in the sensitivity for sour in the lung cancer group. No significant differences were noted concerning sweet, bitter or salty tastes, although there were individuals with recognition levels that differed considerably from controls. It was concluded that diet therapy management for lung cancer patients should be individualized, in order to maintain the diary amount of protein and calories (23).

Turcott et al. evaluated changes in the thresholds for detecting and recognizing sweet, bitter and umami tastes in patients with non-small cell lung cancer (NSCLC) receiving CT treatments of cisplatin and paclitaxel-based, as well as their association with nutritional and HRQoL parameters. It was concluded that taste buds' impairment and disturbance of renewal cell processes might increase the detection thresholds for sweet, sour, salty, bitter or umami. On the other hand, higher sensitivity to umami

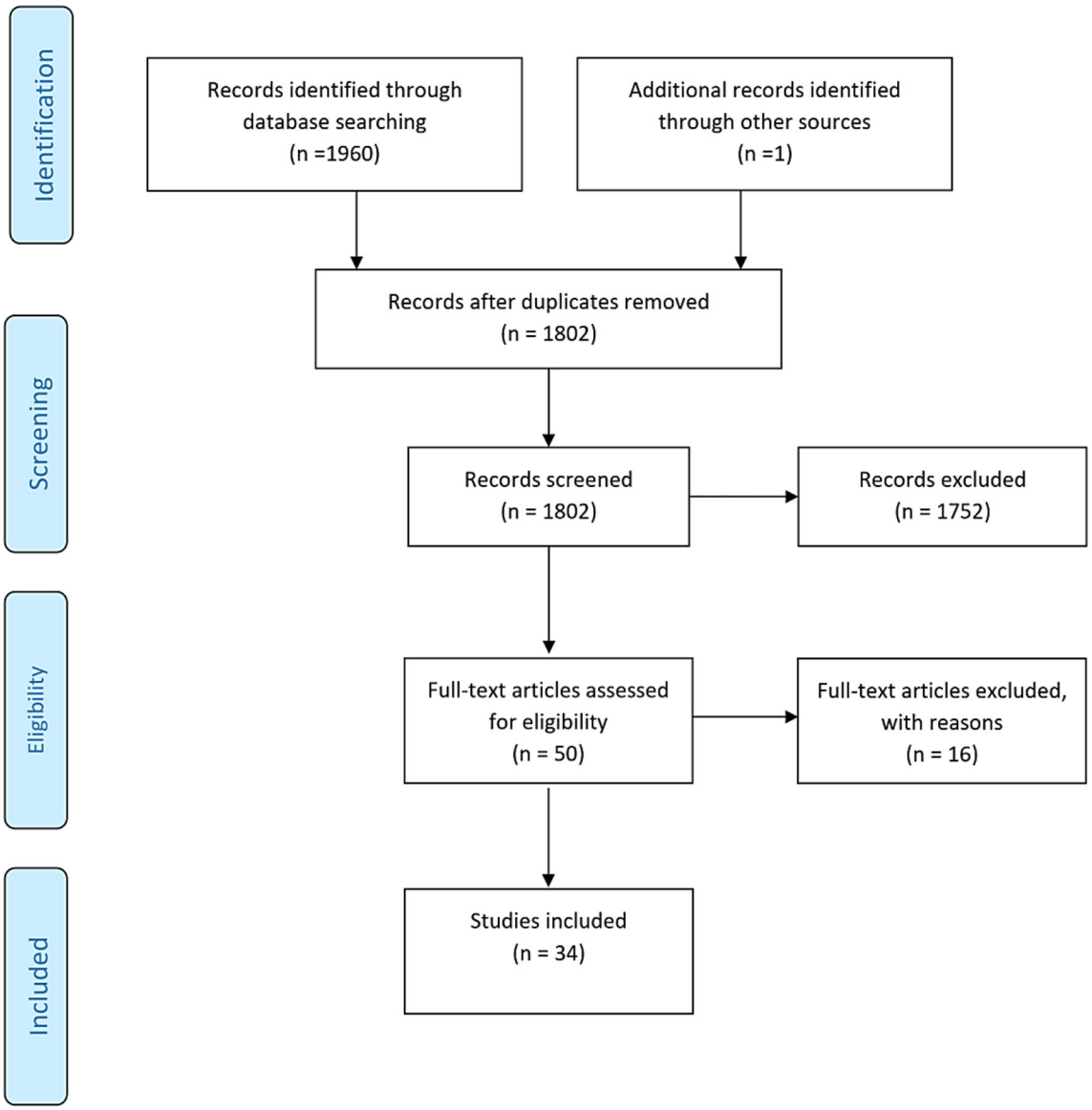

FIGURE 1 | PRISMA flowchart outlining the process for selecting the included articles.

recognition (hypergeusia) had significant association with a global HRQoL status deterioration and loss of appetite (p=0.016 and 0.115 respectively) (24).

McGreevy et al. investigated the characteristics of severe TSAs reported by 89 lung cancer patients undergoing CT. Patients reporting TSAs were younger and more frequently smokers. Gender was a statistically significant variable, with higher numbers of women reporting TSAs (25).

On the other hand, Yoshimoto et al. investigated CT impact on the smell and taste of 35 Japanese patients with lung cancer through the use of questionnaires, identifying no statistically significant associations between smell alterations and age, gender or smoking history. Patients became more sensitive to sweet and salty tastes, but less so for umami and bitter. This might have been influenced by patients' psychological stress, oral hygiene and smoking status, as well as the study's small sample size (11).

Amézaga et al. also found no statistically significant differences in taste and smell alterations between older and younger patients (3).

Zabernigg et al. found that elderly patients or patients with nicotine abuse reported fewer TAs, which might be explained by the fact that these two groups already tend to suffer from hypogeusia of some degree, making CT-induced changes less noticeable (10).

Taste and Smell Alterations in Treatment- Naïve Lung Cancer Patients

Table 2 summarizes the existing evidence on TSAs in treatment-naïve lung cancer patients, included in the review. Turcott et al.

TABLE 2 | Summary of evidence concerning treatment-naïve lung cancer patients included in the review.

Authors	Year	Type of Study	Sample Size	Variables Assessed	Method used to evaluate TSAs	Main Results
Turcott et al. (2**)**	2020	Cross-sectional, unicentric	N= 65 treatment-naïve non-small-cell lung cancer (SCLC) pts	-Dysgeusia -HRQL -Nutritional Status	Self-reporting taste Questionnaire	-35% prevalence of self-reported dysgeusia -Pts with dysgeusia had less lean body mass (p=0.027); higher fat mass (p=0.027); nausea (p=0.042); anorexia (p=0.004); early satiety (p<0.0001); clinically significant alterations in HRQL
Belqaid et al. (13**)**	2014	Prospective, observational, unicentric	N=215 pts under investigation for lung cancer, of which N=117 were diagnosed with lung cancer	-TSAs -Nutritional Status	Taste and Smell Survey	-38% prevalence of TSAs in pts with and without lung cancer; generally mild - Pts with lung cancer reporting TSAs had higher frequency of weight loss ≥10% (p<0.05)
Williams & Cohen (23**)**	1978	Prospective, observational, unicentric	N=60; 30 male pts with lung cancer and 30 male healthy controls	- Taste Acuity	Method of Henkin	-Lung cancer pts had lower sensitivity for sour (p=0.05)
Singh et al. (30**)**	2009	Case Report	–	–	–	- Case report of concomitant dysgeusia, hyponatremia and SCLC. - Dysgeusia is rarely seen with SIAD; various reports on its association with lung cancer, mostly with SCLC histology.
Nakazato et al. (27**)**	2006	Case Report	–	–	–	- Case report of dysgeusia (sweet taste of nearly all food) and hyponatremia related to SIAD, found to be associated with large-cell lung carcinoma. -Dysgeusia might have been caused by the tumor producing an unknown taste modifying substance, leading to structural changes in the taste receptor membrane when the extracellular sodium levels decreased. Miraculin could be a potential candidate substance.
Karthik et al. (29**)**	2004	Case Report	–	–	–	- Case report of dysgeusia as paraneoplastic syndrome related with lung adenocarcinoma.
Croghan et al. (28**)**	2003	Case Report	–	–	–	-Case report of dysgeusia (constant sweet taste sensation) and hyponatremia, found to be associated with a diagnosis of SCLC.
Ishimaru et al. (26**)**	1999	Case Report	–	–	–	-Case report of a lung cancer metastasized to the right frontal lobe, causing compression of the olfactory sulcus. The average olfaction recognition threshold improved after craniotomy.
Panayiotou et al. (22**)**	1995	Case series (3 case reports)	–	–	–	-Changes in the extracellular sodium concentration may modulate the sweet receptor. - The onset of persistent dysgeusia (especially if unpleasant sweet taste) should prompt measurement of serum sodium concentration and the consideration of lung carcinoma.
Kamoi et al. (39**)**	1987	Case Report	–	–	–	- Case report of SCLC associated with hyponatremia, renal sodium loss and inappropriate antidiuresis, due to increased secretion of atrial natriuretic peptide (ANP) by the atrial tissue. The natriuretic activity led to the glomerular filtration rate increasing and a decrease in tubular sodium resorption, increasing the renal fractional excretion of sodium.

Pts, patients; SIAD, Syndrome of Inappropriate Antidiuresis; SCLC, Small Cell Lung Cancer; TSAs, Taste and Smell Alterations.

found a 35% prevalence of self-reported dysgeusia among 65 treatment-naïve non-small cell lung cancer patients submitted to self-reporting taste and smell questionnaires and a rinse stimuli technique. A minimal concentration of taste stimuli was required for most patients to perceive the stimuli; however they commonly could not recognize the taste. Patients with dysgeusia presented with a significantly reduced lean-body mass (p=0.027), a significant increase in fat mass (p=0.027) and gastrointestinal symptoms, including nausea (p=0.042), anorexia (p=0.004), early satiety (p<0.0001) and reduced food consumption (p=0.01). They also had clinically significant alterations in HRQoL scales (2).

In another study, Turcott et al. found self-reported dysgeusia was prevalent in 37.5% of NSCLC treatment-naïve patients, and a 34.5% prevalence post-CT, revealing a drastically high rate of taste disorders prior to CT, comparing to that of the general population (0.07-1.7%) - meaning that dysgeusia could be caused by the disease itself (24).

An observational study by Belqaid et al. involving 215 patients under investigation for lung cancer, found a self-reported TSA prevalence of 38% in the group of patients diagnosed with lung cancer (n=117), and symptoms were in general mild (13).

Ishimaru et al. described a case report of reversible hyposmia, after removal of a right frontal lobe lung cancer metastasis which was causing slight compression and swelling of the olfactory area in the brain (26).

Also, a triad of taste distortion with prominent sweet taste, hyponatremia and lung cancer diagnosis was firstly reported in a case series by Panayiotou et al., in 1995 (22).

Since then, few other reports have described the diagnosis of lung cancer in the context of dysgeusia with unpleasant sweet taste, with concomitant hyponatremia as the sole biochemical anomaly (27–30).

It is necessary to consider the lung cancer induced syndrome of inappropriate antidiuresis (SIAD) when cryptogenic dysgeusia is identified, particularly if patients report an unpleasant sweet taste (27).

For SIAD to be diagnosed, the osmolality of the patient's urine when the effective plasma osmolality is low must exceed 100 mOsm per kilogram of water. Additionally, it is essential for clinical euvolemia to be present. Eliminating the underlying cause is the only definitive treatment for SIAD. For the majority of SIAD cases caused by malignant disease, effective antineoplastic treatment is typically the best course of action (31).

The most frequently implicated histological type is the small cell lung carcinoma. In all cases, dysgeusia seemed to disappear rapidly with normalization of serum sodium concentration (27–30).

One explanation for this is that extracellular sodium levels may modulate sweet receptors. Hyponatremia may decrease lingual sweetness receptor thresholds, although the sole cause of taste alteration cannot be completely attributed to a low sodium level alone. Nakazato et al. hypothesized that an unknown taste modifying substance could be produced by the tumor causing all foods to be interpreted by patients as sweet. This might occur due to structural changes in the taste receptor membrane when extracellular sodium levels decreased, allowing attachment of the taste modifier to sites on the sweet receptor (27). A candidate substance could be miraculin, a glycoprotein extracted from the West African berries *Richadella dulcifera*, which modifies taste through the alteration of taste receptor configuration (27, 30).

Taste and Smell Alterations in Lung Cancer Patients Undergoing Treatment

Multiple factors contribute to the risk of CT leading to toxic effects in the oral cavity, including the high renewal rates of oral tissues, damage to the mucosal microflora, salivary glands and development of neuropathy, where axonal degeneration of nerve conduction velocity occurs in up to 80% of cases affecting taste sensitivity and contributing to dysgeusia. The glossopharyngeal, facial and vagus nerves give rise to the corda tympani and greater petrosal nerves, all involved in the taste pathway (24).

Table 3 summarizes the evidence on TSAs in lung cancer patients undergoing systemic treatment, included in the review. A study by Zabernigg et al. investigated the prevalence of taste alterations (TAs) in 197 cancer patients undergoing CT, of which 54.3% had lung cancer. Almost 70% of patients reported TAs at least once during the study period, with 17.6% reporting moderate to severe TAs (10).

CT for lung cancer may involve a platinum-based compound and a third–generation agent, such as paclitaxel. Approximately two thirds of patients reported some type of dysgeusia when treated with paclitaxel-based CT (24).

In a study by Amézaga et al., CT with docetaxel led to the highest taste alteration scores in patient self-assessments (3). Steinbach et al. in Amézaga et al. found CT based on taxanes resulted in more severe taste disorders, particularly for the salt tastant. Metallic tastes, bad tastes in mouth and xerostomia have been reported in higher frequencies with paclitaxel, vinorelbine, anthracyclines and carboplatin. However, conclusions are limited by the use of a non-validated questionnaire to measure TAs. The exact mechanism causing metallic taste in patients receiving CT is unknown, but it can be generated from the CT substances being secreted in saliva and thus coming into contact with taste receptors (3).

Joussain et al. evaluated the olfactory performance of 15 lung cancer patients receiving cisplatin-based CT, concluding that whilst cisplatin did not influence odor identification and detection, a reduction in the pleasantness of food odors was evident, impairing food-related hedonic pleasure and ultimately, QoL (32).

Minakata et al. reported a case of severe gustatory disorder following the administration of a combination of cisplatin and etoposide CT (33). It had previously been reported by Henkin et al. in Minakata et al. (33) that cisplatin can displace zinc from its normal binding site and induce the inactivation of gustin, with consequent hypogeusia. Kanda et al. in Minakata et al. (33) hypothesized that cisplatin-induced gustatory disorder could be caused by disturbance to a receptor or a peripheral nerve. Cisplatin and/or etoposide could suppress gustatory receptor function, as well as leading to the occurrence of some dysfunction of the central nervous system (33).

Radiotherapy aims to destroy cancer cells by directly breaking the DNA helix strands, leading to cell death. Radiation to the chest affects the significantly radiosensitive epithelial cells lining the esophagus and pharynx. This can lead to radiation-induced side effects that can affect swallowing by disruption of the normal mucosal barrier and predisposition to fungal infection. Although typically resolving within 2 weeks after treatment conclusion, esophagitis and self-reported taste changes can continue to affect patients for weeks to months (34).

As the epidermal growth factor receptor (EGFR) is fundamental to epidermal and epithelial cells homeostasis, cutaneous or mucosal toxicities are commonly associated with the majority of anti-EGFR-treated patients (35).

Anaplastic lymphoma kinase (ALK) and ROS1 rearrangements also represent an established molecular alterations in a small subset of NSCLC (36).

Oral events induced by anti-EGFR TKIs are underreported compared to skin toxicities. Monotherapy with Erlotinib leads to an incidence of mucositis in patients of 8-20%, ranging between 17-24% with Gefitinib (35).

Crizotinib is a small-molecule, orally available tyrosine kinase inhibitor, that can suppress the activity of ALK and oncogene ROS1 kinases, causing cell cycle arrest at G1/S phase (37).

TABLE 3 | Summary of evidence concerning lung cancer patients undergoing systemic treatment included in the review.

Authors	Year	Type of Study	Sample Size	Variables Assessed	Method used to evaluate TSAs	Main Results
Nolden et al. (12**)**	2019	Systematic Scoping Review	11 studies including 578 participants (380 with cancer and 198 controls); all of the studies evaluated taste change and 5 also evaluated smell changes	- Taste changes (detection and recognition thresholds) for sweet, sour, bitter, salty and umami, and their relationship between food behavior in patients undergoing cancer treatment. - Smell changes (identification, sensitivity and discrimination) and their relationship between food behavior in patients undergoing cancer treatment.	- Whole mouth, filter paper disks and taste strips - Sniffin' Sticks	- Cancer patients with appetite loss were more likely to prefer reduced sweetness levels; compared with patients without a reduced appetite. Effect sizes showed that sweet taste had the highest empirical evidence for food behavior involvement, with reduced appetite and overall lower energy intake. - The authors did not report any significant relationships between food behavior and olfactory measures.
Yoshimoto et al. (11**)**	2019	Cross-sectional, unicentric	N=35 Japanese lung cancer patients	- TSAs	-Self-reporting taste Questionnaire	- No significant associations between change in the sense of taste and CT cycles, age or BMI, were found. There was a trend towards an association with current smoking (p=0.083). - Patients reported a higher sensitivity to salty and sweet tastes and a lower sensitivity to umami after the start of CT. - No significant associations between change in the sense of smell and age, gender or smoking history were found. - Despite less favorable taste, Japanese patients did not change their dietary habits.
Belqaid et al. (21**)**	2018	Qualitative Interview Study	N=17 lung cancer patients; 13 women, 4 men	- Patients behavior while experiencing treatment-related TSAs	- Qualitative Interview	- TSAs implied coming to terms with the presence of these symptoms and finding new personal strategies to overcome them. - Health-care professionals' involvement was generally described as limited. More normalizing information, emotional support and practical advice concerning dysgeusia could help better dealing with TSAs.
Amézaga et al. (3**)**	2018	Prospective, observational, unicentric	N=151 patients undergoing CT (13.2% with lung cancer)	- TSAs	- Interviewer-assisted TSAs' Questionnaire	- Prevalence of 76% of taste disorders and 45% of smell alterations. - Anthracyclines, paclitaxel, docetaxel and carboplatin produced highest taste disturbance rates of all CT agents. - Xerostomia was the most frequent symptom reported, strongly associated with bad taste in mouth and taste loss. - Age did not significantly influence the occurrence of TSAs.
Schalk et al. (40**)**	2018	Cross-sectional, unicentric	N=138 patients; n= 42 with cancer (2.4% lung cancer patients), n= 57 with inflammatory disease, n=39 healthy controls	- Taste Acuity	- Tastant solutions through a "whole mouth method"	- Cancer patients had significantly increased detection thresholds for tastants sweet (p=0.024), salty (p=0.031) and umami (p=0.007) compared to healthy individuals; and for sweet (p=0.004) and sour (p=0.039), compared to patients with inflammatory disease. - No significant differences were found between treatment-naive cancer patients vs patients submitted to CT.
Vigarios et al. (35**)**	2017	Review	–	-Oral toxicities induced by targeted therapies and immune checkpoint inhibitors	–	- The incidence of mucositis was found to be between 8-20% with Erlotinib and between 17 to 24% with Gefitinib. - Crizotinib has been associated with moderate dysgeusia (grade 1-2) in 11-26% of treated patients. - The incidence of moderate dysgeusia (grade 1 or

(Continued)

TABLE 3 | Continued

Authors	Year	Type of Study	Sample Size	Variables Assessed	Method used to evaluate TSAs	Main Results
						2) with immune checkpoint inhibitors has been documented in 3% of PD-1 and PD-L1 treated patients. Xerostomia (generally grade 1-2) has been reported in about 6% of patients treated with Nivolumab and 4-7.2% of patients treated with Pembrolizumab.
Ponticelli et al. (8)	2016	Cross-sectional, unicentric	N=289 patients (8.7% with lung cancer)	- Taste Acuity - HRQL	- Taste Questionnaire	- Prevalence of dysgeusia during or after CT of 64%. - There was a statistically significant correlation between type of cancer and dysgeusia (p=0.012). - There was a statistically significant correlation between type of CT and occurrence of dysgeusia (p=0.031). - Patients with dysgeusia had a worse HRQL (p=0.002).
Turcott et al. (24)	2016	Cohort, unicentric	N=40 patients with lung cancer undergoing CT with Cisplatin/Paclitaxel	- Taste Acuity - Nutritional Status - HRQL	- Rinsing technique	- Prevalence of self-reported dysgeusia in treatment-naive lung cancer patients 37.5%; post-CT 34.5%. - CT induced a tendency for an increase in taste acuity for umami (p=0.109) and sweet (p=0.092), and an increase for bitter (p=0.02).
Belqaid et al. (19)	2016	Cohort, unicentric	N= 52 lung cancer patients under anti-cancer treatment	- Taste Acuity - Nutritional Status	- Taste and Smell Survey	- TSA characteristics changed over time, relative to the start of localized or systemic treatment. Patients' experiences must be taken into account in order to adapt advice and support individual's needs.
McGreevy et al. (25)	2014	Cohort (timepoint for data analysis 'when TSAs were most severe'), unicentric	N= 89 patients under treatment for lung cancer	- TSAs - Nutritional Status	- Taste and Smell Survey	- 69% prevalence of TSAs after the start of cancer treatment -Patients reporting TSAs were on average more frequently smokers and younger -Women reported stronger TSAs -Patients with TSAs suffered more from loss of appetite, early satiety and nausea.
Joussain et al. (32)	2013	Cohort, unicentric	N=30 male patients; 15 patients with lung cancer; 15 controls	- Olfactory performance	- ETOC	- Cisplatin CT in lung cancer patients impaired the pleasure of perceived food odors (p<0.03), but not odor identification nor detection thresholds.
Zabernigg et al. (10)	2010	Cohort, unicentric	N= 197 cancer patients (54.3% with lung cancer) undergoing CT	- Taste Acuity - HRQL	- EORTC QLQ-C30 + 2 questions directed to TAs	- 69.9% of patients reported TAs in at least at one assessment time; 14.6% reported TAs in all assessment times. - 17.6% of patients reported moderate to severe TSAs. - TAs decreased significantly with age (p<0.001); - Patients with nicotine abuse reported less TAs (p=0.002) - Gender was not significantly associated with TAs. - TAs were significantly associated with appetite loss, fatigue, nausea/vomiting and cognitive functioning.
Kassem et al.	2019	Systematic Review	N = 2793 patients considered eligible from 14 studies	- Adverse Events	- CTCAE v4.0	- Systematic review reporting a rate of dysgeusia with Crizotinib and Alectinib ranging between 11-52%. - The most common AEs observed with ALK inhibitors were gastrointestinal toxicities. - There were differences between the toxicity patterns, with increased hepatic and gastrointestinal toxicities with Ceritinib, Crizotinib leading to more visual disorders, both Crizotinib and Alectinib

(Continued)

TABLE 3 | Continued

Authors	Year	Type of Study	Sample Size	Variables Assessed	Method used to evaluate TSAs	Main Results
						causing more dysgeusia and Brigatinib causing more respiratory complications. -Low grade AEs were most commonly observed, and deaths related to treatment occurred in 0-1% of patients.
Ueno et al. (36)	2019	Prospective, Observational, Real-world data (Post-marketing surveillance: follow-up 52 weeks)	N = 2028 Japanese patients with ALK fusion gene-positive NSCLC treated with Crizotinib	- Adverse Events	- CTCAE v4.0	- Reported incidence rate of dysgeusia of 16.8%.
Koizumi et al. (38)	2015	Case report	–	–	–	- Case report on Grade 3 dysgeusia and anorexia, developing 5 days after starting treatment with Crizotinib. Toxicity completely regressed after switching to Alectinib. - Crizotinib is a multi-target receptor TKI for ALK, ROS1 and MET whereas, conversely, Alectinib targets ALK very selectively without activity against ROS1 and MET. -It remains unclear whether MET and ROS1 signals could be involved in oral tissues or cell impairment.
Minakata et al. (33)	2002	Case report	–	–	–	- Case report of severe gustatory disorder following the administration of cisplatin and etoposide CT combination. - It had been previously reported that cisplatin could lead to zinc displacement from its typical binding site, with gustin inactivation and subsequent hypogeusia. - Cisplatin-induced gustatory disorder could also be caused by disturbance to a peripheral nerve or receptor. The function of gustatory receptors could be suppressed either by cisplatin and/or etoposide. Some central nervous system dysfunction may also occur. - Gustatory disorders induced by anticancer agents usually reduce patients quality of life.

AEs. Adverse Events; CiTAS. Chemotherapy-induced Taste Alteration Scale; CT. Chemotherapy; CTCAE. Common Terminology Criteria for Adverse Events; EORTC QLQ-C30. European Organization for Research and Treatment of Cancer; ETOC. European Test of Olfatory Capabilities; HRQL. Health Related Quality of Life; NSCLC. Non-Small Cell Lung Cancer; RECIST. Response Evaluation Criteria in Solid Tumors; TAs. Taste Alterations; TSAs. Taste and Smell Alterations.

In a Crizotinib post-marketing surveillance performed in Japan, the incidence rate of dysgeusia was 16.8% (36).

A systematic review on ALK inhibitor studies, including Crizotinib and Alectinib, reported a rate of dysgeusia ranging between 11-52%. Despite none of them reporting high-grade dysgeusia, this might be a cause of patient uncompliance (37).

Qian et al. in Koizumi et al. (38) conducted a meta-analysis of Crizotinib published clinical trials and reported that the Crizotinib doses must be lowered or discontinued in 6.5% of patients due to toxicity. Koizumi et al. reported a case of G3 taste alteration and loss of appetite after 5 days of treatment with Crizotinib 250mg (twice daily), leading to a discontinuation of the drug. Toxicity completely regressed after switching to Alectinib 300mg (twice daily). It remains unclear whether dysgeusia could be dependent on the dose of Crizotinib. Whereas Crizotinib is a multi-target receptor TKI for ALK, MET and ROS1, Alectinib is highly selective for ALK without activity against MET and ROS1. It also remains unclear whether MET and ROS1 signals could be involved in oral tissues or cells impairment (38).

Moderate dysgeusia (grade 1 or 2) has been noted in fewer than 3% of PD-1 and PD-L1-treated patients (35).

Management and Treatment of Taste and Smell Alterations

Due to the increased risk of TSAs in lung cancer patients coupled with the related risks of experiencing weight loss and malnutrition, there is a high medical need for clinical trials

TABLE 4 | Summary of interventions to prevent or treat dysgeusia in cancer patients undergoing systemic treatment included in the review.

Authors	Year	Type of study	Sample size	Variables assessed	Method used to evaluate TSAs	Main results
Nutritional Counseling						
Belqaid et al. (21)	2018	Qualitative Interview Study	N=17 lung cancer patients; 13 women, 4 men	- Patients behavior while experiencing treatment-related TSAs	- Qualitative Interview	- TSAs implied coming to terms with the presence of these symptoms and finding new personal strategies to overcome them - Health-care professionals' involvement was generally described as limited; clinicians should be supported in providing more practical advice, normalizing information, and emotional support to better support patients manage TSAs.
Taste and Smell Training						
Von Grundherr et al. (20)	2019	Phase II pilot trial, unicentric	N = 62 cancer patients undergoing CT (n=2 with lung cancer): - Intervention group (n=30): Taste and smell training + individual nutritional counseling - Non-intervention group (n=32): General nutritional information	- TSAs - Nutritional Status - HRQL	-"Taste Strips" method and "taste score" - MUST - EORTC QLQ-C30	- After 12 weeks, a clinically significant improvement of >2 points in the taste score were observed in 92% (n=23) of the intervention group patients, meeting the study's primary endpoint. - Median QoL score did not significantly change in the intervention group at week 12 (p= 0.811), although a relevant clinical improvement was observed in 24% of patients (n=6).
Schiffman et al. (41)	2007	Randomized Controlled Trial, unicentric	N=107 elderly cancer patients (n=95 with lung cancer) - Experimental group (n=54): Flavor enhancement products + Nutritional information - Control group (n=53): Nutritional information	- TSAs - Nutritional Status - QoL - Immune Parameters	- Taste and Smell Questionnaire, evaluation of taste and olfatory thresholds; - Mini Nutritional Assessment (MNA) - EORTC QLQ-C30 - Lymphocyte counts	- In the experimental group, MNA scores and physical function improved at the 8 months timepoint compared to the control group.
Zinc Supplementation						
Hoppe et al. (42)	2021	Systematic Review	N=1120 patients undergoing cancer treatment from a total of 19 publications included. Types of cancer were not specified	Effect of Zinc Supplementation on: - Chemotherapy –induced mucositis -Radiotherapy –induced mucositis - Oral pain -Xerostomia - Dysgeusia	- Quantitative and qualitative methods	- Zinc supplementation revealed the occurrence, onset or severity of oral mucositis due to CT were not significantly affected by the intake of zinc; although positive effects on oral pain and severity and frequency of xerostomia were found. - For patients receiving RT or radio-chemotherapy, zinc had a significant impact on the onset, severity and duration of oral mucositis (except in nasopharyngeal carcinoma patients). - There was a common trend to taste improvement during radiotherapy, but not chemotherapy. - There was no observed impact on measured QoL, weight, fatigue, and survival.
Fujii et al. (45)	2018	Retrospective, unicentric	N=634 patients (n=47 with lung cancer) receiving cancer CT - Patients with dysgeusia (n=80):	- Grade 2 dysgeusia	- CTCAE v 4.0	- In patients who received oral Polaprezinc, the grade 2 dysgeusia's 90 day recovery rates post symptom onset was 60%, significantly higher compared to the follow-up observation group (p=0.0007). - Grade 2 dysgeusia median recovery time was significantly lower in the Polaprezinc group than in patients in the follow-up

(Continued)

TABLE 4 | Continued

Authors	Year	Type of study	Sample size	Variables assessed	Method used to evaluate TSAs	Main results
			Polaprezinc (150mg twice a day) until symptom disappearance - Patients without dysgeusia (n=554): Observation			group. - Polaprezinc was not as effective in elderly patients (≥65 years). - Pancreatic cancer patients were less responsive to Polaprezinc. - The patients with the highest Polaprezinc response were those suffering with colorectal cancer.
Doi et al. (43)	2018	Review	-Cites 4 RCTs on the effect of zinc and Polaprezinc on the management of dysgeusia in cancer patients; only 2 involving lung cancer patients (Yamagata et al. being the only trial involving lung cancer patients exclusively; Lyckholm et al. involving 10 lung cancer patients from a sample of 41 patients with multiple cancer types)	-Taste Alterations	- Quantitative and qualitative methods	- Yamagata et al. explored the intravenous infusion of zinc during chemotherapy as a strategy for preventing taste disorders in patients receiving CT for lung cancer, with successful results. - Lyckholm et al. reported the failure of using oral zinc sulfate at 220 mg twice a day in improving CT-related taste alteration, loss or distortion of taste and smell, compared with placebo. - The studies demonstrated varied administration routes and dosing of zinc and Polaprezinc and included subjective forms of assessment of dysgeusia. Further studies with large samples using objective measures on taste testing should be conducted to support zinc use.
Yamagata et al. (44)	2003	Randomized Controlled Trial, unicentric	N= 12 lung cancer patients under CT - Group A (n=7): CT + intravenous drip infusion containing zinc - Group B (n=5): CT + intravenous drip infusion without zinc	- Taste Acuity	- Electrogustometer (quantitative measurement)	- After 2 weeks of treatment, taste thresholds in all group B patients worsened at the corda tympani nerve area, whereas two thirds of patients in group A showed an improvement. Electrical taste thresholds significantly differed between both groups, after 2 and 4 weeks ($p<0.05$). - Although not significant, patients in group A revealed an improvement on the electrical taste thresholds in the glossopharyngeal nerve area, at 2 weeks. At 4 weeks, there wasn't a significant difference in the taste characteristics in the glossopharyngeal nerve area between groups.
Amifostine						
Komaki et al. (47)	2004	Randomized Controlled Trial, unicentric	N=62 patients with inoperable stage II or III NSCLC -Arm 1 (n=31): Chemoradiotherapy without Amifostine -Arm 2 (n=31): Chemoradiotherapy with Amifostine	- Toxicity from chemoradiotherapy - Survival outcomes	- NCI Common Toxicity Criteria	- Amifostine significantly reduced the rate of mild, moderate and severe esophageal toxicity ($p=0.021$), as well as the rate of severe pneumonitis ($p=0.020$) and neutropenic fever ($p=0.046$). - Mild hypotension ($p<0.001$), sneezing ($p=0.039$) and dysgeusia ($p=0.029$) were significantly more frequent in the Amifostine arm. - Amifostine had no apparent effect on survival.

CT, Chemotherapy; CTCAE, Common Terminology Criteria for Adverse Events; EORTC QLQ-C30, European Organization for Research and Treatment of Cancer; HRQL, Health Related Quality of Life; MNA, Mini Nutritional Assessment; NCI, National Cancer Institute; NSCLC, Non-Small Cell Lung Cancer; PZ, Polaprezinc; Pts, patients; QoL, Quality of Life; RECIST, Response Evaluation Criteria in Solid Tumours; TSAs, Taste and Smell Alterations; RT, Radiotherapy.

focused on novel interventions to improve taste and smell. No guidelines for the treatment of smell and taste disorders are available, with general nutritional counselling that is offered to patients not earnestly addressing this subject (20). **Table 4** provides the summary of interventions to prevent or treat TSAs in lung cancer patients, included in the review.

Nutritional Counselling

To ensure appropriate nutritional counselling, information related to possible taste changes that patients could experience should be made clear before starting treatment. This necessitates providing clinicians with evaluation measures that have been validated and ensuring they receive appropriate training in their use (12).

Belquaid et al. performed a qualitative interview to 17 lung cancer patients in order to understand what strategies or resources were used to deal with cancer-related TSAs. It was concluded that limited support from health-care professionals was provided, and that the majority of patients initiated management strategies by themselves, including coming to terms with TSAs, modifying their taste and smell experiences and finding emotional support in family and friends. As part of treatment, normalizing information about TSAs seemed to be

TABLE 5 | Summary of the excluded articles with reasons.

References	Year	Study type	Reasons for exclusion
Gift et al.	2003	Retrospective, secondary analysis	Background article
Turcott et al.	2018	Abstract poster	Full article included in this review
Lederhandler et al.	2018	Case report	Wrong outcome (refers specifically to oral mucositis)
Paule J.V. et al.	2020	Prospective, longitudinal	Background article
Catania et al.	2020	Short Communication	Wrong outcome (refers specifically to dysgeusia and anosmia related to SARS-COV2 infection)
Frowen J. et al.	2020	Cross-sectional study	Background article
Simeone et al.	2019	Review article	Background article
Van der Werf et al.	2018	Pilot Study	Small sample and not exclusively related to lung cancer
Sasaki et al.	2017	Prospective study	Wrong outcome (non-physical concerns) and not exclusively related to lung cancer
Wagland et al.	2016	Cross sectional	Background article
Thorne et al.	2015	Review article	Background article
Boltong et al.	2012	Systematic review	Background article
Watters et al.	2011	Review	Background article
Vadhan-Raj et al.	2010	Randomized Controlled Trial	Wrong outcome (refers specifically to oral mucositis)
Sanchez-Lara et al.	2010	Cross-sectional study	Background article
Ishinaga et al.	2018	Cross-sectional study	Small sample and very specific to Japanese population

important in promoting acceptance and adjustment to this reality, empowering patients to find their own solutions (21).

Maintaining protein intake is important for patients during treatment. Therefore, adding high protein foods into a patient's diet should be encouraged, including eggs, dairy products, peanut butter, mild-tasting fish, chicken and soy meat substitutes (34).

Additionally, patients suffering from ageusia can try other techniques, such as flavoring meat, fish or chicken through sweet juice marination, sweet wine, and other sources including sweet-and-sour and Italian dressing. If nutritional supplements are too sweet, patients can try other options, including unflavored supplements or supplements that are based on juice or yogurt. CT-related metallic taste can be overcome by using plastic utensils, instead of metal ones (34).

For elderly patients or those suffering from umami hypogeusia, umami savoriness could help reduce any additional salt, sugar and fat consumption (24).

Taste and Smell Training

A clinical prospective pilot trial (the "TASTE trial") assessed the possible short-term impacts of training taste and smell by applying the "Taste Strips Test" plus individual nutritional counseling to a group of cancer patients undergoing chemotherapy (<= or "CT"), 3% (n=2) having lung cancer. After 12 weeks, the study's endpoint was met when a clinically significant improvement of >2 points was observed in 92% (n=23) of the intervention group patients (20).

A study by Schiffman et al. enrolled 107 cancer patients above 55 years old, the majority with lung cancer, to an experimental arm of flavor enhancement with aromas of actual foods plus nutritional counseling (n=54) and compared it with a control arm receiving nutritional information only (n=53). It was concluded that flavor enhancement plus nutritional counseling could improve patients' nutritional status and QoL, suggesting that it is possible to minimize some chemosensory losses by providing cancer patients with the knowledge to improve the flavor of their foods (41).

Zinc Supplementation

Despite multiple investigations into how zinc can impact cancer treatment toxicities, there remains a lack of evidence to form a common consensus on its role (42).

To synthesize gustin, a salivary protein that is important in ensuring the integrity of taste buds, sufficient levels of zinc are required. Zinc deficiencies, therefore, can cause impaired taste and odor sensitivity. Maeda et al. in Cranganu *et al.* (34) investigated the impact of taste alterations in 36 advanced lung cancer patients, and found higher taste abnormalities in patients with reduced serum zinc levels compared with the normal zinc level patient group (34).

A systemic review was performed by Hoppe et al. to evaluate the role of systemic zinc supplementation as complementary treatment for cancer patients (including 16 patients with lung cancer). Zinc was found to have no significant effects on chemotherapy-related oral mucositis or dysgeusia, although it seems to have positive effects on the prevention, severity and duration of RT or CT-induced oral xerostomia, mucositis and dysgeusia (42).

Polaprezinc is a chelating compound and anti-ulcer drug composed of a zinc ion, L-histidine, L-carnosine, and a β-alanine dipeptide. It has been observed to have antioxidant properties and to scavenge free radicals. Several preclinical and clinical studies showed its efficacy in reducing radiation-induced normal tissue damage. One review concluded that systemic Polaprezinc may be an acceptable option for reducing toxicities from chemoradiotherapy, being highly promising for preventing normal tissue damage in this context (43).

Yamagata et al. suggested that administering zinc intravenously during CT for lung cancer could help in preventing taste disorders and aiding patients in maintaining their QoL. Interestingly, a direct correlation between taste sensation and plasma zinc concentration could not be established, and the administration of zinc did not parallel an increase in the plasma zinc concentration (44).

A single-center retrospective study evaluated how zinc affects cancer patients' taste disorders in which subjects with different types of cancer (including 47 patients with lung cancer) suffering from grade 2 CT-related taste disorders were given 150mg of zinc twice daily orally until symptoms disappeared, *vs* a placebo comparison group. The median recovery time was significantly lower in the group where patients received zinc (63 *vs* 112 days; p=0.019) (45).

Amifostine

Amifostine is a potent exogenous, free-radical scavenger and an established radioprotectant particularly for the prevention of radiation-induced xerostomia (43). It is currently the only US Food and Drug Administration (FDA) treatment for preventing moderate to severe radiation-induced xerostomia. Additionally, for patients with NSCLC or advanced ovarian cancer receiving repeated doses of cisplatin, it reduces the cumulative renal toxicity associated with treatment. Investigators have been interested in using this drug to prevent or reduce the severity of mucositis, but its effectiveness remains controversial (46).

One study examined the impact of amifostine on NSCLC patients receiving concurrent CT and RT and whether it impacted the acute toxicity associated with treatment. Interestingly, it demonstrated that in patients given amifostine, dysgeusia was more commonly present than in the control group patients (47).

DISCUSSION

From examining the literature, we believe no other reviews of dysgeusia and dysosmia in lung cancer patients have been conducted. TSAs are common in this particular population and may follow the diagnosis of the malignancy or develop during the course of cancer treatment, leading to a decrease in nutrient intake, weight loss, poor health-related quality of life (HRQoL) and worse disease prognosis.

TSAs' intensity tends to change over time throughout the course of lung cancer treatment. Individual and contextual factors influence TSAs, including the presence of additional symptoms, side-effects of treatment and the overall life-situation of the patient (19).

Typically upon lung cancer diagnosis, a range of symptoms are present and can remain for the duration of the disease. These include weakness, fatigue, appetite and weight loss, nausea, vomiting and taste alterations (48).

On this basis, detection of these symptoms should warrant prompt assessment of chemosensory alterations (18).

In addition, it appears that the most predictive signal for the number of symptoms clustering in a patient is the stage of cancer the patient is experiencing (48).

Qualitative reports on TSAs changes are quite miscellaneous. The underlying mechanism for chemosensory alterations in cancer patients is not completely understood. This results from cancer population study heterogeneity, the multifactorial nature of odor and taste abnormalities, as well as the lack of standardized measurement tools for TSAs (3).

Taste disturbances seem to be present not only in cancer patients, but also, in patients suffering from inflammatory disorders, suggesting that taste perception deterioration can be linked to systemic inflammation inducing changes in interferon, toll-like receptor pathway and lipopolysaccharide, reducing taste progenitor cell proliferation and shortening taste bud cell lifespan (40).

For neoplastic disease, inflammation processes are induced by the release of multiple pro-inflammatory cytokines, which could be linked to the onset of taste disturbances. In this context, lung cancer may lead to changes in cell volume or osmolar content in central nervous system neurons, altering the sense of taste (22).

Upon observation of cryptogenic dysgeusia in lung cancer patients, it is necessary to consider the syndrome of inappropriate antidiuresis (SIAD), particularly if patients report unpleasantly sweet taste (27).

Interestingly, Kamoi et al. reported a case of a small cell lung cancer associated with hyponatremia, renal sodium loss and inappropriate antidiuresis unrelated to abnormal ADH plasma levels produced by the tumor. In this case, they were associated with an increased secretion of atrial natriuretic peptide (ANP) by the atrial tissue, resulting in a glomerular filtration rate increase and a decrease in tubular resorption of sodium (39).

TSAs may also develop as a consequence of CT, TKIs or RT-related side effects, through salivary gland damage and neuropathy, alteration of the structure of taste pores or conditioned aversions. A common complication of cytotoxic RT and/or CT is oral mucositis, being associated with dysgeusia, severe pain, odynophagia, malnutrition and dehydration. Contributing factors to smell and taste perception reductions include insufficient oral hygiene, xerostomia, older age, and alcohol or nicotine abuse. Other possible causes of unpleasant taste alterations arise from infection and gastrointestinal reflux leading to the production of extraneous substances (9).

In PD-1 and PD-L1-treated patients, moderate dysgeusia (grade 1 or 2) has also been observed in a minority of patients. One of the various immune-related adverse events to be aware of is pneumonitis (35). In the COVID-19 era, respiratory complaints, dysgeusia and anosmia are possible symptoms of SARS-CoV-2 viral infection, which can act as confounding factors in patients under immunotherapy when identifying treatment toxicities (49).

In lung cancer patients undergoing treatment with immune checkpoint inhibitors, the differential diagnosis between pulmonary toxicity induced by drugs, infective pneumonitis and tumor progression can be a major challenge (49).

Two randomized controlled trials (RCTs) investigated how the incidence and severity of oral side effects of cancer therapy, including dysgeusia, were affected by providing patients with dietary counseling and educational tapes. However, overall, dietary counseling as a single intervention only provided limited benefit to some patients, and the manner of delivery of the educational material to patients did not have a large impact (9).

On the other hand, nutritional counseling combined with taste and smell training and food enhancement may help the treatment of taste alterations before further problems or complications arise, particularly major weight loss and malnutrition (20, 40, 41).

Umami is regarded as the signal for protein-rich food and nutritious food, developing when meat and vegetables are cooked or roasted, resulting in the release of glutamate in food. Glutamate helps stimulate saliva production and appetite, reducing the craving

for salt and sugar. A possible correlation between lower perception of umami and observed reductions in cancer patient meat consumption could exist. Testing of glutamate could be a predictor of a patient's protein intake and its addition to a dish may increase savory perception. This has potential implications for supporting elderly cancer patients with healthier nutrition (40).

Despite conflicting results, studies reveal that systemic zinc supplementation or zinc-based solutions may help prevent and treat chemoradiotherapy-induced tissue damage, consequent mucositis and taste disorders (50).

In line with these data, Yanase et al. retrospectively evaluated the use of a 150 mg oral zinc solution 3 times per day before meals in patients with NSCLC under weekly administration of carboplatin and paclitaxel CT and concurrent chest RT. Grade ≥ 2 radiation esophagitis development was significantly delayed by oral zinc supplementation (HR, 0.397; 95% CI, 0.160–0.990; $p = 0.047$) at the point of reached cumulative radiation dose of 40Gy (51, 52).

Despite the fact that mucositis and xerostomia are frequently associated with taste alterations, we cannot necessarily assume that by treating the first we will be able to improve the latter, as it is reflected in various interventions improving oral mucositis, but not TSAs.

Many unanswered questions remain to fully understand the impact of lung cancer on taste and smell. Currently, standardized methods are unavailable to accurately and consistently measure taste and smell dysfunction across different clinical settings. This makes it more difficult to analyze and interpret study results given that self-reported taste and smell function is often not objective. Without understanding taste and smell tissue development, regeneration and degeneration at a cellular level, it is not possible to identify and develop treatments to target the sources of sensory dysfunction. For example, a consistent method for regrowing human taste receptor cells or olfactory neurons after injury or illness remains elusive, nor a method for reconnecting those cells to the areas of the brain responsible for taste and smell perception. Also, little progress has been made in analyzing the fluids specific to each type of tissue (saliva for taste, mucus for smell) for inflammation-related biomarkers or cellular dysfunction (4).

So far, no guidelines for the treatment of taste disorders are available, while there is a large need for trials to improve cancer patient's smell and taste with alternative interventions, as dietary counseling alone seems to be of modest benefit to some patients (9).

CONCLUSIONS

Given the high frequency of TSAs and their impact on nutritional status, treatment tolerance and QoL, normalizing and promoting adequate adjustment to TSAs in lung cancer patients is relevant. Potential taste and smell changes prior to lung cancer treatment should be communicated clearly to patients, requiring clinicians to be appropriately trained and provided with validated evaluation measures. Food enhancement through taste and smell training plus personalized nutritional counseling combined with zinc supplementation or use of oral zinc-based solutions seem to be helpful in preventing and treating mucositis and taste disorders in lung cancer patients under chemo-radiation treatment, although adequately powered prospective RCTs are still lacking. Overall, more work is needed to compensate for the lack of methods to standardize smell and taste dysfunction measurement across different clinical settings and the lack of understanding of the increased risk of taste alterations associated with some patient and clinical characteristics. Finally, it is critical to better understand, at the cellular level, the development and regeneration of smell and taste tissues. This could significantly help identify the sources of sensory dysfunction and support the creation of targeted strategies for treating taste and smell disorders in this cancer population.

DATA AVAILABILITY STATEMENT

The original contributions presented in the study are included in the article/supplementary material. Further inquiries can be directed to the corresponding author.

AUTHOR CONTRIBUTIONS

All authors made substantial contribution for the writing of this systematic review. PR inspired and encouraged the first author to review this topic. ASS and DSD were responsible for systematically reviewing the literature ensuring an independent selection of all the papers included. ASS was the main responsible for the conception, planning and writing of the first draft. MLC provided major support in coordinating and structuring the manuscript itself. PR, AM and FP helped to comprehensively and critically write the final draft; together with TS and PMN, who analyzed the manuscript, rectifying the language and validating the integrity and structure of the content included in this review. All authors contributed to the article and approved the submitted version.

REFERENCES

1. The Global Cancer Observatory. *Cancer Today - Fact Sheets* (2021). Available at: https://gco.iarc.fr/today/data/factsheets/populations/900-world-fact-sheets.pdf.
2. Turcott JG, Juárez-Hernández E, Sánchez-Lara K, Flores-Estrada D, Zatarain-Barrón ZL, Arrieta O. Baseline Dysgeusia in Chemotherapy-Naïve Non-Small Cell Lung Cancer Patients: Association With Nutrition and Quality of Life. *Nutr Cancer* (2020) 72(2):194–201. doi: 10.1080/01635581.2019.1633362
3. Amézaga J, Alfaro B, Ríos Y, Larraioz A, Ugartemendia G, Urruticoechea A, et al. Assessing Taste and Smell Alterations in Cancer Patients Undergoing Chemotherapy According to Treatment. *Support Care Cancer Off J Multinatl Assoc Support Care Cancer* (2018) 26(12):4077–86. doi: 10.1007/s00520-018-4277-z
4. Mainland JD, Barlow LA, Munger SD, Millar SE, Vergara MN, Jiang P, et al. Identifying Treatments for Taste and Smell Disorders: Gaps and Opportunities. *Chem Senses* (2020) 45(7):493–502. doi: 10.1093/chemse/bjaa038

5. Wang T, Glendinning J, Grushka M, Hummel T, Mansfield K. From the Cover: Drug-Induced Taste Disorders in Clinical Practice and Preclinical Safety Evaluation. *Toxicol Sci* (2017) 156(2):315–24. doi: 10.1093/toxsci/kfw263
6. Pashkovski SL, Iurilli G, Brann D, Chicharro D, Drummey K, Franks KM, et al. Structure and Flexibility in Cortical Representations of Odour Space. *Nat* (2020) 583(7815):253–8. doi: 10.1038/s41586-020-2451-1
7. Spotten LE, Corish CA, Lorton CM, Ui Dhuibhir PM, O'Donoghue NC, O'Connor B, et al. Subjective and Objective Taste and Smell Changes in Cancer. *Ann Oncol Off J Eur Soc Med Oncol* (2017) 28(5):969–84. doi: 10.1093/annonc/mdx018
8. Ponticelli E, Clari M, Frigerio S, De Clemente A, Bergese I, Scavino E, et al. Dysgeusia and Health-Related Quality of Life of Cancer Patients Receiving Chemotherapy: A Cross-Sectional Study. *Eur J Cancer Care (Engl)* (2017) 26 (2):1–7. doi: 10.1111/ecc.12633
9. Hovan AJ, Williams PM, Stevenson-Moore P, Wahlin YB, Ohrn KEO, Elting LS, et al. A Systematic Review of Dysgeusia Induced by Cancer Therapies. *Support Care Cancer Off J Multinatl Assoc Support Care Cancer* (2010) 18 (8):1081–7. doi: 10.1007/s00520-010-0902-1
10. Zabernigg A, Gamper E-M, Giesinger JM, Rumpold G, Kemmler G, Gattringer K, et al. Taste Alterations in Cancer Patients Receiving Chemotherapy: A Neglected Side Effect? *Oncologist* (2010) 15(8):913–20. doi: 10.1634/theoncologist.2009-0333
11. Yoshimoto N, Inagaki M, Sekiguchi Y, Tomishima Y, Masuko K. Chemotherapy Alters Subjective Senses of Taste and Smell But Not Dietary Patterns in Japanese Lung Cancer Patients. *Support Care Cancer Off J Multinatl Assoc Support Care Cancer* (2020) 28(4):1667–74. doi: 10.1007/s00520-019-04958-z
12. Nolden AA, Hwang L-D, Boltong A, Reed DR. Chemosensory Changes From Cancer Treatment and Their Effects on Patients' Food Behavior: A Scoping Review. *Nutrients* (2019) 11(10):1–17. doi: 10.3390/nu11102285
13. Belqaid K, Orrevall Y, McGreevy J, Månsson-Brahme E, Wismer W, Tishelman C, et al. Self-Reported Taste and Smell Alterations in Patients Under Investigation for Lung Cancer. *Acta Oncol* (2014) 53(10):1405–12. doi: 10.3109/0284186X.2014.895035
14. Frowen J, Hughes R, Skeat J. The Prevalence of Patient-Reported Dysphagia and Oral Complications in Cancer Patients. *Support Care Cancer Off J Multinatl Assoc Support Care Cancer* (2020) 28(3):1141–50. doi: 10.1007/s00520-019-04921-y
15. Mantzorou M, Koutelidakis A, Theocharis S, Giaginis C. Clinical Value of Nutritional Status in Cancer: What Is Its Impact and How it Affects Disease Progression and Prognosis? *Nutr Cancer* (2017) 69(8):1151–76. doi: 10.1080/01635581.2017.1367947
16. Joseph PV, Nolden A, Kober KM, Paul SM, Cooper BA, Conley YP, et al. Fatigue, Stress, and Functional Status are Associated With Taste Changes in Oncology Patients Receiving Chemotherapy. *J Pain Symptom Manage* (2021) 62(2):373–382.e2. doi: 10.1016/j.jpainsymman.2020.11.029
17. Sasaki H, Tamura K, Naito Y, Ogata K, Mogi A, Tanaka T, et al. Patient Perceptions of Symptoms and Concerns During Cancer Chemotherapy: "Affects My Family" Is the Most Important. *Int J Clin Oncol* (2017) 22 (4):793–800. doi: 10.1007/s10147-017-1117-y
18. Spotten L, Corish C, Lorton C, Dhuibhir PU, O'Donoghue N, O'Connor B, et al. Subjective Taste and Smell Changes in Treatment-Naive People With Solid Tumours. *Support Care Cancer Off J Multinatl Assoc Support Care Cancer* (2016) 24(7):3201–8. doi: 10.1007/s00520-016-3133-2
19. Belqaid K, Tishelman C, McGreevy J, Månsson-Brahme E, Orrevall Y, Wismer W, et al. A Longitudinal Study of Changing Characteristics of Self-Reported Taste and Smell Alterations in Patients Treated for Lung Cancer. *Eur J Oncol Nurs Off J Eur Oncol Nurs Soc* (2016) 21:232–41. doi: 10.1016/j.ejon.2015.10.009
20. von Grundherr J, Koch B, Grimm D, Salchow J, Valentini L, Hummel T, et al. Impact of Taste and Smell Training on Taste Disorders During Chemotherapy - TASTE Trial. *Cancer Manag Res* (2019) 11:4493–504. doi: 10.2147/CMAR.S188903
21. Belqaid K, Tishelman C, Orrevall Y, Månsson-Brahme E, Bernhardson B-M. Dealing With Taste and Smell Alterations-A Qualitative Interview Study of People Treated for Lung Cancer. *PloS One* (2018) 13(1):e0191117. doi: 10.1371/journal.pone.0191117
22. Panayiotou H, Small SC, Hunter JH, Culpepper RM. Sweet Taste (Dysgeusia). The First Symptom of Hyponatremia in Small Cell Carcinoma of the Lung. *Arch Intern Med* (1995) 155(12):1325–8. doi: 10.1001/archinte.155.12.1325
23. Williams LR, Cohen MH. Altered Taste Thresholds in Lung Cancer. *Am J Clin Nutr* (1978) 31(1):122–5. doi: 10.1093/ajcn/31.1.122
24. Turcott JG, Juárez-Hernández E, de la Torre-Vallejo M, Sánchez-Lara K, Luvian-Morales J, Arrieta O. Value: Changes in the Detection and Recognition Thresholds of Three Basic Tastes in Lung Cancer Patients Receiving Cisplatin and Paclitaxel and Its Association With Nutritional and Quality of Life Parameters. *Nutr Cancer* (2016) 68(2):241–9. doi: 10.1080/01635581.2016.1144075
25. McGreevy J, Orrevall Y, Belqaid K, Wismer W, Tishelman C, Bernhardson B-M. Characteristics of Taste and Smell Alterations Reported by Patients After Starting Treatment for Lung Cancer. *Support Care Cancer Off J Multinatl Assoc Support Care Cancer* (2014) 22(10):2635–44. doi: 10.1007/s00520-014-2215-2
26. Ishimaru T, Miwa T, Nomura M, Iwato M, Furukawa M. Reversible Hyposmia Caused by Intracranial Tumour. *J Laryngol Otol* (1999) 113 (8):750–3. doi: 10.1017/S0022215100145104
27. Nakazato Y, Imai K, Abe T, Tamura N, Shimazu K. Unpleasant Sweet Taste: A Symptom of SIADH Caused by Lung Cancer. *J Neurol Neurosurg Psychiatry* (2006) 77(3):405–6. doi: 10.1136/jnnp.2005.073726
28. Croghan CL, Salik RM. Undiagnosed Lung Cancer Presenting With Dysgeusia. *Am J Emergency Med United States;* (2003) 21:604–5. doi: 10.1016/j.ajem.2003.08.021
29. Karthik S, Roop R, Mediratta NK. Adenocarcinoma of Lung Presenting With Dysgeusia. *Thorax* (2004) 59:84. doi: 10.1136/thx.2004.001479
30. Singh NK, Hayes S, Hahs S, Varney A. Dysgeusia in Symptomatic Syndrome of Inappropriate Antidiuretic Hormone Secretion: Think of Lung Cancer. *BMJ Case Rep* (2009) 2009:1–4. doi: 10.1136/bcr.02.2009.1567
31. Ellison DH, Berl T. Clinical Practice. The Syndrome of Inappropriate Antidiuresis. *N Engl J Med* (2007) 356(20):2064–72. doi: 10.1056/NEJMcp066837
32. Joussain P, Giboreau A, Fontas M, Laville M, Hummel T, Souquet PJ, et al. Cisplatin Chemotherapy Induces Odor Perception Changes in Bronchial Cancer Patients. *Lung Cancer* (2013) 82(1):168–70. doi: 10.1016/j.lungcan.2013.06.009
33. Minakata Y, Yamagata T, Nakanishi H, Nishimoto T, Nakanishi M, Mune M, et al. Severe Gustatory Disorder Caused by Cisplatin and Etoposide. *Int J Clin Oncol* (2002) 7(2):124–7. doi: 10.1007/s101470200017
34. Cranganu A, Camporeale J. Nutrition Aspects of Lung Cancer. *Nutr Clin Pract Off Publ Am Soc Parenter Enter Nutr* (2009) 24(6):688–700. doi: 10.1177/0884533609352249
35. Vigarios E, Epstein JB, Sibaud V. Oral Mucosal Changes Induced by Anticancer Targeted Therapies and Immune Checkpoint Inhibitors. *Support Care Cancer Off J Multinatl Assoc Support Care Cancer* (2017) 25 (5):1713–39. doi: 10.1007/s00520-017-3629-4
36. Ueno N, Banno S, Endo Y, Tamura M, Sugaya K, Hashigaki S, et al. Treatment Status and Safety of Crizotinib in 2028 Japanese Patients With ALK-Positive NSCLC in Clinical Settings. *Jpn J Clin Oncol* (2019) 49(7):676–86. doi: 10.1093/jjco/hyz049
37. Kassem L, Shohdy KS, Lasheen S, Abdel-Rahman O, Ali A, Abdel-Malek RR. Safety Issues With the ALK Inhibitors in the Treatment of NSCLC: A Systematic Review. *Crit Rev Oncol Hematol* (2019) 134:56–64. doi: 10.1016/j.critrevonc.2018.11.004
38. Koizumi T, Fukushima T, Tatai T, Kobayashi T, Sekiguchi N, Sakamoto A, et al. Successful Treatment of Crizotinib-Induced Dysgeusia by Switching to Alectinib in ALK-Positive Non-Small Cell Lung Cancer. *Lung Cancer* (2015) 88(1):112–3. doi: 10.1016/j.lungcan.2015.01.018
39. Kamoi K, Ebe T, Hasegawa A, Sato F, Takato H, Iwamoto H, et al. Hyponatremia in Small Cell Lung Cancer. Mechanisms Not Involving Inappropriate ADH Secretion. *Cancer* (1987) 60(5):1089–93. doi: 10.1002/1097-0142(19870901)60:5<1089::AID-CNCR2820600528>3.0.CO;2-U
40. Schalk P, Kohl M, Herrmann HJ, Schwappacher R, Rimmele ME, Buettner A, et al. Influence of Cancer and Acute Inflammatory Disease on Taste Perception: A Clinical Pilot Study. *Support Care Cancer Off J Multinatl Assoc Support Care Cancer* (2018) 26(3):843–51. doi: 10.1007/s00520-017-3898-y
41. Schiffman SS, Sattely-Miller EA, Taylor EL, Graham BG, Landerman LR, Zervakis J, et al. Combination of Flavor Enhancement and Chemosensory Education Improves Nutritional Status in Older Cancer Patients. *J Nutr Health Aging* (2007) 11(5):439–54.
42. Hoppe C, Kutschan S, Dörfler J, Büntzel J, Büntzel J, Huebner J. Zinc as a Complementary Treatment for Cancer Patients: A Systematic Review. *Clin Exp Med* (2021) 21(2):297–313. doi: 10.1007/s10238-020-00677-6

43. Doi H, Kuribayashi K, Kijima T. Utility of Polaprezinc in Reducing Toxicities During Radiotherapy: A Literature Review. *Future Oncol* (2018) 14(19):1977–88. doi: 10.2217/fon-2018-0021
44. Yamagata T, Nakamura Y, Yamagata Y, Nakanishi M, Matsunaga K, Nakanishi H, et al. The Pilot Trial of the Prevention of the Increase in Electrical Taste Thresholds by Zinc Containing Fluid Infusion During Chemotherapy to Treat Primary Lung Cancer. *J Exp Clin Cancer Res* (2003) 22(4):557–63.
45. Fujii H, Hirose C, Ishihara M, Iihara H, Imai H, Tanaka Y, et al. Improvement of Dysgeusia by Polaprezinc, a Zinc-L-Carnosine, in Outpatients Receiving Cancer Chemotherapy. *Anticancer Res* (2018) 38(11):6367–73. doi: 10.21873/anticanres.12995
46. Chambers MS, Garden AS, Martin JW, Kies MS, Weber RS, Lemon JC. Oral and Orofacial Considerations in Oncology. In: S-CJ Yeung, CP Escalante, RF Gagel, editors. *Internal Medical Care of Cancer Patients*. Shelton, Connecticut: People's Medical Publishing House (2009). p. 307–19.
47. Komaki R, Lee JS, Milas L, Lee HK, Fossella FV, Herbst RS, et al. Effects of Amifostine on Acute Toxicity From Concurrent Chemotherapy and Radiotherapy for Inoperable non-Small-Cell Lung Cancer: Report of a Randomized Comparative Trial. *Int J Radiat Oncol Biol Phys* (2004) 58 (5):1369–77. doi: 10.1016/j.ijrobp.2003.10.005
48. Gift AG, Stommel M, Jablonski A, Given W. A Cluster of Symptoms Over Time in Patients With Lung Cancer. *Nurs Res* (2003) 52(6):393–400. doi: 10.1097/00006199-200311000-00007
49. Catania C, Stati V, Spitaleri G. Interstitial Pneumonitis in the COVID-19 Era: A Difficult Differential Diagnosis in Patients With Lung Cancer. *Tumori* (2021) 107(3):267–9. doi: 10.1177/0300891620951863
50. Thorne T, Olson K, Wismer W. A State-of-the-Art Review of the Management and Treatment of Taste and Smell Alterations in Adult Oncology Patients. *Support Care Cancer Off J Multinatl Assoc Support Care Cancer* (2015) 23(9):2843–51. doi: 10.1007/s00520-015-2827-1
51. Hewlings S, Kalman D. A Review of Zinc-L-Carnosine and Its Positive Effects on Oral Mucositis, Taste Disorders, and Gastrointestinal Disorders. *Nutrients* (2020) 12(3):1–11. doi: 10.3390/nu12030665
52. Yanase K, Funaguchi N, Iihara H, Yamada M, Kaito D, Endo J, et al. Prevention of Radiation Esophagitis by Polaprezinc (Zinc L-Carnosine) in Patients With Non-Small Cell Lung Cancer Who Received Chemoradiotherapy. *Int J Clin Exp Med* (2015) 8(9):16215–22.

Conflict of Interest: Author FP was employed by company BlueClinical.

The remaining authors declare that the research was conducted in the absence of any commercial or financial relationships that could be construed as a potential conflict of interest.

frontiers in Oncology

REVIEW
published: 15 December 2021
doi: 10.3389/fonc.2021.766659

EGFR-Dependent Extracellular Matrix Protein Interactions Might Light a Candle in Cell Behavior of Non-Small Cell Lung Cancer

Sarah Sayed Hassanein[1,2*‡], *Ahmed Lotfy Abdel-Mawgood*[1†‡] *and Sherif Abdelaziz Ibrahim*[2†‡]

[1] Biotechnology Program, Basic and Applied Sciences (BAS) Institute, Egypt-Japan University of Science and Technology (E-JUST), Alexandria, Egypt, [2] Zoology Department, Faculty of Science, Cairo University, Giza, Egypt

Lung cancer remains the leading cause of cancer-related death and is associated with a poor prognosis. Lung cancer is divided into 2 main types: the major in incidence is non-small cell lung cancer (NSCLC) and the minor is small cell lung cancer (SCLC). Although NSCLC progression depends on driver mutations, it is also affected by the extracellular matrix (ECM) interactions that activate their corresponding signaling molecules in concert with integrins and matrix metalloproteinases (MMPs). These signaling molecules include cytoplasmic kinases, small GTPases, adapter proteins, and receptor tyrosine kinases (RTKs), particularly the epidermal growth factor receptor (EGFR). In NSCLC, the interplay between ECM and EGFR regulates ECM stiffness, angiogenesis, survival, adhesion, migration, and metastasis. Furthermore, some tumor-promoting ECM components (e.g., glycoproteins and proteoglycans) enhance activation of EGFR and loss of PTEN. On the other hand, other tumor-suppressing glycoproteins and -proteoglycans can inhibit EGFR activation, suppressing cell invasion and migration. Therefore, deciphering the molecular mechanisms underlying EGFR and ECM interactions might provide a better understanding of disease pathobiology and aid in developing therapeutic strategies. This review critically discusses the crosstalk between EGFR and ECM affecting cell behavior of NSCLC, as well as the involvement of ECM components in developing resistance to EGFR inhibition.

Keywords: epidermal growth factor receptor (EGFR), extracellular matrix (ECM), non-small cell lung cancer (NSCLC), integrin receptors, proteoglycans, glycoproteins, matrix metalloproteinases (MMPs), tyrosine kinase inhibitors (TKIs).

OPEN ACCESS

Edited by:
Paul Takam Kamga,
Université de Versailles Saint-Quentin-en-Yvelines, France

Reviewed by:
Jelena Stojsic,
University of Belgrade, Serbia
Loredana Urso,
University of Padua, Italy

****Correspondence:***
Sarah Sayed Hassanein
sarah.hassanein@ejust.edu.eg;
ssara@sci.cu.edu.eg

†ORCID:
Sarah Sayed Hassanein
0000-0003-0545-4215
Ahmed L. Abdelmawgood
0000-0001-9784-1014
Sherif A. Ibrahim
0000-0001-6403-7345

‡These authors have contributed equally to this work and share senior authorship

Specialty section:
This article was submitted to Thoracic Oncology, a section of the journal Frontiers in Oncology

Received: *29 August 2021*
Accepted: *23 November 2021*
Published: *15 December 2021*

Citation:
Hassanein SS, Abdel-Mawgood AL and Ibrahim SA (2021) EGFR-Dependent Extracellular Matrix Protein Interactions Might Light a Candle in Cell Behavior of Non-Small Cell Lung Cancer. Front. Oncol. 11:766659. doi: 10.3389/fonc.2021.766659

1 INTRODUCTION

Globally, lung cancer is the foremost cause of cancer-related death, accounting for 2.09 million cases and 1.76 million deaths in 2018, according to GLOBOCAN (1). Two types of lung cancer are known: non-small cell lung cancer (NSCLC) and small cell lung cancer (SCLC), with an incidence rate of 85% and 14%, respectively. According to histological characteristics, NSCLC is divided into lung adenocarcinoma (ADC), squamous cell carcinoma (SqCC), and large cell carcinoma (LCC) (2). Most likely, lung cancer is

diagnosed at locally advanced or metastatic stages in 70% of patients, leading to a low 5-year survival rate (15%) (3). Lung cancer metastasis is the primary cause of death in most patients, including metastasis to the brain (20–40%), bones (30–40%); however, the mechanism has yet remained unclear (4, 5). The latest advances in technology have helped determine genetic, epigenetic, and proteomic alterations in different cancers (6). The epidermal growth factor receptor (EGFR) signaling pathway plays a crucial role in NSCLC progression (7, 8).

The EGFR is a transmembrane glycoprotein receptor that belongs to the ErbB family of receptor tyrosine kinases (RTKs). There are four types of EGF receptors (HER1/EGFR/ErbB1, HER2/ErbB2, HER3/ErbB3, and HER4/ErbB4) that comprise a cysteine-rich extracellular ligand-binding domain (LBD), an α-helix transmembrane domain (single-pass), a C-terminal domain, and except HER3, a cytoplasmic tyrosine kinase (TK) domain (8). The EGFR signaling pathway is multifaceted, with more than 13 extracellular ligands. Upon ligand-receptor binding, the dimerization of the receptor either with the same (homodimerization) or another receptor (heterodimerization) of the EGFR family takes place (9, 10). Upon EGFR dimerization, it activates one or more downstream cascades, including the phosphatidylinositol-3-kinase/protein kinase B (PI3K/AKT), mitogen-activated protein kinase (MAPK), extracellular signal-regulated kinase (MEK/ERK), mammalian target of rapamycin (mTOR), and signal transducer and activator of transcription (STAT) pathways through autophosphorylation of the receptor as well as the cytoplasmic protein binding (11, 12). EGFR is normally downregulated after receptor activation by an endocytic pathway, resulting in receptor degradation or recycling. The uncontrolled EGFR pathway induces aberrant signaling linked with many airway illnesses, including extreme airway proliferation, hypersecretion, mucus overproduction, and advanced distal lung fibrosis and cancer (13, 14). Lung SqCC and ADC patients can harbor abnormal EGFR pathway activation and conserved *ErbB1* gene mutations (15) that are approximately 90% in exons 18–21 of its kinase domain, besides an additional 5% denoted to an in-frame deletion in exons 2–7 (13). Tumor extracellular matrix (ECM) composition can play a role in EGFR-dependent lung cancers.

ECM is a significant part of all tissues' microenvironment. It offers physical support for the neighboring cells, binds growth factors, and controls cell behavior under physiological and pathological conditions (16). ECM is composed of a non-cellular network of proteins, proteoglycans, glycoproteins, and polysaccharides that constitute the interstitial matrix (IM) and the basement membrane (BM) (17). The latter is a well-structured membrane, underlining epithelial and endothelial cells under healthy conditions to separate them from the IM, which constitutes the main stroma and plays a significant role in cell adhesion, cell migration, tissue development, angiogenesis, and repair (18). It is well-known that carcinogenesis is multistep genetic and epigenetic variations, resulting in oncogenes overexpression and downregulation of tumor suppressor genes (19). These aberrations induce cancer cells to stimulate adjacent stromal cells and augment the release of ECM proteins, growth factors, cytokines, angiogenic factors, and proteolytic enzymes into tumor stroma to form a tumor-supportive microenvironment (**Figure 1**) (20, 21). The development of resistance to EGFR tyrosine kinase inhibitors (TKIs) is still a critical problem in lung cancer, and the underlying mechanisms remain fully unexplored (22). Although TKI-induced or –selected genetic alterations are known to cause chemoresistance, other poorly understood mechanisms in tumor cells can drive this resistance. In the absence of genetic alterations, ECM components are players in TKI resistance (23). **I**n the following sections, we highlight the different types of ECM proteins and their roles in mediating EGFR signaling to pinpoint their significance in NSCLC as biomarkers for diagnosis and prognosis and their potential as druggable targets.

2 ECM-KEY STRUCTURAL AND SIGNALING COMPONENTS MODULATE EGFR ACTIVATION AND AFFECT CELL BEHAVIOR OF NSCLC

2.1 Glycoproteins

2.1.1 Fibulins (FBLNs)

Emerging data have indicated that the fibulin (FBLN) family comprising seven members (fibulin-1–7) of widely expressed ECM proteins is associated with lung cancer invasion and metastasis. FBLNs are ECM glycoproteins consisting of EGF-like domain repeats crucial for normal organogenesis and embryonic development (24). They are vital for these biological processes as they regulate cell-to-matrix communication and ECM structure stabilization through intermolecular bridges that bind to several supramolecular structures (25, 26). Besides their structural role, FBLNs are linked to many cellular signaling events and complex biologic processes, including cellular proliferation, adhesion, and migration (25, 27).

Fibulin-1 (FBLN1) expression levels are substantially downregulated in NSCLC (28). The role of FBLNs in regulating the EGFR function is shown in **Figure 2**. Harikrishnan *et al.* used siRNA to knock down *FBLN1C* and *FBLN1D* expression in NSCLC Calu-1 cells to examine if FBLN1 isoforms could play a role in controlling EGFR signaling and function (28). Without affecting overall EGFR expression levels, *FBLN1C* and *FBLN1D* expression loss significantly increases basal (with serum) and EGF-mediated EGFR activation. Conversely, overexpression of FBLN1D and FBLN1C inhibits EGFR activation, indicating a regulatory crosstalk between the two proteins.

FBLN3's functions and signaling mechanisms in lung cancer stem cells (CSCs) were investigated (29). Moreover, FBLN3 was downregulated in the lung (30) and nasopharyngeal carcinomas (31). Forced expression of FBLN3 reduces the expression of epithelial-mesenchymal transition (EMT) activators, including N-cadherin and Snail, which inhibit ADC cell invasion and migration. FBLN3 inhibits the stemness activities of ADC cells, as shown by a decline in spheroid formation and the levels of stemness markers, including SRY-like HMG box (Sox2) and β-catenin. FBLN3 effects are mediated by the glycogen synthase

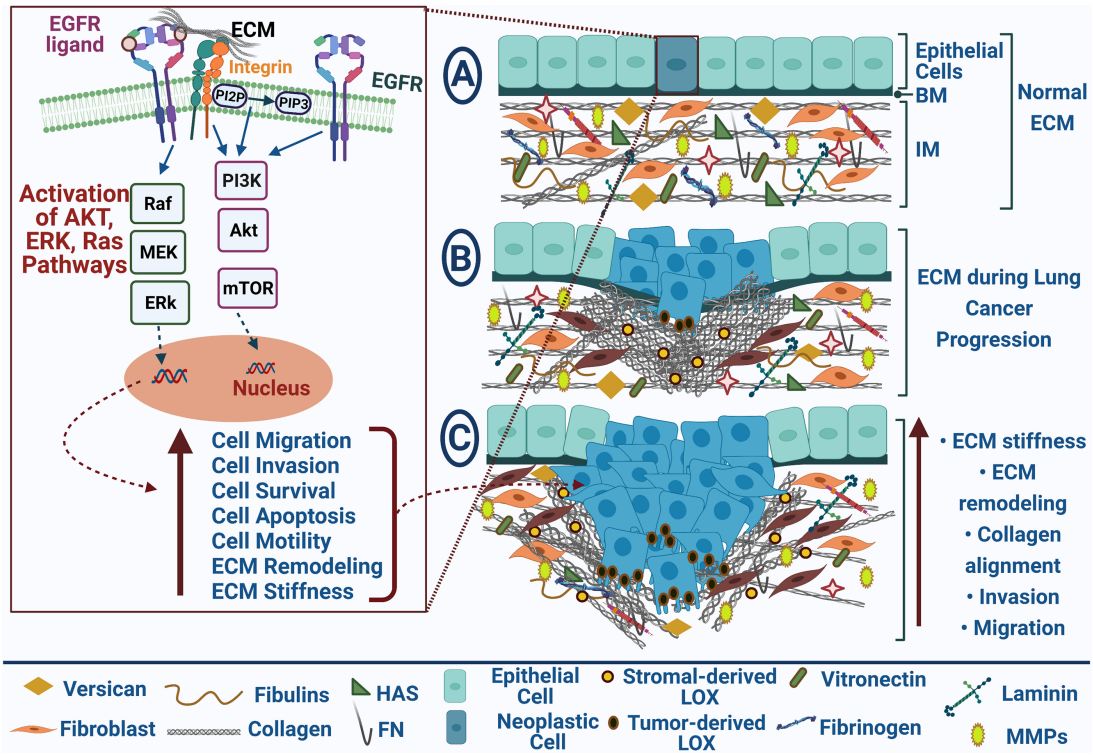

FIGURE 1 | EGFR-mediated ECM remodeling during lung cancer progression. EGFR and ECM receptors, integrins, results in Akt, Erk, and Ras pathways' activation that participate in increasing cell migration, invasion, survival, and motility and repressing cell apoptosis; **(A)** Normal ECM in healthy tissue; **(B)** Neoplastic cells with uncontrolled cell growth promote ECM remodeling during lung cancer progression; **(C)** Tumor migration and invasion are mediated by collagen alignment and ECM stiffness. Blue arrows point to stimulation, upright-directed red arrows point to increase effect, and dashed red arrows point to cellular effect.

kinase-3β (GSK3β)/β-catenin pathway and the upstream regulators of GSK3β such as (PI3K)/AKT and insulin-like growth factor receptor (IGF1R). Furthermore, *IGF1R* was discovered to be a direct target of FBLN3, which inhibits the action of IGF. Further, FBLN3 inhibits lung CSC and EMT by modulating the IGF1R/PI3K/AKT/GSK3 pathway, and that FBLN3 may be used as a CSC-centered therapeutic alternative (29). FBLN3 could attenuate the invasion of NSCLC A549 cells by inhibiting the transcription of matrix metalloproteinase-*(MMP)-7* and *MMP-2* (32). Again, Chen et al. revealed the function of FBLN3 and FBLN5 as suppressors of lung cancer invasion and metastasis through the inhibition of Wnt/β-catenin and ERK signaling pathways (33) that, in turn, downregulate MMP-2 and MMP-7 expression (32) and inhibit lung cancer cell survival, proliferation, and metastasis (34, 35). Moreover, FBLN3 overexpression notably decreased the activities of MMP-2 and MMP-9 and repressed the invasion of NSCLC A549 cells; thus, it could be used as a therapeutic strategy for NSCLC (36).

FBLN5 (DANCE), a vascular integrin receptor ligand, is a distinct member of fibulins harboring the RGD (Arg-Gly-Asp) motif associated with endothelial cell adhesion (37). FBLN5 can also depend on RGD to attenuate angiogenesis (38). It interacts directly with elastic fibers *in vitro*, and its amino-terminal domain serves as a ligand for cell surface integrins αvβ3, α9β1, and αvβ5 (39–41). FBLN5 expression is induced under pathological conditions, including pulmonary hypertension and lung injury (42), and is controlled by transforming growth factor-β (TGF-β) (43). FBLN5 was discovered to be a suppressor of lung cancer invasion and metastasis *via* inhibiting MMP-7. Indeed, FBLN5 knockdown induces cell invasion and MMP-7 expression. In lung tumors, the expression levels of FBLN5 and MMP-7 are inversely associated. FBLN5 suppresses MMP-7 expression through the ERK pathway, which is mediated by an integrin-binding RGD motif. FBLN5 overexpression in H460 lung cancer cells also prevents metastasis in mice. These findings indicate that epigenetically silenced *FBLN5* promotes lung cancer invasion and metastasis by inducing MMP-7 expression through the ERK pathway (44).

2.1.2 Mucins

Mucins (MUCs) are high M.wt glycoproteins synthesized by many epithelial tissues (45). They are categorized into two major groups: secretory mucins and membrane-bound mucins. There are 11 membrane-bound mucins (MUC1, MUC3A, MUC3B, MUC4, MUC12, MUC13, MUC15, MUC16, MUC17, MUC20, and MUC21) and seven secreted mucins (MUC2, MUC5AC, MUC5B, MUC6, MUC7, MUC8, and MUC19) (46). MUCs are involved in the normal development of the lungs and are

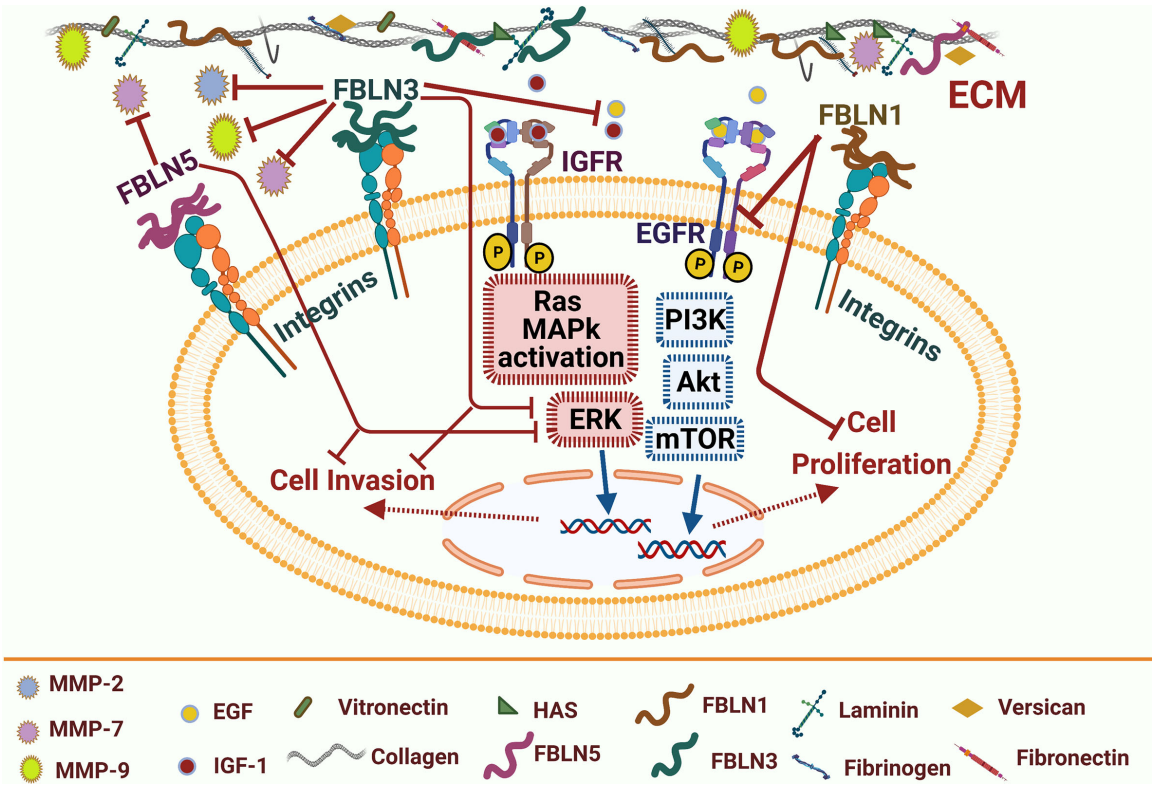

FIGURE 2 | Fibulins-mediated EGFR signaling pathways and matrix metalloproteinases in lung cancer. Fibulin (FBLN) family includes many types such as FBLN1,3&5 serve as tumor-suppressor proteoglycans. FBLN1 can inhibit EGFR activation and thus suppress cell proliferation. FBLN3 can compete with EGF and IGF-1 binding to their receptors; it also can inhibit transcription of oncogenic matrix metalloproteinases (MMP2& MMP9). FBLN3/5 can inhibit MMP7 and Erk pathway activation and thus inhibit cell invasion. Blue arrows for stimulation; dashed red arrows for cellular effect, and red "T" sign for inhibition.

expressed during the embryonic stages of lung development. The cytoplasmic domain of MUC1-C contains i) a YEKV motif: a substrate for EGFR phosphorylation and a SRC SH2 binding site (47), ii) a YHPM motif: a binding site for PI3K and the AKT pathway activation (48, 49), and iii) a YTNP motif: Upon tyrosine phosphorylation, it interacts with Grb2, which binds MUC1-C to son of sevenless (SOS) and thereby activating the RAS→MEK→ERK pathway (49).

MUC1 is an oncogenic glycoprotein that binds to EGFR, serving as a substrate, and that MUC1 expression can enhance EGFR-dependent signaling. MUC1 expression can prevent degradation of EGFR in breast epithelial cells using overexpression constructs and RNAi-mediated knockdown of MUC1, increasing total cellular pools of EGFR (50). The MAPS (MUC1-associated proliferation signature) includes a cytoplasmic domain of MUC1 (MUC1-CD)-dependent genes, including cyclin B1 (*CCNB1*), cyclin-dependent kinase inhibitor 3 (*CDKN3*), cell division cycle protein (*CDC2*, *CDC20*), mitotic arrest deficient 2-like protein 1 (*MAD2L1*), protein regulator of cytokinesis 1 (*PRC1*), and ribonucleoside-diphosphate reductase subunit M2 (*RRM2*), which are involved in cell cycle and proliferation regulation and have been linked to poor outcomes in patients with lung adenocarcinoma (51). MUC1 is expressed as MUC1-N and MUC1-C, a non-covalent heterodimer of N-terminal and C-terminal subunits, respectively (46). MUC1 overexpression, in association with MUC1-C, contributes to activation of the nuclear factor Kappa-activated B cells (NF-κB) (52), Wnt/β-catenin/TCF4 (transcription factor 4) (53), and STAT1/3 pathways in NSCLC (54). In NSCLC, the heterodimeric protein MUC1 is abnormally overexpressed, resulting in gene signatures linked to poor patient survival (48). The cytoplasmic domain of MUC1-C is associated with PI3K p85 in NSCLC cells.

Blocking the interaction of MUC1-C with PI3K p85 *via* cell-penetrating peptides suppresses Akt phosphorylation and its downstream effector mTOR. Treatment of NSCLC cells with GO-203, a MUC1-C peptide inhibitor, results in downregulation of PI3K-Akt signaling, growth inhibition, an increase in reactive oxygen species (ROS), and necrosis induction *via* a ROS-dependent mechanism. Furthermore, in H1975 (EGFR L858R/T790M) mutant cells and A549 (K-Ras G12S) xenografts developed in nude mice after treatment with GO-203, tumor regressions were observed. These data suggest that MUC1-C is needed for PI3K-Akt pathway activation and survival in NSCLC cells (48). Galectin-3 is a β-galactoside binding protein that has also been linked to human cancer development. Glycosylation of

the C-terminal subunit of Asn-36 is necessary for galectin-3 upregulation. Two Sentences have been transferred to section no. 8. Galectin-3 binds to MUC1-C at the glycosylated Asn-36 site. Galectin-3 acts as a bridge between EGFR and MUC1, besides galectin-3 is needed for EGF-mediated interactions between MUC1 and EGFR that support the importance of the MUC1-C-galectin-3 interaction (55).

In *EGFR* mutant NSCLC, MUC5B-positive patients had significantly longer overall survival and relapse-free survival than MUC5B-negative patients. MUC5B appears to be a novel prognostic biomarker in NSCLC patients with EGFR mutations (56). Lung ADC subtypes, including invasive mucinous adenocarcinoma (IMA) and lepidic predominant adenocarcinoma (LPA) are associated with MUC expression. In this regard, MUC1 is expressed in LPA, whereas MUC5B, MUC5AC and MUC6 are expressed in IMA (57). Also, *EGFR* and *KRAS* (Kirsten Rat Sarcoma viral oncogene homolog) mutations and Hnf4α expression may participate in mucin expression profiles in these lung ADC subtypes (57). The overexpression of MUC21 proteins with a particular glycosylation state is implicated in developing *EGFR*-mutated lung ADCs associated with a high frequency of lymphatic vessels invasion and lymph node metastasis (58). Additionally, MUC5AC is linked to poor prognosis and would be a prospective therapeutic target in lung ADC due to its role in enhancing tumor heterogeneity with mucin production (59). Therefore, developing treatment strategies targeting MUCs' expression and functions to manage NSCLC progression are under investigation (60).

2.1.3 Fibronectin

Fibronectin (FN) is present in multiple isoforms through alternative splicing, where 20 isoforms in humans have been discovered (61) and are involved in mediating many cellular interactions with the ECM (62). It is primarily synthesized by CAFs and polymerized into ECM fibrils that act as scaffolds for ECM binding molecules such as growth factors and cell surface receptors (63). FN is overexpressed in the stroma of NSCLC and can promote cancer cell adhesion, growth, differentiation, migration, invasion, survival, and resistance to chemotherapy (64). FN-dependent molecular pathways can control the tumor cell response to the stromal matrix and represent potential targets for managing chemo-resistant tumors (65). FNIII-1c, a peptide mimetic, can activate Toll-like receptors (TLRs) to promote NF-κB activation and release inflammatory cytokine in fibroblasts (**Figure 3**) (66, 67). Notably, the PI3K/Akt pathway is the main pathway by which most cytokines and growth factors activate mTOR and its downstream targets. In NSCLC H1838 and H1792 cells, FN induces phosphorylation of eukaryotic initiation factor 4E–binding protein 1 (4E-BP1) and p70S6K1 (two downstream targets of mTOR), and Akt phosphorylation (an upstream inducer of mTOR), whereas it inhibits the tumor suppressor protein phosphatase that antagonizes the PI3K/Akt signal (68). Furthermore, FN inhibits liver kinase B1 (LKB1) mRNA and protein expression, as well as the phosphorylation of AMP-activated protein kinase (AMPK), both of which are known to inhibit mTOR. These data indicate that NSCLC cell proliferation induced by FN is mediated by Akt/mTOR/p70S6K pathway activation and LKB1/AMPK signaling inhibition (68).

2.1.4 Laminin

Laminins (Lns) are heterotrimeric extracellular glycoproteins found in all BMs. So far, more than 17 Ln isoforms have been identified with a cross-shaped and specific arrangement of α, β, and γ subunits (69). Ln-332 and Ln5 consist of heterogeneous α3, β3, and γ2 chains and serve as BMs' essential structural constituent. Ln5 plays a crucial role in cellular migration and tumor invasion (70, 71). NSCLC patients with positive Ln5 expression had a slightly lower survival rate than Ln5-negative expression counterparts. Besides, positive Ln5 expression combined with the loss of PTEN, positive active EGFR expression, or positive active Akt expression has a significantly different overall survival. According to Cox regression analysis, the co-expression of Ln5, PTEN, and p-Akt are the three most independent prognostic markers in NSCLC patients. The findings illustrate the intricate tumorigenesis relationship between key signaling pathway molecules and ECM proteins (71) (**Figure 3**). A Ln receptor, namely integrin α6β4, triggers carcinoma progression through cooperation with various GFRs to facilitate invasion and metastasis (72). Using a lung cancer tissue microarray and immunohistochemistry (IHC), Stewart et al. discovered that SqCC has a higher integrin β4 (*ITGB4*) expression than ADC, and these data were verified in external gene expression data sets. Overexpression of *ITGB4* is also linked to venous invasion and a lower overall patient survival rate. The most highly 50 altered genes related to ITGB4 identified in SqCC were Lns, *CD151*, collagens, *PI3K*, and *EGFR*-associated pathway genes, other recognized signaling partners using cBioPortal. Finally, they show that ITGB4 is overexpressed in NSCLC and is an unfavorable prognostic factor (72). Overall, these data suggest a potential correlation between Lns and EGFR in lung cancer prognosis; however, further studies are still required to profile expression patterns of different Ln types in NSCLC to underscore their clinical relevance.

2.1.5 Fibrinogen

Fibrinogen is a 350 kDa glycoprotein synthesized mainly by the liver epithelium (73). It comprises two similar sets of three polypeptide chains, including Aα, Bβ, and γ, linked by five symmetrical disulfide bridges (74). Many proteins and cytokines such as vascular endothelial growth factor (VEGF) and fibroblast growth factor-2 (FGF-2) bind to fibrinogen affecting its biological behavior (75, 76). Lungs produce fibrinogen by inflammatory stimuli (77). Fibrinogen changed into insoluble fibrin *via* activated thrombin considerably affects blood clotting, inflammatory response, wound healing, fibrinolysis and neoplasia. Increased fibrinogen activity considerably affects cancer cell growth, progression, and metastasis (78).

Accumulating evidence indicates a correlation between fibrinogen and EGFR in lung cancer (79–81). A study by Shang et al. discovered a novel serum protein, fibrinogen alpha chain isoform 2 (FGA2), in lung ADC patients with mutated EGFR using microarray data analysis of 41,472 antibodies coupled with mass spectrometry analysis (79). Further, plasma

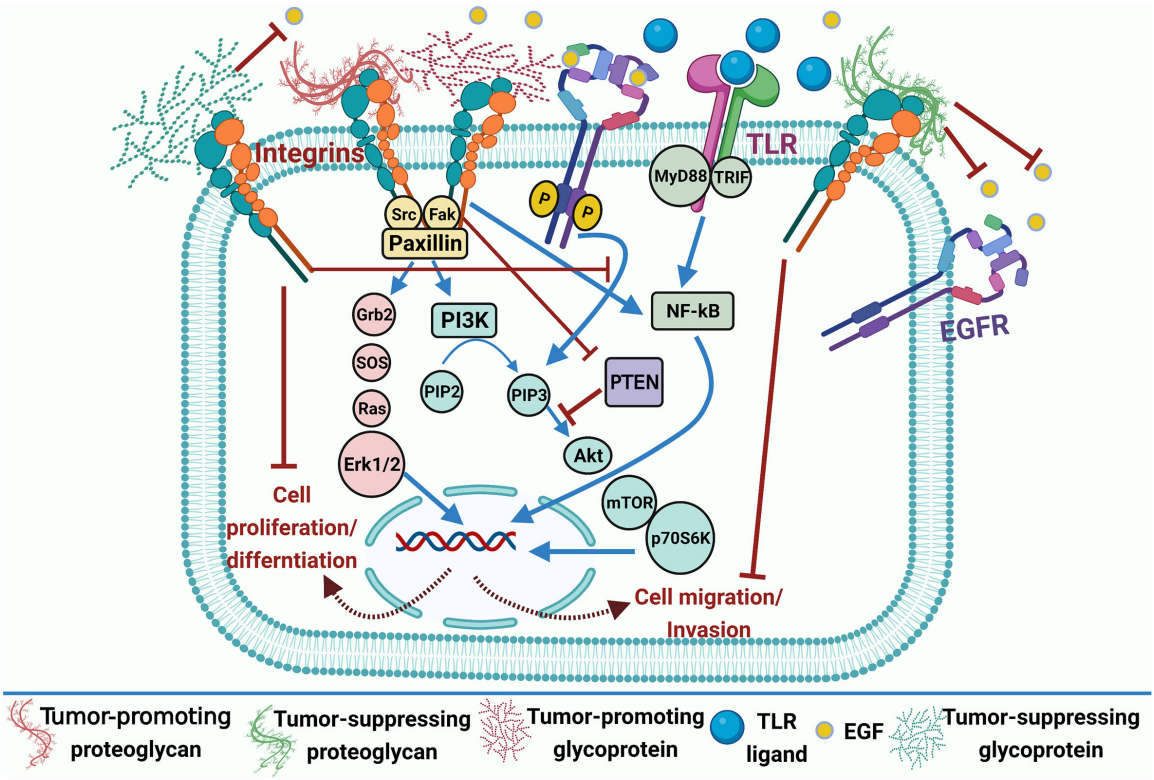

FIGURE 3 | Dual effect of ECM glycoproteins and proteoglycans in lung cancer. Tumor-promoting glycoproteins (e.g., laminin 5 and fibronectin); laminin expression enhances phospho-EGFR or phospho-Akt expression and loss of PTEN; fibronectin activates toll-like receptors (TLRs) to promote NF-κB activation as well as EGFR-dependent Akt/mTOR/p70S6K signaling pathway; and thus, it stimulates cell proliferation and differentiation in lung cancer. Tumor-promoting proteoglycans (e.g., GPC5) prompted cell migration and metastasis. Tumor-suppressing glycoproteins (e.g., fibulins1,3, and 5) compete with EGF and inhibit EGFR activation. Tumor-suppressing proteoglycans (e.g., GPC3 and SDC-1) can regulate EGF and many intracellular signaling pathways inhibiting cell invasion and migration. Blue arrows for stimulation; dashed red arrows for cellular effect; and red "T" sign for inhibition.

FGA2 levels were remarkably downregulated in *EGFR*-mutated patients relative to those with the wild-type *EGFR* (81). In the same study, hyperfibrinogenemia was linked to distant metastasis and lymphatic tissue metastasis. A multivariate model based on fibrinogen and smoking history was also used to predict *EGFR* mutation status in NSCLC patients (81). Furthermore, Fibrinogen-like protein 1 (FGL1) is significantly overexpressed in the gefitinib-resistant NSCLC cell line PC9/GR more than in the gefitinib-sensitive NSCLC cell line PC9 with an *EGFR* mutation. However, FGL1 knockdown reduces cell viability, decreases gefitinib IC50, and increases apoptosis in PC9/GR and PC9 cells after gefitinib therapy. FGL1 knockdown in PC9/GR tumor cells increases gefitinib's inhibitory and apoptosis-inducing effects in a mouse xenograft model. Gefitinib's possible mechanism for inducing apoptosis in PC9/GR cells includes suppressing FGL1 and activating Poly (ADP-Ribose) Polymerase 1 (PARP1) and caspase 3 pathways. By regulating the PARP1/caspase 3 pathway, FGL1 promotes acquired resistance to gefitinib in the PC9/GR NSCLC cell line. As a result, FGL1 may be a possible therapeutic option for NSCLC patients who have developed resistance to gefitinib (80).

2.1.6 Other ECM Glycoproteins

Tenascin-C (TN-C) is a glycoprotein composed of 4 distinct domains interacting with matrix constituents, cell surface proteins, soluble factors, and pathogenic components. TN-C affects pulmonic blood vessel invasions by decreasing apoptosis and promoting cancer cell plasticity, thus, increasing lung metastasis (82). TN-C also binds to more than 25 different molecules, including EGF-L repeats (a low-affinity ligand for the EGFR, MAPK, and phospholipase-C gamma (PLC)-γ signaling). Besides, TN-C binds to FNIII, aggrecan, integrins, and perlecan, along with growth factors such as FGF, platelet-derived growth factor (PDGF), and TGF-β families (83). Again, receptor-type tyrosine-protein phosphatase zeta (PTPRζ1), fibrinogen-like globe (FBG) that can bind to integrins, and TLR4 are TN-C-related molecules (83). These diverse interactions render TN-C a significant driver for many processes such as cell attachment, cell migration, cell spreading, cell survival, focal adhesion, neurite outgrowth, protease, and matrix assembly, and pro-inflammatory cytokine synthesis (83). However, a correlation between TN-C and EGFR has not yet been elucidated in NSCLC.

Periostin (Postn, PN, or osteoblast-specific factor OSF-2) is a vital ECM protein known for its complex role in tumorigenesis (84). It can directly bind to many ECM proteins, including TN-C, FN, collagen, and Postn itself (85). Also, it acts as a ligand for numerous integrins such as $\alpha_v\beta_3$, $\alpha_v\beta_5$, and $\alpha_6\beta_4$ to participate in cell adhesion, survival, and migration (85, 86). Postn affects tumor progression by regulating cellular survival, angiogenesis, invasion, and metastasis in epithelial tumors (85). Periostin is overexpressed and enhances metastatic growth in colon cancer by inhibiting stress-induced apoptosis in cancer cells and increasing endothelial cell survival to boost angiogenesis. Although there is no direct association between Postn and EGFR in lung cancer, Postn can regulate EGFR interacting partners or its downstream signaling. Periostin increases cellular survival at the molecular level by activating the Akt/PKB signaling pathway through $\alpha_v\beta_3$ integrins (87). In lung cancer, high Postn expression is positively associated with the EMT markers Snail and Twist and lung cancer stage, according to IHC results. Further, recombinant Postn causes EMT in lung cancer cells through the p38/ERK pathway, and that pretreatment with chemical inhibitors prevents Postn-induced EMT (88). Moreover, the increased Postn expression in the NSCLC A549 cells is one form of cellular response to chemical-mimic hypoxia stress, and this effect can be controlled by hypoxia-inducible growth factors like TGF-α and bFGF, which trigger the RTK/PI3-K pathway leading to upregulation of Postn, and in turn, facilitating the survival of A549 cells in a hypoxic microenvironment *via* the Akt/PKB pathway (89). Collectively, these data indicate that Postn may serve as a therapeutic target in NSCLC.

Vitronectin (VTN) is a multifunctional glycoprotein found in blood and ECM. It binds collagen, glycosaminoglycans, the urokinase-receptor, and plasminogen and stabilizes plasminogen activation inhibitor-1 (PAI-1)'s inhibitory conformation. VTN can potentially control the ECM proteolytic degradation through its localization in the ECM and binding to PAI-1. VTN also binds to complement, heparin, and thrombin-antithrombin III complexes, suggesting an immune response role and clot formation control (90). VTN is mostly overexpressed in smaller and well-differentiated tumors (91). EGF promotes carcinoma cell metastasis by phosphorylating p130 CAS in an Src-dependent manner, activating Ras-related protein 1 (Rap1), a small GTPase implicated in integrin activation. Src activity induced by EGFR causes phosphorylation of the CAS substrate, required for Rap1 and αvβ5 activation (92). EGFR activation of Src initiates αvβ5-mediated migration in FG (express stably mutational active Y527F (SrcA) pancreatic carcinoma cells. EGF causes cell metastasis and αvβ5-mediated Rap1 activation. Rac1 and Rap1 activity are increased in FG cells plated on anti-β5, but not anti-β1, integrin antibodies after EGF therapy. Rap1 knockdown on vitronectin but not fibronectin prevents EGF-induced cell migration. In the chick CAM model, knocking down integrin β5 expression prevents EGF-induced pulmonary metastasis but not primary tumor weight (92).

Nidogen (NID1 and NID2) are present in the BM and help maintain its stability by connecting COLIV and Ln networks in the ECM (93, 94). The determination of NID2 methylation represents a biomarker for NSCLC diagnosis (95). The lung metastasis of NID1– or 2–deficient mice were studied after being intravenously injected with B16 murine melanoma cells. The authors demonstrated that the depletion of NID2, but not NID1, facilitates melanoma cell lung metastasis. According to histological and ultrastructural examination, the morphology and ultrastructure of BMs, including vessel BMs, are not different in NID1– and 2–deficient lungs. Furthermore, there is no difference in the deposition and distribution of the main BM components between the two mouse strains. These findings indicate that the absence of NID2 can cause subtle changes in endothelial BMs in the lung, allowing tumor cells to move through these BMs more quickly, resulting in a higher risk of metastasis and larger tumors (96). Further, NID2 inhibits liver metastasis in a significant way. NID2 suppresses the EGFR/Akt and integrin/focal adhesion kinase (FAK)/PLC metastasis-related pathways; these data shed light on NID2's critical tumor metastasis-suppression functions in cancer (97). The roles of NID1 and NID2 in NSCLC have not yet been fully characterized.

2.2 Proteoglycans

Proteoglycans, key molecular effectors of cell surface and pericellular microenvironments, perform multiple roles in health and diseases because of their polyhedric structure and ability to interact with ligands and receptors that control neoplastic growth and neovascularization (98, 99). Some proteoglycans, like perlecan, have pro- and anti-angiogenic properties, while others, like syndecans and glypicans, can directly influence cancer growth by modulating key signaling pathways. Several groups of enzymes in the tumor microenvironment further regulate the bioactivity of these proteoglycans: (i) various proteinases, which cleave the protein core of pericellular proteoglycans, (ii) endosulfatases and heparanases which change the structure and bioactivity of various heparan sulfate proteoglycans and their bound growth factors, and (iii) sheddases, which cleave transmembrane or cell-associated syndecans and glypicans. On the other hand, small leucine-rich proteoglycans like lumican and decorin serve as tumor suppressors by physically antagonizing RTK such as EGFR and c-Met (receptor for HGF), evoking antisurvival and proapoptotic pathways (98).

Proteoglycans, including serglycin (100), perlecan (101), versican (102), aggrecans (103), decorin (104), lumican (105), syndecans (106), testicans (107), endocan (108), and glypicans (109) are involved in EGFR signaling pathways in lung cancer (108). For example, endocan is known to be a RTK ligand enhancer in tumorigenesis. Higher endocan levels are observed in lung tumors relative to non-neoplastic tissues, and these levels are associated with a poor prognosis in NSCLC patients with mutant EGFR. Circulating endocan levels are also significantly higher in patients with mutant EGFR than those with wild-type EGFR. Endocan enhances tumor growth driven by mutated EGFR by facilitating EGFR signaling through direct binding and enhancing the EGF-EGFR interaction. Through the Janus kinase (JAK)/STAT3 and ERK/ELK cascades, activated EGFR upregulates endocan expression, creating a positive regulatory

loop of endocan-EGFR signaling. These results point to a novel relationship between EGFR and endocan and new strategies to target the endocan-EGFR regulatory axis in NSCLC patients with TKI-resistant (108). Another example is decorin, small leucine-rich proteoglycans (SLRP) that control cell growth and migration in several tumor cell lines (104). Up-regulation of decorin inhibits proliferation, arrests the cell cycle at G1, and reduces invasive activity in the NSCLC A549 cells. Further, upregulating decorin substantially reduces EGFR phosphorylation, cyclin D1, TGF-1 expression and increases *p53* and *P21* expression; whereas, decorin downregulation could reverse the effects (104). In the following section, we discuss the available data for syndecans and glypicans as examples for proteoglycans.

2.2.1 Glypicans

Glypicans (GPCs), a heparan sulfate proteoglycan (HSPG) family, consist of core proteins (60- to 70-kDa), heparan sulfate (HS) chains, and a glycosylphosphatidylinositol linkage (110). There are six known GPCs (GPC1-GPC6) in humans. GPCs participate in cell growth by regulating Wnt (111), development by modifying morphogen gradient formation (112), and other multiple signaling pathways. GPCs are abnormally expressed in multiple types of cancer and are crucial for cancer cell growth and progression. The expression of GPC5 is regulated to control cell growth and differentiation throughout mammalian development (113). Also, genetic variations of *GPC5* may share in the increased risk of never-smokers (114). *GPC5* mRNA and protein levels are overexpressed in A549 and H3255 cells. Using shRNA-mediated knockdown or overexpression of *GPC5*, the migration rates of A549 and H3255 cells transfected with pRNAT-shRNA-*GPC5* are lower than controls employing scratch and transwell assays. Using immunohistochemical staining, the high GPC5 expression level in NSCLC is linked to respiratory symptoms of lung cancer, regional lymph node metastasis, poor differentiation, vascular invasion, and a higher TNM stage. According to the Kaplan-Meier analysis, NSCLC patients with high levels of GPC5 expression have a shorter overall survival time relative to those with low levels of GPC5 expression (115). Conflicting data indicated that GPC5 is downregulated and linked to a poor prognosis in lung ADC tissues. Further, the loss of GPC5 expression is controlled by its hypermethylation, according to de-methylation experiments. GPC5 overexpression inhibits lung cancer cell proliferation, migration, and invasion *in vitro* and slows tumor growth *in vivo*, whereas GPC5 knockdown reverses these effects. Moreover, *via* binding Wnt3a on the cell surface, GPC5 inhibits Wnt/β-catenin signaling, thereby mediating tumor suppressor action (113). Therefore, targeting particular GPCs in the tumor microenvironment that acts as ligands for inducing oncogenic pathways represents an effective cancer therapy strategy (100). Although the functions of GPCs have been assigned in different tumors, including lung (116), colon (117), and breast (118) cancers, esophageal squamous cell (119) carcinoma, and pancreatic ductal adenocarcinoma (120), their interaction with EGFR in NSCLC remains yet to be explored.

2.2.2 Syndecans

The syndecan (SDC) family is a transmembrane protein that possesses HS chains on their extracellular domains (121) and consists of four members (SDC1-SDC4). SDC-1 is frequently misexpressed in cancer and associated with invasion, metastasis, angiogenesis, and dedifferentiation (122–128). SDC-1 acts as a coreceptor for a wide range of growth factors (129), including bFGF and HB-EGF (130). A recent study reported that lung cancer has noticeable SDC-1, yet its expression does not associate with lung cancer patients' survival rate (121). However, a study by Shah et al. revealed that the expression of either NSCLC subtype classifiers EGFR and SDC-1 determined by tissue microarray is correlated with a 30% reduction in the risk of death. Loss of expression of these histologic classifiers is linked to aggressiveness in lung tumors and a poor prognosis (106). Besides, Zhu and colleagues interestingly reported that NSCLC patients with both a SDC4-ROS1 rearrangement and an activating EGFR mutation might acquire resistance to EGFR-TKIs. Although the coexistence of two driver gene mutations in NSCLC is uncommon, triggering alterations of *EGFR, ROS1, ALK*, and *KRAS* have recently been recorded (131, 132).

2.3 Non-proteoglycan Polysaccharides

2.3.1 Hyaluronan (HA)

HA is a plentiful constitute of the pericellular matrix that plays a vital role in regulating tissue homeostasis and cancer progression through its interaction with the cell surface receptor CD44 (133). HA synthesis is controlled by growth factors (e.g., EGF) and cytokines such as IL-1β (133). Three hyaluronan synthases (HAS) isoforms, including HAS1, HAS2, and HAS3, are known. CD44-HA interaction can modulate a variety of intracellular signaling by forming coreceptor complexes with many RTKs (e.g., EGFR) (134) that induce oncogenic pathways involved in cancer cell invasion, migration, and metastasis in the human MCF7 and TamR breast cancer cells (135). HA and CD44 are overexpressed in NHLFs/LCAFs (normal human lung fibroblasts vs. lung cancer-associated fibroblasts), followed by NSCLC cells. In NSCLC cells, exogenous HA somehow rescues the fault in cell proliferation and survival. Further, simultaneous silencing of *HAS2* and *HAS3* or *CD44* suppresses the EGFR/AKT/ERK signaling pathway, cell proliferation, and survival (136, 137). Of note, dual targeting CD44/EGFR by HA-based nanoparticles along with systemic administration of plasmid DNA expressing wild-type (wt-) p53 and microRNA-125b (miR-125b) in a genetically engineered mouse model of lung cancer led to an increase of wild-type *p53* and *miR-125b* gene up to 20-fold associated with elevated caspase-3 and *APAF-1* expression-induced apoptosis; thus it may represent an effective gene therapy for NSCLC (138).

Interestingly, treatment with EGF and IL-1β, either alone or combined with TGF-β in ADC, can stimulate HA production in A549 cell line, where treatment with TGF-β/IL-1β changed cell morphology, induced EMT with altered vimentin and E-cadherin gene expression. Also, *HAS3* overexpression induces HA synthesis, MMP9 expression, EMT phenotype, and MMP2 activities and increases invasion of epithelial ADC cell line H358

(133). Induction of HA in H358 cells and adding exogenous HA in A549 cells significantly improved resistance to EGFR inhibitor Iressa. These results propose that increased HA production can promote EMT and Iressa resistance in NSCLC (133). Thus, regulating HA expression in NSCLC can be a new therapeutic strategy (133). Again, HA is implicated in EMT through EGF or TGF-β1 signaling in lung cancer cell line A549, where TGF-β1 upregulates HAS1, HAS2, and HAS3 expressions and augments CD44 expression interacts with EGFR, leading to the activation of the downstream signaling AKT and ERK pathways (139). On the contrary, pretreatment with HAS inhibitors such as 4-methylumbelliferone (4-MU) can suppress TGF-β1's impact on the expression of CD44 and EGFR and inhibit the CD44-EGFR interaction. Collectively, these data indicate that HA/CD44 interaction mediated by TGF-β1 transactivates EGFR signaling, resulting in EMT induction in NSCLC cells (139).

2.4 Fibrous ECM Proteins

2.4.1 Collagens

Collagens (COLs) are the major ECM proteins (up to 30% of the total protein mass) in the human body. They are arranged in a relaxed meshwork and possess elasticity to extreme tensile strength owing to their surrounding proteins like elastin and glycoproteins (140). The individual structure of COLs can also create an intricate network that enables them to interact with each other and the surroundings (141). There are 28 known COL types and divided into specific subgroups according to their supramolecular assemblies, including a) fibrillar-forming COLs: the IM significant components such as COL type I, II, III, V, XI, XXVI, XXVII; b) the network-forming COLs: the main components of basement membrane such as type IV, VIII, X, and XVIII COLs (142). Of note, COLI, COLIII, and COLV are predominantly fibroblasts-derived COLs, while COLIV is mainly expressed by epithelial and endothelial cells (143); c) fibril-associated COLs with interrupted triple helices (FACITs) (e.g., IX, XII, XIV, XVI, XIX, XX, XXI, XXII, XXIV); and d) MACITs (membrane-anchored collagens with interrupted triple helices) such as type XIII, XVII, XXIII, and XXV COLs (144–146). COLIV is upregulated in NSCLC stroma, promoting the *in vitro* impairment of cell apoptosis and multidrug resistance. For example, NSCLC cells expressing COLIV are resistant to cis-platinum (DDP), which is mechanistically attributed to the PI3K pathway (147).

Notably, many studies addressed the significant effect of CAFs in tumorigenesis (148, 149). CAFs are the key players in COL dysregulation and turnover, resulting in desmoplasia (tumor fibrosis), where COLs deposit excessively in the tumor surroundings, crosslink, and linearize, thus increasing tissue stiffness (150). This influences the behavior of the nearby tumor cells and controls cell differentiation, proliferation, migration, gene expression, invasion, metastasis, and survival; thereby, directly affecting the cancer hallmarks (151). Tumor tissue with considerable fibroblast-derived COLs is correlated with poor outcomes (152–154). A study by Li et al. reported that the regulation of autocrine COLI expression for sustaining lung cancer cell growth in 3D cultures with fibroblasts provides a new insight for lung cancer targeted therapy (155). CAFs and other molecules can regulate COLs' expression in cancer cells, such as transcription factors, mutated genes, receptors, and signaling pathways; these molecules can also affect tumor cell behavior by integrins, RTKs (e.g., EGFR), and discoidin domain receptors (156).

In healthy tissues, the biosynthesis of COLs is highly controlled by a great counterbalance of many enzymes, including MMPs and their inhibitors and lysyl oxidases (LOX) (157, 158). In lung tumors, the stroma comprises a stiffer matrix than normal lung tissues due to more collagen modifications (159) mediated by lysyl hydroxylase-2 or procollagen-lysine, 2-oxoglutarate 5-dioxygenase 2 (PLOD2) enzyme enhancing cell invasion and metastasis (160). Fibrotic collagen is primarily modified by PLOD2. PLOD2 was elevated in NSCLC specimens and was linked to a poor prognosis in NSCLC patients. PLOD2 directly enhances NSCLC metastasis by promoting migration and indirectly by inducing COL reorganization, evident by gain- and loss-of-function experiments and an orthotopic implantation metastasis model. In addition, PLOD2 regulation is achieved by PI3K/AKT-FOXA1 axis. The transcription factor FOXA1 directly binds to the PLOD2 promoter for the transcription of PLOD2. These findings indicated that the NSCLC metastasis mechanism could be regulated by EGFR-PI3K/AKT-FOXA1-PLOD2 pathway and PLOD2 can be a therapeutic target for NSCLC treatment (161).

3 INTEGRINS -ECM-INTERACTING CELL MEMBRANE RECEPTORS

In tumorigenesis, a complex relationship is established between ECM proteins and key signaling pathway molecules (71). Cell–ECM interactions are implicated in the intracellular signals that control gene expression, cell cycle progression, survival, movement, and physical support (162). Notably, these processes are governed by cell surface receptors that bind to ECM proteins called integrins. They are α,β heterodimeric transmembrane proteins implicated in many physiological and pathological processes such as adhesion to ECM, proliferation, survival, differentiation, and migration (163). Some integrins bind to the RGD motif on the ECM proteins, and the specificity of integrin binding to various ECM proteins is determined, partially through other amino acids neighboring the RGD sequence (164). Integrin cytoplasmic tails do not possess a kinase activity but activate specific intracellular non-receptor tyrosine kinases, such as FAK; thus, they recruit the Src kinase (165). Src phosphorylates several FAK-associated proteins, including tensin, paxillin, and the adaptor $p130^{Cas}$ (Crk-Associated Substrate). To some extent, FAK activation results in the recruitment of other SH2-containing proteins, including PLC-γ, PI3K, and the adapter proteins Grb2 and Grb7, mediate ERK activation (165). The FAK/Src complex modulates small GTPase activity, leading to actin cytoskeleton remodeling required for cell adhesion and migration (166).

Upon integrins-ECM binding, numerous signaling molecules are activated, including cytoplasmic kinases, small GTPases, adapter proteins, and growth factor-RTKs (167). The ECM-

and EGFR-activated signaling pathways have a high degree of functional interdependence. When EGFR interacts with ECM proteins, autophosphorylation increases in various cell types, including fibroblasts, smooth muscle, and kidney epithelial cells (168, 169)., This type of overlapping signaling is thought to help or improve a variety of ECM and RTK-controlled cell functions, such as proliferation and survival (170). ECM interaction has been discovered to be essential for many EGF-mediated biological responses besides modulating EGFR signaling. EGF, for example, controls integrin-mediated cell migration, an actin-based mechanism that relies entirely on ECM component co-presentation (171).

Numerous studies have suggested that integrin-RTK cooperation exists and plays an important role in cancer progression by controlling proliferation, invasion, and survival (172). Various mechanisms could control the crosstalk between integrins and RTKs, regardless of α or β subunit catalytic activity. The integrins' ability to induce EGFR activation led to the regulation of Erk and Akt activation, which permitted adhesion-dependent induction of p21, cyclin D1 and Rb phosphorylation, and cdk4 activation in epithelial cells in the absence of exogenous growth factors. Epithelial cell adhesion to the ECM fails to efficiently induce p27 degradation, cdk2 activity, or cyclin A and Myc synthesis, and as a result, cells do not progress into the S phase. Treatment of ECM-adherent cells with EGF (to induce EMT), or overexpression of EGFR or Myc, resulted in restoring late-G1 cell cycle events and progression into the S phase. These findings suggest that integrin receptor-mediated partial activation of EGFR is significant in mediating events triggered by epithelial cell attachment to ECM (173). There are three major categories of integrin/RTK interactions (174) (**Figure 4**): (1) Integrins can physically bind to RTKs; (2) integrins clustering upon ECM binding can enhance signaling pathways triggered after ligand-dependent RTK activation, and (3) integrins and RTKs regulate their surface expression in a reciprocal manner (174). EGFR can interact with many integrins in different cancers, such as α6β4 (175), β1 (170), and αvβ3 (176), probably by forming a multimeric complex that also includes Src and the adaptor protein $p130^{Cas}$ (176). This type of interaction is ligand-independent activation of the EGFR, leading to signaling involved in cell survival and proliferation in response to ECM (170) (**Figure 4**).

Emerging data indicate integrins' importance as essential EGFR signaling regulators in NSCLC (72, 177–179). For example, β1 integrin silencing in human NSCLC A549 cells showed a defective activation of the EGFR signaling cascade, resulting in enhanced sensitivity to Gefitinib and cisplatin, reduced migration, and invasive behavior, and decreased *in vitro* proliferation and *in vivo* tumor growth. This silencing also increases the amount of cell surface EGFR, implying that β1 integrin is required for efficient constitutive EGFR turnover at the cell membrane. Despite having no effect on the EGF internalization rate and recycling in silenced cells, EGFR signaling is recovered only by the Rab-coupling protein (RCP) expression, suggesting that β1 integrin maintains the endocytic machinery required for EGFR signaling (177). Also, Integrin β4 (ITGB4) expression is overexpressed in SCC compared with adenocarcinoma and associated with the presence of venous invasion, low overall patient survival. Using cBioPortal, a network map demonstrates the 50 most highly altered genes neighboring ITGB4 in SCC, which included genes in the EGFR and PI3K pathways and other known signaling partners as well as laminins, collagens, and CD151 (72). Moreover, CD151 drives cancer progression depending on integrin α3β1 through EGFR signaling in NSCLC. In detail, a high CD151 mRNA expression level is detected in NSCLC tissues and cell lines, and its high

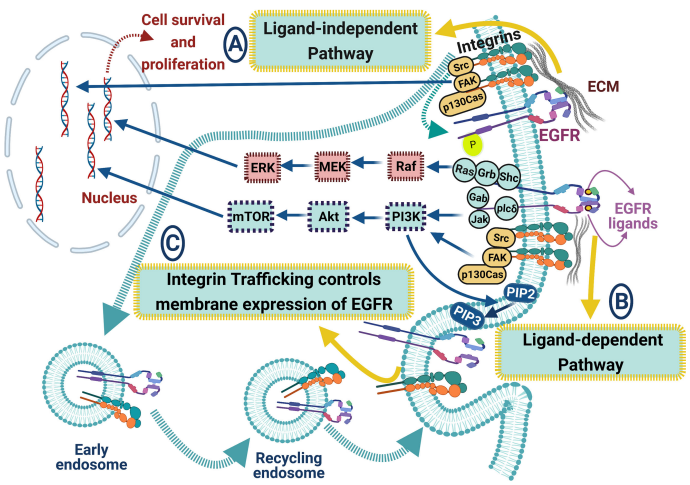

FIGURE 4 | ECM proteins and integrins regulate EGFR signaling pathways in lung cancer. The crosstalk between EGFR and integrins includes many signaling pathways: **(A)** ligand-independent pathway, where integrins can biochemically bind to EGFR leading to its activation. EGFR can interact with integrins via forming a multimeric complex (Src, FAK, and the adaptor protein p130Cas), leading to cell survival and proliferation, **(B)** ligand-dependent pathway, where integrin clustering enhances EGFR signaling cascades upon EGFR ligand binding, resulting in enhancing Akt, ERK, and Ras signaling pathways, and **(C)** integrin trafficking controls the membrane expression of EGFR. Blue arrows for stimulation; dashed red arrows for cellular effect, and red "T" sign for inhibition.

expression was substantially related to the poor prognosis of NSCLC patients. Also, CD151 knockdown *in vitro* suppressed tumor proliferation, migration, and invasion. Further, overexpression of CD151 enhanced NSCLC growth in a mice model. NSCLC cells overexpressing CD151 exhibit migratory and invasive phenotype via interacting with integrins and regulating the downstream signaling pathways of EGFR/ErbB2 (179). Interestingly, the inhibition of EGFR in NSCLC cell lines reduces tyrosine phosphorylation of neural precursor cell expressed, developmentally down-regulated 9 (NEDD9), an integrin signaling adaptor protein that consists of multiple domains serving as substrate for various tyrosine kinases. Overexpression of constitutively active EGFR, in the absence of integrin stimulation, leads to tyrosine phosphorylation of NEDD9, which plays a pivotal role in the *in vitro* cell migration and invasion of NSCLC cells. Moreover, NEDD9 overexpression promoted lung metastasis of an NSCLC cell line in NOD/Shi-scid, IL-2Rγ(null) mice (NOG) mice (178). Overall, these data show that integrins-dependent EGFR interactions might represent a prognostic marker and potential therapeutic targets in NSCLC.

4 KEY ECM REMODELING ENZYMES

Matrix degradation is a finely regulated process that occurs simultaneously with the formation of new ECM molecules. Tissue integrity is achieved through the actions of matrix-degrading enzymes such as matrix metalloproteinases (MMPs) and their endogenous inhibitors (TIMPs), adamalysin group (ADAMs and ADAMTS), cathepsins, plasminogen activation system components, and glycolytic enzymes such as heparanase (HPSE) and hyaluronidases (HYALs) that cleave heparan sulfate (HS)/heparin chains on hyaluronan (HA) and proteoglycans (PGs) (180, 181). Elastase, dipeptidyl peptidase IV (DPPIV), and tissue kallikrein are ECM serine proteases that play distinct functions in matrix proteolysis and have been linked to cancer progression (182–184). MMPs are the major catabolic matrix endopeptidases linked to a number of normal processes such as wound healing, immunological response, differentiation, tissue homeostasis, and diseases such as osteoarthritis neuroinflammation, atherosclerosis, and cancer (185). The human genome contains 24 MMP members, which are classified into secreted and membrane-bound MMPs. MMPs are categorized as matrilysins, gelatinases, furin-activated collagenases, stromelysins, and other MMPs based on substrate specificity (186, 187). MMPs are mediators of the tumor microenvironment alternations during cancer growth because they enhance EMT, cancer cell signaling, migration, invasion, autophagy, and angiogenesis, which aid tumor progression and metastasis (188). We focus on the functional interplay between MMPs and EGFR in NSCLC in the next sections.

4.1 Metalloproteinases (MMPs)

MMPs are a group of 24 proteinases, also known as matrix MMPs, matrixins, and zinc-dependent endopeptidases (189). Transcription of most matrixins is regulated by growth factors, hormones, cytokines, and cellular transformation. MMPs' proteolytic activities are tightly controlled during their activation from their precursors and inhibition by the endogenous inhibitors TIMPs and a-macroglobulins (190). Aberrant expression of MMPs is associated with many diseases, including lung cancer (191). MMPs perform their proteolytic activity autonomously in the alveolar space for any changes in the cleaved protein properties (192). Cancer cells secrete many MMPs that remodel and degrade the BM in lung cancer tissue, creating a dynamic flow of pro- and antitumor signals (190, 191). The regulation of MMPs expression occurs by triggering inflammatory molecules and hormones and intercellular and matrix interactions (190). MMPs are present in low levels in normal adult tissues, yet the MMPs expression is upregulated during wound healing, tissue repair, or remodeling under pathogenic conditions (192).

When the ECM collagen becomes abundant, large amounts of MMPs are secreted in tumor tissues, and BM remodeling occurs (193, 194), leading to complex chaos of pro-and antitumor signals originating from BM degradation products and enhancing the invasive phenotype of malignant cells (195). In both mouse and human NSCLC, MMP14 is significantly upregulated in intratumoral myeloid compartments and tumor epithelial cells. In an orthotopic ($K\text{-}Ras^{G12D/+}p53^{-/-}$) mouse model of lung cancer, overexpression of a soluble dominant-negative MMP14 (DN-MMP14) or pharmacological inhibition of MMP14 blocks the invasion of lung cancer cells in collagen I matrix *in vitro* and reduces tumor incidence. MMP14 activity also triggers the proteolytic processing and activation of Heparin-Binding EGF-like growth factor (HB-EGF), which stimulates the EGFR signaling pathway and increases tumor proliferation and growth. These data pinpoint the potential for developing therapeutic strategies that target MMP14 in NSCLC, specifically targeting the MMP14-HB-EGF axis (191). Increased expression of MMP-9 *in vitro* and *in vivo* has been linked to tumor progression. Cox et al. linked the EGFR expression with MMP-9 upregulation in tumor cells *in vitro* in NSCLC patients. MMP-9 expression strongly correlated with EGFR expression and EGFR membranous expression, but not with cytoplasmic EGFR expression. MMP-9 and EGFR co-expression is associated with a poorer prognosis in NSCLC patients. Also, MMP-9 and EGFR are expressed in a large proportion of NSCLC tumors. The presence of these markers together indicates a poor prognosis. These findings suggest that the EGFR signaling pathway, *via* specific up-regulation of MMP-9, can play a key role in NSCLC invasion (196).

5 EFFECT OF ECM COMPONENTS' EXPRESSION AND INTERACTIONS ON SENSITIVITY TO TKI THERAPY

The biological features of the tumor microenvironment are affected by cancer cells, non-cancerous cells, and ECM (197). The interactions between different cell types within the tumor microenvironment play a key role in developing resistance to the

anticancer drugs (198). The most abundant matrix protein in the cancer stroma, COLI, promotes tumor progression by facilitating cancer cell growth, invasion, and metastasis (199, 200). Also, COLI supports anticancer drug resistance through the integrin signaling pathway (201). Besides, COLI induces EGFR-TKI resistance in EGFR-mutated cancer cells (202). Moreover, the results of Wang *et al.* reported that COLI drives EGFR-TKI resistance through integrin-β (23). Knockdown of integrin-β1 significantly suppresses the resistance driven by both COLI and de-cellularized ECM, indicating that COLI and integrin-β1 could mediate the resistance-driving function of ECM and might be useful interventional therapeutic strategies. Further, a collagen synthesis inhibitor, CHP (cis-4-Hydroxy-L-proline), efficiently inhibiting collagen production and synergizing with osimertinib, leads to growth suppression of GFP-labeled H1975 cells co-cultured with parental H1975 cells or fibroblasts (23). Interleukin-6 (IL-6) plays a vital role in developing interstitial fibroblastic proliferation induced by EGFR-TKI. In lung cancer, A549 cell lines treated with EGFR-TKIA reduce cell viability *via* increment of IL-6 mRNA and protein expression. IL-6 treatment increases α-actin and collagen expression, fibrosis markers, in lung fibroblast cells using a co-culture model. These findings indicate that IL-6 plays a role in EGFR-TKI-induced interstitial fibroblastic proliferation. Therefore, inhibiting IL-6 could be helpful to cancer patients receiving EGFR-TKI treatment to reduce the risk of side effects (203). Further, in EGFR mutated lung ADC patients, FG2A level was related to EGFR-TKI response, and FGA2 represented a predictor of targeted therapy for EGFR-mutated lung (79). Furthermore, integrin β1 promotes Src-Akt pathway activation and induces erlotinib resistance (201). COLI is dysregulated in the bone, and other solid tumors influence tumor cell behavior inducing EMT, including the lung (204) and breast (205). The sensitivity of EGFR-TKI in EGFR-mutated cancer cells cultured with COLI was investigated when COLI activated mTOR *via* Akt and ERK1/2-independent pathway in NSCLC, leading to EGFR-TKI resistance. Combining EGFR-TKI and mTOR inhibitors may be a viable option for combating such resistance (206). ECM components are internalized and used as nutrients by cells through several mechanisms. For example, the degradation of ECM proteins into peptides by MMPs and internalization of the degraded peptide fragments by cells. Another mechanism involves endocytosis of ECM macromolecules (207, 208). Rac1 inhibition reduces COLI uptake in mutated lung cancer cells (PC-9) and restores their sensitivity to EGFR-TKI. Rac1 is needed for micropinocytosis and reduction of COLI uptake. Thus, EGFR-TKI resistance can evolve in EGFR-mutated lung cancer cells *via* COLI uptake mediated by micropinocytosis (202).

EMT is characterized by the downregulation of epithelial markers, especially E-cadherin, and upregulation of mesenchymal markers such as vimentin, N-cadherin, and fibronectin (209). EMT is essential in the primary resistance of erlotinib in the EGFR-TKI responsive EGFR-mutant lung cancer cell line (210, 211). The expression of EGFR and EMT-related proteins are noticeably modulated in the peripheral leading edge of NSCLCs associated with poor prognosis (212). In NSCLC, EMT is a key player in controlling sensitivity or resistance to EGFR inhibition. NSCLC lines expressing E-cadherin showed higher sensitivity to EGFR inhibition *in vitro* and xenografted models, whereas NSCLC lines expressing vimentin and/or fibronectin showed resistance to the growth inhibitory effects of EGFR kinase inhibition (210).

FBLN1 isoforms regulate EGFR signaling and function in NSCLC. FBLN1 loss, using siRNA mediated knockdown of FBLN1C and FBLN1D, in NSCLC Calu-1 cells significantly increased EGF mediated EGFR activation, inhibited EGFR activation, promoted EGFR-dependent cell migration that inhibited upon Erlotinib treatment. Notably, FBLN1C and FBLN1D knockdown cells show a substantial increase in EGF-mediated EGFR activation, which promotes cell adhesion reduced by Erlotinib treatment. These data point out that FBLN1C/1D, as an ECM protein, can bind and regulate EGFR function and activation in NSCLC Calu-1 cells, highlighting tumor ECM role in affecting EGFR dependent lung cancers (6). In H1975/EGFR (L858R/T790M) cells, stable silencing of MUC1-C downregulates AKT signaling and inhibits colony formation, growth, and tumorigenicity. Similar results were found during MUC1-C silencing in gefitinib-resistant PC9GR cells that express EGFR (delE746_A750/T790M). Further, inhibition of MUC1-C suppresses the activation of EGFR (T790M), AKT, ERK, and MEK activation, colony formation, and tumorigenicity. Treatment of PC9GR and H1975 cells with GO-203 inhibits MUC1-C homodimerization, results in EGFR, AKT, and MEK/ERK signaling inhibition, as well as loss of survival. The combination of GO-203 and the irreversible EGFR inhibitor afatinib acts in synergism to inhibit the growth of NSCLC cells harboring activating EGFR (T790M) or EGFR (delE746-A750) mutants (213).

The activation of many signaling pathways imperils the clinical efficacy of EGFR-TKIs in EGFR-mutated NSCLC (214–218). The interactions between tumor cells and the extracellular environment are regulated by an integrin-linked kinase (ILK) to promote cell proliferation, migration, and EMT. Src homology 2 domain-containing phosphatase 2 (SHP2) is essential for MAPK pathway and RTK signaling activation. In baseline tumor specimens, highly expressed ILK mRNA is associated with poor prognostic factors for patient-free survival in the univariate and multivariate Cox regression models (214). Integrin β3 was significantly and consistently overexpressed in acquired osimertinib- or gefitinib-resistant lung cancer *in vitro* and *in vivo* and involved in the progression of lung ADC. Antagonizing integrin β3 improved the TKI sensitivity *in vitro* and *in vivo*, inhibiting anoikis resistance, proliferation, and EMT phenotype in lung cancer cells. Integrin β3 overexpression was also linked to the enhanced cancer stemness implicated in resistance development. Mechanistically, integrin β3 is induced by increased levels of TGFβ1 in acquired TKI-resistant lung cancer, which indicates the TGFβ1/integrin β3 axis as a potential target for combination therapy in EGFR-mutant lung cancer to overcome acquired resistance to EGFR TKIs (215). Furthermore, azurin, an anticancer therapeutic protein, controls integrin β1 levels, and its appropriate membrane localization suppressed the intracellular downstream signaling cascades of integrins and the invasiveness of NSCLC A549 cells. Further,

azurin combined with erlotinib and gefitinib enhances the sensitivity of NSCLC A549 cells to azurin. The stiffness of A549 lung cancer cells decreased with exposure to azurin and gefitinib using Young's module (E), suggesting that the changes in the membrane properties are the principal of the broad anticancer activity of azurin, and it may be relevant as an adjuvant to enhance the effects of other clinical anticancer agents (216). The expression levels of EGFR and integrin α2 and β1 subunits were significantly elevated in Ionizing radiation (IR) cells. Importantly, functional blockade of integrin α2β1 or treatment with EGFR-TKI, PD168393, resulted in a round morphology of cells and revoked their invasion in the collagen matrix. Further, higher activation of Erk1/2 and Akt signaling molecules in IR cells. Inhibition of Akt activation by treating with PI3K inhibitor LY294002 decreased IR cell invasion, yet MEK inhibitor U0126 did not inhibit Erk1/2 activation, which indicates integrin α2β1 and EGFR mutually promote higher invasiveness mediated by the PI3K/Akt signaling pathway in IR-survived lung cancer cells and might provide alternative targets along with radiotherapy (217). Recently, EGFR inhibitors' resistance was delayed by co-delivering EGFR and integrin αvβ3 inhibitors with nanoparticles in NSCLC. The enhanced expression of integrin αvβ3 is observed in tumor tissues of patients resistant to EGFR inhibitors. Further, integrin αvβ3-positive NSCLC cells unveiled significant EGFR inhibitor resistance, leading to activating Galectin-3/KRAS/RalB/TBK1/NF-κB signaling pathway. Interestingly, co-encapsulating erlotinib and cilengitide by MPEG-PLA (Erlo+Cilen/PP) nanoparticles enhanced the drug delivery system, leading to reduced systemic toxicity and superior anti-cancer effects (218).

6 CONCLUSION AND FUTURE PERSPECTIVES

ECM components, along with integrin and MMPs, regulate many cellular processes relevant to lung cancer progression, including cell proliferation, adhesion, and migration through their direct or indirect interactions with EGFR. ECM proteins associated with poor NSCLC prognosis *via* crosstalk with EGFR, including COLs, MMP-9, MUC1, MUC5AC, Ln 5, and GPC5. Many ECM proteins can be used as therapeutic targets, such as COLs, PLOD2, FBLN3, MUC5AC, FN, FAG2, FG, GPC3, and HA by modulating their interaction with EGFR. ECM proteins can be tumor-suppressing or -promoting depending on their signaling context with EGFR and many signaling molecules. Despite the emerging data revealing the role of ECM components or/and EGFR in NSCLC, many gaps still exist in EGFR-ECM interactions. The correlation between EGFR and many ECM proteins, including COLI, COLIV, FBLN1, FBLN3, FBLN5 MUC1, MUC5, MUC6, and Ln5 was revealed, yet EGFR interactions with other types of COLs, MUC and Ln, FG, TN, Postn, VTN, NID, TSP, and versican in NSCLC still need further investigations. A future better understanding of the interactions between ECM components and EGFR-TKI might provide new insights for developing new therapeutic strategies for NSCLC patients.

AUTHOR CONTRIBUTIONS

Conceptualization, SH and SI. Literature searches, SH and SI. Data curation, SI, SH, and AA. Investigation, SH, SI, and AA. Supervision, AA and SI. Figures design, SH. Writing—original draft, SH and SI. Writing—review and editing, SH, SI, and AA. This article is based primarily on the student MSc. thesis, SH. All authors have read and agreed to the published version of the manuscript.

ACKNOWLEDGMENTS

All the figures were created with BioRender.com.

REFERENCES

1. Ferlay J, Colombet M, Soerjomataram I, Mathers C, Parkin DM, Piñeros M, et al. Estimating the Global Cancer Incidence and Mortality in 2018: GLOBOCAN Sources and Methods. *Int J Cancer* (2019) 144:1941–53. doi: 10.1002/ijc.31937
2. Travis WD, Brambilla E, Nicholson AG, Yatabe Y, Austin JHM, Beasley MB, et al. The 2015 World Health Organization Classification of Lung Tumors: Impact of Genetic, Clinical and Radiologic Advances Since the 2004 Classification. *J Thorac Oncol* (2015) 10:1243–60. doi: 10.1097/JTO.0000000000000630
3. Molina JR, Yang P, Cassivi SD, Schild SE, Adjei AA. Non-Small Cell Lung Cancer: Epidemiology, Risk Factors, Treatment, and Survivorship. *Mayo Clin Proc* (2008) 83(5):584–94. doi: 10.4065/83.5.584
4. Fidler IJ. Critical Determinants of Metastasis. *Semin Cancer Biol* (2002) 12:89–96. doi: 10.1006/scbi.2001.0416
5. Minna JD, Roth JA, Gazdar AF. Focus on Lung Cancer. *Cancer Cell* (2002) 1:49–52. doi: 10.1016/S1535-6108(02)00027-2
6. Spivey KA, Banyard J, Solis LM, Wistuba II, Barletta JA, Gandhi L, et al. Collagen XXIII: A Potential Biomarker for the Detection of Primary and Recurrent Non-Small Cell Lung Cancer. *Cancer Epidemiol Biomarkers Prev* (2010) 19:1362–72. doi: 10.1158/1055-9965.EPI-09-1095
7. Vallath S, Hynds RE, Succony L, Janes SM, Giangreco A. Targeting EGFR Signalling in Chronic Lung Disease: Therapeutic Challenges and Opportunities. *Eur Respir J* (2014) 44:513–22. doi: 10.1183/09031936.00146413
8. Zhang H, Berezov A, Wang Q, Zhang G, Drebin J, Murali R, et al. ErbB Receptors: From Oncogenes to Targeted Cancer Therapies. *J Clin Invest* (2007) 117:2051–8. doi: 10.1172/JCI32278
9. Graus-Porta D, Beerli RR, Daly JM, Hynes NE. ErbB-2, the Preferred Heterodimerization Partner of All ErbB Receptors, is a Mediator of Lateral Signaling. *EMBO J* (1997) 16:1647–55. doi: 10.1093/emboj/16.7.1647
10. Lemmon MA. Ligand-Induced ErbB Receptor Dimerization. *Exp Cell Res* (2009) 315:638–48. doi: 10.1016/j.yexcr.2008.10.024
11. Yarden Y, Sliwkowski MX. Untangling the ErbB Signalling Network. *Nat Rev Mol Cell Biol* (2001) 2:127–37. doi: 10.1038/35052073
12. Jorissen RN, Walker F, Pouliot N, Garrett TPJ, Ward CW, Burgess AW. Epidermal Growth Factor Receptor: Mechanisms of Activation and Signalling. *Exp Cell Res* (2003) 284:31–53. doi: 10.1016/S0014-4827(02)00098-8
13. Bethune G, Bethune D, Ridgway N, Xu Z. Epidermal Growth Factor Receptor (EGFR) in Lung Cancer: An Overview and Update. *J Thorac Dis* (2010) 2(1):48–51.
14. Burgel PR, Nadel JA. Epidermal Growth Factor Receptor-Mediated Innate Immune Responses and Their Roles in Airway Diseases. *Eur Respir J* (2008) 32(1):1068–81. doi: 10.1183/09031936.00172007

15. Lynch TJ, Bell DW, Sordella R, Gurubhagavatula S, Okimoto RA, Brannigan BW, et al. Activating Mutations in the Epidermal Growth Factor Receptor Underlying Responsiveness of Non–Small-Cell Lung Cancer to Gefitinib. *N Engl J Med* (2004) 350:2129–39. doi: 10.1056/nejmoa040938
16. Yue B. Biology of the Extracellular Matrix: An Overview. *J Glaucoma* (2014) 23:S20–3. doi: 10.1097/IJG.0000000000000108
17. Järveläinen H, Sainio A, Koulu M, Wight TN, Penttinen R. Extracellular Matrix Molecules: Potential Targets in Pharmacotherapy. *Pharmacol Rev* (2009) 61:198–223. doi: 10.1124/pr.109.001289
18. Theocharis AD, Skandalis SS, Gialeli C, Karamanos NK. Extracellular Matrix Structure. *Adv Drug Deliv Rev* (2016) 97:4–27. doi: 10.1016/j.addr.2015.11.001
19. Lv H, Liu R, Fu J, Yang Q, Shi J, Chen P, et al. Epithelial Cell-Derived Periostin Functions as a Tumor Suppressor in Gastric Cancer Through Stabilizing P53 and E-Cadherin Proteins *via* the Rb/E2F1/p14ARF/Mdm2 Signaling Pathway. *Cell Cycle* (2014) 13:2962–74. doi: 10.4161/15384101.2014.947203
20. Wong GS, Rustgi AK. Matricellular Proteins: Priming the Tumour Microenvironment for Cancer Development and Metastasis. *Br J Cancer* (2013) 108:755–61. doi: 10.1038/bjc.2012.592
21. Mueller MM, Fusenig NE. Friends or Foes - Bipolar Effects of the Tumour Stroma in Cancer. *Nat Rev Cancer* (2004) 4:839–49. doi: 10.1038/nrc1477
22. Hassanein SS, Ibrahim SA, Abdel-Mawgood AL. Cell Behavior of Non-Small Cell Lung Cancer Is at EGFR and MicroRNAs Hands. *Int J Mol Sci* (2021) 22 (22):12496. doi: 10.3390/IJMS222212496
23. Wang Y, Zhang T, Guo L, Ren T, Yang Y. Stromal Extracellular Matrix is a Microenvironmental Cue Promoting Resistance to EGFR Tyrosine Kinase Inhibitors in Lung Cancer Cells. *Int J Biochem Cell Biol* (2019) 106:96–106. doi: 10.1016/j.biocel.2018.11.001
24. De Vega S, Iwamoto T, Yamada Y. Fibulins: Multiple Roles in Matrix Structures and Tissue Functions. *Cell Mol Life Sci* (2009) 66:1890–902. doi: 10.1007/s00018-009-8632-6
25. Gallagher WM, Currid CA, Whelan LC. Fibulins and Cancer: Friend or Foe? *Trends Mol Med* (2005) 11:336–40. doi: 10.1016/j.molmed.2005.06.001
26. Twal WO, Czirok A, Hegedus B, Knaak C, Chintalapudi MR, Okagawa H, et al. Fibulin-1 Suppression of Fibronectin-Regulated Cell Adhesion and Motility - PubMed. *J Cell Sci* (2001) 114:4587–98. doi: 10.1242/jcs.114.24.4587
27. Obaya AJ, Rua S, Moncada-Pazos A, Cal S. The Dual Role of Fibulins in Tumorigenesis. *Cancer Lett* (2012) 325:132–8. doi: 10.1016/j.canlet.2012.06.019
28. Harikrishnan K, Joshi O, Madangirikar S, Balasubramanian N. Cell Derived Matrix Fibulin-1 Associates With Epidermal Growth Factor Receptor to Inhibit Its Activation, Localization and Function in Lung Cancer Calu-1 Cells. *Front Cell Dev Biol* (2020) 8:522. doi: 10.3389/fcell.2020.00522
29. Kim IG, Kim SY, Choi SI, Lee JH, Kim KC, Cho EW. Fibulin-3-Mediated Inhibition of Epithelial-to-Mesenchymal Transition and Self-Renewal of ALDH+ Lung Cancer Stem Cells Through IGF1R Signaling. *Oncogene* (2014) 33:3908–17. doi: 10.1038/onc.2013.373
30. Yue W, Dacic S, Sun Q, Landreneau R, Guo M, Zhou W, et al. Frequent Inactivation of RAMP2, EFEMP1 and Dutt1 in Lung Cancer by Promoter Hypermethylation. *Clin Cancer Res* (2007) 13:4336–44. doi: 10.1158/1078-0432.CCR-07-0015
31. Hwang CF, Chien CY, Huang SC, Yin YF, Huang CC, Fang FM, et al. Fibulin-3 is Associated With Tumour Progression and a Poor Prognosis in Nasopharyngeal Carcinomas and Inhibits Cell Migration and Invasion *via* Suppressed AKT Activity. *J Pathol* (2010) 222:367–79. doi: 10.1002/path.2776
32. Kim EJ, Lee SY, Woo MK, Choi SI, Kim TR, Kim MJ, et al. Fibulin-3 Promoter Methylation Alters the Invasive Behavior of Non-Small Cell Lung Cancer Cell Lines *via* MMP-7 and MMP-2 Regulation. *Int J Oncol* (2012) 40:402–8. doi: 10.3892/ijo.2011.1191
33. Chen X, Meng J, Yue W, Yu J, Yang J, Yao Z, et al. Fibulin-3 Suppresses Wnt/β-Catenin Signaling and Lung Cancer Invasion. *Carcinogenesis* (2014) 35:1707–16. doi: 10.1093/carcin/bgu023
34. You L, He B, Xu Z, Uematsu K, Mazieres J, Mikami I, et al. Inhibition of Wnt-2-Mediated Signaling Induces Programmed Cell Death in Non-Small-Cell Lung Cancer Cells. *Oncogene* (2004) 23:6170–4. doi: 10.1038/sj.onc.1207844
35. Nguyen DX, Chiang AC, Zhang XHF, Kim JY, Kris MG, Ladanyi M, et al. WNT/TCF Signaling Through LEF1 and HOXB9 Mediates Lung Adenocarcinoma Metastasis. *Cell* (2009) 138:51–62. doi: 10.1016/j.cell.2009.04.030
36. Xu S, Yang Y, Sun YB, Wang HY, Sun CB, Zhang X. Role of Fibulin-3 in Lung Cancer: *In Vivo* and *In Vitro* Analyses. *Oncol Rep* (2014) 31:79–86. doi: 10.3892/or.2013.2799
37. Nakamura T, Ruiz-Lozano P, Lindner V, Yabe D, Taniwaki M, Furukawa Y, et al. DANCE, a Novel Secreted RGD Protein Expressed in Developing, Atherosclerotic, and Balloon-Injured Arteries. *J Biol Chem* (1999) 274:22476–83. doi: 10.1074/jbc.274.32.22476
38. Albig AR, Neil JR, Schiemann WP. Fibulins 3 and 5 Antagonize Tumor Angiogenesis *in vivo*. *Cancer Res* (2006) 66:2621–9. doi: 10.1158/0008-5472.CAN-04-4096
39. Nakamura T, Lozano PR, Ikeda Y, Iwanaga Y, Hinek A, Minamisawa S, et al. Fibulin-5/DANCE Is Essential for Elastogenesis In Vivo. *Nature* (2002) 415:171–5.
40. Timpl R, Sasaki T, Kostka G, Chu ML. Fibulins: A Versatile Family of Extracellular Matrix Proteins. *Nat Rev Mol Cell Biol* (2003) 4:479–89.
41. Yanagisawa H, Davis EC, Starcher BC, Ouchi T, Yanagisawa M, Richardson JA, et al. Fibulin-5 Is an Elastin-binding Protein Essential for Elastic Fiber Development In Vivo. *Nature* (2002) 415:168–71.
42. Kuang P-P, Goldstein RH, Liu Y, Rishikof DC, Jean J-C, Joyce-Brady M. Coordinate Expression of Fibulin-5/DANCE and Elastin During Lung Injury Repair. *Am J Physiol Lung Cell Mol Physiol* (2003) 285:1147–52. doi: 10.1152/ajplung.00098.2003.-Fibulin-5
43. Schiemann WP, Blobe GC, Kalume DE, Pandey A, Lodish HF. Context-Specific Effects of Fibulin-5 (DANCE/EVEC) on Cell Proliferation, Motility, and Invasion. Fibulin-5 is Induced by Transforming Growth Factor-β and Affects Protein Kinase Cascades. *J Biol Chem* (2002) 277:27367–77. doi: 10.1074/jbc.M200148200
44. Yue W, Sun Q, Landreneau R, Wu C, Siegfried JM, Yu J, et al. Fibulin-5 Suppresses Lung Cancer Invasion by Inhibiting Matrix Metalloproteinase-7 Expression. *Cancer Res* (2009) 69:6339–46. doi: 10.1158/0008-5472.CAN-09-0398
45. Lee HK, Kwon MJ, Seo J, Kim JW, Hong M, Park HR, et al. Expression of Mucins (MUC1, MUC2, MUC5AC and MUC6) in ALK-Positive Lung Cancer: Comparison With EGFR-Mutated Lung Cancer. *Pathol Res Pract* (2019) 215:459–65. doi: 10.1016/j.prp.2018.12.011
46. Kufe DW. Mucins in Cancer: Function, Prognosis and Therapy. *Nat Rev Cancer* (2009) 9:874–85. doi: 10.1038/nrc2761
47. Li Y, Ren J, Yu WH, Li Q, Kuwahara H, Yin L, et al. The Epidermal Growth Factor Receptor Regulates Interaction of the Human DF3/MUC1 Carcinoma Antigen With C-Src and β-Catenin. *J Biol Chem* (2001) 276:35239–42. doi: 10.1074/jbc.C100359200
48. Raina D, Kosugi M, Ahmad R, Panchamoorthy G, Rajabi H, Alam M, et al. Dependence on the MUC1-C Oncoprotein in Non-Small Cell Lung Cancer Cells. *Mol Cancer Ther* (2011) 10:806–16. doi: 10.1158/1535-7163.MCT-10-1050
49. Yao M, Zhang W, Zhang Q, Xing L, Xu A, Liu Q, et al. Overexpression of MUC1 Enhances Proangiogenic Activity of Non-Small-Cell Lung Cancer Cells Through Activation of Akt and Extracellular Signal-Regulated Kinase Pathways. *Lung* (2011) 189:453–60. doi: 10.1007/s00408-011-9327-y
50. Pochampalli MR, Bejjani RME, Schroeder JA. MUC1 Is a Novel Regulator of ErbB1 Receptor Trafficking. *Oncogene* (2007) 26:1693–701. doi: 10.1038/sj.onc.1209976
51. MacDermed DM, Khodarev NN, Pitroda SP, Edwards DC, Pelizzari CA, Huang L, et al. MUC1-Associated Proliferation Signature Predicts Outcomes in Lung Adenocarcinoma Patients. *BMC Med Genomics* (2010) 3:16. doi: 10.1186/1755-8794-3-16
52. Ahmad R, Raina D, Joshi MD, Kawano T, Ren J, Kharbanda S, et al. MUC1-C Oncoprotein Functions as a Direct Activator of the Nuclear Factor-κb P65 Transcription Factor. *Cancer Res* (2009) 69:7013–21. doi: 10.1158/0008-5472.CAN-09-0523
53. Huang L, Chen D, Liu D, Yin L, Kharbanda S, Kufe D. MUC1 Oncoprotein Blocks Glycogen Synthase Kinase 3β-Mediated Phosphorylation and Degradation of β-Catenin. *Cancer Res* (2005) 65:10413–22. doi: 10.1158/0008-5472.CAN-05-2474

54. Ahmad R, Rajabi H, Kosugi M, Joshi MD, Alam M, Vasir B, et al. MUC1-C Oncoprotein Promotes STAT3 Activation in an Autoinductive Regulatory Loop. *Sci Signal* (2011) 4(160):ra9. doi: 10.1126/scisignal.2001426
55. Ramasamy S, Duraisamy S, Barbashov S, Kawano T, Kharbanda S, Kufe D. The MUC1 and Galectin-3 Oncoproteins Function in a MicroRNA-Dependent Regulatory Loop. *Mol Cell* (2007) 27:992–1004. doi: 10.1016/j.molcel.2007.07.031
56. Wakata K, Tsuchiya T, Tomoshige K, Takagi K, Yamasaki N, Matsumoto K, et al. A Favourable Prognostic Marker for EGFR Mutant non-Small Cell Lung Cancer: Immunohistochemical Analysis of MUC5B. *BMJ Open* (2015) 5(7):e008366. doi: 10.1136/bmjopen-2015-008366
57. Michaël D, Martine A, Nathalie R, Anita R, Anne MLF, Roger L, et al. Lepidic Predominant Adenocarcinoma and Invasive Mucinous Adenocarcinoma of the Lung Exhibit Specific Mucin Expression in Relation With Oncogenic Drivers. *Lung Cancer* (2017) 109:92–100. doi: 10.1016/j.lungcan.2017.05.007
58. Matsumura M, Okudela K, Nakashima Y, Mitsui H, Denda-Nagai K, Suzuki T, et al. Specific Expression of MUC21 in Micropapillary Elements of Lung Adenocarcinomas - Implications for the Progression of EGFR-Mutated Lung Adenocarcinomas. *PLoS One* (2019) 14(4):e0215237. doi: 10.1371/journal.pone.0215237
59. Dong Y, Dong Y, Zhou L, Zhao D, Li K, Liu Z, et al. MUC5AC Enhances Tumor Heterogeneity in Lung Adenocarcinoma With Mucin Production and is Associated With Poor Prognosis. *Jpn J Clin Oncol* (2020) 50:701–11. doi: 10.1093/jjco/hyaa016
60. Lakshmanan I, Ponnusamy MP, Macha MA, Haridas D, Majhi PD, Kaur S, et al. Mucins in Lung Cancer: Diagnostic, Prognostic, and Therapeutic Implications. *J Thorac Oncol* (2015) 10:19–27. doi: 10.1097/JTO.0000000000000404
61. Singh P, Carraher C, Schwarzbauer JE. Assembly of Fibronectin Extracellular Matrix. *Annu Rev Cell Dev Biol* (2010) 26:397–419. doi: 10.1146/annurev-cellbio-100109-104020
62. Zollinger AJ, Smith ML. Fibronectin, the Extracellular Glue. *Matrix Biol* (2017) 60–61:27–37. doi: 10.1016/j.matbio.2016.07.011
63. Pankov R, Yamada KM. Fibronectin at a Glance. *J Cell Sci* (2002) 115:3861–3. doi: 10.1242/jcs.00059
64. Cho C, Horzempa C, Longo CM, Peters DM, Jones DM, McKeown-Longo PJ. Fibronectin in the Tumor Microenvironment Activates a TLR4-Dependent Inflammatory Response in Lung Cancer Cells. *J Cancer* (2020) 11:3099–105. doi: 10.7150/jca.39771
65. Wang JP, Hielscher A. Fibronectin: How its Aberrant Expression in Tumors may Improve Therapeutic Targeting. *J Cancer* (2017) 8:674–82. doi: 10.7150/jca.16901
66. You R, Zheng M, McKeown-Longo PJ. The First Type III Repeat in Fibronectin Activates an Inflammatory Pathway in Dermal Fibroblasts. *J Biol Chem* (2010) 285:36255–9. doi: 10.1074/jbc.C110.176990
67. Kelsh RM, McKeown-Longo PJ. Topographical Changes in Extracellular Matrix: Activation of TLR4 Signaling and Solid Tumor Progression. *Trends Cancer Res* (2013) 9:1–13.
68. Han SW, Khuri FR, Roman J. Fibronectin Stimulates Non-Small Cell Lung Carcinoma Cell Growth Through Activation of Akt/mammalian Target of Rapamycin/S6 Kinase and Inactivation of LKB1/AMP-Activated Protein Kinase Signal Pathways. *Cancer Res* (2006) 66:315–23. doi: 10.1158/0008-5472.CAN-05-2367
69. Mori T, Ono K, Kariya Y, Ogawa T, Higashi S, Miyazaki K. Laminin-3B11, a Novel Vascular-Type Laminin Capable of Inducing Prominent Lamellipodial Protrusions in Microvascular Endothelial Cells. *J Biol Chem* (2010) 285:35068–78. doi: 10.1074/jbc.M110.146126
70. Miyazaki K. Laminin-5 (Laminin-332): Unique Biological Activity and Role in Tumor Growth and Invasion. *Cancer Sci* (2006) 97:91–8. doi: 10.1111/j.1349-7006.2006.00150.x
71. An SJ, Lin QX, Chen ZH, Su J, Cheng H, Xie Z, et al. Combinations of Laminin 5 With PTEN, P-EGFR and P-Akt Define a Group of Distinct Molecular Subsets Indicative of Poor Prognosis in Patients With Non-Small Cell Lung Cancer. *Exp Ther Med* (2012) 4:226–30. doi: 10.3892/etm.2012.577
72. Stewart RL, West D, Wang C, Weiss HL, Gal T, Durbin EB, et al. Elevated Integrin α6β4 Expression is Associated With Venous Invasion and Decreased Overall Survival in Non-Small Cell Lung Cancer. *Hum Pathol* (2016) 54:174–83. doi: 10.1016/j.humpath.2016.04.003
73. Kim I, Kim HG, Kim H, Kim HH, Park SK, Uhm CS, et al. Hepatic Expression, Synthesis and Secretion of a Novel Fibrinogen/Angiopoietin-Related Protein That Prevents Endothelial-Cell Apoptosis. *Biochem J* (2000) 346:603–10. doi: 10.1042/0264-6021:3460603
74. Courtney M, Stoler M, Marder V, Haidaris P. Developmental Expression of mRNAs Encoding Platelet Proteins in Rat Megakaryocytes. *Blood* (1991) 77:560–8. doi: 10.1182/blood.v77.3.560.560
75. Sahni A, Simpson-Haidaris PJ, Sahni SK, Vaday GG, Francis CW. Fibrinogen Synthesized by Cancer Cells Augments the Proliferative Effect of Fibroblast Growth Factor-2 (FGF-2). *J Thromb Haemost* (2007) 6:176–83. doi: 10.1111/j.1538-7836.2007.02808.x
76. Sahni A, Francis CW. Vascular Endothelial Growth Factor Binds to Fibrinogen and Fibrin and Stimulates Endothelial Cell Proliferation. *Blood* (2000) 96:3772–8. doi: 10.1182/blood.v96.12.3772
77. Guadiz G, Sporn LA, Simpson-Haidaris PJ. Thrombin Cleavage-Independent Deposition of Fibrinogen in Extracellular Matrices. *Blood* (1997) 90:2644–53. doi: 10.1182/blood.v90.7.2644
78. Mosesson MW. Fibrinogen and Fibrin Structure and Functions. *J Thromb Haemost* (2005) 3:1894–904. doi: 10.1111/j.1538-7836.2005.01365.x
79. Shang Z, Niu X, Zhang K, Qiao Z, Liu S, Jiang X, et al. FGA Isoform as an Indicator of Targeted Therapy for EGFR Mutated Lung Adenocarcinoma. *J Mol Med* (2019) 97:1657–68. doi: 10.1007/s00109-019-01848-z
80. Sun C, Gao W, Liu J, Cheng H, Hao J. FGL1 Regulates Acquired Resistance to Gefitinib by Inhibiting Apoptosis in Non-Small Cell Lung Cancer. *Respir Res* (2020) 21(1):210. doi: 10.1186/s12931-020-01477-y
81. Guan J, Xiao N, Qiu C, Li Q, Chen M, Zhang Y, et al. Fibrinogen Is Associated With EGFR Mutation Status and Lymphatic Metastasis in Non-Small Cell Lung Cancer. *Oncol Lett* (2019) 17:739–46. doi: 10.3892/ol.2018.9652
82. Sun Z, Velázquez-Quesada I, Murdamoothoo D, Ahowesso C, Yilmaz A, Spenlé C, et al. Tenascin-C Increases Lung Metastasis by Impacting Blood Vessel Invasions. *Matrix Biol* (2019) 83:26–47. doi: 10.1016/j.matbio.2019.07.001
83. Giblin SP, Midwood KS. Tenascin-C: Form Versus Function. *Cell Adhes Migr* (2015) 9:48–82. doi: 10.4161/19336918.2014.987587
84. Ruan K, Bao S, Ouyang G. The Multifaceted Role of Periostin in Tumorigenesis. *Cell Mol Life Sci* (2009) 66:2219–30. doi: 10.1007/s00018-009-0013-7
85. Kudo Y, Siriwardena BSMS, Hatano H, Ogawa I, Takata T. Periostin: Novel Diagnostic and Therapeutic Target for Cancer. *Histol Histopathol* (2007) 22:1167–74. doi: 10.14670/HH-22.1167
86. Baril P, Gangeswaran R, Mahon PC, Caulee K, Kocher HM, Harada T, et al. Periostin Promotes Invasiveness and Resistance of Pancreatic Cancer Cells to Hypoxia-Induced Cell Death: Role of the β4 Integrin and the PI3k Pathway. *Oncogene* (2007) 26:2082–94. doi: 10.1038/sj.onc.1210009
87. Bao S, Ouyang G, Bai X, Huang Z, Ma C, Liu M, et al. Periostin Potently Promotes Metastatic Growth of Colon Cancer by Augmenting Cell Survival *via* the Akt/PKB Pathway. *Cancer Cell* (2004) 5:329–39. doi: 10.1016/S1535-6108(04)00081-9
88. Hu WW, Chen PC, Chen JM, Wu YM, Liu PY, Lu CH, et al. Periostin Promotes Epithelial-Mesenchymal Transition *via* the MAPK/miR-381 Axis in Lung Cancer. *Oncotarget* (2017) 8:62248–60. doi: 10.18632/oncotarget.19273
89. Ouyang G, Liu M, Ruan K, Song G, Mao Y, Bao S. Upregulated Expression of Periostin by Hypoxia in Non-Small-Cell Lung Cancer Cells Promotes Cell Survival *via* the Akt/PKB Pathway. *Cancer Lett* (2009) 281:213–9. doi: 10.1016/j.canlet.2009.02.030
90. Schvartz I, Seger D, Shaltiel S. Vitronectin. *Int J Biochem Cell Biol* (1999) 31:539–44. doi: 10.1016/S1357-2725(99)00005-9
91. Böger C, Kalthoff H, Goodman SL, Behrens HM, Röcken C. Integrins and Their Ligands are Expressed in non-Small Cell Lung Cancer But Not Correlated With Parameters of Disease Progression. *Virchows Arch* (2014) 464:69–78. doi: 10.1007/s00428-013-1506-1
92. Ricono JM, Huang M, Barnes LA, Lau SK, Weis SM, Schlaepfer DD, et al. Specific Cross-Talk Between Epidermal Growth Factor Receptor and Integrin α Vβ 5 Promotes Carcinoma Cell Invasion and Metastasis. *Cancer Res* (2009) 69:1383–91. doi: 10.1158/0008-5472.CAN-08-3612

93. Kohfeldt E, Sasaki T, Göhring W, Timpl R. Nidogen-2: A New Basement Membrane Protein With Diverse Binding Properties. *J Mol Biol* (1998) 282:99–109. doi: 10.1006/jmbi.1998.2004
94. Miosge N, Holzhausen S, Zelent C, Sprysch P, Herken R. Nidogen-1 and Nidogen-2 are Found in Basement Membranes During Human Embryonic Development. *Histochem J* (2001) 33:523–30. doi: 10.1023/A:1014995523521
95. Geng J, Sun J, Lin Q, Gu J, Zhao Y, Zhang H, et al. Methylation Status of NEUROG2 and NID2 Improves the Diagnosis of Stage I NSCLC. *Oncol Lett* (2012) 3:901–6. doi: 10.3892/ol.2012.587
96. Mokkapati S, Bechtel M, Reibetanz M, Miosge N, Nischt R. Absence of the Basement Membrane Component Nidogen 2, But Not of Nidogen 1, Results in Increased Lung Metastasis in Mice. *J Histochem Cytochem* (2012) 60:280–9. doi: 10.1369/0022155412436586
97. Chai AWY, Cheung AKL, Dai W, Ko JMY, Ip JCY, Chan KW, et al. Metastasis-Suppressing NID2, an Epigenetically-Silenced Gene, in the Pathogenesis of Nasopharyngeal Carcinoma and Esophageal Squamous Cell Carcinoma. *Oncotarget* (2016) 7:78859–71. doi: 10.18632/oncotarget.12889
98. Iozzo RV, Sanderson RD. Proteoglycans in Cancer Biology, Tumour Microenvironment and Angiogenesis. *J Cell Mol Med* (2011) 15:1013–31. doi: 10.1111/j.1582-4934.2010.01236.x
99. Gassar ES, Ibrahim SA, Götte M. Heparan Sulfate Proteoglycans in Cancer Therapy. In: Pavã M. (eds) *Glycans in Diseases and Therapeutics*. Springer, Berlin, Heidelberg: Biology of Extracellular Matrix. doi: 10.1007/978-3-642-16833-8_6
100. Guo JY, Chiu CH, Wang MJ, Li FA, Chen JY. Proteoglycan Serglycin Promotes non-Small Cell Lung Cancer Cell Migration Through the Interaction of its Glycosaminoglycans With CD44. *J BioMed Sci* (2020) 27:2. doi: 10.1186/s12929-019-0600-3
101. Nackaerts K, Verbeken E, Deneffe G, Vanderschueren B, Demedts M, David G. Heparan Sulfate Proteoglycan Expression in Human Lung-Cancer Cells. *Int J Cancer* (1997) 74:335–45. doi: 10.1002/(SICI)1097-0215(19970620)74:3<335::AID-IJC18>3.0.CO;2-A
102. Pirinen R, Leinonen T, Böhm J, Johansson R, Ropponen K, Kumpulainen E, et al. Versican in Nonsmall Cell Lung Cancer: Relation to Hyaluronan, Clinicopathologic Factors, and Prognosis. *Hum Pathol* (2005) 36:44–50. doi: 10.1016/j.humpath.2004.10.010
103. Fernandez-Madrid F, Karvonen RL, Kraut MJ, Czelusniak B, Ager JW. Autoimmunity to Collagen in Human Lung Cancer. *Cancer Res* (1996) 56 (1):121–6.
104. Liang S, Xu JF, Cao WJ, Li HP, Hu CP. Human Decorin Regulates Proliferation and Migration of Human Lung Cancer A549 Cells. *Chin Med J (Engl)* (2013) 126:4736–41. doi: 10.3760/cma.j.issn.0366-6999.20130207
105. Nikitovic D, Papoutsidakis A, Karamanos NK, Tzanakakis GN. Lumican Affects Tumor Cell Functions, Tumor-ECM Interactions, Angiogenesis and Inflammatory Response. *Matrix Biol* (2014) 35:206–14. doi: 10.1016/j.matbio.2013.09.003
106. Shah L, Walter KL, Borczuk AC, Kawut SM, Sonett JR, Gorenstein LA, et al. Expression of Syndecan-1 and Expression of Epidermal Growth Factor Receptor are Associated With Survival in Patients With Nonsmall Cell Lung Carcinoma. *Cancer* (2004) 101:1632–8. doi: 10.1002/cncr.20542
107. Reka AK, Chen G, Jones RC, Amunugama R, Kim S, Karnovsky A, et al. Epithelial-Mesenchymal Transition-Associated Secretory Phenotype Predicts Survival in Lung Cancer Patients. *Carcinogenesis* (2014) 35:1292–300. doi: 10.1093/carcin/bgu041
108. Yang YC, Pan KF, Lee WJ, Chang JH, Tan P, Gu CC, et al. Circulating Proteoglycan Endocan Mediates EGFR-Driven Progression of non-Small Cell Lung Cancer. *Cancer Res* (2020) 80:3292–304. doi: 10.1158/0008-5472.CAN-20-0005
109. Fei X, Zhang J, Zhao Y, Sun M, Zhao H, Li S. MiR-96 Promotes Invasion and Metastasis by Targeting GPC3 in non-Small Cell Lung Cancer Cells. *Oncol Lett* (2018) 15:9081–6. doi: 10.3892/ol.2018.8507
110. Bernfield M, Götte M, Park PW, Reizes O, Fitzgerald ML, Lincecum J, et al. Functions of Cell Surface Heparan Sulfate Proteoglycans. *Annu Rev Biochem* (1999) 68:729–77. doi: 10.1146/annurev.biochem.68.1.729
111. Capurro M, Martin T, Shi W, Filmus J. Glypican-3 Binds to Frizzled and Plays a Direct Role in the Stimulation of Canonical Wnt Signaling. *J Cell Sci* 127(Pt 7):1565–75. doi: 10.1242/jcs.140871
112. Häcker U, Nybakken K, Perrimon N. Heparan Sulphate Proteoglycans: The Sweet Side of Development. *Nat Rev Mol Cell Biol* (2005) 6:530–41. doi: 10.1038/nrm1681
113. Yuan S, Yu Z, Liu Q, Zhang M, Xiang Y, Wu N, et al. GPC5, a Novel Epigenetically Silenced Tumor Suppressor, Inhibits Tumor Growth by Suppressing Wnt/β-Catenin Signaling in Lung Adenocarcinoma. *Oncogene* (2016) 35:6120–31. doi: 10.1038/onc.2016.149
114. Li Y, Sheu CC, Ye Y, de Andrade M, Wang L, Chang SC, et al. Genetic Variants and Risk of Lung Cancer in Never Smokers: A Genome-Wide Association Study. *Lancet Oncol* (2010) 11:321–30. doi: 10.1016/S1470-2045(10)70042-5
115. Li Y, Miao L, Cai H, Ding J, Xiao Y, Yang J, et al. The Overexpression of Glypican-5 Promotes Cancer Cell Migration and is Associated With Shorter Overall Survival in non-Small Cell Lung Cancer. *Oncol Lett* (2013) 6:1565–72. doi: 10.3892/ol.2013.1622
116. Cai Z, Grobe K, Zhang X. Role of Heparan Sulfate Proteoglycans in Optic Disc and Stalk Morphogenesis. *Dev Dyn* (2014) 243:1310–6. doi: 10.1002/dvdy.24142
117. Ellina MI, Bouris P, Aletras AJ, Theocharis AD, Kletsas D, Karamanos NK. EGFR and HER2 Exert Distinct Roles on Colon Cancer Cell Functional Properties and Expression of Matrix Macromolecules. *Biochim Biophys Acta - Gen Subj* (2014) 1840:2651–61. doi: 10.1016/j.bbagen.2014.04.019
118. Tsonis AI, Afratis N, Gialeli C, Ellina MI, Piperigkou Z, Skandalis SS, et al. Evaluation of the Coordinated Actions of Estrogen Receptors With Epidermal Growth Factor Receptor and Insulin-Like Growth Factor Receptor in the Expression of Cell Surface Heparan Sulfate Proteoglycans and Cell Motility in Breast Cancer Cells. *FEBS J* (2013) 280:2248–59. doi: 10.1111/febs.12162
119. Harada E, Serada S, Fujimoto M, Takahashi Y, Takahashi T, Hara H, et al. Glypican-1 Targeted Antibody-Based Therapy Induces Preclinical Antitumor Activity Against Esophageal Squamous Cell Carcinoma. *Oncotarget* (2017) 8:24741–52. doi: 10.18632/oncotarget.15799
120. Qian JY, Tan YL, Zhang Y, Yang YF, Li XQ. Prognostic Value of Glypican-1 for Patients With Advanced Pancreatic Cancer Following Regional Intra-Arterial Chemotherapy. *Oncol Lett* (2018) 16:1253–8. doi: 10.3892/ol.2018.8701
121. Toyoshima E, Ohsaki Y, Nishigaki Y, Fujimoto Y, Kohgo Y, Kikuchi K. Expression of Syndecan-1 is Common in Human Lung Cancers Independent of Expression of Epidermal Growth Factor Receptor. *Lung Cancer* (2001) 31:193–202. doi: 10.1016/S0169-5002(00)00184-7
122. Ibrahim SA, Hassan H, Reinbold R, Espinoza-Sanchez NA, Greve B, Götte M. Role of Syndecan-1 in Cancer Stem Cells. In: Götte M, Forsberg-Nilsson K. (eds) *Proteoglycans in Stem Cells. Biology of Extracellular Matrix*, vol 9. Springer, Cham. doi: 10.1007/978-3-030-73453-4_12
123. Katakam SK, Tria V, Sim W-C, Yip GW, Molgora S, Karnavas T, et al. The Heparan Sulfate Proteoglycan Syndecan-1 Regulates Colon Cancer Stem Cell Function *via* a Focal Adhesion Kinase—Wnt Signaling Axis. *FEBS J* (2021) 288:486–506. doi: 10.1111/FEBS.15356
124. Hassan H, Greve B, Kiesel L, Ibrahim S, Götte M. Syndecan-1 Modulates IL-6- and Beta-Integrin- Dependent Functions in Breast Cancer Cell Adhesion and Migration. *Exp Clin Endocrinol Diabetes* (2013) 121:OP5_31. doi: 10.1055/S-0033-1336639
125. Nassar E, Hassan N, El-Ghonaimy EA, Hassan H, Abdullah MS, Rottke TV, et al. Syndecan-1 Promotes Angiogenesis in Triple-Negative Breast Cancer Through the Prognostically Relevant Tissue Factor Pathway and Additional Angiogenic Routes. *Cancers* (2021) 13:2318. doi: 10.3390/CANCERS13102318
126. Ibrahim SA, Gadalla R, El-Ghonaimy EA, Samir O, Mohamed HT, Hassan H, et al. Syndecan-1 is a Novel Molecular Marker for Triple Negative Inflammatory Breast Cancer and Modulates the Cancer Stem Cell Phenotype *via* the IL-6/STAT3, Notch and EGFR Signaling Pathways. *Mol Cancer* (2017) 16(1):57. doi: 10.1186/s12943-017-0621-z
127. Ibrahim SA, Yip GW, Stock C, Pan J-W, Neubauer C, Poeter M, et al. Targeting of Syndecan-1 by microRNA miR-10b Promotes Breast Cancer Cell Motility and Invasiveness *via* a Rho-GTPase- and E-Cadherin-Dependent Mechanism. *Int J Cancer* (2012) 131:E884–96. doi: 10.1002/IJC.27629
128. Nikolova V, Koo C-Y, Ibrahim SA, Wang Z, Spillmann D, Dreier R, et al. Differential Roles for Membrane-Bound and Soluble Syndecan-1 (CD138) in

Breast Cancer Progression. *Carcinogenesis* (2009) 30:397–407. doi: 10.1093/CARCIN/BGP001
129. Ruoslahti E, Yamaguchi Y. Proteoglycans as Modulators of Growth Factor Activities. *Cell* (1991) 64:867–9. doi: 10.1016/0092-8674(91)90308-L
130. Aviezer D, Yayon A. Heparin-Dependent Binding and Autophosphorylation of Epidermal Growth Factor (EGF) Receptor by Heparin-Binding EGF-Like Growth Factor But Not by EGF. *Proc Natl Acad Sci U.S.A.* (1994) 91:12173–7. doi: 10.1073/pnas.91.25.12173
131. Zhu YC, Xu CW, Zhang QX, Wang WX, Lei L, Zhuang W. Syndecan 4-C-Ros Oncogene 1 Fusion as a Mechanism of Acquired Resistance in Epidermal Growth Factor Receptor Mutant Lung Adenocarcinoma. *Chin Med J (Engl)* (2019) 132:3015–7. doi: 10.1097/CM9.0000000000000555
132. Zeng L, Yang N, Zhang Y. GOPC-ROS1 Rearrangement as an Acquired Resistance Mechanism to Osimertinib and Responding to Crizotinib Combined Treatments in Lung Adenocarcinoma. *J Thorac Oncol* (2018) 13:e114–6. doi: 10.1016/j.jtho.2018.02.005
133. Mulshine JL, Chow G, Tauler J. Cytokines and Growth Factors Stimulate Hyaluronan Production: Role of Hyaluronan in Epithelial to Mesenchymal-Like Transition in non-Small Cell Lung Cancer. *J BioMed Biotechnol* (2010) 2010:485468. doi: 10.1155/2010/485468
134. Hiraga T, Ito S, Nakamura H. Cancer Stem-Like Cell Marker CD44 Promotes Bone Metastases by Enhancing Tumorigenicity, Cell Motility, and Hyaluronan Production. *Cancer Res* (2013) 73:4112–22. doi: 10.1158/0008-5472.CAN-12-3801
135. Hiscox S, Baruha B, Smith C, Bellerby R, Goddard L, Jordan N, et al. Overexpression of CD44 Accompanies Acquired Tamoxifen Resistance in MCF7 Cells and Augments Their Sensitivity to the Stromal Factors, Heregulin and Hyaluronan. *BMC Cancer* (2012) 12:458. doi: 10.1186/1471-2407-12-458
136. Song JM, Im J, Nho RS, Han YH, Upadhyaya P, Kassie F. Hyaluronan-CD44/RHAMM Interaction-Dependent Cell Proliferation and Survival in Lung Cancer Cells. *Mol Carcinog* (2019) 58:321–33. doi: 10.1002/mc.22930
137. Song JM, Molla K, Anandharaj A, Cornax I, Gerard O'Sullivan M, Kirtane AR, et al. Triptolide Suppresses the *In Vitro* and *In Vivo* Growth of Lung Cancer Cells by Targeting Hyaluronan-CD44/RHAMM Signaling. *Oncotarget* (2017) 8:26927–40. doi: 10.18632/oncotarget.15879
138. Talekar M, Trivedi M, Shah P, Ouyang Q, Oka A, Gandham S, et al. Combination Wt-P53 and MicroRNA-125b Transfection in a Genetically Engineered Lung Cancer Model Using Dual CD44/EGFR-Targeting Nanoparticles. *Mol Ther* (2016) 24:759–69. doi: 10.1038/mt.2015.225
139. Li L, Qi L, Liang Z, Song W, Liu Y, Wang Y, et al. Transforming Growth Factor-β1 Induces EMT by the Transactivation of Epidermal Growth Factor Signaling Through HA/CD44 in Lung and Breast Cancer Cells. *Int J Mol Med* (2015) 36:113–22. doi: 10.3892/ijmm.2015.2222
140. Frantz C, Stewart KM, Weaver VM. The Extracellular Matrix at a Glance. *J Cell Sci* (2010) 123:4195–200. doi: 10.1242/jcs.023820
141. Nissen NI, Karsdal M, Willumsen N. Collagens and Cancer Associated Fibroblasts in the Reactive Stroma and its Relation to Cancer Biology. *J Exp Clin Cancer Res* (2019) 38(1):115. doi: 10.1186/s13046-019-1110-6
142. O'Reilly MS, Boehm T, Shing Y, Fukai N, Vasios G, Lane WS, et al. Endostatin: An Endogenous Inhibitor of Angiogenesis and Tumor Growth. *Cell* (1997) 88:277–85. doi: 10.1016/S0092-8674(00)81848-6
143. Qiu S, Deng L, Liao X, Nie L, Qi F, Jin K, et al. Tumor-Associated Macrophages Promote Bladder Tumor Growth Through PI3K/AKT Signal Induced by Collagen. *Cancer Sci* (2019) 110:2110–8. doi: 10.1111/cas.14078
144. Sampath Narayanan A, Page RC. Synthesis of Type V Collagen by Fibroblasts Derived From Normal, Inflamed and Hyperplastic Human Connective Tissues. *Top Catal* (1985) 5:297–304. doi: 10.1016/S0174-173X(85)80019-4
145. Zou Y, Zhang R-Z, Sabatelli P, Chu M-L, Bönnemann CG. Muscle Interstitial Fibroblasts Are the Main Source of Collagen VI Synthesis in Skeletal Muscle: Implications for Congenital Muscular Dystrophy Types Ullrich and Bethlem. *J Neuropathol Exp Neurol* (2008) 67:144–54. doi: 10.1097/nen.0b013e3181634ef7
146. Ricard-Blum S. The Collagen Family. *Cold Spring Harb Perspect Biol* (2011) 3:1–19. doi: 10.1101/cshperspect.a004978
147. Xu Y, Zhao Y, Su B, Chen Y, Zhou C. Expression of Collagen IV, Fibronectin, Laminin in non-Small Cell Lung Cancer and its Correlation With Chemosensitivities and Apoptosis. *Chinese-German J Clin Oncol* (2006) 5:58–62. doi: 10.1007/s10330-005-0440-3
148. Kalluri R. The Biology and Function of Fibroblasts in Cancer. *Nat Rev Cancer* (2016) 16:582–98. doi: 10.1038/nrc.2016.73
149. Kalluri R, Zeisberg M. Fibroblasts in Cancer. *Nat Rev Cancer* (2006) 6:392–401. doi: 10.1038/nrc1877
150. Pankova D, Chen Y, Terajima M, Schliekelman MJ, Baird BN, Fahrenholtz M, et al. Cancer-Associated Fibroblasts Induce a Collagen Cross-Link Switch in Tumor Stroma. *Mol Cancer Res* (2016) 14:287–95. doi: 10.1158/1541-7786.MCR-15-0307
151. Pickup MW, Mouw JK, Weaver VM. The Extracellular Matrix Modulates the Hallmarks of Cancer. *EMBO Rep* (2014) 15:1243–53. doi: 10.15252/embr.201439246
152. Bager CL, Willumsen N, Leeming DJ, Smith V, Karsdal MA, Dornan D, et al. Collagen Degradation Products Measured in Serum can Separate Ovarian and Breast Cancer Patients From Healthy Controls: A Preliminary Study. *Cancer Biomarkers* (2015) 15:783–8. doi: 10.3233/CBM-150520
153. Willumsen N, Bager CL, Leeming DJ, Smith V, Christiansen C, Karsdal MA, et al. Serum Biomarkers Reflecting Specific Tumor Tissue Remodeling Processes are Valuable Diagnostic Tools for Lung Cancer. *Cancer Med* (2014) 3:1136–45. doi: 10.1002/cam4.303
154. Leeming DJ, Koizumi M, Qvist P, Barkholt V, Zhang C, Henriksen K, et al. Serum N-Terminal Propeptide of Collagen Type I is Associated With the Number of Bone Metastases in Breast and Prostate Cancer and Correlates to Other Bone Related Markers. *biomark Cancer* (2011) 3:15–23. doi: 10.4137/BIC.S6484
155. Li J, Li X, Lan T, Qi C, He X. Type I Collagen Secreted by Lung Cancer Cells Promotes Cancer Cell Growth in a Three- Dimensional Culture System - PubMed. *Nan Fang Yi Ke Da Xue Xue Bao* (2014) 34(8):1129–34.
156. Xu S, Xu H, Wang W, Li S, Li H, Li T, et al. The Role of Collagen in Cancer: From Bench to Bedside. *J Transl Med* (2019) 17(1):309. doi: 10.1186/s12967-019-2058-1
157. Bonnans C, Chou J, Werb Z. Remodelling the Extracellular Matrix in Development and Disease. *Nat Rev Mol Cell Biol* (2014) 15:786–801. doi: 10.1038/nrm3904
158. Mason SD, Joyce JA. Proteolytic Networks in Cancer. *Trends Cell Biol* (2011) 21:228–37. doi: 10.1016/j.tcb.2010.12.002
159. Chen Y, Terajima M, Yang Y, Sun L, Ahn YH, Pankova D, et al. Lysyl Hydroxylase 2 Induces a Collagen Cross-Link Switch in Tumor Stroma. *J Clin Invest* (2015) 125:1147–62. doi: 10.1172/JCI74725
160. Chen Y, Guo H, Terajima M, Banerjee P, Liu X, Yu J, et al. Lysyl Hydroxylase 2 is Secreted by Tumor Cells and can Modify Collagen in the Extracellular Space. *J Biol Chem* (2016) 291:25799–808. doi: 10.1074/jbc.M116.759803
161. Du H, Chen Y, Hou X, Huang Y, Wei X, Yu X, et al. PLOD2 Regulated by Transcription Factor FOXA1 Promotes Metastasis in NSCLC. *Cell Death Dis* (2017) 8:e3143. doi: 10.1038/cddis.2017.553
162. Humphries MJ. Integrin Cell Adhesion Receptors and the Concept of Agonism. *Trends Pharmacol Sci* (2000) 21:29–32. doi: 10.1016/S0165-6147(99)01410-8
163. Barczyk M, Carracedo S, Gullberg D. Integrins. *Cell Tissue Res* (2010) 339:269–80. doi: 10.1007/s00441-009-0834-6
164. Ruoslahti E. RGD AND OTHER RECOGNITION SEQUENCES FOR INTEGRINS. *Annu Rev Cell Dev Biol* (1996) 12:697–715. doi: 10.1146/annurev.cellbio.12.1.697
165. Zhao X, Guan JL. Focal Adhesion Kinase and its Signaling Pathways in Cell Migration and Angiogenesis. *Adv Drug Delivery Rev* (2011) 63:610–5. doi: 10.1016/j.addr.2010.11.001
166. Mitra SK, Schlaepfer DD. Integrin-Regulated FAK-Src Signaling in Normal and Cancer Cells. *Curr Opin Cell Biol* (2006) 18:516–23. doi: 10.1016/j.ceb.2006.08.011
167. Giancotti FG, Ruoslahti E. Integrin Signaling. *Sci (80-)* (1999) 285:1028–32. doi: 10.1126/science.285.5430.1028
168. Cybulsky AV, McTavish AJ, Cyr MD. Extracellular Matrix Modulates Epidermal Growth Factor Receptor Activation in Rat Glomerular Epithelial Cells. *J Clin Invest* (1994) 94:68–78. doi: 10.1172/JCI117350
169. Miyamoto S, Teramoto H, Gutkind JS, Yamada KM. Integrins can Collaborate With Growth Factors for Phosphorylation of Receptor Tyrosine Kinases and MAP Kinase Activation: Roles of Integrin

Aggregation and Occupancy of Receptors. *J Cell Biol* (1996) 135:1633–42. doi: 10.1083/jcb.135.6.1633
170. Moro L, Venturino M, Bozzo C, Silengo L, Altruda F, Beguinot L, et al. Integrins Induce Activation of EGF Receptor: Role in MAP Kinase Induction and Adhesion-Dependent Cell Survival. *EMBO J* (1998) 17:6622–32. doi: 10.1093/emboj/17.22.6622
171. Li J, Lin ML, Wiepz GJ, Guadarrama AG, Bertics PJ. Integrin-Mediated Migration of Murine B82L Fibroblasts is Dependent on the Expression of an Intact Epidermal Growth Factor Receptor. *J Biol Chem* (1999) 274:11209–19. doi: 10.1074/jbc.274.16.11209
172. Desgrosellier JS, Cheresh DA. Integrins in Cancer: Biological Implications and Therapeutic Opportunities. *Nat Rev Cancer* (2010) 10:9–22. doi: 10.1038/nrc2748
173. Bill HM, Knudsen B, Moores SL, Muthuswamy SK, Rao VR, Brugge JS, et al. Epidermal Growth Factor Receptor-Dependent Regulation of Integrin-Mediated Signaling and Cell Cycle Entry in Epithelial Cells. *Mol Cell Biol* (2004) 24:8586–99. doi: 10.1128/mcb.24.19.8586-8599.2004
174. Ivaska J, Heino J. Cooperation Between Integrins and Growth Factor Receptors in Signaling and Endocytosis. *Annu Rev Cell Dev Biol* (2011) 27:291–320. doi: 10.1146/annurev-cellbio-092910-154017
175. Mariotti A, Kedeshian PA, Dans M, Curatola AM, Gagnoux-Palacios L, Giancotti FG. EGF-R Signaling Through Fyn Kinase Disrupts the Function of Integrin α6β4 at Hemidesmosomes: Role in Epithelial Cell Migration and Carcinoma Invasion. *J Cell Biol* (2001) 155:447–57. doi: 10.1083/jcb.200105017
176. Moro L, Dolce L, Cabodi S, Bergatto E, Erba EB, Smeriglio M, et al. Integrin-Induced Epidermal Growth Factor (EGF) Receptor Activation Requires C-Src and p130Cas and Leads to Phosphorylation of Specific EGF Receptor Tyrosines. *J Biol Chem* (2002) 277:9405–14. doi: 10.1074/jbc.M109101200
177. Morello V, Cabodi S, Sigismund S, Camacho-Leal MP, Repetto D, Volante M, et al. β1 Integrin Controls EGFR Signaling and Tumorigenic Properties of Lung Cancer Cells. *Oncogene* (2011) 30:4087–96. doi: 10.1038/ONC.2011.107
178. Kondo S, Iwata S, Yamada T, Inoue Y, Ichihara H, Kichikawa Y, et al. Impact of the Integrin Signaling Adaptor Protein NEDD9 on Prognosis and Metastatic Behavior of Human Lung Cancer. *Clin Cancer Res* (2012) 18:6326–38. doi: 10.1158/1078-0432.CCR-11-2162
179. Zhu J, Cai T, Zhou J, Du W, Zeng Y, Liu T, et al. CD151 Drives Cancer Progression Depending on Integrin α3β1 Through EGFR Signaling in non-Small Cell Lung Cancer. *J Exp Clin Cancer Res* (2021) 40(1):192. doi: 10.1186/S13046-021-01998-4
180. Karamanos NK, Theocharis AD, Neill T, Iozzo RV. Matrix Modeling and Remodeling: A Biological Interplay Regulating Tissue Homeostasis and Diseases. *Matrix Biol* (2019) 75–76:1–11. doi: 10.1016/J.MATBIO.2018.08.007
181. Iozzo RV, Gubbiotti MA. Extracellular Matrix: The Driving Force of Mammalian Diseases. *Matrix Biol* (2018) 71–72:1–9. doi: 10.1016/J.MATBIO.2018.03.023
182. Borgoño CA, Diamandis EP. The Emerging Roles of Human Tissue Kallikreins in Cancer. *Nat Rev Cancer* (2004) 4:876–90. doi: 10.1038/NRC1474
183. Yang X, Zhang X, Wu R, Huang Q, Jiang Y, Qin J, et al. DPPIV Promotes Endometrial Carcinoma Cell Proliferation, Invasion and Tumorigenesis. *Oncotarget* (2017) 8:8679–92. doi: 10.18632/ONCOTARGET.14412
184. Deryugina E, Carré A, Ardi V, Muramatsu T, Schmidt J, Pham C, et al. Neutrophil Elastase Facilitates Tumor Cell Intravasation and Early Metastatic Events. *iScience* (2020) 23(12):101799. doi: 10.1016/J.ISCI.2020.101799
185. Piperigkou Z, Manou D, Karamanou K, Theocharis AD. Strategies to Target Matrix Metalloproteinases as Therapeutic Approach in Cancer. *Methods Mol Biol* (2018) 1731:325–48. doi: 10.1007/978-1-4939-7595-2_27
186. Visse R, Nagase H. Matrix Metalloproteinases and Tissue Inhibitors of Metalloproteinases: Structure, Function, and Biochemistry. *Circ Res* (2003) 92:827–39. doi: 10.1161/01.RES.0000070112.80711.3D
187. Verma RP, Hansch C. Matrix Metalloproteinases (MMPs): Chemical-Biological Functions and (Q)SARs. *Bioorg Med Chem* (2007) 15:2223–68. doi: 10.1016/J.BMC.2007.01.011
188. Gialeli C, Theocharis AD, Karamanos NK. Roles of Matrix Metalloproteinases in Cancer Progression and Their Pharmacological Targeting. *FEBS J* (2011) 278:16–27. doi: 10.1111/J.1742-4658.2010.07919.X
189. Cathcart J, Pulkoski-Gross A, Cao J. Targeting Matrix Metalloproteinases in Cancer: Bringing New Life to Old Ideas. *Genes Dis* (2015) 2:26–34. doi: 10.1016/j.gendis.2014.12.002
190. Nagaset H, Woessner JF. Matrix Metalloproteinases. *J Biol Chem* (1999) 274:21491–4. doi: 10.1074/jbc.274.31.21491
191. Stawowczyk M, Wellenstein MD, Lee SB, Yomtoubian S, Durrans A, Choi H, et al. Matrix Metalloproteinase 14 Promotes Lung Cancer by Cleavage of Heparin-Binding EGF-Like Growth Factor. *Neoplasia (United States)* (2017) 19:55–64. doi: 10.1016/j.neo.2016.11.005
192. Merchant N, Nagaraju GP, Rajitha B, Lammata S, Jella KK, S.Buchwald Z, et al. Matrix Metalloproteinases: Their Functional Role in Lung Cancer. *Carcinogenesis* (2017) 38:766–80. doi: 10.1093/carcin/bgx063
193. Nerenberg PS, Salsas-Escat R, Stultz CM. Collagen-A Necessary Accomplice in the Metastatic Process. *Cancer Genomics Proteomics* (2007) 4(5):319–28.
194. Chen P, Cescon M, Bonaldo P. Collagen VI in Cancer and Its Biological Mechanisms. *Trends Mol Med* (2013) 19(7):410–7. doi: 10.1016/j.molmed.2013.04.001
195. Kalluri R. Basement Membranes: Structure, Assembly and Role in Tumour Angiogenesis. *Nat Rev Cancer* (2013) 3(6):422–33. doi: 10.1038/nrc1094
196. Cox G, Jones JL, O'byrne KJ. Matrix Metalloproteinase 9 and the Epidermal Growth Factor Signal Pathway in Operable Non-Small Cell Lung Cancer 1. *Clin Cancer Res* (2000) 6(6):2349–55.
197. Ishii G, Ochiai A, Neri S. Phenotypic and Functional Heterogeneity of Cancer-Associated Fibroblast Within the Tumor Microenvironment. *Adv Drug Delivery Rev* (2016) 99:186–96. doi: 10.1016/J.ADDR.2015.07.007
198. Yoshida T, Ishii G, Goto K, Neri S, Hashimoto H, Yoh K, et al. Podoplanin-Positive Cancer-Associated Fibroblasts in the Tumor Microenvironment Induce Primary Resistance to EGFR-TKIs in Lung Adenocarcinoma With EGFR Mutation. *Clin Cancer Res* (2015) 21:642–51. doi: 10.1158/1078-0432.CCR-14-0846
199. Provenzano PP, Inman DR, Eliceiri KW, Knittel JG, Yan L, Rueden CT, et al. Collagen Density Promotes Mammary Tumor Initiation and Progression. *BMC Med* (2008) 6:11. doi: 10.1186/1741-7015-6-11
200. Kakkad SM, Solaiyappan M, O'Rourke B, Stasinopoulos I, Ackerstaff E, Raman V, et al. Hypoxic Tumor Microenvironments Reduce Collagen I Fiber Density. *Neoplasia* (2010) 12:608. doi: 10.1593/NEO.10344
201. Kanda R, Kawahara A, Watari K, Murakami Y, Sonoda K, Maeda M, et al. Erlotinib Resistance in Lung Cancer Cells Mediated by Integrin β1/Src/Akt-Driven Bypass Signaling. *Cancer Res* (2013) 73:6243–53. doi: 10.1158/0008-5472.CAN-12-4502
202. Yamazaki S, Su Y, Maruyama A, Makinoshima H, Suzuki J, Tsuboi M, et al. Uptake of Collagen Type I *via* Macropinocytosis Cause mTOR Activation and Anti-Cancer Drug Resistance. *Biochem Biophys Res Commun* (2020) 526:191–8. doi: 10.1016/j.bbrc.2020.03.067
203. Ishiguro Y, Ishiguro H, Miyamoto H. Epidermal Growth Factor Receptor Tyrosine Kinase Inhibition Up-Regulates Interleukin-6 in Cancer Cells and Induces Subsequent Development of Interstitial Pneumonia. *Oncotarget* (2013) 4:550–9. doi: 10.18632/oncotarget.939
204. Shintani Y, Maeda M, Chaika N, Johnson KR, Wheelock MJ. Collagen I Promotes Epithelial-to-Mesenchymal Transition in Lung Cancer Cells *via* Transforming Growth Factor-β Signaling. *Am J Respir Cell Mol Biol* (2008) 38:95–104. doi: 10.1165/rcmb.2007-0071OC
205. Gilles C, Polette M, Seiki M, Birembaut P, Thompson EW. Implication of Collagen Type I-Induced Membrane-Type 1-Matrix Metalloproteinase Expression and Matrix Metalloproteinase-2 Activation in the Metastatic Progression of Breast Carcinoma. *Lab Investig* (1997) 76:651–60.
206. Yamazaki S, Higuchi Y, Ishibashi M, Hashimoto H, Yasunaga M, Matsumura Y, et al. Collagen Type I Induces EGFR-TKI Resistance in EGFR-Mutated Cancer Cells by mTOR Activation Through Akt-Independent Pathway. *Cancer Sci* (2018) 109:2063–73. doi: 10.1111/cas.13624
207. Finicle BT, Jayashankar V, Edinger AL. Nutrient Scavenging in Cancer. *Nat Rev Cancer* (2018) 18:619–33. doi: 10.1038/S41568-018-0048-X
208. Ha KD, Bidlingmaier SM, Liu B. Macropinocytosis Exploitation by Cancers and Cancer Therapeutics. *Front Physiol* (2016) 7:381. doi: 10.3389/FPHYS.2016.00381

209. Huber MA, Kraut N, Beug H. Molecular Requirements for Epithelial-Mesenchymal Transition During Tumor Progression. *Curr Opin Cell Biol* (2005) 17:548–58. doi: 10.1016/j.ceb.2005.08.001
210. Thomson S, Buck E, Petti F, Griffin G, Brown E, Ramnarine N, et al. Epithelial to Mesenchymal Transition is a Determinant of Sensitivity of Non-Small-Cell Lung Carcinoma Cell Lines and Xenografts to Epidermal Growth Factor Receptor Inhibition. *Cancer Res* (2005) 65:9455–62. doi: 10.1158/0008-5472.CAN-05-1058
211. Suda K, Tomizawa K, Fujii M, Murakami H, Osada H, Maehara Y, et al. Epithelial to Mesenchymal Transition in an Epidermal Growth Factor Receptor-Mutant Lung Cancer Cell Line With Acquired Resistance to Erlotinib. *J Thorac Oncol* (2011) 6:1152–61. doi: 10.1097/JTO.0b013e318216ee52
212. Mahmood MQ, Ward C, Muller HK, Sohal SS, Walters EH. Epithelial Mesenchymal Transition (EMT) and non-Small Cell Lung Cancer (NSCLC): A Mutual Association With Airway Disease. *Med Oncol* (2017) 34(3):45. doi: 10.1007/s12032-017-0900-y
213. Kharbanda A, Rajabi H, Jin C, Tchaicha J, Kikuchi E, Wong KK, et al. Targeting the Oncogenic MUC1-C Protein Inhibits Mutant EGFR-Mediated Signaling and Survival in non-Small Cell Lung Cancer Cells. *Clin Cancer Res* (2014) 20:5423–34. doi: 10.1158/1078-0432.CCR-13-3168
214. Karachaliou N, Cardona AF, Bracht JWP, Aldeguer E, Drozdowskyj A, Fernandez-Bruno M, et al. Integrin-Linked Kinase (ILK) and Src Homology 2 Domain-Containing Phosphatase 2 (SHP2): Novel Targets in EGFR-Mutation Positive non-Small Cell Lung Cancer (NSCLC). *EBioMedicine* (2019) 39:207–14. doi: 10.1016/J.EBIOM.2018.11.036
215. Wang C, Wang T, Lv D, Li L, Yue J, Chen HZ, et al. Acquired Resistance to EGFR TKIs Mediated by Tgfβ1/Integrin β3 Signaling in EGFR-Mutant Lung Cancer. *Mol Cancer Ther* (2019) 18:2357–67. doi: 10.1158/1535-7163.MCT-19-0181
216. Bernardes N, Abreu S, Carvalho FA, Fernandes F, Santos NC, Fialho AM. Modulation of Membrane Properties of Lung Cancer Cells by Azurin Enhances the Sensitivity to EGFR-Targeted Therapy and Decreased β1 Integrin-Mediated Adhesion. *Cell Cycle* (2016) 15:1415–24. doi: 10.1080/15384101.2016.1172147
217. Li X, Ishihara S, Yasuda M, Nishioka T, Mizutani T, Ishikawa M, et al. Lung Cancer Cells That Survive Ionizing Radiation Show Increased Integrin α2β1- and EGFR-Dependent Invasiveness. *PLoS One* (2013) 8(8):e70905. doi: 10.1371/journal.pone.0070905
218. He F, Wang Y, Cai W, Li M, Dong L. Reversal of EGFR Inhibitors' Resistance by Co-Delivering EGFR and Integrin αvβ3 Inhibitors With Nanoparticles in non-Small Cell Lung Cancer. *Biosci Rep* (2019) 39(8):BSR20181259. doi: 10.1042/BSR20181259

Conflict of Interest: The authors declare that the research was conducted in the absence of any commercial or financial relationships that could be construed as a potential conflict of interest.

Publisher's Note: All claims expressed in this article are solely those of the authors and do not necessarily represent those of their affiliated organizations, or those of the publisher, the editors and the reviewers. Any product that may be evaluated in this article, or claim that may be made by its manufacturer, is not guaranteed or endorsed by the publisher.

GLOSSARY

ADC	Adenocarcinoma
AKT	Protein Kinase B
ALK	Anaplastic Lymphoma Kinase
AMPK	5' Adenosine Monophosphate-activated Protein Kinase
APAF-1	Apoptotic Peptidase Activating Factor 1
BM	Basement Membrane
CAFs	Cancer-Associated Fibroblasts
CCNB1	Cyclin B1
CD151	Cluster of Differentiation 151
CDC	cell division cycle protein
CDKN3	Cyclin-dependent kinase inhibitor 3
COLs	Collagens
CSCs	Cancer Stem Cells
Cdk4	cyclin-dependent kinase 4
ECM	Extra Cellular Matrix
EGF	Epidermal Growth Factor
EGFR	Epidermal Growth Factor Receptor
EMT	Epithelial-Mesenchymal Transition
ERK	Extracellular Signal-regulated Kinase
FACITs	Fibril-Associated COLs with Interrupted Triple helices
FAK	Focal Adhesion Kinase
FBG	Fibrinogen-like Globe
FBLN	Fibulin
FGA2	Fibrinogen Alpha chain isoform 2
FGF	Fibroblast Growth Factor
FN	Fibronectin
FOXA1	Fork-head box protein A1
GFRs	Growth Factor Receptors
GPC	Glypican
Grb2	Growth factor Receptor-Bound protein 2
HA	Hyaluronan
HAS	Hyaluronan Synthases
HB-EGF	Heparin-Binding EGF-like growth factor
Hnf4α	Hepatocyte Nuclear Factor 4α
HSPG	Heparan Sulfate Proteoglycan
IGF1R	Insulin-like Growth Factor 1 Receptor
IL-1β	Interleukin-1β
IL-6	Interleukin 6
IM	Interstitial Matrix
IMA	Invasive Mucinous Adenocarcinoma
ITGB4	Integrin Subunit Beta 4
JAK	Janus kinaes
KRAS	Ki-ras2 Kirsten Rat Sarcoma viral oncogene homolog
LPA	Lepidic Predominant Adenocarcinoma
LCC	Large Cell Carcinoma
LKB1	Liver Kinase B1
lncRNA	Long noncoding RNA
Ln	Laminins
LOX	Lysyl Oxidases
MACITs	Membrane-Anchored Collagens with Interrupted Triple helices
MAD2L1	Mitotic Arrest Deficient 2-Like Protein 1
MEK	MAPK Kinase
MMPs	Matrix Metalloproteinases
mTOR	Mammalian Target of Rapamycin
MUCs	Mucins
NF-κB	Nuclear Factor Kappa-light-chain-enhancer of activated B cells
NID	Nidogen
NSCLC	Non-small Cell Lung Cancer
OSF-2	Osteoblast-Specific Factor-2
PARP1	Poly(ADP-Ribose) Polymerase 1
PDGF	Platelet-Derived Growth Factor
PI3K	Phosphatidylinositol-3-Kinase
PKB	Protein kinase B
PLC-γ	Phospholipase C-gamma
PLOD2	Procollagen-Lysine, 2-Oxoglutarate 5-Dioxygenase 2
Postn	Periostin
PRC1	Protein Regulator of cytokinesis 1
PTEN	Phosphatase and Tensin homolog
PTPRζ1	Receptor-type Tyrosine-Protein phosphatase Zeta
$p130^{Cas}$	p130 Crk-Associated Substrate
p70S6K	70 kDa ribosomal protein S6 kinase
Rac1	Ras-related C3 botulinum toxin substrate 1
Rap1	Ras-related protein 1
ROBO2	Roundabout homolog 2
ROS1	ROS proto-oncogene 1
RRM2	Ribonucleoside-Diphosphate Reductase Subunit M2
RTKs	Receptor Tyrosine Kinases
SCLC	Small Cell Lung Cancer
SDC	Syndecan
SLRP	Small Leucine-Rich Proteoglycans
Sox2	SRY-like HMG box
SOS	Son of Sevenless
Src	Sarcoma viral oncogene
STAT	Signal Transducer and Activator of Transcription
SqCC	Squamous Cell Carcinoma
TCF4	Transcription factor 4
TGF-β	Transforming Growth Factor-β
TKIs	Tyrosine Kinase Inhibitors
TN-C	Tenascin-C
TLRs	Toll-like receptors
TSP	Thrombospondin
VTN	Vitronectin

frontiers in Oncology

ORIGINAL RESEARCH
published: 28 February 2022
doi: 10.3389/fonc.2022.835881

Impact of an Embedded Palliative Care Clinic on Healthcare Utilization for Patients With a New Thoracic Malignancy

*Kelly C. Gast[1], Jason A. Benedict[2], Madison Grogan[1], Sarah Janse[2], Maureen Saphire[3], Pooja Kumar[3], Erin M. Bertino[1], Julia L. Agne[4] and Carolyn J. Presley[1]**

[1] Division of Medical Oncology, The Ohio State University James Comprehensive Cancer Center, Columbus, OH, United States, [2] Center for Biostatistics, The Ohio State University Wexner Medical Center, Columbus, OH, United States, [3] Department of Pharmacy, The Ohio State University James Comprehensive Cancer Center, Columbus, OH, United States, [4] Division of Palliative Medicine, The Ohio State University Wexner Medical Center, Columbus, OH, United States

OPEN ACCESS

Edited by:
Lizza E. L. Hendriks, Maastricht University Medical Centre, Netherlands

Reviewed by:
Eleonora Anna Mess, Wroclaw Medical University, Poland
Daisy J. A. Janssen, Ciro, Netherlands

***Correspondence:**
Carolyn J. Presley
carolyn.presley@osumc.edu

Specialty section:
This article was submitted to Thoracic Oncology, a section of the journal Frontiers in Oncology

Received: *15 December 2021*
Accepted: *07 February 2022*
Published: *28 February 2022*

Citation:
Gast KC, Benedict JA, Grogan M, Janse S, Saphire M, Kumar P, Bertino EM, Agne JL and Presley CJ (2022) Impact of an Embedded Palliative Care Clinic on Healthcare Utilization for Patients With a New Thoracic Malignancy. Front. Oncol. 12:835881. doi: 10.3389/fonc.2022.835881

Introduction: Palliative care is beneficial for patients with advanced lung cancer, but the optimal model of palliative care delivery is unknown. We investigated healthcare utilization before and after embedding a palliative care physician within a thoracic medical oncology "onco-pall" clinic.

Methods: This is a retrospective cross-sectional cohort study comparing healthcare outcomes in two cohorts: "pre-cohort" 12 months prior to and "post-cohort" 12-months after the onco-pall clinic start date. Patients were included if they had a new diagnosis of lung cancer and received care at The Ohio State University Thoracic Oncology Center, and resided in Franklin County or 6 adjacent counties. During the pre-cohort time period, access to palliative care was available at a stand-alone palliative care clinic. Palliative care intervention in both cohorts included symptom assessment and management, advance care planning, and goals of care discussion as appropriate. Outcomes evaluated included rates of emergency department (ED) visits, hospital admissions, 30-day readmissions, and intensive care unit (ICU) admissions. Estimates were calculated in rates per-person-years and with Poisson regression models.

Results: In total, 474 patients met criteria for analysis (214 patients included in the pre-cohort and 260 patients in the post-cohort). Among all patients, 52% were male and 48% were female with a median age of 65 years (range 31-92). Most patients had non-small cell lung cancer (NSCLC - 17% stage 1-2, 20% stage 3, 47% stage 4) and 16% had small cell lung cancer. The post-cohort was older [median age 66 years vs 63 years in the pre-cohort (p-value: < 0.01)]. The post-cohort had a 26% reduction in ED visits compared to the pre-cohort, controlling for age, race, marital status, sex, county, Charlson score at baseline, cancer type and stage (adjusted relative risk: aRR: 0.74, 95% CI: 0.58-0.94,

p-value = 0.01). Although not statistically significant, there was a 29% decrease in ICU admissions (aRR: 0.71, 95% CI: 0.41-1.21, p-value = 0.21) and a 15% decrease in hospital admissions (aRR: 0.85, 95% CI: 0.70-1.03, p-value = 0.10). There was no difference in 30-day readmissions (aRR: 1.03, 95% CI: 0.73-1.45, p-value = 0.85).

Conclusions: Embedding palliative care clinics within medical oncology clinics may decrease healthcare utilization for patients with thoracic malignancies. Further evaluation of this model is warranted.

Keywords: thoracic, healthcare utilization, embedded, palliative care, lung cancer

INTRODUCTION

Multiple randomized trials have demonstrated that patients with advanced lung cancer benefit from early palliative care (within 8 weeks of diagnosis) concurrently with standard oncology care (1–4). These benefits include improved health-related quality of life (1–3, 5) and survival (1, 6). As a result, the American Society of Clinical Oncology guidelines recommend all patients with advanced cancer receive early interdisciplinary palliative care services (7). Despite the known benefits to early palliative care, there have been challenges in implementing this recommendation. These challenges include resource availability, financial constraints, increased clinic appointments, patient and caregiver fatigue, and patient and provider perceptions of end-of-life care (8, 9).

Although access to palliative care has increased in recent years, the optimal model of palliative care delivery is unknown. There has been a significant increase in outpatient palliative care clinics at National Cancer Institute (NCI)-designated cancer centers (95% in 2018 compared to 59% in 2009) (10). However, the vast majority of NCI-designated cancer centers offer stand-alone outpatient clinics (82.7%) while a smaller proportion offer palliative care in oncology clinics (38.5%) (10).

Several studies have evaluated the feasibility and impact of this newer model of embedded palliative care delivery (11–14). Embedded care models increased palliative care referral rates, resulted in palliative care intervention earlier in the disease course, and improved symptom burden (11, 12). While embedded palliative care in oncology clinics improves access, reported results on the effect on healthcare outcomes is mixed. Multiple studies have reported that the embedded palliative care model improves advanced care planning discussions (13, 14). One study showed increased hospice referral rates (13), while two studies demonstrated no difference (12, 14). There was no difference reported between embedded and stand-alone palliative clinic models with respect to end-of-life quality metrics including hospital or intensive care unit (ICU) admissions in the last 30 days of life (13, 14), emergency department (ED) visits (14), or receipt of chemotherapy in the last 14 days of life (12, 14). In addition to improving the accessibility of palliative care, there has been increased focus on improving the quality of palliative care services (15). A few studies have evaluated the effect of early vs delayed palliative care on improving healthcare outcomes prior to death. However, these studies found no difference in hospitalizations, ICU admissions, ED visits, or chemotherapy in the last 14 days of life (6, 16).

As embedded palliative care clinics become more prevalent within the oncology field, more research is necessary to demonstrate what effect this model may have on healthcare utilization outcomes. To address this knowledge gap, we evaluated the effect of the onco-pall embedded care model on healthcare utilization outcomes across the course of the disease rather than limited to the immediate days preceding end-of-life. In this study, we investigated the effect of a new onco-pall embedded care model available to providers within one Thoracic Oncology clinic at a large NCI-designated cancer center on healthcare utilization outcomes compared to a stand-alone palliative care clinic model. We hypothesized that an embedded onco-palliative care model would decrease ED visits, hospital admissions, ICU admissions, and 30-day readmissions compared to a stand-alone palliative care clinic model.

MATERIALS AND METHODS

Study Design

This was a retrospective study of patients with a diagnosis of thoracic malignancy seen by Thoracic Medical Oncology at The Ohio State University both before and after the establishment of a new embedded palliative care provider within the Thoracic Oncology clinic. Prior to development of this embedded onco-pall clinic, outpatient palliative care was only available *via* stand-alone clinic model that operates independently and in a separate location from oncology clinics. The stand-alone palliative clinic has its own dedicated interdisciplinary team including nursing staff, social work, chaplain, and clinical pharmacist. The embedded palliative care clinic model included one palliative care physician who shared clinical workspace with the medical oncology team two full days per week. The palliative care physician was flexible in scheduling and was available to evaluate the patient at the most convenient time within the clinic flow (before, after, or with the medical oncologist, or during the infusion visit). Oncology clinical resources, including nursing staff, scheduling assistants, case managers, social workers, and pharmacists, were shared with the embedded palliative physician. In both clinic models, palliative

clinic referrals are ordered per discretion of the oncology team without triggering referral guidelines. Patients seen in both the stand-alone and embedded clinic models received the same content of palliative care intervention including symptom assessment and management, advance care planning, and goals of care discussion as appropriate. End of life discussions in the embedded clinic model differed in that oncology and palliative providers frequently shared these encounters with the patient and family. All palliative clinic patients are seen monthly until symptom management has stabilized and then every 6-8 weeks thereafter unless sooner follow up is requested by the patient or oncology team. The Ohio State University Institutional Review Board approved this retrospective cross-sectional cohort study.

Patient Population

Patients included in this retrospective cohort were ≥ 18 years of age with a diagnosis of lung cancer and visited the Thoracic Oncology clinic in the designated time frame per cohort. Patients were excluded from the study if they had visited the Thoracic Oncology clinic in the preceding 1 year prior to the respective study period. This allowed for only new patients to be included in each respective study period. Patients were required to be established patients with at least two visits during the study period. Patients were required to reside within the same county (Franklin County) or one of six counties adjacent to the academic medical center (hospital catchment area). Patients may have received systemic treatment, surgery, and radiation. Systemic treatment included chemotherapy, immunotherapy, and targeted therapy. Patients evaluated between September 1, 2017 and August 31, 2018 in the Thoracic Oncology clinic were included in the pre-cohort. During this time, palliative care was available by referral to a free-standing outpatient clinic located approximately 2 miles away from the Thoracic Oncology clinic. The embedded clinic opened on September 1, 2018 in a limited capacity. There was a five-month ramp-up period until the embedded palliative care clinic was functioning at full capacity. Therefore, patients were included in the post-cohort if they were evaluated in the Thoracic Oncology clinic between February 1, 2019 and January 31, 2020.

Data Collection

Data was abstracted from the electronic medical record and included baseline demographics including age, gender, race/ethnicity, marital status, zip code, and county of residence. Clinical variables included cancer diagnosis at baseline, cancer stage at baseline, cancer treatment, Charlson comorbidity index at baseline, ED visits, hospital admissions, ICU admissions, 30-day readmissions, palliative care referral orders, and palliative care referral completion (defined as patient having been evaluated by palliative care at least once).

Statistical Analyses

Descriptive statistics were used for baseline demographics and clinical variables. Categorical variables were summarized by counts and proportions and Fisher's exact test was used for comparisons between the two cohorts. Continuous variables were summarized by median and range and comparisons between the cohorts were made using the Wilcoxon rank-sum test. Healthcare utilization outcomes, including estimates for ED visits, hospital admissions, ICU admissions, and 30-day readmissions, were calculated in rates-per-person years. Poisson regression models with robust sandwich-type standard errors and time as an offset were used for statistical analyses (17).

Patients were considered at risk for ED visits, hospital admissions, and ICU admissions following their first visit to the Thoracic Oncology clinic. For the outcome of 30-day readmissions, patients became at risk for the first 30 days following the discharge date of each hospital admission that was identified as an emergency or urgent admission unless a discharge occurred for the following reasons: 1) left against medical advice or discontinued care; 2) discharged/transferred to a designated cancer center; and 3) discharged/transferred to a short-term general hospital for inpatient care. If a patient returned within 30 days of their previous hospital discharge due to an elective procedure, this visit was not counted as a 30-day readmission. For each outcome of interest, patients exited the study when there was loss of follow-up, the patient died, or the study period ended for their cohort.

Models were adjusted for potential confounding by patient age, race (non-Hispanic white vs other), marital status (married vs unmarried), sex (male vs female), location (patient primary address within Franklin County vs adjacent county), Charlson score at baseline, and cancer type and stage at baseline (NSCLC stage 1 or 2, NSCLC stage 3, NSCLC stage 4, or SCLC). All confidence intervals are two-sided and presented at their nominal level. P-values < 0.05 were considered statistically significant. All analyses were performed in R version 4.0.0.

RESULTS

Study Sample

The final analytical sample included 474 patients, 214 patients in the pre-cohort and 260 patients in the post-cohort **(Figure 1).** Among all patients, 52% were male and 48% were female with a median age of 65 years (y) (range 31-92 y). The majority of patients were non-Hispanic white (80%). The majority of patients (66%) resided within the same county as the academic medical center and 34% resided within a county adjacent to the academic medical center (hospital catchment area). Cancer type and stage included 17% NSCLC stage 1 or 2, 20% NSCLC stage 3, 47% NSCLC stage 4, and 16% SCLC. Treatment types included surgery (3%), radiation (26%), chemotherapy (35%), immunotherapy (20%), and other (3%). Patients in the post-cohort tended to be older and to have a higher Charlson comorbidity score. Additional details on patient characteristics, tumor characteristics, and treatment characteristics are available in **Table 1**.

Healthcare Utilization Outcomes

Table 2 provides healthcare utilization outcomes for ED visits, hospital admissions, ICU admissions, and 30-day readmissions. Events per-person-year were decreased in the post-cohort

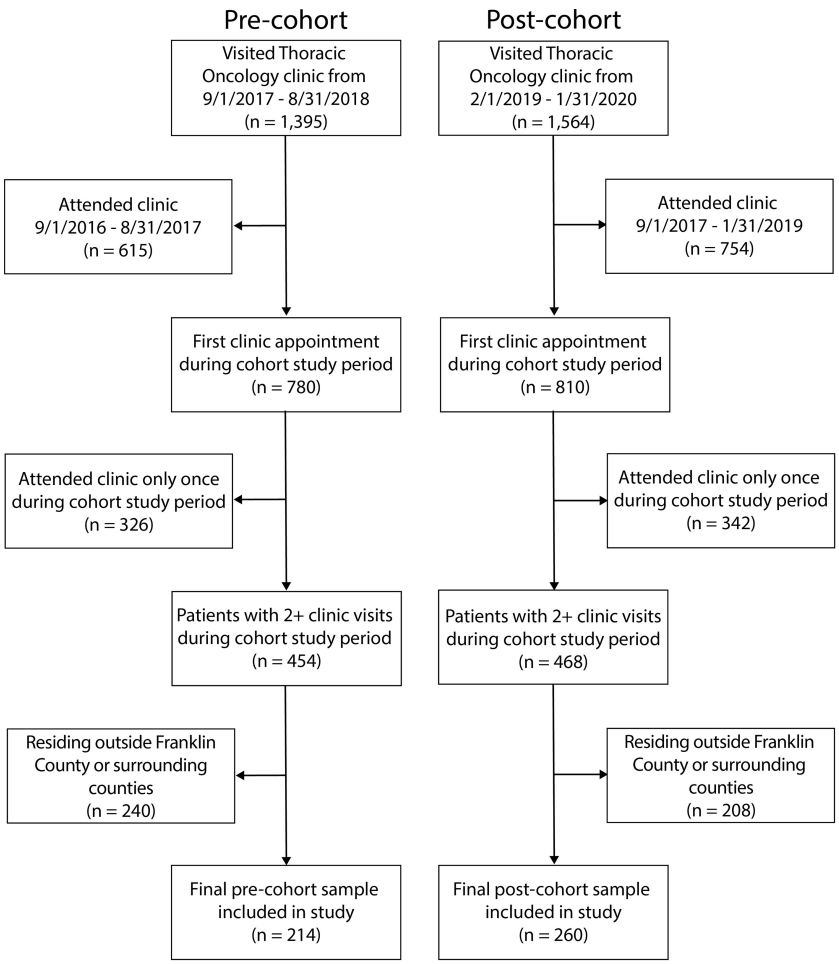

FIGURE 1 | Cohort development.

relative to the pre-cohort for ED visits (2.54 vs. 3.43), hospital admissions (3.77 vs. 4.39) and ICU admissions (0.31 vs 0.46). There was no decrease in events per-person year for 30-day readmissions observed in the post-cohort (6.71) relative to the pre-cohort (6.58). There was a statistically significant 26% reduction in ED visits in the post-cohort relative to the pre-cohort (adjusted relative risk: 0.74, 95% CI: 0.58-0.94, p-value = 0.01). Although not statistically significant, we also observed a 29% reduction in ICU admissions (adjusted relative risk: 0.71, 95% CI: 0.41-1.21, p-value = 0.21) and a 15% reduction in hospital admissions (adjusted relative risk: 0.85, 95% CI: 0.70-1.03, p-value = 0.10) in the post-cohort relative to the pre-cohort. As this study was performed at a single site, it is likely that patients who live further from the site would be less likely to be captured in the analytic data as they may preferentially visit hospitals closer to their residences. Therefore, we performed a sensitivity analysis by re-analyzing all healthcare outcomes for patients residing only within Franklin County. This analysis yielded similar results **(Appendix Table 2)**.

Palliative Care Referrals

The proportion of palliative care referrals did not differ between the two cohorts, as 16% (34/214) of patients in the pre-cohort and 18% (48/260) of patients in the post-cohort had an ambulatory palliative care referral placed. Patients in the post-cohort were more likely to complete the ambulatory palliative care referral within the 1-year observation time period 75% (36/48) compared to the pre-cohort 50% (17/34). The median time from initial medical oncology appointment to placement of a palliative care referral was decreased in the post-cohort compared to the pre-cohort (12 days vs 21 days) (**Figure 2A**). Additionally, the median time from palliative care referral to palliative referral completion was also decreased in the post-cohort compared to the pre-cohort (22 days vs 29 days) (**Figure 2B**). With both earlier referrals and earlier palliative appointment completions following the referral, the median time from initial medical oncology appointment to palliative referral completion was substantially lower in the post-cohort compared to the pre-cohort (5.8 weeks vs 23.6 weeks) (**Figure 2C**).

TABLE 1 | Patient characteristics.

Characteristic[1]	Overall (n = 474)	Pre-cohort (n = 214)	Post-cohort (n = 260)	P-value[3]
Age, median (min-max)	65 (31-92)	63 (31-86)	66 (37-92)	<0.01
Age				0.06
Under 65	228 (48.1)	116 (54.0)	112 (43.1)	
65+ and under 70	87 (18.4)	33 (15.4)	54 (20.8)	
70+ and under 75	77 (16.2)	37 (17.3)	40 (15.4)	
75+ and under 80	59 (12.4)	21 (9.8)	38 (14.6)	
80+	23 (4.9)	7 (3.3)	16 (6.2)	
Sex				>0.95
Female	227 (47.9)	102 (47.7)	125 (48.1)	
Male	247 (52.1)	112 (52.3)	135 (51.9)	
Race/ethnicity				0.82
Non-Hispanic white	377 (80.0)	172 (80.8)	205 (79.5)	
Other	94 (20)	41 (19.2)	53 (20.5)	
Unknown	3	1	2	
Marital status				0.41
Unmarried	229 (48.3)	108 (50.5)	121 (46.5)	
Married	245 (51.7)	106 (49.5)	139 (53.5)	
Residing location				0.85
Within Franklin County	312 (65.8)	142 (66.4)	170 (65.4)	
Surrounding Franklin County	162 (34.2)	72 (33.6)	90 (34.6)	
Charlson comorbidity at baseline, median (min-max)	6 (0-24)	5 (1-14)	6 (0-24)	0.07
Cancer type and stage at baseline				0.53
NSCLC Stage 1 or 2	82 (17.3)	40 (18.8)	42 (16.2)	
NSCLC Stage 3	94 (19.9)	40 (18.8)	54 (20.7)	
NSCLC Stage 4	222 (46.9)	104 (48.8)	118 (45.4)	
SCLC	75 (15.9)	29 (13.6)	46 (17.7)	
Unknown	1	1	0	
Treatment undergone during study[2]				
Chemotherapy	165 (34.8)	84 (39.3)	81 (31.2)	0.07
Radiation	125 (26.4)	61 (28.5)	64 (24.6)	0.35
Immunotherapy	95 (20.0)	42 (19.6)	53 (20.4)	0.91
Surgery	15 (3.2)	10 (4.7)	5 (1.9)	0.11
Other therapy	15 (3.2)	12 (5.6)	3 (1.2)	0.01

[1]*Presented as n (%) unless otherwise indicated.*
[2]*Patients could undergo more than one treatment during the course of the study.*
[3]*P-values calculated using Fisher's exact test for categorical variables and Wilcoxon rank-sum test for continuous variables.*
NSCLC, non-small cell lung cancer.
SCLC, small-cell lung cancer.

TABLE 2 | Healthcare utilization comparing pre- versus post-cohort.

	Number of events	Total person-years of exposure	Events per-person-year (95% CI)	Relative risk (95% CI)	Adjusted relative risk (95% CI)[1]
ICU admissions					
Pre-cohort	36	78.8	0.46 (0.32-0.63)	Reference	Reference
Post-cohort	30	96.4	0.31 (0.21-0.44)	0.68 (0.40-1.16)	0.71 (0.41-1.21)
ED visits					
Pre-cohort	270	78.8	3.43 (3.03-3.86)	Reference	Reference
Post-cohort	245	96.4	2.54 (2.23-2.88)	0.74 (0.58-0.94)	0.74 (0.58-0.94)
Hospital Admissions					
Pre-cohort	346	78.8	4.39 (3.94-4.88)	Reference	Reference
Post-cohort	363	96.4	3.77 (3.39-4.17)	0.86 (0.71-1.03)	0.85 (0.70-1.03)
30-day readmissions[2]					
Pre-cohort	74	11.2	6.58 (5.17-8.26)	Reference	Reference
Post-cohort	69	10.3	6.71 (5.22-8.49)	1.02 (0.71-1.46)	1.03 (0.73-1.45)

[1]*Adjusted for age, race (Non-Hispanic white vs other), marital status (married vs unmarried), sex (male vs female), location (patient primary address within Franklin County vs adjacent county), Charlson score at baseline, cancer type and cancer stage at baseline (NSCLC stage 1 or 2, NSCLC stage 3, NSCLC stage 4, or SCLC).*
[2]*Individuals had at most 30 days of risk of a hospital readmission after each hospital admission.*
ICU, intensive care unit.
ED, emergency department.
CI, confidence interval.

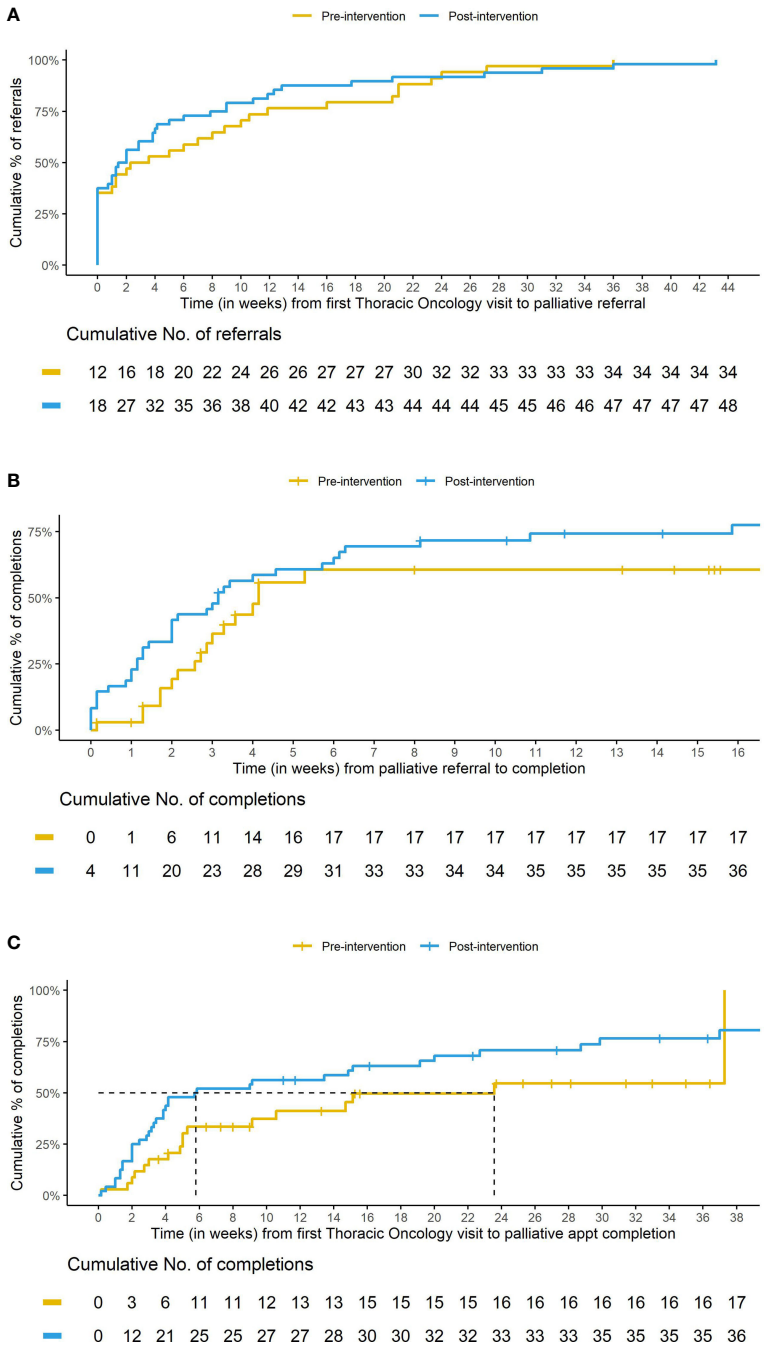

FIGURE 2 | Cumulative incidence curves comparing pre- versus post-cohort. Caption: **(A)** Time (in weeks) from first Thoracic Oncology visit to palliative referral for patients with a palliative referral. Caption **(B)** Time (in weeks) from palliative referral to palliative appointment completion. Caption **(C)** Time (in weeks) from first Thoracic Oncology visit to palliative appointment completion for those with a palliative referral. Note the shorter length of time to median palliative appointment completion for those in the post- cohort. This decrease is likely due to patients being referred earlier **(A)** and completing their palliative appointment sooner **(B)**.

To further evaluate the impact of embedded palliative care on ED visits, we analyzed emergency department visits before and after palliative care intervention in both cohorts (**Table 3**). This analysis included only those patients who completed a palliative care referral in the respective study period which consisted of 17 patients in the pre-cohort and 36 patients in the post-cohort. ED visits before palliative care consultation included any ED visit that occurred after the first Thoracic Oncology visit and prior to the patient being evaluated by palliative care and ED visits after palliative care consultation included any ED visit that occurred

after a patient's initial palliative care appointment and prior to the end of the study period. ED visits per-person-year decreased following palliative care intervention in both cohorts. ED visits decreased by approximately 50% in the pre-cohort (8.6 vs 4.1) and approximately 80% in the post-cohort (7.5 vs 1.5). ED visits following palliative care intervention decreased in the post-cohort, after the establishment of the embedded clinic model, compared to the pre-cohort, when only the stand-alone model existed (1.5 vs 4.1).

DISCUSSION

To our knowledge, this is the first study to evaluate the impact of a newly embedded onco-pall care model on healthcare utilization across the course of disease and not specifically focusing on end-of-life quality metrics. Early palliative care intervention is beneficial for patients with a new thoracic malignancy but there are still many challenges in care delivery. Prior research by Agne et al. identified "time burden to patients" as the primary logistical barrier to outpatient palliative care referral (18). In an effort to overcome this barrier, we established a palliative care clinic embedded within the thoracic medical oncology clinic. In contrast to prior studies (14), we found the embedded clinic model resulted in decreased healthcare utilization compared to the stand-alone clinic model.

We found a statistically significant decrease in ED visit rates in the post-cohort study period. This decrease may be due to improved access to palliative care and symptom management earlier in the disease course. Although only the outcome of ED visits was statistically significantly lowered, this study may not have been powered to detect a statistically significant difference in ICU and hospital admissions. However, using point estimates from the models, this translates into a 29% decrease in ICU admissions ($980k), 15% decrease in hospitalizations ($1.6 million), and a 26% decrease in ED visits ($86k) for a total of 2.7 million in annual savings. This observed decrease in healthcare utilization is both fiscally and clinically important. Additional research is warranted to further evaluate the fiscal impact of the embedded clinic model. Although ED visits, ICU visits, and hospital admissions were decreased, there was no observable impact on 30-day readmissions. One possible explanation for the lack of impact on 30-day readmissions is that patients are readmitted to the hospital shortly after discharge prior to being evaluated in the onco-pall clinic.

While there was no observed difference in the proportion of palliative care referral orders between the pre-cohort and the post-cohort, the frequency of completion of palliative care referral was increased in the post-cohort and the time from initial medical oncology appointment to completed palliative care appointment was substantially decreased in the post-cohort. Both the increased involvement of palliative care as well as the earlier involvement of palliative care could potentially contribute to the decrease in healthcare utilization outcomes observed in the post-cohort, as patients referred to palliative care had an outsized impact on healthcare utilization. For example, although 17% of all patients seen in the onco-pall clinic in the two years of the study were referred to palliative care, these patients accounted for 30% of all ED visits **(Appendix Table 2)**.

The involvement of multidisciplinary teams is recommended to provide high-quality cancer care and has been found to enhance communication among and improve knowledge among healthcare providers (19). Therefore, it is possible that the shared workspace for palliative care and medical oncology permitted additional informal input from palliative care which may have improved symptom control and contributed to the decrease in healthcare utilization even for those not formally seen by palliative care **(Appendix Table 2)**. For this reason, all patients seen in the onco-pall clinic in the respective time periods were included in the study rather than only those referred to palliative care. There is some evidence of this multidisciplinary team effect in our study in that patients seen in the pre-cohort who were never referred to palliative care had increased healthcare utilization compared to patients seen in the post-cohort who were never referred to palliative care.

Though it should be considered exploratory due to the small number of patients, data regarding the frequency of ED visits both before and after palliative care intervention provide additional support that the development of the embedded clinic model decreased rates of ED visits. When only the stand-alone clinic model was available, ED visits for patients seen by palliative care decreased by a factor of 2. After the development of the embedded clinic model, ED visits for patients seen by palliative care decreased by a factor of 5. While these results should be interpreted with caution due to the small sample size, patients referred to palliative care likely have advanced disease and greater symptom burden and therefore have a greater potential for high healthcare utilization. One possible explanation for the decrease in ED visits seen in the embedded clinic model is that this model may facilitate easier access to palliative care for those patients who may otherwise be too sick

TABLE 3 | Emergency department (ED) visits comparing pre- and post-cohort before and after palliative care consultation.

	Pre-cohort (n = 17)	Post-cohort (n = 36)
Before palliative consultation		
Number of ED visits	24	41
Total observation time, years	2.8	5.5
ED visits per-person years	8.6	7.5
After palliative consultation		
Number of ED visits	19	17
Total observation time, years	4.7	11.4
ED visits per-person years	4.1	1.5

ED, emergency department.

and less likely to complete palliative care or continue to seek care through the stand-alone model. Additionally, after establishing with palliative care, patients gain access to additional resources including palliative care pharmacists and palliative phone triage for additional symptom management.

Limitations of our study include the relatively small analytic sample size and inability to obtain healthcare utilization data that occurred at a site other than the academic medical center. The study also may not have been powered to detect differences in the healthcare utilization outcomes of hospital admissions and ICU admissions. Although this study would benefit from additional years of data, the impact of the COVID-19 pandemic would likely confound the results of this study. While we identified and controlled for several confounders, it is possible there were additional unmeasured confounders that affected these results. Additionally, reasons for palliative care referral were not collected as a part of this study and palliative care intervention in the embedded clinic model was provided by one palliative care physician. More details regarding reasons for palliative care referral and expansion of the embedded model to involve additional palliative care providers would be of benefit.

In conclusion, embedding palliative care within medical oncology has the potential to decrease healthcare utilization for patients with thoracic malignancies earlier in the disease course in addition to end-of-life outcomes.

DATA AVAILABILITY STATEMENT

The raw data supporting the conclusions of this article will be made available by the authors, without undue reservation.

ETHICS STATEMENT

The studies involving human participants were reviewed and approved by The Ohio State University Institutional Review Board. Written informed consent for participation was not required for this study in accordance with the national legislation and the institutional requirements.

AUTHOR CONTRIBUTIONS

EB, JA, and CP: conceptualization. KG, JB, MG, SJ, MS, PK, EB, JA, and CP: data collection. JB and SJ: data analysis. KG and JB: drafting original version. EB, JA, and CP: supervision. All authors read and approved the final version of this manuscript.

FUNDING

Funding for the development of the onco-pall clinic provided by private donor, Vicky Lippert. Research support was provided by the REDCap project and The Ohio State University Center for Clinical and Translational Science grant support (National Center for Advancing Translational Sciences, Grant UL1TR002733). CP is currently supported by the National Institute of Aging: 1K76AB074923-01. Research reported in this publication was supported by The Ohio State University Comprehensive Cancer Center and the National Institutes of Health under grant number P30 CA016058. We thank the Biostatistics Shared Resource (BSR) at The Ohio State University Comprehensive Cancer Center, Columbus, OH, for biostatistical support of this study. The funders were not involved in the study design, collection, analysis, interpretation of data, the writing of this article or the decision to submit it for publication.

ACKNOWLEDGMENTS

The authors wish to acknowledge the contributions of Kamila Jaroniec, M.F.A., Technical Editor, Division of Medical Oncology, Department of Internal Medicine, The Ohio State University Wexner Medical Center, in the revision of this manuscript.

SUPPLEMENTARY MATERIAL

The Supplementary Material for this article can be found online at: https://www.frontiersin.org/articles/10.3389/fonc.2022.835881/full#supplementary-material

REFERENCES

1. Temel JS, Greer JA, Muzikansky A, Gallagher ER, Admane S, Jackson VA, et al. Early Palliative Care for Patients With Metastatic Non-Small-Cell Lung Cancer. *N Engl J Med* (2010) 363(8):733–42. doi: 10.1056/NEJMoa1000678
2. Temel JS, Greer JA, El-Jawahri A, Pirl WF, Park ER, Jackson VA, et al. Effects of Early Integrated Palliative Care in Patients With Lung and GI Cancer: A Randomized Clinical Trial. *J Clin Oncol* (2017) 35(8):834–41. doi: 10.1200/JCO.2016.70.5046
3. Vanbutsele G, Pardon K, Van Belle S, Surmont V, De Laat M, Colman R, et al. Effect of Early and Systematic Integration of Palliative Care in Patients With Advanced Cancer: A Randomised Controlled Trial. *Lancet Oncol* (2018) 19 (3):394–404. doi: 10.1016/S1470-2045(18)30060-3
4. Zimmermann C, Swami N, Krzyzanowska M, Hannon B, Leighl N, Oza A, et al. Early Palliative Care for Patients With Advanced Cancer: A Cluster-Randomised Controlled Trial. *Lancet* (2014) 383(9930):1721–30. doi: 10.1016/S0140-6736(13)62416-2
5. Ferrell B, Sun V, Hurria A, Cristea M, Raz DJ, Kim JY, et al. Interdisciplinary Palliative Care for Patients With Lung Cancer. *J Pain Symptom Manage* (2015) 50(6):758–67. doi: 10.1016/j.jpainsymman.2015.07.005
6. Bakitas MA, Tosteson TD, Li Z, Lyons KD, Hull JG, Dionne-Odom JN, et al. Early Versus Delayed Initiation of Concurrent Palliative Oncology Care: Patient Outcomes in the ENABLE III Randomized Controlled Trial. *J Clin Oncol* (2015) 33(13):1438–45. doi: 10.1200/JCO.2014.58.6362
7. Ferrell BR, Temel JS, Temin S, Smith TJ. Integration of Palliative Care Into Standard Oncology Care: ASCO Clinical Practice Guideline Update Summary. *J Oncol Pract* (2017) 13(2):119–21. doi: 10.1200/JOP.2016.017897
8. Hui D, Hannon BL, Zimmermann C, Bruera E. Improving Patient and Caregiver Outcomes in Oncology: Team-Based, Timely, and Targeted Palliative Care. *CA Cancer J Clin* (2018) 68(5):356–76. doi: 10.3322/caac.21490
9. Hui D, Cerana MA, Park M, Hess K, Bruera E. Impact of Oncologists' Attitudes Toward End-Of-Life Care on Patients' Access to Palliative Care. *Oncologist* (2016) 21(9):1149–55. doi: 10.1634/theoncologist.2016-0090

10. Hui D, de la Rosa A, Chen J, Dibaj S, Delgado Guay M, Heung Y, et al. State of Palliative Care Services at US Cancer Centers: An Updated National Survey. *Cancer* (2020) 126(9):2013–23. doi: 10.1002/cncr.32738
11. Muir JC, Daly F, Davis MS, Weinberg R, Heintz JS, Paivanas TA, et al. Integrating Palliative Care Into the Outpatient, Private Practice Oncology Setting. *J Pain Symptom Manage* (2010) 40(1):126–35. doi: 10.1016/j.jpainsymman.2009.12.017
12. Einstein DJ, DeSanto-Madeya S, Gregas M, Lynch J, McDermott DF, Buss MK. Improving End-Of-Life Care: Palliative Care Embedded in an Oncology Clinic Specializing in Targeted and Immune-Based Therapies. *J Oncol Pract* (2017) 13(9):e729–e37. doi: 10.1200/JOP.2016.020396
13. Walling AM, D'Ambruoso SF, Malin JL, Hurvitz S, Zisser A, Coscarelli A, et al. Effect and Efficiency of an Embedded Palliative Care Nurse Practitioner in an Oncology Clinic. *J Oncol Pract* (2017) 13(9):e792–9. doi: 10.1200/JOP.2017.020990
14. Yennurajalingam S, Prado B, Lu Z, Naqvi S, Williams JL, Lim T, et al. Outcomes of Embedded Palliative Care Outpatients Initial Consults on Timing of Palliative Care Access, Symptoms, and End-Of-Life Quality Care Indicators Among Advanced Nonsmall Cell Lung Cancer Patients. *J Palliat Med* (2018) 21(12):1690–7. doi: 10.26226/morressier.5afadd8bf314ac000849b2ec
15. National Quality Forum. National Voluntary Consensus Standards: Palliative Care and End-Of-Life Care, A Consensus Report. (2012). Available at: https://www.qualityforum.org/Publications/2012/04/Palliative_Care_and_End-of-Life_Care%E2%80%.
16. Vanbutsele G, Van Belle S, Surmont V, De Laat M, Colman R, Eecloo K, et al. The Effect of Early and Systematic Integration of Palliative Care in Oncology on Quality of Life and Health Care Use Near the End of Life: A Randomised Controlled Trial. *Eur J Cancer* (2020) 124:186–93. doi: 10.1016/j.ejca.2019.11.009
17. White H. A Heteroskedasticity-Consistent Covariance Matrix Estimator and a Direct Test for Heteroskedasticity. *Econometrica* (1980) 48(4):21. doi: 10.2307/1912934
18. Agne JL, Bertino EM, Grogan M, Benedict J, Janse S, Naughton M, et al. Too Many Appointments: Assessing Provider and Nursing Perception of Barriers to Referral for Outpatient Palliative Care. *Palliat Med Rep* (2021) 2(1):137–45. doi: 10.1089/pmr.2020.0114
19. Devitt B, Philip J, McLachlan SA. Team Dynamics, Decision Making, and Attitudes Toward Multidisciplinary Cancer Meetings: Health Professionals' Perspectives. *J Oncol Pract* (2010) 6(6):e17–. doi: 10.1200/JOP.2010.000023

Conflict of Interest: The authors declare that the research was conducted in the absence of any commercial or financial relationships that could be construed as a potential conflict of interest.

Publisher's Note: All claims expressed in this article are solely those of the authors and do not necessarily represent those of their affiliated organizations, or those of the publisher, the editors and the reviewers. Any product that may be evaluated in this article, or claim that may be made by its manufacturer, is not guaranteed or endorsed by the publisher.

frontiers in Oncology

ORIGINAL RESEARCH
published: 31 March 2022
doi: 10.3389/fonc.2022.835582

A Geriatric Assessment Intervention to Reduce Treatment Toxicity Among Older Adults With Advanced Lung Cancer: A Subgroup Analysis From a Cluster Randomized Controlled Trial

Carolyn J. Presley[1], Mostafa R. Mohamed[2], Eva Culakova[3], Marie Flannery[4], Pooja H. Vibhakar[1], Rebecca Hoyd[1], Arya Amini[5], Noam VanderWalde[6], Melisa L. Wong[7], Yukari Tsubata[8], Daniel J. Spakowicz[1] and Supriya G. Mohile[2,3]*

[1] Division of Medical Oncology, Department of Internal Medicine, The Ohio State University, Columbus, OH, United States, [2] Department of Medicine, University of Rochester Medical Center, Rochester, NY, United States, [3] Department of Surgery, University of Rochester Cancer Center National Cancer Institute (NCI) Community Oncology Research Program (NCORP) Research Base, Rochester, NY, United States, [4] Department of Radiation Oncology, School of Nursing, University of Rochester, Rochester, NY, United States, [5] Department of Radiation Oncology, City of Hope Comprehensive Cancer Center, Duarte, CA, United States, [6] West Cancer Center & Research Institute, Memphis, TN, United States, [7] Divisions of Hematology/Oncology and Geriatrics, Department of Medicine, University of California, San Francisco, San Francisco, CA, United States, [8] Division of Medical Oncology and Respiratory Medicine, Department of Internal Medicine, Shimane University Faculty of Medicine, Izumo, Japan

OPEN ACCESS

Edited by:
Jessica Desiree Menis, Integrated University Hospital Verona, Italy

Reviewed by:
Francesco Cuccia, Sacro Cuore Don Calabria Hospital (IRCCS), Italy
Andrea Camerini, Azienda Usl Toscana Nord Ovest, Italy

***Correspondence:**
Carolyn J. Presley
carolyn.presley@osumc.edu

Specialty section:
This article was submitted to Thoracic Oncology, a section of the journal Frontiers in Oncology

Received: *14 December 2021*
Accepted: *04 March 2022*
Published: *31 March 2022*

Citation:
Presley CJ, Mohamed MR, Culakova E, Flannery M, Vibhakar PH, Hoyd R, Amini A, VanderWalde N, Wong ML, Tsubata Y, Spakowicz DJ and Mohile SG (2022) A Geriatric Assessment Intervention to Reduce Treatment Toxicity Among Older Adults With Advanced Lung Cancer: A Subgroup Analysis From a Cluster Randomized Controlled Trial. Front. Oncol. 12:835582. doi: 10.3389/fonc.2022.835582

Introduction: More older adults die from lung cancer worldwide than breast, prostate, and colorectal cancers combined. Current lung cancer treatments may prolong life, but can also cause considerable treatment-related toxicity.

Objective: This study is a secondary analysis of a cluster-randomized clinical trial which evaluated whether providing a geriatric assessment (GA) summary and GA-guided management recommendations can improve grade 3-5 toxicity among older adults with advanced lung cancer.

Methods: We analyzed participants aged ≥70 years(y) with stage III & IV (advanced) lung cancer and ≥1 GA domain impairment starting a new cancer treatment with high-risk of toxicity within the National Cancer Institute's Community Oncology Research Program. Community practices were randomized to the intervention arm (oncologists received GA summary & recommendations) versus usual care (UC: no summary or recommendations given). The primary outcome was grade 3-5 toxicity through 3 months post-treatment initiation. Secondary outcomes included 6-month (mo) and 1-year overall survival (OS), treatment modifications, and unplanned hospitalizations. Outcomes were analyzed using generalized linear mixed and Cox proportional hazards models with practice site as a random effect. ***Trial Registration:*** NCT02054741.

Results & Conclusion: Among 180 participants with advanced lung cancer, the mean age was 76.3y (SD 5.1), 39.4% were female and 82.2% had stage IV disease. The proportion of patients who experienced grade 3-5 toxicity was significantly lower in the

intervention arm vs UC (53.1% vs 71.6%, P=0.01). More participants in the intervention arm received lower intensity treatment at cycle 1 (56.3% vs 35.3%; P<0.01). Even with a cycle 1 dose reduction, OS at 6mo and 1 year was not significantly different (adjusted hazard ratio [HR] intervention vs. UC: 6mo HR=0.90, 95% CI: 0.52-1.57, P=0.72; 1 year HR=0.89, 95% CI: 0.58-1.36, P=0.57). Frequent toxicity checks, providing education and counseling materials, and initiating direct communication with the patient's primary care physician were among the most common GA-guided management recommendations. Providing a GA summary and management recommendations can significantly improve tolerability of cancer treatment among older adults with advanced lung cancer.

Keywords: treatment toxicities, geriatric assessment, lung cancer, older adult, clinical trial

INTRODUCTION

Over 75% of all new non-small cell lung cancer (NSCLC) diagnoses are among adults ≥65 years of age (1). As lung cancer is generally a disease of older adults, cancer and aging research is significant because the population of older adults is large and growing. By 2030, nearly two-thirds of all cancer diagnoses will be among older adults (2, 3). More older adults die from lung cancer worldwide than any other cancer type (1). In the United States, among adults ≥65 years, 289 men and women per 100,000 will develop lung cancer (4). However, clinical trials include almost exclusively younger adults, thereby limiting external generalizability of clinical results to older adults, particularly in regard to toxicity and response to novel cancer drugs (5, 6). With the rapid approval of novel cancer drugs, the lack of evidence among older adults in pivotal trials continues to grow (7). A lack of clinical trial evidence perpetuates uncertainty for clinicians, patients, and families regarding important clinical outcomes such as treatment-related toxicity among older adults receiving lung cancer treatment within the community oncology setting. In addition, clinical trials include the healthiest older adults with little to no information on older adults with complex geriatric conditions.

Prior research has demonstrated that older adults with cancer have a high prevalence of characteristics that are associated with a greater risk of chemotherapy toxicity (8, 9). A geriatric assessment (GA) can identify areas of vulnerability (e.g., functional impairment, cognitive impairment, polypharmacy) and thus direct GA-guided management for older adults receiving cancer treatment (10–13). The GA has great potential to identify areas of vulnerability and develop recommendations that could help improve outcomes (e.g., treatment toxicity) among older adults with cancer (14–16). However, this type of evaluation is not routinely incorporated into the oncology clinical evaluation. A critical knowledge gap exists in respect to whether provision of GA information along with GA-guided management recommendations to the oncology treatment team would improve outcomes among older adults with advanced lung cancer receiving cancer treatment with a high risk of toxicity.

Balancing the benefits and risks of chemotherapy in the older adult patient population with advanced cancer is challenging because of the dearth of evidence-based data to guide these decisions (17, 18). Furthermore, older patients who are treated with chemotherapy are at high risk for adverse outcomes, including chemotherapy toxicity and functional and physical consequences (19–21). In addition, older adults are more susceptible to toxicity from combination chemotherapy plus newer immunotherapy or targeted kinase inhibitors (22–25). In a randomized controlled trial by Corre et al, GA-guided lung cancer treatment strategies have been shown to lower symptomatic toxicities and improve other clinical outcomes among older adults receiving chemotherapy for advanced lung cancer (26). There was no difference seen in overall survival between the GA-directed arm versus usual care; yet, 23% of the patients treated in the GA-directed arm did not receive chemotherapy. A more recent large cluster-randomized controlled trial (GAP-70+) demonstrated that GA-guided management recommendations could decrease the proportion of older adults who experienced a serious grade 3-5 toxicity from a new cancer treatment regimen for advanced cancer (>80% had stage IV disease) (27). A lower proportion of patients in the intervention arm experienced grade 3-5 toxicity (177/349; 50.7%) than in usual care (263/369; 71.3%); relative risk (RR) was 0.74 (95% CI: 0.64-0.86; p<0.001) (27). GA-guided recommendations can focus on managing symptomatic toxicities from cancer treatment among patients with functional impairments or can be interventions that are known to improve outcomes of older adults with geriatric syndromes (e.g., physical therapy and fall prevention education in patients who are falling or who are at risk for falling).

The primary goal of this secondary GAP-70+ analysis was to evaluate whether providing a GA summary and GA-guided management recommendations could decrease grade 3-5 toxicity specifically among older adults with advanced lung cancer.

METHODS

Study Design

This is a secondary data analysis of the participants with lung cancer from the cluster-randomized clinical trial entitled "Geriatric Assessment for Patients 70 years and older (GAP-70

+; NCT02054741)." Community oncology practices within the National Cancer Institute Community Oncology Research Program (NCORP) were randomized to the intervention arm (oncologists received GA summary & management recommendations) or usual care (UC: no summary or recommendations given; notifications were provided to oncologists for patients who screened positive for depression and severe cognitive impairment). NCORP practices were recruited through the University of Rochester National Cancer Institute (NCI) Research Base network (UR NCORP). NCORP is a national network of community cancer clinical trial practice sites in the United States (https://ncorp.cancer.gov/about/). Practice clusters were comprised of NCORP-affiliated community oncology practices. Participating practice clusters represent a large geographic area across the United States of which 33/40 practices enrolled patients with lung cancer. The UR Research Base coordinated study activities, but the UR did not enroll participants. The UR (Rochester, NY, USA) and all participating practice clusters obtained approval from their institutional review boards. All patients completed informed consent.

Participants

Participants were recruited from July 2014-March 2019. Participants aged ≥70 years(y) with advance solid tumors or lymphoma and ≥1 GA domain impairment (other than polypharmacy) starting a new cancer treatment regimen with a high risk of toxicity within 4 weeks of enrollment were included. Participants were required to be able to understand English and provide written informed consent independently or with a healthcare proxy. For inclusion in this secondary analysis, participants with advanced (non-surgical stage III/IV) lung cancer, either NSCLC or extensive stage small cell lung cancer (ES-SCLC), were selected. Treatment regimens had to include at least one chemotherapy agent or have a >50% prevalence of grade 3-5 toxicity as determined by the primary oncologist with review and approval by a clinical team blinded to study arm at the Research Base (27, 28). The treating oncologists selected the specific treatment regimen, dosing, and schedules.

Procedures

Community oncology practice clusters were randomized to the GA intervention versus UC arm, stratified by large or small based on prior accrual records. Participants in both arms completed a GA and were asked about proposed treatment plan before starting a new treatment regimen. Participants in the intervention arm were additionally given recommendations before starting a new treatment regimen. Oncologists in the intervention arm were provided with a tailored GA summary and GA-guided management recommendations before any cancer treatment was initiated. The GA evaluated 8 domains: comorbidity, cognition, physical performance, functional status, nutritional status, social support, polypharmacy, and psychological health. The recommendations provided based on GA domain impairment can be found in detail in the supplemental documents of Mohile et al. (27) Oncologists in the UC arm received notification for depression or severe cognitive impairment on screening tests, but no management recommendations were provided. There was no patient or provider blinding as this study evaluated a model of care rather than a particular treatment agent; however, all research investigators were blinded to the site assignment when the treatment and toxicity data were reviewed centrally.

Outcomes

The primary outcome was grade 3-5 toxicity within 3 months of starting a new treatment regimen. Secondary outcomes included unplanned hospitalizations, subsequent dose reduction, dose delay, treatment discontinuation, overall survival (OS) at 6-month (mo) and 1-year in addition to cycle 1 treatment intensity (standard vs reduced). Practice staff prospectively captured toxicities over 3 months using NCI's Common Terminology Criteria for Adverse Events (V4.0). Blinded oncology clinicians reviewed medical records to verify all treatment and toxicity data. At UR NCORP, two blinded clinicians reviewed each enrolled patient's medical record and treatment regimen and used guidelines and clinical trials to determine standard dosing and length for treatment regimens. We evaluated the proportion of patients who received a reduced intensity regimen (e.g., lower dose or omission of an agent compared to standard) at cycle one. Standard treatment was evaluated according to National Comprehensive Cancer Network guidelines (29) of published phase II/III clinical trials. The blinded clinicians also reviewed medical records to evaluate unplanned hospitalizations (an overnight hospital stay for any reason that was not scheduled), dose reductions, dose delays, and treatment discontinuation. These were assessed by comparing what the patient received compared to what was planned by the oncologist at the start of treatment. Outcomes captured those changes related to clinical reasons (e.g., toxicity, patient preference) but not logistical reasons (e.g., holiday).

Statistical Analysis

Descriptive statistics were performed to summarize demographics, GA measures, baseline clinical characteristics, and outcome measures. Bivariate analyses using chi-square tests for categorical variables and *t* tests for continuous variables were done to compare differences between study arms. A Generalized Linear Mixed Model (GLMM) was applied to analyze the primary outcome of grade 3-5 toxicity within 3 months with practice site as a random effect and study arm as a fixed effect. Proportions of patients who experienced grade 3-5 toxicity in the intervention vs UC arm were calculated by odds ratio adjusted for practice site. Kaplan-Meier method was used to estimate 6-month and 1-year OS and the effect of the intervention on OS was assessed by Cox Shared Frailty Model with practice sites as random effects. Similar to the primary outcome, GLMMs were applied to evaluate secondary outcomes (hospitalization, subsequent dose reduction, dose delay, treatment discontinuation, and reduced treatment intensity at cycle 1). Two-sided p values of <0.05 were considered statistically significant. All analyses were conducted using SAS 9.4 (SAS Institute, Cary, NC).

RESULTS

Among 180 participants with advanced lung cancer (NSCLC + ES-SCLC), the mean age was 76.3y (range 70-91, SD 5.1), 39.4% were female and 82.2% had stage IV disease. Patients in both arms (64 participants in the intervention and 116 participants in the UC arm) had similar baseline characteristics including age, sex, race/ethnicity, marital status, education, and income (**Table 1**). The majority of participants received platinum doublet chemotherapy (>70%). The GA domain impairments had similar distributions across arms. The mean number of geriatric impairments was 4.7 (SD: 1.5) and did not differ between study arms. The physical performance domain impairment was the most prevalent GA impaired domain (>90% in both arms). This was followed by polypharmacy, comorbidity, functional status, and nutritional domain impairment (**Table 1**).

TABLE 1 | Patient Characteristics by Study Arm.

	All patients (N = 180)	Intervention arm (N = 64)	Usual care arm (N = 116)	P-values
Age (mean [standard deviation])	76.3 (5.1)	76.3 (5.3)	76.2 (4.9)	0.88
70-79	138 (76.7%)	46 (71.9%)	92 (79.3%)	0.12*
80-89	37 (20.6%)	17 (26.6%)	20 (17.2%)	
≥90	4 (2.2%)	0 (0.0%)	4 (3.5%)	
Missing	1 (0.6%)	1 (1.6%)	0 (0.0%)	
Sex				0.34
Male	108 (60.0%)	41 (64.1%)	67 (57.8%)	
Female	71 (39.4%)	22 (34.4%)	49 (42.2%)	
Missing	1 (0.6%)	1 (1.6%)	0 (0.0%)	
Race/Ethnicity				0.22*
Non-Hispanic White	164 (91.1%)	55(85.9%)	109 (94.0%)	
Black	7 (3.9%)	3 (4.7%)	4 (3.5%)	
Others	8 (4.4%)	5 (7.8%)	3 (2.6%)	
Missing	1 (0.6%)	1 (1.6%)	0 (0.0%)	
Marital Status				0.46*
Single, Never Married	3 (1.7%)	2 (3.1%)	1 (0.86%)	
Married/Domestic Partnership	111 (61.7%)	40 (62.5%)	71 (61.2%)	
Separated/Widowed/Divorced	65 (36.1%)	21 (32.8%)	44 (37.9%)	
Missing	1 (0.6%)	1 (1.6%)	0 (0.0%)	
Education				0.99
<High school	36 (20.0%)	13 (20.3%)	23 (19.8%)	
High school graduate	58 (32.2%)	20 (31.3%)	38 (32.8%)	
Some college or above	85 (47.2%)	30 (46.9%)	55 (47.4%)	
Missing	1 (0.6%)	1 (1.6%)	0 (0.0%)	
Income				0.49
≤$50,000	100 (55.6%)	39 (60.9%)	61 (52.6%)	
>$50,000	39 (21.7%)	12 (18.8%)	27 (23.3%)	
Decline to answer	40 (22.2%)	12 (18.8%)	28 (24.1%)	
Missing	1 (0.6%)	1 (1.6%)	0 (0.0%)	
Cancer stage and lung cancer type				0.05*
Stage III NSCLC	30 (16.7%)	16 (25.0%)	14 (12.1%)	
Stage IV NSCLC	148 (82.2%)	48 (75.0%)	100 (86.2%)	
ES-SCLC	2 (1.1%)	0 (0.0%)	2 (1.7%)	
Prior chemotherapy	28 (15.6%)	7 (10.9%)	21 (18.1%)	0.16
Treatment Regimen (Chi-square test)				
Chemo platinum doublet	134(74.4%)	45 (70.3%)	89 (76.7%)	0.38
Chemo+ immunotherapy	21 (11.7%)	8 (12.5%)	13 (11.2%)	
Single agent chemo	21 (11.7%)	8 (12.5%)	13 (11.2%)	
Other**	4 (2.2%)	3 (4.7%)	1 (0.8%)	
Number of Impaired Geriatric Assessment Domains (mean [SD])**	4.7 (1.5)	4.8 (1.5)	4.7 (1.4)	0.59
Physical performance domain impairment	167 (92.8%)	58 (90.6%)	109 (94.0%)	0.41
Polypharmacy domain impairment	151 (83.9%)	55 (85.9%)	96 (82.8%)	0.58
Comorbidity domain impairment	125 (69.4%)	45 (70.3%)	80 (69.0%)	0.85
Functional status domain impairment	115 (63.9%)	39 (60.9%)	76 (65.5%)	0.54
Nutrition domain impairment	124 (68.9%)	46 (71.9%)	78 (67.2%)	0.52
Cognition domain impairment	61 (33.9%)	23 (35.9%)	38 (32.8%)	0.67
Social support domain impairment	45 (25·0%)	20 (31.3%)	25 (21.6%)	0.15
Psychological status domain impairment	61 (33.9%)	21 (32.8%)	40 (34.5%)	0.82

33% of the cells have expected counts less than 5. Chi-Square may not be a valid test.

**other included: targeted, targeted + chemo, or multiple chemo (no platinum).*

Sixty-five percent of all participants experienced a grade 3-5 toxicity (**Figure 1**). The proportion of patients who experienced grade 3-5 toxicity was lower in the intervention vs. UC arm (53.1% vs 71.6%, P=0.01). After accounting for practice sites as a random effect, the odds of any grade 3-5 toxicity were lower in the intervention vs. UC arm (Adjusted odds ratio=0.45 95% CI: 0.24-0.86, P=0.01, **Figure 2**). More participants in the intervention group received lower intensity treatment at cycle 1 (56.3% vs 35.3%; P<0.01). Unplanned hospitalizations, dose delay, and early discontinuation were similar across groups. Subsequent dose reduction post-C1 was significantly higher in the UC arm (P=0.02, **Table 2**).

The OS at 6mo and 1 year was not significantly different between arms (**Figures 3A, B**: adjusted hazard ratio [HR] interventions vs. UC: 6mo HR=0.90, 95% CI: 0.52-1.57, P=0.72; 1 year HR=0.89, 95% CI: 0.58-1.36, P=0.57). Frequent toxicity checks, providing education and counseling materials, and initiating direct communication with the patient's primary care physician were among the most common GA-guided interventions recommended and acknowledged by the treating oncologist (**Table 3**).

DISCUSSION

Providing GA information and recommendations can improve tolerability of cancer treatment among older adults with advanced lung cancer. Despite a significant difference in C1 dose reduction between arms (56.3% in the intervention arm versus 35.3% in the UC arm), there was no significant difference in 6-month or 1-year OS. However, there was a significantly decreased risk of grade 3-5 toxicity for the intervention arm. The majority of participants received a platinum-based chemotherapy regimen which is explained by the standard-of-care treatment at the time this study was conducted. The current standard-of-care is a platinum doublet with immunotherapy for most patients depending on PD-L1 status. Yet, our findings are still relevant to current treatment recommendations. With the addition of immunotherapy now to standard platinum doublets, the risk of toxicities is potentially even higher (30). Unfortunately, the proportion of older adults comprise only 41-55% of all patients with NSCLC included in the phase III clinical trials that led to the drug approvals (30), which are the healthiest of older adults. The incidence of high-grade toxicities among older adults with GA domain impairment receiving chemotherapy + immunotherapy is currently unknown.

This study confirms the utility of a GA among older adults with advanced lung cancer. The decrease in toxicity is similar to lung cancer outcome data presented by Corre et al. in the ESOGIA-GFPC-GECP 08-02 Study (26). Yet, a distinct difference is that GAP70+ is one of the first studies in the United States to provide geriatric domain-focused recommendations while letting the oncology team decide the final cancer treatment regimen. This is very distinct from the ESOGIA study that used the GA to dictate the lung cancer treatment regimen. The former approach is likely a much more palatable design for oncology clinicians in the United States, where personal and professional autonomy is culturally prioritized over algorithmic pathway approaches. This approach is also consistent with a current emphasis on shared patient-provider decision-making.

The majority of the GA was completed from patient-reported information. This may cause a barrier to implementation if the resources are not available either in-person or electronically to capture the patient-reported information. There are alternative GA tools (31, 32) such as the G8, the CARG, and CRASH tools that are shorter than the GA performed in this study; yet, many are not validated with the use of newer cancer therapeutics and do not include recommendations to the oncology team.

For advanced NSCLC in the United States, single agent immunotherapy (IO) is now a Food & Drug Administration-approved treatment option. Fewer patients who received single

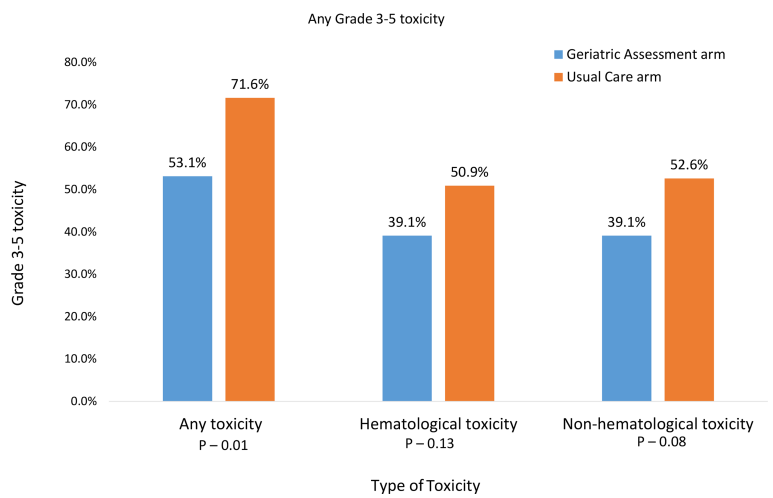

FIGURE 1 | Prevalence of grade 3-5 toxicities over 3 months after the start of new treatment for advanced stage III/IV lung cancer.

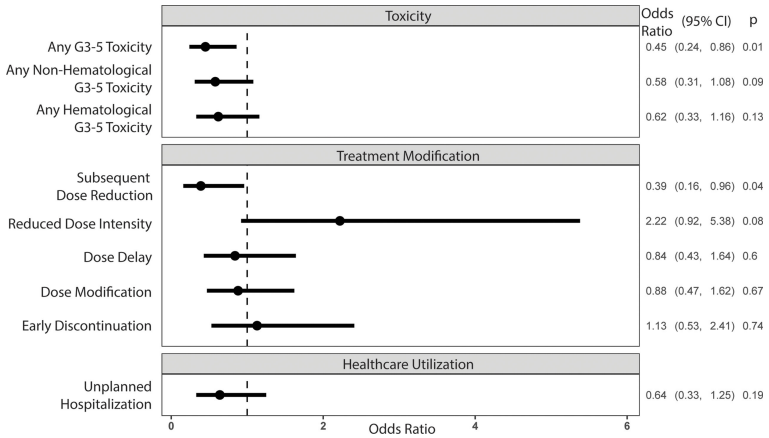

FIGURE 2 | Odds ratios of outcome variables associated with the intervention arm, controlling for the site cluster (random effect)*. *All outcomes except reduced dose intensity at cycle 1 were assessed at 3 months of treatment.

TABLE 2 | GAP Study Lung Cancer Treatment Secondary Outcomes by Study Arm.

	All patients (n = 180)	GA arm (n = 64)	Usual care arm (n = 116)	P values
Unplanned Hospitalization	62 (34.4%)	18 (28.1%)	44 (37.9%)	0.19
Dose delay	55 (30.6%)	18 (28.1%)	37 (31.9%)	0.60
Subsequent dose reduction	40 (22.2%)	8 (12.5%)	32 (27.6%)	0.02
Early discontinuation of treatment	37 (20.6%)	14 (21.9%)	23 (19.8%)	0.74
Reduced dose intensity at cycle 1	77 (42.8%)	36 (56.3%)	41 (35.3%)	<0.01
Overall Survival at 6 months*	124 (68.9%)	45 (70.3%)	79 (68.1%)	0.76
Overall Survival at 1 year*	82 (45.6%)	31 (48.4%)	51 (44.0%)	0.56

Censoring is not considered.

agent IO experienced grade 3-5 adverse events at 5 years of follow-up compared to those who received chemotherapy alone for PD-L1 positive (≥50%) disease (33). However, the trial comparing chemotherapy + IO versus IO alone (INSIGNA NCT NCT03793179) is ongoing. The PACIFIC study (34) also demonstrated an improvement in overall survival with the addition of durvalumab after concurrent chemoradiation. Unfortunately, over half of all older adults with advanced lung cancer are excluded from clinical trials (35). Future directions will hopefully explore GA-guided recommendations in a prospective clinical trial design among older adults with GA impairment receiving chemotherapy + IO for stage IV and chemoradiation therapy for stage III NSCLC. Whether to use concurrent versus sequential chemoradiation is controversial, but may have equivalent outcomes for older adults (36).

The majority of patients experienced impairment in physical performance and issues with polypharmacy. This is similar to the findings of Gomes et al. in a study of 70 older adults

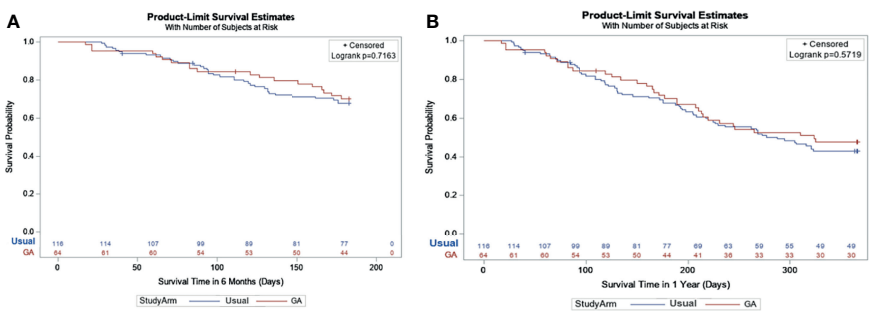

FIGURE 3 | **(A)** Survival at 6 months based on Kaplan-Meier Estimates and Cox Model*. *Geriatric Assessment Intervention: 70.1% vs. Usual Care: 67.7%; Adjusted Hazard Ratio: 0.90 95% CI: (0.52-1.57), P = 0.72. **(B)** Survival at 1 year based on Kaplan-Meier Estimates and Cox Model*. *Geriatric Assessment Intervention: 47.8% vs. Usual Care: 43.1%; Adjusted Hazard Ratio: 0.89 95% CI: (0.58-1.36), P = 0.57.

TABLE 3 | Geriatric assessment (GA) recommendations by domain.

Domains	Prevalence of the most common GA-guided management recommendations chosen by oncologists in the intervention arm
Comorbidity (n = 45 impaired in intervention arm)	- Initiate direct communication (written, electronic, or phone) with patient's primary care physician about the plan for the patient's cancer (90.0%) - Modify treatment choices if applicable to the individual patient. Examples: 1) History of diabetes - avoid neurotoxic agents if another option is equivalent (27.5%); 2) History of heart failure - minimize volume of agents and/or administer treatments at slower infusion rate (22.5%); 3) History of renal impairment-adjust as appropriate (25.0%) - Modify dosage or schedule if there is concern about how the patient will tolerate therapy or if there is a concern about worsening of comorbidities (42.5%) - Provide smoking cessation counseling if the patient currently smokes (7.5%)
Cognition (n = 23 impaired in intervention arm)	- Provide explicit and written instructions for appointments, medications, and treatment (77.3%) - Medication review - minimize psychoactive and high-risk medications (72.7%) - Assess decision-making capacity and elicit health care proxy information and input if the patient lacks decision- making capacity (45.5%) Cancer treatment decision – 1) modify dosage (e.g. 20% dose reduction with escalation as tolerated (40.9%); 2) modify treatment choice (consider starting with single agent with escalation to doublet if standard at second cycle depending on tolerance) (18.6%); 3) modify treatment regimen (e.g., use an option with demonstrated safety and efficacy in older and/or frail adults) (27.3%) - Give patient/family member handout on delirium risk counseling (22•9%) - Referral: refer to clinician experienced in memory care (9.1%) - Confirm someone else will help fill pillbox (54.5%)
Physical performance* (n = 58 impaired in intervention arm)	- Conduct frequent toxicity checks (89.7%) - Provide information on exercise and exercise prescription (87.2%) - Provide fall counselling hand-out/information (79.5%) - Provide hand-out on energy conservation (79.5%)
Functional status* (n = 39 impaired in intervention arm)	- Medication Review: minimize psychoactive meds including those used for supportive care (28.2%); minimize duplicative medications (41.0%) - Treatment modification: consider modification of treatment dose or choice. Examples: 1) consider single agent rather than doublet therapy if appropriate (20.5%): 2) modify dosage (e.g., 20% dose reduction with escalation as tolerated) (51.3%); 3) modify treatment regimen (e.g., use an option with demonstrated safety and efficacy in older and/or frail adults) (46.2%) - Referrals: refer to 1) physical therapist (outpatient or home-based depending on eligibility for home care) (17.9%); 2) occupational therapist (7.7%); 3) aide services (7.7%); 4) personal emergency response information (25.6%); 5) vision specialist if difficulties (12.8%) - Physical Examination: check orthostatic blood pressure (23.1%) and decrease or eliminate blood pressure meds if blood pressure is low or low normal (12.8%)
Nutritional status (n = 46 impaired in intervention arm)	- Conduct frequent toxicity checks (95.5%)- Give Nutrition hand-out (77.3%)- Give mucositis hand-out (72.7%)- Cancer Treatment: 1) use caution with highly emetogenic regimens and use another option if appropriate (81.8%); 2) utilize aggressive anti-emetic therapy (86.4%)- Referrals: refer to: 1) Nutritionist/Clinical Dietician (29.5%); 2) dentist if poor dentition or denture issues (2.3%); 3) speech and swallow if difficulty with swallowing (4.5%)
Social Support (n = 20 impaired in intervention arm)	- Confirm documented health care proxy is in medical record (77.8%) - Modify treatment choice and/or dosage (66.7%) - Provide referral or information on 1) Social worker *via* on-site or visiting nurse services (38.9%); 2) visiting nurse service or home health aide (if meets criteria) (16.7%); 3) transportation or ride services (22.2%); 4) medical insurance advising, advocacy, and negotiation (11•1%); 5) community resource mobilization (16.7%)
Polypharmacy (n = 55 impaired in intervention arm)	- Ask patient to bring in prescribed and over-the-counter medications and supplements to review at the next visit (45.3%) - Contact primary care provider to help reduce regimen complexity (17.0%) - Reduce medicines solely used for hypertension or diabetes if appropriate (including dose and number of medications) (17.0%) - Consult the pharmacist who fills the patient's scripts to synchronize medication refills whenever possible (3.8%) - Have pharmacist meet with the patient to evaluate drug interactions and medication counseling (7.5%) - Recommend pillbox and/or medication calendar (30.2%) - Provide written instructions (at the sixth-grade level) to patient/caregiver for taking new medications (60.4%) - Provide hand out on polypharmacy (79.2%)
Psychological health (n = 21 impaired in intervention arm)	- Provide written or verbal communication with primary care physician (41•1%) - Referral: refer to 1) counseling or psychotherapy (9.5%); 2) social work (14.3%); 3) spiritual counseling or Chaplaincy services (14.3%); 4) palliative care if other physical and/or cancer symptoms are present (14.3%). - Initiate pharmacologic therapy if appropriate in conjunction with primary care provider (14.3%)

**Recommendations for physical performance and functional status impairments are combined and presented together.*
ADL, Activity of Daily Living; OARS, Older American Resources and Services; TSH, thyroid stimulating hormone.

receiving IO for advanced NSCLC or malignant melanoma (37). Similarly, a study of over 200 older adults with lung cancer receiving treatment and GA demonstrated that handgrip strength was the most commonly impaired domain in octogenarians (38). Targeted interventions to improve both polypharmacy and physician impairment among other GA domain impairments are possible and should be incorporated into future research.

LIMITATIONS

A very small number of older adults with ES-SCLC were included, which is not representative of the percentage of patients with SCLC in the United States. The majority received a platinum-based chemotherapy regimen, which was standard-of-care treatment at the time this study was conducted. This high number of platinum doublet may be higher than that of other

countries and may not be necessarily generalizable to other countries or geographic regions. The standard of care treatment has also changed since the study period, and now includes a combination of chemotherapy + IO; in addition, older adults may have received single agent IO, which would not have met the high-toxicity regimen inclusion criteria. There was a higher number of stage IIIB patients in the intervention than the usual care arm, which could affect the secondary survival endpoints. Future studies would need to use survival as the primary endpoint and stage as a stratification factor for randomization. This study required a full GA assessment, which is often not possible in routine clinical cancer care. Due to the nature of this secondary data analysis and small sample size of the subgroup of patients with lung cancer, the analysis focusing on hematologic and non-hematologic toxicities separately and the secondary endpoints analyses may be lacking sufficient statistical power. Future prospective properly powered study may be needed to confirm these promising results. These limitations may reduce the overall generalizability of the study results.

CONCLUSION

The use of a GA assessment and recommendations can result in upfront treatment dose reduction and a decrease in high-grade toxicity among older adults with advanced lung cancer without compromising survival outcomes. This is one of the first subset analyses in the United States to demonstrate the importance of GA recommendations in geriatric oncology treatment among older adults with advanced lung cancer.

DATA AVAILABILITY STATEMENT

The raw data supporting the conclusions of this article will be made available by the authors, without undue reservation.

ETHICS STATEMENT

The studies involving human participants were reviewed and approved by The University of Rochester (Rochester, NY, USA) and all participating practice clusters obtained approval from their institutional review boards. The patients/participants provided their written informed consent to participate in this study.

AUTHOR CONTRIBUTIONS

SM and CP: conceptualization. SM, EC, MF, and MM: data collection. MM, EC, RH, and DS: data analysis. CP and PV: drafting original version. CP and SM: supervision. All authors read and approved the final version of this manuscript.

FUNDING

This work was supported by the National Cancer Institute: R01CA177592, U01CA233167, UG1CA189961, The Ohio State University Comprehensive Cancer Center, and The National Institute of Aging (CP, 1K76AB074923-01, MW, K76AG064431, SM, K24AG056589, R33AG059206, DS, 1K01AG070310-01A1). Research reported in this publication was supported by The Ohio State University Comprehensive Cancer Center and the National Institutes of Health under grant number P30 CA016058.

ACKNOWLEDGMENTS

The authors wish to acknowledge the contributions of Kamila Jaroniec, M.F.A., Technical Editor, Div. of Medical Oncology, Dept. of Internal Medicine, The Ohio State University Wexner Medical Center, in the revision of this manuscript. We thank the patients for their participation.

REFERENCES

1. Siegel RL, Miller KD, Fuchs HE, Jemal A. Cancer Statistics, 2021. *CA: A Cancer J Clin* (2021) 71:7–33. doi: 10.3322/caac.21654
2. Smith BD, Smith GL, Hurria A, Hortobagyi GN, Buchholz TA. Future of Cancer Incidence in the United States: Burdens Upon an Aging, Changing Nation. *J Clin Oncol* (2009) 27:2758–65. doi: 10.1200/JCO.2008.20.8983
3. Hurria A, Naylor M, Cohen H. Improving the Quality of Cancer Care in an Aging Population: Recommendations From an Iom Report. *JAMA* (2013) 310:1795–6. doi: 10.1001/jama.2013.280416
4. Howlader N, Noone AM, Krapcho M, Miller D, Brest A, Yu M, et al. *SEER Cancer Statistics Review, 1975-2017*. Bethesda, MD: National Cancer Institute (2021).
5. Hutchins LF, Unger JM, Crowley JJ, Coltman CA Jr, Albain KS. Underrepresentation of Patients 65 Years of Age or Older in Cancer-Treatment Trials. *N Engl J Med* (1999) 341:2061–7. doi: 10.1056/NEJM199912303412706
6. Murthy VH, Krumholz HM, Gross CP. Participation in Cancer Clinical Trials: Race-, Sex-, and Age-Based Disparities. *JAMA* (2004) 291:2720–6. doi: 10.1001/jama.291.22.2720
7. Sedrak MS, Freedman RA, Cohen HJ, Muss HB, Jatoi A, Klepin HD, et al. Older Adult Participation in Cancer Clinical Trials: A Systematic Review of Barriers and Interventions. *CA: A Cancer J Clin* (2021) 71:78–92. doi: 10.3322/caac.21638
8. Mohile SG, Xian Y, Dale W, Fisher SG, Rodin M, Morrow GR, et al. Association of a Cancer Diagnosis With Vulnerability and Frailty in Older Medicare Beneficiaries. *J Natl Cancer Inst* (2009) 101:1206–15. doi: 10.1093/jnci/djp239
9. Mohile SG, Fan L, Reeve E, Jean-Pierre P, Mustian K, Peppone L, et al. Association of Cancer With Geriatric Syndromes in Older Medicare Beneficiaries. *J Clin Oncol* (2011) 29:1458–64. doi: 10.1200/JCO.2010.31.6695
10. Kenis C, Bron D, Libert Y, Decoster L, Van Puyvelde K, Scalliet P, et al. Relevance of a Systematic Geriatric Screening and Assessment in Older Patients With Cancer: Results of a Prospective Multicentric Study. *Ann Oncol* (2013) 24:1306–12. doi: 10.1093/annonc/mds619
11. Repetto L, Fratino L, Audisio RA, Venturino A, Gianni W, Vercelli M, et al. Comprehensive Geriatric Assessment Adds Information to Eastern Cooperative Oncology Group Performance Status in Elderly Cancer Patients: An Italian Group for Geriatric Oncology Study. *J Clin Oncol* (2002) 20:494–502. doi: 10.1200/JCO.2002.20.2.494
12. Kenis C, Decoster L, Van Puyvelde K, De Grève J, Conings G, Milisen K, et al. Performance of Two Geriatric Screening Tools in Older Patients With Cancer. *J Clin Oncol* (2014) 32:19–26. doi: 10.1200/JCO.2013.51.1345
13. Cuccia F, Mortellaro G, Mazzola R, Donofrio A, Valenti V, Tripoli A, et al. Prognostic Value of Two Geriatric Screening Tools in a Cohort of Older

Patients With Early Stage Non-Small Cell Lung Cancer Treated With Hypofractionated Stereotactic Radiotherapy. *J Geriatr Oncol* (2020) 11:475–81. doi: 10.1016/j.jgo.2019.05.002
14. Rodin MB, Mohile SG. A Practical Approach to Geriatric Assessment in Oncology. *J Clin Oncol* (2007) 25:1936–44. doi: 10.1200/JCO.2006.10.2954
15. Hurria A, Cirrincione CT, Muss HB, Kornblith AB, Barry W, Artz AS, et al. Implementing a Geriatric Assessment in Cooperative Group Clinical Cancer Trials: CALGB 360401. *J Clin Oncol* (2011) 29:1290–6. doi: 10.1200/JCO.2010.30.6985
16. Pal SK, Katheria V, Hurria A. Evaluating the Older Patient With Cancer: Understanding Frailty and the Geriatric Assessment. *CA Cancer J Clin* (2010) 60:120–32. doi: 10.3322/caac.20059
17. Dale W, Mohile SG, Eldadah BA, Trimble EL, Schilsky RL, Cohen HJ, et al. Biological, Clinical, and Psychosocial Correlates at the Interface of Cancer and Aging Research. *J Natl Cancer Inst* (2012) 104:581–9. doi: 10.1093/jnci/djs145
18. Hurria A, Mohile SG, Dale W. Research Priorities in Geriatric Oncology: Addressing the Needs of an Aging Population. *J Natl Compr Canc Netw* (2012) 10:286–8. doi: 10.6004/jnccn.2012.0025
19. Hoppe S, Rainfray M, Fonck M, Hoppenreys L, Blanc JF, Ceccaldi J, et al. Functional Decline in Older Patients With Cancer Receiving First-Line Chemotherapy. *J Clin Oncol* (2013) 31:3877–82. doi: 10.1200/JCO.2012.47.7430
20. Kenis C, Decoster L, Bastin J, Bode H, Van Puyvelde K, De Grève J, et al. Functional Decline in Older Patients With Cancer Receiving Chemotherapy: A Multicenter Prospective Study. *J Geriatr Oncol* (2017) 8:196–205. doi: 10.1016/j.jgo.2017.02.010
21. Presley CJ, Arrato NA, Janse S, Shields PG, Carbone DP, Wong ML, et al. Functional Disability Among Older Versus Younger Adults With Advanced Non–Small-Cell Lung Cancer. *JCO Oncol Practice:OP* (2021) 17(6):e848–58. doi: 10.1200/OP.20.01004
22. Kyriakou F KP, Papamichael D. Targeted Agents: Review of Toxicity in the Elderly Metastatic Colorectal Cancer Patients. *Targeted Oncool* (2011) 6:245–51. doi: 10.1007/s11523-011-0198-1
23. Meoni G CFL, Lucherini E, Di Costanzo F. Medical Treatment of Advanced non-Small Cell Lung Cancer in Elderly Patients: A Review of the Role of Chemotherapy and Targeted Agents. *J Geriatric Oncol* (2013) 4:282–90. doi: 10.1016/j.jgo.2013.04.005
24. Zustovich F, Novara G. Advanced Kidney Cancer: Treating the Elderly. *Expert Rev Anticancer Ther* (2013) 13:1389–98. doi: 10.1586/14737140.2013.846095
25. Grothey A VCE, Sobrero A, Siena S, Falcone A, Ychou M, et al. Regorafenib Monotherapy for Previously Treated Metastatic Colorectal Cancer (CORRECT): An International, Multicentre, Randomised, Placebo-Controlled, Phase 3 Trial. *Lancet* (2013) 381:303–12. doi: 10.1016/S0140-6736(12)61900-X
26. Corre R, Greillier L, Caër HL, Audigier-Valette C, Baize N, Bérard H, et al. Use of a Comprehensive Geriatric Assessment for the Management of Elderly Patients With Advanced Non–Small-Cell Lung Cancer: The Phase III Randomized ESOGIA-GFPC-GECP 08-02 Study. *J Clin Oncol* (2016) 34:1476–83. doi: 10.1200/JCO.2015.63.5839
27. Mohile SG, Mohamed MR, Xu H, Culakova E, Loh KP, Magnuson A, et al. Evaluation of Geriatric Assessment and Management on the Toxic Effects of Cancer Treatment (GAP70+): A Cluster-Randomised Study. *Lancet* (2021) 398(10314):1894–904. doi: 10.1016/S0140-6736(21)01789-X
28. Mohamed MR, Kyi K, Mohile SG, Xu H, Culakova E, Loh KP, et al. Prevalence of and Factors Associated With Treatment Modification at First Cycle in Older Adults With Advanced Cancer Receiving Palliative Treatment. *J Geriatr Oncol* (2021) 12(8):1208–13. doi: 10.1016/j.jgo.2021.06.007
29. Ettinger DS, Wood DE, Aisner DL, Akerley W, Bauman JR, Bharat A, et al. NCCN Guidelines Insights: Non-Small Cell Lung Cancer, Version 2.2021. *J Natl Compr Canc Netw* (2021) 19:254–66. doi: 10.6004/jnccn.2021.0013
30. Presley CJ, Gomes F, Burd CE, Kanesvaran R, Wong ML. Immunotherapy in Older Adults With Cancer. *J Clin Oncol* (2021) 39:2115–27. doi: 10.1200/JCO.21.00138
31. Almodovar T, Teixeira E, Barroso A, Yin T, Liang Y. Elderly Patients With Advanced NSCLC: The Value of Geriatric Evaluation and the Feasibility of CGA Alternatives in Predicting Chemotherapy Toxicity. *Pulmonology* (2019) 25:40–50. doi: 10.1016/j.pulmoe.2018.07.004
32. Gridelli C, Balducci L, Ciardiello F, Di Maio M, Felip E, Langer C, et al. Treatment of Elderly Patients With Non-Small-Cell Lung Cancer: Results of an International Expert Panel Meeting of the Italian Association of Thoracic Oncology. *Clin Lung Cancer* (2015) 16:325–33. doi: 10.1016/j.cllc.2015.02.006
33. Brahmer JR, Rodriguez-Abreu D, Robinson AG, Hui R, Csőszi T, Fülöp A, et al. LBA51 KEYNOTE-024 5-Year OS Update: First-Line (1L) Pembrolizumab (Pembro) vs Platinum-Based Chemotherapy (Chemo) in Patients (Pts) With Metastatic NSCLC and PD-L1 Tumour Proportion Score (TPS) ≥50%. *Ann Oncol* (2020) 31:S1181–2. doi: 10.1016/j.annonc.2020.08.2284
34. Antonia SJ, Villegas A, Daniel D, Vicente D, Murakami S, Hui R, et al. Durvalumab After Chemoradiotherapy in Stage III Non–Small-Cell Lung Cancer. *N Engl J Med* (2017) 377:1919–29. doi: 10.1056/NEJMoa1709937
35. Tang M, Pearson SA, Schaffer AL, Lewis CR, John T, Simes RJ, et al. Are Clinical Trial Eligibility Criteria Representative of Older Patients With Lung Cancer? A Population-Based Data Linkage Study. *J Geriatr Oncol* (2021) 12:930–6. doi: 10.1016/j.jgo.2021.02.003
36. Maggiore RJ, Zahrieh D, McMurray RP, Feliciano JL, Samson P, Mohindra P, et al. Toxicity and Survival Outcomes in Older Adults Receiving Concurrent or Sequential Chemoradiation for Stage III Non-Small Cell Lung Cancer in Alliance Trials (Alliance A151812). *J Geriatric Oncol* (2020) 12(4):563–71. doi: 10.1016/j.jgo.2020.09.005
37. Gomes F, Lorigan P, Woolley S, Foden P, Burns K, Yorke J, et al. A Prospective Cohort Study on the Safety of Checkpoint Inhibitors in Older Cancer Patients – the ELDERS Study. *ESMO Open* (2021) 6(1):100042. doi: 10.1016/j.esmoop.2020.100042
38. Couderc A-L, Tomasini P, Rey D, Israel T, Esnault H, Guyard A, et al. Octogenarians Treated for Thoracic and Lung Cancers: Impact of Comprehensive Geriatric Assessment. *J Geriatric Oncol* (2021) 12:402–9. doi: 10.1016/j.jgo.2020.10.005

Conflict of Interest: MW receives royalties from UpToDate and immediate family member is an employee of Genentech with stock ownership. Dr. Flannery reports grants from NIH NCI RO1 CA 177592, grants from NIH NCI UO1 CA 233167, grants from NIH NCI UG1 CA189961, during the conduct of the study. YT received grant and personal fees from Daiichi Sankyo Co., Ltd and AstraZeneca K.K. and personal fees from Chugai Pharmaceuticals Inc. outside the submitted work.

The remaining authors declare that the research was conducted in the absence of any commercial or financial relationships that could be construed as a potential conflict of interest.

Publisher's Note: All claims expressed in this article are solely those of the authors and do not necessarily represent those of their affiliated organizations, or those of the publisher, the editors and the reviewers. Any product that may be evaluated in this article, or claim that may be made by its manufacturer, is not guaranteed or endorsed by the publisher.

frontiers | Frontiers in Oncology

ORIGINAL RESEARCH
published: 31 May 2022
doi: 10.3389/fonc.2022.835844

Impact of Introducing Intensity Modulated Radiotherapy on Curative Intent Radiotherapy and Survival for Lung Cancer

Isabella Fornacon-Wood[1†], Clara Chan[2†], Neil Bayman[2], Kathryn Banfill[1,2], Joanna Coote[2], Alex Garbett[2], Margaret Harris[2], Andrew Hudson[2], Jason Kennedy[3], Laura Pemberton[2], Ahmed Salem[1,2], Hamid Sheikh[2], Philip Whitehurst[4], David Woolf[2], Gareth Price[1,4‡] and Corinne Faivre-Finn[1,2‡]*

[1] Division of Cancer Sciences, University of Manchester, Manchester, United Kingdom, [2] Department of Clinical Oncology, The Christie Hospital NHS Foundation Trust, Manchester, United Kingdom, [3] Radiotherapy Related Research, The Christie Hospital NHS Foundation Trust, Manchester, United Kingdom, [4] Christie Medical Physics and Engineering, The Christie Hospital NHS Foundation Trust, Manchester, United Kingdom

OPEN ACCESS

Edited by:
Meng Xu Welliver, The Ohio State University, United States

Reviewed by:
Stephanie Tanadini-Lang, University Hospital Zürich, Switzerland
Tomas Kron, Peter MacCallum Cancer Centre, Australia

***Correspondence:**
Clara Chan
Clara.Chan@nhs.net

[†]*These authors share first authorship*

[‡]*These authors share last authorship*

Specialty section:
This article was submitted to Thoracic Oncology, a section of the journal Frontiers in Oncology

Received: *15 December 2021*
Accepted: *03 May 2022*
Published: *31 May 2022*

Citation:
Fornacon-Wood I, Chan C, Bayman N, Banfill K, Coote J, Garbett A, Harris M, Hudson A, Kennedy J, Pemberton L, Salem A, Sheikh H, Whitehurst P, Woolf D, Price G and Faivre-Finn C (2022) Impact of Introducing Intensity Modulated Radiotherapy on Curative Intent Radiotherapy and Survival for Lung Cancer. Front. Oncol. 12:835844. doi: 10.3389/fonc.2022.835844

Background: Lung cancer survival remains poor. The introduction of Intensity-Modulated Radiotherapy (IMRT) allows treatment of more complex tumours as it improves conformity around the tumour and greater normal tissue sparing. However, there is limited evidence assessing the clinical impact of IMRT. In this study, we evaluated whether the introduction of IMRT had an influence on the proportion of patients treated with curative-intent radiotherapy over time, and whether this had an effect on patient survival.

Materials and Methods: Patients treated with thoracic radiotherapy at our institute between 2005 and 2020 were retrospectively identified and grouped into three time periods: A) 2005-2008 (pre-IMRT), B) 2009-2012 (selective use of IMRT), and C) 2013-2020 (full access to IMRT). Data on performance status (PS), stage, age, gross tumour volume (GTV), planning target volume (PTV) and survival were collected. The proportion of patients treated with a curative dose between these periods was compared. Multivariable survival models were fitted to evaluate the hazard for patients treated in each time period, adjusting for PS, stage, age and tumour volume.

Results: 12,499 patients were included in the analysis (n=2675 (A), n=3127 (B), and n=6697 (C)). The proportion of patients treated with curative-intent radiotherapy increased between the 3 time periods, from 38.1% to 50.2% to 65.6% (p<0.001). When stage IV patients were excluded, this increased to 40.1% to 58.1% to 82.9% (p<0.001). This trend was seen across all PS and stages. The GTV size increased across the time periods and PTV size decreased. Patients treated with curative-intent during period C had a survival improvement compared to time period A when adjusting for clinical variables (HR=0.725 (0.632-0.831), p<0.001).

Conclusion: IMRT was associated with to more patients receiving curative-intent radiotherapy. In addition, it facilitated the treatment of larger tumours that historically would have been treated palliatively. Despite treating larger, more complex tumours with curative-intent, a survival benefit was seen for patients treated when full access to IMRT was available (2013-2020). This study highlights the impact of IMRT on thoracic oncology practice, accepting that improved survival may also be attributed to a number of other contributing factors, including improvements in staging, other technological radiotherapy advances and changes to systemic treatment.

Keywords: IMRT, lung cancer, radiotherapy, real-world data, big data

INTRODUCTION

Lung cancer is the third most common cancer and the leading cause of cancer death in the UK (1). For some time it has been recognised that better treatments are urgently required to improve lung cancer survival. Over the last two decades, increasing knowledge regarding the biology of lung cancer has led to the development of new systemic agents such as tyrosine kinase inhibitors and immunotherapy, leading to improvements in survival in locally advanced and metastatic non-small cell lung cancer. However outcome of lung cancer patients remains poor compared to the majority of other cancer types (2, 3).

Radiotherapy (RT) plays an important role in the management of lung cancer with over 50% patients receiving this modality at some point during their cancer journey (4). Radiotherapy can either be given with palliative intent to control symptoms, or radically with curative intent – in patients with early and locally advanced disease.

Radiotherapy treatment planning is a careful balancing act between optimal tumour control and limitation of damage to normal tissue. In order to avoid undue toxicity, dose constraints are placed on the normal tissues such as the lungs, heart, oesophagus and spinal cord to minimise functional damage. The radiotherapy dose delivered to the tumour is therefore often limited by the dose that can be safely delivered to the normal tissues. This is particularly challenging in patients who have large volume disease and/or disease close to critical normal structures, such as the spinal cord. In some situations this can lead to patients being treated with a safer, lower, but ultimately palliative dose. As local control correlates with improved survival (5, 6), these patients naturally have a poorer outcome.

Over the last two decades, great advancements have been made in radiotherapy technology (7, 8). Prior to the 1980's radical lung patients were planned with fluoroscopy, however the introduction of computed tomography (CT) allowed improved tumour localisation and conformal planning. In addition, the advent of the multi-leaf collimator (MLC) enabled fields to be shaped around a target volume. This three-dimensional conformal radiotherapy (3DCRT) has been the gold standard for radical RT to the lung since the 1980's. Subsequently, 4D planning was introduced which incorporates tumour motion into the radiotherapy planning process, allowing more bespoke plans based on tumour motion and a reduction in margins. In addition there have been improved methods of image guidance, allowing the verification of the tumour position during the treatment course with increasing accuracy. This again has allowed a reduction in tumour margins and therefore dose delivered to normal tissue (9). Despite these improvements in technology, there are still a significant proportion of lung cancer patients, in particular those with locally advanced disease, who are treated with a palliative approach either due to the treatment volume or its proximity to a critical structure (10).

Intensity-modulated radiotherapy (IMRT) is an advanced form of 3DCRT that modifies the intensity of the radiation across each beam, sculpting the high-dose volume around the site of disease and thereby sparing adjacent organs at risk. This technology has been available since the early 2000s, however the routine implementation of IMRT in the setting of lung cancer treatment has been slow, due partly to the increased planning and quality assurance time required by this techniques, and a perceived lack of evidence for using it (11). To date there are a handful of large retrospective studies evaluating 3DCRT against IMRT in lung cancer, and only one publication in a randomised, prospective setting which addresses this issue (12). There is a lack of data on the impact of modern RT technology on patient management and outcome, particularly for patients that are typically excluded from clinical trials (13).

We have been treating lung cancer patients in our institution routinely with IMRT for over a decade. This study aims to evaluate whether the introduction of IMRT has had an influence on the proportion of patients we are able to treat with curative intent over time, and whether this has had any impact on patient survival.

METHODS AND MATERIALS

A retrospective review of patients in our institution treated with thoracic RT for lung cancer between 2005-2020 was carried out. Approval was granted to collect and analyse this patient data by the UK Computer Aided Theragnostics (ukCAT) Research Database Management Committee (REC reference: 17/NW/0060).

Patients between 2005-2012 were identified by ICD-10 codes on MOSAIQ and patients between 2013-2020 were identified *via*

the Christie web portal (CWP – an in house e-record system designed to collect structured data on patients, tumour characteristics and outcome data). For all patients, data on age, sex, ECOG performance status (PS), stage, gross tumour volume (GTV), planning target volume (PTV) and survival were collected. For patients planned using 4D-CT imaging, GTV data was synthesized from the internal gross tumour volume (iGTV) using a previously published method (14).

Patients were grouped into 3 time periods, determined by the year the first radiotherapy fraction was delivered: A (2005-2008, pre IMRT), B (2009-2012, some availability IMRT) and C (2013-2020, full access IMRT). SABR was introduced in 2011 in our institution. Any patient who received an absolute physical dose of greater than 40Gy was classed as having 'curative-intent' thoracic RT. This dose was chosen to cover patients receiving radical doses such as 45Gy/30 fractions twice-daily (EQD2 43.1 Gy) or 40Gy/15 fractions daily (EQD2 42.2 Gy) for limited stage small cell lung cancer (SCLC). For patients receiving palliative radiotherapy, records were manually checked to ensure these patients received palliative radiotherapy to the lung (and not a site of metastatic disease). Those that had not were excluded from this study.

The proportion of patients treated with curative-intent RT was compared between the 3 time periods and the Chi-squared test was used to compare differences between the groups. We performed 2 analyses, one including all stages and the other including only patients with stage I-III. The proportion of patients treated with curative-intent RT was also compared across all PS groupings and stages of disease. For curative-intent patients, the trend of tumour volume treated over time was reviewed and the Mann–Whitney U test used to compare GTV and PTV across time periods. Survival curves were generated using the Kaplan-Meier method and compared using the log-rank test. Univariable and multivariable cox survival models were fitted to evaluate the hazard of being treated in one of the 3 time periods, adjusting for baseline PS, stage at diagnosis, age at the start of treatment and GTV. These analyses were then repeated excluding patients who had received stereotactic radiotherapy (SABR). All statistical analyses were performed in R 4.0.0 (15) with package *survival* v3.1-12 (16).

RESULTS

In total, 12499 patients were identified as having received radiotherapy to the lung between 2005 and 2020; 2675 in group A (2005-2008, pre IMRT), 3127 in group B (2009-2012, some availability IMRT) and 6697 in group C (2013-2020, full access IMRT). Patients in time period B receiving IMRT were planned with this technique only if 3D conformal radiotherapy was unable to achieve a dosimetrically acceptable radical plan.

Baseline characteristics are presented in **Table 1**. Median age was 70 (63-77), 71 (64-78) and 72 (65-78) in each group respectively. 985 patients received SABR, 0 in group A, 33 in group B and 952 in group C.

There was a progressive increase in the proportion of patients receiving curative-intent radiotherapy year on year since 2005, with a step wise change occurring from 2011 as shown in **Figure 1**. This increase in the proportion of patients receiving a curative dose was highlighted further when patients were grouped into the 3 previously specified time periods (**Figure 2**). Patients receiving curative-intent RT increased between groups A (2005-2008) and B (2009-2013) (38.1% to 50.2%, p<0.0001), and B and C (2014-2020) (50.2% to 65.6%, p<0.0001). Results were similar when the patients treated with SABR were removed from the analysis (**Supplementary Figures 1**, **2**). These percentages increased when only stage I-III patients were examined (**Figure 3**) with patients receiving curative-intent RT increasing from 40.1% to 58% to 82.9% in A, B and C respectively.

Further sub-classification according to PS and stage are presented in **Tables 2**, **3** respectively. The proportion of patients treated with curative-intent radiotherapy increased between the three time periods, regardless of PS and stage of disease. Stage IV patients have been included to reflect the increasing use of 'radical' radiotherapy to achieve optimal local disease control, typically in the setting of oligometastatic disease. Results were similar when patients treated with SABR were removed from the analysis (**Supplementary Tables 1, 2**). **Table 4** presents sub-classification according to PS for stage III patients only, showing that the proportion of curative-intent patients has increased across all PS for these patients.

GTV data was available for 4306 patients treated with curative-intent. The distribution of GTVs in each time period is presented in **Figure 4A**, showing larger GTVs have been treated in group C compared to A and B. Median GTV was 35.5 cm^3 [16.8, 60.1], 39.2 cm^3 [15.1, 82.9] and 32.5 cm^3 [9.9, 91.8] for groups A, B and C respectively. There was a significant decrease in median GTV between time periods B and C (p=0.00597). However, when patients treated with SABR (n=546) were removed from the analysis (violin plot in **Figure 4B**), median GTV was 35.5 cm^3 [16.8, 60.1], 41.7 cm^3 [16.3, 85.8] and 47.6 cm^3 [17.6, 112.1] for groups A, B and C respectively, showing a significant increase in GTV size in each time period in non-SABR patients (A to B, p=0.00383; B to C, p=0.00136). The maximum treated GTV also increased across each time period, from 254.0 cm^3 to 534.4 cm^3 to 916.3 cm^3.

PTV data was available for 4915 curative-intent patients. The distribution of PTVs in each time period is presented in **Figure 5**. Median PTV was 319.2 cm^3 [225.8, 433.2], 326.3 cm^3 [202.3, 502.2] and 235.9 cm^3 [97.8, 401.7] for groups A, B and C respectively. There was a significant decrease in PTV between time periods B and C (p<0.0001). When patients treated with SABR were removed from the analysis, median PTV was 319.2 cm^3 [225.8, 433.2], 334.1 cm^3 [211.8, 506.7] and 282.2 cm^3 [169.7, 438.9] for groups A, B and C respectively, again showing a significant decrease in PTV between time periods B and C (p<0.0001).

Univariable survival analysis showed that the survival of patients treated with curative-intent radiotherapy has significantly improved in time period C compared to A

TABLE 1 | Baseline characteristics.

	A: 2005-2008 n=2675	B: 2009-2012 n=3127	C: 2013-2020 n=6697
Age at start of treatment [median (IQR)]	70.00 [63.00, 77.00]	71.00 [64.00, 78.00]	72.00 [65.00, 78.00]
Sex [n (%)]			
Male	1527 (57.8)	1729 (56.0)	3435 (52.3)
Female	1117 (42.2)	1358 (44.0)	3139 (47.7)
Treatment intent [n (%)]			
Curative	1018 (38.1)	1570 (50.2)	4391 (65.6)
Palliative	1657 (61.9)	1557 (49.8)	2306 (34.4)
SABR [n (%)]	0 (0.0)	33 (1.1)	952 (14.2)
ECOG Performance status [n (%)]			
0	284 (10.6)	281 (9.0)	588 (8.8)
1	852 (31.9)	1071 (34.3)	2301 (34.4)
2	474 (17.7)	762 (24.4)	2012 (30.0)
3	167 (6.2)	348 (11.1)	813 (12.1)
4	3 (0.1)	5 (0.2)	17 (0.3)
Missing	895 (33.5)	660 (21.1)	966 (14.4)
Stage [n (%)]			
I	321 (12.0)	443 (14.2)	1490 (22.2)
II	158 (5.9)	243 (7.8)	628 (9.4)
III	552 (20.6)	810 (25.9)	1875 (28.0)
IV	142 (5.3)	512 (16.4)	1706 (25.5)
Missing	1502 (56.1)	1119 (35.8)	998 (14.9)

SABR, stereotactic ablative radiotherapy; ECOG, Eastern Cooperative Oncology Group.

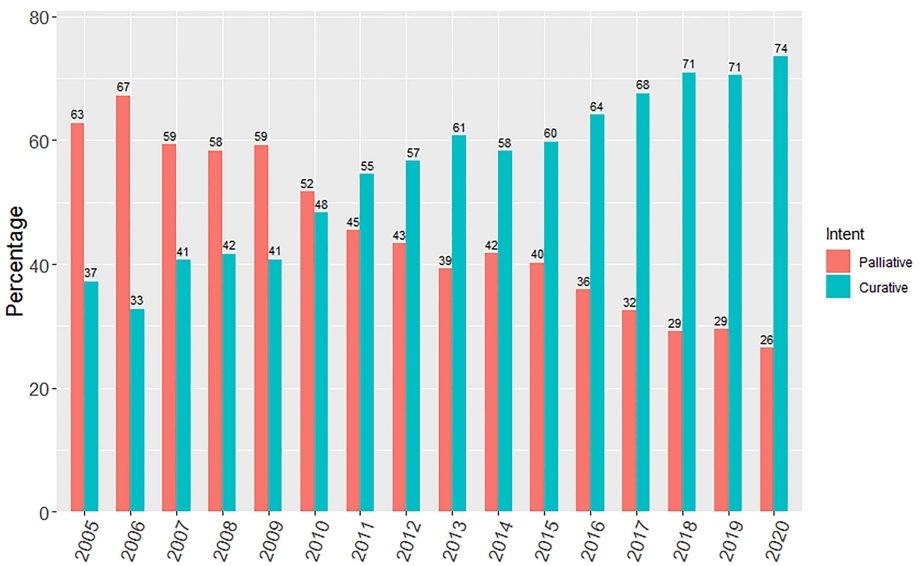

FIGURE 1 | Yearly percentage of patients treated with curative versus palliative intent radiotherapy from 2005 to 2020.

(HR=0.847 (0.786-0.913), p<0.001). When patients treated with SABR were removed from the analysis, there was only a survival benefit for patients in time period B compared to A (HR=1.09 (1.00-1.18), p=0.0486), not for time period C compared to A (HR=0.949 (0.879-1.02), p=0.180). Kaplan-Meier curves are presented in **Figure 6** for all curative-intent patients and curative-intent without SABR. Multivariable survival analysis, however, showed a survival benefit for patients treated in time period C compared to A for all curative-intent patients (HR=0.725 (0.632-0.831), p<0.001) as well as when patients treated with SABR were removed from the analysis (HR=0.757 (0.658-0.870), p<0.001). Full results are presented in **Supplementary Tables 3, 4**.

We conducted an analysis in patients with stage III disease. Kaplan-Meier curve is presented in **Figure 7** for patients with stage III treated with curative-intent. Univariable survival analysis showed no significant improvement or worsening of survival for time period C compared to A (HR=0.969 (0.832, 1.13), p=0.683). Multivariable survival analysis however, showed a survival benefit for patients treated in time period C compared

FIGURE 2 | Percentage of patients treated with curative versus palliative intent radiotherapy (whole population) in each of the pre-specified time periods.

FIGURE 3 | Percentage of patients treated with curative versus palliative intent radiotherapy (stages I-III) in each of the pre-specified time periods.

to A for patients with stage III disease treated with curative-intent (HR=0.740 (0.600-0.913), p=0.00489). Full results are presented in **Supplementary Table 5**.

DISCUSSION

In this big data analysis, there has been a steady increase in the proportion of patients treated with curative-intent radiotherapy, across all PS groups and stages of disease. In addition, survival improved in the era when there was full access to IMRT (2013-2020) compared to no access to IMRT (2005-2008) when clinical variables were adjusted for. The introduction of IMRT has allowed the delivery of curative-intent doses to patients with tumours previously considered to be unsuitable for such an approach due to large volume or proximity to critical organs at risk. In addition, the normal tissue sparing that IMRT facilitates enabled the treatment of patients with poorer performance status due to better tolerance of the treatment.

Our analysis showed that the proportion of patients with stage III lung cancer receiving curative-intent treatment has increased over the time periods, across all PS. This change has been partly facilitated by IMRT which allows the treatment of large and complex volumes. Other factors may have played a role, such as 4D CT planning (introduced 2011) facilitating more individualised treatment volumes, and also availability of

TABLE 2 | Proportion of patients treated with curative-intent radiotherapy across each PS and time period.

PS	A: 2005-2008 % curative-intent (n curative-intent/n total)	B: 2009-2012 % curative-intent (n curative-intent/n total)	C: 2013-2020 % curative-intent (n curative-intent/n total)
0	52.1	65.5	71.3
(n=1153)	(148/284)	(184/281)	(419/588)
1	43.9	60.5	70.7
(n=4224)	(374/852)	(648/1071)	(1627/2301)
2	34.8	51.3	67.8
(n=3248)	(165/474)	(391/762)	(1365/2012)
3	15.6	21.8	47.8
(n=1328)	(26/167)	(76/348)	(389/813)

radiotherapy at new satellite centres from 2010, allowing more patients (particularly the elderly and patients with poorer PS) to be treated nearer home. Accepting this, we still feel that as GTV volumes increased over the time periods studied, the introduction of IMRT is likely to have contributed greatly towards the proportion of patients able to receive curative-intent treatment. Baseline PET imaging has been standard at our institution since 2001 and so should not account for differences observed between the groups.

The survival benefit demonstrated on multivariable analysis was not seen in the unadjusted analysis, reflecting that patients with poorer performance status and larger tumours are being treated in the latest time period. As lung cancer outcome is associated with tumour volume (17, 18), it was expected that the survival in this group might have been worse in comparison to earlier time frames. However, survival improved for patients in the latest time period despite larger gross tumour volumes and an increased number of patients with poorer PS suggesting that planning with IMRT leads to at least non-inferior survival. In particular, when patients treated with SABR were removed from the analysis we showed that despite a significant increase in GTV in patients treated with curative-intent, the survival benefit in the latest time period remained.

Whilst this survival gain could be partly attributed to IMRT it is important to recognise that other changes in lung cancer management have occurred in the intervening time period we examined, and so we cannot claim that IMRT has directly led to an improvement in survival. Technological advances such as SABR, 4D radiotherapy and image guidance radiotherapy have allowed reduced radiotherapy planning margins, leading to reduced normal tissue doses. The doses we used for curative intent stayed the same throughout the study. In our series, median PTV volumes were lower in the later timeframe (C) compared to either of the earlier timeframes, even when patients treated with SABR were excluded. This is likely to reflect a change in our CTV-PTV expansion margins which were introduced in the later time period following a move to daily image verification. It is unlikely that this reduction in PTV volume is responsible for the increased survival seen in the later timeframe, as although the difference was found to be statistically significant, in clinical terms the differences in PTV volume seen between group C and groups A and B is small. Also, GTV volume is known to be an independent prognostic factor for lung cancer survival, and we have previously demonstrated that this parameter increased between the three time periods.

Non-radiotherapy factors such as improved diagnostic imaging techniques, endobronchial ultrasound (EBUS) and associated stage migration, a change in staging classification, improvements in systemic therapy and supportive care may all have led to better outcomes. With regards to systemic therapy, the last 15 years have seen better integration of radiotherapy and systemic treatment, as well as the development of more targeted agents and immunotherapy that can be used on progression. Unfortunately due to the fact that this study started in 2005 data on chemotherapy were not as complete in the first time period due to lack of availability of electronic records for systemic therapy at the time. It was therefore not possible to guarantee a full, accurate and therefore meaningful collection of data on systemic treatment the patient may have received at the time of radiotherapy, or subsequently on progression. It is worth noting however that systemic treatment in the context of concurrent chemoradiotherapy had not changed significantly until the introduction of adjuvant Durvalumab,

TABLE 3 | Proportion of patients treated with curative-intent radiotherapy across each stage and time period.

Stage	A: 2005-2008 % curative-intent (n curative-intent/n total)	B: 2009-2012 % curative-intent (n curative-intent/n total)	C: 2013-2020 % curative-intent (n curative-intent/n total)
I	76.9	91.4	97.5
(n=2254)	(247/321)	(405/443)	(1453/1490)
II	70.3	84.8	91.6
(n=1029)	(111/158)	(206/243)	(575/628)
III	40.4	66.4	75.9
(n=3237)	(223/552)	(538/810)	(1424/1875)
IV*	2.11	9.96	14.9
(n=2360)	(3/142)	(51/512)	(255/1706)

**Patients with oligometastatic disease treated with curative intent.*

TABLE 4 | Proportion of patients treated with curative-intent radiotherapy across each PS and time period for stage III patients only.

PS	A: 2005-2008 % curative-intent (n curative-intent/n total)	B: 2009-2012 % curative-intent (n curative-intent/n total)	C: 2013-2020 % curative-intent (n curative-intent/n total)
0	66.7	79.4	87.2
(n=451)	(48/72)	(77/97)	(246/282)
1	46.0	77.9	85.2
(n=1430)	(116/252)	(306/393)	(669/785)
2	28.7	57.6	72.1
(n=819)	(31/108)	(110/191)	(375/520)
3	10.5	32.9	34.1
(n=296)	(4/38)	(27/82)	(60/176)

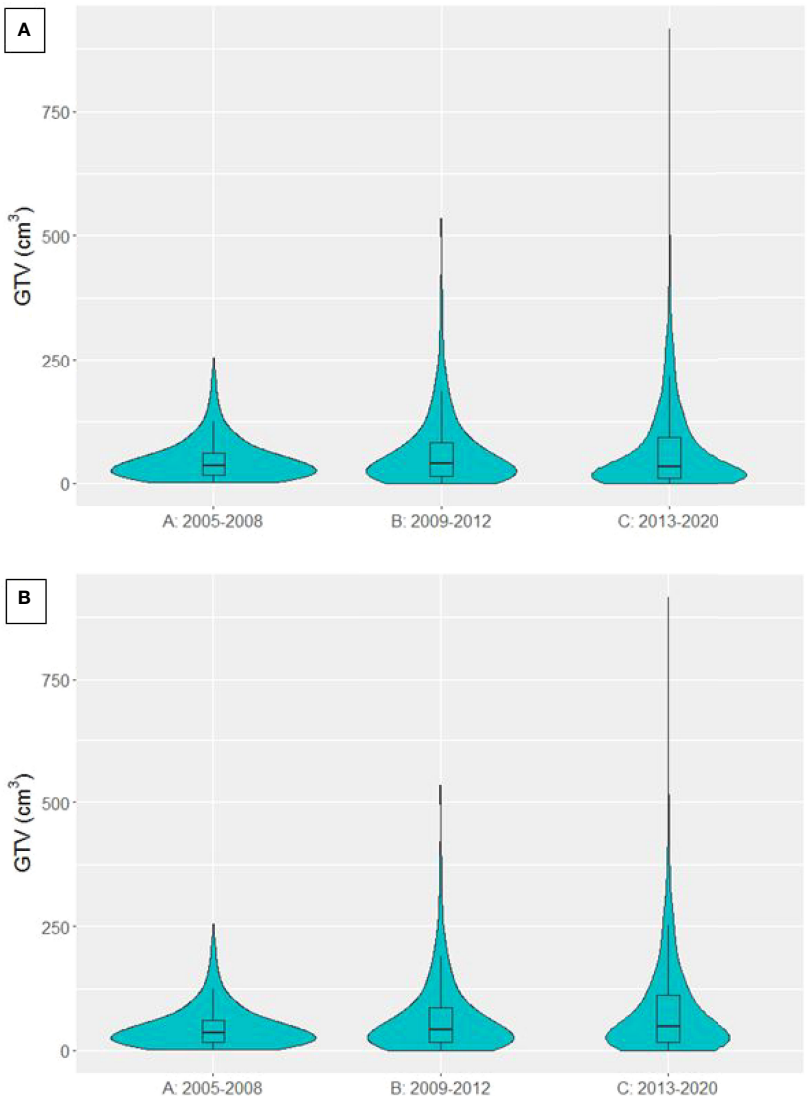

FIGURE 4 | Violin plot presenting the distribution of GTVs in patients treated with curative-intent radiotherapy in each time period. **(A)** SABR patients included **(B)** SABR patients excluded.

which has only been in routine use in the U.K. since 2019 (the latter part of our latest time period).

There are other limitations to this study including its retrospective design, and as is always the case when performing big data analyses, there is a significant amount of missing data within the clinical variables, including the lack of data on systemic therapy. This was more evident in the earlier time frames which were prior to our in house electronic e-record being created, which

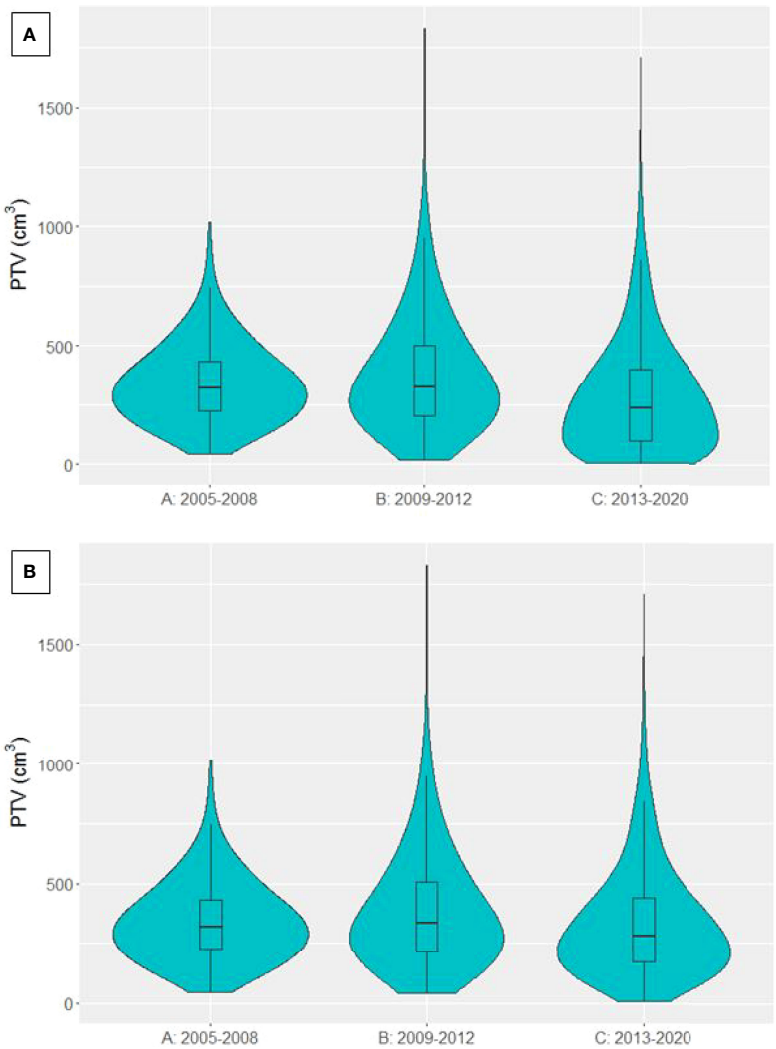

FIGURE 5 | Violin plot presenting the distribution of PTVs from patients treated with curative-intent radiotherapy in each time period. **(A)** SABR patients included **(B)** SABR patients excluded.

facilitated the prospective collection of key data on outcome forms. We feel the large number of patients included in this analysis in part mitigates the issue of missing data (19). Furthermore, this study reports on a unique dataset that evaluates real-world data from patients that are typically excluded from clinical trials. It is also worth noting that we have purposefully included a heterogenous population of lung cancer patients with differing histologies into this analysis as we were interested in evaluating the impact of IMRT on curative-intent treatment. Admittedly the dose threshold for curative intent of greater than 40Gy may also have included patients with NSCLC who did not fully complete their treatment, but in the context of such a large study, the numbers of patients whom this applies to are expected to be low.

These results are of particular importance in the UK, following publication of the most recent national lung cancer audit (10). This highlighted that the majority of stage III NSCLC patients are receiving best supportive care or palliative treatment, even when patients have a PS of 0/1. In addition, there was a large regional variation in the percentage of patients receiving curative intent treatment from 8-80% (10). It has been suggested that the centres offering a greater proportion of patients curative intent treatment may have better access to optimal radiotherapy planning techniques and image guided treatment (20). Indeed, in the Royal College of Radiologists (RCR) published consensus statements for radiotherapy for lung cancer, it is recommended that patients receiving radical radiotherapy are planned with advanced techniques such as IMRT or VMAT (21).

The implementation of IMRT for the curative-intent treatment of lung cancer has lagged behind that of other disease sites such as head& neck cancers. This may stem from a perceived lack of high level evidence for using the technique. To date, there has only been one prospective study looking at the

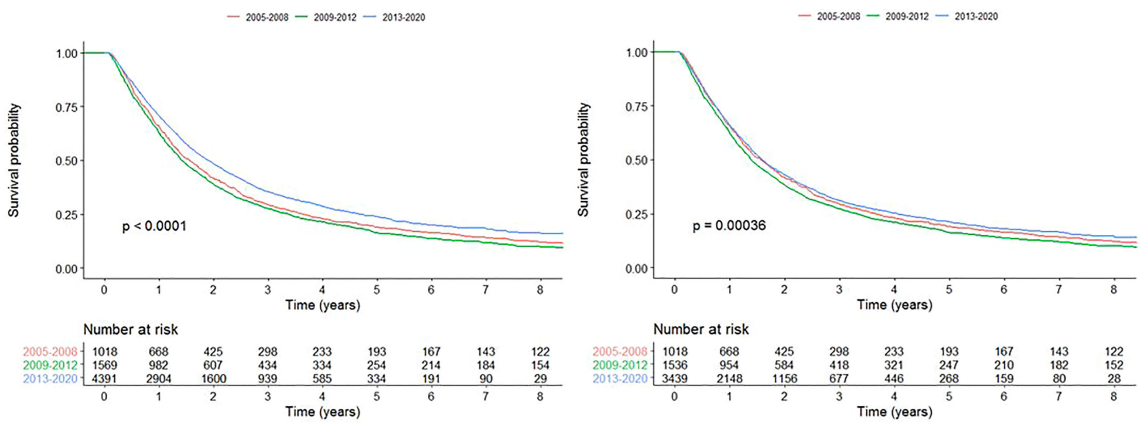

FIGURE 6 | Kaplan-Meier survival curves for each time period for all patients treated with curative-intent radiotherapy (left) and curative-intent without SABR (right).

impact of IMRT on treatment toxicity and survival (12). Chun et al. compared the outcome of patients treated with IMRT to 3D-CRT within the RTOG 0617 trial, reporting that despite larger planning target volumes in the IMRT group, patients had a lower rates of grade 3+ pneumonitis and higher cardiac doses, however no difference in survival between the groups was observed (12). A retrospective study by Yom et al. showed that patients treated with IMRT had larger GTVs compared to matched patients treated with 3D-CRT. Similarly to Chun et al., they reported lower rates of grade 3+ pneumonitis in the IMRT group (22). On the other hand, due to the complexity and cost of delivering IMRT, it has been suggested that 3D-CRT is still an equally sound option for locally advanced NSCLC, particularly for less experienced centres (23). A meta-analysis of studies comparing IMRT to 3D-CRT reported survival to be similar between the two techniques, however there were reduced incidence of grade 2 pneumonitis and increased grade 3 oesophagitis in the IMRT group (24). Overall the available data suggests that IMRT facilitates treatment of larger volumes, does not lead to inferior survival in NSCLC patients and should be employed to reduce dose to organs at risk, particularly to the heart and lung (12, 24).

IMRT and other advanced radiotherapy planning techniques offer the opportunity to achieve more than just treating larger volumes. Due to its ability to sculpt dose around the treatment volume, it may be possible to safely deliver a higher dose to the tumour, without compromising normal tissue toxicity. The hypothesis is that higher dose should equate to improved local control, and subsequently better survival. The RTOG 0617 study results however suggested that dose escalating with conventional

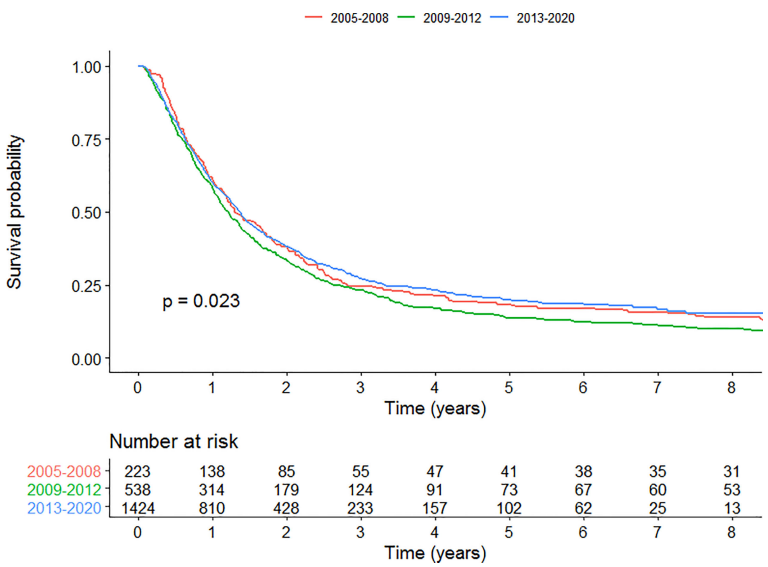

FIGURE 7 | Kaplan-Meier survival curves for each time period for patients with stage III disease curative-intent radiotherapy.

fractionation does not seem to offer a benefit. It should be noted that only 47% patients in this study were planned with IMRT, dose to the heart was not prioritised in radiotherapy planning and further analysis has shown that higher cardiac dose in this trial is associated with worse survival (12). Since the publication of RTOG 0617, further studies have demonstrated that excess radiation dose to the heart is associated with a decrease in survival (25). A number of studies are have addressed the question of isotoxic dose escalation and dose painting based on FDG PETCT which are facilitated by the use of IMRT (26).

Looking forward, it may be possible in the future to perform causal inference analyses, which would help establish whether the increased proportion of patients treated with curative intent, and their improved survival, is indeed attributable to the introduction on IMRT. The data could also be enhanced by including treatment related toxicity, something that can now be achieved through the use of patient reported outcomes (ePROMS) and proactive, prospective clinician reported toxicity, which we are now documenting at our centre on an eform at each outpatient visit (27).

In summary, this big data analysis has demonstrated that the introduction of IMRT was associated with an increasing proportion of patients with lung cancer receiving curative-intent radiotherapy, across all PS and stages of disease. Despite treating larger, more complex tumours with curative-intent, and more patients with poor performance status, a survival benefit was seen for patients treated when full access to IMRT was available. This study highlights the impact IMRT has had on our practice, acknowledging that other contributing factors such as improvement in staging, technical radiotherapy and systemic therapy may have also contributed to the improved survival. We would recommend that IMRT is available for routine use for lung cancer patients who are being considered for treatment with curative intent. Current evidence suggests that this technique, at the very least, leads to non-inferior outcomes, and may facilitate improved outcomes firstly through the greater number of patients with stage III disease being able to receive a curative-intent dose, and secondly through a reduction of dose to the normal tissues.

DATA AVAILABILITY STATEMENT

The raw data supporting the conclusions of this article will be made available by the authors, without undue reservation.

AUTHOR CONTRIBUTIONS

All authors contributed to the article and approved the submitted version.

FUNDING

This work was supported by CRUK *via* the funding to Cancer Research UK Manchester Centre: [C147/A18083] and [C147/A25254]. CF-F is supported by NIHR Manchester Biomedical Research Centre.

SUPPLEMENTARY MATERIAL

The Supplementary Material for this article can be found online at: https://www.frontiersin.org/articles/10.3389/fonc.2022.835844/full#supplementary-material

REFERENCES

1. Bray F, Ferlay J, Soerjomataram I, Siegel RL, Torre LA, Jemal A. Global Cancer Statistics 2018: GLOBOCAN Estimates of Incidence and Mortality Worldwide for 36 Cancers in 185 Countries. *CA Cancer J Clin* (2018) 68 (6):394–424. doi: 10.3322/caac.21492
2. Siegel RL, Miller KD, Jemal A. Cancer Statistics, 2019. *CA Cancer J Clin* (2019) 69(1):7–34. doi: 10.3322/caac.21551
3. Cancer Research UK. *Lung Cancer Survival Statistics* (2010). Available at: https://www.cancerresearchuk.org/health-professional/cancer-statistics/statistics-by-cancer-type/lung-cancer/survival (Accessed February 19, 2020).
4. Department of Health Cancer Policy Team. *Radiotherapy Services in England 2012*. Department of Health (2012).
5. Aupérin A, Le Péchoux C, Rolland E, Curran WJ, Furuse K, Fournel P, et al. Meta-Analysis of Concomitant Versus Sequential Radiochemotherapy in Locally Advanced Non - Small-Cell Lung Cancer. *J Clin Oncol* (2010) 28 (13):2181–90. doi: 10.1200/JCO.2009.26.2543
6. Machtay M, Paulus R, Moughan J, Komaki R, Bradley JE, Choy H, et al. Defining Local-Regional Control and its Importance in Locally Advanced Non-Small Cell Lung Carcinoma. *J Thorac Oncol* (2012) 7(4):716–22. doi: 10.1097/JTO.0b013e3182429682
7. Connell PP, Hellman S. Advances in Radiotherapy and Implications for the Next Century: A Historical Perspective. *Cancer Res* (2009) 69(2):383–92. doi: 10.1158/0008-5472.CAN-07-6871
8. Diwanji TP, Mohindra P, Vyfhuis M, Snider JW, Kalavagunta C, Mossahebi S, et al. Advances in Radiotherapy Techniques and Delivery for Non-Small Cell Lung Cancer: Benefits of Intensity-Modulated Radiation Therapy, Proton Therapy, and Stereotactic Body Radiation Therapy. *Transl Lung Cancer Res* (2017) 6(2):131–47. doi: 10.21037/tlcr.2017.04.04
9. Brown S, Banfill K, Aznar MC, Whitehurst P, Finn CF. The Evolving Role of Radiotherapy in Non-Small Cell Lung Cancer. *Br J Radiol* (1104) 2019:92. doi: 10.1259/bjr.20190524
10. Adizie JB, Khakwani A, Beckett P, Navani N, West D, Woolhouse I, et al. Stage III Non-Small Cell Lung Cancer Management in England. *Clin Oncol* (2019) 31(10):688–96. doi: 10.1016/j.clon.2019.07.020
11. Chan C, Lang S, Rowbottom C, Guckenberger M, Faivre-Finn C. Intensity-Modulated Radiotherapy for Lung Cancer: Current Status and Future Developments. *J Thorac Oncol* (2014) 9(11):1598–608. doi: 10.1097/JTO.0000000000000346
12. Chun SG, Hu C, Choy H, Komaki RU, Timmerman RD, Schild SE, et al. Impact of Intensity-Modulated Radiation Therapy Technique for Locally Advanced Non-Small-Cell Lung Cancer: A Secondary Analysis of the NRG Oncology RTOG 0617 Randomized Clinical Trial. *J Clin Oncol* (2017) 35 (1):56–62. doi: 10.1200/JCO.2016.69.1378
13. Van Loon J, Grutters J, Macbeth F. Evaluation of Novel Radiotherapy Technologies: What Evidence Is Needed to Assess Their Clinical and Cost Effectiveness, and How Should We Get It? *Lancet Oncol* (2012) 13(4):e169–77. doi: 10.1016/S1470-2045(11)70379-5

14. Johnson C, Price G, Khalifa J, Faivre-Finn C, Dekker A, Moore C, et al. A Method to Combine Target Volume Data From 3D and 4D Planned Thoracic Radiotherapy Patient Cohorts for Machine Learning Applications. *Radiother Oncol* (2018) 126(2):355–61. doi: 10.1016/j.radonc.2017.11.015
15. R Core Team. *R: A Language and Environment for Statistical Computing*. Vienna, Austria: R Foundation for Statistical Computing (2018).
16. Therneau TM. *A Package for Survival Analysis in R. R Package Version 3.1-12* (2020). R Foundation for Statistical Computing, Vienna, Austria. Available at: https://cran.r-project.org/package=survival.
17. Ball DL, Fisher RJ, Burmeister BH, Poulsen MG, Graham PH, Penniment MG, et al. The Complex Relationship Between Lung Tumor Volume and Survival in Patients With Non-Small Cell Lung Cancer Treated by Definitive Radiotherapy: A Prospective, Observational Prognostic Factor Study of the Trans-Tasman Radiation Oncology Group (TROG 99.05). *Radiother Oncol* (2013) 106(3):305–11. doi: 10.1016/j.radonc.2012.12.003
18. Zhang J, Gold KA, Lin HY, Swisher SG, Xing Y, Lee JJ, et al. Relationship Between Tumor Size and Survival in Non-Small-Cell Lung Cancer (NSCLC): An Analysis of the Surveillance, Epidemiology, and End Results (SEER) Registry. *J Thorac Oncol* (2015) 10(4):682–90. doi: 10.1097/JTO.0000000000000456
19. Kang H. The Prevention and Handling of the Missing Data. *Korean J Anesthesiol* (2013) 64(5):402–6. doi: 10.4097/kjae.2013.64.5.402
20. Mcdonald F, Senan S, Faivre-Finn C, Hatton M. Curative Radiotherapy for Non-Small Cell Lung Cancer: Practice Changing and Changing Practice? *Clin Oncol* (2019) 31(10):678–80. doi: 10.1016/j.clon.2019.07.025
21. RCR. *Radiotherapy for Lung Cancer RCR Consensus Statements*. Royal Collage of Radiologists (2020).
22. Yom SS, Liao Z, Liu HH, Tucker SL, Hu CS, Wei X, et al. Initial Evaluation of Treatment-Related Pneumonitis in Advanced-Stage Non-Small-Cell Lung Cancer Patients Treated With Concurrent Chemotherapy and Intensity-Modulated Radiotherapy. *Int J Radiat Oncol Biol Phys* (2007) 68(1):94–102. Royal Collage of Radiologists. doi: 10.1016/j.ijrobp.2006.12.031
23. Ball D, MacManus M, Siva S, Plumridge N, Bressel M, Kron T. Routine Use of Intensity-Modulated Radiotherapy for Locally Advanced Non-Small-Cell Lung Cancer is Neither Choosing Wisely Nor Personalized Medicine. *J Clin Oncol* (2017) 35(13):1492. doi: 10.1200/JCO.2016.71.3156
24. Hu X, He W, Wen S, Feng X, Fu X, Liu Y, et al. Is IMRT Superior or Inferior to 3DCRT in Radiotherapy for NSCLC? A Meta-Analysis. *PloS One* (2016) 11 (4):1–15. doi: 10.1371/journal.pone.0151988
25. Banfill K, Giuliani M, Aznar M, Franks K, McWilliam A, Schmitt M, et al. Cardiac Toxicity of Thoracic Radiotherapy: Existing Evidence and Future Directions. *J Thorac Oncol* (2021) 16(2):216–27. doi: 10.1016/j.jtho.2020.11.002
26. Christodoulou M, Bayman N, McCloskey P, Rowbottom C, Faivre-Finn C. New Radiotherapy Approaches in Locally Advanced Non-Small Cell Lung Cancer. *Eur J Cancer* (2014) 50(3):525–34. doi: 10.1016/j.ejca.2013.11.027
27. Crockett C, Gomes F, Faivre-Finn C, Howell S, Kasipandian V, Smith E, et al. The Routine Clinical Implementation of Electronic Patient-Reported Outcome Measures (ePROMs) at The Christie NHS Foundation Trust. *Clin Oncol* (2021) 33(12):761–4. doi: 10.1016/j.clon.2021.06.004

Conflict of Interest: The authors declare that the research was conducted in the absence of any commercial or financial relationships that could be construed as a potential conflict of interest.

Publisher's Note: All claims expressed in this article are solely those of the authors and do not necessarily represent those of their affiliated organizations, or those of the publisher, the editors and the reviewers. Any product that may be evaluated in this article, or claim that may be made by its manufacturer, is not guaranteed or endorsed by the publisher.

frontiers | Frontiers in Oncology

ORIGINAL RESEARCH
published: 07 June 2022
doi: 10.3389/fonc.2022.805538

Continuous Vaginal Bleeding Induced By EGFR-TKI in Premenopausal Female Patients With EGFR Mutant NSCLC

Min Yu[1], *Xiaoyu Li*[1,2], *Xueqian Wu*[1], *Weiya Wang*[3], *Yanying Li*[1], *Yan Zhang*[1], *Shuang Zhang*[4] *and Yongsheng Wang*[1,2*]

[1] Department of Thoracic Oncology of Cancer Center, West China Hospital, Sichuan University, Chengdu, China, [2] Institute of Drug Clinical Trials, West China Hospital, Sichuan University, Chengdu, China, [3] Department of Pathology, West China Hospital, Sichuan University, Chengdu, China, [4] Department of Biotherapy, Cancer Center, West China Hospital, Sichuan University, Chengdu, China

OPEN ACCESS

Edited by:
Meng Xu Welliver, The Ohio State University, United States

Reviewed by:
Yuqing Lou, Shanghai Jiaotong University, China
Tianqing Chu, Shanghai Jiaotong University, China

***Correspondence:**
Yongsheng Wang
wangys@wchscu.cn

Specialty section:
This article was submitted to Thoracic Oncology, a section of the journal Frontiers in Oncology

Received: *30 October 2021*
Accepted: *07 April 2022*
Published: *07 June 2022*

Citation:
Yu M, Li X, Wu X, Wang W, Li Y, Zhang Y, Zhang S and Wang Y (2022) Continuous Vaginal Bleeding Induced By EGFR-TKI in Premenopausal Female Patients With EGFR Mutant NSCLC. Front. Oncol. 12:805538. doi: 10.3389/fonc.2022.805538

EGFR-TKI is widely used for EGFR-mutant NSCLC patients. Bleeding is reported as a neglected adverse effect induced by EGFR-TKI. Female patients with lung adenocarcinoma have a high frequency of EGFR mutations. This study investigated the effect of EGFR-TKI on the menstrual cycle, especially on bleeding, in women of childbearing age. The underlying mechanism was further investigated in a patient with severe bleeding. We retrospectively investigated the effects on menstrual cycle in premenopausal female NSCLC patients who underwent EGFR-TKI treatment during 2013 to 2019. Menstrual changes including cycle disorders and prolonged bleeding were investigated *via* questionnaire survey. EGFR signaling, ER, PR and tissue factor expression were analyzed in endometrium tissue obtained from a 43-year-old patient who suffered from continuous vaginal bleeding during treatment with erlotinib and osimertinib. Among 42 premenopausal female patients taking EGFR tyrosine kinase inhibitor, 69.05% patients experienced abnormal menstruation. In women with abnormal menstruation, 41.37% had profuse menstruation and 20.69% had irregular menstruation. In most cases, the abnormal vaginal bleeding stopped when suspending EGFR-TKI. The EGFR-TKI induced abnormal vaginal bleeding might be associated with low progesterone level, decreased EGFR activation and tissue factor (TF) expression in endometrial tissues. EGFR-TKI unusually induce abnormal vaginal bleeding in premenopausal female NSCLC patients, which may be attributed to progesterone/EGFR/TF signaling. Megestrol acetate may be an available and effective drug for the uncommon adverse effect.

Keywords: vaginal bleeding, non-small cell lung cancer, EGFR tyrosine kinase inhibitor, epidermal growth factor receptor, premenopausal female

BACKGROUND

Epidermal growth factor receptor (EGFR) activation mutation has been demonstrated to be driver genes in non-small cell lung cancer (NSCLC) that can benefit from oral EGFR tyrosine kinase inhibitors (1, 2). Most of EGFR tyrosine kinase inhibitor (EGFR-TKI) have been developed to block autophosphorylation and subsequent signal transduction, including both wild type and mutant EGFR signaling (3, 4). Therefore, EGFR-TKI inevitably generate some adverse events, including skin toxicity, gastrointestinal reactions, and so on, owing to extensive EGFR expression in both tissue and normal tissue (5).

Clinically, some female patients complained of menstrual abnormalities, even prolonged or continuous bleeding. As known, EGFR mutation rate was significantly higher in women, especially in younger women, while these population may have normal menstruation (6). Previous studies have shown that EGF/EGFR signaling is closely related to growth, differentiation of human endometrium and even hemostasis in the menstrual cycle (7). Abnormal menstruation, especially vaginal bleeding, is a common but possibly severe gynecological symptom. In this situation, it is necessary to clarify whether EGFR-TKI induces the continuous bleeding of the menstrual cycle and its underlying mechanism for clinical treatment.

Herein, we investigated menstrual changes in premenopausal women after receiving EGFR-TKI treatment, in particular prolonged and increased bleeding, and explored potential mechanisms in a severe vaginal bleeding patient.

METHODS

Patient and Clinical Data Collection

Premenopausal female patients with EGFR-mutant NSCLC and received EGFR-TKI during 2013 to 2019 were investigated whether there was an abnormal menstruation. Clinical characteristics and the following data were collected: bleeding pattern of the vaginal bleeding (duration, volume, frequency), types of EGFR inhibitor, applied medical interventions to stop the bleeding, and the subsequent outcome of the bleeding. The Ethics Committee of West China Hospital has exempted informed consent.

Endometrial Sample Analysis

A 43-year-old patient who suffered from continuous vaginal bleeding and diagnostic curettage during treatment with erlotinib and osimertinib. Endometrial sample in the typical case was used for the examination of EGFR, p-EGFR and TF expression by immunohistochemistry. Two samples from non-cancer patients were used as controls.

RESULTS

Patients and Clinical Data

We retrospectively analyzed the menstrual status in 42 premenopausal women during EGFR-TKI treatment. It indicated that 69.05% women experienced abnormal menstruation. Among women with abnormal menstruation, 20.69% women had irregular menstruation, 41.37% had profuse menstruation, and 37.94% had scanty menstruation (**Figure 1**).

A Case Report and Case-Based Mechanism

A 43-year-old female Chinese never-smoker was admitted to local hospital in February 2014, for severe headache and vomiting. Radiological investigations showed intracranial space occupying lesion suggestive of metastasis. The patient underwent craniotomy and excision of the lesion. Histological examination and CT scan revealed a brain metastasis of lung adenocarcinoma. After 2 cycles of chemotherapy using docetaxel and nedaplatin, CT image suggested that adenocarcinoma of the left lung had increased dramatically. The patient was admitted to our hospital in May 2014. CT image showed a 4.0 cm diameter mass in the upper lobe of the left lung, with multiple nodules of different sizes in both lungs. Targeted next-generation sequencing (NGS) was performed on DNA extracted from the tumor biopsy specimen, revealing that the tumor harbored EGFR exon 19 deletion. The patient was treated with erlotinib, 150 mg daily from 18 May 2014. After 5 weeks of treatment, chest CT showed mass in the upper lobe of the left lung shrunk significantly (**Figure 2A**). Nevertheless, the patient complained of continuous vaginal bleeding for 2 weeks, with a volume of more than 10 ml daily. The hemorrhage worsened over time, and the patient was in hemorrhagic shock caused by massive bleeding. It is worth noting that conventional hemostatic drugs did not work. The bleeding reduced after the diagnostic curettage, and no malignant cells were found in the pathological examination. She tried to stop taking erlotinib, and bleeding stopped 3 days later. She suffered from vaginal bleeding again after erlotinib

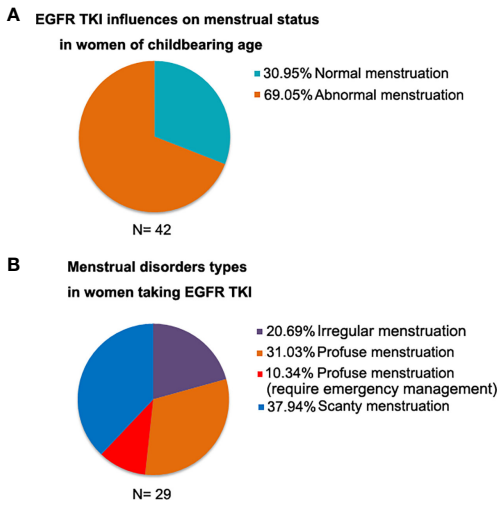

FIGURE 1 | The menstrual status in 42 premenopausal women during EGFR-TKI treatment. **(A)** 69.05% women experienced abnormal menstruation; **(B)** Among women with abnormal menstruation, 41.37% had profuse menstruation.

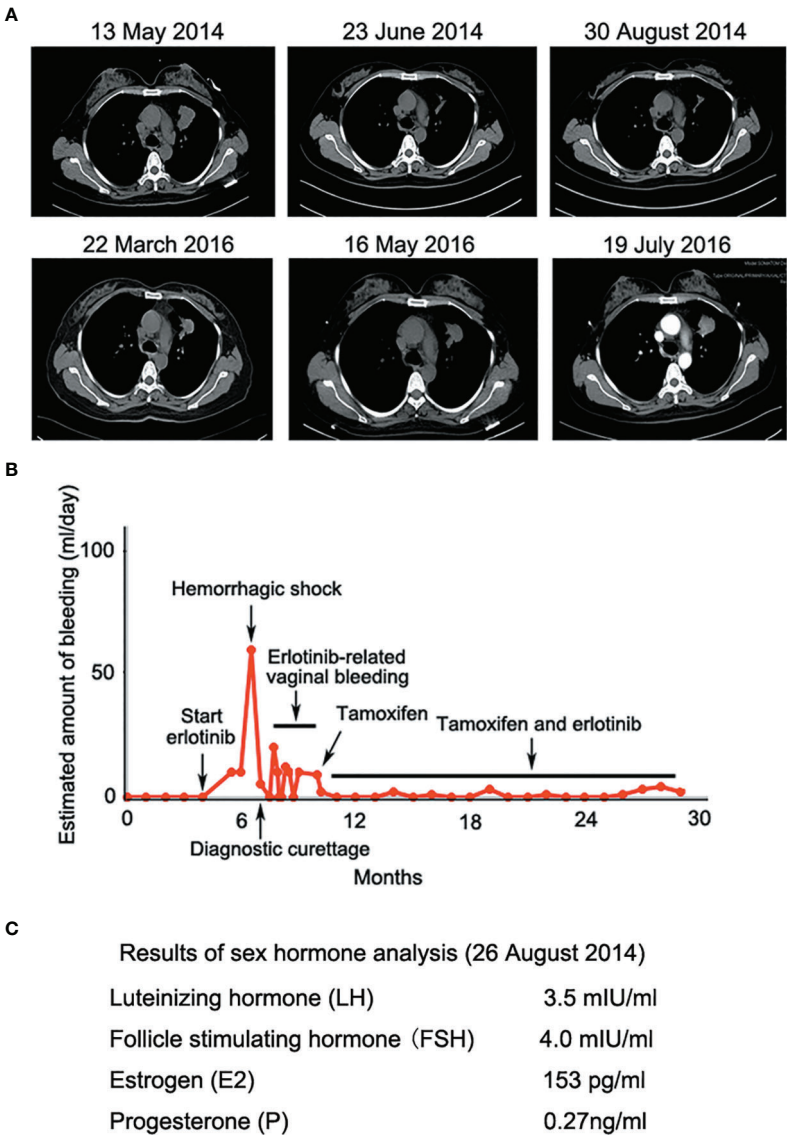

FIGURE 2 | **(A)** Erlotinib decreased lesion in the upper lobe of the left lung significantly at the early stage of treatment; **(B)** Erlotinib-related vaginal bleeding during the treatment; **(C)** Sex hormone tests showed low levels of progesterone during luteal stages of the menstrual cycle.

rechallenge, then bleeding stopped entirely after the ending of taking erlotinib. Erlotinib-related vaginal bleeding recurred three times (**Figure 2B**). Laboratory data were generally unremarkable except for mild anemia and low progestin level during luteal stages of the menstrual cycle (**Figure 2C**). The patient had no previous gynecological symptom and was excluded from gynecological diseases by gynecologist. She also refused to replace erlotinib owing to significant clinical benefit. The bleeding was not controlled even after the erlotinib dose was changed to 75 mg daily. The patient was then treated with tamoxifen 10 mg daily without ceasing erlotinib. Vaginal bleeding stopped 5 days after taking tamoxifen. The patient intermittently took tamoxifen due to side effects such as gastrointestinal discomfort. Vaginal bleeding did not stop completely, but the amount of bleeding was significantly decreased, which supported continuing use of erlotinib for about 20 months.

Given that erlotinib also targets wild-type EGFR, we detected EGFR expression and activation in endometrial tissues by curettage. Compared with normal endometrial tissues, immunohistochemical results showed that the expression levels of EGFR, p-EGFR and TF in endometrial tissues of the case decreased significantly (**Figures 3**, **4**). In July 2016, lung lesion was found to be progressive, and the patient was switched to 80 mg osimertinib once daily. Vaginal bleeding recurred after taking osimertinib, and bleeding completely stopped soon after subcutaneous injection of progesterone. However, the severe bleeding reoccurred when she stopped progesterone, and she had to receive another curettage.

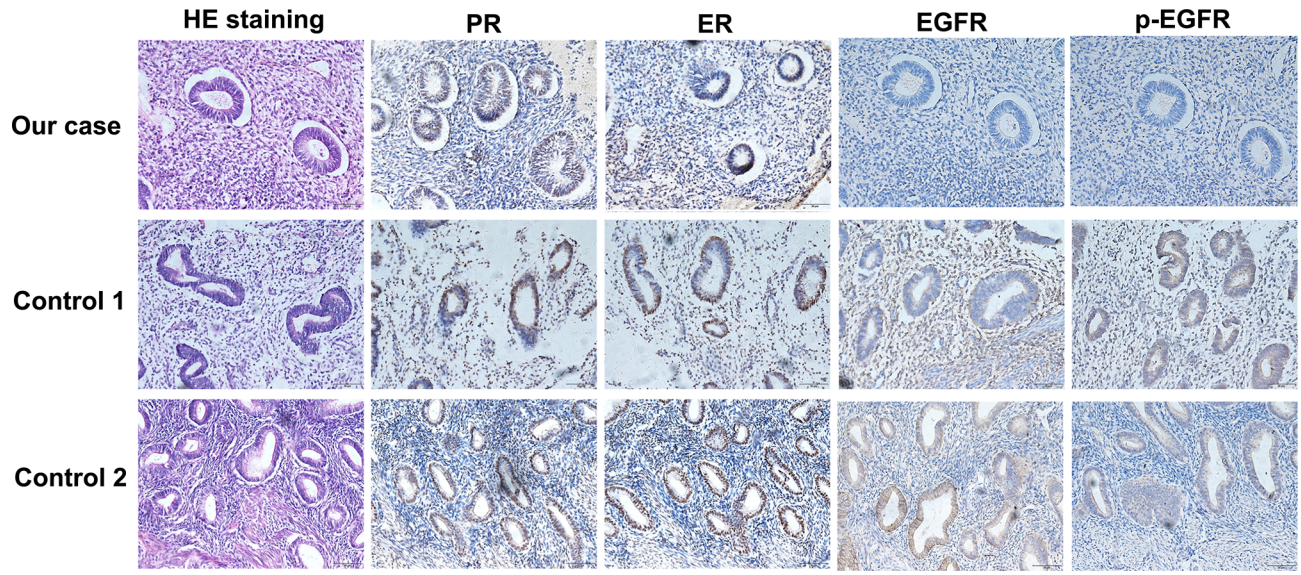

FIGURE 3 | Compared with normal endometrial tissues, immunohistochemical results showed that the expression levels of EGFR and p-EGFR in endometrial tissues of the case decreased significantly.

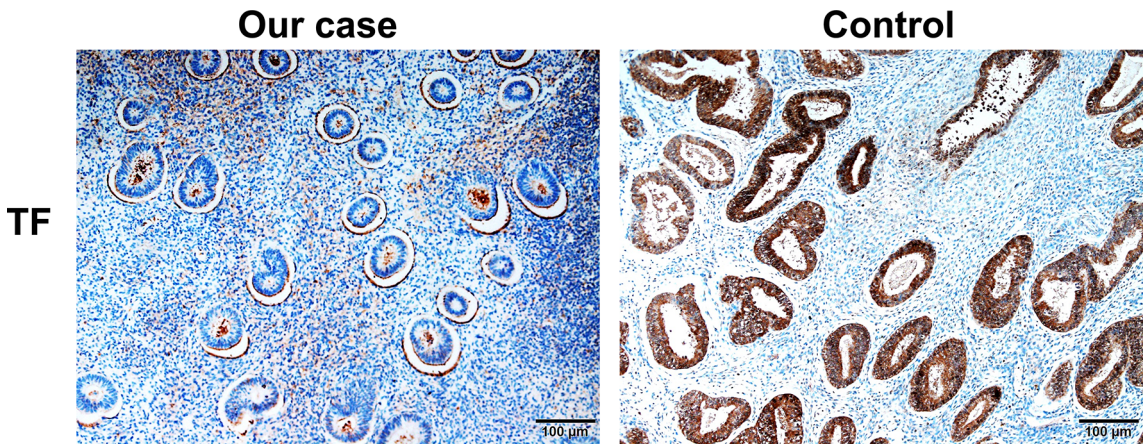

FIGURE 4 | Compared with normal endometrial tissues, immunohistochemical results showed that the expression levels of TF in endometrial tissues of the case decreased significantly.

Then, she had to take tamoxifen again since osimertinib brought tumor shrinkage and vaginal bleeding again (**Figure 5**). In November 2017, progressive pulmonary lesions and new liver lesions were detected by CT scan. EGFR exon 19 deletion (2.71% mutation abundances) was found by NGS in plasma, and she tried to rechallenge with 150 mg erlotinib daily in January 2018. Vaginal bleeding occurred during erlotinib treatment, and she stopped taking erlotinib, then liver and pulmonary lesions deteriorated in February 2018 (**Figure 6A**). The patient subsequently underwent CT-guided percutaneous lung biopsy of pulmonary lesion, which revealed adenocarcinoma with EGFR exon 19 deletion without EGFR T790M and other resistant mutations. Pemetrexed/carboplatin combined with bevacizumab was administrated in March 2018. Three days after discharge, the patient developed vaginal bleeding with a volume greater than 100 mL daily. This time, the bleeding was stopped by conventional hemostatic drugs including carbazochrome sodium sulfonate (**Figure 6B**). After bleeding stopped, the patient continued to receive pemetrexed/carboplatin, but liver and lung lesions progressed after 2 cycles of chemotherapy (**Figure 6A**). The patient then took 30 mg afatinib daily, and vaginal bleeding started again soon. The bleeding stopped soon 2 days after administration of 320 mg megestrol daily. One

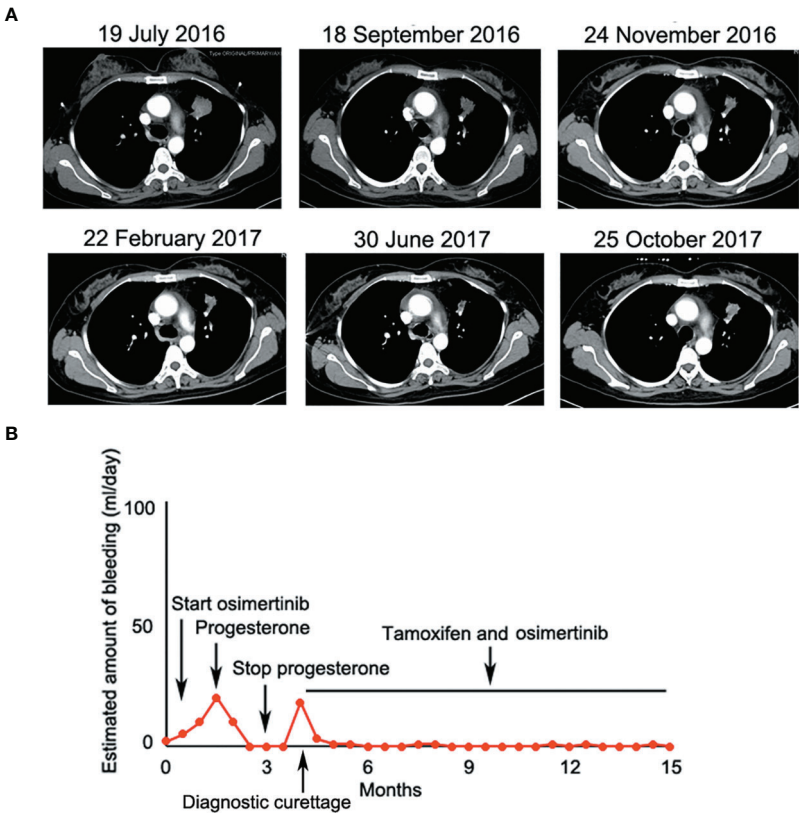

FIGURE 5 | **(A)** Osimertinib decreased lesion in the upper lobe of the left lung significantly at the early stage of treatment; **(B)** Osimertinib-related vaginal bleeding during the treatment.

month after administration of afatinib, progressive disease was confirmed owing to the increase of pulmonary, liver and intracranial lesions (**Figure 6A**). In June 2018, the patient received a daily 12 mg anlotinib, a novel multi-targeting tyrosine kinase inhibitor. The treatment lasted for one week, and the patient stopped the therapy due to adverse reactions such as fatigue, vomiting, and vaginal bleeding again (**Figure 6B**). Finally, she received nivolumab but did not show efficacy and died in July 2018. The overall survival of the patient was 53 months (**Figure 6C**).

DISCUSSION

Clinically, EGFR-TKI-induced gastrointestinal bleeding is very rare though several studies reported EGFR-TKI-induced hemorrhage such as gastrointestinal bleeding (5). However, it is not uncommon for female patients to complain of menstrual abnormalities and even prolonged vaginal bleeding. It is very important to verify whether these clinical manifestations were induced by EGFR-TKI and explore the underlying mechanism and potential treatment. We investigated the menstrual changes in premenopausal women during EGFR-TKI treatment. It indicated that 69.05% women experienced abnormal vaginal bleeding. Especially, in the reported case, the patient experienced EGFR-TKI treatment, bleeding, dosage reduction, discontinuation, rechallenge, and repeated bleeding. Nevertheless, most of female patients do not want to talk about these symptoms or can tolerate these changes, and continue to EGFR-TKI treat, resulting in both clinicians and patients to ignore this symptom. Our research suggests that we should pay attention to EGFR-TKI-induced menstruation abnormalities, notably prolonged and increased bleeding.

The mechanisms for EGFR-TKI-induced menstruation abnormalities remainunclear. In this study, the typical case provided some clues to help us to understand the underlying mechanism. In this case, it is very clear for the relationship between vaginal bleeding and EGFR-TKI including erlotinib, osimertinib and afatinib since bleeding recurred several times after the initiation of EGFR tyrosine kinase inhibitor and stopped exactly after drug withdrawal. Previous studies demonstrated that synthesis and expression of human endometrial EGF and EGFR played important role in the menstrual cycle, and EGF and EGFR levels were significantly increased at the luteal stages compared with the early follicular stage (8). TF is the primary initiator of hemostasis, which is strategically positioned to counteract the threat of hemorrhage during endovascular trophoblast invasion

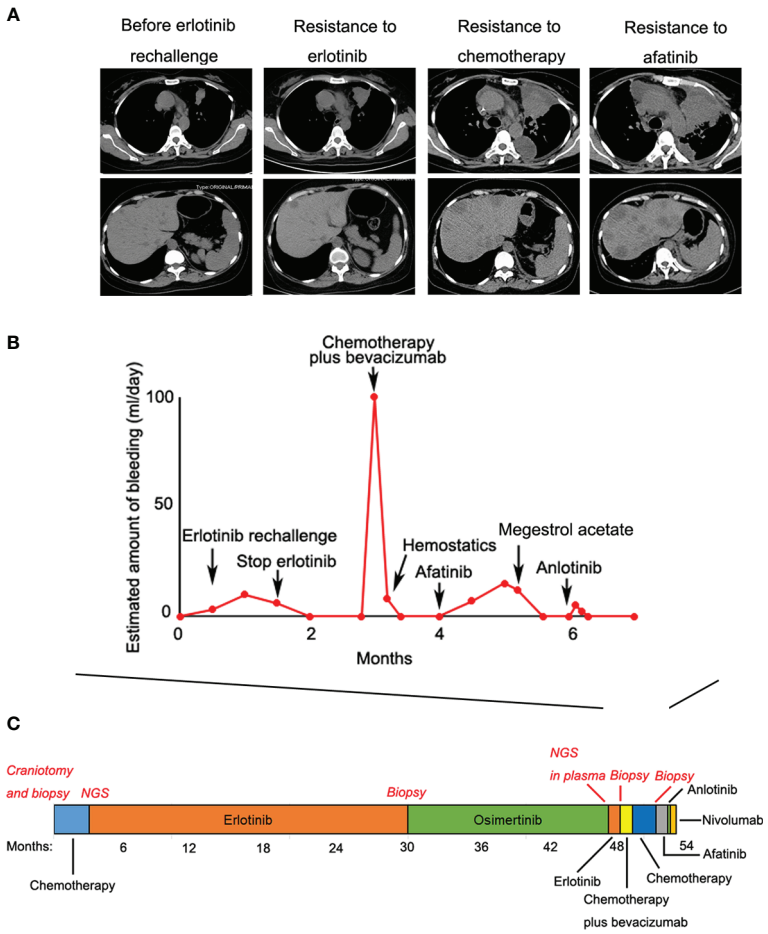

FIGURE 6 | **(A)** Liver and pulmonary lesions deteriorated during the subsequent treatments; **(B)** Vaginal bleeding during the subsequent treatments; **(C)** Treatment summary and the overall survival of the patient was 53 months.

and subsequent induces thrombin formation. In human endometrial stromal cells, progestin increased TF mRNA and protein levels, and EGFR agonist plus progestin further enhanced TF expression (7, 9). Therefore, progestin, EGF/EGFR and TF play joint roles in menstrual cycle. The patient had low progestin level even in the luteal stages. Besides, we found that expression levels of EGFR, p-EGFR and TF in endometrial tissues of our case decreased significantly. This all indicated that low progestin and inhibition of EGFR signaling may result in decreased of TF expression. More importantly, treatment with progesterone or megestrol completely remit vaginal bleeding induced by osimertinib and afatinib. Therefore, we speculate that the downregulated EGFR signaling and low progestin level mediated decreased TF expression, which led to prolonged vaginal bleeding in our case. Progesterone or megestrol administration alleviated vaginal bleeding, this provided convincing evidence in the molecular mechanism.

We initially used tamoxifen to treat vaginal bleeding in the hope of using tamoxifen's side effect that may induce cessation of menstruation. Besides, tamoxifen plus erlotinib resulted in cytotoxicity and cell growth inhibition synergistically in NSCLC cell lines (10). In this case, tamoxifen is effective for EGFR-TKI-induced vaginal bleeding though it does not completely solve the problem. These findings may support the combined administration of tamoxifen and EGFR inhibitor. Mechanically, however, we tend to select megestrol to combine with EGFR-TKI for better control of bleeding.

Treatment guidelines are insufficient and the optimal treatment for this uncommon drug-induced bleeding has not yet been established. As small molecular targeted therapies become an attractive therapeutic option in oncology, our study helps to recognize the unnoticeable side effects and apply the potentially effective treatment.

DATA AVAILABILITY STATEMENT

The raw data supporting the conclusions of this article will be made available by the authors, without undue reservation.

ETHICS STATEMENT

The studies involving human participants were reviewed and approved by The Ethics Committee of West China Hospital. Written informed consent for participation was not required for this study in accordance with the national legislation and the institutional requirements.

AUTHOR CONTRIBUTIONS

MY and SZ collected, analyzed the patient data, and wrote the manuscript. XL, YL and YZ collected the clinical data. WW and XW performed histological examinations. YW designed the study, revised the article, and approved for the final version to be submitted. All authors read and approved the final manuscript.

FUNDING

This work was supported by the National Science and Technology Major Project (2017ZX09304023) and National Natural Science Foundation (81472197) of China.

ACKNOWLEDGMENTS

We owe thanks to the patient and her family.

SUPPLEMENTARY MATERIAL

The The Supplementary Material for this article can be found online at: https://www.frontiersin.org/articles/10.3389/fonc.2022.805538/full#supplementary-material

REFERENCES

1. Shepherd FA, Rodrigues Pereira J, Ciuleanu T, Tan EH, Hirsh V, Thongprasert S, et al. Erlotinib in Previously Treated non-Small-Cell Lung Cancer. *N Engl J Med* (2005) 353:123–32. doi: 10.1056/NEJMoa050753
2. Wu YL, Zhou CC, Lu S, Qin S, Pan H, Wu G, et al. Erlotinib Versus Gemcitabine/Cisplatin in Chinese Patients With EGFR Mutation-Positive Advanced non-Small-Cell Lung Cancer: Crossover Extension and Post-Hoc Analysis of the ENSURE Study. *Lung Cancer* (2019) 130:18–24. doi: 10.1016/j.lungcan.2019.01.016
3. Laurie SA, Goss GD. Role of Epidermal Growth Factor Receptor Inhibitors in Epidermal Growth Factor Receptor Wild-Type non-Small-Cell Lung Cancer. *J Clin Oncol* (2013) 31:1061–9. doi: 10.1200/JCO.2012.43.4522
4. Winther-Larsen A, Fledelius J, Sorensen BS, Meldgaard P. Metabolic Tumor Burden as Marker of Outcome in Advanced EGFR Wild-Type NSCLC Patients Treated With Erlotinib. *Lung Cancer* (2016) 94:81–7. doi: 10.1016/j.lungcan.2016.01.024
5. Bai H, Liu Q, Shi M, Zhang J. Erlotinib and Gefitinib Treatments of the Lung Cancer in an Elderly Patient Result in Gastrointestinal Bleeding. *Pak J Med Sci* (2013) 29:1278–9. doi: 10.12669/pjms.295.3661
6. Lee SH, Kim WS, Choi YD, Seo JW, Han JH, Kim MJ, et al. Analysis of Mutations in Epidermal Growth Factor Receptor Gene in Korean Patients With Non-small Cell Lung Cancer: Summary of a Nationwide Survey. *J Pathol Transl Med* (2015) 49:481–8. doi: 10.4132/jptm.2015.09.14
7. Schatz F, Krikun G, Caze R, Rahman M, Lockwood CJ. Progestin-Regulated Expression of Tissue Factor in Decidual Cells: Implications in Endometrial Hemostasis, Menstruation and Angiogenesis. *Steroids* (2003) 68:849–60. doi: 10.1016/s0039-128x(03)00139-9
8. Imai T, Kurachi H, Adachi K, Adachi H, Yoshimoto Y, Homma H, et al. Changes in Epidermal Growth Factor Receptor and the Levels of its Ligands During Menstrual Cycle in Human Endometrium. *Biol Reprod* (1995) 52:928–38. doi: 10.1095/biolreprod52.4.928
9. Taketani Y, Ishihara S, Miyauchi A, Mizuno M. Roles of Epidermal Growth Factor (EGF) in the Growth and Differentiation of Human Endometrium. *Hum Cell* (1989) 2:260–4.
10. Ko JC, Chiu HC, Syu JJ, Jian YJ, Chen CY, Jian YT, et al. Tamoxifen Enhances Erlotinib-Induced Cytotoxicity Through Down-Regulating AKT-mediated Thymidine Phosphorylase Expression in Human non-Small-Cell Lung Cancer Cells. *Biochem Pharmacol* (2014) 88:119–27. doi: 10.1016/j.bcp.2014.01.010

Conflict of Interest: The authors declare that the research was conducted in the absence of any commercial or financial relationships that could be construed as a potential conflict of interest.

Publisher's Note: All claims expressed in this article are solely those of the authors and do not necessarily represent those of their affiliated organizations, or those of the publisher, the editors and the reviewers. Any product that may be evaluated in this article, or claim that may be made by its manufacturer, is not guaranteed or endorsed by the publisher.

frontiers | Frontiers in Oncology

ORIGINAL RESEARCH
published: 18 July 2022
doi: 10.3389/fonc.2022.815737

Loss of Frizzled 9 in Lung Cells Alters Epithelial Phenotype and Promotes Premalignant Lesion Development

*Kayla Sompel[1], Lori D. Dwyer-Nield[2], Alex J. Smith[1], Alamelu P. Elango[1], Lauren A. Vanderlinden[3], Katrina Kopf[4], Robert L. Keith[1,5] and Meredith A. Tennis[1]**

[1] School of Medicine, University of Colorado Anschutz Medical Campus, Aurora, CO, United States, [2] Skaggs School of Pharmacy, University of Colorado Anschutz Medical Campus, Aurora, CO, United States, [3] School of Public Health, University of Colorado Anschutz Medical Campus, Aurora, CO, United States, [4] Office of Academic Affairs, National Jewish Health, Denver, CO, United States, [5] Division of Pulmonary Sciences and Critical Care Medicine, Rocky Mountain Regional Medical Center, Aurora, CO, United States

OPEN ACCESS

Edited by:
Meng Xu Welliver, Comprehensive Cancer Center, The Ohio State University, United States

Reviewed by:
Farrah Kheradmand, Baylor College of Medicine, United States
Melissa V Gammons, MRC Laboratory of Molecular Biology (LMB), University of Cambridge, United Kingdom

***Correspondence:**
Meredith A. Tennis
Meredith.Tennis@cuanschutz.edu
orcid.org/0000-0002-0619-6732

Specialty section:
This article was submitted to Thoracic Oncology, a section of the journal Frontiers in Oncology

Received: *15 November 2021*
Accepted: *21 June 2022*
Published: *18 July 2022*

Citation:
Sompel K, Dwyer-Nield LD, Smith AJ, Elango AP, Vanderlinden LA, Kopf K, Keith RL and Tennis MA (2022) Loss of Frizzled 9 in Lung Cells Alters Epithelial Phenotype and Promotes Premalignant Lesion Development. Front. Oncol. 12:815737. doi: 10.3389/fonc.2022.815737

The transmembrane receptor Frizzled 9 (FZD9) is important for fetal neurologic and bone development through both canonical and non-canonical WNT/FZD signaling. In the adult lung, however, Fzd9 helps to maintain a normal epithelium by signaling through peroxisome proliferator activated receptor γ (PPARγ). The effect of FZD9 loss on normal lung epithelial cells and regulators of its expression in the lung are unknown. We knocked down FZD9 in human bronchial epithelial cell (HBEC) lines and found that downstream EMT targets and PPARγ activity are altered. We used a FZD9$^{-/-}$ mouse in the urethane lung adenocarcinoma model and found FZD9$^{-/-}$ adenomas had more proliferation, increased EMT signaling, decreased activation of PPARγ, increased expression of lung cancer associated genes, increased transformed growth, and increased potential for invasive behavior. We identified PPARγ as a transcriptional regulator of FZD9. We also demonstrated that extended cigarette smoke exposure in HBEC leads to decreased FZD9 expression, decreased activation of PPARγ, and increased transformed growth, and found that higher exposure to cigarette smoke in human lungs leads to decreased FZD9 expression. These results provide evidence for the role of FZD9 in lung epithelial maintenance and in smoking related malignant transformation. We identified the first transcriptional regulator of FZD9 in the lung and found FZD9 negative lesions are more dangerous. Loss of FZD9 creates a permissive environment for development of premalignant lung lesions, making it a potential target for intervention.

Keywords: Frizzled 9, lung cancer, transformed growth, EMT, premalignant lesions

INTRODUCTION

Frizzled 9 (FZD9) is a G protein-coupled transmembrane receptor commonly expressed in brain, testis, skeletal muscle and renal tissue (1). FZD9 is in the chromosomal region 7q11.23 and alterations are associated with Williams-Beuren syndrome, while loss of FZD9 in mouse models has been associated with slight abnormality in B-cell development, impaired osteoblast function, and learning defects (2). Alterations in FZD9 have been associated with cancers including astrocytoma,

osteosarcoma, acute myeloid leukemia, and hepatocellular carcinoma (3–7). FZD9 interacts with several WNT ligands in tumors to activate β-catenin signaling, including WNT2, WNT5a, and WNT3a, and to promote EMT and invasiveness. In contrast, in the lung FZD9 interacts with WNT7a to activate tumor suppressive signaling. WNT7a binds to FZD9 and signals to peroxisome proliferator activated receptor gamma (PPARγ) through an Erk5-dependent cascade, leading to anti-tumor signaling, including increasing epithelial and reducing mesenchymal gene expression (3, 8). Loss of FZD9 in NSCLC cell lines leads to increased transformed growth and decreased PPARγ signaling, but these studies did not investigate the effect of FZD9 loss in a normal lung epithelium (9).

In matched human lung tumor and normal tissues, 77% of tumors had less FZD9 than normal tissues, suggesting that FZD9 is a lung tumor suppressor (10). In serial endobronchial biopsies, FZD9 expression is higher in regressive endobronchial dysplasia compared to progressive or persistent endobronchial dysplasia (10). Urethane and smoke exposed mice have decreased FZD9 expression (10). In an *in vitro* model using a human bronchial epithelial cell line (HBEC), FZD9 expression decreases with short and long term cigarette smoke condensate (CSC) exposure (10). Mutations in Frizzled receptors are not common in lung cancer and regulation of FZD9 in the lung is largely unknown. A few studies have identified regulators in other contexts, such as leukemia and bone formation (5, 11). To further characterize FZD9 in the lung and investigate its preventive and therapeutic potential, we studied the effects of FZD9 loss on normal lung cells and how it is affected by cigarette smoke using *in vitro* and *in vivo* models and human lung biopsies.

MATERIALS AND METHODS

Cell Culture

Non-transformed human bronchial epithelial cells (HBEC3KT and HBEC2KT) (a gift from the lab of Dr. John Minna, UT Southwestern) were cultured in Keratinocyte Serum Free Medium (GIBCO) (12). All HBEC cell cultures were grown and handled in a dedicated incubator. Human embryonic kidney 293T (HEK293T) cell line (purchased from the American Type Culture Collection) was cultured in DMEM (GIBCO) with 10% FBS. All cell lines were cultured at 37°C in a humidified 5% CO2 incubator and passaged twice per week. To generate cigarette smoke condensate (CSC), filters from a TE-10 smoking machine (Teague Enterprises) were weighed before and after smoking ten cigarettes and then soaked in DMSO to recover cigarette smoke particulate. For CSC exposure, 24 hours after seeding HBEC3KT, cells were treated with 5μg/mL of CSC or equal volume vehicle control (DMSO). Treatment was repeated after each passage, two times per week for one to 24 weeks and conducted in triplicate. Adenoma cell lines were created as previously described from WT and $FZD9^{-/-}$ urethane treated mice (13). After they were established, adenoma lines were cultured in DMEM (GIBCO) with 10% FBS and 1% of 10,000U/mL of Pen/Strep (Gibco) and 1% of 25ug/mL of AmphotericinB (Gibco) at 37°C in a humidified 5% CO2 incubator and passaged twice per week. For the migration assay, wild type and $FZD9^{-/-}$ adenoma cell lines were cultured in a 24 well plate with a 500μm silicone insert (Ibidi) and grown to 90% confluency around the insert. The insert was removed, and cells were imaged at 0, 4, 8, and 24 hours. Migration was captured on Nikon TMS microscope fitted with an AmScope digital camera. For the transformed growth assay, tumor cell lines were grown on a low-attachment plate (S-BIO) at a concentration of 1000 cells/well. At 72 hours, cell growth was analyzed using the CellTiter Glo Assay (Promega) (14). Statistical analysis was done by two-tailed t-test or one way ANOVA with Tukey's *post hoc* analysis in GraphPad Prism (RRID : SCR_002798, version 9.0.2).

qPCR

Mouse lung tissue and lesions were collected in RNA Later (Qiagen) at the time of harvest. Cell line and tissue RNA were extracted with the RNeasy Plus kit (Qiagen). qPCR Prime PCR Assays (Bio-Rad) for mouse included: NFKB, EZH2, FZD9, FN1, VIM, COX2, IL1β, ESR1, ESR2, SNAI1, PLK1, Cyclin D1, BCL2, NCAD, ECAD, VEGFA, COL1α2, and PPARγ. qPCR was conducted using standard protocol for SsoAdvanced SYBR Green Master Mix (Bio-Rad) on a CFX96 Touch (Bio-Rad). All gene expression data was normalized to the reference gene RPS18 and fold changes were calculated using the $2^{-\Delta\Delta Ct}$ method. PCR analysis was conducted in triplicate and statistical analysis was done by two-tailed t-test or one way ANOVA with Tukey's *post hoc* analysis in GraphPad Prism.

Western Blot, ELISA, Dot Blot

Mouse lung tissue was collected and flash frozen in liquid nitrogen at the time of harvest. Protein was extracted from 10mg of tissue and for western blots, 20ug per sample was used to measure vimentin, COX2, e-cadherin, and β-actin (vimentin, 1:1000 Cell Signaling Technologies#D21H3; COX2, 1:500 Protein Tech#6635-1-Ig; e-cadherin, 1:3000 Protein Tech#20874-1-AP; β-actin, Biorad #MCA5775GA). Quantitative analysis was performed on triplicate experiments by creating a ratio between the band intensity for the protein of interest and its corresponding β-actin band intensity. Additional protocol details for western blots are included in the supplementary methods. For the active β-catenin ELISA, protein was extracted from 10mg of flash frozen mouse tissue and 80% confluent 100mm plates of tumor cells using Symansis MKA buffer (Symansis). After protein quantification by BCA assay, the ELISA was performed with 100μg of mouse tissue protein or 30μg of tissue lysate per manufacturer instructions (Symansis). Fluorescence was measured on a Glomax Instrument (Promega). For the apoptosis protein dot blot, protein was extracted from tumor cells using RIPA buffer (Thermo Scientific) with HALT protease inhibitor (Thermo Scientific). After protein quantification by BCA assay, one apoptosis dot blot assay was performed for each sample per the manufacturer's instructions (RayBiotech, #AAM-APO-1-8) with 500μg of cell lysate. Blots were imaged with chemiluminescence settings on a BioRad ChemiDoc Imager. Relative differences in protein were determined by normalizing the positive control intensity between membranes.

Transfections

For PPRE assays, HBEC3KT and HBEC2KT cells were seeded at 5000 cells/well in a 96 well plate with triplicates for each experimental group. After 24 hours, wells were transfected with PPARγ response element luciferase (PPRE; a gift from Bruce Spiegelman; Addgene plasmid #1015) (45ng) and renilla control reporter vector (Promega) (5ng) using TransIT-X2 transfection reagent (Mirus Bio) per the manufacturer's protocol. After 48 hours, PPRE (firefly) and control reporter (renilla) were measured using the Dual-Luciferase Reporter assay kit (Promega) on a Glomax instrument (Promega). For CSC experiments in HBEC3KT, cells were treated with 5μg/ml of CSC for 48 hours or two weeks before luciferase analysis. For FZD9 promoter experiments, HBEC3KT were transfected with a luciferase vector containing the complete Fzd9 promoter, PPARγ plasmid (Genecopoeia), or control plasmid (Genecopoeia), with activity measured by the Secret-Pair Dual Luminescence Assay kit (Genecopoeia) on a Glomax. siRNA experiments were transfected with FZD9 siRNA (Genecopoeia), PPARγ siRNA (Qiagen), or Allstar negative siRNA control (Qiagen). Experiments were conducted in triplicate. Significance of luciferase assays was assessed by two-tailed t-test or one way ANOVA with Tukey's *post hoc* analysis in GraphPad Prism.

In Vivo Mouse Studies

The methods for generation and genotyping of $FZD9^{-/-}$ FVBN mice are in the supplementary methods. Male and female $FZD9^{-/-}$ mice were generated for experiments by breeding $FZD9^{-/-}$ males with $FZD9^{-/-}$females to produce 100% knockout litters and were housed in a pathogen-free facility in the Veterinary Care Unit at the Rocky Mountain Regional VA Medical Center (RMRVAMC). Mice were injected IP with 100μl of 1 mg urethane/g body weight dissolved in 0.9% saline vehicle or with 100ul saline. Mice were weighed daily for 7 days after urethane injection and weekly for the remainder of the experiment. After 16 weeks of urethane exposure, mice were sacrificed by a lethal dose of Fatal Plus. Lungs from three mice were inflated with formalin and fixed. Lesions were dissected from surrounding lung tissue and diameters were measured with digital calipers. The surrounding lung tissue was saved for RNA extraction. For the six-week smoke study, one group of mice was exposed to whole body cigarette smoke (CS) at particulate levels of 35 mg/m^3 and the other to ambient air in Teague Enterprises TE-10 smoking machines for 6 hour/day, 5 days/week for 6 weeks. Mice were weighed daily during the first 3 weeks of CS exposure, and weekly thereafter. CS exposure was suspended in mice experiencing 15-20% weight loss, until they regained weight. RNA was extracted from whole lung tissues. Statistical analysis using a two-tailed t-test or one way ANOVA with Tukey's *post hoc* analysis was conducted using GraphPad Prism. Studies were carried out in accordance with the recommendations in the NIH Guide for the Care and Use of Laboratory Animals and were approved by the RMRVAMC Animal Care and Use Committee. microCT imaging is described in the supplementary methods. Wild type and $FZD9^{-/-}$ tumor cell lines were generated by dissecting 24-week urethane induced tumors, chopping tumors into 1mm sections, and culturing in DMEM, low glucose, 10% FBS media until cells grew consistently in a 100mm dish and had 20+ passages.

Immunohistochemistry

5μm lung sections were used for Ki67 staining (1:2000 dilution, Abcam 15580). Tumor area was measured and Ki67-positive nuclei/mm^2 were counted in each tumor. Replicate blinded counts were conducted. The Ki67+ nuclei/mm^2 tumor area for each tumor was averaged by group. A one-way ANOVA with Tukey's *post hoc* analysis in GraphPad Prism was used to determine statistical differences between groups. H&E stains were done on 5μm lung sections from WT and $FZD9^{-/-}$, urethane and saline groups. Additional protocol details are included in the supplementary methods.

Serum PPARγ Activity Assay

Serum was collected by intracardiac puncture immediately after euthanizing each mouse. HEK293T cells were seeded at 2,000 cells/well in a 96 well plate. After twenty-four hours, the cells were transfected with 45ng of PPRE and 5ng renilla control reporter vector using TransiT-X2 transfection reagent and Opti-MEM media, per the manufacturer's protocol. Cells were treated with 10μl mouse serum at 24 hours and 48 hours post transfection (15). Serum treatments were conducted in triplicate and included empty and mock transfection controls. Luciferase activity was measured after 48 hours using the Dual-Luciferase Reporter assay kit on the Glomax. PPRE activity was normalized to renilla activity and analyzed relative to untreated controls. Significance was assessed by two tailed t-test in GraphPad Prism.

Analysis of Human Lung Biopsy Samples

The oral iloprost lung cancer chemoprevention study was a Phase II, placebo-controlled trial of iloprost in current and former smokers at increased risk for lung cancer (NCT00084409). The characteristics of the population, protocol, and the results have been reported in detail (16). Biopsies were collected at baseline and after six months of treatment with iloprost or placebo. Pre- and post-treatment biopsies were collected for 125 subjects and 413 total tissues were available for analysis. RNA *in situ* hybridization (RISH) was conducted to measure FZD9 and PPARγ in biopsy tissues, which were deidentified and used with approval of the Colorado Multiple Institutional Review Board. RNAscope GAPDH (positive control), dapB (negative control), FZD9, and PPARγ probes were used according to the manufacturer's protocol (ACDBio). Percent of epithelial cells with signal in each sample were counted and samples were included in analysis if the positive control and targets had at least 10% more positive cells than the negative control. RISH Data Pre-processing and Quality Control: Quantitation of gene expression was used by summing up the number of slides with the gene present. GAPDH was a reference gene and if the negative control was more than 5 units above GAPDH (n=14) or the expression for GAPDH was missing (n=25), the samples was removed from the dataset. Further QC was done on the individual gene level with any samples missing removed from analysis (FZD9 n = 14, PPARγ n = 24). Gene expression, after adjustment for GAPDH, was used moving forward for all statistical modeling.

Baseline Statistical Model

In our baseline model, gene expression was dichotomized into low or high gene expression based on the median value. Pack years and quit time were dichotomized into either high or low based on the median value for each variable. Each smoking variable of interest (smoking status, pack years and quit time), a logistic mixed-model was run (lme4, v.1.1-26) using gene expression as the outcome and smoking variable as the predictor while adjusting for sex and accounting for random effects of subject. For quit time, we flipped the OR for comparison purposes with the other smoking variables (i.e., high smoking exposure is the risk factor modeled).

RESULTS

Loss of FZD9 in Normal Lung Epithelial Cells Alters EMT and PPARγ Pathways

Loss of FZD9 in NSCLC cell lines leads to decreased PPARγ activity, but the effect of FZD9 loss on non-transformed cells is unknown (9). We knocked down expression of FZD9 in two human bronchial epithelial cell lines (HBEC3KT and HBEC2KT) using an siRNA approach (**Figure 1A**). HBEC cells are immortalized by co-transfecting with cyclin-dependent kinase 4 (CDK4) and human telomerase reverse transcriptase (hTERT). This allows HBEC cells to replicate continuously with epithelial-like features but without becoming malignant (17). Loss of FZD9 in these cell lines altered expression of lung cancer associated genes and targets of PPARγ, a downstream measure of FZD9 activity (**Figure 1B**). In both cell lines, loss of FZD9 led to significant increases in IL1β, VEGFA, and COX2 and in the HBEC3KT cell line, NFKβ and EZH2 also had significantly increased expression. Loss of FZD9 led to alterations in EMT gene expression in both cell lines (**Figure 1C**). Mesenchymal gene vimentin (VIM) increased in both cell lines, while snail increased in HBEC2KT and MMP9 increased in HBEC3KT. Epithelial gene e-cadherin (ECAD) decreased slightly with FZD9 loss in HBEC3KT. Gene expression changes varied between the two cell lines but shared some similarities and both demonstrated effects of FZD9 loss. Loss of FZD9 in both cell

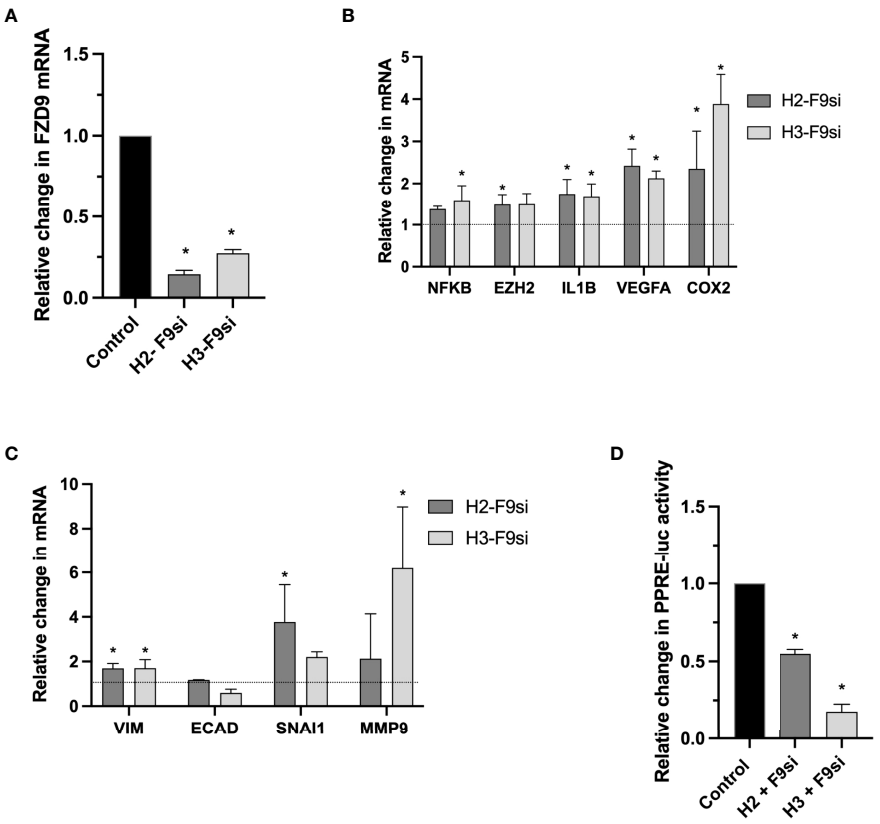

FIGURE 1 | Loss of FZD9 alters downstream targets in HBEC. siRNA was used to knock down FZD9 expression in HBEC3KT and HBEC2KT cell lines and results are shown relative to a scramble siRNA control. **(A)** FZD9 expression measured by qPCR. Results are normalized to GAPDH. **(B)** Gene expression with FZD9 siRNA transfection was measured for NFKB, EZH2, IL1B, VEGFA and COX2. Results are normalized to GAPDH and relative to a scramble siRNA control (dotted line). **(C)** Expression of VIM, ECAD, SNAI1 and MMP9 was measured after FZD9 siRNA transfection. Results are normalized to GAPDH and relative to a scramble siRNA control (dotted line). **(D)** Change in PPRE-luciferase activity. Each cell line is shown relative to its own control transfection (set to 1). Transfections and qPCR were conducted in triplicate. H2-F9si, HBEC2KT + FZD9 siRNA; H3-F9si, HBEC3KT + FZD9 siRNA. Statistical significance was measured by a two tailed t-test relative to each cell line's control. Significance is *p<0.05 compared to control.

lines decreased the activity of PPARγ as measured by PPRE (**Figure 1D**). These results demonstrate that loss of FZD9 in lung epithelial cells leads to changes associated with lung cancer and could support EMT. FZD9 loss in combination with a carcinogen exposure could augment tumor promotion.

Loss of FZD9 *In Vivo* Increases Adenoma Multiplicity

To validate *in vitro* effects of FZD9 loss in normal lung cells, we used a CRISPR approach to generate an FVB/N FZD9$^{-/-}$ mouse. Loss of FZD9 had no significant physiologic or anatomic effects up to one year of age. FZD9$^{-/-}$ mice, along with wild type controls, were used in an established lung adenocarcinoma model, where animals are given a single injection of urethane or saline control and develop adenomas starting at 6 weeks, with carcinomas developing at 20 weeks (18). There were no differences in animal weights during the experiment (**Figure 2A**). **Figure 2B** shows a 3D image generated from microCT imaging that is representative of adenoma development in wild type and FZD9$^{-/-}$ mice treated with urethane. Urethane exposure in wild type or FZD9$^{-/-}$ mice leads to increased adenoma multiplicity compared to saline controls (**Figure 2C**). Adenoma multiplicity in FZD9$^{-/-}$ urethane mice compared to wild type urethane mice trended higher (p=0.08) (**Figure 2C**). Adenoma diameter did not differ between urethane exposed wild type or FZD9$^{-/-}$ mice (**Figure 2D**). Ki67 proliferation staining in adenomas was not significantly different between urethane exposed wild type and FZD9$^{-/-}$ mice (**Figure 2E**). FZD9$^{-/-}$ adenomas displayed a wide range of Ki67 staining, suggesting there may be subsets of FZD9$^{-/-}$ lesions with other alterations that stimulate proliferation (Representative Ki-67 images, **Supplementary Figure 1**). **Figure 2F** shows representative H&E stains of whole lung and 10x magnification from wild type saline, FZD9$^{-/-}$ saline, wild type urethane, and FZD9$^{-/-}$ urethane animals.

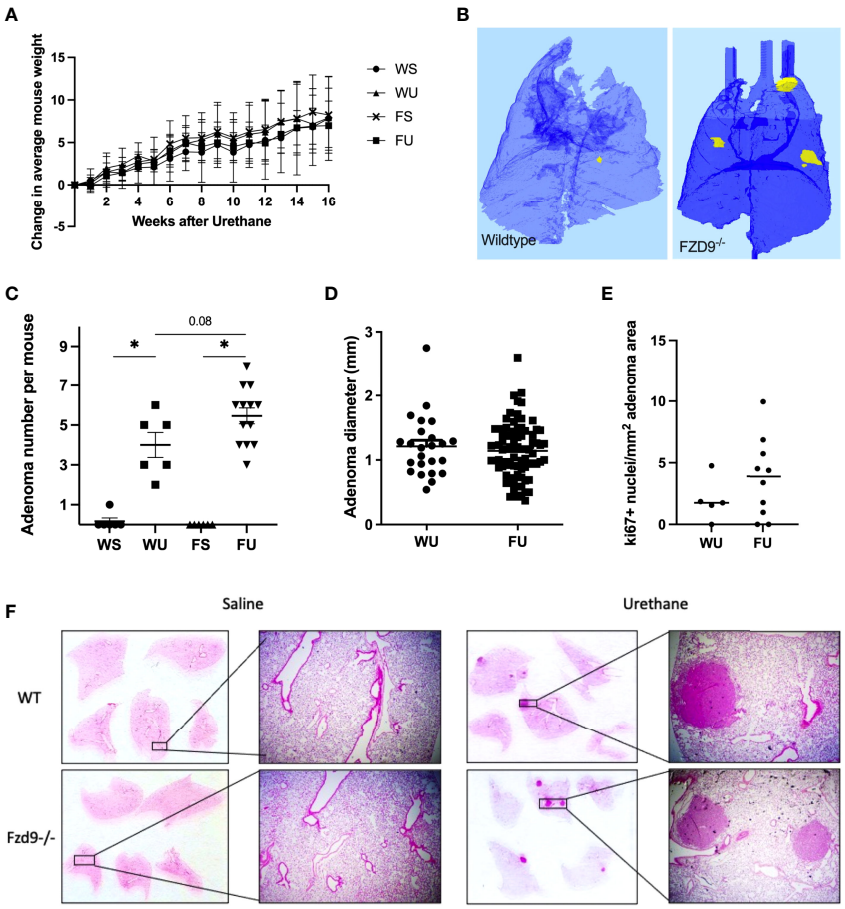

FIGURE 2 | Loss of FZD9 increases adenoma multiplicity *in vivo*. **(A)** Mice were weighed weekly after urethane exposure and average change each week was calculated for each group. **(B)** Representative microCT image of wild type and FZD9$^{-/-}$ mouse lungs 16 weeks after urethane exposure. Yellow indicates presence of an adenoma. **(C)** Wild type and FZD9$^{-/-}$ mice were exposed to 16 weeks of urethane or saline control and lesions were counted after sacrifice. Statistical significance was measured by one way ANOVA with Tukey's *post hoc* analysis and *p<0.05. **(D)** The diameter of each lesion was measured and compared between wild type and FZD9$^{-/-}$ mice. **(E)** Positive Ki-67 nuclei per mm^2 lesion area from adenomas in wild type or FZD9$^{-/-}$ mice exposed to urethane. **(F)** Representative H&E stains of whole lungs and 10x magnification from each group. WS, wild type saline; WU, wild type urethane; FS, FZD9$^{-/-}$ saline; FU, FZD9$^{-/-}$ urethane.

Downstream Gene Expression and Activity Is Affected by FZD9 Loss *In Vivo*

FZD9 activates PPARγ, which is associated with reducing inflammatory signals and reversing EMT signals. We measured gene expression markers of EMT and inflammation in whole lung samples from wild type saline, FZD9$^{-/-}$ saline, wild type urethane, and FZD9$^{-/-}$ urethane mice. We found that mesenchymal marker fibronectin (FN1) increased significantly with loss of FZD9 compared to wild type mice (**Figure 3A**). FN1 also increased, though non significantly, with exposure to urethane in wild type mice and was slightly higher in FZD9$^{-/-}$ mice with urethane. Mesenchymal marker vimentin (VIM) significantly increased in wild type urethane mice compared to wild type saline mice and was elevated in FZD9$^{-/-}$ saline mice similarly to wild type urethane exposure (**Figure 3B**). Inflammatory marker COX2 was significantly elevated with urethane in wild type mice and trended toward increased levels in FZD9$^{-/-}$ mice with saline or urethane (**Figure 3C**). Inflammatory marker IL1β was non-significantly elevated with urethane in wild type mice and with FZD9 loss, but was significantly higher in FZD9$^{-/-}$ mice exposed to urethane compared to wild type mice exposed to urethane (**Figure 3D**). Previous gene expression screening suggested estrogen receptor expression may be increased by FZD9 loss and alterations in estrogen receptors have been associated with lung cancer, so we measured expression of estrogen receptor α (ESR1) and β (ESR2) (19). We found no difference in ESR1 expression in female or male wild type mice exposed to urethane but detected significantly elevated expression of ESR1 in female FZD9$^{-/-}$ mice exposed to urethane compared to female Fzd9$^{-/-}$ saline mice and to male FZD9$^{-/-}$ urethane exposed mice (**Figure 3E**). Expression of ESR2 was significantly elevated in female FZD9$^{-/-}$ urethane mice compared to wild type urethane mice and compared to male Fzd9$^{-/-}$ urethane mice (**Figure 3F**). In male

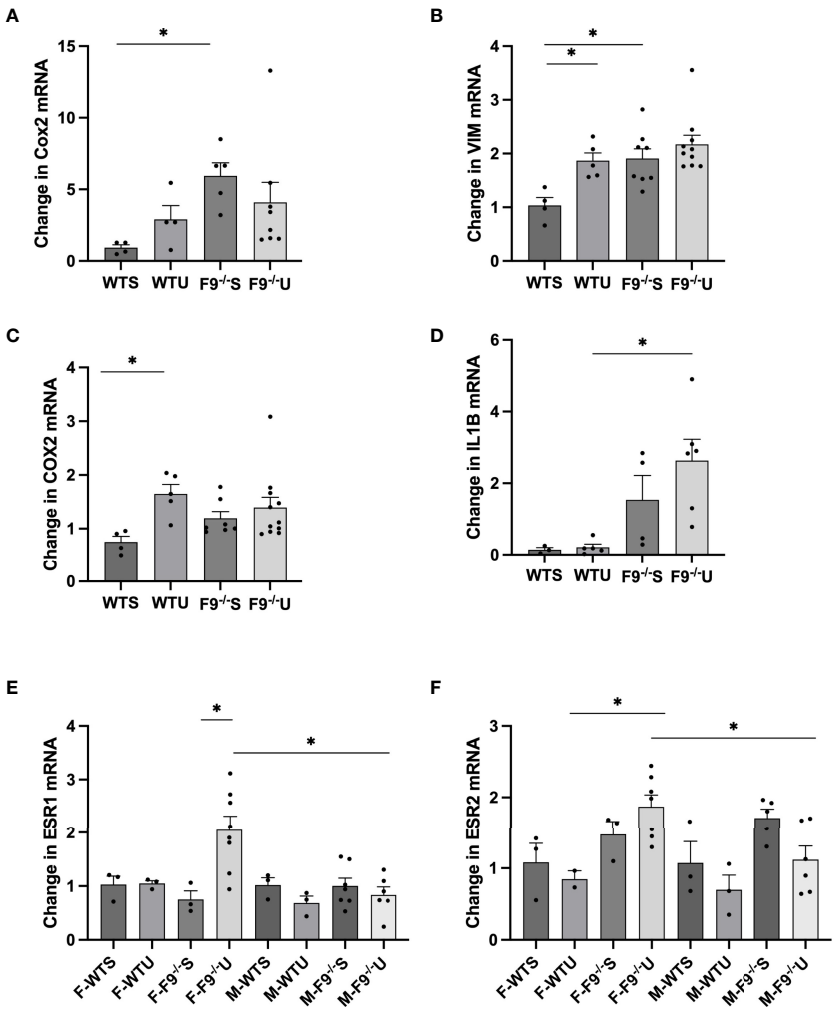

FIGURE 3 | FZD9 loss *in vivo* alters mRNA expression of downstream targets. RNA from mouse lung was harvested from wild type saline (WTS), wild type urethane (WTU), FZD9$^{-/-}$ saline (F9$^{-/-}$S), and FZD9$^{-/-}$ urethane (F9$^{-/-}$U) groups and gene expression measured by qPCR. **(A)** FN1, **(B)** VIM, **(C)** COX2, **(D)** IL1B, **(E)** ESR1, **(F)** ESR2. PCR was normalized to RPS18 and measured in triplicate. F-, Female; M-, Male. Significance was measured by one-way ANOVA and *p<0.05.

mice, expression of ESR2 trended toward an increase in FZD9$^{-/-}$ saline mice compared to wild type saline mice and toward a decrease with urethane exposure in both genotypes (**Figure 3F**).

To measure effects of FZD9 loss on downstream PPARγ activity, serum was collected from wild type and FZD9$^{-/-}$ mice and used to treat HEK293t cells transfected with PPRE (15). PPRE activity resulting from treatment with serum from FZD9$^{-/-}$ was significantly lower than wild type mice, indicating that there is a lower level of PPARγ activation when FZD9 is lost *in vivo* (**Figure 4A**). To further explore the downstream effects of FZD9 loss *in vivo*, we measured protein levels of mesenchymal marker VIM and inflammatory marker COX2 in whole lung protein extracts from wild type saline, FZD9$^{-/-}$ saline, wild type urethane, and FZD9$^{-/-}$ urethane mice. Loss of FZD9 increased COX2 expression with urethane exposure when compared to saline (**Figure 4B**).

VIM expression increased with urethane exposure in wild type mice and was higher in FZD9$^{-/-}$ mice (**Figure 4B**). FZD9 in the lung epithelium does not activate canonical β-catenin signaling, but pro-tumorigenic β-catenin activation may be a contributor to the tumor supportive conditions that accompany FZD9 loss (3, 8, 9, 20). In **Figure 4C**, we show increased active β-catenin in whole lung with exposure to urethane in both wild type and FZD9$^{-/-}$ mice. There was no difference in active β-catenin with FZD9 loss in saline or urethane mice compared to wild type. Together, these data suggest the environment in FZD9$^{-/-}$ lungs has altered gene expression and downstream activity that may support development of lung adenomas, but that loss of Fzd9 expression alone does not increase β-catenin activity.

FZD9$^{-/-}$ Adenomas Have More Characteristics of Tumors

In the urethane lung cancer mouse model at 16 weeks after injection, FVB/N mice have multiple hyperplasias and adenomas, while saline controls typically have none. We collected adenomas from wild type urethane and FZD9$^{-/-}$ urethane mice, extracted RNA, and used qPCR to measure expression of lung cancer associated genes. FZD9$^{-/-}$ adenomas had significantly higher expression of polo-like kinase 1 (PLK1) and cyclin D1, which are associated with altered cell cycle control in lung cancer (**Figure 5A**). Increased PLK1 is also associated with persistent squamous dysplasias (21). BCL2 is elevated in FZD9$^{-/-}$ adenomas, suggesting increased avoidance of apoptosis (**Figure 5A**). Significantly elevated N-cad, FN1, and VEGF may contribute to increased potential of FZD9$^{-/-}$ adenomas for

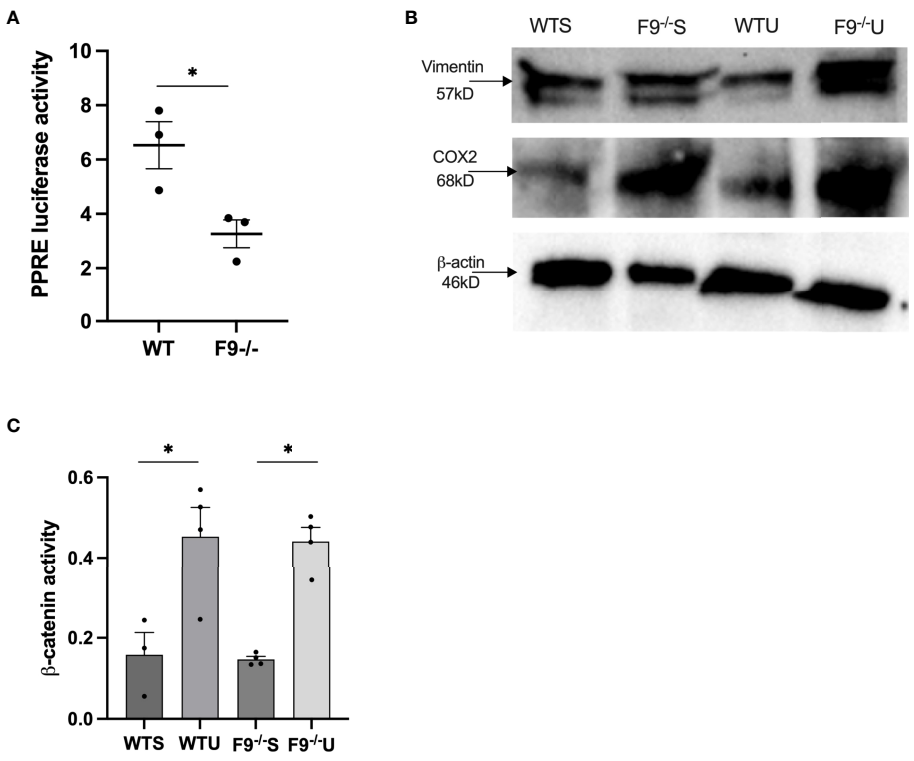

FIGURE 4 | Loss of FZD9 *in vivo* alters downstream target activity. **(A)** HEK293t cells were transfected with PPRE-luc and treated with 10ul mouse serum from wild type or FZD9$^{-/-}$ mice. Significance was measured by two-tailed t-test and *p<0.05 **(B)** Protein was extracted from whole lung samples from wild type or FZD9$^{-/-}$ mice exposed to saline or urethane and analyzed for vimentin and COX2 protein expression, with β-actin as a loading control. **(C)** Active β-catenin was measured by ELISA in wild type or FZD9$^{-/-}$ mice treated with saline or urethane. The assay was conducted in triplicate. Significance was measured by one-way ANOVA with Tukey's *post hoc* analysis and *p>0.05. WT, wild type; F9-/-, FZD9 knockout; WTS, wild type saline; F9$^{-/-}$S, FZD9$^{-/-}$ saline; WTU, Wild type urethane; F9$^{-/-}$U, FZD9$^{-/-}$ urethane.

progression to carcinoma (**Figure 5A**). Increased COL1a2 may result from the presence of cancer associated fibroblasts in FZD9$^{-/-}$ adenomas and is associated with poor prognosis (22). ESR1 is overexpressed in NSCLC and promotes proliferation, migration, and invasion of lung cancer cells (23). ESR1 was not detected in male FZD9$^{-/-}$ adenomas and was significantly elevated in female FZD9$^{-/-}$ adenomas (**Figure 5A**). ESR2 expression is higher in normal lung, is associated with poor prognosis of NSCLC, and is elevated in male adenocarcinomas (19). Here, ESR2 was elevated significantly in male FZD9$^{-/-}$ adenomas and non-significantly in female FZD9$^{-/-}$ adenomas (**Figure 5A**). We generated cell lines from adenomas collected from wild type and FZD9$^{-/-}$ mice. These cell lines were compared for differences in protein expression of downstream targets and for changes in cell behavior. Increased BCL2 in FZD9-/- adenomas suggested an effect of FZD9 loss on cell survival, so we measured apoptosis proteins in the WT and FZD9$^{-/-}$ adenoma cell lines by protein dot blot. In the FZD9$^{-/-}$ adenoma cell lines compared to the WT cell line, we found increased IGF-1, BCL-W and HSP60, and decreased p53, IGFBP2, and TRAILR2, all supporting that loss of FZD9 contributes to increased cell survival in adenomas (**Figure 5B**)

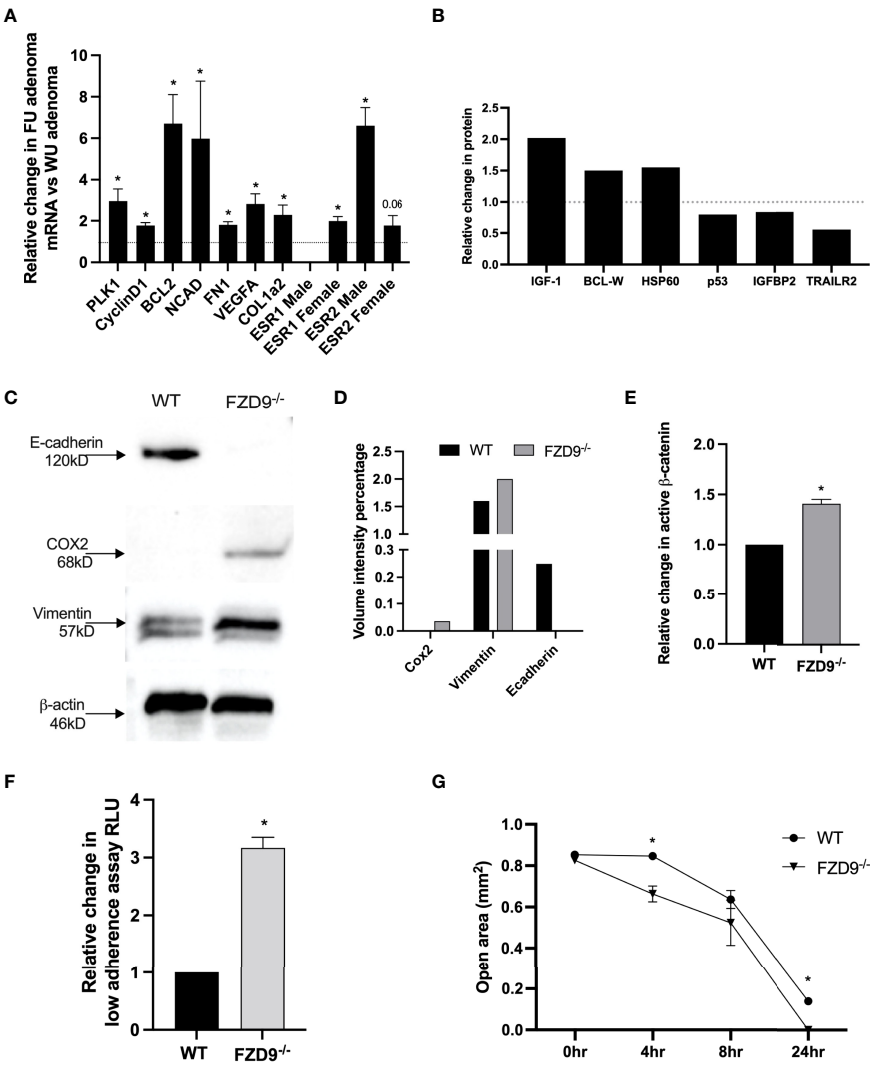

FIGURE 5 | Urethane induced FZD9$^{-/-}$ adenomas have a more tumor-like phenotype. **(A)** Change in gene expression in FZD9$^{-/-}$ (FU) adenomas relative to wild type (WU) adenomas, measured by qPCR. Data is normalized to RPS18 and assays were conducted in triplicate. **(B)** Changes in apoptosis pathway proteins was measured by dot blot, normalized to dot blot positive controls, and quantified. (n=1) **(C)** Change in protein expression measured by western blot of FZD9$^{-/-}$ and WT adenoma cell lines. β-actin is a loading control. **(D)** Quantification of bands from western blot in **(C)**. **(E)** Active β-catenin was measured by ELISA in a Fzd9$^{-/-}$ adenoma cell line and is shown relative to a WT adenoma cell line. The assay was conducted in triplicate. **(F)** Growth on low adherence plates measured by fluorescence viability assay in a FZD9$^{-/-}$ adenoma cell line and shown relative to a WT adenoma cell line. Assay was conducted in triplicate. **(G)** Migration was measured in triplicate by quantifying the open area left by a silicone insert in cells cultured over 24 hours. WT, wild type tumor cell line; F9$^{-/-}$, FZD9 knockout tumor cell line. Statistical significance was measured by a two-tailed t-test and *p<0.05.

(Dot blot images are in **Supplementary Figure 2**). Western blot protein analysis of the adenoma cell lines indicated higher expression of e-cadherin in wild type adenoma cells and higher expression of COX2 and VIM in FZD9$^{-/-}$ adenoma cells (**Figures 5C, D**). An active β-catenin ELISA detected increased active β-catenin in the FZD9$^{-/-}$ adenoma cells compared to the wild type adenoma cells (**Figure 5E**). Adenoma cell lines were cultured for 48 hours on a low-adherence plate to measure transformed growth. FZD9$^{-/-}$ adenoma cells had significantly higher growth compared to wild type adenoma cells (**Figure 5F**). To measure the migration capacity of the adenoma cell lines, a silicone insert was used to generate identical spaces while cells grew to 90% confluency around the insert. Over 24 hours, FZD9$^{-/-}$ adenoma cells moved into an empty space on a tissue culture plate faster than wild type adenoma cells (**Figure 5G**) (Representative images of the migration assay are in **Supplementary Figure 3**). Together, these data suggest that FZD9$^{-/-}$ adenomas have increased capacity for aggressive behavior and have higher levels of factors that promote tumor progression.

CSC Decreases FZD9 Expression and Downstream Activity

In vivo, exposure to cigarette smoke carcinogens, including urethane and one week of smoke exposure, decreased FZD9 expression (10). Here, we measured FZD9 expression in FVB/N mice after six weeks of cigarette smoke exposure and found decreased FZD9 expression compared to mice exposed only to ambient air (**Figure 6A**). Exposure to CSC alters expression of FZD9 in HBEC3KT after 24 weeks of exposure (10). We investigated the effects of two weeks of CSC exposure on HBEC3KT. Expression of FZD9 and ECAD decreased significantly, while VIM expression increased (**Figure 6B**). We also demonstrated that two weeks of CSC exposure in HBEC3KT led to decreased PPARγ activity and increased growth in low adherence conditions (**Figures 6C, D**). This was also validated with protein extraction, where ECAD was decreased and VIM was increased after the cells were exposed to CSC (**Figure 6E**).

To understand effects of cigarette smoke on FZD9 and PPARγ expression in human lung epithelium, we used RNA *in situ* hybridization (RISH) to measure expression in lung biopsies from the oral iloprost clinical trial (16). We conducted RISH for GAPDH (positive control), dapB (negative control), PPARγ, and FZD9 on baseline and follow up biopsies from 125 patients (Representative staining, **Figure 6F**). We compared FZD9 and PPARγ expression in epithelial cells at baseline with smoking parameters, including smoking status (current or former), smoking pack years, and smoking quit time, to determine if there is an effect of cigarette smoke exposure on FZD9 or PPARγ expression. All analyses were adjusted for sex. Baseline model analysis of FZD9 produced non-significant results, however, we see a trend in all models where higher smoke exposure leads to lower FZD9 expression at baseline (**Figure 6G**). The estimated odds ratios (OR) for current smoking status and lower quit time were 0.97 (p=0.933) and 0.78 (p=0.577), respectively. The OR for pack years approached significance at 0.55 (p=0.086). PPARγ baseline models also resulted in non-significant results, where current smoking status and lower quit time led to higher expression of PPARγ (**Figure 6G**). The ORs for current smoking status and lower quick time were 2.21 (p=0.192) and 1.41 (p=0.582)), respectively. In contrast, higher pack years resulted in a lower expression of PPARγ that neared significance with a OR of 0.36 (p=0.08), which agrees with the FZD9 baseline model analysis. Analysis of the effect of cigarette smoke on the lung epithelium in human cells and tissue suggests that FZD9 expression is a target of cigarette smoke induced carcinogenesis.

CSC Alters Expression of FZD9 Through PPARγ

PPARγ activation in the lung epithelium occurs when Wnt7a binds FZD9, but if FZD9 expression is decreased by CSC, we hypothesized that PPARγ activity would also be lost. Loss of PPARγ occurs *in vitro* in lung epithelial cells with 16 weeks of CSC exposure and *in vivo* with urethane exposure (24). Here, we show decreased PPARγ expression with six weeks of cigarette exposure in mice (**Figure 7A**) and decreased expression in HBEC3KT with 1-24 weeks of CSC exposure (**Figure 7B**). We also found that 48 hours of CSC exposure in HBEC3KT significantly reduces PPRE activity compared to control cells (**Figure 7C**). Regulation of FZD9 transcription in the lung epithelium by transcription factors has not been described. We transfected HBEC3KT with a PPARγ expression plasmid, confirmed increased PPARγ expression, and found that FZD9 expression also increased (**Figure 7D**). To determine if PPARγ is necessary for FZD9 expression, we transfected a PPARγ siRNA into HBEC3KT and confirmed significantly decreased PPARγ, which was associated with significantly decreased FZD9 expression (**Figure 7E**). We identified putative PPRE binding sites in the Fzd9 promoter and hypothesized that, in addition to being a target of FZD9 signaling, PAPRγ could act as a transcription factor for FZD9 (**Figure 7F**) (25). To determine if PPARγ binds to the FZD9 promoter and is sufficient to activate transcription, we transfected a PPARγ plasmid into HBEC3KT cells along with a luciferase containing the complete Fzd9 promoter and found that luciferase activity significantly increased with PPARγ compared to a control plasmid (**Figure 7G**). Transfection of PPARγ siRNA with the FZD9 promoter luciferase did not significantly decrease activity of the luciferase (data not shown), suggesting the presence of additional factors that may compensate for PPARγ loss. **Figure 7H** depicts the effects of carcinogen exposure and Fzd9 loss in lung epithelial cells. Together, these data demonstrate that PPARγ activates transcription of FZD9 and that cigarette smoke exposure may reduce FZD9 expression in part by decreasing PPARγ expression and activity.

DISCUSSION

Frizzled receptors have oncogenic and tumor suppressive activity depending on the specific Frizzled, tissue, or disease investigated

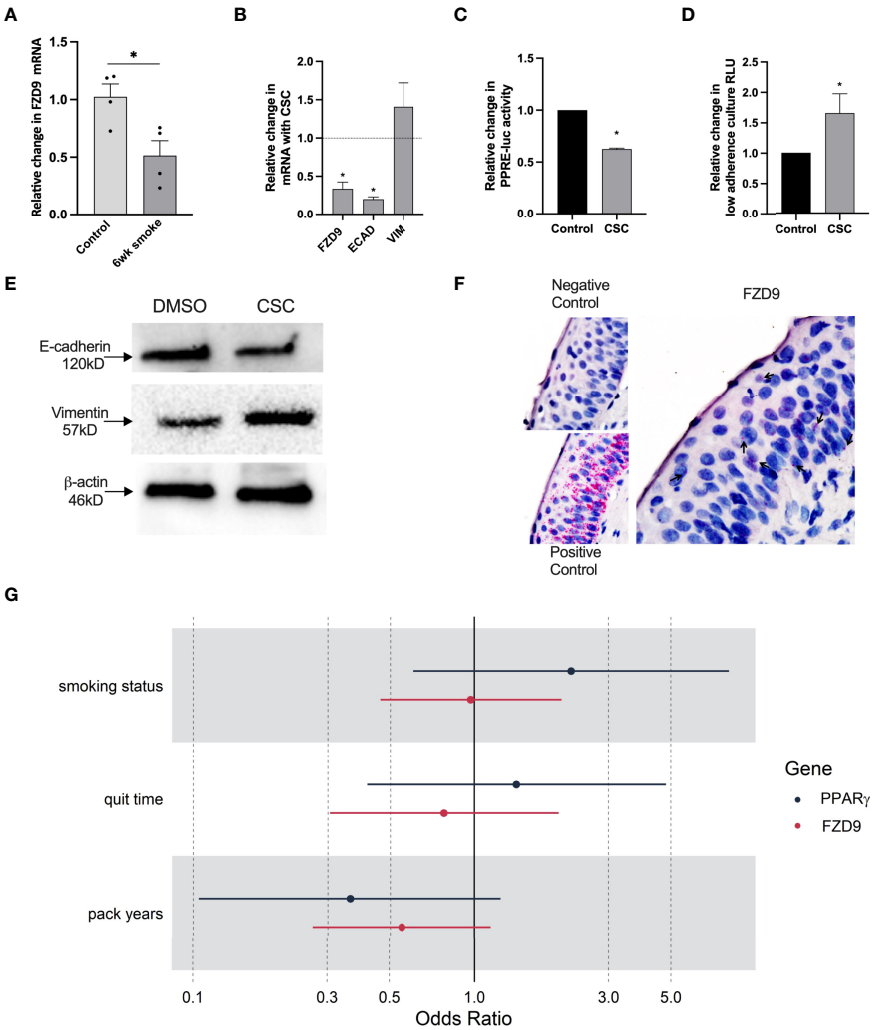

FIGURE 6 | FZD9 expression decreases with smoke exposure. **(A)** Change in FZD9 expression in mice after six weeks of exposure to cigarette smoke or ambient air control, measured by qPCR. Results are normalized to RPS18 and conducted in triplicate. **(B–D)** HBEC3KT were treated with 5ug/ml CSC or DMSO every 48 hours for two weeks and analyzed for **(B)** FZD9, Ecad, and VIM expression by qPCR, **(C)** PPRE-luc activity by transfection, **(D)** viability in a low-adherence culture, and **(E)** Ecad and VIM protein expression by western blot, with β-actin loading control. Significance in A-E was measured by a two-tailed t-test and *p<0.05. CSC, cigarette smoke condensate. Treatments, transfections, luciferase assays, and qPCR was conducted in triplicate. qPCR results are normalized to GAPDH. Data is shown relative to control. **(F)** Representative images for RISH signal in negative control, positive control, and FZD9. **(G)** Odds ratios for the effect of smoking characteristics on FZD9 and PPARγ expression at baseline, where someone with higher pack year exposure to smoke has lower odds of high FZD9 expression.

(26). For example, FZD1 is oncogenic in lymphoma and neuroblastoma but in prostate cancer is methylated early in lesion progression, suggesting a suppressive role (27–29). In mesenchymal glioblastoma, FZD6 is overexpressed, but in gastric cancer, overexpression of FZD6 reduced tumorigenesis (30, 31). Interest in the role of FZD9 in the lung was initiated by the discovery that FZD9 and Wnt7a induced non-canonical and tumor suppressive signaling in NSCLC cells, in contrast with studies in osteosarcoma and hepatocellular carcinoma (3, 7, 32). We engineered loss of FZD9 in two HBEC cell lines and found changes in EMT genes that had previously been associated with FZD9 negative NSCLC cell lines, suggesting that persistence of early changes may contribute to lesion progression (9). EMT associated with Frizzleds may also be targeted for chemoprevention (33). We also discovered changes in the expression of new targets of FZD9, including EZH2, IL1β, and VEGFA, all of which are associated with lung cancer. EZH2 is associated with carcinogen-induced transformation of HBEC and its depletion prevents progression from hyperplasia to adenoma in an NNK mouse model (34). IL1β induces EMT in NSCLC cells and is reduced with iloprost chemoprevention (35, 36). VEGF is overexpressed in bronchial dysplasia and is associated with persistent lesions (21, 37). Increased expression of these genes in normal epithelial cells likely contributes to initiation or promotion of early lesions with FZD9 loss.

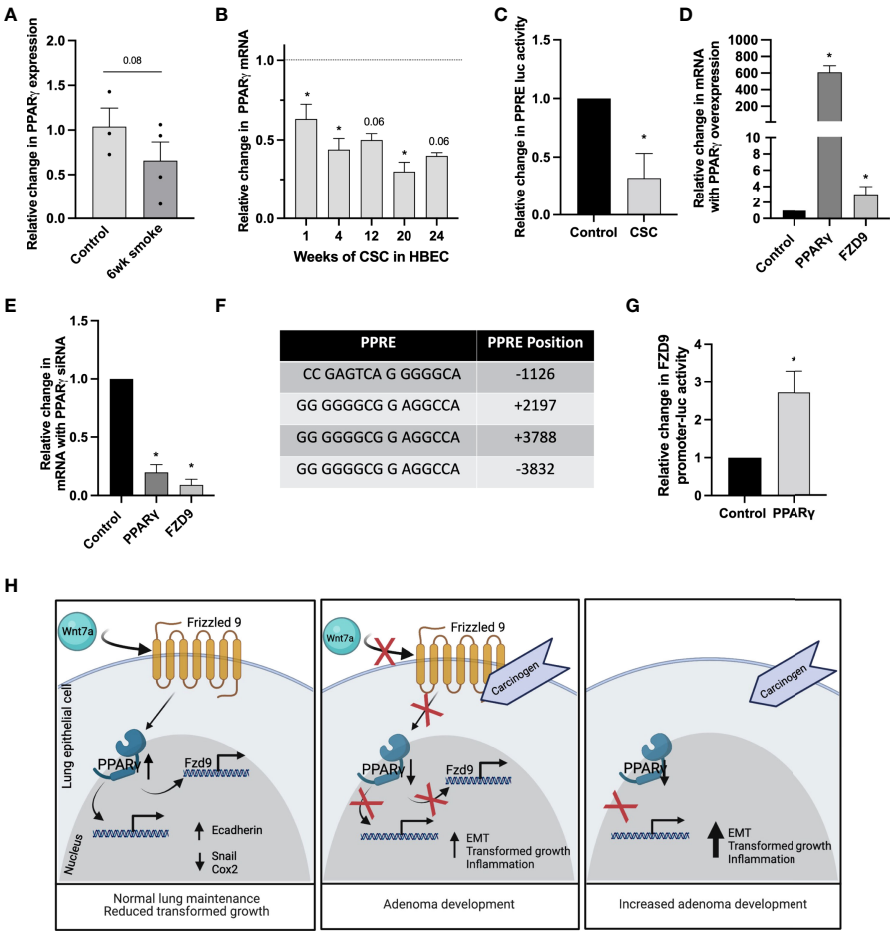

FIGURE 7 | Transcription of FZD9 is decreased by CSC and increased by PPARγ. **(A)** Change in PPARγ expression in mice after six weeks of exposure to cigarette smoke or ambient air control measured by qPCR. Results are normalized to RPS18 and measured in triplicate. **(B)** Change in PPARγ expression in HBEC3KT with 1-24 weeks exposure to CSC relative to DMSO control at each time point (dotted line), measured by qPCR. Results are normalized to GAPDH and conducted in triplicate. **(C)** Change in PPRE-luc activity after 48 hours of CSC exposure relative to DMSO control in HBEC3KT. Transfections and luciferase assays were conducted in triplicate. **(D, E)** Fold change in PPARγ and FZD9 expression in HBEC3KT measured by qPCR after transfection in triplicate with **(D)** PPARγ or **(E)** PPARγ siRNA. Results are normalized to GAPDH, relative to control, and conducted in triplicate. **(F)** Putative PPREs in the TSS-flanking region of FZD9. **(G)** FZD9 promoter luciferase activity vs control in HBEC3KT after transfection with a PPARγ plasmid. **(H)** Diagram of the effects of carcinogen exposure and Fzd9 loss in lung epithelial cells. Diagram created with Biorender.com. Transfections and luciferase assays were conducted in triplicate. Statistical significance was determined by a two-tailed t-test or one-way ANOVA with Tukey's *post hoc* analysis and *p<0.05. CSC, cigarette smoke condensate.

With the current study, we present the first investigation of effects of FZD9 loss in the urethane lung adenocarcinoma model. Loss of FZD9 increased tumor multiplicity *in vivo* with carcinogen exposure, however, this trend was not significant (p=0.08), which reduces the impact of this data. When the FZD9$^{-/-}$ urethane group in this study is compared to a larger wild type urethane group from a different urethane FZD9$^{-/-}$ study conducted in parallel (under review), there is a significant difference between adenoma number, suggesting that a larger wildtype urethane group in this study would have led to significance. Unfortunately, additional animals could not be included for this report and we acknowledge this limitation. FZD9 loss induced expression of EMT genes VIM and FN1 and inflammatory genes COX2 and IL1β. This correlates with *in vitro* data from this study and supports previous data from carcinogen exposure *in vitro* and *in vivo* (24). FZD9$^{-/-}$ female mice exhibited higher mRNA levels of ESR1 and ESR2 in both whole lung and adenomas when compared to all male mouse groups and to wild-type female groups. This is the first observation of an association between FZD9 and estrogen in the lung. Estradiol is elevated in NSCLC, and tobacco smoke activates metabolism of 17β-estradiol to the carcinogenic metabolite 4-OH-E (19). The role of estrogen receptors in lung cancer is not as clear, but lung cancer is considered estrogen positive, with predominant ESR2 expression, and in females ESR2 is associated with a worse prognosis (38). Estrogen receptors regulate components of the tumorigenic β-catenin signaling pathway to modulate NSCLC progression (39). Increased tumor promoting characteristics in

$FZD9^{-/-}$ lung tissue and adenomas could be due to loss of regulation of estrogen receptor expression and subsequent activation of receptor signaling networks that promote cancer development. These results support investigations into the role of estrogen in development of premalignant lung lesions and the potential for anti-estrogen therapy to block progression to lung cancer.

When FZD9 binds to Wnt7a in the lung epithelium and initiates anti-cancer signaling through PPARγ, it does not activate canonical β-catenin signaling (3). In whole lung analysis from mice in this study, active β-catenin was increased with urethane but was not higher in $FZD9^{-/-}$ tissue compared to wild type, suggesting that loss of FZD9 alone in the uninvolved tissue surrounding adenomas does not contribute to increased β-catenin signaling. In this first examination of a FZD9 negative, urethane-induced, lung adenoma cell line, we found that compared to a wildtype urethane-induced adenoma cell line, loss of FZD9 led to increased expression of apoptosis inhibiting, proliferation promoting, and EMT genes. We also found changes in protein expression that would lead to suppression of apoptosis in $FZD9^{-/-}$ adenomas. In contrast to whole lung analysis, the $FZD9^{-/-}$ adenoma cell line had increased active β-catenin compared to the wild type adenoma cell line, which may lead to the increased cyclinD1 observed in $FZD9^{-/-}$ adenomas. Increased β-catenin could also lead to transcription of c-Myc, a frequently dysregulated oncogene in lung cancer (40). $FZD9^{-/-}$ adenoma cells had increased ability to grow in an anchorage independent environment and to migrate, suggesting a more dedifferentiated phenotype. FZD9 may have a role in the development of early lung lesions and loss of FZD9 could lead to early lesions more likely to progress to carcinoma through several associated mechanisms.

In an *in vitro* model using HBEC, FZD9 expression decreases during short- and long-term CSC exposure. In cells treated with CSC followed by removal of CSC with 4 weeks of iloprost, a chemopreventive prostacyclin analogue, FZD9 expression increases while cells with continued CSC maintain low FZD9 (10). This result mirrors the oral iloprost chemoprevention trial, in which current smokers did not have improved endobronchial histology with iloprost but former smokers did (16). Examination of cell, animal, and human samples in the current study confirms that cigarette smoke exposure decreases FZD9 expression. This establishes a contribution by FZD9 to early changes in the lung epithelium that occur with cigarette smoke exposure. FZD9 also plays a key role in the activity of iloprost, where it is required for iloprost's activation of PPARγ and downstream anti-cancer signaling (9). We demonstrated decreased activation of PPRE with FZD9 loss or CSC in HBEC and with FZD9 loss in mouse serum. Regulation of FZD9 by transcription factors in the lung is largely unknown, but Frizzleds can be regulated by non-coding RNA and we previously demonstrated that miR-31 indirectly and miR-520a-5p directly decrease FZD9 expression (10, 41, 42). Here we show evidence of PPARγ acting as a transcription factor for FZD9. FZD9 and PPARγ expression is increased by iloprost, suggesting feedback loops that propagate a response to iloprost. In the presence of cigarette smoke, however, increased FZD9 and PPARγ expression and activation are inhibited, preventing a response to iloprost and leading to persistence of early lesions in the lung epithelium. Additional studies are needed to offer a more detailed appraisal of the relationship between FZD9, PPARγ, and cigarette smoke.

Loss of FZD9 from cigarette smoke carcinogen exposure interferes with maintenance of a normal lung epithelium and could promote premalignant lesion development and progression. Recent work suggests that, contrary to previously held opinions, FZD receptors could be direct targets for small molecule drugs (43). The smoothened agonist SAG1.3 binds Fzd6 to stimulate activation and interactions in the Fzd6 signaling pathway (44). There is also evidence suggesting that the chemoprevention drug iloprost binds to FZD9 (9). FZD9 may be a target for intercepting early lung lesion development and progression. To explore the potential of FZD9 as a therapeutic or preventive target, further investigation is required to understand the regulation of FZD9 by PPARγ and other factors at the transcriptional and translational levels, and to clarify how cigarette smoke alters FZD9 expression in the lung.

DATA AVAILABILITY STATEMENT

The raw data supporting the conclusions of this article will be made available by the authors, without undue reservation.

ETHICS STATEMENT

Ethical review and approval was not required for the study on human participants in accordance with the local legislation and institutional requirements. Written informed consent for participation was not required for this study in accordance with the national legislation and the institutional requirements. The animal study was reviewed and approved by Institutional Animal Care and Use Committee, Rocky Mountain Regional Veterans Affairs Medical Center Veterinary Medical Unit.

AUTHOR CONTRIBUTIONS

Conceptualization: MT, LD-N, and RK; Methodology: KK and LV; Investigation: KS, AS, AE, and L-DN; Analysis: LV, KS, AE, and MT; Funding acquisition: MT; Project administration: KS, AE, and MT; Supervision: MT and LN; Writing – original draft: KS and MT; Writing – review and editing: KS, AE, MT, L-DN, and RK. All authors contributed to the article and approved the submitted version.

FUNDING

This work was supported by the National Cancer Institute (R01CA214531) (MT), an NIH CURE Diversity Supplement (AS), the Regional Mouse Genetics Core Facility (National

Jewish Health and the University of Colorado Anschutz Medical Campus), and the University of Colorado Cancer Center Cell Technologies shared resource funded by the National Cancer Institute through a Cancer Center Support Grant (P30CA046934).

SUPPLEMENTARY MATERIAL

The Supplementary Material for this article can be found online at: https://www.frontiersin.org/articles/10.3389/fonc.2022.815737/full#supplementary-material

REFERENCES

1. Wang YK, Spörle R, Paperna T, Schughart K, Francke U. Characterization and Expression Pattern of the Frizzled Gene Fzd9, the Mouse Homolog of FZD9 Which Is Deleted in Williams-Beuren Syndrome. *Genomics* (1999) 57 (2):235. doi: 10.1006/geno.1999.5773
2. Wang Y, Chang H, Rattner A, Nathans J. Frizzled Receptors in Development and Disease. *Curr Top Dev Biol* (2016) 117:113–39. doi: 10.1016/bs.ctdb.2015.11.028
3. Winn RA, Marek L, Han SY, Rodriguez K, Rodriguez N, Hammond M, et al. Restoration of Wnt-7a Expression Reverses Non-Small Cell Lung Cancer Cellular Transformation Through Frizzled-9-Mediated Growth Inhibition and Promotion of Cell Differentiation. *J Biol Chem* (2005) 280(20):19625–34. doi: 10.1074/jbc.M409392200
4. Zhang Z, Schittenhelm J, Guo K, Buhring HJ, Trautmann K, Meyermann R, et al. Upregulation of Frizzled 9 in Astrocytomas. *Neuropathol Appl Neurobiol* (2006) 32(6):615–24. doi: 10.1111/j.1365-2990.2006.00770.x
5. Albers J, Schulze J, Beil FT, Gebauer M, Baranowsky A, Keller J, et al. Control of Bone Formation by the Serpentine Receptor Frizzled-9. *J Cell Biol* (2011) 192(6):1057–72. doi: 10.1083/jcb.201008012
6. Zhang Y, Jiang Q, Kong X, Yang L, Hu W, Lv C, et al. Methylation Status of the Promoter Region of the Human Frizzled 9 Gene in Acute Myeloid Leukemia. *Mol Med Rep* (2016) 14(2):1339–44. doi: 10.3892/mmr.2016.5387
7. Fujimoto T, Tomizawa M, Yokosuka O. SiRNA of Frizzled-9 Suppresses Proliferation and Motility of Hepatoma Cells. *Int J Oncol* (2009) 35(4):861–6. doi: 10.3892/ijo_00000400
8. Winn RA, Van Scoyk M, Hammond M, Rodriguez K, Crossno JTJr., Heasley LE, et al. Antitumorigenic Effect of Wnt 7a and Fzd 9 in non-Small Cell Lung Cancer Cells Is Mediated Through ERK-5-Dependent Activation of Peroxisome Proliferator-Activated Receptor Gamma. *J Biol Chem* (2006) 281(37):26943–50. doi: 10.1074/jbc.M604145200
9. Tennis MA, Van Scoyk M, Heasley LE, Vandervest K, Weiser-Evans M, Freeman S, et al. Prostacyclin Inhibits non-Small Cell Lung Cancer Growth by a Frizzled 9-Dependent Pathway That Is Blocked by Secreted Frizzled-Related Protein 1. *Neoplasia* (2010) 12(3):244–53. doi: 10.1593/neo.91690
10. Tennis MA, New ML, McArthur DG, Merrick DT, Dwyer-Nield LD, Keith RL. Prostacyclin Reverses the Cigarette Smoke-Induced Decrease in Pulmonary Frizzled 9 Expression Through miR-31. *Sci Rep* (2016) 6:28519. doi: 10.1038/srep28519
11. Raffoux E, Cras A, Recher C, Boelle PY, de Labarthe A, Turlure P, et al. Phase 2 Clinical Trial of 5-Azacitidine, Valproic Acid, and All-Trans Retinoic Acid in Patients With High-Risk Acute Myeloid Leukemia or Myelodysplastic Syndrome. *Oncotarget* (2010) 1(1):34–42. doi: 10.18632/oncotarget.100518
12. Sato M, Larsen JE, Lee W, Sun H, Shames DS, Dalvi MP, et al. Human Lung Epithelial Cells Progressed to Malignancy Through Specific Oncogenic Manipulations. *Mol Cancer Res* (2013) 11(6):638–50. doi: 10.1158/1541-7786.MCR-12-0634-T
13. Malkinson AM, Dwyer-Nield LD, Rice PL, Dinsdale D. Mouse Lung Epithelial Cell Lines–Tools for the Study of Differentiation and the Neoplastic Phenotype. *Toxicology* (1997) 123(1-2):53–100. doi: 10.1016/S0300-483X(97)00108-X
14. Rotem A, Janzer A, Izar B, Ji Z, Doench JG, Garraway LA, et al. Alternative to the Soft-Agar Assay That Permits High-Throughput Drug and Genetic Screens for Cellular Transformation. *Proc Natl Acad Sci U S A* (2015) 112 (18):5708–13. doi: 10.1073/pnas.1505979112
15. Edwards L, Watt J, Webster TF, Schlezinger JJ. Assessment of Total, Ligand-Induced Peroxisome Proliferator Activated Receptor Gamma Ligand Activity in Serum. *Environ Health* (2019) 18(1):45. doi: 10.1186/s12940-019-0486-2
16. Keith RL, Blatchford PJ, Kittelson J, Minna JD, Kelly K, Massion PP, et al. Oral Iloprost Improves Endobronchial Dysplasia in Former Smokers. *Cancer Prev Res (Phila)* (2011) 4(6):793–802. doi: 10.1158/1940-6207.CAPR-11-0057
17. Ramirez RD, Sheridan S, Girard L, Sato M, Kim Y, Pollack J, et al. Immortalization of Human Bronchial Epithelial Cells in the Absence of Viral Oncoproteins. *Cancer Res* (2004) 64(24):9027–34. doi: 10.1158/0008-5472.CAN-04-3703
18. Fritz JM, Tennis MA, Orlicky DJ, Lin H, Ju C, Redente EF, et al. Depletion of Tumor-Associated Macrophages Slows the Growth of Chemically Induced Mouse Lung Adenocarcinomas. *Front Immunol* (2014) 5:587. doi: 10.3389/fimmu.2014.00587
19. Musial C, Zaucha R, Kuban-Jankowska A, Konieczna L, Belka M, Marino Gammazza A, et al. Plausible Role of Estrogens in Pathogenesis, Progression and Therapy of Lung Cancer. *Int J Environ Res Public Health* (2021) 18(2):648. doi: 10.3390/ijerph18020648
20. Karasawa T, Yokokura H, Kitajewski J, Lombroso PJ. Frizzled-9 Is Activated by Wnt-2 and Functions in Wnt/beta -Catenin Signaling. *J Biol Chem* (2002) 277(40):37479–86. doi: 10.1074/jbc.M205658200
21. Merrick DT, Edwards MG, Franklin WA, Sugita M, Keith RL, Miller YE, et al. Altered Cell-Cycle Control, Inflammation and Adhesion in High-Risk Persistent Bronchial Dysplasia. *Cancer Res* (2018) 78(17):4971–83. doi: 10.1158/0008-5472.CAN-17-3822
22. Zeng Y, Li N, Zheng Z, Chen R, Peng M, Liu W, et al. Screening of Hub Genes Associated With Pulmonary Arterial Hypertension by Integrated Bioinformatic Analysis. *BioMed Res Int* (2021) 2021:6626094. doi: 10.1155/2021/6626094
23. Liau CS, Mogan P, Thomas W. Oestrogen Actions Contribute to Female Gender-Specific Risks in the Development of Lung Carcinoma. *J Steroid Biochem Mol Biol* (2021) 208:105786. doi: 10.1016/j.jsbmb.2020.105786
24. New ML, White CM, McGonigle P, McArthur DG, Dwyer-Nield LD, Merrick DT, et al. Prostacyclin and EMT Pathway Markers for Monitoring Response to Lung Cancer Chemoprevention. *Cancer Prev Res (Phila)* (2018) 11 (10):643–54. doi: 10.1158/1940-6207.CAPR-18-0052
25. Fang L, Zhang M, Li Y, Liu Y, Cui Q, Wang N. PPARgene: A Database of Experimentally Verified and Computationally Predicted PPAR Target Genes. *PPAR Res* (2016) 2016:6042162. doi: 10.1155/2016/6042162
26. Zeng CM, Chen Z, Fu L. Frizzled Receptors as Potential Therapeutic Targets in Human Cancers. *Int J Mol Sci 19(5)* (2018) 19(5):1543. doi: 10.3390/ijms19051543
27. Flahaut M, Meier R, Coulon A, Nardou K, Niggli F, Martinet D, et al. The Wnt Receptor FZD1 Mediates Chemoresistance in Neuroblastoma Through Activation of the Wnt/β-Catenin Pathway. *Oncogene* (2009) 28(23):2245–56. doi: 10.1038/onc.2009.80
28. Mathur R, Sehgal L, Braun FK, Berkova Z, Romaguerra J, Wang M, et al. Targeting Wnt Pathway in Mantle Cell Lymphoma-Initiating Cells. *J Hematol Oncol* (2015) 8(1):1–12. doi: 10.1186/s13045-015-0161-1
29. Devaney JM, Wang S, Funda S, Long J, Taghipour DJ, Tbaishat R, et al. Identification of Novel DNA-Methylated Genes That Correlate With Human Prostate Cancer and High-Grade Prostatic Intraepithelial Neoplasia. *Prostate Cancer Prostatic Dis* (2013) 16(4):292–300. doi: 10.1038/pcan.2013.21
30. Huang T, Alvarez AA, Pangeni RP, Horbinski CM, Lu S, Kim SH, et al. A Regulatory Circuit of miR-125b/miR-20b and Wnt Signalling Controls Glioblastoma Phenotypes Through FZD6-Modulated Pathways. *Nat Commun* (2016) 7:12885. doi: 10.1038/ncomms12885
31. Sheh A, Ge Z, Parry NM, Muthupalani S, Rager JE, Raczynski AR, et al. 17beta-Estradiol and Tamoxifen Prevent Gastric Cancer by Modulating Leukocyte Recruitment and Oncogenic Pathways in Helicobacter Pylori-

Infected INS-GAS Male Mice. *Cancer Prev Res (Phila)* (2011) 4(9):1426–35. doi: 10.1158/1940-6207.CAPR-11-0219
32. Wang Q, Liu H, Wang Q, Zhou F, Liu Y, Zhang Y, et al. Involvement of C-Fos in Cell Proliferation, Migration, and Invasion in Osteosarcoma Cells Accompanied by Altered Expression of Wnt2 and Fzd9. *PLoS One* (2017) 12(6):e0180558. doi: 10.1371/journal.pone.0180558
33. Sompel K EA, Smith AJ, Tennis MA. Cancer Chemoprevention Through Frizzled Receptors and EMT. *Discover Oncol* (2021) 12(32):32. doi: 10.1007/s12672-021-00429-2
34. Tellez CS, Picchi MA, Juri D, Do K, Desai DH, Amin SG, et al. Chromatin Remodeling by the Histone Methyltransferase EZH2 Drives Lung Pre-Malignancy and Is a Target for Cancer Prevention. *Clin Epigenet* (2021) 13 (1):44. doi: 10.1186/s13148-021-01034-4
35. Li R, Ong SL, Tran LM, Jing Z, Liu B, Park SJ, et al. Chronic IL-1beta-Induced Inflammation Regulates Epithelial-to-Mesenchymal Transition Memory Phenotypes *via* Epigenetic Modifications in non-Small Cell Lung Cancer. *Sci Rep* (2020) 10(1):377. doi: 10.1038/s41598-019-57285-y
36. Tennis MA, Smith AJ, Dwyer-Nield LD, Keith RL. Intranasal Iloprost Prevents Tumors in a Murine Lung Carcinogenesis Model. *Cancer Prev Res (Phila)* (2021) 15(1):11– 6. doi: 10.1158/1940-6207.CAPR-21-0086
37. Merrick DT, Haney J, Petrunich S, Sugita M, Miller YE, Keith RL, et al. Overexpression of Vascular Endothelial Growth Factor and its Receptors in Bronchial Dypslasia Demonstrated by Quantitative RT-PCR Analysis. *Lung Cancer* (2005) 48(1):31–45. doi: 10.1016/j.lungcan.2004.07.049
38. Chen H, Yan M, Shi W, Shi J, Duan C, Fan Q, et al. Expression of Estrogen Receptor Beta and Overall Survival in non-Small Cell Lung Cancer Patients: Protocol for a Systematic Review and Meta-Analysis of Cohort Studies. *Med (Baltimore)* (2019) 98(43):e17559. doi: 10.1097/MD.0000000000017559
39. Gao X, Cai Y, Wang Z, He W, Cao S, Xu R, et al. Estrogen Receptors Promote NSCLC Progression by Modulating the Membrane Receptor Signaling Network: A Systems Biology Perspective. *J Transl Med* (2019) 17(1):308. doi: 10.1186/s12967-019-2056-3
40. Chanvorachote P, Sriratanasak N, Nonpanya N. C-Myc Contributes to Malignancy of Lung Cancer: A Potential Anticancer Drug Target. *Anticancer Res* (2020) 40(2):609–18. doi: 10.21873/anticanres.13990
41. Smith AJ, Do P, Sompel K, Elango A, Tennis MA. miR-520a-5p Regulates Frizzled 9 Expression and Mediates Effects of Cigarette Smoke and Iloprost Chemoprevention. *Sci Rep* (2022) 12(1):2388. doi: 10.1038/s41598-022-06292-7
42. Smith AJ, Sompel KM, Elango A, Tennis MA. Non-Coding RNA and Frizzled Receptors in Cancer. *Front Mol Biosci* (2021) 8:712546. doi: 10.3389/fmolb.2021.712546
43. Schulte G, Wright SC. Frizzleds as GPCRs - More Conventional Than We Thought! *Trends Pharmacol Sci* (2018) 39(9):828–42. doi: 10.1016/j.tips.2018.07.001
44. Kozielewicz P, Turku A, Bowin CF, Petersen J, Valnohova J, Canizal MCA, et al. Structural Insight Into Small Molecule Action on Frizzleds. *Nat Commun* (2020) 11(1):414. doi: 10.1038/s41467-019-14149-3

Conflict of Interest: The authors declare that the research was conducted in the absence of any commercial or financial relationships that could be construed as a potential conflict of interest.

Publisher's Note: All claims expressed in this article are solely those of the authors and do not necessarily represent those of their affiliated organizations, or those of the publisher, the editors and the reviewers. Any product that may be evaluated in this article, or claim that may be made by its manufacturer, is not guaranteed or endorsed by the publisher.

Advantages of publishing in Frontiers

OPEN ACCESS
Articles are free to read for greatest visibility and readership

FAST PUBLICATION
Around 90 days from submission to decision

HIGH QUALITY PEER-REVIEW
Rigorous, collaborative, and constructive peer-review

TRANSPARENT PEER-REVIEW
Editors and reviewers acknowledged by name on published articles

Frontiers
Avenue du Tribunal-Fédéral 34
1005 Lausanne | Switzerland

Visit us: www.frontiersin.org
Contact us: frontiersin.org/about/contact

REPRODUCIBILITY OF RESEARCH
Support open data and methods to enhance research reproducibility

DIGITAL PUBLISHING
Articles designed for optimal readership across devices

FOLLOW US
@frontiersin

IMPACT METRICS
Advanced article metrics track visibility across digital media

EXTENSIVE PROMOTION
Marketing and promotion of impactful research

LOOP RESEARCH NETWORK
Our network increases your article's readership